Insulinotropic and glucose-lowering peptides from phylogenetically ancient fish with potential for therapy of type 2 diabetes

A thesis presented for the degree of

Doctor of Philosophy

In the

School of Biomedical Sciences

Faculty of Life and Health Sciences

Galyna Graham B.Sc.

February 2019

Dedication

I dedicate my thesis to my family, teachers and friends

CONTENTS

ACKNOWLEDGEMENTS

I would like to thank my supervisors Prof Peter Flatt, Prof Michael Conlon and Dr Yasser Abdel-Wahab for the opportunity to join as a PhD student in Diabetes Research Group at Ulster University. I would like to express my gratitude to them for providing excellent supervision, valuable guidance, support and patience throughout these years. I am also greatly appreciative of all the staff members of the DRG group and BBRU for their support.

The wish to thank Professor Bernard Thorens (University of Lausanne, Switzerland) for GLP-1 receptor-transfected CHL cells, Professor Cecilia Unson (The Rockefeller University, USA) for glucagon receptor transfected HEK293 cells and Jaqueline Naylor (MedImmune, Cambridge, UK) for CRISPR/Cas9-engineered INS-1 cells.

I am grateful for Ulster University for awarding me with the DEL scholarship and providing world-class research facilities.

Summary

This thesis investigates the in vivo and in vitro ability of glucagon-related molecules isolated from a wide range of fish species including sea lamprey, dogfish, ratfish, paddlefish, zebrafish and trout, to exert antidiabetic actions by acting on multiple GPCR receptors in a mammalian system. Overall, the piscine peptides with the most potential were glucagon and GLP-1 from sea lamprey and paddlefish, and oxyntomodulin from dogfish. These proglucagon-derived molecules showed insulinotropic activities in rat clonal pancreatic beta cells (BRIN-BD11), human-derived pancreatic beta cells (1.1B4) and isolated mouse islets similarly to human GLP-1. The dual agonist properties of fish hormones were demonstrated *in vitro* using glucagon and GLP-1 receptors antagonists, GLP-1R-transfected CHL and glucagonR-transfected HEK293 cells as well as CRISPR/Cas9-engineered cells bearing either GLP-1R or glucagonR knock-out. Acute administration of fish peptides to normal mice produced significant beneficial antihyperglycaemic and insulinotropic changes, however, the actions were limited due to rapid enzymatic degradation in plasma by DPP-IV

Structural modifications including the stereochemical configuration and the addition of a γ-glutamyl spacer to the selective fish glucagon and GLP-1 sequences were used to develop novel enzymatically stable analogues namely [D-Ser^2]-lamprey glucagon-Lys^{30}-gamma-glutamyl-pal, [D-Ser^2]-paddlefish glucagon-Lys^{30}-gamma-glutamyl-pal, [D-Ala^2]-lamprey GLP-1-Lys^{31}-gamma-glutamyl-pal and [D-Ala^2]-paddlefish GLP-1-Lys^{28}-gamma-glutamyl-pal. The most promising analogues, [D-Ala^2]-lamprey GLP-1-Lys^{31}-gamma-glutamyl-pal and [D-Ser^2]-paddlefish glucagon-Lys^{30}-gamma-glutamyl-pal retained the potent biological properties of the native peptides as indicated in acute in vitro and in vivo studies. Moreover, chronic administration of [D-

Ala^{2}]-lamprey GLP-1-Lys^{31}-gamma-glutamyl-pal and [D-Ser^{2}]-paddlefish glucagon-Lys^{30}-gamma-glutamyl-pal analogues improved metabolic status, islet morphology and the expression genes involved in insulin secretion in diet-induced obese mice and showed positive effects on beta-cell transdifferentiation in genetically modified GluCreRosa26-YFP mice.

To conclude, this thesis outlines the ability of fish glucagon-derived peptides and their analogues to modulate simultaneously multiple receptor signalling pathways resulting in prominent antidiabetic effects and illustrates the potential of the peptides to be developed into therapeutic agents for the treatment of type 2 diabetes-obesity.

ABBREVIATIONS

AAC	Area above the curve
ABCC	ATP binding cassette subfamily C member 8
ADP	Adenosine diphosphate
AGIs	Alpha-glucosidase inhibitors
AKT1	Protein Kinase B
ANOVA	Analysis of variance
ATP	Adenosine triphosphate
AUC	Area under the curve
BMC	Bone mineral content
BMD	Bone mineral density
BSA	Bovine serum albumin
bw	Body weight
BYA	Billion years ago
$CaCl_2.2H_2O$	Calcium chloride dihydrate
CACNA1C	Calcium voltage-gated channel subunit alpha1 C
cAMP	Cyclic adenosine monophosphate
CCK	Cholecystokinin
cDNA	Complementary DNA
CH_2Cl_2	Dichloromethane

cm	Centimetre
CO_2	Carbon dioxide
CoA	Coenzyme A
cpm	Counts per minutes
CPT-1	Carnitine palmitoyltransferase 1
Da	Dalton
DAG	Diacylglycerol
DAPI	4' 6-diamidino-2-phenylindole
DCC	Dextran-coated charcoal
DIDS	4 4-diisothiocyanostilbene-2 2-disulfonic acid
DM	Diabetes mellitus
DMEM	Dulbecco's Modified Eagle's medium
DPP-IV	Dipeptidyl peptidase IV
DUK	Diabetes United Kingdom
DEXA	Dual-energy X-ray absorptiometry
EC50	Half maximal effective concentration
EDTA	Ethylenediamine tetraacetic acid
EGTA	Ethylene glycol-bis-N N N'N'-tetraacetic acid
ELISA	Enzyme-linked immunosorbent assay
ER	Endoplasmic reticulum

FBS	Foetal bovine serum
FFA	Free fatty acids
g	Gram
GCK	Glucokinase
GCG	Glucagon
GIP	Glucose-dependent insulinotropic peptide
GLP-1	Glucagon-like peptide 1
GLUT2	Glucose transporter 2
GLUT4	Glucose transporter 4
GRP	Gastrin-releasing peptide
GTT	Glucose tolerance test
HBSS	Hanks balanced salt solution
HCl	Hydrochloric acid
HDL	High density lipoprotein
HEPES	4-(2-hydroxyethyl)-1-piperazineethanesulfonic acid
HLA	Human leukocyte antigen
HOMA-IR	Homeostatic model assessment of insulin resistance
HPLC	High-performance liquid chromatography
IBMX	1-methyl-3-(2-methylpropyl)-7H-purine-2 6-dione
IDF	International Diabetes Federation

IFNγ	Interferon-gamma
IGT	Impaired glucose tolerance
IL-1β	Interleukin 1 beta
INS	Insulin gene
INSR	Insulin receptor
InsP3	Inositol 1, 4, 5-triphosphate
IPGTT	Intraperitoneal glucose tolerance test
IRS1	Insulin receptor substrate 1
IRS2	Insulin receptor substrate 2
IUCN	International Union for Conservation of Nature
KCl	Potassium chloride
KCNJ11	Potassium inwardly-rectifying channel subfamily J member 11
kg	Kilogram
KH_2PO_4	Potassium dihydrogen orthophosphate
KRBB	Kreb's ringer bicarbonate buffer
kV	Kilovolt
L	Litre
LDH	Lactate dehydrogenase
LDL	Low-density lipoprotein
m/z	Mass per charge

MALDI-TOF MS	MS Matrix-assisted laser desorption/ionization mass spectrometry
mCi	Millicurie
mg	Milligram
$MgSO_4$	Magnesium sulphate
MHC	Major Histocompatibility Complex
min	Minute
ml	Millilitre
mM	Millimolar
mmol	Millimole
MW	Molecular weight
MYA	Million years ago
N	Normal
Na_2HPO_4	Disodium hydrogen orthophosphate
NaCl	Sodium chloride
NAD	Nicotinamide adenine dinucleotide
NADH	Nicotinamide adenine dinucleotide reduced
$NaHCO_3$	Sodium bicarbonate
Na125I	Radioactive sodium iodide
NaOH	Sodium hydroxide
NEFAs	Non-esterified fatty acids

ng	Nanogram
NHS	National Health Service
nm	Nanometer
nmol	Nanomole
nM	Nanomolar
OD	Optical density
O_2	Oxygen
OGTT	Oral glucose tolerance test
OXM	Oxyntomodulin
PBS	Phosphate buffer saline
PC	Prohormone convertase
PDK1	3-phosphinositide dependent protein kinase 1
PDX-1	Pancreatic and duodenal homeobox 1
PI3KCA	Phosphoinositide-3-kinase catalytic alpha polypeptide
PKA	Protein kinase A
PKB	Protein kinase B
PKC	Protein kinase C
PLC	Phospholipase C
pM	Picomole
PP	Pancreatic polypeptide

PPARγ	Peroxisome proliferator-activated receptor γ
PTB 1	Protein phosphatase 1B
RFU	Relative fluorescence unit
RIA	Radioimmunoassay
RLU	Relative light units
ROS	Reactive oxygen species
rpm	Revolutions per minute
RPMI	Roswell Park Memorial Institute
SEM	Standard error of mean
SGLT2	Sodium-glucose transporter 2
SLC2A4	Glucose transporter 4
SLC2A2	Glucose transporter 2
STAT1	Signal transducer and activator of transcription 1, isoform 1
STZ	Streptozotocin
SUR1	Sulphonylurea receptor 1
T1D	Type 1 diabetes mellitus
T2D	Type 2 diabetes mellitus
TCA	Tricarboxylic acid cycle
TEA	Triethanolamine
TFA	Trifluoroacetic acid

TNF α	Tumour necrosis factor α
TUNEL	Terminal deoxynucleotidyl transferase dUTP nick end labelling
TZDs	Thiazolidinediones
UDP	Uridine diphosphate
UK	United Kingdom
UKPDS	United Kingdom Prospective Diabetes Study
USA	United States of America
µg	Microgram
µl	Microlitre
µM	Micromolar
V	Volts
v/v	Volume/volume
VDCC	Voltage dependent calcium channel
VLDL	Very low-density lipoprotein
WHO	World Health Organization
w/v	Weight per volume
zfGIP	Zebrafish GIP

List of amino acids and their abbreviations

Amino Acid	3-Letter	1-Letter	Side-chain polarity	Side-chain charge (pH 7.4)
Alanine	Ala	A	Nonpolar	Neutral
Arginine	Arg	R	Polar	Positive
Asparagine	Asn	N	Polar	Neutral
Aspartic acid	Asp	D	Polar	Negative
Cysteine	Cys	C	Nonpolar	Neutral
Glutamic acid	Glu	E	Polar	Negative
Glutamine	Gln	Q	Polar	Neutral
Glycine	Gly	G	Nonpolar	Neutral
Histidine	His	H	Polar	Positive
Isoleucine	Ile	I	Nonpolar	Neutral
Leucine	Leu	L	Nonpolar	Neutral
Lysine	Lys	K	Polar	Positive
Methionine	Met	M	Nonpolar	Neutral
Phenylalanine	Phe	F	Nonpolar	Neutral
Proline	Pro	P	Nonpolar	Neutral
Serine	Ser	S	Polar	Neutral
Threonine	Thr	T	Polar	Neutral
Tryptophan	Trp	W	Nonpolar	Neutral
Tyrosine	Try	Y	Polar	Neutral
Valine	Val	V	Nonpolar	Neutral

PUBLICATIONS ARISING FROM THE THESIS

Full-Length Scientific Papers

1. Graham GV; Conlon JM; Abdel-Wahab YH; Gault VA; Flatt PR “Evaluation of the insulinotropic and glucose-lowering actions of zebrafish GIP in mammalian systems: Evidence for involvement of the GLP-1 receptor”, Peptides, Volume 100: 182-189; 2018.

2. Graham, GV; Conlon JM; Abdel-Wahab YH; Flatt PR "Glucagon-like peptides-1 from phylogenetically ancient fish show potent anti-diabetic activities by acting as dual GLP1R and GCGR agonists", Molecular and Cellular Endocrinology, Volume 480: 54-64; 2018.

3. Graham GV; Conlon JM; Abdel-Wahab YH; Flatt PR “Glucagon-related peptides from phylogenetically ancient fish reveal new approaches to the development of dual GCGR and GLP1R agonists for Type 2 diabetes therapy” Volume: 110, 19-29; 2018.

These published papers form the basis for Chapters 3, 4 and 7

DECLARATION

"I hereby declare that for two years from the date, on which the thesis is deposited in the library of the Ulster University, the thesis shall remain confidential with access or copying prohibited. Following the expiry of this period, I permit the Librarian of the University to allow the thesis to be copied in whole or in part without reference to me on the understanding that such authority applies to the provision of single copies made for study purposes or inclusion within the stock of another library. This restriction does not apply to British Library Service (which, subject to the expiry of the period of confidentiality, is permitted to copy the thesis on demand for loan or sale under the terms of a separate agreement) nor to the copying or publication of the title and abstract of the thesis.

IT IS A CONDITION OF USE OF THIS DISSERTATION THAT ANYONE WHO CONSULTS IT MUST RECOGNISE THAT THE COPYRIGHT RESTS WITH THE AUTHOR AND THAT NO QUOTATION FROM THE DISSERTATION AND NO INFORMATION DERIVED FROM IT MAY BE PUBLISHED UNLESS THE SOURCE IS PROPERLY ACKNOWLEDGED"

Chapter 1

General Introduction

1.1 History of Diabetes: from ancient times to the discovery of insulin

1.1.1 In Antiquity

Diabetes Mellitus is an ancient disease. The earliest recognised record of the clinical feature characterised as "too great emptying of the urine" was noted on third-dynasty Egyptian papyrus by physician Hesy-Ra in 1552 BCE (Zajac et al. 2010; Bhaskar et al. 2010). For the treatment of this disease, ancient Egyptian physicians recommended using wheat grains, fruit, and sweet beer (Zajac et al. 2010).

At around the same time, ancient Indian physicians developed what can be described as the first clinical test for diabetes after discovering that the urine from affected individuals attracted ants and flies. They named the condition *Madhumeha* (passing a large volume of sweet urine).

Around 230 BCE, Apollonius of Memphis originally described the term *diabetes* meaning from Greek "*pass through*" (dia – through, betes – to go) as the condition drained more fluid than a person could consume (Das et al. 2011). He attributed diabetes to a disease of the kidneys and recommended bloodletting and dehydration for the treatments (Zajac et al. 2010).

In 30–50 CE, a Roman medical writer, Aulus Cornelius Celsus, made the first complete clinical description of diabetes and included it his monumental eight-volume work entitled *De medicina* (Poretsky 2010; Zajac et al. 2010). However, only in early 2nd century Aretaeus of Cappadocia, a Greek physician provided a detailed and accurate account of diabetes in his work *On the Causes and Indications of Acute and Chronic Diseases*. Medical historians believed that Aretaeus of Cappadocia re-introduced the prefix 'diabetes' when he described the differences in polyuria between

the clinical picture of what is now known as type 1 diabetes (T1D) and diabetes insipidus (Nwanery 2015).

A Greek physician of the Roman Empire, Claudius Galenus, referred to as Galen (129-200 CE) supported the work of Apollonius of Memphis by attributing the development of the condition to the weakness of the kidney (Eknoyan et al. 2005).

In the 5th century, Indian physicians, Sushruta and Charaka, noted differences in the clinical picture of patients and identified two types of conditions associated with youth or obesity, later to be named T1D and T2D respectively (Ramachandran et al. 2009). Sushruta included exercise in the prescription to treat the disease and promoted physical activities to minimise the consequences of obesity and diabetes (Tipton 2008).

Although Galen defined diabetes as a rare disease and only investigated two cases, Maimonides, the most prominent Jewish medieval physician claimed to have seen more than 20 individuals suffering from this illness (Rosner 2002; Sanders et al. 2002). Meanwhile, in medieval Persia, Avicenna (980–1037 CE), an Arabo-Islamic physician and medical writer, provided a detailed account for diabetes in his book *The Canon of Medicine.* He recognised primary and secondary diabetes, as well as explained some complications of diabetes such as sexual dysfunction and diabetic gangrene. For the treatment of diabetes, Avicenna used a mixture of herbal remedies which are still recognised in modern time (Lakhtakia 2013; Eboh et al. 2014; Mahdizadeh et al. 2015; Sharofova et al. 2017).

1.1.2 Renaissance and After

A fundamental change in the basic concepts of understanding diabetes was made in the 16th century, when the Renaissance physician Paracelsus (1493-1541) challenged the medical doctrine describing the condition as a constitutional disease that "irritates the kidneys" and provokes polyuria. Having evaporated the urine from a diabetic patient, Paracelsus discovered an excessive residue which he incorrectly called "salt" particles (Eknoyan et al. 2005). It was only much later, in 1670, that an English doctor, Thomas Willis noticed the sweet taste of urine of patients with diabetes and added the word *mellitus* - the Latin word for honey (Ahmed 2002). This observation was not new due to, as mentioned earlier, the sweetness of urine was already described in ancient Indian texts and noted by Paracelsus and Avicenna (Eknoyan et al. 2005; Zajac et al. 2010). Thomas Willis attributed diabetes to the disease of the blood arguing that the sweetness appears first in the blood before it reaches the urine (Eknoyan et al. 2005). In 1776, British physiologist Matthew Dobson (1713–1784) identified that the sweet-tasting substance in the urine of diabetic patients was sugar serum and published his work as *Experiments and Observations on the Urine in Diabetics*. He also discovered hyperglycaemia while noticing the sweet taste of blood serum in diabetic sufferers which supported the theory of diabetes being a systemic disease (Eknoyan et al. 2005; Macfarlane 2014). A decade after, in 1788, Thomas Cawley performed the autopsy of patients with diabetes and observed that their pancreatic tissue was damaged which indicated the involvement of the pancreas in the pathogenesis of disease (Stylianou et al. 2009).

1.1.3 The 19th and the Early 20th Century: Discovery of Insulin

Although diabetes and its treatment attempts have been known since ancient times, the important elements of current understanding of diabetes mellitus can be traced to the 19th century, the time when modern scientific disciplines and chemical methods were invented (Zajac et al. 2010; Poretsky 2010). A French chemist, Eugene Chevreul, studied the sugar isolated from diabetic urine and discovered that it was identical to "grape sugar". (Tattersall 2009; Dods 2013). In 1815, he proved that this sugar was glucose (Zajac et al. 2010). By this time in history, glycosuria was accepted criteria for the diagnosis of diabetes and first quantitative tests were invented. However, the source of glucose and the metabolic process in the body remained unknown (Zajac et al. 2010; Dods 2013). One of the hypotheses suggested that glucose was transported by the lymphatic system into the blood and metabolised there. Others proposed that the lungs were involved in the process of "burning" of the sugar (Jorgens et al. 2013). In 1857, a French physiologist, Claude Bernard (1813–1878), questioned these strange hypotheses after discovering that the liver stored a starch-like substance (that he baptized "glycogen") and secreted a sugary substance into the blood affecting blood sugar levels (Sanders at al. 2002; Jorgens et al. 2013). He received wide acceptance after proposing that over-secretion of this substance leads to diabetes (Zajac et al. 2010). Indeed, it was the work of Claude Bernard that promoted the study of diabetes which over the next 50 years evolved into the discipline of endocrinology. It also made a crucial contribution to the discovery of the role of the pancreas in diabetes by Oscar Minkowski (1858-1931) and Joseph von Mering (1849-1908) in 1889. The scientists observed signs of diabetes in the dogs after total pancreatectomy. (Eknoyan et al. 2005; Karamanou et al. 2016).

To prove that the impaired exocrine pancreatic secretion was not involved in the pathogenesis of diabetes, dog's pancreatic duct was ligated which led to the development of digestive problems but not elevated blood glucose.

After French investigator, Edouard Hedon (1863–1933), confirmed similar findings in 1893, it became clear that the internal pancreatic secretion was the main cause of the disease (Zajac et al. 2010). At the same year, French scientist Gustave–Edouard Laguesse (1861–1927) proposed that the pancreatic islet cells discovered by Paul Langerhans in 1869, might be the source of the substance involved in blood glucose control. (Zajac et al. 2010; Alam et al. 2017). In 1923, Frederick Banting and John MacLeod received the Nobel Prize in Physiology or Medicine for the insulin' discovery which was a fundamental step in the history of diabetes. (Karamanou et al. 2016).

Over the next years, there was an improvement in the methods of insulin purification leading to new insulin formulations such as Protamine–zinc insulin or long-acting insulin (Engelhardt 1989; Karamanou et al. 2016). However, the discovery of insulin did not provide the world with a cure for diabetes and did not prevent complications such as retinopathy, nephropathy, neuropathy, and coronary and peripheral angiopathy (Stylianou et al. 2009). Hence, diabetes mellitus continues to be one of the major healthcare challenges of the 21st century.

1.2 Classification of Diabetes Mellitus

The existence of clinically different types of diabetes had been evident from historical Indian texts. In the 19th century a French pharmacist, Apollinaire Bouchardat pioneered a systematic treatment regimen for obese patients after noticing that weight loss and physical activity helped to promote metabolic control. Another French

physician, Étienne Lancereaux, described patients as having ‘diabète maigre’ (lean diabetes) or ‘diabète gras’ (fat diabetes) (Watkins et al. 2008). However, in 1936, Harold (Harry) Percival Himsworth was the first to link clinical symptoms with insulin sensitivity and thus scientifically identified the differences between type 1 and type 2 diabetes and developed a test to distinguish between them (Furdell et al. 2008; Bryder et al. 2013).

1.2.1 Type 1 diabetes (T1D)

Type 1 diabetes (T1D) is a chronic disease caused by specific immune-mediated destruction targeting the endocrine unit of the pancreas, insulin-producing pancreatic β-cells, which leads to a subsequent reliance on exogenous insulin load (Yoon et al. 2005; Simmons et al. 2015). T1D is one of the most common metabolic and endocrine illnesses among children and young adults. The incidence of the disease continues to increase, especially in children less than five years of age (Simmons et al. 2015).

In 1997, the Committee of Experts of the American Diabetes Association developed a further classification of TD1 dividing it into Type 1A diabetes and Type 1 B (idiopathic). The former represents the vast majority of cases (70–90%) and involves immune-mediated responses whereas the aetiology of the latter is unknown (Echeverri et al. 2013 and Simmons et al. 2015). Unless otherwise stated, the term T1D refers to autoimmune T1D in this thesis.

T1D is associated with the presence of biomarkers of autoimmunity: humoral (auto-antibodies) and cellular (T-cells) responses occurring many months or years before symptom onset (Simmons et al. 2015). The immune system of affected individual target one or several autoantigens — islet cells, insulin, 65 kDa glutamic acid decarboxylase (GAD65; also known as glutamate decarboxylase 2), insulinoma-

associated protein 2 (IA2) or zinc transporter 8 (ZNT8) (Pihoker 2005 and Simmons et al. 2015). Immunosuppressive drugs such as cyclosporine and azathioprine can slow the progression of pancreatic islet destruction indicating the critical role of the immune system in the development of T1D (Fu et al. 2013).

Individuals with genetic predispositions have a higher risk to develop T1D. The Human Leukocyte Antigen (HLA) genes encoding cell surface proteins responsible for the interaction with immune cells are the major contributors to the presence of various autoantibodies in T1D sufferers (Rich 2015). The HLA Class II region is considered to be the most critical. People with class II HLA-risk genotypes, specifically with HLA DR3/4 and HLA DQ2/8 allelic variations have a 50% chance to develop two or more autoantibodies and T1D (Zhou et al. 2016 and Katsarou et al. 2017). Gene polymorphism in other non-HLA T1D loci encoding the insulin (*INS*), protein tyrosine phosphatase nonreceptor type 22 (*PTPN22)*, cytotoxic T-lymphocyte-associated antigen-4 (*CTLA4)*, interleukin 2 receptor alpha *(IL2RA)* and interferon induced with helicase C domain 1 (*IFIH1)* genes have also been suggested to be associated with T1D susceptibility (Kavvoura et al. 2005; Steck et al. 2011; Yang et al. 2012; Giza et al. 2013; Tang et al. 2015).

There is a 15-fold higher risk for siblings of a diabetic individual to develop T1D than the risk for T1D in the general population. Moreover, the concordance rates for T1D in monozygotic twins are approximately 50% while in dizygotic twins these rates are only 6-10% (Steck et al. 2011).

The genetic predisposition for T1D is combined with undefined environmental factors – including viral infections, the timing of solid food introduction, and development of food sensitisation and gestational events. (Gillespie et al. 2006; Erlich et al. 2008;

Steck et al. 2011; Katsarou et al. 2017). T1D usually has a rapid onset with the symptoms including elevated blood glucose, polyuria, polydipsia, extreme thirst, weight loss, abdominal symptoms, headaches and ketoacidosis (Katsarou et al. 2017). Hyperglycemia represents a clinically significant manifestation of the final stage of insulitis with only 10 to 20% of functional beta cells (Eisenbarth et al. 2005; Echeverri et al. 2013). Management of T1D in the past 30 years since the Diabetes Control and Complications Trial (DCCT), and Epidemiology of Diabetes Interventions and Complications (EDIC) studies has been focused on intensive insulin therapy that aims to maintain glucose levels as close to the nondiabetic range as safely possible and avoid hypoglycaemia (Nathan 2014; Gubitosi-Klug 2016; Katsarou et al. 2017)

1.2.2 Type 2 diabetes (T2D)

Type 2 D diabetes (T2D) is characterised by sustained hyperglycaemia as a result of ineffective pancreatic insulin production, insulin resistance or both. The chronic hyperglycaemia in diabetic subjects affects various organs, especially the eyes, kidneys, nerves, heart, and blood vessels (Olokoba et al. 2012; Prasad et al. 2015). This results in complications such as retinopathy with a risk of blindness; nephropathy linked to kidney failure; peripheral neuropathy which may progress to foot ulcers and amputations; and autonomic neuropathy associated with gastrointestinal, genitourinary, and cardiovascular abnormality as well as sexual dysfunction (American Diabetes Association 2009). The incidence of disability associated with T2D has increased significantly since 1990 among people aged 15–69 years (Zheng et al. 2018).

Analysis of recent statistical data reveals that the growing pandemic of T2D exhibits specific demographic characteristics. As such a steady increase in diabetes prevalence

is observed in developed countries whereas in developing countries it has become an alarming issue with a rapid rate of increase. The Asian population is contributing to more than 60% of the world's diabetes cases (Ramachandran et al. 2012; Wu et al. 2014; Nanditha et al. 2016). Moreover, it is becoming more frequently diagnosed in children, teenagers and adolescents as a result of increasing rates of childhood obesity or overweight (Wu et al. 2014).

The development of T2D is closely related to the interaction between multiple genes scattered all across the genome and environmental factors such as obesity, sedentary lifestyle and stress as well as low birth weight and ageing (Ali 2013; Mi et al. 2017; Zheng et al. 2018). The involvement of genetic factors has a clear impact on disease occurrence and progression. Some individuals appear to be more susceptible to developing diabetes than others even when exposed to the same environmental factors. The risk of developing T2D also increases if both parents are affected. The concordance rate in monozygotic twins is approximately 70% while the rates in dizygotic twins are only 20%-30%. Heritability of obesity contributes to the vast majority of diabetes cases (Ali 2013).

Segregation analysis revealed that T2D is a polygenic disorder. The identification of the genetic markers linked to the disease represents an ongoing challenge (Ali 2013). A large-scale genetic association study identified linkage of an SNP within intron 3 of calpain 10 (*CAPN10*) to susceptibility to T2D. The mechanisms by which genetic variation in this gene leads to T2D are still unknown (Sorimachi at al. 2013 and Melmed 2016). Moreover, polymorphism of transcription factor 7-like 2 (*TCF7L2*), encoding T-cell specific, HMG-box is confirmed to be a genetic risk factor according to multiple Genome-wide association studies (Ali 2015). Other genes linked to T2D

risk include *CDKAL1* (CDK5 regulatory subunit associated protein 1-like 1), *HMGA2* (high mobility group AT-hook 2), *KCNQ11* (potassium voltage-gated channel, KQT like subfamily, member 1), *IGF2BP2* (insulin-like growth factor 2 mRNA binding protein 2), *CDKN2A/B* (Cyclin-dependent kinase inhibitor 2A/B) and *NOTCH2-ADAM30* (Notch 2-ADAM metallopeptidase domain 30). The exact contribution of these genes to the pathophysiology of T2D remains mostly unknown (Ali 2013).

1.2.3 Novel subgroups of adult-onset diabetes

The classification of diabetes mainly relies on the presence (T1D) or absence (T2D) of autoantibodies targeting several pancreatic islet β-cell-related antigens and age at diagnosis. As a result, most of the patients are classified as having T2D. A third subgroup, latent autoimmune diabetes in adults (LADA, 10% of all diabetes cases, characterised by the presence antibodies targeting GAD65 autoantigen), phenotypically resembles type 2 diabetes at diagnosis but becomes increasingly similar to T1D with time. Interestingly, T1D and T2D could be further divided into different subtypes, according to recent research studies investigating cases of nearly 9,000 people with diabetes in Sweden and Finland (Ahlqvist et al. 2018).

Five clusters were identified. Cluster 1 labelled as severe autoimmune diabetes (SAID) overlapped with T1D and LADA, whereas cluster 2 and cluster 3 named as severe insulin-deficient diabetes (SIDD) and severe insulin-resistant diabetes (SIRD) respectively, represent two new, severe forms of diabetes previously masked within T2D. SIDD and SIRD were associated with an increased risk of kidney disease and retinopathy compared to the other clusters. Clusters 4 and 5, labelled as obesity-related diabetes (MOD), and mild age-related diabetes (MARD) respectively, corresponded to T2D (Ahlqvist et al. 2018).

The new clustering approach is superior to the classic diabetes classification which could improve outcomes of the disease by identifying patients at high risk of diabetic complications and potentially reduce the risk of diabetes-related complications in the future through personalising treatments (Ahlqvist et al. 2018).

1.3 Architecture of Endocrine Pancreas

In humans, the pancreas is a large solitary retroperitoneal organ originated from the embryonic foregut after the fusion of the ventral and dorsal buds. The organ is 14-18 cm long, 2-9 cm wide and 2-3 cm thick, weighing 50-125 g. It is usually divided for descriptive purposes into the head, neck, body and the tail regions. These regions, in contrast to the well-defined outer borders, have no clear-cut off borders between them (Dolensek et al. 2016; El-Gohary et al. 2018). The pancreas consists of exocrine and endocrine compartments. The exocrine pancreatic component represents 98% of the pancreatic tissue and consists of acinar cells which produce digestive enzymes secreted through a ductal network. The endocrine compartment is represented by three-dimensional clusters of cells, islets of Langerhans, surrounded by the exocrine part of the gland. These unique micro-organs exhibit complex cytoarchitecture and have a defined glucoregulatory function (Paniccia et al. 2017). Although pancreatic islets compromise only 2% of the total pancreatic volume, they are highly vascularized and receive approximately 10% of the blood supply (Rorsman et al. 2013). There are approximately 1 million islets scattered throughout the pancreas in humans, whereas the mouse pancreas contains approximately 1000-5000 islet cells. (Hruban et al. 2009; El-Gohary et al. 2018). In mammals, despite differences in the size of the pancreas and islet composition, the size distribution closely overlaps and lies between 100 and 200 μm regardless of species (Jo et al. 2007; Kim et al. 2009). Human pancreatic islets

consist of five cell subtypes: β-cells (50 % of the cells in human islets), α-cells (35–40%), δ-cells (10–15%), ε-cells (<10%) and pancreatic polypeptide (PP) cells (<10%) that synthesise and secrete glucagon, insulin, somatostatin, ghrelin and pancreatic polypeptide respectively (El-Gohary et al 2018). In addition to the hormone-secreting endocrine cells, other types of cells such as vascular cells, resident immune cells, and, in many species, neurons and glial cells of the neuroinsular complex are also found in the islets (Kilimnik et al. 2011; Caicedo et al. 2013). The composition of islet cells varies according to the region within the pancreas and among different species. Human islets have a superior proportion of alpha cells (38%) compared to mouse islets (18%). In humans, more alpha-cells intermingle with beta-cells, delta-cells cells or both whereas in mouse islet beta-cells are located in the central core with fewer alpha-cells residing in the periphery (Kilimnik et al. 2011; Caicedo et al. 2013). Moreover, the proportions of endocrine cells also differ between males and females of the same species (Gannon et al. 2018).

In addition to hormone-secreting endocrine cells, there are also other types of cells that are found in pancreatic islets such as vascular cells, resident immune cells, and, in many species, neurons and glial cells of the neuroinsular complex (Kilimnik et al. 2011 and Caicedo et al. 2013).

1.4 Insulin

1.4.1 Insulin synthesis

Insulin is the blood glucose-lowering hormone which is coded on the short arm of chromosome 11. It is originally synthesised as preproinsulin in the rough ER of the pancreatic β cells. Preproinsulin is transformed into an 86 amino acid peptide proinsulin by proteolytic action of cleaving enzymes. Finally, the proinsulin is then

transported to the Golgi complex, where it matures into active polypeptide hormone, insulin, and a 31 amino acid C-peptide. This step is catalyzed by several enzymes: prohormone convertases 1 and 2 (PC1 and PC2) and carboxypeptidase-H (Patil et al. 2014; Sun et al. 2017). In the healthy beta cells, the vast majority (> 95%) of proinsulin is converted to insulin and C-peptide. Insulin molecule consists of two polypeptide chains: chain A (21 a.a) and chain B (30 a.a) which are linked by disulfide bonds and have a molecular weight of 6 kDa (Patil et al. 2014). Mature granules containing equimolar amounts of C-peptide and insulin are secreted into the circulation by exocytosis (Scheen 2004; Wilcox 2005; Mielke et al. 2011). Although insulin is a relatively small polypeptide, it has been associated with more Nobel Prizes than any other molecules: an award in 1923 to Banting and colleagues for insulin isolation, an award in 1958 to Sanger for insulin sequencing, an award in 1964 to Dorothy Hodgkin for identification of the atomic structure of insulin and other biomolecules, and an award in 1977 to Yalow for technology leading to insulin-sensitive measurement (Mielke et al 2011; Jaskolski et al 2014).

1.4.2 Insulin secretion

Approximately, 50%-60% of the insulin secreted by the pancreatic beta cells into the portal vein is removed during the first passage through the liver. This causes higher levels of the hormone in the portal vein compared with its concentration in a peripheral vein. Basal pancreatic insulin release is important for the maintenance of basal euglycaemia. Both, basal insulin secretion and meal-related insulin release are controlled by glucose. However, other nutrients (other monosaccharides, amino acids, and fatty acids), hormones and neural factors are also important in maintaining glucose homeostasis (Scheen et al. 2004). Indeed, evolutionarily glucose is the primary

secretagogue in some animal species, accumulating immediately after food ingestion (Fu et al. 2013). Pancreatic beta cells employ several sensing mechanisms for measuring circulating glucose. Membrane-bound glucose transporters (GLUT) are parts of the cellular sensing apparatus. Out of the 14 GLUT family members so far identified, human pancreatic β-cells principally express GLUT1 (encoded by *SLC2A1*) and GLUT3 (encoded by *SLC2A3*) glucose transporters, which mediates facilitated diffusion of glucose regardless of the extracellular sugar concentration. Conversely, in rodent β cells glucose uptake occurs predominantly through Glut2 (encoded by *Slc2a2*) glucose transporter (Schuit et al. 2001; Rorsman et al.; 2013; Pingitore et al. 2017).

These GLUTs exhibit different affinities for glucose entry into β-cells. GLUT1 and GLUT3 transporters have high affinity with low capacity Km values of 1-4mM, whereas low affinity, GLUT2 has a K_m of > 15mM is most active at higher glucose concentrations. The differences in the glucose-sensing apparatus indicate species-specific regulation of glucose homeostasis (Pingitore et al. 2017).

After glucose enters β-cells, an additional element of the glucose sensing system, glucokinase (GCK) initiates glucose metabolic degradation. GCK is a rate-limiting enzyme which exhibits relatively low affinity for glucose. Its K_m is only 6 mmol/L, falling in the middle of the normal blood glucose range (4-10 mmol/l). GCK phosphorylates the reaction forming glucose 6 phosphate (Fu et al. 2013). Metabolism of glucose-6-phosphate via glycolysis, the endpoint of which is the metabolic substrate pyruvate. Pyruvate is then oxidized through the tricarboxylic acid *cycle* in mitochondria to produce ATP which subsequently leads to an increased intracellular ATP-to-ADP ratio (Schmeltz et al. 2007).

Elevated intracellular ATP closes KATP channels, depolarizes the membrane, and opens voltage-dependent Ca2+ channels. This results in an influx of Ca2+ which leads to the fusion of insulin-containing secretory granules with the plasma membrane and exocytosis of insulin into the portal circulation (Schmeltz et al. 2007; Fu et al. 2013).

The intermediates, NADPH, malonyl-CoA, and glutamate, derived in these processes can act as signals to further amplify K_{ATP} channel-dependent insulin secretion (Figure 1.1).

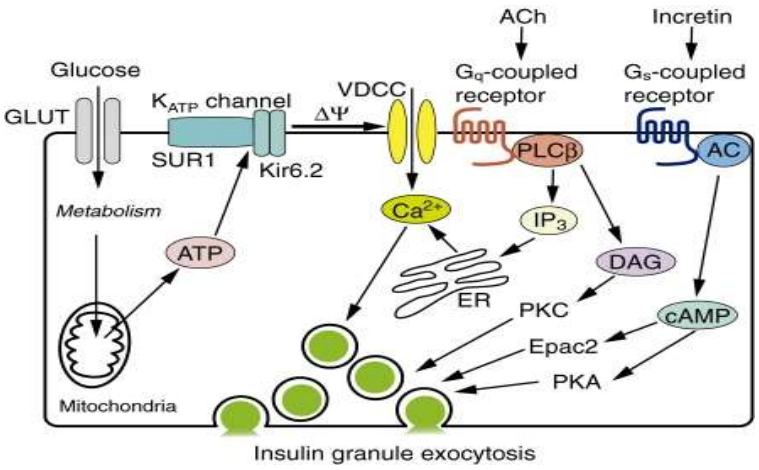

Figure 1.1 Mechanism of insulin secretion in the pancreatic β-cell (Fajans et al. 2001).

Moreover, additional glucose signals result from the generation of glycerol-3-phosphate (Gly3P) synthesized by reducing dihydroxyacetone phosphate (DHAP), a glycolysis intermediate, with glycerol-3-phosphate dehydrogenase. Gly3P is important for producing lipid metabolic coupling factors such as long-chain acyl-CoA and diacylglycerol (DAG) which can amplify insulin secretion. Elevated glucose also triggers insulin biosynthesis by increasing the transcription rate of the insulin gene (Schmeltz et al. 2007).

As mentioned earlier, apart from glucose other nutrients can act as secretagogues. Individual amino acids act as poor insulin secretagogues at physiological concentrations. Some combinations (combination of glutamine with leucine) or higher concentration (alanine) of amino acids stimulate insulin release from beta cells. Alanine and glutamine can indirectly influence pancreatic insulin release during the fasting period. These amino acids are released into the blood triggering glucagon secretion which results in elevation of blood glucose levels and subsequent insulin release. In addition, dietary amino acids influence insulin release through the incretin-dependent process. Ingestion of nutrients results in secretion of glucagon-like peptide-1 (GLP-1) and gastric inhibitory polypeptide (GIP) peptide hormones from intestinal cells which activate specific receptors expressed on the beta cells leading to elevation of cAMP generated from ATP. The cAMP amplifies insulin secretion via PKA phosphorylation which brings the type 2 ryanodine receptor RY_2 receptor to an excitable state increasing Ca^{2+} concentration (Islam et al. 2002; Tengholm et al. 2017).

Amplification of glucose-stimulated insulin secretion is also triggered by free fatty acids (FFAs), which is particularly operative in situations of increased insulin need as a consequence of insulin resistance in type 2 diabetes (Nolan et al. 2006; Fu et al. 2013) A membrane free fatty acid receptor, Gq protein-coupled receptor (FFAR-1/GPR40) expressed on beta cells was recently discovered. Elevated levels of FFA result in the increased concentration of long-chain acyl-CoA and DAG, which act directly by acylation of proteins (i.e. synaptosomal-associated protein-25 (SNAP-25) and synaptogamin) responsible for granule fusion the exocytotic machinery or indirectly by activating essential enzymes, such as protein kinase C respectively (Mingrone et al. 2006). Many hormones including cholecystokinin (CCK), estrogen, melatonin, leptin and growth hormone can also influence insulin release from beta

cells (Fu et al. 2013). Insulin-releasing medicines include sulfonylureas and glinides (Section 1.7.3)

1.4.3 Insulin action

1.4.3.1 Insulin action overview

Insulin controls glucose and lipid metabolism by binding to the insulin receptor (IR) on the membrane of target cells (Peterson et al. 2018). IR is a heterotetrameric receptor which belongs to the receptor tyrosine kinase family consisting of two extracellular α subunits (bind insulin) and two transmembrane β subunits (with tyrosine kinase domains) joined by disulfide bonds (Meyts 2016; Peterson 2018). The IR messenger RNA (mRNA) undergoes alternative splicing of exon 11 generating two isoforms (IR-A and IR-B). Out of these two IR isoforms, the IR-B is more specific for metabolic regulation, and it is primarily expressed in the liver, muscle and white adipose tissue (Boucher et al. 2014; Belfiore et al.2015; 2017; Peterson et al. 2018). The IR-A isoform is highly expressed in foetal cells such as foetal fibroblasts, muscle, liver and kidney where it regulates embryonic growth and development (Frasca et al. 1999; Boucher et al. 2014).

Structure-function studies of insulin analogues suggest that IR contains two insulin binding sites, however, due to its negative cooperativity, affinity for the ligand decreases. Hence, only one insulin molecule can bind and activate one IR (Whittaker et al. 2008; Peterson et al. 2018). Following ligand binding to the α subunits, IR undergoes a conformational change in the β subunit which accounts for transactivation of the tyrosine kinase activity through autophosphorylation of the activation loop of the kinase domain that contains tyrosines Tyr 1162, Tyr 1158, and Tyr 1163 (McDonald at al. 1995; Peterson et al. 2018). This process results in further tyrosine

phosphorylation on residues including Tyr 972 in the juxtamembrane region which importantly leads to recruitment of receptor substrates (IRS). These substrates (IRS 1-6) are members of the insulin receptor substrate family of proteins which act as an adaptor molecule that triggers signalling cascades by generating the molecular complexes. There are two main insulin signalling pathways: mitogenic and metabolic. Metabolic, the phosphatidylinositol-3-kinase (PI3K)/Akt, also known as protein kinase B (PKB), the pathway is initiated by insulin receptor substrate (IRS) proteins and SH2B2/APS. The pathway regulates glycolytic metabolism including glucose transport stimulation, glycogen and protein synthesis and adipogenesis (Gutiérrez-Rodelo et al. 2017). The central role in this signalling pathway belongs to Akt kinase which has three isoforms (Akt 1, 2 and 3). Isoform Akt 2 is responsible for insulin metabolic actions, including the incorporation of GLUT-4 from intracellular compartments into the plasma membrane of the cell muscle and adipose cells to facilitate glucose uptake.

On the other hand, mitogenic, mitogen-activated protein kinases/Ras pathway (MAPK/Ras), pathway is responsible for regulation of gene expression and insulin-associated mitogenic effects such as proliferation, differentiation and growth initiated by phosphorylation of growth factor receptor-bound protein 2 (GRB2) and SH2 domain-containing protein (SHC) (Gutiérrez-Rodelo et al 2017).

The positive feedback mechanism of the proximal insulin signalling pathway (Figure 1.2) is represented by feedforward amplification via Gα-interacting, vesicle-associated protein (GIV) potentiation of phosphoinositide-3-kinase (PI3K)-AKT signalling, and phosphatase inhibition by NAD(P)H oxidase 4 (NOX4)-derived H2O2] (Petersen et al. 2018). Insulin action is regulated by the concentration of circulating insulin. Negative feedback involves stabilisation and recruitment of GRB10 to the IR, and

activation of S6 kinase 1 (S6K1) to phosphorylate and inhibit IRS proteins). Liver clearance of insulin involves receptor-mediated insulin endocytosis and degradation via an IRS in the liver known as the carcinoembryonic antigen-related cell adhesion molecule 1 (CEACAM1) (Najjar 2002).

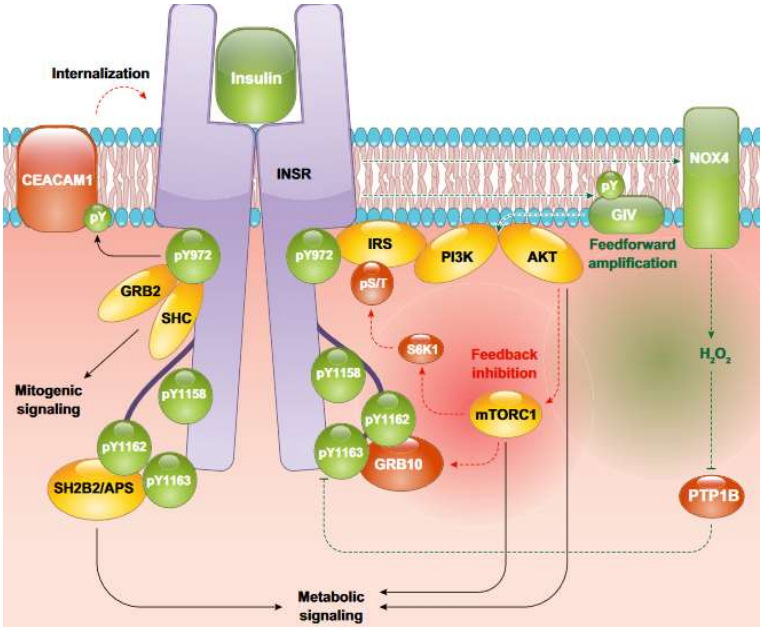

Figure 1. 2 Proximal insulin signalling (Petersen et al. 2018).

1.4.3.2 Insulin signalling in the skeletal muscle

When glucose is abundant, the skeletal muscle receives insulin signals to initiate the myocyte insulin signalling cascade responsible for promoting glucose uptake and glycogen synthesis/storage (Figure 1.3). Muscle accounts for about 60–70% of whole-body insulin-mediated uptake (Wilcox 2005). The cells uptake glucose via translocation of GLUT4-containing storage vesicles (GSVs) to the plasma membrane controlled by PI3K. This results in the generation of intracellular glucose-6-phosphate by cytosolic hexokinase enzyme. The molecule of glucose-6-phosphate is then converted to glycogen for storage via several enzymatic reactions involving

phosphoglucomutase, glucose 1-phoshate uridylyltransfertase and glycogen synthase (GS). Additionally, coordinated dephosphorylation of glycogen metabolic proteins such as glycogen synthase kinase 3 (GKS3) occurs during glycogen synthesis (Bouskila et al. 2008 and Petersen et al. 2018).

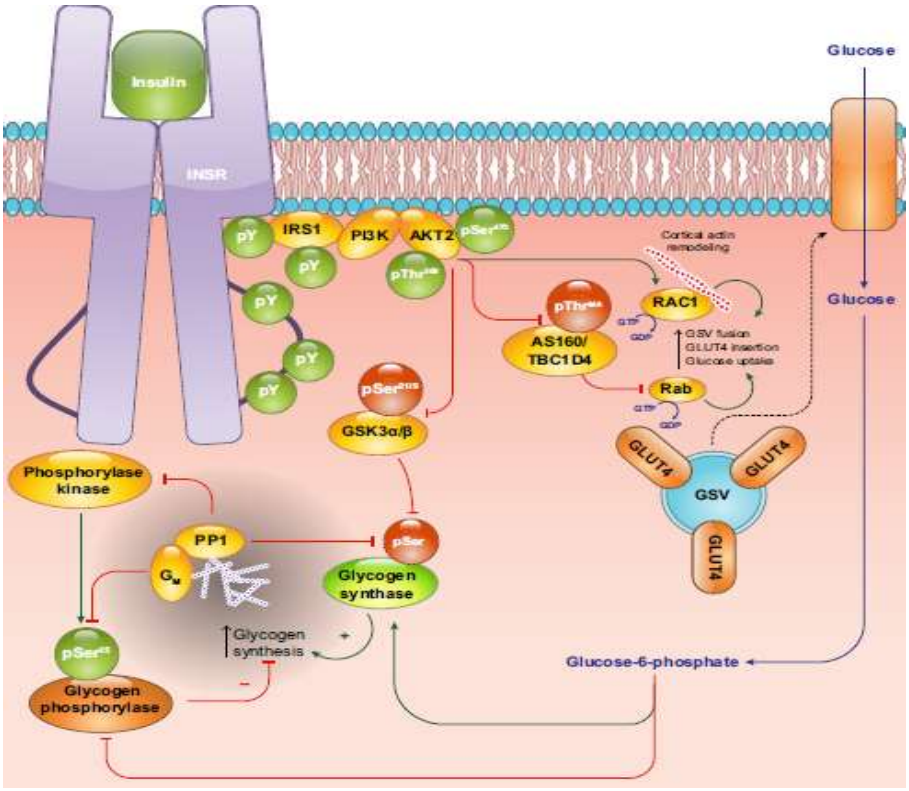

Figure 1. 3 Insulin signalling in skeletal muscle (Petersen et al. 2018).

1.4.3.3 Insulin signalling in the liver

Liver exposure to insulin concentrations is two- to threefold higher than other tissue types in the general circulation. Hepatic insulin signalling is initiated similarly to other cell types. The central molecule of hepatocellular insulin action is AKT activated due to PI3 production (Figure 1.4). AKT phosphorylates transcription factor, Forkhead box protein O1 (FOXO1), at Thr24, Ser253 and Ser316 causing nuclear exclusion and which results in inhibition of FOXO-dependent transcription, i.e. suppression of gluconeogenesis and activating the glycogen and protein synthesis.

FOXO1 is active in the fasted state where it is dephosphorylated at the Akt sites and localised in the nucleus resulting in increased hepatic glucose production via expression of two gluconeogenic enzymes, G6Pc (Glucose-6-phosphatase catalytic subunit) and PEPCK (phosphoenolpyruvate carboxykinase).

Additionally, insulin upregulates the transcription of sterol regulatory element binding protein 1c (SREBP-1c), which subsequently promotes de novo lipogenesis (DNL). Insulin also increases the proteolytic cleavage of SREBP-1c and nuclear translocation leading to increased transcription of the target genes such as fatty acid synthase (*Fasn*), glycerol-3-phosphate acyltransferase 1(*Gpam*) and acetyl-CoA carboxylase (*Acaca*) (Matsuzaka et al. 2013; Petersen et al. 2018).

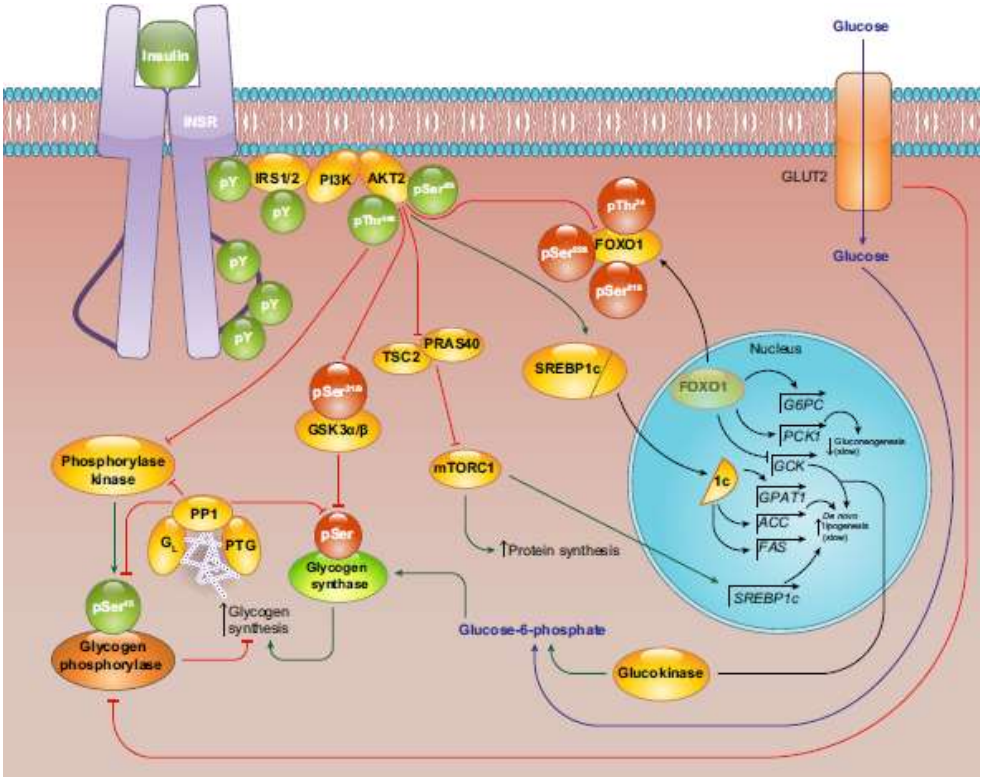

Figure 1. 4 Insulin signalling in the liver (Petersen et al. 2018).

1.4.3.4 Insulin signalling in the white adipose tissue

White adipocytes store dietary energy in highly concentrated form as triglycerides in a large unilocular lipid droplet (Nishimoto et al. 2017). Insulin stimulates adipocyte differentiation and adipose tissue expansion (Madsen et al. 2010). Hence, insulin receptor activation results in suppression of lipolysis, stimulation of de novo fatty acid synthesis and glucose and FFA uptake in white adipose tissue as well as reduction of plasma nonesterified fatty acid (NEFA) levels (Figure 1.5) (Madsen et al. 2010; Petersen et al. 2018). The antilipolytic function of insulin occurred via activation of phosphodiesterase 3B (PDE3B) which subsequently phosphorylates perilipin (PLIN) and facilitates maximal lipolysis by hormone-sensitive lipase (*HSL*) and adipose triglyceride lipase which decrease of intracellular cAMP-levels. Glucose uptake by white adipocytes is achieved via phosphoinositide-3-kinase (PI3K)-dependent and PI3Kindependent pathways which stimulates plasma membrane fusion of *GLUT4* glucose transporter-containing vesicles (Huang et al. 2005; Madsen et al.; 2010 and Petersen 2018).

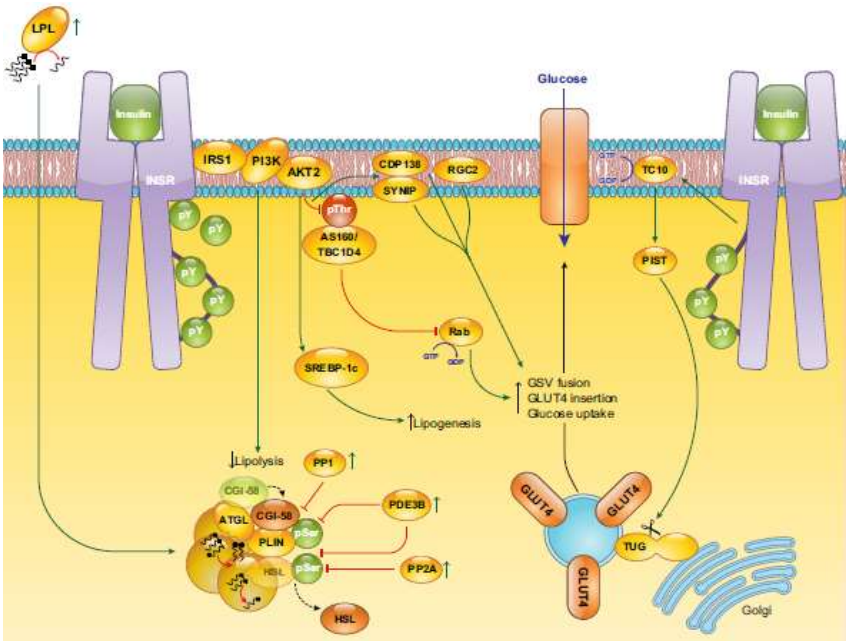

Figure 1. 5 Insulin signalling in the white adipocytes (Petersen et al. 2018).

1.5 Beta-cell dysfunction

A decline in beta-cell function is triggered by different factors such as cytokine-induced inflammation, obesity and insulin resistance, and excess consumption of saturated fat and FFA leading to loss of beta cell mass and development of diabetes (Cerf et al. 2013).

Pro-inflammatory cytokines, IL-1β, TNFα and IFNγ, are released by macrophages and T-cells from infiltrated pancreatic islets. This leads to nitrosative and oxidative stresses which interrupt mitochondrial function and consequently result in the induction of the caspase cascade and β-cell death via apoptosis (Kacheva et al. 2011; Fu et al. 2013).

Chronic hyperglycaemia in T2D leads to glucotoxicity as a result of impaired ß-cell proliferation and increased apoptosis (Stolarczyk et al. 2007). It also results in elevation of cytosolic Ca^{2+} levels, increased production of IL-1β, and activation of NF-kB leading to DNA fragmentation and β-cell injury. Moreover, glycation that occurs non-enzymatically during long-term hyperglycaemia leads to the generation of advanced glycation end products (AGEs). Overexposure of pancreatic β-cells to AGEs results in reduced insulin release and cell apoptosis (You et al. 2016).

Increased release of inflammatory mediators is also observed in obese visceral tissue suggesting the ongoing chronic inflammation due to increased expression of TNFα and inducible nitric oxide synthase in macrophages (Corgosinho et al. 2015). This leads to the increased adipocyte secretion of cytokines and adipokines such as TNF-α, IL-6, leptin, resistin and adiponectin which are toxic to β-cells.

Chronic exposure to fatty acids combined with high glucose levels has a negative impact on β-cell function. Glucolipotoxicity is a complex event which plays a central role in combining multiple factors and pathways including the formation of toxic compounds (e.g., ceramide), formation, oxidative stress, unfolded protein response, and the inflammatory events (Fu et al. 2013).

1.6 Insulin resistance

The ability to store dietary energy as glycogen or fat to use at a later time is an incredibly adaptable mechanism that has supported the development of animal life for nearly 600 million years. However, human evolution encountered some major dietary shifts which include meat eating, food preparation, and the changes related to plant and animal domestication (Luca et al. 2010; Samuel et al. 2012). In a remarkably short period, humanity has altered an environment of caloric deficiency and high caloric demands into one with a reduction in nutritional diversity, excess caloric availability and very little caloric needs. There is clear evidence that obesity rates are increasing dramatically around the world. The epidemic of obesity has been associated with increased rates of serious life-long conditions such as metabolic syndrome, nonalcoholic fatty liver disease (NAFLD), T2D and atherosclerotic heart disease (Wahba et al. 2007; Mitchell et al. 2012; Samuel et al. 2012). Insulin resistance is the main feature of many of these modern diseases. Hence, understanding its pathogenesis has become increasingly important to guide the development of future treatment (Samuel et al. 2012).

In 1963 Randle and colleagues after conducting the studies using rodent heart and diaphragm, suggested a primary role for increased FFA availability and the development of insulin resistance (Ragheb et al. 2011; Samuel et al. 2012). Since then,

Randle's hypothesis was supported by different studies, and the link between disturbances in lipid metabolism and insulin resistance has been widely recognised. Elevated concentrations of circulating fatty acids accumulate within the insulin-sensitive tissues such as muscle, liver and adipose. Due to impaired insulin-mediated skeletal muscle glucose uptake, glucose is diverted to the liver which is also affected by increased lipid profile. A failure of insulin to increase hepatic glucose utilisation and to suppress gluconeogenesis as well as increase delivery in dietary glucose and lipogenesis leads to nonalcoholic fatty liver disease (Samuel et al. 2012). Increased lipolysis in adipose tissue as well as increased secretion of cytokines and adipokines such as TNF-α, IL-6, promotes re-esterification of lipids in other tissues and leads to the toxicity of cells (Samuel et al. 2012; Corgosinho et al. 2015).

Insulin resistance in many patients is believed to be triggered by errors in downstream of the insulin signalling cascade such as genetic polymorphisms of tyrosine or inhibition of phosphorylation of the IR, IRS proteins or PIP-3 kinase, as well as the defective function of GLUT 4 (Wilcox 2005). Early studies have reported that high-fat diet results in an accumulation of intracellular triglyceride which contribute to the onset of insulin resistance. This biochemical parameter is considered to be one of the most consistent markers of whole body insulin resistance. Other major molecules involved in the pathogenesis are the lipid intermediates such as long-chain fatty acyl CoAs (LCACoAs), diacylglycerol (DAG) and ceramides (Ragheb et al. 2011).

1.6.1 The role of counterregulatory hormones in insulin resistance

Physiologically, the actions of insulin are influenced by other circulating factors that either promote or reduce the biological effects of insulin and, therefore, attenuate or induce insulin resistance (Byne 2001; Wilcox 2005). Insulin, the main regulator of

blood glucose balance in the fed state. It decreases postprandial blood glucose by increasing glucose uptake by peripheral tissues and decreasing gluconeogenesis (Kim et al. 2017). On the other hand, agents opposing the actions of insulin include all known counterregulatory hormones such as cortisol, epinephrine, growth hormone, glucagon, and catecholamines. These hormones are realised during the fasting state and stressful situations to regulate metabolic processes are considered to be a defence mechanism against hypoglycaemia (Hupfeld et al. 2010). Chronic stress and adaptation to changes in homeostasis promote the production of the primary mediators such as elevated levels cortisol and increased inflammatory cytokines. Secondary outcomes of these events include elevated blood pressure, overweight and insulin resistance. Repetitive chronic stress leads to tertiary outcomes which are represented by obesity, diabetes, hypertension and other disorders (Chovatiya et al. 2014; Lee at al. 2015). Also, conditions such as Cushing's disease and acromegaly excessive levels of stress hormones can promote the insulin-resistant diabetic state. However, in the usual case of obesity or type 2 diabetes, increased levels of these hormones are not an important contributory factor to insulin resistance as they do not account for the vast majority of insulin-resistant cases (Wilcox 2005; Hupfeld et al. 2010).

1.7 Current antidiabetic drugs

The management of diabetes has changed dramatically during the past several thousand years from the ancient primitive treatment options (a mixture of "water from the bird pond," elderberry, fibres from the asit plant, milk, beer, cucumber flower, and green dates), to the significantly effective current pharmaceutical medications. However, with ongoing research and treatment development, modern antidiabetic agents will likely be considered arcane by our successors 100 years (White et al. 2014). The history of diabetes medications from 1915 to 2015, is shown in Figure 1.6.

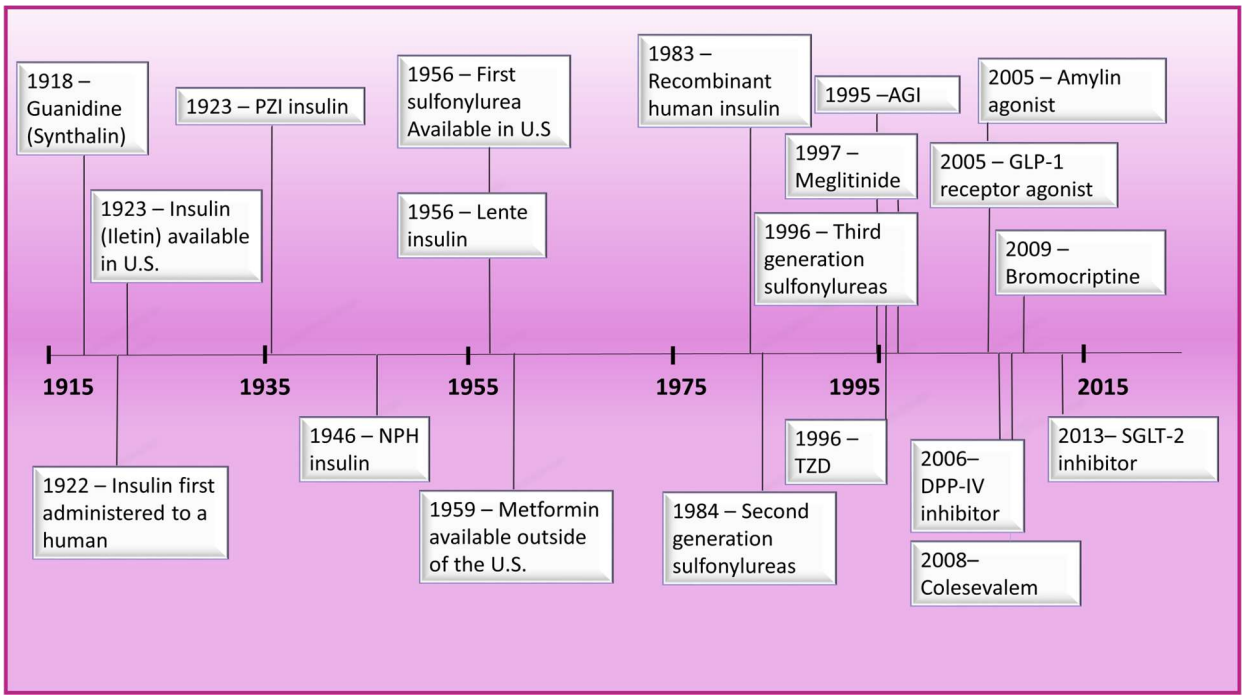

Figure 1.6 History of Diabetes Medications (Cavaiola et al. 2017).

1.7.1 Insulin and insulin analogues

Before the discovery in 1921, there were no effective pharmacological agents for the management of diabetes and T1D was a fatal disorder. A successful insulin crystallisation in 1926, opened the door to insulin formulation modifications (White 2014). Injectable insulin is the most effective agent in lowering glucose levels in the blood which is utilised in the treatment of individuals with all types of diabetes. This medication can be used as monotherapy or in combination with other antidiabetic drugs. However, due to insulin resistance in T2D, larger insulin doses are required to achieve the therapeutic effects. Insulin treatment does not imitate endogenous insulin release and is associated with weight gain and a risk of hypoglycaemia.

The first commercially available, extended-action insulin, PZI (protamine zinc insulin), was released in 1936 and is currently used in cats with diabetes. All insulin

containing medications produced before 1983 were derived from animal sources (primarily beef and pork). In 1983, the first insulin utilising rDNA technology, Humulin® R (rapid) and N (NPH, intermediate-acting), were developed. However, these medications were unable to mimic the basal and prandial insulin secretion (Quianzon et al. 2012)

In the mid-1990s to early 2000s, modification of the site of amino acids in the insulin changed the pharmacokinetics and led to the development of improved insulin analogues. Insulin lispro and insulin aspart (very rapid-acting insulin analogues for pre-meal coverage) and insulin glargine (a long-acting insulin analogue), have increased the flexibility of diabetes management (Marin-Penalver et al. 2017). Inhalable insulin was approved in 2006 (Exubera) but was shortly withdrawn from the clinical use due to commercial reason. The choice of insulin analogues has been broadened since 2014 (Figure 1.7) (Blind et al. 2018).

1.7.2 Biguanides (Metformin)

The use of biguanide can be traced back to the medieval times when a plant, French lilac, or goat's rue (*Galega officinalis*) was used as a folk remedy for diabetes in Southern and Eastern Europe (White 2014). In the early 20th century, the antihyperglycemic component of this herb, guanidine, was extracted. However, guanidine and its homologues compounds synthesised between 1920 and 1930, appeared to be toxic for clinical use. In the 1950s, three biguanides: metformin, phenformin, and buformin, were introduced. Although phenformin and buformin were used clinically, they were withdrawn from the market in the late 1970s due to the high risk of lactic acidosis. The only biguanide that is available for commercial use to date is metformin (Quianzon et al. 2012a).

Metformin is a bisubstituted, short-chain hydrophilic guanidine derivative, which is recommended as initial therapy for most newly diagnosed patients with T2D according to American Diabetes Association/European Association for Study of Diabetes guidelines (Mkele et al. 2013; Weiss et al. 2014; Wang et al. 2017). It was first approved for use in the UK in 1958 and the US in 1995 with doses ranging from 500 to 2,500 mg/day (Wang et al. 2017). Metformin works by suppressing glucose production in the liver, decreasing intestinal glucose absorption, improving glucose uptake by the target tissue, lowering fasting plasma insulin levels and promoting weight loss in some patients by improving hepatic and muscle insulin sensitivity. Metformin action results in improvement of hyperglycaemia and glycosylated HbA1c levels without causing overt hypoglycaemia (Weiss et al. 2014). Although some believe that this medication stimulates weight loss due to a primary anorectic effect. Metformin is associated with more gastrointestinal side effects contraindicated with renal insufficiency than other single medications for T2D (Poretsky 2010; JMEC for Clinical 2011; Benett et al. 2011).

1.7.3 Sulfonylureas and Glinides (Meglitinides)

Sulfonylureas (glibenclamide/glyburide, gliclazide, glimepiride and glipizide) and glinides (repaglinide and nateglinide) are two different, structurally unrelated, classes, of oral hypoglycaemic drugs which share a common mechanism of action. The history of the sulfonylureas began in 1937 with the discovery of the hypoglycaemic properties of synthetic sulfur compounds. Further studies confirmed hypoglycaemia in patients receiving treatment for typhoid containing these compounds (Quianzon et al. 2012a).

In 1956 the first sulfonylurea, tolbutamide, was introduced to the market in Germany which was followed by the commercialisation of other first-generation agents

(chlorpropamide, acetohexamide and tolazamide) in Europe. The next advanced and more potent second-generation of sulfonylureas (glipizide and glyburide) became available in approved the United States in 1984. Finally, glimepiride, which is sometimes referred to as a third-generation agent, was released in 1995 (White 2014).

Currently, sulfonylureas are utilised as a classic first or second-line therapy for patients with T2D. Both, sulfonylureas and glinides (non-sulfonylurea insulin secretagogues with a short half-life), stimulate pancreatic beta cells to release insulin following the closure of the beta-cell K_{ATP} channel. Glinides target a different subunit binding site within the sulfonylurea receptor in the pancreas. They have a more rapid absorption with a shorter circulating half-life, hence require more frequent dosing.

Although both of these types of drugs are rapidly effective, they continue to stimulate insulin secretion even in the absence of hyperglycaemia. Therefore these agents carry a risk of severe episodes of hypoglycaemia accompanied by coma or seizure (Marin-Penalver et al. 2017; Marks 2018).

1.7.4 Thiazolidinediones (TZDs, PPAR γ Agonists or Glitazones)

TZDs (e.g. pioglitazone, rosiglitazone) increase insulin sensitivity by acting on the target tissue cells such as muscle, adipose tissue and liver, to increase glucose metabolism and decrease glucose production. TZDs were initially introduced to the US market in 1996 (White 2014). These drugs enhance skeletal muscle insulin sensitivity and suppress hepatic glucose production. TZDs function as selective ligands for nuclear hormone receptor peroxisome proliferator-activated receptor gamma (PPAR γ), a transcriptional factor that controls the expression of a large number of regulatory genes in lipid and glucose metabolism (Bertin et al. 2013 and Marin-Penalver et al. 2017). Troglitazone was the first agent in this category to be

approved by the FDA. However, it was shortly removed from the market due to increased risks of hepatic failure. Two other STZs, pioglitazone and rosiglitazone have been linked to nonhypoglycemic issues (White 2014). In Europe, since 2010, rosiglitazone was withdrawn from the market by the European Medicines Agency, because of the toxic effect on the liver. Pioglitazone was suspended in France and Germany in 2011 (Marin-Penalver et al. 2017). The adverse effects of pioglitazone include peripheral oedema, fluid retention and fracture risk in women (Mazzola et al. 2012).

1.7.5 Alpha-Glucosidase Inhibitors (AGIs)

Alpha-Glucosidase inhibitors, acarbose, voglibose and miglitol, have a unique mode of action compared to other antidiabetic compounds. AGIs exhibit structural identity to natural oligosaccharides with higher affinity for alpha-glucosidases enzymes that convert oligosaccharides into monosaccharides. These medications lower the rate of digestion of carbohydrates in the intestine via reversible inhibition of membrane-bound intestinal alpha-glucoside hydrolase enzymes and are most effective for postprandial hyperglycemia without causing hypoglycaemia.

Acarbose was the first drug in this category to be approved by the FDA in 1995. This was followed by the introduction of miglitol to clinical use in 1996 (White 2014). These drugs are less effective than metformin and sulfonylureas and are known to cause side effects such as abdominal pain, diarrhoea and flatulence (Marin-Penalver et al. 2017).

1.7.6 Incretin-Based Therapies: GLP-1 Receptor Agonists and Dipeptidyl Peptidase-IV (DPP-IV) Inhibitors

There are two incretin drug classes that are based on glucoregulatory effects of incretins: incretin mimetics (exenatide, liraglutide, dulaglutide, lixisenatide, albiglutide and semaglutide) and DPP-IV inhibitors (sitagliptin, vildagliptin, saxagliptin, linagliptin and alogliptin).

GLP-1 receptor agonists mimic the biological function of incretin hormones such as stimulation of glucose-dependent insulin secretion and inhibition of glucagon secretion in response to nutrient inputs. Exenatide, a synthetic form of exendin-4 (peptide produced exclusively by the salivary glands of Gila Monster *Heloderma suspectum*), was the first GLP-1 receptor agonist to become available in the market in 2005. A second GLP-1 receptor agonist, liraglutide, was approved in 2010. Shortly after, in 2012, a long-acting (once-weekly) form of exenatide was introduced for clinical use (White 2014). Semaglutide represents the most recently authorized drug from this category (approved in 2018) (Figure 1.7) (Blind et al. 2018).

GLP-1 mimetics are all administered subcutaneously. However, an oral version of semaglutide, is currently undergoing a primary endpoint in the PIONEER 1 phase 3a trial (Abbasi 2018; Aroda et al. 2018).

Incretin-based agents are generally associated with 0.5–1% reductions in A1C levels as well as weight loss. However, these compounds are also linked to significant gastrointestinal side effects, particularly early in therapy (White 2014).

DPP-IV inhibitors prevent enzymatic degradation of GLP-1 and GIP by blocking the activity of DPP-IV enzymes. The first of these agents, sitagliptin, was approved in 2006 in the United States. This was followed by the release of saxagliptin and

linagliptin and other compounds. DPP-IV inhibitors are shown to reduce A1C by ~ 0.8% and do not cause hypoglycaemia (White 2014). Development of a new DPP-IV inhibitor intended for once-weekly use (omarigliptin) was discontinued in 2016 after being tested in phase 3 clinical trial (Blind et al. 2018)

Incretin-based medications are usually prescribed in combination with first-line metformin therapy. (Cernea et al. 2011 and Kazafeos et al. 2011)

1.7.7 Amylinomimetics

Amylin agonist (pramlintide) is a synthetic analogue that mimics actions of an endogenous neuroendocrine hormone, amylin. Amylin was discovered in 1987 and is known to be co-secreted in equimolar amounts with insulin from the pancreatic β cells in response to food intake (Ryan et al. 2005). Pramlintide (approved by FDA in 2005) is co-administrated with primary insulin therapy. This medication controls hyperglycaemia by reducing postprandial glucagon secretion, slowing gastric emptying, and reducing appetite in patients with T2D (Asmar et al. 2010). Long-term safety for pramlintine is yet to be established. It is associated with gastrointestinal side effects, weight loss and hypoglycaemia. This medication should only be administered before food intake that contains at least 250 calories or 30 g of carbohydrates (Olokoba et al. 2012; Marin-Penalver et al. 2017).

1.7.8 Sodium-glucose cotransporter 2 (SGLT2) inhibitors

Sodium-glucose cotransporter 2 (SGLT2) inhibitors (dapagliflozin, canagliflozin, **e**mpagliflozin and ertugliflozin) are novel groups of compounds, four of which were approved between 2012 and 2018 (Figure 1.7) (Blind et al. 2018). SGLT2s increase renal elimination of glucose, increase its excretion and reduce hyperglycaemia in patients with T2D. (Mazzola et al. 2012). A high-capacity, low-affinity SGLT2

transporter protein is located in the kidney proximal tubule and is responsible for about 90% of glucose reabsorption (White 2014). The medication inhibits glucose reabsorption, increases its excretion in the urine and promotes weight loss. SGLT2 inhibitors may be less effective in patients with renal impairment. The primary side effects include the urogenital tract infections, euglycaemic ketoacidosis, and orthostatic hypotension and the volume depletion.

1.7.9 Other antidiabetic medications

Other antidiabetic medications include Colesevelam, which exhibits a dual effect of lowering LDL cholesterol and reducing blood glucose level, and a dopamine agonist Bromocriptine, which was approved as antihyperglycemic medication in 2009 (White 2014).

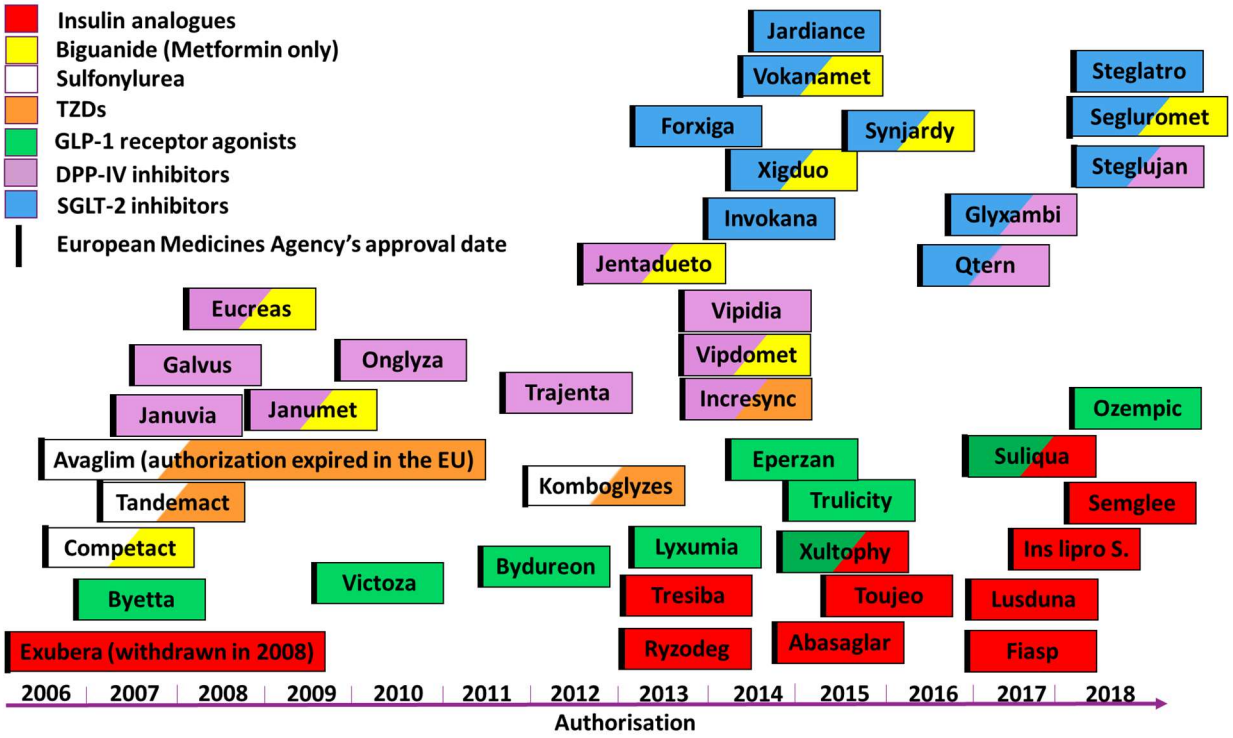

Figure 1.7 European Medicines Agency's approval of new products for the treatment of T2D since 2005 (Blind et al. 2018)

1.8 The history of the incretin concept

1.8.1 Incretin effect

Incretin hormones are gut-derived peptides secreted in response to nutrient intake mainly glucose and fats. In humans, there are two incretin hormones known as glucagon-like peptide (GLP-1) and glucose-dependent insulinotropic polypeptide (GIP). Together they are responsible for the so-called incretin effect which describes the fact that a greater rate of insulin release is achieved after oral administration of glucose than if the same amount of sugar was infused intravenously to match the glycaemic excursion (Deacon et al. 2011; Usser et al. 2012). In healthy individuals, the incretin effect can account for at least 50% of the total insulin secreted after oral glucose, depending on the size of the stimulus. Hence, these hormones exhibit insulinotropic effects at usual physiological concentrations (Kim et al. 2008).

1.8.2 Pre-discovery

It has been more than a century-long since the concept of incretins was introduced. In 1850-1900, European physiologists began to investigate the mechanisms of the external and internal pancreatic secretion. During these times, Joseph von Mering and Oskar Minkowski discovered the role of the pancreas in diabetes, and Claude Bernard revealed that significantly larger quantities of glucose could be administrated orally than intravenously without excretion of sugar in the urine (Rehfeld et al. 2018). Therefore, Claude Bernard suggested that after intestinal absorption, a considerable amount was taken up by the liver during the first portal circulation (Jorpes and Mutt 1973). This theory was recognised up to the 1950s (Rehfeld et al. 2018).

1.8.3 The birth of gastrointestinal endocrinology

A breakthrough came at the beginning of the 19th century with William Bayliss and Ernest Starling discovery of secretin. This time has become associated with the birth of gastrointestinal endocrinology in the history of incretins (Creutzfeldt 2005; Rehfeld 2018).

The scientists proposed that intestinal mucosa contained a factor which stimulated the exocrine secretion of the pancreas through the blood flow. The conclusion was established following infusion of the acid chyme from the stomach, or hydrochloric acid alone into the digestive system which resulted in the release of a chemical substance into the blood leading to the exocrine pancreatic secretion even after the nerves supply to the intestine was removed (Sherwood et al. 2000).

The hallmark discovery of secretin by Bayliss and Starling revolutionised physiology with a new concept (Modlin et al. 2001). It was shown that gastric acid secretion was regulated not only via neural reflexes but also involved hormonal stimuli. However, this became the subject of debate for decades, beginning with Ivan Pavlov, a Russian physiologist which argued that the function of the pancreas was mediated entirely by the nerves (Smith 2000; Creutzfeldt 2005; Walton 2009).

In his renowned "Cronian Lectures" for the Royal Society, Starling coined the expression "hormone" (from Greek "hormoa": I arouse to activity) for chemical substances which are released from one site and act on the function of a distant organ on another site via the blood circulation (Creutzfeldt 2005; Rehfeld 2018). The fact that some of the gastrointestinal hormones are also found in nerve and brain cells has later led to the concept of a gut-brain axis (Track 1980).

Starling further suggested that the duodenal mucosa contained other substances which could act on the pancreas. However, at the time, in 1906, this hypothesis was tested by Moore and colleagues which involved oral administration of gut extracts to patients with diabetes. Although some success was achieved as a reduction of the levels of urine sugars was observed in some patients, overall results were negative and inconclusive due to effects of proteolytic enzymes of gastric juice on the peptides (Seino et al. 2010; Seewoodhary et al. 2010; Reusch et al. 2013; Scott et al. 2014; Rehfeld 2018).

After insulin was discovered and harvested from pancreatic islets by Banting and Best in 1921, several attempts were taken to investigate the effects of gut extracts on oral or injected glucose concentrations (Kim et al. 2008).

Promising results were obtained by La Barre and Still in 1930 after the processing of duodenal extracts *in vitro* led to the discovery of two interesting fractions. One fraction was crude secretin with well-known actions on pancreatic duct secretion, and the other contained a compound which lowered blood glucose levels and had no stimulatory effects on the exocrine pancreas. This observation had led to the suggestion that the antihyperglycaemic effect was due to stimulated insulin release (Rehfeld 2018).

In 1932, La Barre coined the name, "incrétine" ("intestine, secretion, insulin"), for a substance extracted from the upper gut mucosa and proposed the use of incretin for treatment of diabetes mellitus in future (La Barre 1932). But he did not prove incontrovertibly that incretins existed (Kim et al. 2008).

1.8.4 Re-birth of incretin concepts

The inconsistent literature on the existence of incretins made between 1902 and 1940 encouraged Andrew C. Ivy, who was president of the American Physiological Society

known for his experiments on gastrointestinal hormones as well as CCK discovery, to reinvestigate the questionable matter in controlled experiments. The outcome of his work resulted in the entire incretin hypothesis losing its credibility and remaining so until rekindled some 25 years later once radioimmunoassays (RIA) for insulin invented by Yalow and Berson became available (Yalow and Berson 1960; Kim et al. 2008; Marks 2018). The RIA technique allowed for the first time to accurately measure molecules including peptide hormones present at minute concentrations in plasma (Rehfeld 2018). In 1960, insulin was first quantified by the RIA technology. One year later, RIA assay was successfully modified for measuring glucagon by Roger Unger and colleagues. During the following decade, this technique continued to be effectively adapted for novel gastrointestinal hormones (Rehfeld 2018). With the progress in modern methods for purification and sequencing and development of highly specific sensitive RIA assay, interest in the investigation of insulinotropic intestinal factors regained its popularity (Creutzfeldt 2005).

At the beginning of the 1960s, Neil McIntyre together with Derrick Holdsworth and Desmond Turner in London, UK and Elrick and co-workers in Denver, the US in similar experiments independently reported that administration of glucose orally stimulates considerably superior insulin than intravenous glucose (McIntyre et al 1964). Hence, confirming the existence of incretin mechanism (Rehfeld 2018). Simultaneously, John Dupre was working with secretin (Dupre 1964), and Vincent Marks and Ellis Samols were investigating the insulinotropic effects of glucagon in 1964 (Marks 1978; Marks 2018). Makman and Sutherland had described a substance with similar biological properties to glucagon that was found in the human blood before the discovery of glucagon's insulinotropic properties (Makman and Sutherland 1964).

By 1965 glucagon had gained popularity in diabetes research. Samols and colleagues observed that the rates of plasma immunoreactive glucagon levels (IRG) in blood were increased in response to oral glucose (Marks 2018). They suspected that the rise in the plasma immunoreactive glucagon in response to oral glucose might have originated from the gut and even represent hypothetical incretin (Marks 2018).

1.8.5 Discovery of GIP

At the end of the 1960s, all known gastrointestinal hormones such as secretin, cholecystokinin-pancreozymin, gastrin, and the uncharacterised immunoreactive gut glucagon-like material were the main candidates for the role of incretin. Careful investigation revealed that none of the known peptides met the criteria (Creutzfeldt 2005; Marks 2018). The factor responsible for the incretin effect remained unknown until the late 1960s were when John Brown and Victor Mutt isolated a new peptide from a crude porcine cholecystokinin extract (Creutzfeldt 2005; Gault 2018). The peptide was named gastric inhibitory polypeptide (GIP) on the basis of its ability to block gastric acid secretion (Tseng et al. 2004).

However, as more studies were performed using accessible RIA, the insulinotropic activity of GIP at physiological concentrations in response to glucose and triglycerides was revealed (Morgan et al. 1978; Morgan et al. 1988). Acronym GIP was suggested to be read as “glucose-dependent insulinotropic polypeptide”. This discovery could not explain the source of the entire gut hormonal effect on insulin release in response to oral glucose due to complete GIP removal from rat gut extracts decreased the incretin effect by just 50% (Creutzfeldt 2005; Seino et al. 2010; Müller et al. 2017; Rehfeld 2018).

In the next 15 years, the role of GIP in pathophysiology and its biological properties were established. Although studies have shown that the insulin-releasing properties of GIP are severely diminished in people with T2D, it is thought to be involved in the regulation of lipid as well as carbohydrate metabolism (Marks 2018; Gault 2018).

1.8.6 Discovery of GLP-1

Several indicators suggested the existence of additional incretin agent which influenced scientists to look deeply into the investigation of incretin nature of immunoreactive glucagon substances using modern molecular biology techniques.

In the 1970s, glicentin a 69 amino-acid glucagon-like peptide and oxyntomodulin were identified and characterised. However, both peptides exhibited only a weak insulinotropic activity (Creutzfeldt 2005; Marks 2018).

The success of these efforts has been facilitated by the cloning and sequencing of mammalian glucagon genes by Graeme Bell and colleagues in 1983. The sequence of cDNA of proglucagon in addition to glucagon also contained the sequences of two novel glucagon-like peptides, named GLP-1 and GLP-2.

Since then, numerous studies worldwide have demonstrated beneficial insulinotropic, and most importantly antidiabetic, effects of GLP-1 and its analogues in patients with T2D (Creutzfeldt 2005; Rehfeld 2018).

1.9 Glucagon-like peptide 1 (GLP-1)

Glucagon-like peptide (GLP-1), a 30 amino acid long peptide, was first identified in its inactive (1-37 and 1-36 amide) form, during the cloning and sequencing of proglucagon genes isolated from the pancreas of bony fish (anglerfish) and birds (chicken) in the early 1980s (Irwin et al 1999). The biologically active truncated GLP-

1 molecule (7–37 and 7–36 amide) was then discovered by sequencing of the peptides purified from gut extraction in the late 1980s. GLP-1 belongs to the glucagon family of peptide hormones which include glucagon, GLP-2, glucose-dependent insulinotropic polypeptide (GIP) and glucagon-related peptides (GCRP) (Takei et al. 2015; Sekar et al. 2016; On et al. 2016). GLP-1 is highly homologous to glucagon, displaying identity at 14 positions (45% identity) (Pan et al. 2006).

In humans, during fasting state levels of circulating GLP-1 range between 5-15 pmol/L and rises 2-4 fold post meal consumption. Postprandial GLP-1 release is regulated by nutritional and neuroendocrine factors. The initial secretory phase is detectable 10 to 15 min after food consumption and is believe to be influenced by vagal nerves. The second phase of GPL-1 secretion occurs 30-60 minutes in response to nutrient contact by L-cells. The secretion reaches its peak after approximately 60 minutes (Bodnaruc et al. 2016).

1.9.1 Post-transcriptional processing of preproglucagon.

The preproglucagon gene encodes proglucagon, a 160 amino acid inactive precursor of several peptide hormones. Its post-transcriptional modification depends upon to the tissue-specific expression of prohormone convertases (PC) 1/3 and 2. In the pancreatic α-cells, PC 2, encoded by *PCSK2* gene*,* cleaves the precursor to generate glucagon, glicentin-related pancreatic polypeptide (GRPP), intervening peptide 1 (IP1), and a proglucagon fragment. Whereas, in the intestinal L-cell and specific CNS neurons, (PC1/3), encoded by Proprotein Convertase Subtilisin/Kexin Type 1 (*PCSK1)* gene, regulates the post-translational processing of proglucagon producing GLP-1, GLP-2, oxyntomodulin, glicentin, and IP2 (Figure 1.8) (Irwin 2010; Sandoval et al. 2015; Bodnaruc et al. 2016).

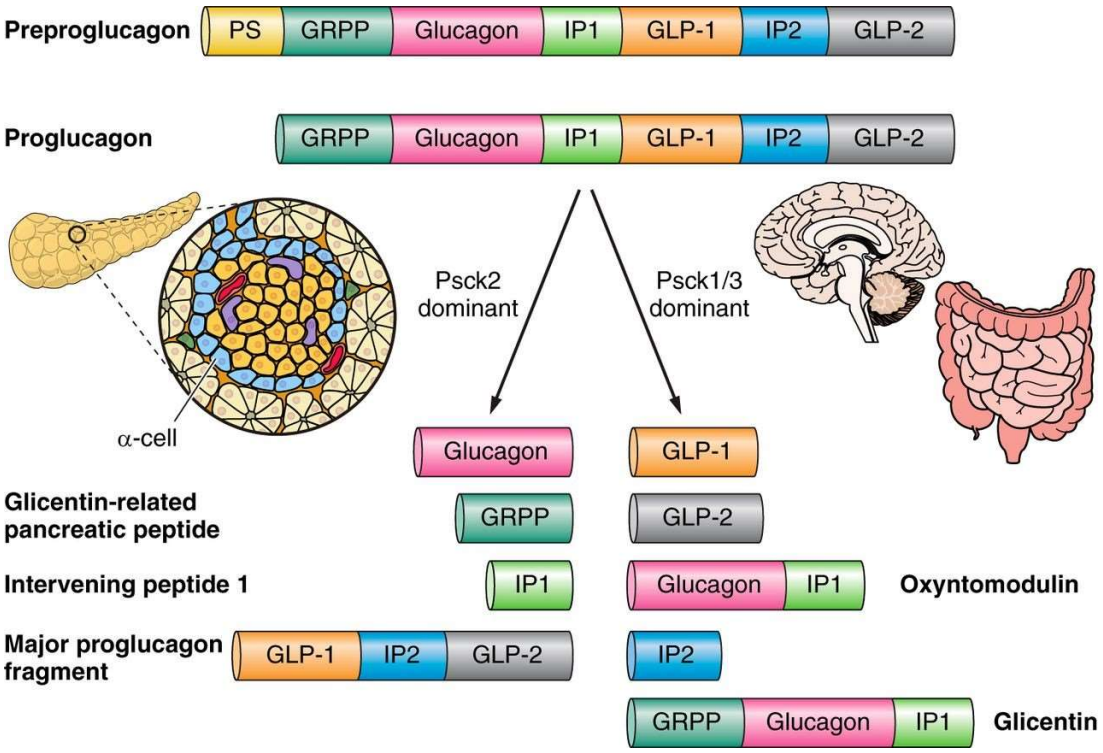

Figure 1. 8 Posttranslational processing of preproglucagon (Sandoval et al. 2015).

1.9.2 GLP-1 synthesis

GLP-1 is mainly produced in enteroendocrine L-cells of the gut by differential processing of proglucagon gene which is expressed in these cells (Holst et al. 2007). GLP-1 is also synthesised in the central nervous system (CNS), mainly in the brainstem. In the brain, preproglucagon is generated in the neuronal cells in nucleus tractus solitarius (NTS) from where it is extended to the hypothalamus, some thalamic and cortical areas (Simsir et al. 2018). In some species, such as dog, chicken, and amphibians, the proglucagon gene is also expressed in the stomach (Irwin 2010).

Multiple mechanisms are involved in the regulation of proglucagon transcription. Studies have shown that GLP-1 and 2 are absent in intestinal tissues from *PCSK1* knockout mice which results in a severe block in the production of both peptides as well as model development of massive obesity and glucose intolerance

related to impaired insulin secretion (Zhu et al. 2002; Bandsma et al. 2013). Patients with PC1/3 deficiency are reported to have significant abnormalities in intestinal and enteroendocrine function (Bandsma et al. 2013).

Abnormalities in a transcription factor, Pax6, responsible for the binding to the promoter region of the proglucagon gene, are also associated with impaired GLP-1 synthesis, according to the gene expression studies using mice homozygous for a dominant-negative form of Pax6. Moreover, MEK-ERK signalling may also regulate gene expression via cAMP-dependent Epac2.

1.9.3 GLP-1 secretion and elimination

GLP-1 is a gut-derived peptide secreted from enteroendocrine L-cells in response to injection of nutrients. L-cells are predominantly located in the ileum and colon but can also be found in the duodenum (Lim et al. 2006; Spreckley et al. 2015).

Being open-type epithelial cells, L-cells possess microvilli on their apical surface which express several transporters, such as sodium glucose cotransporter-1 (SGLT-1) and amino acid (AA) transporter, and G-protein coupled receptors (GPCRs) including GPR40, GPR41, GPR43, GPR119 and GPR120. L-cells may also express sweet taste receptor T1R2 + T1R3 coupled to G-protein α gustducin, phospholipase Cβ2, and the calcium-sensitive channel Trpm5. The importance of taste receptors in the regulation of plasma insulin and glucose is also evident. Mice lacking the α-gustducin receptor fail to secrete GLP-1 in response to ingestion of glucose and show abnormalities in glucose homeostasis (Jang et al. 2007).

The aforementioned important cellular devices serve as chemical sensors during direct contact with nutrients and other substrates present in the intestinal lumen. GPCRs and

transporters exhibit close interaction with vascular factors and the enteric nervous system allowing the L-cell to be affected by both neural and hormonal stimuli (Lim et al. 2006, Habib et al. 2012, Pais et al. 2016 and Zufall et al. 2016). Glucose is transported into the L-cell via SGLT-1, which is coupled with Na+ influx, depolarizing the cell membrane opening L-type calcium channels leading to calcium release from intracellular stores and increase in cAMP levels (Habib et al. 2012 and Cho et al. 2014). GLP-1 is stored in secretory granules of L-cells as well as synthesized to a lesser extent by neurons of the nucleus tractus solitarius (NTS) of the brainstem (Bodnaruc et al. 2016). Elevation of intracellular cAMP potentiates downstream signals leading to the exocytosis of hormone-containing vesicles at the L-cells basolateral face (Cho et al. 2014 and Spreckley et al. 2015). Further amplification of GLP-1 secretion results from the closure of KATP channels due to elevated intracellular ATP arising from glucose metabolism (Cho et al. 2014). A similar mechanism occurs via AA transporters. Other signalling molecules such as free fatty acids (FFA), bile acids, and short-chain fatty acids (SCFA) activate GPRs leading to intracellular calcium release and/or activating protein kinase C (aPKC) which triggers GLP-1 release Genetic modifications of aPKC in the intestine results in altered response to oral administration of oleic acid *in vivo*. Also, GLP-1 release is also regulated by neural stimuli through muscarinic receptors such as M1R, M2R (Cho et al. 2014).

Some physiological and experimental conditions, such as stress, islet transplantation or *in vivo* streptozotocin or high-fat treatments, and ex-vivo chronic exposure to high glucose concentrations are known to trigger the secretion of bioactive, GLP-1(7–36) amide or GLP-1(7–37), and N-terminally extended GLP-1 from pancreatic α-cells. This process may be achieved by overexpression of PC 1/3, which is normally minute

in α-cells resulting in increased production of GLP-1 as a growth factor promoting superior glucose-dependent insulin release, β-cell survival and function under extreme metabolic conditions such as diabetes (Cho et al. 2013 and Nakashima et al. 2018).

Bioactive GLP-1 is rapidly metabolised and inactivated in the bloodstream by the catalytic activity of the enzyme dipeptidyl-peptidase IV, which cleaves two NH_2-terminal amino acids of the hormone to produce noninsulinotropic GLP-1 (9–36) amide and GLP-1 (9–37). As a result plasma half-life of GLP-1 is less than 2 min and only 10–15% of circulating hormone remains bioactive by the time it reaches the pancreas. This raises the possibility that some of the effects of GLP-1 are transmitted through sensory neurons in the guts and the liver expressing the GLP-1R. The hormone and its truncated product are further cleaved by neutral endopeptidase 24.11 (Cho et al. 2013, Simsir et al. 2018 and Nakashima et al. 2018).

1.9.4 GLP-1 pleiotropic actions

GLP-1 exerts activities via binding and activating the GLP-1R which is expressed in various tissues such as the pancreas, lung, brain, pituitary, stomach, heart and kidney (Figure 1.9). The human GLP-1R consists of 463 amino acids (~63 kDa) and exhibits 90% sequence homology with the rat GLP-1R (Cho et al. 2013).

GLP-1 is well-recognised for its ability to potentiate insulin secretion from pancreatic β-cells in response to food intake and increase insulin gene transcription and biosynthesis. Receptor binding results in increased production of cAMP activating second messenger pathways, such as the protein kinase A (PKA) and Epac pathways. This results in elevation of intracellular cAMP and PKA raising cytosolic calcium concentrations which subsequently leads to insulin exocytosis from secretory granules (Seetho et al. 2014; Bodnaruc et al. 2016).

GLP-1R antagonists such as exendin-4(9– 39) are demonstrated to reduce glucose-induced insulin secretion and impair glucose tolerance in rodents and humans. Similar effects are observed in GLP-1R KO mice models.

The peptide has trophic effects on β-cells, inducing differentiation and proliferation of progenitor cells in the pancreas and protecting from β-cell apoptosis via the activation of phosphatidy-linositol 3 kinase (PI3K) and mitogen-activated protein kinase (MAPK) pathways leads to the expression of genes involved in cellular growth, repair and differentiation (Simsir et al. 2018).

GLP-1 also inhibits glucagon secretion by direct interaction with glucagon receptors on the α-cells in healthy subjects and patients with T1D and T2D. This process is known to be partly regulated by the raised insulin and somatostatin release from pancreatic islets in response to nutrient intake (Bodnaruc et al. 2016).

In addition to its pancreatic functions, the peptide exhibits pleiotropic extrapancreatic roles. GLP-1 decreases food intake, and appetite increases satiety and controls body weight. GLP-1Rs are widely expressed in the brain such as the hypothalamic nuclei, thalamus, hippocampus, lateral septum, and subfornical organ, which are involved in the regulation of appetite and satiety.

GLP-1 in the brain is synthesised in neurons in the nucleus tractus solitaries (NST) from where these cells extend into the paraventricular nucleus and interact with their receptors, resulting in satiety, appetite and anorexia. They can also extend to the arcuate nucleus and transmit vagal motor signals to the pancreas. GLP-1 freely crosses the blood-brain barrier which allows it to regulate cellular pathways in the CNS such as neuroinflammation, mitochondrial function, and cellular proliferation.

It is thought that GLP-1 also affects neurological and cognitive functions. Positive effects of GLP-1 receptor agonists on neurodegenerative diseases such as Alzheimer's disease has previously been reported in vivo and preclinical studies (reviewed in Simsir et al. 2018). Other beneficial properties of GLP-1 include regulation of blood pressure, cholesterol levels, postprandial triglyceride concentration, coagulability, and inflammation and improvement of vascular endothelial function and bone profile.

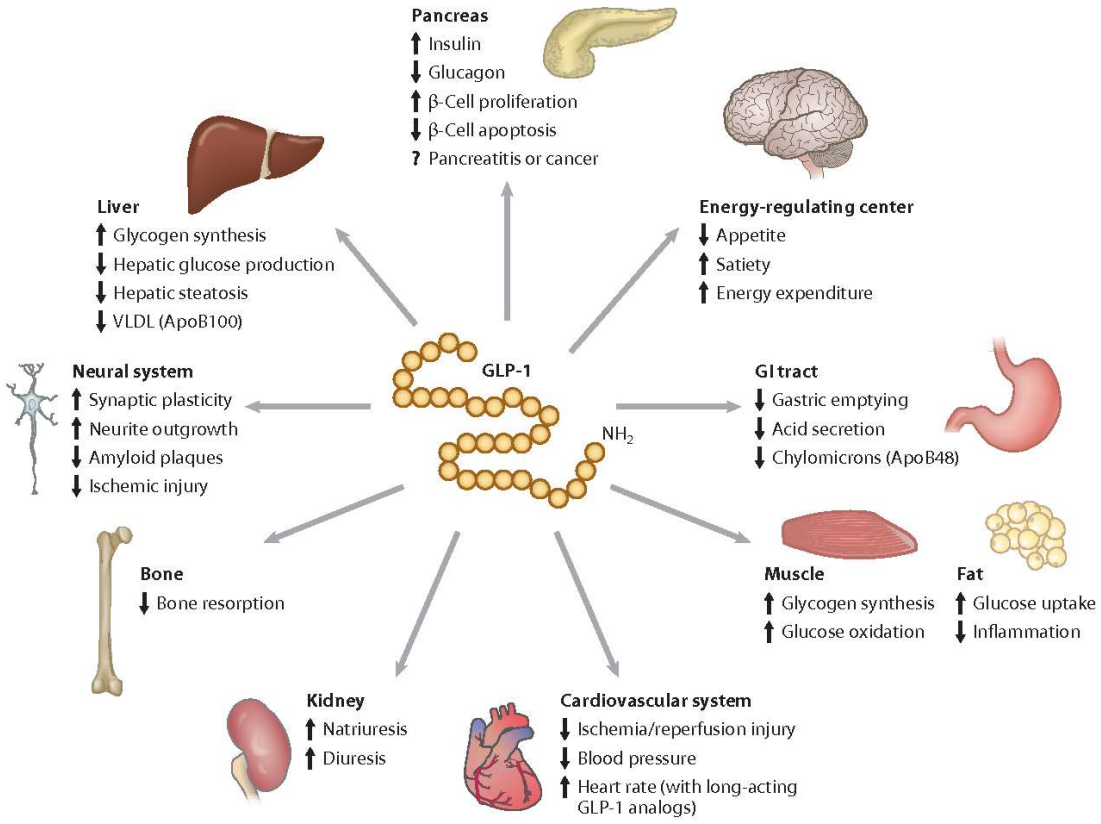

Figure 1.9 Pleiotropic functions of GLP-1 (Cho et al. 2013)

1.10 GIP

GIP is produced by enteroendocrine K-cells located in the proximal small intestine (duodenum and jejunum), and its secretion is regulated largely by food ingestion, primarily dietary carbohydrate and fat (Gault 2017). GIP is also known to be expressed in the CNS in rodents and pancreatic α-cells in rodents and humans (Finan et al. 2016).

The peptide consists of 42 amino acids and is derived from a 153 amino acid preprohormone precursor (proGIP) comprising a putative signal peptide (21 amino acids), N-terminal peptide (30 amino acids), GIP coding region (42 amino acids) and C-terminal peptide (60 amino acids) (Gault et al 2017). PC 1/3, which is expressed in K-cells, cleaves the 51 N-terminal residues and the 60 C-terminal residues of proGIP to for mature GIP $_{(1-42)}$ sequence.

In a subset of K-cells and α-cells, the precursor can undergo alternative processing by PC2 resulting in a C-terminally truncated form of GIP known as GIP $_{(1-30)}$ which is shown to exhibit insulinotropic effects in mice comparable to GIP $_{(1-42)}$.

GIP provokes an insulinotropic response via activation of GIPR which is abundantly expressed in β-cells. Apart from being expressed in the pancreas, GIPR mRNA has also been found in other tissue types such as adipose tissue, small intestine, adrenal cortex, lung, pituitary, heart, testis, bone and brain. In addition to its insulinotropic effects, GIP has been shown to promote proliferation and protect from apoptosis of pancreatic β-cells, inhibit hepatic glucose production, stimulate lipogenesis, enhance fatty acid and glucose uptake by adipocytes, and improve bone strength, as well as stimulate neuronal proliferation and protects from β-amyloid plaque formation in the cortex (Gault et al. 2017). Limitation of GIP such as short plasma half-life and most importantly diminished incretin effects in T2D resulted in little enthusiasm for the promotion of GIP action for T2D therapies.

However, several recent studies revealed that reduction of the high level of glucose using established glucose-lowering agents can restore GIP insulinotropic effects and therefore show that the peptide can still exhibit possible therapeutic potential (Gault et al. 2017). Moreover, a novel GIP/GLP-1 receptor agonist has recently been reported

to exhibit significantly better efficacy in glucose control and weight loss compared to dulaglutide (Frias et al.2018).

1.11 Glucagon

1.11.1 History of Glucagon

Its existence of glucagon first came to light as a contaminant of insulin, in 1922, when Charles Kimball and John Murlina isolated a pancreatic fraction which exhibited hyperglycaemic effects after being injected in rabbits and dogs. They concluded that this pancreatic substance is secreted to oppose hypoglycaemia caused by insulin and named it glucagon ("the glucose agonist"). Nevertheless, the term "glucagon" did not enter general usage until much later (Plisetskaya et al. 1996). Bürger and colleagues reclassified the molecule as the "the hyperglycaemic-glycogenolytic (H–G) factor" after discovering glycogenolytic properties of glucagon on the liver in 1929. Due to this "factor" persisted in the pancreas of animals treated with a toxic glucose analogue, aloxan, (i.e., after the selective destruction of insulin-producing cells), pancreatic α-cells and similar argentophile cells in the upper two-thirds of the gastric mucosa of the dog were correctly suggested to be the source of glucagon (Plisetskaya et al 1996). More than 20 years passed before a pure crystalized glucagon (from a pig) was reported by Behrens and colleagues in 1953 (Chabenne et al. 2010; Müller et al. 2017) and 4 years later Bromer and co-workers reported its primary amino acid structure (Plisetskaya et al. 1996). Following the development of the RIA, quantitative detection of glucagon found its medicinal application in the management of severe hypoglycaemia. The technique also resulted in a finding of a series of structurally related peptides which presented a troublesome interference with the initial assay. The studies of the mechanism of glucagon biosynthesis were directed

towards a search of larger precursors and their conversion to native peptide due to the presence of this large glucagon-like immunoreactivity found in the plasma and pancreatic extracts of dogs and humans (Lefebvre 1983). In 1980 two molecules, glicentin (100 amino acid and oxyntomodulin were found to be responsible for the majority of intestinal glucagon-like immunoreactivity (Holst et al. 1997). Subsequently, it was discovered that glucagon and GLPs are all produced from a common precursor, now named proglucagon.

In the 1970s Roger Unger used a newly developed radioimmunoassay, reported that diabetic individuals exhibited elevated levels of glucagon (Unger et al. 1970). This led to the conclusion that glucose fails to suppress glucagon action which could contribute to the development of hyperglycaemia and the development of diabetes in these patients. From 1970 to 1990, new roles of glucagon which fall beyond glucose metabolism were established including regulation of energy intake, stimulation of brown adipose tissue thermogenesis, suppression of gastric motility, activation of lipolysis and inhibition of lipid synthesis, and promote autophagy (Müller et al. 2017).

1.11.2 Glucagon synthesis and secretion

Glucagon is predominantly expressed in the pancreatic α-cells, but small amounts are also produced in intestinal L-cells and a subset of neurons in the nucleus tractus solitarius (NTS) of the brain stem (Drucker et al. 1988; Müller et al. 2017). The proglucagon gene promoter region exhibits selective DNA control elements which are necessary for specific binding of distinct transcription factors enabling for α-cell-specific expression of the molecule (Müller et al. 2017). Glucagon is cleaved from proglucagon by PC 2, the enzyme which is expressed in α-cells under normal conditions. It has been previously reported that extreme conditions, such as STZ

treatment, results in increased levels of immunoreactive PC1 in rat α-cells leading to increased synthesis of GLP-1 in these cells and consequently improving islet survival. (Nie et al. 2000).

The secretion of glucagon is triggered under conditions of hypoglycaemia and subsequently decreases during hyperglycaemia. In humans, the mechanism of glucagon secretion is similar to that of insulin secretion from β-cells. However, β-cells are electrically inactive at basal glucose levels due to their open K_{ATP} channels and hyperpolarized membrane potential, and thus do not release insulin. On the other hand, α-cells are active at a basal rate of glucose due to increased ATP/ADP ratio in these cells. This results in closure of most (but not all) K_{ATP} channels and a depolarized membrane potential that leads to opening of Na^+ and Ca^{2+} (VDCC) channels. The subsequent Ca^{2+} and Na^+ influx trigger the release of glucagon through exocytosis of glucagon containing secretory granules. Under conditions of high plasma glucose concentration, glucose enters α-cells via the GLUT1 transporters where it is metabolised via glycolysis and mitochondrial oxidative metabolism which subsequently results in further increase in the intracellular ATP/ADP ratio and closure of K_{ATP} channels leading to further depolarisation of the membrane and the depolarization-dependent inactivation of Na^+ channels and VDCCs. Paracrine factors secreted from β-cells and pancreatic δ-cells are also responsible for the suppression of glucagon release due to their interaction with putative α-cell metabolic sensors (i.e., PASK and AMPK) (Gaisano et al. 2012).

1.11.3 Mechanism of glucagon action

Once glucagon binds to its receptor in the hepatocytes, it leads to activation of the Gs-alpha catalytic subunit of the membrane-bound enzyme adenylate cyclase, which

catalyzes the conversion of ATP to cAMP, which subsequently activates intracellular kinase which activates several downstream signalling pathways: (i) glycogenolysis, (ii) gluconeogenesis, and (iii) ketogenesis. For glycogenolysis, subsequent phosphorylation of phosphorylase results in its activation leading to desphosphorylation of glycogen synthase and its inactivation. Thus, glycogen formation is inhibited, and glycogen breakdown stimulated. In the case of gluconeogenesis, the initiation of the pathway is more complex and involves several steps. Glucagon stimulates the liver to uptake amino acids, but its main effect is intrahepatic which involves the production of phosphoenolpyruvate and suppression of its disposal by pyruvate kinase (Gosmanov et al. 2000).

Glucagon is the primary hormone in the induction of fatty acid oxidation and ketogenesis (Foster et al. 1984). During the periods of fasting, inhibition of glycolysis results in activation of glycogenolysis due to reduced activity of glycolytic enzymes and reduced activity of acetyl CoA carboxylase which subsequently leads to the reduction of malonyl-CoA concentration. The decreasing concentration of intracellular malonyl-CoA results in activation of mitochondrial transport system responsible for ß-oxidation of fatty acids leading to raised levels of acetyl CoA which stimulate ketogenesis (Barnett et al. 2003).

1.11.4 Role of glucagon in the pathology of diabetes

Glucagon is known to exhibit lipolytic effect and the ability to promote the reduction of weight via modulation of calories intake and energy expenditure. Thus, glucagon receptor agonism has recently become a potentially attractive target for pharmacological weight management. On the other hand, glucagon also has diabetogenic nature due to its potent ability to stimulate glucose production by the

liver. Several lines of evidence show that elevated glucagon levels play a pathophysiological role in the development of chronic hyperglycemia (Müller et al. 2017). In 1975 Unger and Orci suggested that that diabetes is a bihormonal disease caused by both insulin abnormality and glucagon excess (Unger et al. 1975; Unger 1978). Indeed, in both T1D and T2D, there are inappropriately high levels of plasma glucagon which correlates with hyperglycaemia even when plasma insulin concentration is similar to normal control. Plasma fasting levels of glucagon are also shown to be increased in patients with diabetes (Kulina et al. 2016).

Moreover, when somatostatin was administrated to healthy fasting individuals, mild suppression of insulin and glucagon followed by marginal hyperglycaemia was observed. However, the additional minimal dose of glucagon to somatostatin normalised basal glucagon levels and resulted in significant and sustained hyperglycemia, mimicking the scenario seen in T2D (Lins et al. 1983). Exaggerated glucagon response to ingested amino acids and therefore high hepatic glucagon production is also observed in patients with T2D compared to nondiabetic controls (Kulina et al. 2016).

Other studies revealed that nonsuppression of glucagon after meals contributes to postprandial hyperglycemia in patients with diabetes. This indicates that glucagon excess is the key factor in the pathogenesis of the condition and inhibition of glucagon action might improve hyperglycemia in diabetic individuals (Shah et al. 2000; Unger et al. 2012; Kulina et al. 2016; Müller et al. 2017).

1.12 Evolution of glucagon-like sequences and their receptors

1.12.1 The Glucagon-like subfamily

Glucagon, GLP-1 and GIP are glucagon-like sequences which share sequence similarity with a small number of other consists of structurally related brain-gut short peptides hormones belonging to the secretin gene superfamily (Figure 1.10) (Irwin 2010). These hormones are produced in the intestine, pancreas, and the central and peripheral nervous systems and act as ligands for the class B1 G protein-coupled receptors (GPCR superfamily) to exhibit various biological functions such as neurotransmission.

In mammals, currently there are 10 known peptide members of the secretin superfamily which are further divided into two major subfamilies: i) PACAP-like subfamily which includes PACAB, GH-releasing hormone (GHRH, also known as growth-hormone-releasing factor, GRF), PACAP-related peptide (PRP also called GHRG-like peptide, GHRH-LP), vasoactive intestinal polypeptide (VIP), peptide histidine methionine or peptide histidine isoleucine (PHI/PHM) and secretin (SCT) and ii) glucagon-like subfamily which includes glucagon (GCG), GLP-1, GLP-2 and GIP (Sherwood et al. 2000; Cardoso et al. 2010; Moody et al. 2011; Takei 2015; Sekar et al. 2017). Other non-mammalian important members include exendin-3 and -4 helospectin-1 and -2, helodermin isolated from lizard (Heloderma) venom (Figure 1.10).

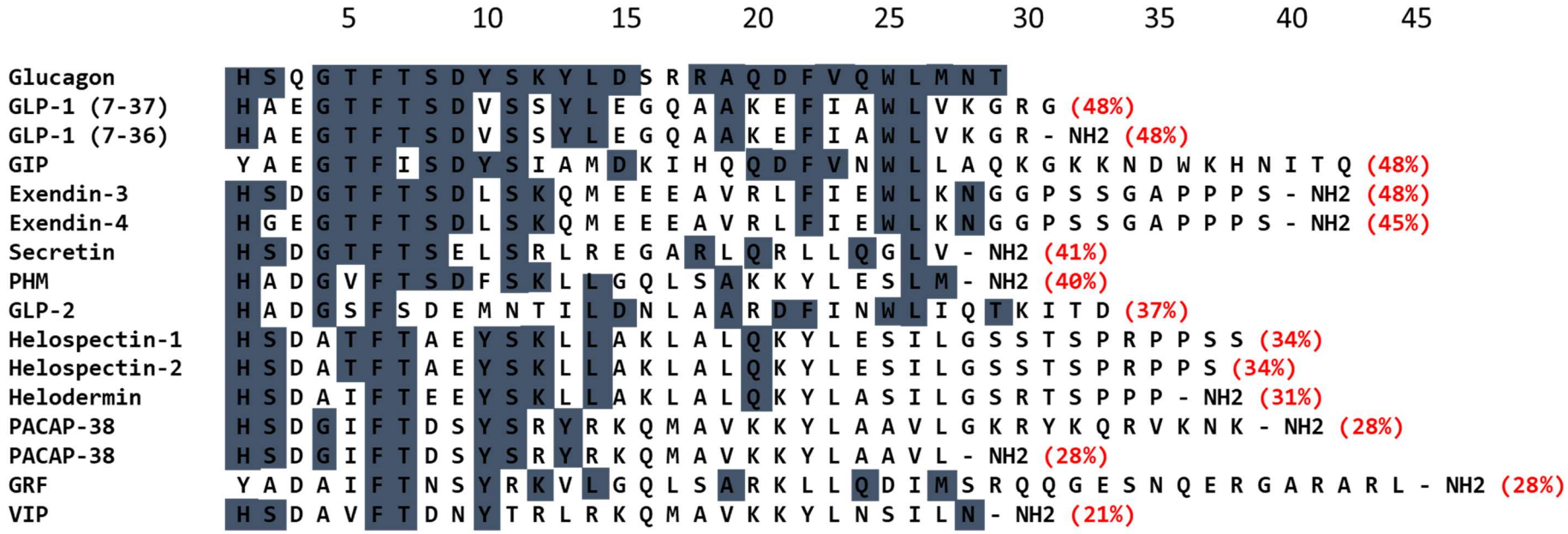

Figure 1.10 Amino acid sequences of the members of the superfamily of secretin/PACAP/ glucagon peptides. Residues similar to those of glucagon in the same position are represented in blue. The values in parentheses show % sequence identity with glucagon.

In mammals, six genes have been identified to encode glucagon-like sequences. This is due to some of these genes such as *GCG* and *VIP* encode three (glucagon, GLP-1 and -2) and two (PMH/PHI and VIP) bioactive peptides respectively, whereas the *ADCYAP*, *GHRH (GRF)*, *SCT*, and *GIP* genes encode only a single bioactive peptides: PACAP, GRF, secretin and GIP respectively (Sherwood et al. 2000; Irwin 2010). Additionally, *ADCYAP* gene also encodes a PRP, the function of which remains an enigma to date (Tam et al. 2007). These peptides are suggested to have evolved from a common ancestor exon via exon and gene/chromosome duplication events in the chordate radiation (Figure 1.11) (Cardoso et al. 2010). At least one gene duplication event gave rise to the novel exendin family which has been identified only in a few lizards (Gila monster) (Sherwood et al. 2000).

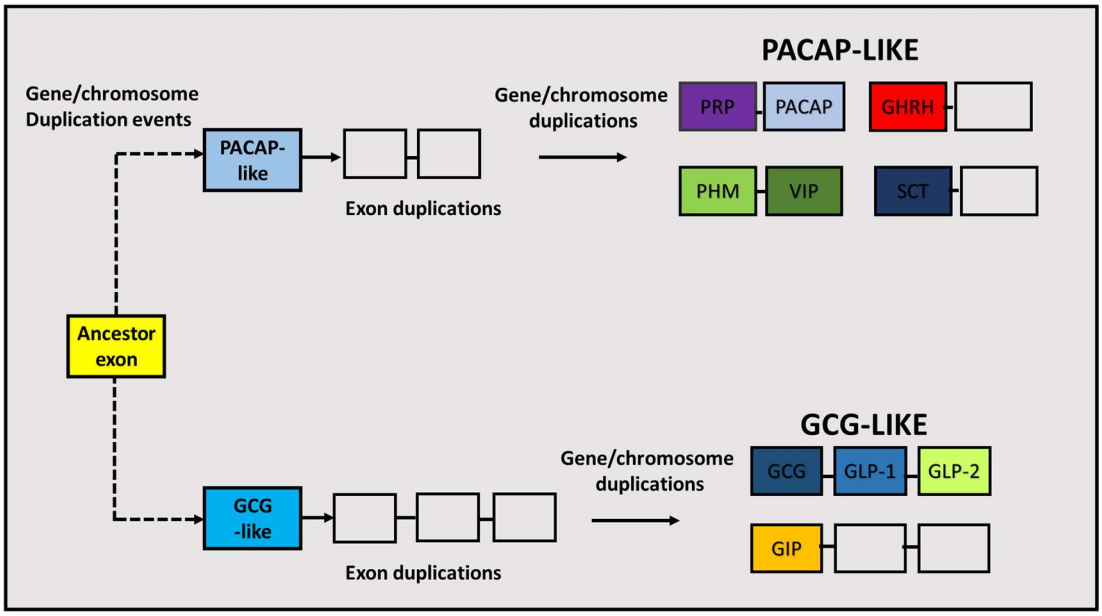

Figure 1.11 Evolutionary model of PACAP-like and Glucagon members. Boxes represent exons and lines introns. Coding exons are indicated by peptide abbreviations (Adapted from Cardoso et al. 2010).

Phylogenetic hypothesis previously suggested that the *ADCYAP* and *GHRH* were evolved via gene duplication specific to the mammalian lineage. However, more recent evidence suggests that these genes can be found in the genomes of diverse vertebrates and therefore should be regarded as two separate genes in all vertebrate species (Tam et al. 2007; Irwin 2010).

Despite being the first hormone discovered secretin's evolutionary origin remains unresolved. It is known that secretin sequence exhibits moderate similarity in tetrapods, however, in mammals, it is highly conserved (81.5–96.3% identity). Therefore, this suggests a rapid evolution of *SCT* along the tetrapod lineage until the mammals began to diverge resulting in only 9.3–51.9% secretin peptide sequence similarity compared to mammalian secretin. Interestingly, even though *SCT* has already emerged before the divergence of osteichthyans, it was lost in fish and retained only in land vertebrates. The secretin-like receptor has been identified in both actinopterygian fish (zebrafish) and sarcopterygian fish (lungfish) however in zebrafish it is demonstrated to be inactive (Tam et al. 2014). Although secretin was originally considered to be a gastrointestinal peptide, it has also been found in the gonads, brain, and developing pancreas (Sherwood et al. 2000).

Unlike SCT, the genes encoding GCG, GIP, VIP, have been describing in both fish and mammalian genomes. The current hypothesis suggests that the proglucagon and GIP arose during one of the two whole genome duplications (2R theory) events that took place in the early vertebrate evolution. Indeed, novel software tools such as Synteny analyses and reconstruction of phylogeny and ancestral genomes confirmed that most peptide hormones and receptor families in many vertebrate and invertebrate species evolved via two rounds of whole genome duplication and local duplications before and after 2R. Moreover, these evolutionary events were followed by

modification and loss of gene sequences. Hormone/receptor orthologues exhibit specific alterations in their sequences which may guide their selective interactions and discriminate against paralogous hormone/receptors (Park et al. 2013).

The sequence structures of the secretin superfamily members are highly conserved with anywhere from 21% to 48% amino acid identity with glucagon sequence (Figure 1.10). According to the phylogenetic analysis, PACAP, VIP and glucagon appeared to be the most conserved members of the secretin superfamily, whereas PRP, GLP2, and SCT are demonstrated to be most divergent. The elements of a secondary structure belonging to these peptide hormones form a random N-terminal and a C-terminal alpha helix. Notably, although exhibiting a high degree of sequence homology, the function of these peptide hormones differ significantly, even in those that are co-encoded within the same precursor (such as GLP-1 and glucagon derived from proglucagon).

1.12.2 Evolution of glucagon-like sequences

Glucagon, GLP-1 and GLP-2 are the main products of the invertebrate proglucagon gene, the expression of which is tissue-specific and vary between species. The sequences of the proglucagon peptide trio display the structural similarity but regulate distinct physiological processes.

Glucagon and GLP-1 peptides have been isolated from various vertebrate species (including different species of fish (Table 1.1)), whereas GLP-2 sequence has only been purified from mammalian species. Phylogenetic analysis has suggested that sequence of GLP-2 was subject of rapid evolution on the early mammalian lineage acquiring a role of a nutrient-responsive growth factor that stimulates intestinal epithelial cells growth. Due to having highly conserved nature GLP-2 is proposed to

be produced and function in the intestine of most vertebrates. Glucagon is the counter-regulatory hormone of insulin that has a main role to maintain blood glucose levels during fasting by inducing the liver to produce glucose, whereas the role of GLP-1 is to decrease hyperglycaemia by stimulating the secretion of insulin. Together, these peptides are suggested to have a common evolutionary origin descending from an ancient exon that arose one billion years ago with the functions evolved separately following the divergence of the sequences (Figure 1.12) (Ng 2010).

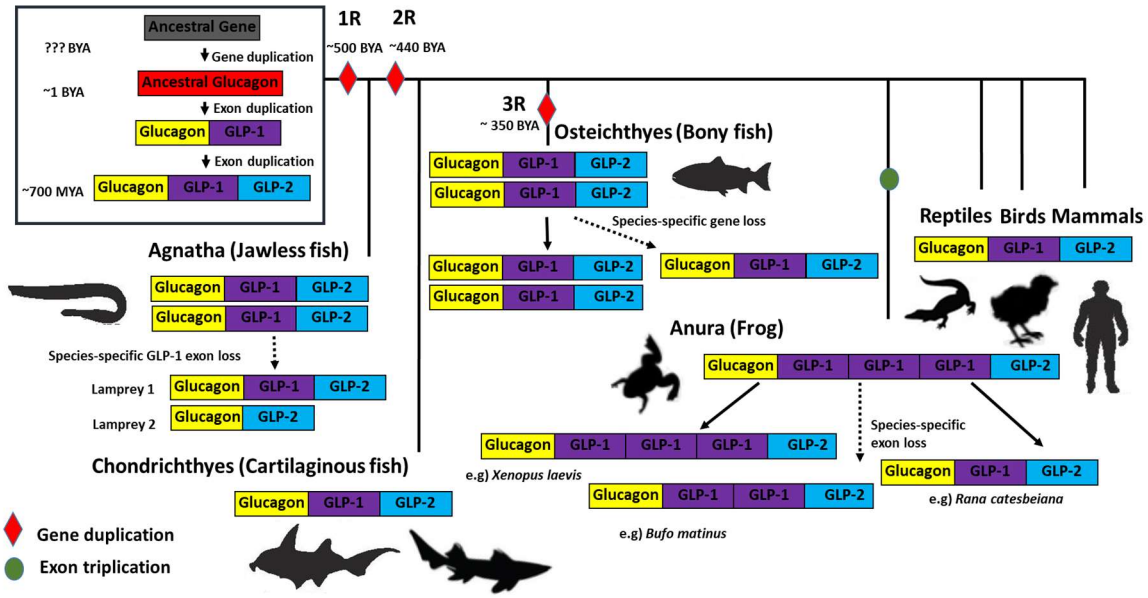

Figure 1. 12 An evolutionary scheme of proglucagon-derived peptides in vertebrates. Unknown or unclear events are represented by dotted lines. The phylogenetic timeline for the events are not to scale (Adapted from Ng et al. 2010).

Duplication of exon within the ancestral glucagon presumably occurred next, resulting in GLPs that subsequently diverged into GLP-1 and GLP-2 about ~700 million years ago (Figure 1.12). The primary structures of GLP-1 and GLP-2 were deduced from

cDNA sequences before their physiological role was discovered (Plisetskaya et al. 1996).

It appears that intestinal peptides with gastrointestinal hormone activities arose early in vertebrate evolution (class Agnatha). The glucagon-like molecule is also present in extracts of some invertebrate chordates, including both tunicates and cephalochordates (Norris et al. 2013).

Proglucagon-derived peptides are speculated to be subject to the genome and gene duplication events, which is responsible for the changes in the structure of the vertebrate sequences observed today.

In mammals, birds and reptiles, only a single set consisting of three proglucagon-derive hormones are known to exist (Figure 1.12). However, amphibian and some fish (jawless fish and bony fish) exhibit multiple proglucagon-related sequences which are represented by multiple genes or additional peptide sequences encoded within the gene (Figure 1.12) (Ng et al. 2010). As an example, proglucagon genes of some frog species encode five glucagon-like sequences, whereas bony fish such as zebrafish, have two proglucagon genes, one of which reflects the standard scenario of three glucagon-like peptides and the second gene only encodes glucagon and GLP-1.

This variation results in multiple proglucagon mRNA being produced in non-mammalian species which may also be due to alternative splicing process which is known to occur in fish, chicken and reptiles such as Gila monster.

Comparison of the sequences of the proglucagon genes between multiple species revealed conserved coding sequences which correlate with conservation of function.

Different rates of evolution could be linked to greater levels of divergent sequences resulting in alteration of function of the peptides in specific species. This can be

observed in Hystricognath rodents (guinea pig) in which glucagon sequence underwent evolutionary changes, such as multiple substitutions, resulting in hormone with attenuated function (Irwin et al. 2010).

Mammalian GLP-1 sequence is shown to be highly conserved within the species except for the monotremes (platypus and echidnas). A recent study has shown that in the monotremes a single *GCG* encodes a GLP-1 peptide with two functions, one in venom and the other in the gut (Tsend-Ayush et al. 2016). In other vertebrates (fish and amphibians) a greater variation in sequences is reported. Interestingly, the function of GLP-1 is not conserved. In fish, the effects of GLP-1 resembles the actions of glucagon rather than classical incretin effects observed in mammals. (Sherwood et al. 2000; Irwin 2010; Ng 2010; Irwin 2012). The inability of GLP-1 to function as an incretin hormone in fish is suggested to be due to the redundancy of GLP-1 as a result of duplicated sequences found in these species.

1.12.3 Evolution of receptors for glucagon subfamily

Four cognate receptors (*Gcgr*, *Glp1r*, *Glp2r* and *Gipr*) belonging to the Secretin G-protein coupled receptor (GPCR) has been characterised for the mammalian glucagon-like peptides.

Structural features of this family of receptors include 7 transmembrane domains (TMD) and a long extracellular N-terminal domain (ECD) with 6 conserved cysteine residues responsible for peptide binding and receptor activation and signalling. All of the peptide ligands bind the ECD with their C-terminal a helix. The C terminus of the peptide initiates recognition with the ECD of the receptor, which allows the peptide's N terminus to bind the TMD ligand-binding pocket subsequently activating the receptor and prompting downstream signalling pathways (de Graaf et al. 2017).

As opposed to the tissue-specific expression of the glucagon-like hormone precursors in mammals, the receptors exhibit a widespread tissue distribution in vertebrates (Cardoso et al. 2018).

In addition to the aforementioned mammalian receptor members, the gene encoding GCG-related peptide receptor (*Grpr*), as well as the gene for its ligand, have been found in representative tetrapod taxa such as anole lizard, chicken, and *Xenopus*, and in lampreys and teleosts including medaka, fugu, tetraodon, and stickleback. However, these genes are known to be absent in mammals and zebrafish (Park et al. 2013; Cardoso et al. 2018).

In the case of incretin receptors, most of the characterisation studies have been performed in mammalian species with only a few nonmammalian receptors have been functionally described. Similarly, *Gcgr* from a small number of fish species and a frog have been isolated and partially characterized revealing a close relation to mammalian glucagon receptors. Moreover, piscine *Gipr*-encoding gene shows similarity to that of mammals (Irwin 2010).

Interestingly, *Glp1r*-encoding gene has been known to be missing from the fish genomic sequence. However, a recent gene analysis has suggested that lampreys are the only fish in which putative glp1r gene persisted. Moreover, in teleost fish, GLP-1 does not exhibit incretin effects. Instead, it acts similarly to glucagon stimulating the production of glucose by hepatocytes, activating receptors which are more closely related to mammalian *Gcgr* genes rather than to *Glp1r*. *Glp1r* has been proposed to be encoded by a duplicate copy of the *Gcgr* due to fish-specific genome duplication thus GLP-1 molecule has gained new glucagon-like biological effects.

1.13 Structure of Endocrine Pancreas in Fish

There are 5 types of pancreatic islet morphology in vertebrates: (I) cyclostome type, (II) primitive gnathostome type, (III) actinopterygian type, (IV) lungfish type, and (V) tetrapod type. Mammals, birds, amphibians and reptiles have distinct pancreatic organs consisting of both exocrine compartments and islet tissues. The most primitive anatomical arrangement of the endocrine pancreas belongs to lampreys (agnathas/jawless fish) (Figure 1.13). In these ancient fish species, the follicles of Langerhans are partially embedded in the gut lining. In contrast, other jawless fishes, the primitive hagfishes, exhibit a definite endocrine pancreatic organ. Glucagon-immunoreactive cells are not found the islet organ of agnathas and only exist in the gut mucosa in these species. GLP-1 immunopositive cells are known to be located in the intestine of juvenile and up upstream migrant marine lamprey (Plisetskaya et al. 1996).

Cartilaginous fishes (sharks, rays, skates and chimaeras) and *Latimeria* (coelacanth) are (Figure 1.13) known to have the primitive gnathostome type of endocrine pancreas. It has been reported that in the pancreas (and in gut) of ratfish (chimaera) two types of cells exhibiting distinct glucagon immunoreactivity were observed, which strongly suggested the existence of two different populations of glucagon – one closely related to glucagon and another possibly close to oxyntomodulin (due to reactivity with C- and N-terminally directed anti-glucagon sera). In all other fishes, including elasmobranchs (sharks, rays and skates) and actinopterygians (ray-finned fishes), the endocrine pancreas produces both glucagon and GLP-1 (Plisetskaya et al. 1996).

The pancreas of many teleosts (Figure 1.14) exhibits a unique arrangement represented by almost complete separation of endocrine from exocrine compartments. (Plisetskaya

et al. 1966). The piscine endocrine tissue cells are condensed into a few large rounded bodies called “the principal islet”, surrounded by only a thin rim of exocrine tissue, thus lack an acinar (exocrine) pancreas (Norris et al. 2013). In addition to these islets a few smaller ones are scattered in the mesentery (Khanna et al. 1971). The collection of islet tissues is so-called Brockmann body, named after Heinrich Brockmann, who first described an endocrine organ in sculpin (*Cottus scorpius*) and cod (*Gadus cullarius*) in 1846. Brockmann bodies are anatomically located close to the gall bladder duct and are visible to the naked eye as whitish or pinkish round structures (Plisetskaya et al. 1996). Indeed, this structural uniqueness greatly facilitates isolation of high purity fish pancreatic hormones due to minimal risk of contamination with endocrine tissue.

1.14 Piscine Proglucagon-derived Peptides: Discovery and Scientific Value

Fish are valuable experimental models which have made significant contributions to the research of pancreatic hormones and other gastrointestinal peptides. The first piscine (tuna, *Thunnus germo*, and anglerfish, *Lophius piscatorius*) hyperglycaemic substances were discovered simultaneously by Mialhe, and Audy and colleagues in 1952. A few years later, the hyperglycaemic effects of extracts isolated from the Brockmann bodies of tuna (*Thunnus thymus*) were connected to the action of glucagon. The first attempted to purify and characterise anglerfish proglucagon peptide was made by Trakatellis and colleagues in early 1970s (Lefebvre 1983). The endocrine parenchyma of anglerfish became an organ of choice for studying glucagon biosynthesis as well as investigating the metabolism of the endocrine pancreas. Anglerfish islets were used for investigation of glucagon-like immunoreactivity found in the plasma and pancreatic extracts. Lund and co-workers first cloned proglucagon cDNA from anglerfish islets in the 1980s and following its sequencing, mammalian

version was determined from cattle, hamster, rat and human in the 1980s (Kastin 2013). The proglucagon sequence was found encode three related peptides: glucagon, GLP-1 and -2) glucagon-related peptides. The first native GLP-1 to be isolated from any source coming from the pancreas of the channel catfish (*Zctulurus punctutus*) (Table 1.1) (Andrews et al. 1985; Plisetskaya et al. 1996).

1.15 Consequences of fish-specific evolution on glucagon-like peptides

1.15.1 Agnathas

The Agnatha, or jawless fish, represent the first vertebrates whose line of evolution diverged from jawed vertebrates (gnathostomes) about 550-500 million years ago (Figure 1.13) (Woods et al. 2005). The fossil record suggests that the Agnatha were numerous during the Silurian/Devonian period, however only one class called Cyclostomata whose members include the extant lampreys (Petromyzontiformes) and hagfish (Myxinoformes) have survived to date and are known to be the oldest living vertebrates (Conlon et al. 1993, Kuraku et al. 2006, Ng et al. 2010). The divergence of lampreys and hagfish occurred 470-390 million years ago. The taxonomic analysis suggests that the lampreys are more closely related to gnathostomes than either is to hagfishes (Conlon et al. 1993). At present, lampreys are divided into 3 families: the Petromyzontidae (34 species), the Mordaciidae (3 species) and Geotriidae (1 species).

The appearance characteristics of lampreys are very primitive, and their endocrine pancreas can reflect the earliest state of islet hormones evolution and development in the vertebrates (Xu et al. 2016). The endocrine elements in these animals originate from intestinal and bile-duct epithelia and are represented by an aggregate of submucosal islets (Youson et al. 2000). Previously, glucagon and GLP-1 peptides from intestines parasitic phase *Petromyzon marinus* (sea lamprey) (Table 1.1) (Conlon

et al. 1993) and glucagon from intestines of *Lampetra fluviatilis* (river lamprey) (Conlon et al. 1995) well as two forms of glucagon from lamprey *Geotria australis* (Wang et al. 1999) were purified and characterised.

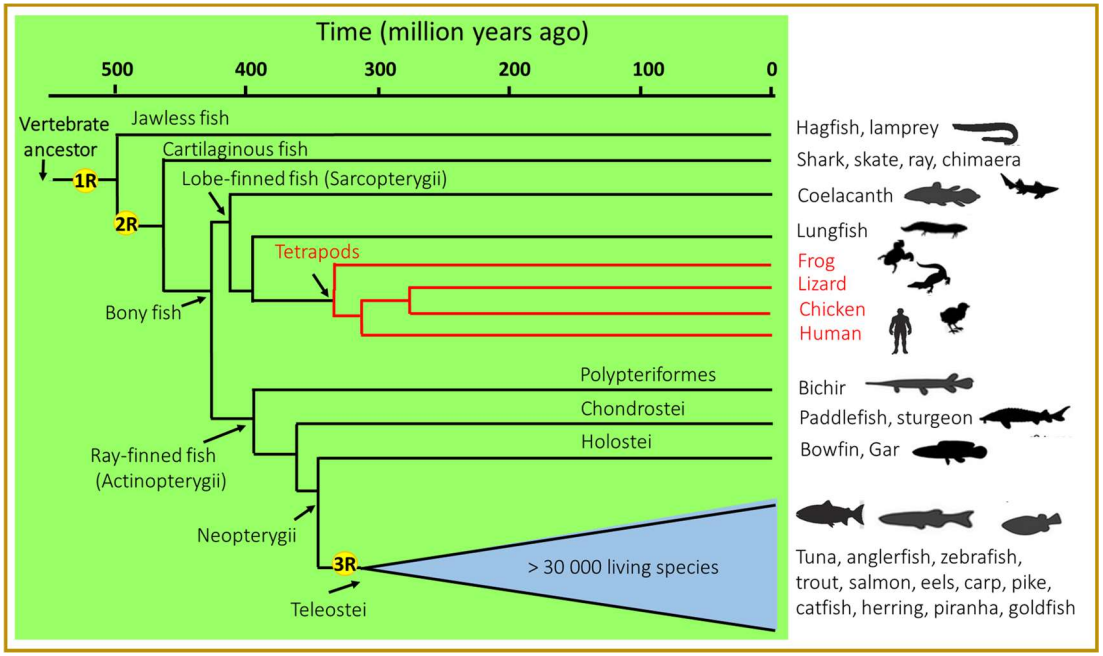

Figure 1.13 A simplified phylogenetic tree of vertebrates. Yellow circles represent the whole-genome duplication (WGD) events.

Indeed, lampreys possess the most ancient glucagon-like system among the vertebrates. The genome of these fish species contains two unique proglucagons: i) proglucagon I encoding glucagon, GLP-1 and GLP-2 and ii) proglucagon II which only encodes glucagon and GLP-2 (Figure 1.12) (TG et al. 2010). The origin of the peptide trio is suggested to occur before the divergence of jawed and jawless vertebrates as glucagon sequences isolated from *Petromyzon marinus* and *Geotria australis* glucagons differ by six amino acid residues (Wang et al. 1999). This may also reflect the divergence event between Petromyzontidae and Geotriidae about 220–280 million years ago). A large number of chromosomes suggests that genome

duplication event has occurred early in the lamprey lineage but before the divergence of modern lampreys.

1.15.2 Chondrichthyes

Chondrichthyes (cartilaginous fish) represent the oldest group of jawed vertebrates that diverged from a common ancestor of Osteichthyes (bony vertebrates) about 440 million years ago, near the Devonian–Silurian boundary (Figure 1.13) (Inoue et al. 2010; Amaral et al. 2018). The early Devonian period is associated with the second duplication event that occurred after the split of lampreys but before the split of cartilaginous fish from the main vertebrate lineage (Hallbook et al. 1998).

The extant cartilaginous fishes are divided into two subclasses: Elasmobranchii (shark, skates and rays) and Holocephali (chimaeras). The Elasmobranchii group represents the most diverse class of large predatory fishes (about 1200 species) (Amaral et al. 2018). The modern holocephalans are marine fishes found in the world's oceans except for the Arctic and are represented by only 39 species (Inoue et al. 2010). These species represent the first vertebrate in evolution to develop a pancreas containing the 4 kinds of islets hormones found in mammals (Conlon et al. 1994). Currently, the sequence of a single copy proglucagon peptide is known for the small number of cartilaginous fishes including the electric ray (*Torpedomar morata*), dogfish (*Scyliorhinus canicula*), Pacific ratfish *(Hydrolagus colliei*), and elephant-fish (*Callorhynchus milii*) (Table 1.1). It has been suggested that the duplicate proglucagon gene is either lost or silenced in the cartilaginous lineage (Ng et al. 2010).

Proglucagon gene from cartilaginous fish was recently predicted to produces 3 GLPs; in addition to glucagon, GLP-1 and GLP-2, a novel glucagon-like peptide, named GLP-3 was identified in elephant shark and the elasmobranch *Rhincodon typus* (whale

shark). Previously, only a single GLP-1 was identified in extracts of pancreata in *Scyliorinus canicula* (dogfish) (Conlon et al. 1994) *Hydrolagus colliei* (and ratfish) (Conlon et al. 1989). It has been suggested that GLP-3 evolved in the early vertebrate, before the origin of cartilaginous fish and could be lost from the genome of the ancestor of tetrapods and Actinopterygii (ray-finned fish) (Irwin et al. 2018).0

1.15.3 Osteichthyes

Osteichthyes (bony vertebrates) is a group consisting of Actinopterygii fishes (ray-finned) and lobe-finned fishes plus Sarcopterygii (tetrapods) (Figure 1.13). Actinopterygii fishes are the habitats of aquatic environments over the world, from deep ocean trenches to high mountain streams, and thrive in extreme acidic, subzero, hypersaline, hypoxic, temporary and fast-flowing water conditions (Hughes et al. 2018).

Ray-finned fishes diverged early, about 476 to 423 million years ago, from the main stem of the phylogeny (Sarcopterygii-Actinopterygii split).

The phylogenetically ancient Actinopterygii include 18 living species of Polypteriformes (reedfishes), 30 species of sturgeons and paddlefishes (Acipenseriformes) 7 species of gars (Lepisosteiformes), and a single species of bowfin (Amiiformes) (Broughton et al. 2013).

Previously, glucagon-like peptides were isolated from the endocrine pancreas of *Amia calva* (bowfin) (glucagon and GLP-1) (Table 1.1) (Conlon et al. 1993b), *Polyodon spathula* (paddlefish) (two glucagon peptides and GLP-1) (Nguyen et al. 1994), *Lepisosteus spatula* (alligator gar) (glucagon and GLP-1). The pancreatic extract of alligator gar also contained oxyntomodulin whose primary structures was determined (Pollock et al. 1988).

The third, teleost specific, genome duplication occurred approximately 350 million years ago early in the ray-finned lineage before teleost diversification (Figure 14). Teleostei appeared about 284 million years ago and included at least 30,000 living species inhabiting diverse environments with different access to nutrients and life histories.

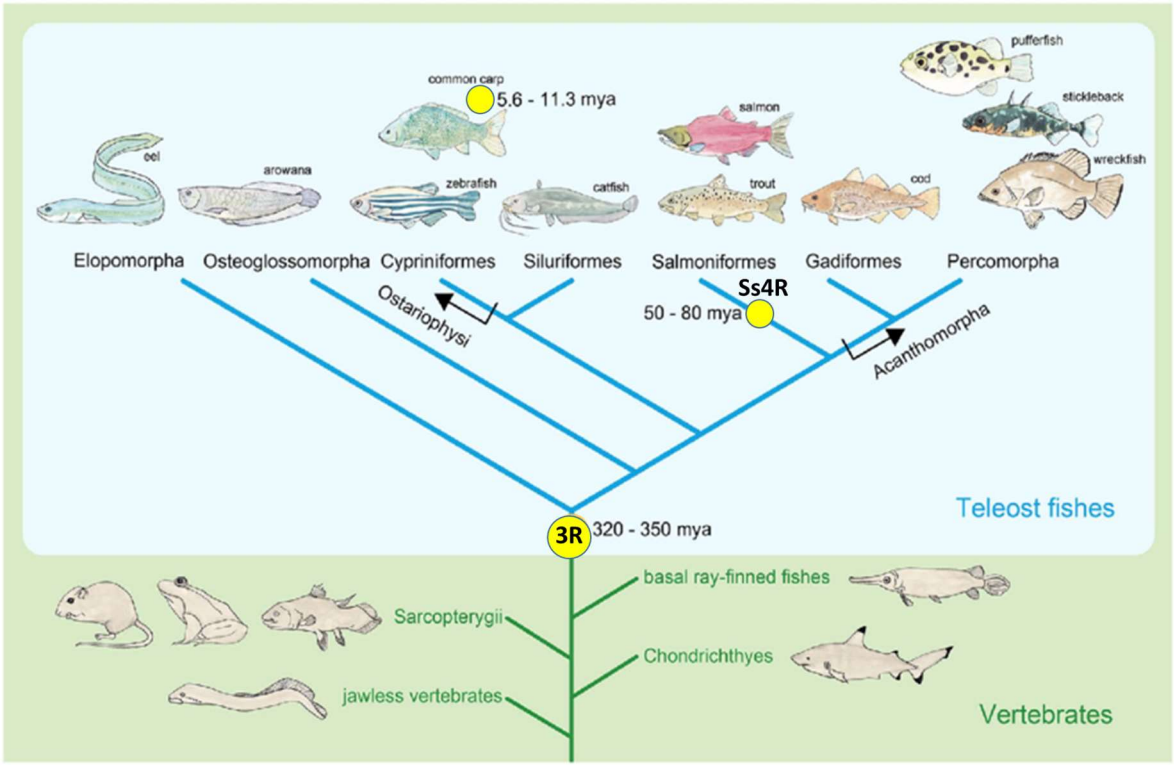

Figure 1.14 A simplified phylogenetic tree focusing on the evolution of teleost fishes (Glasauer et al. 2014). Yellow circles represent the whole-genome duplication (WGD) events.

The systematic evaluation of the developmentally important and well-conserved Hox gene clusters supported the theory of the teleost-specific whole genome duplication event. The existence of many duplicated Hox genes was identified in zebrafish (7 Hox clusters) and pufferfish (6 Hox clusters) as well as in most basal extant groups of teleost fishes the Elopomorpha (including eels and tarpons) and Osteoglossomorpha

(including bony tongues and elephant-fish) to the already known ones from tetrapods. Markedly, the modern eels (European and Japanese eel) are presently the only fishes in which the complete set of the original 8 Hox clusters has been identified. Whole-genome sequencing of some fish genomes has also provided conclusive evidence for at least one teleost-specific genome duplication event (Glasauer et al. 2014).

Three major teleost stem lineages, Elopomorpha, Osteoglossomorpha and Clupeocephala, diverged in the Middle Permian. Through the Late Permian and Early Triassic, there are few cladogenic events, but in the Late Triassic, crown groups Elopomorpha, Osteoglossomorpha, Otomorpha and Euteleosteomorpha all begin to diversify (Broughton et al. 2013).

Phylogenetic analysis of the proglucagon coding sequence revealed that most teleost proglucagon genes separate into two groups: gcga and gcgb which in some teleost fish have differing coding potential and are thought to occur due to fish-specific genome duplication suggesting that the divergence between gcga and gcgb preceded the radiation of teleost fish (Irwin et al. 2018).

Multiple proglucagon gene copies are found in several bony fish: rainbow trout (*Oncorhynchus mykiss*), anglerfish, sculpin (*Cottus scorpius*) and eel (*Anguilla anguilla*) as well as fugu (*Takifugu rubripes*), pufferfish (Tetraodon nigroviridis), medaka (*Orzyzias latipes*) and stickleback (*Gasterosteus aculeatus*). In these species where one proglucagon encodes for all three derived peptides, and the other encodes for glucagon and GLP-1 (Ng et al. 2010). Moreover, additional and relatively recent duplication events occurred at the base of Salmonifarms 50–80 million years ago (Berthelot et al. 2014) and in a closely related ancestor of the common carp 5.6–11.3 million years ago (Figure 14) (Glasauer et al. 2014). Rediploidization or gene

fractionation (the loss of duplicated genes after whole genome duplication) by mutations and deletions to return to a mostly diploid state, is an ongoing process in the species of the *Salmonidae family* (rainbow trout) genome which represents a particular interest for the research (Bobe et al. 2016).

1.16 Hypothesis:

Glucagon-related peptides (glucagon, GLP-1, oxyntomodulin and GIP) isolated from various fish ranging from phylogenetically ancient to recently evolved species, may exhibit unique sequence substitutions allowing them to activate multiple GPCRs for glucagon, GLP-1 and GIP located in the mammalian pancreas which may lead to a discovery of a therapeutically exploitable unimolecular multi-agonist with the potential to become an agent for improvement of T2D treatment.

1.17 Aims:

The primary aims of this thesis are to assess of the insulinotropic and antihyperglycaemic potential of fish glucagon-related peptides *in vitro* and *in vivo*, to identify their target receptors, and to identify the most promising molecules to serve as templates for the development of long-acting fish glucagon-derived analogues.

1.18 Objectives:

1. To purify and perform *in vitro* and *in vivo* studies of glucagon-related peptides from sea lamprey, dogfish, ratfish, paddlefish, bowfin, zebrafish and trout (Figure 1.15).

2. To delineate which hormone receptors and responses are achieved by the fish glucagon-derived peptides and the mechanisms underlying their actions using receptor transfected and receptor KO cells.

3. To examine *in vivo* metabolic effects of native fish peptides in normal mice to identify the most promising molecules the sequences could be used as templates for further modifications.

4. To design and test synthetic analogues of these molecules with improved plasma stability and explore their antidiabetic properties using various cell lines as well as normal, genetically modified and high fat fed mice models.

1.19 Plan of investigation

A brief plan of investigation includes purification of crude synthetic peptides, confirmation of molecular masses and *in vitro* and *in vivo* biological testing in order to select the most promising compound for further studies (Figure 1.15).

.

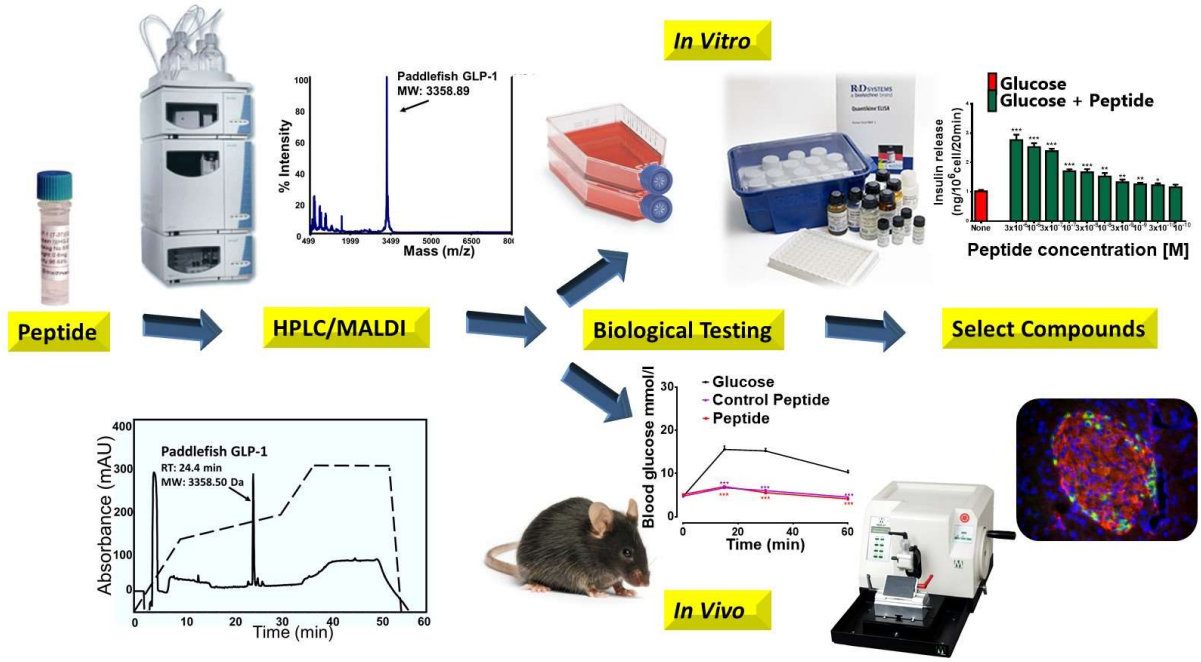

Figure 1.15 Plan of Investigation

1.20 Why specific fish glucagon-related peptides were selected for the study

The sequences of the synthetic peptides used in this study are based on the structures of glucagon, oxyntomodulin, GLP-1 and GIP isolated from fish species that occupy different positions in the vertebrate evolution including the primitive jawless fish (sea lamprey), two cartilaginous fish (dogfish and ratfish) which represent the first jawed vertebrates, two early diverging ray-finned (paddlefish and bowfin), and two recently evolved teleost species (zebrafish and trout). The structure-function studies described in this thesis are based on the sequence differences between the selected fish glucagon-related peptides and the corresponding human peptides (Figure 1.16) as well as on the core sequence similarities between each fish peptide sequence and human glucagon, GLP-1 and GIP.

```
Human GLP-1             HAEGTFTSDVSSYLEGQAAKEFIAWLVKGR-NH2
Lamprey GLP-1           HADGTFTNDMTSYLDAKAARDFVSWLARSDKS
Dogfish GLP-1           HAEGTYTSDVDSLSDYFKAKRFVDSLKSY
Ratfish GLP-1           HADGIYTSDVASLTDYLKSKRFVESLSNYNRKQNDRRM
Paddlefish GLP-1        HADGTYTSDASSFLQEQAARDFISWLKKGQ
Bowfin GLP-1            YADAPYISDVYSYLQDQVAKKWLKSGQDRRE
Trout GLP-1             HADGTYTSDVSTYLQDQAAKDFVSWLKSGRA

Human Glucagon          HSQGTFTSDYSKYLDSRRAQDFVQWLMNT
Lamprey glucagon        HSEGTFTSDYSKYLENKQAKDFVRWLMNA
Dogfish oxyntomodulin   HSEGTFTSDYSKYMDNRRAKDFVQWLMSTKRNG
Ratfish oxyntomodulin   HTDGIFSSDYSKYLDNRRTKDFVQWLLSTKRNGANT
Paddlefish glucagon     HSQGMFTNDYSKYLEEKRAKEFVEWLKNGKS
Trout glucagon          HSEGTFSNDYSKYQLERMAQDFVQWLMNS

Human GIP               YAEGTFISDYSIAMDKIHQQDFVNWLLAQKGKKNDWKHNITQ
Zebrofish GIP           YAESTIASDISKIVDSMVQKNFVNFLLNQRE
```

Figure 1.16 Comparison of fish glucagon-derived sequences with the corresponding human peptides. Structural differences are highlighted in yellow.

Table 1.1 Glucagon, GLP-1 and oxyntomodulin peptides and proglucagon cDNA isolated from fish.

	Glucagon	GLP-1	OXM	Proglucagon	References
Agnatha					
Pouched lamprey (*G. australis*)	Intestine (29) I, II				(Andoh et al. 2000)
Sea lamprey (*P.marinus*)	Intestine (29)	Intestine (32)		Intestine I, II (cDNA)	(Conlon et al. 1993a; Irwin et al. 1999)
River lamprey (*L.fluviatilis*)	Intestine (29)				(Conlon et al. 1995)
Cartilaginous					
Dogfish (*S. canicula*)	Pancreas (29) Intestine (29)	Pancreas (29) Intestine (29)	Pancreas (33)		(Conlon et al. 1987 and 1994)
Ray (*T. marmorata*)	Pancreas (29)				(Conlon et al. 1985)
Pacific ratfish (*H. colliei*)		Pancreas (38, 35)	Pancreas (36)		(Conlon et al. 1989)
Elephant shark (*C.milii*)	Pancreas (29)				(Berks et al. 1989)
Ray-finned					
Alligator gar (*L.spatula*)	Pancreas (29, 35)	Pancreas (34)			(Pollock et al. 1988
American eel (*A. rostrata*)		Pancreas (30)			(Conlon et al. 1991)
European eel (*A. anguilla*)	Pancreas (29, 35)				(Conlon et al. 1988)
Anglerfish (*L. americanus*)	Pancreas (29)	Pancreas (31)		Pancreas a, b (cDNA)	(Lund et al. 1982 and 1983; Andrews et al. 1986; Nichols et al. 1988)

Coho salmon (*O. kisutch*)	Pancreas (29)	Pancreas (31)		(Plisetskaya et al. 1986)
Channel catfish (*I.punctata*)	Pancreas (29)	Pancreas (34)		(Andrews et al. 1985)
Daddy sculpin (*C. scorpius*)	Pancreas (29)	Pancreas (31)		Conlon et al. 1987; Cutfield, 1993)
Bowfin (*A. calva*)	Pancreas (29)	Pancreas (31)		(Conlon et al. 1993b)
Bigeye tuna (*T.obesus*)	Pancreas (29)			Navarro et al. 1991
Flounder (*P. jlesus*)	Pancreas (29)			(Conlon et al. 1987)
Paddlefish (*P.spathula*)	Pancreas (29)	Pancreas (31)		Nguyen et al. 1994
Kaluga sturgeon (*H. dauricus*)	Pancreas (29, 34, 35)			Andoh et al. 2000)
Rainbow trout (*O. mykiss*)	cDNA (29)	cDNA (31)	Intestine (a) Pancreas (b) (cDNA)	Irwin and Wong, 1995)
Goldfish (*C. auratus*)			Intestine (cDNA)	(Yuen et al. 1997)
Ya-fish (*S. prenanti*)			Intestine (cDNA)	Lin et al. 2015
Copper rockfish (*S.caurinus*)	Pancreas (29)	Pancreas (31, 34)	Intestine and brain (a, b) (cDNA)	(Busby and Mommsen, 2016)

The length (a.a) of the isolated peptides, proglucagon isoforms (a, b or I, II) and tissue of origin are indicated (Cardoso et al. 2018).

Chapter 2

General Materials and Methods

2.1 Materials

2.1.1 Chemical Reagents

Ultrapure water used in the experiments was obtained from the Elga PURELAB Ultra system (Elga, Celbridge, Ireland) with the purity of 18.2 MΩ-cm. All the chemicals used in the thesis, as well as suppliers' names are listed in Table 2.1.

2.1.2 Peptides

Synthetic lamprey glucagon, dogfish oxyntomodulin, ratfish oxyntomodulin, paddlefish glucagon, trout glucagon, lamprey GLP-1, dogfish GLP-1, ratfish GLP-1, paddlefish GLP-1, bowfin GLP-1, zebrafish GIP and exendin-4 peptides were supplied by EZBiolab Inc. (Carmel, IN, USA) in a crude form, whilst four crude synthetic fish peptide analogues derived from modified sequences of lamprey and paddlefish glucagon and GLP-1 (1. [D-Ser^{2}]-lamprey glucagon-Lys^{30}-gamma-glutamyl-pal, 2. [D-Ala^{2}]-lamprey GLP-1-Lys^{31}gamma-glutamyl-pal, 3. [D-Ser^{2}]-paddlefish glucagon-Lys^{30}-gamma-glutamyl-pal and 4. [D-Ala^{2}]-paddlefish GLP-1-Lys^{28}gamma-glutamyl-pal) were purchased from Synpeptide Co. Ltd. (Shanghai, China). The fish analogues contained a substitution of either L-Ser for D-Ser or L-Ala for D-Ala at the position 2. Additionally, a gamma-glutamyl with palmitate adjunct was added to the side-chains of the lysine residues. The remaining synthetic peptides: human glucagon, human GLP-1, human oxyntomodulin, human GIP, liraglutide and trout GLP-1 were obtained from Synpeptide Co. Ltd. (Shanghai, China) at >95% purity which was confirmed by reversed-phase HPLC and MALDI-TOF. All crude peptides were purified to > 98% homogeneity by reversed-phase HPLC, and their structures were confirmed by MALDI-TOF.

2.2 Purification and characterisation of peptides

2.2.1 Reversed-phase high-performance liquid chromatography (RP-HPLC) purification of crude peptides

HPLC purification of native fish proglucagon-derived peptides and exendin-4 was performed using HPLC Spectra System Instrument containing Manual Dual Mode Sample injector, P2000 binary pump, UV 1000 detector and vacuum membrane degasser (Thermo Separation Products, Inc. New Jersey, USA). The chromatogram was generated using a BD 12E dual channel compact flatbed chart recorder (Kipp&Zonen Delf, Netherlands). Crude native fish peptides and exendin-4 were dissolved in 15% – 35% of acetonitrile (3mg/ml), depending on hydrophobicity and injected into a (2.2 cm x 25 cm) Vydac 218TP1022 (C18) column (Grace, Deerfield, IL, USA) equilibrated with 21% – 35% acetonitrile and 0.1% TFA/water. The program run was adjusted to each individual peptide, raising the concentration of acetonitrile in eluting solvent from 21% – 35% to 56% – 70% over 50 min using a linear gradient. Absorbance was measured at 214 nm, and the flow rate was 6 ml/min.

Purification of fish peptide analogues, [D-Ser^2]-lamprey glucagon-Lys^{30}gamma-glutamyl-pal, [D-Ala^2]-lamprey GLP-1-Lys^{31}gamma-glutamyl-pal, [D-Ser^2]-paddlefish glucagon-Lys^{30}-gamma-glutamyl-pal and [D-Ala^2]-paddlefish GLP-1-Lys^{28}gamma-glutamyl-pal, was performed using the Thermo Scientific Surveyor Plus HPLC System controlled by PC-based ChromQuest 5.0 data system (Thermo Fisher Scientific Inc. Waltham, Massachusetts, USA). The instrument system contained Manual Dual Mode Sample injector, Quaternary Low-Pressure Surveyor LC Pump with a built-in Vacuum Degasser and Surveyor UV/Vis Plus Detector. Peptides were dissolved in 15% acetonitrile (3mg/ml) injected onto a (2.2 cm x 25 cm) Vydac

218TP1022 (C18) column (Grace, Deerfield, IL, USA) equilibrated with 0.12% TFA/water. The concentration of acetonitrile in the eluting solvent from 0% to 35% over 10 min and from 35% – 70% over 50 min using a linear gradient. Absorbance was measured at 214 nm, and the flow rate was 6 ml/min. The peaks were collected manually into 15 ml Falcon^{tm} conical centrifuge tubes (Fisher Scientific, Loughnorough, UK). Acetonitrile was removed using vacuum concentrator SPD2010 (Integrated SpeedVac Systems, MA, USA) set to 45^{o}C, 5.1 Torr/min for 2 hours.

The purity of purified preparatius of the crude peptides as well as those that were received already at a purity of >95%, was confirmed by Luna 5u C8 250x4.6mm column and MALDI-TOF MS.

2.2.2 Confirmation of molecular masses using matrix-assisted laser desorption ionisation time-of-flight (MALDI-TOF) MS

The molecular masses of the purified crude peptides were confirmed by MALDI-TOF MS using Voyager-DE Biospectrometry Workstation (PerSpective Biosystems, Framingham, Massachusetts, USA). The instrument was calibrated with the reference compounds (internal standards) in the same spectrum as the tested peptide samples. Each peptide HPLC fraction was mixed (1:1 ratio) to matrix consisting of α-CHCA (10mg/ml in 50:50 acetonitrile/0.1%TFA (aq.). The sample/matrix solution (1.5µl) was placed on an appropriate position of the 100-well stainless-steel sample plate and allowed to dry at room temperature to obtain the maximum hydrophobic effect. The mass of the samples was obtained by measuring the mass-to-charge ratio (m/z) against signal intensity and compared with the theoretical masses of the peptides.

2.3 Enzymatic degradation of proglucagon-derived peptides and their analogues

2.3.1. DPP-4 and plasma degradation of fish peptides and peptide analogues

Peptides (30 µg or 100 µg depending on the experiment) were incubated in 50mM/l TEA-HCl buffer (pH 7. 8) with purified porcine DPP-IV (5 mU) or mouse plasma for 0 and 4 h on an orbital shaker at 37 °C. The reaction was terminated with 10% TFA (aq.), and the samples were stored at -20 °C. HPLC degradation was performed on the Thermo Scientific Surveyor Plus HPLC System controlled by PC-based ChromQuest 5.0 data system (Thermo Fisher Scientific Inc. Waltham, Massachusetts, USA) with a Luna 5u C8 250x4.6mm column using various linear gradients, depending on the hydrophobicity of the peptides/analogues. For the native fish peptides and human glucagon, GLP-1 and GIP the concentration of acetonitrile in the eluting solvent was raised from 0% to 42% (over 50 min), from 42% to 70% (over 10 min) for the total run time of 60 min. For the fish peptide analogues concentration of acetonitrile in the eluting solvent was raised from 0% to 35% (over 10 min), from 35% to 42% (over 20 min), from 42 to 70% (over 5 min), and 70% (over 25 min) for the total run time of 60 min. Absorbance was measured at 214nm, and the flow rate was set to 1.0 ml/min.

2.3.2 Conformation of molecular masses using matrix-assisted laser desorption ionisation time-of-flight (MALDI-TOF) MS

The molecular masses of the HPLC fractions of intact peptides and peptide fragments were identified by MALDI-TOF MS as previously described in Section 2.2.2.

2.3.3 Calculation of the intact peptide percentage

Percentage of the intact peptide was calculated from the peak area under the curve data generated by the Thermo Scientific Surveyor Plus HPLC System controlled by a PC-based ChromQuest 5.0 data system.

2.4 Cell culture

2.4.1 Culturing BRIN-BD11 and 1.1B4 cells

BRIN-BD11 rat clonal β-cells and 1.1B4 human-derived pancreatic β-cells are two different insulin-secreting cell lines. BRIN-BD11 cell line was produced by electrofusion of RINm5f cells with New England Deaconess Hospital rat pancreatic islet cells (McClenaghan *et al.,* 1996), whereas 1.1B4 was generated by electrofusion of freshly isolated human pancreatic beta cells and PANC-1, an immortal human ductal epithelial cell line (McCluskey *et al.,* 2011). The cell lines (approximately $1x10^6$) were stored in the cryopreservation store in 2ml screw-cap plastic cryogenic vials (Sterilin Limited, Hounslow, UK) in vapour phase liquid nitrogen below -135 ^{0}C maintained at Ulster University, Coleraine. The freezing medium contained 10% sterilised DMSO, 10% RPMI-1640 medium and 80% FBS.

Cryogenic vials were removed from liquid nitrogen tank, quickly embedded onto crushed ice and thawed rapidly using hand heat and water bath set at 37^{0}C to prevent crystal formation. Using aseptic techniques in a Vertical Laminar Airflow hood, the cell suspension was transferred into 15 ml Falcon^{tm} conical centrifuge tubes and 10 ml of pre-warmed RPMI-1640 medium supplemented with 10% (v/v) FBS and 1% (v/v) antibiotics – penicillin (100 U/ml) and streptomycin (0.1 mg/l) was diluted slowly, with continual swirling, into the cells to avoid osmotic shock. The cell suspension was

then centrifuged at 900 rpm for 5 min. After decanting of the supernatant, fresh 10 ml pre-warmed RPMI-1640 medium (supplemented as previously described) was added to the cell pellet which was then homogenously resuspended and transferred into a sterile 75 cm^2 tissue culture flask (Nunc, Roskilde, Denmark). Additional 15 ml of pre-warmed medium was added into the tissue flask prior to incubation at 37 °C, 5% CO_2 and 95% air (LEEC secure CO_2 incubator, LEEC, Nottingham) to allow the cells to adhere to the tissue flask wall and develop monolayers with the epithelioid characteristic. For passaging the cells, media was removed from the tissue flask containing adherent cells which were then washed with 10 ml HBSS solution (diluted to1X concentration using purified water) prior to dissociation with 3 ml of trypsin (diluted to 1X concentration using 1X HBSS) and incubated for 3-4 minutes at 37 °C. Fresh media (10ml) was added to the detached cells to inhibit the action of trypsin. The cell suspension was transferred into 25 ml universal tube and centrifuged at 900 rpm for 5 min. The supernatant was removed, and the pellet was resuspended in pre-warmed fresh medium (25-30ml). Assessment of cell viability was performed by mixing 100 µl of the cell suspension with 100 µl of 0.4% trypan blue dye in a 0.5 ml Eppendorf Safe-Lock microcentrifuge tube (Sigma-Aldrich, Pool, UK) prior loading the sample in the Neubauer haemocytometer chamber. The number of viable cells exhibiting unstained and bright appearance due to intact membranes was then determined for further analysis. To maintain the cells, 1 ml of cell suspension was transferred back to the flask with the addition of 25 ml of pre-warmed medium and stored in the incubator. BRIN-BD11 cells used in the experiments had passages between 16 and 35. For 1.1B4 cells, the passage was between 25 and 40.

2.4.2 Culturing of Chinese Hamster Lung (CHL) and Human Embryonic Kidney (HEK293) receptor transfected cell lines

CHL cells transfected with GLP-1 receptor (Thorens et al., 1993) and HEK293 cells transfected with glucagon receptor (Ikegami et al., 2001) were stored in the cryopreservation store in 2 ml cryogenic vials (approximately $1x10^6$/vial) in vapour phase liquid nitrogen below 135^0C maintained at Ulster University, Coleraine. The freezing medium contained 10% sterilized DMSO, 10% DMEM tissue culture medium and 80% FBS.

The transfected cells were cultured as described for BRIN-BD11 and 1.1B4 cells (Section 2.4.1) with the exception that the DMEM medium supplemented with 10% (v/v) FBS and 1% (v/v) antibiotics – penicillin (100 U/ml), streptomycin (0.1 mg/l) and gentamycin (0.1 mg/ml) was used instead of RPMI-1640. CHL cells passages were between 58 and 65 for GLP-1 receptor transfected cells and between 15 and 16 for GIP receptor transfected cells. For HEK293 the passage was between 12 and 14.

2.4.3 Culturing of wild-type INS-1 832/3 rat clonal pancreatic β-cells and CRISPR/Cas9-engineered cells with knock-out of the GLP-1 receptor (GLP1R KO), glucagon receptor (GCGR KO) and GIP receptor (GIPR KO)

Wild-type INS-1 832/3 rat clonal pancreatic β-cells and CRISPR/Cas9-engineered cells with the knock-out of the GLP-1 receptor (GLP1R KO), GIP receptor (GIPR KO) (Naylor et al., 2016) and glucagon receptor (GCGR KO) (generated in our laboratory) were stored and cultured as described for BRIN-BD11 cells (Section 2.4.1) with the addition of 1 mM sodium pyruvate and 50 mM 2-mercaptoethanol to the medium. Wild-type cells used in the experiment were between passages between 55

and 60. The passage was between 17 and 25 for GLP1R KO cells; between 18 and 25 for GIPR KO cells; and between 44 and 50 for GCGR KO cells.

2.5 *In vitro* insulinotropic activity studies

2.5.1 Insulin release studies using BRIN-BD11 cells

The cells were cultured, detached from the cell flask and counted as previously described (Section 2.4.1). The cells were seeded (150,000 cells/well) into 24-well plates (Nunc, Roskilde, Denmark) and allowed to attach overnight at 37 °C, 5% CO_2, and 95% air. The culture medium was replaced with the Krebs-Ringer Bicarbonate (KRB) buffer (115 mM NaCl, 4.7 mM KCl, 1.28 mM $CaCl_2.2H_2O$, 1.2 mM KH_2PO_4, 1.2 mM $MgSO_4.7H_2O$, 20 mM HEPES and 25 mM $NaHCO_3$) supplemented with 1.1 mM D-glucose and 0.5% (w/v) BSA (pH 7.4) and the cells were pre-incubated for 40 min at 37 °C. The buffer was then removed, and the cells were incubated for 20 min at 37 °C with the test solutions containing KRB buffer supplemented with 5.6 mM D-glucose, 0.5% (w/v) BSA (pH 7.4) and test peptides at a concentration from 0 to 3μM. After the incubation the test solutions were collected into 3.5-ml plastic tubes and stored at -20 °C before measuring the insulin concentration by radioimmunoassay.

2.5.2 Receptor antagonist studies using BRIN-BD11 cells

The cells were seeded and pre-incubated as previously described (Section 2.5.1). The cells were incubated for 20 min at 37 °C with the test solution containing KRB buffer supplemented with 5.6 mM D-glucose, 0.5% (w/v) BSA (pH 7.4) and 0.1 μM of peptides alone or in the presence of 1 μM of either exendin-4 (9-39) (GLP-1 receptor antagonist), GIP(6-30)Cex-K40[Pal] (GIP receptor antagonist) or des-His1,Pro4-Glu9-glucagon amide (glucagon receptor antagonist). After the incubation the test

solutions were collected into 3.5-ml plastic tubes and stored at -20 °C before measuring the insulin concentration by radioimmunoassay.

2.5.3 Insulin release studies using 1.1B4 cells

The cells were cultured, detached from the cell flask and counted as previously described (Section 2.4.1). The cells were seeded (150,000 cells/well) into 24-well plates (Nunc, Roskilde, Denmark) and allowed to attach overnight at 37 °C, 5% CO_2, and 95% air. The culture medium was replaced with the Krebs-Ringer Bicarbonate KRB buffer supplemented with 1.4 mM D-glucose and 0.5% (w/v) BSA (pH 7.4). The cells were pre-incubated for 40 min at 37 °C. The buffer was then removed, and the cells were incubated for 20 min at 37 °C with the test solutions containing KRB buffer supplemented with 16.7 mM D-glucose, 0.5% (w/v) BSA (pH 7.4), and 10 nM or 1μM test peptide. Samples were stored at −20 °C prior to the insulin release determination by radioimmunoassay.

2.5.4 Insulin release studies using receptor knockout cells

The cells were cultured, detached from the cell flask and counted as previously described (Section 2.4.1). The cells were seeded (150,000 cells/well) into 24-well plates (Nunc, Roskilde, Denmark) and allowed to attach overnight at 37 °C, 5% CO_2, and 95% air. The culture medium was replaced with the Krebs-Ringer Bicarbonate KRB buffer supplemented with 1.1 mM D-glucose and 0.5% (w/v) BSA (pH 7.4). The cells were pre-incubated for 40 min at 37 °C. The buffer was then removed, and the cells were incubated for 20 min at 37 °C with the test solutions containing KRB buffer supplemented with 5.6 mM D-glucose, 0.5% (w/v) BSA (pH 7.4), and 10 nM or 1μM test peptide. Samples were stored at -20 °C prior the insulin release analysis by radioimmunoassay Section 2.5.7).

2.5.5 Insulin-release and insulin content studies using mouse islets

2.5.5.1 Isolation of pancreatic islets

All procedures were performed by following the rules and regulations of the UK Animals (Scientific Procedures) Act 1986. Pancreatic islets were isolated from adult NIH Swiss mice and processed by the collagenase digestion method (Lacy et., al 1967). Animals were sacrificed by cervical dislocation immediately before harvest. The pancreas was carefully removed from the abdominal cavity and placed in an ice-cold collagenase solution (5ml/pancreas) containing Collagenase P (1.4mg/ml) in HBSS buffer (8 g/l NaCl, 0.4 g/l KCl, 0.14 g/l $CaCl_2$, 0.1 g/l $MgSO_4.7H_2O$, 0.1 g/l $MgCl_2.6H2O$, 0.06 g/l $Na_2HPO_4.H_2O$, 0.006 g/l, KH_2PO_4, 1 g/l glucose, 0.02 g/l phenol red, 0.35 g/l $NaHCO_3$). The pancreas was then chopped into small pieces in the collagenase solution and placed in the water bath at for 10 min at 37 °C to aid the digestion. Series of washing steps were performed using an ice-cold collagenase-free HBSS buffer supplemented with 0.1% BSA. The supernatant was removed after centrifugation at 1200 rpm for 2 min repeated two times. Fresh wash buffer was added to evenly distribute the pellet which was then filtered through a strainer to separate any debris, and the sample was centrifuged at 1200 rpm for 2 min. After the supernatant was discarded, approximately 10 ml of pre-warmed RPMI-1640 medium supplemented with 10% (v/v) FBS and 1% (v/v) antibiotics – penicillin (100 U/ml) and streptomycin (0.1 mg/l) was added to the pellet and evenly distributed onto a petri dish with additional 15 ml of media. The islets were cultured for 48 h at 37 °C, 5% CO_2 and 95% air before an acute study of insulin release and insulin content.

2.5.5.2 Acute insulin release studies from isolated mouse islets

Pancreatic islets were isolated from adult NIH Swiss mice and digested with collagenase P obtained from *Clostridium histolyticum* as previously described (Section 2.5.5.1). The islets were cultured for 48 h at 37 °C, 5% CO_2 and 95% air and carefully transferred into a 1.5 ml Eppendorf tube (10 islets/tube) and centrifuged at 1200 rpm for 5 min to remove any remaining media. The cells were pre-incubated with KRB buffer (pH 7.4) supplemented with 0.5% BSA and 1.4 mM glucose (500µl/tube) for 60 min at 37 ◦C. The samples were centrifuged at 1200 rpm for 5 min and the supernatant was replaced with the test solutions (500µl/tube) containing KRB buffer (pH 7.4) supplemented with 0.5% BSA and 16.7 mM glucose, and the test peptides (1µM or 10 nM) for the 60 min incubation at 37◦C followed by centrifugation at 1200 rpm for 5 min. The test solutions were then collected into 2.5 ml tubes and stored at -20 ◦C for insulin release determination by radioimmunoassay.

2.5.5.3 Determination of islet insulin content

Islets were isolated, incubated and treated with the test solutions as described in Section 2.5.5.1 and Section 2.5.5.2. Insulin content of islets was determined using the acid ethanol method (Otani et al., 2003). Following the incubation and centrifugation steps, the test solutions were collected from the treated islets for the insulin release determination and the pellets containing islets were incubated overnight at 4 °C with an acid–ethanol solution containing 75% ethanol, 23.5% H_2O and 1.5% HCl (500µl/tube) to extract cellular insulin content. The samples were then centrifuged at 1200 rpm for 2 min at 4 °C to remove any cell debris. The supernatant was aliquoted into fresh tubes and stored at -20 °C for measuring insulin content by radioimmunoassay.

2.5.6 Iodination of insulin

Chlorine-containing compound, 1,3,4,6-tetrachloro-3α,6α-diphenyl glycoluril, trade name Iodogen, was used for iodination of bovine insulin. This method of iodination was firstly proposed by Fraker and Speck in 1978.

Iodogen (2mg) was added to 10 ml of dichloromethane. The prepared solution was aliquoted into 1.5 ml Eppendorf tubes (200µl/tube) and allowed to evaporate in the water bath for 5 min at 37 °C for to pre-coat the insoluble iodogen onto the surface of the reaction vessel. Insulin solution containing bovine insulin (1mg/ml in 10 mM HCl) was diluted (1:8) to 125 µg/ml in 500 mM phosphate buffer (pH 7). Procedures involving reaction mixture preparation were carried out in a fume hood situated in the specifically designed RIA premises. 20 µl of bovine insulin (125 µg/ml) and 5 µl of sodium iodide ($Na^{125}I$ 100 mCi/ml) were added into the reaction tubes coated with iodogen. The reaction tubes were placed into an ice-box for 15 min with gentle agitation every 3 min. The sample was transferred from the reaction vessel to a fresh tube, and 50 mM sodium phosphate buffer (500µl/tube) was added to the sample to terminate iodide oxidation.

^{125}I-bovine insulin was then purified from the unbound sodium iodide ($Na^{125}I$) using RP HPLC instrument (LKB Bromma, Sweden). The reaction mixture was injected into a Vydac C-8 (4.6 x 250 mm) analytical HPLC column equilibrated with 0.12% TFA/water. The concentration rate of acetonitrile in the eluting solvent was raised from 0% to 56% over 10 min and from 56% to 70% over 10 min at a flow rate of 1 ml/min. The fractions (1ml each) were collected over 67 min of HPLC run using the fraction collector (Frac-100, LKB) set to 1-min intervals (Figure 1.1).

5 µl aliquots of each fraction were checked for radioactivity using the gamma counter (Wizard™ 1470 automatic gamma counter, Perkin Elmer, USA). The fractions with the highest counts per minute were diluted (1:1) with working RIA buffer. The binding test was carried out using various antibody dilutions (1:25,000, 1:35,000, 1:45,000) to identify and pool together the fractions with appropriate binding ability. The ^{125}I-bovine insulin was then stored at 4 °C.

2.5.7 Insulin radioimmunoassay (RIA)

Insulin concentration was measured by the dextran-coated charcoal radioimmunoassay (RIA) method (Albano et al., 1972; Flatt and Bailey 1981), using crystalline rat insulin as a standard. All procedures involved in RIA required pre-assay preparation. RIA buffer was prepared by adjusting the pH of a basic solution, containing 40 mM disodium hydrogen orthophosphate, 0.2 g/l thimerosal and 3 g/l NaCl, to 7.4 by adding an acidic solution containing 40 mM sodium dihydrogen orthophosphate. Insulin standards were prepared in RIA buffer (supplemented with 0.5% BSA) by making serial dilutions of insulin standard ranging either from 20 ng to 0.039 ng/ml (rat) or from 5 ng /ml to 0.009 ng/ml (human) depending on the experiment. The standards and unknown samples were aliquoted in triplicates and duplicated respectively (200µl/tube). Guinea pig anti-porcine antibody was diluted in a RIA buffer supplemented with 0.5% BSA. The dilution of antibodies was selected within the range varying from 1:25,000 to 1:45,000 depending on the binding ability of the appropriate radiolabelled insulin stock. The antibody solution was added (100µl/tube) to the standards and the unknown samples. Radiolabelled insulin was diluted in the RIA buffer supplemented with 0.5% BSA to achieve ~10,000 counts per minute (CPM) for every 100 µl of the buffer solution which was then distributed to

each tube containing the standards and the unknown samples. In addition to the various insulin concentration, the standard set included triplicates of the tubes for the total count identification (containing 100µl of the radioactive label solution alone), tubes for the nonspecific binding measurement (300 µl of assay buffer and 100 µl of the radioactive label solution), and tubes with the zero standards (containing assay buffer, antibody solution and radioactive label solution (100 µl each)). The sample tubes loaded with the reaction mixture were then incubated at 4 °C for 48. Stock dextran-coated charcoal (DCC) containing 50 g of activated charcoal and 5 g dextran T 70 dissolved in 1 litre of 40 Mm sodium phosphate buffer was further diluted with the same buffer (1:4) to prepare working DCC which was stirred for 30 min before use. Woking DCC was distributed into the reaction mixture tubes (1ml/tube) except for the standard triplicate containing 100µl of the radioactive label solution only. The samples were incubated for 20 min at 4 °C and centrifuged (Model J-6B centrifuge, Beckman Instruments Inc., UK) at 2500 rpm for 20 min. After the centrifugation supernatant was decanted. The pellet contained charcoal bound to free radiolabelled insulin the amount of which was measured in the gamma counter against the known standard values of insulin concentration using a spine fitting algorithm.

2.6 Adenosine 3'5'-cyclic monophosphate (cAMP) production studies using transfected cell lines

2.6.1 Preparation of cell lysate

Chinese hamster lung (CHL) cells transfected with the human GLP-1 receptor (GLP-1R) and human embryonic kidney (HEK293) cells transfected with the human glucagon receptor (CGCR) were used to assess effects of peptides on cAMP production. Cells were cultured as previously described (Section 2.4.2). The cells were

seeded (75,000 cells per well) into 24-well plates and incubated for 21 hours at 37 °C in an atmosphere of 5% CO_2 and 95% air to form monolayers. The cells were then pre-incubated for 40 minutes with KRB buffer supplemented with 0.1% BSA and 1.1 mM glucose, before incubation with test peptides (10 nM and 1μM) in the presence of 200 μM 3-isobutyl-1-methylxanthine (IBMX) for 60 min at 37°C. After incubation, the medium was removed, and cells were washed with cold 0.9% phosphate-buffered saline (PBS) buffer tree times. The cells were then lysed (200 μl/well) with the cell lysis buffer diluted (1:5) with water (R&D Systems, Abingdon, UK) before measurement of cAMP using a Parameter cAMP assay kit (R&D Systems, Abingdon, UK).

2.6.2 Measuring of cAMP

According to the manufacturer's instructions, a 96-well goat anti-mouse microplate was incubated primary antibody solution (50μl/well), except the non-specific binding (NSB) wells, for 60 min at room temperature on a horizontal orbital microplate shaker set at 500 rpm ± 50 rpm. After the incubation, the plate was washed four times with assay wash buffer (400μl/well). A cAMP Conjugate solution was added to the wells (50 μl/well). The standards and the unknown samples were added to the 96-well plate (100 μl/well) within 15 minutes of addition of the cAMP Conjugate. The standard was made using 100 μl of the standard stock (2400 p/mol) dissolved in the cell lysis buffer. Serial dilutions were prepared from 240 p/mol to 3.75 p/mol. The plate was incubated for 2 hours at room temperature on the shaker. After the incubation, the four-wash step was repeated. Substrate Solution was added to the wells (200 μl/well) and incubated for 30 min at room temperature on the bench top (protected from light). 100 μL of Stop Solution was added to each well changing the colour in the wells from blue to

yellow. The optical density of each well was measured within 30 minutes, using a microplate reader set to 450 nm and 540 nm. The wavelength was corrected by subtracting 540 nm reading from the readings measured at 450 nm. The cAMP concentration of unknown samples was determined using the standard curve with known values created by plotting the mean absorbance for each standard on a linear y-axis against the concentration on a logarithmic x-axis in Prism 5 program. A typical cAMP curve is shown in Figure 1.2.

2.7 Apoptosis and cell proliferation study

2.7.1 Analysis of apoptosis using TUNEL assay

BRIN-BD11 cells were cultured, harvested and counted as previously described (Section 2.4.1). The cells were carefully seeded onto sterile round glass coverslips inserted inside of the wells of a 12-well plate (4000 cells/well). The cells were treated with cytokine mixture (containing 200 U tumour-necrosis factor-α, 20 U interferon-γ and 100 U interleukin-1β dissolved in RPMI-1640 media) in the presence and absence of test peptides (10nM and 1 μM) and incubated for 20 hours at 37 °C. After the incubation, the test solutions were removed, and the cells were washed in PBS. The cells were fixed with 4% paraformaldehyde and treated with 0.1 M sodium citrate buffer (pH 6.0) in a water bath at 94 °C for 20. The plates were then allowed to cool on the bench for 20 min. using *In situ* Cell Death Detection Kit (Roche Diagnostics, Burgess Hill, UK) following the manufacturer's instruction. After the buffer was removed, the *In situ* Cell Death Detection Kit (Roche Diagnostics, Burgess Hill, UK) was used to investigate the positive protective effects of peptides from the DNA damage caused by cytokines. After the sodium citrate buffer was removed, the TUNEL reaction mixture from the kit was added to the wells (50 μl/well) and

incubated for 60 min at 37 °C (protected from light) according to the manufacturer's instruction. The wells were then washed with PBS three times for 5 minute. Each cover glass with fixed treated cells was removed from the wells and mounted on the slide with a drop of a mounting solution containing 1:1 glycerol/PBS (2 over glass/slide). The slides were analysed using the 488 nm filter of the fluorescent microscope containing a DP70 camera adapter system controlled by Multi-fluorescence imaging system Cell ^ F (Olympus System Microscope; model BX51, Southend-on-Sea, UK).

2.7.2 Assessment of cell proliferation

BRIN-BD11 cells were seeded, incubated with the test peptides, fixed with paraformaldehyde and treated with sodium citrate buffer as previously described (Section 2.7.1). The cells were washed with Ki-67 primary antibody (Abcam, Cambridge, UK). The cells were treated with 1.1% BSA (300 µl/well) for 30 min at room temperature before incubation with Ki-67 primary antibody (Abcam, Cambridge, UK) for 2 hours at 37 °C. The cells were then washed three times with PBS for 5 min and treated with Alexa Fluor 594 secondary antibody (Abcam. Cambridge, UK). The slides were mounted as previously described (Section 2.7.1) and analysed (~150 cells/replicate) with the 594nm filter using the fluorescent microscope.

2.8 *In vivo* studies

All *in vivo* studies were carried out in the Biomedical and Behavioural Research Unit (BBRU) at Ulster University in accordance with the UK Animals (Scientific Procedures) Act 1986 and EU Directive 2010/63EU and approved by Ulster University Animal Ethics Review Committee. The mice were age-matched and housed individually in a group of 6-8 animals (depending on the experimental

protocol) under controlled laboratory environment (12:12 light/darkness cycle, 22±2ºC).

2.8.1 Animal models

2.8.1.1 Standard diet normal National Institute of Health (NIH) Swiss mice

Acute *in vivo* studies were carried out using 8-12 week-old male National Institutes of Health (NIH) Swiss mice (Envigo, Huntingdon, UK). Animals had free access to drinking water and standard laboratory chow (10% fat, 30% protein, 60% carbohydrate; percentage of total energy 12.99 KJ/g; Trouw Nutrition, Cheshire, UK). For food consumption studies mice were readily trained to have a time-restricted 3-hour feeding at a specific time every day (free access to food was given from 10 am to 1 pm every day)

2.8.1.2 High-fat fed mice

A 21-day peptide treatment *in vivo* experiment was performed using 8-12 week-old male TO mice (Envigo, Huntingdon, UK). Free access to water and high chow (45% fat, 20% protein, and 35% carbohydrate (total energy, 26.15 KJ/g; composition: casein, 26.533; choline bitartrate, 0.296; L-cystine, 0.399; lard, 17.895; rice starch, 28.344; cellulose, 6.171; soya oil, 4.319; sucrose, 10.490; mineral mix, 4.319; and vitamin mix, 1.234; Special Diets Service, Essex, UK) was provided for at least 3 month prior to the start of experiments to develop dietary-induced type 2 diabetes animal model with increased beta-cell loss. The body weight and glucose parameters were monitored regularly. High-fat diet triggered weight gain, hyperglycaemia and insulin resistance in mice which started to display the characteristics of obesity. The

animals selected and allocated into groups with matching average body weights and blood glucose levels prior to starting the experiment.

2.8.1.3 Glu-CreRosa26-YFP mouse model

An 11-day peptide treatment study was performed using 10-14 week-old female GluCreRosa26-YFP hybrid transgenic mice (Quoix et al 2007) which express the enhanced yellow fluorescent protein EYFP in alpha cells of the pancreatic islets. The animals were housed individually and had free access to drinking water standard laboratory chow (10% fat, 30% protein, 60% carbohydrate; percentage of total energy 12.99 KJ/g; Trouw Nutrition, Cheshire, UK). Prior starting of the experiment, tamoxifen (approximately 32mg/kg body weight, dissolved in corn oil) was injected (i.p.) to induce recombination. The animals were monitored for any adverse reaction during the 4-day post-injection wait period. Streptozotocin was administrated to overnight fasted mice (50mg/kg dissolved in 7.5 mg/ml citrate buffer, pH 4.5) on each day during a pre-treatment period for subsequent five days. Animals were monitored for hyperglycaemia for further 10 days. The female mice appeared to be resistant to streptozotocin, so an additional 100 mg/kg of streptozotocin was administrated twice within the next 3 weeks before the animals started to show elevated blood glucose levels. Once diabetes was established, the animals were selected and allocated into groups with matching average body weights and blood glucose levels prior starting experiments.

2.8.2 Acute in vivo studies

2.8.2.1 Intraperitoneal glucose tolerance test (IGTT)

Normal male NIH Swiss mice (8-12 week-old) National Institutes of Health (NIH) Swiss mice were housed and grouped as previously described (Section 2.8 and

2.8.1.1). The animals were fasted overnight before an intraperitoneal injection of either glucose (18 mmol/kg body weight) alone or in the presence of peptide (25 or 75 nmol/kg body weight). Blood samples were collected from the tail vein and measured as described in Section 2.8.2.5

2.8.2.2 Oral glucose tolerance test (OGTT)

Normal male NIH Swiss mice (8-12 week-old) National Institutes of Health (NIH) Swiss mice were housed as previously described (Section 2.8 and 2.8.1.1). The test peptides used are shown in Tables 2.3 – 2.7. The animals were fasted overnight before an oral administration (gavage) of glucose (18 mmol/kg body weight) alone or in the presence of peptide (25, 75 or 100 nmol/kg body weight depending on the experiment). Blood samples were collected from the tail vein and measured as described in Section 2.8.2.5

2.8.2.3 Acute duration of action studies

Normal male NIH Swiss mice (8-12 week-old) National Institutes of Health (NIH) Swiss mice were housed as previously described (Section 2.8 and 2.8.1.1). Animals (overnight fasted) received intraperitoneal injection of saline solution (containing 9 g/l (w/v) NaCl) or peptides (25 nmol/kg body weight) dissolved in saline solution two or/and four hours (depending on the experiment) prior to intraperitoneal administration of glucose load (18 mmol/kg body weight). Blood samples were collected from the tail vein and measured at 15, 30 and 60 min post glucose injection as described in Section 2.8.2.5

2.8.2.4 Acute food consumption studies

Normal male TO mice (8-12 week-old) were housed as previously described (Section 2.8 and Section 2.8.1.1). The animals were trained to have a free access to food from 10 am to 1 pm every day. On the day of the experiment at 10 am fasting mice were administrated intraperitoneal injections of either saline solution or peptides (25, 50 or 75 nmol/kg body weight depending on the experiment) and sumitenioisly received pellets of food of known weight. Food weight was recorded over time points of 0, 30, 60, 90, 120, 150 and 180 min (or up to 300 min depending on the experiment). Consumption of water was not restricted in this experiment.

2.8.2.5 Measuring blood glucose and plasma insulin

For IGTT/OGTT *in vivo* studies, blood was obtained from the tail vein before and after peptide administration at different time points: 0, 15, 30 and 60 min to measure glucose concentration using the Ascenacia Counter Blood Glucose Meter (Bayer, Newbury, UK). While measuring glucose parameters, blood was simultaneously collected into heparinised microcentrifuge tubes (Sarstedt, Germany) which were then centrifuged at 13000 rpm at 4ºC for 5 min. Plasma was stored at -20ºC before measuring insulin by RIA (Section 2.5.7).

2.8.3 Long-term in vivo studies using high fat-fed mice

2.8.3.1 Treatment design and monitoring

High fat-fed mice were were housed and grouped as previously described (Section 2.8 and Section +2.8.1.2). The test peptides used are shown in Table 2.5 and 2.6. Animals received twice daily intraperitoneal injections saline solution for three days prior to administration of saline or peptides (25 nmol/kg of body weight) twice daily (09:30

and 17:00 h) over 21 days treatment period. Non-fasting blood glucose, food intake, water intake, body weight, and insulin concentrations were monitored at 3-day intervals at 9 am prior to daily injection of test peptides. Blood was obtained from the tail vein to measure glucose parameters using the glucose meter. For measuring insulin concentration, blood was simultaneously collected into heparinised microcentrifuge tubes (Sarstedt, Germany) which were then centrifuged at 13000 rpm at 4^{o}C for 5 min. Plasma was stored at -20^{o}C prior to insulin radioimmunoassay.

2.8.3.2 Assessment of IGTT and OGTT

After the 21-day study intraperitoneal and oral glucose tolerance were performed. Animals were fasted overnight before intraperitoneal administration or oral gavage of glucose (18 mmol/kg body weight). Blood was obtained from the tail vein before and after glucose administration at different time points: 0, 15, 30, 60, 90 and 120 min to measure glucose concentration using the glucose meter. Plasma was collected and analysed as described previously (Section 2.8.2.5).

2.8.3.3 Assessment of insulin sensitivity

Blood was obtained from the tail vein of non-fasted mice to measure glucose concentration prior to intraperitoneal administration of insulin (50 U/kg body weight). Blood glucose was then measured at 15 and 60 time points after receiving the insulin. Insulin sensitivity was also calculated using the homeostatic model assessment (HOMA) formula:

HOMA-IR = fasting blood glucose x fasting plasma insulin/22.5

HOMA-β = 20 × fasting insulin (μIU/ml)/fasting glucose (mmol/ml) − 3.5

Fasting blood glucose and fasting plasma insulin were obtained as previously described (Section 2.8.3.2).

2.8.3.4 Assessment of body composition by mouse densitometer dual-energy X-ray absorptiometry

Bone mineral density (BMC in gm/cm^2) and body tissue composition of the treated animals were calculated using a Lunar PIXImus DEXA system (Lunar Gorp, Madison, Wisconsin) controlled by integrated computer Software 1.4X. DEXA uses an X-ray generator to produce a beam spanning over a broad spectrum of energy levels. Two distinct energy peaks are then generated by filtering the photon output which results in the separation of bone from soft tissue (Bonnick et al., 2013).The instrument was calibrated with the DEXA phantom control that was placed in the beam path according to the manufacturer's protocol. Animals were sacrificed by cervical dislocation and positioned dorsoventrally on the sticky specimen tray (with heads placed in the tray headset) under the PIXImus beam path. The data was analysed by Lunar Software version 2.0.

2.8.3.5 Terminal blood collection and tissue excision

At the end of the experimental period, terminal non-fasted blood was collected from the tail vein into heparinised microcentrifuge tubes (Sarstedt, Germany) to measure biochemical parameters. Blood tubes which were then centrifuged at 13000 rpm at 4^{o}C for 5 min. Plasma was stored at -20^{o}C until the commencement of assays. Animals were sacrificed by cervical dislocation. A dissection kit was used to open the abdominal cavity and dissect pancreatic tissue. The pancreas was processed for islet isolation (Section 2.5.5.1) and histological investigation (Section 2.13.1). For hormonal content studies, the dissected tissue was covered in aluminium foil and

frozen in a liquid nitrogen container to transport the samples to the -70°C freezer for storage.

2.8.3.6 Islet studies using pancreas from the 21-day treated animals

Pancreatic islets were isolated, cultured and pre-incubated as previously described (Section 2.5.5.1 and Section 2.5.5.2) following the 60-min pre-incubation with 1.4 mM glucose, the samples were centrifuged at 1200 rpm for 5 min. The supernatant was replaced with KRB buffer (500µl/tube) supplemented with 0.5% BSA and 16.7 mM glucose and the test agents (10mM alanine, 20mM KCl, 10mM arginine, 1µM human GLP-1 or 1µM human GIP). Tubes were incubated for 60 min at 37°C followed by centrifugation at 1200 rpm for 5 min. The supernatant was then collected into 2.5 ml test tubes and stored at -20 °C for insulin release determination by radioimmunoassay. The remaining islets were collected from the Petri plate and stored at -70°C for the gene expression studies (Section 2.8.3.13)

2.8.3.7 Plasma amylase activity

Plasma α-amylase activity was measured using an Amylase assay kit (Abcam, Cambridge, UK). According to manufacturer's instructions, 50µl were aliquoted onto a 96 well plate in duplicates. The standard was made using the standard stock (2mM Nitrophenol) dissolved in the assay buffer (Figure 1.3). Standard curve dilutions were prepared from 4 nmol/well to 20 nmol/well. 30µl of water and 20µl of unknown plasma samples were added to the remaining wells. The reaction mixture (100µl) was then added to each well. Absorbance was measured immediately at OD=405 nm in a kinetic mode, every 2 minutes over 60 min at 25°C protected from light using a chemiluminescent plate reader (microlumi XS, Harta instruments, Gaithsberg, MD,

USA). Standards were plotted on a non-linear sigmoidal dose-response curve, and readings were calculated using log analysis.

The activity of amylase was calculated by using the formula:

Amylase Activity = $\left(\frac{B}{\Delta T\ x\ V}\right) * D$

Where B = Nitrophenol amount from the standard curve (nmol).

ΔT = reaction time (T2 – T1) (min).

V = Sample volume

D = sample dilution fact

2.8.3.8 Lipid profile

Plasma total cholesterol, HDL cholesterol, LDH cholesterol and plasma triglycerides were determined using an automated biochemistry analyser I-Lab 650 integrated chemistry system (Instrumentation Laboratory, Warrington, UK).

2.8.3.9 Plasma Alanine Aminotransferase (ALT)

Plasma ALT was measured using an ALT reagent kit (Randox Laboratories, UK) according to the manufacturer's instructions. Standard curve dilutions were prepared from pyruvate standard stock dissolved in water and the assay buffer solution (containing 100mM phosphate buffer (pH 7.4), 2mM L-alanine and 2 mM α-oxoglutarate). The final concentration of the standards corresponded to various transaminase activities from 9 U/l to 87 U/l depending on the dilution. The calibration curve was obtained by plotting the measured absorbance against the transaminase activities in U/l (Figure 1.4). Unknown plasma samples (100µl) were mixed with the

assay buffer solution (500µl) in a reaction tube and incubated for 30 min for 37˚C. 2mM 2,4-dinitrophenylhydrazine (500µl) was then pipetted to the reaction tubes and incubated for exactly 20 min for 20˚C before adding 4mM sodium hydroxide (5ml). The samples were aliquoted into cuvettes, and the absorbance was measured at 546 nm against the reagent blank after 5 min using a Novaspec spectrophotometer Model 4049 (Biochrom Ltd, UK).

2.8.3.10 Plasma glucagon extraction method

Plasma was collected and stored as previously described (Section 2.8.3.5). Glucagon was extracted by adding acetonitrile (225µl/tube) to samples (150µl/tube). The reaction tubes were then vortexed vigorously for 5 seconds. The tubes were let to stand for 20 min on the bench and then centrifuged at 17000xg for 5 minutes. 300µl of the supernatant was removed and transferred to a clean Eppendorf tube which was placed into SpeedVac Concentrator for drying at 80˚C for 2 hours. Dried supernatant was stored at 4˚C prior commencement of assay.

2.8.3.11 Assessment of plasma glucagon

Glucagon was extracted from plasma samples as previously describe (Section 2.8.3.10). Glucagon was measured using an ELISA kit (Millipore Corporation, Germany). Standard stock (2ng/ml) was diluted with the assay buffer according to the manufacturer's protocol chart, to obtain concentrations from 2ng/ml to 0.02 ng/ml. Prior to the experiment, dried samples (Section 2.8.3.10) were hydrated with 30µl of assay buffer. A 96-well plate coated by a pre-titered amount of anchor glucagon antibodies was washed with the assay wash buffer (300µl/well, three times) diluted with water (1:10). 30µl of assay buffer was added to Blank wells and 20µl to the remaining wells. Standards and unknown samples were then added to the plate

(10µl/well in duplicates) prior to adding the antibody mixture solution (20µl/well). The plate was then covered with the plate sealer and incubated for 48 hours on an orbital shaker at 400 rpm, 4°C. After the incubation, the test solutions were decanted, and the plate was washed with the diluted assay wash buffer (300µl/well, three times). The enzyme solution was added to the wells (100µl/well) and incubated (covered with the plate sealer) on a shaker for 30 min at room temperature. The plate was then washed with the diluted assay wash buffer (300µl/well, six times) prior to incubation with the substrate solution (100µl/well) on the shaker for 1 min. Measurements were taken within 5 minutes after adding the substrate using a luminometer plate reader set at 425 nm. Standards were plotted on a non-linear sigmoidal dose-response curve, and readings were calculated using log analysis.

2.8.3.12 Pancreatic insulin and glucagon content

Pancreata were dissected as previously described (Section 2.8.3.5) and homogenised (1 ml/pancreas) in extraction buffer (containing 20 mM Tris-HCl, 150 mM NaCl, 1 mM EDTA, 1 mM EGTA and 0.5% Triton X 100, pH 7.5) using a VWR VDI 12 handheld homogenizer (VWR, UK). Samples were stored at -20 °C until the commencement of assay. The sample was diluted (1:40) in RIA buffer supplemented with 0.5% BSA. Insulin was measured as previously described (Section 2.5.7). Glucagon was extracted using 150 µl of tissue homogenate (Section 2.8.3.10) and analysed using the glucagon ELISA kit (Section 2.8.3.11). Total protein content was determined by incubating the pancreatic extract (5 µl/well) with Bradford reagent (250µl/well) using a 96-well plate at room temperature for 15 min. Absorbance was read at 595 nm. The concentration of unknown samples was determined using a standard curve of known BSA concentrations from 12.5 mg/ml to 0.024 mg/ml).

2.8.3.13 RNA extraction

Animals treated for 21 days were sacrificed as previously described (Section 2.8.3.5). Islets were processed as described in (Sections 2.5.5.1 and 2.8.3.6). Collagenase-digested islet were treated (1ml/0.5 g of cells) with TriPure Isolation Reagent (Roche, UK) and homogenised using VWR VDI 12 handheld homogeniser (VWR, UK). The homogenate was let to stand at room temperature for 5 min prior to the addition of chloroform (0.2 ml/tube). The tubes were then shaken vigorously for 15 sec and incubated for 10 min at 20°C. The samples were centrifuged at 12000 rpm for 15 min at 4 °C to separate the mixture into aqueous and organic interphases. The aqueous phase containing RNA was transferred to an RNase free tubes. Isopropanol (0.5 ml/tube) was added to the tubes, mixed by inversion and incubated for 10 min at 20 °C prior to centrifugation at 12000 rpm for 15 min at 4°C. After the supernatant was decanted, 1 ml of 75% ethanol (diluted in diethylpyrocarbonate (DEPC) treated water was added to the pellet and centrifuged at 7500 rpm for 5 min. The supernatant was discarded, and the pellet was air-dried addition DEPC treated water 30 µl. Nanodrop was used to confirm the quantity and quality of isolated RNA by reading the absorbance of the sample (1 µl) at 260 nm. The samples were stored at -20°C prior to the cDNA synthesis.

2.8.3.14 cDNA synthesis

RNA was isolated from mouse islets and quantified as previously described (Section 2.8.3.13). RNA from each sample (3µg/sample) was then converted to cDNA SuperScript II reverse transcriptase (Invitrogen, Life Technologies; UK) following manufacturer's instruction. The reaction mixture (containing 1 µl of the Oligodt (Invitrogen, Life Technologies), 3 µg of RNA and RNase free water (used to adjust

the total volume to 12 µl)) was prepared in the RNase free tube. The tubes were placed into the G-STORM thermocycler (Gene Technologies, Braintree, UK) and heated at 70˚C for 10 min. 4 µl of 5 X First strand buffer, 2 µl of 0.1 M of DTT (Invitrogen, Life Technologies) and 1 µl of 10 mM dNTP were then added to the reaction tubes and run in the thermocycler at 42 °C for 2 min. In the final step of the experiment, SuperScript II RT (1 µl/tube) was added to the reaction mixture and incubated in the thermocycler at 42 ˚C for 50 min followed by 70 °C for 15. Samples were stored at -20 C.

2.8.3.15 Gene amplification

Real-time polymerase chain reaction (PCR) was performed using Bio-Rad MJ Mini personal Thermal cycler (Bio-Rad Laboratories, UK). PCR reaction mixture (containing 4.5 µl of QuantiFast SYBR green PCR mix (Qiagen, Venlo, Netherlands), 1 µl of forward and 1 µl reverse primers, 3 µl of cDNA (Section 2.8.3.14) and 1 µl of nuclease-free water) was added to the PCR tube strips. DNA denaturation was run at 95°C for 5 min followed by a 40-cycle cDNA amplification with final denaturation at 95°C for 30 sec, annealing at 58 °C for 30 sec and elongation at 72°C for 30 sec. SYBR Green fluorescence was recorded after each cycle. Data were normalised to Beta-actin (Actb) gene expression used as a reference gene and analysed using the ΔΔCt method. The forward/ reverse primers and the genes used in this study are listed in Table 2.2.

2.8.3.16 Immunohistochemistry of pancreas

Animals were sacrificed, and the pancreas was removed as described previously (Section 2.8.3.5). The tissue were placed into plastic cassettes and fixed in 4% paraformaldehyde for 48 hours. The cassettes were then processed overnight using an automated tissue processor Leica TP1020 (Leica Microsystems, Germany), followed

by preparation of paraffin tissue blocks. The sections were cut 7 μm thick using the Finesse 352 manual microtome (Thermo Scientific, UK) and placed on polysine slides (Thermo Scientific, UK).

Prior to staining, the slides were de-waxed using xylene, re-hydrated using gradually decreasing ethanol concentrations (100% for 5 min, 95% for 5 min, 80% for 5 min, 50% for 5 min and 0% (100% water) for 3 min). The slides were then treated with preheated citrate buffer (containing 10mM Sodium Citrate, 0.05% Tween 20, pH 6.0) for 20 min at 93°C in the water bath and 20 min on the bench. The tissue slides were then treated with 2% BSA for 45 min at room temperature before incubating with primary monoclonal mouse anti-insulin antibody (ab6995, 1:400; Abcam, Cambridge, UK) and guinea-pig anti-glucagon antibody (PCA2/4, 1:50; raised in-house) and incubated overnight at 4°C. After the incubations the slides were washed in PBS prior to incubation with secondary antibodies: Alexa Fluor 488 goat anti-guinea pig IgG—1:400 and Alexa Fluor 594 goat anti-mouse IgG—1:400 for 45 min at 37 °C. The slides were washed with PBS (for 5 min, two times) and incubated with 4',6-diamidino-2-phenylindole (DAPI) stain for 15 min at 37 °C followed by additional PBS wash (for 5 min, two times). The slides were mounted with a mounting solution containing 1:1 glycerol/PBS and analysed using a fluorescent microscope (Olympus system microscope, model BX51) with the DP70 camera adapter system. Islet parameters (islet number, islet area, beta cell area, alpha cell area and islet size distribution) were analysed using Cell^F image analysis software (Olympus Soft Imaging Solutions, GmbH).

2.8.4 Long-term in vivo studies using GluCre Rosa26-YFP mice

The animals were housed and diabetes induced as previously described (Sections 2.8.1.3 and Section 2.8.1.4). The mice (n=5) received twice daily intraperitoneal injections of saline or peptides (25 nmol/kg of body weight) over 10 days treatment period. Non-fasting blood glucose, food intake, water intake and body weight were monitored at 3-day intervals prior to daily injection of test peptides. Blood was collected for insulin measurements at the start and end of the experiment. The animals were sacrificed as described previously (Section 2.8.3.5). Pancreatic tissue was processed, de-waxed, re-hydrated and treated as described in Section 2.8.3.16. Three different types of double staining were performed: (i) Insulin-Glucagon (as shown in Section 2.8.3.16), (ii) Insulin-GFP and (iii) Glucagon-GFP. Following primary antibodies were used: mouse anti-insulin (1:400; Abcam ab6995), guinea pig anti-glucagon antibody (PCA2/4, 1:50; raised in house) and rabbit anti-GFP (1:400; Abcam). The slides were incubated and washed as described in Section 2.8.3.16. The slides were then treated with secondary antibodies: (i) Alexa Flour 488 goat anti-mouse; 1:400, (ii) Alexa Flour 594 goat anti-guinea pig; 1:400 and (iii) Alexa Flour 594 rabbit anti-GFP; 1:400. The slides were then incubated, washed and analysed as described in Section 2.8.3.16.

Table 2.1 Chemical reagents used in this thesis

Reagent name A-Z	Vendor
Acetonitrile, HPLC grade (ACN)	Sigma-Aldrich (Poole, UK)
Activated charcoal	Sigma-Aldrich (Poole, UK)
α-Cyano-4-hydroxycinnamic acid (α-CHCA)	Sigma-Aldrich (Poole, UK)
Bovine Serum Albumin (BSA)	Sigma-Aldrich (Poole, UK)
Calcium chloride dihydrate ($CaCl_2.2H_2O$)	Sigma-Aldrich (Poole, UK)
Collagenase-V, *Clostridium histolyticum*	Sigma-Aldrich (Poole, UK)
Dextran T-70	Sigma-Aldrich (Poole, UK)
D-glucose	AMRESCO (Ohio, USA)
Dimethyl sulphoxide (DMSO)	Sigma-Aldrich (Poole, UK)
Dipeptidyl peptidase IV (DPP IV), porcine kidney	Merck Millipore (UK)
Disodium hydrogen orthophosphate (Na_2HPO_4)	VWR International (Belgium)
Dulbecco's Modified Eagles Medium (DMEM)	Gibco Life Technologies Limited (Paisley, Strathclyde, UK)
Ethylenediaminetetraacetic acid (EDTA)	Sigma-Aldrich (Poole, UK)

Ethylene glycol-bis-N,N,N', N'-tetraacetic acid (EGTA)	Sigma-Aldrich (Poole, UK)
Foetal Bovine Serum (FBS)	Gibco Life Technologies Limited (Paisley, Strathclyde, UK)
Gentamycin	Sigma-Aldrich (Poole, UK)
Hanks' Buffered Saline Solution (HBSS) 10x	Gibco Life Technologies Limited (Paisley, Strathclyde, UK)
Hydrochloric acid (HCl)	BDH Chemicals Ltd. (Poole, Dorset, UK)
Insulin, bovine	Sigma-Aldrich (Poole, UK)
Insulin, rat	Novo Industrial (Denmark)
L-Alanine	Sigma-Aldrich (Poole, UK)
Magnesium sulphate ($MgSO_4$)	BDH Chemicals Ltd. (Poole, Dorset, UK)
Penicillin and Streptomycin (Pen & Strep)	Gibco Life Technologies Limited (Paisley, Strathclyde, UK)
Potassium chloride (KCl)	BDH Chemicals Ltd. (Poole, Dorset, UK)
Radiolabelled sodium iodide ($Na^{125}I$)	Perkin Elmer (UK)
Roswell Park Memorial Institute Medium (RPMI-1640)	Gibco Life Technologies Limited (Paisley, Strathclyde, UK)
Sodium bicarbonate ($NaHCO_3$)	Sigma-Aldrich (Poole, UK)

Sodium chloride (NaCl)	Sigma-Aldrich (Poole, UK)
Sodium hydroxide (NaOH)	Sigma-Aldrich (Poole, UK)
Thimerosal	Sigma-Aldrich (Poole, UK)
Triethylamine hydrochloride (TEA-HCl) buffer	Sigma-Aldrich (Poole, UK)
Trifluoroacetic acid (TFA)	Sigma-Aldrich (Poole, UK)
Trypan Blue (0.4%)	Sigma-Aldrich (Poole, UK)
Trypsin (0.5%), no phenol red	Gibco Life Technologies Limited (Paisley, Strathclyde, UK)

Table 2.2: List of the genes and forward/reverse primers used in the gene expression studies

Gene	Common name	Primer sequence
Ins 1	Mus musculus insulin 1	Forward: AAG CTG GTG GGC ATC CAG TA Reverse: GAC AAA AGC CTG GGT GGG TT
Slc2a2	Glucose transporter 2	Forward: GAA GAA GAG TGG TTC GGC CC Reverse: CGC ACA CCG AGG AAG GAA TC
Gck	Glucokinase, Transcript variant 1	Forward: AGG CCC TGA CAG GAG ACA TC Reverse: GCC TCT AGA CGG ACT CAG CA
Abcc8	ATP-binding cassette, sub-family C (CFTR/MRP), member 8	Forward: TGA AGC GCA TCC ACA CAC TC Reverse: ATC TTC TGT CCT GGG GCG AT
Kcnj11	Potassium inwardly-rectifying channel, subfamily J, member 11 (Transcript variant 1)	Forward: TGG GTT GGG GGC TCA GTA AG Reverse: ACC TCT AGG CTG GTA TGC CC
Cacna1c	Calcium channel,voltage-dependent, L-type, alpha 1C subunit	Forward: ACA TGC TTT TCA CCG GCC TC Reverse: GCT CCC AAT GAC GAT GAG GAA G
Glp1r	Glucagon-1 like peptide receptor	Forward: GCT GAG GGT CTC TGG CTA CA Reverse: GGG ACA GGA GCT GTT CCT CA
Gipr	Gastric inhibitory polypeptide receptor	Forward: TGC CCC GAC TAC CGA CTA AG Reverse: GCC TTC AAC CTG TTC CTC CG
Gcgr	Glucagon receptor	Forward: GCC ACC AGG GAC TTC ATC AAC Reverse: CAA GTG ACT GGC ACG AGA TGT

Table 2.3 List of Peptides used in Chapter 3

Peptide	Amino acid sequence
Lamprey GLP-1	HADGTFTNDMTSYLDAKAARDFVSWLARSDKS
Dogfish GLP-1	HAEGTYTSDVDSLSDYFKAKRFVDSLKSY
Ratfish GLP-1	HADGIYTSDVASLTDYLKSKRFVESLSNYNRKQNDRRM
Paddlefish GLP-1	HADGTYTSDASSFLQEQAARDFISWLKKGQ
Bowfin GLP-1	YADAPYISDVYSYLQDQVAKKWLKSGQDRRE
Trout GLP-1	HADGTYTSDVSTYLQDQAAKDFVSWLKSGRA
Human GLP-1	HAEGTFTSDVSSYLEGQAAKEFIAWLVKGR-NH2
Human glucagon	HSQGTFTSDYSKYLDSRRAQDFVQWLMNT
Human GIP	YAEGTFISDYSIAMDKIHQQDFVNWLLAQKGKKNDWKHNITQ
Exendin-4	HGEGTFTSDLSKQMEEEAVRLFIEWLKNGGPSSGAPPPS-NH2

Table 2.4 List of peptides used in Chapter 4

Peptide	Amino acid sequence
Lamprey glucagon	HSEGTFTSDYSKYLENKQAKDFVRWLMNA
Dogfish oxyntomodulin	HSEGTFTSDYSKYMDNRRAKDFVQWLMSTKRNG
Ratfish oxyntomodulin	HTDGIFSSDYSKYLDNRRTKDFVQWLLSTKRNGANT
Paddlefish glucagon	HSQGMFTNDYSKYLEEKRAKEFVEWLKNGKS
Trout glucagon	HSEGTFSNDYSKYQLERMAQDFVQWLMNS
Human GLP-1	HAEGTFTSDVSSYLEGQAAKEFIAWLVKGR-NH2
Human glucagon	HSQGTFTSDYSKYLDSRRAQDFVQWLMNT
Human GIP	YAEGTFISDYSIAMDKIHQQDFVNWLLAQKGKKNDWKHNITQ
Exendin-4	HGEGTFTSDLSKQMEEEAVRLFIEWLKNGGPSSGAPPPS-NH2

Table 2.5 List of peptides used in Chapter 5

Peptide	Amino acid sequence
[D-Ala^{2}]-lamprey GLP-1-Lys^{31}-gamma-glutamyl-pal	HaDGTFTNDMTSYLDAKAARDFVSWLARSD[K-gamma-glutamyl-pal]S-OH
[D-Ala^{2}]-paddlefish GLP-1-Lys^{28}-gamma-glutamyl-pal	HaDGTYTSDASSFLQEQAARDFISWLK[K-gamma-glutamyl-pal]GQ-OH
Human oxyntomodulin	HSQGTFTSDYSKYLDSRRAQDFVQWLMNTKRNKNNIA
Human GLP-1	HAEGTFTSDVSSYLEGQAAKEFIAWLVKGR-NH2
Human glucagon	HSQGTFTSDYSKYLDSRRAQDFVQWLMNT
Human GIP	YAEGTFISDYSIAMDKIHQQDFVNWLLAQKGKKNDWKHNITQ
Exendin-4	HGEGTFTSDLSKQMEEEAVRLFIEWLKNGGPSSGAPPPS-NH2
Liraglutide	HAEGTFTSDVSSYLEGQAAK-(γ-Glu-palmitoyl)-EFIAWLVRGRG-OH

Table 2.6 List of peptides used in Chapter 6

Peptide	Amino acid sequence
[D-Ser^{2}]-lamprey glucagon-Lys^{30}-gamma-glutamyl-pal	HsEGTFTSDYSKYLENKQAKDFVRWLMNA[K-gamma-glutamyl-pal]
[D-Ser^{2}]-paddlefish glucagon-Lys^{30}-gamma-glutamyl-pal	HsQGMFTNDYSKYLEEKRAKEFVEWLKNG[K-gamma-glutamyl-pal]S-OH
Human oxyntomodulin	HSQGTFTSDYSKYLDSRRAQDFVQWLMNTKRNKNNIA
Human GLP-1	HAEGTFTSDVSSYLEGQAAKEFIAWLVKGR-NH2
Human glucagon	HSQGTFTSDYSKYLDSRRAQDFVQWLMNT
Human GIP	YAEGTFISDYSIAMDKIHQQDFVNWLLAQKGKKNDWKHNITQ
Exendin-4	HGEGTFTSDLSKQMEEEAVRLFIEWLKNGGPSSGAPPPS-NH2
Liraglutide	HAEGTFTSDVSSYLEGQAAK-(γ-Glu-palmitoyl)-EFIAWLVRGRG-OH

Table 2.7 List of peptides used in Chapter 7

Peptide	Amino acid sequence
Zebrafish GIP	YAESTIASDISKIVDSMVQKNFVNFLLNQRE
Human glucagon	HSQGTFTSDYSKYLDSRRAQDFVQWLMNT
Human GIP	YAEGTFISDYSIAMDKIHQQDFVNWLLAQKGKKNDWKHNITQ
Exendin-4	HGEGTFTSDLSKQMEEEAVRLFIEWLKNGGPSSGAPPPS-NH2

Figure 1.1 HPLC purification of iodinated bovine insulin

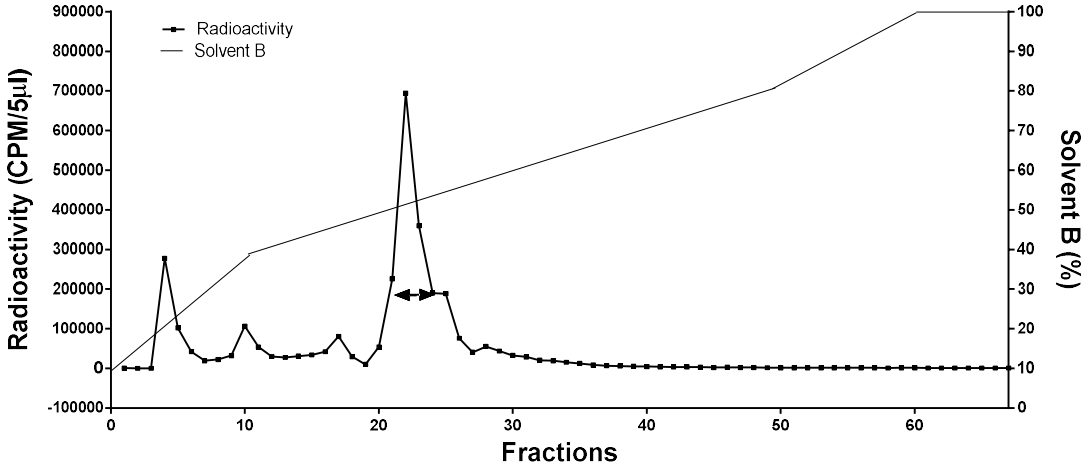

Iodinated ^{125}I - bovine insulin was purified from the reaction mixture using RP-HPLC, at a flow rate of 1 ml/min and an automated fraction collector. Radioactivity of each fraction was determined by Wizard™ 1470 automatic gamma counter (Perkin Elmer, USA).

Figure 1.2 Graph of typical cAMP standard curve

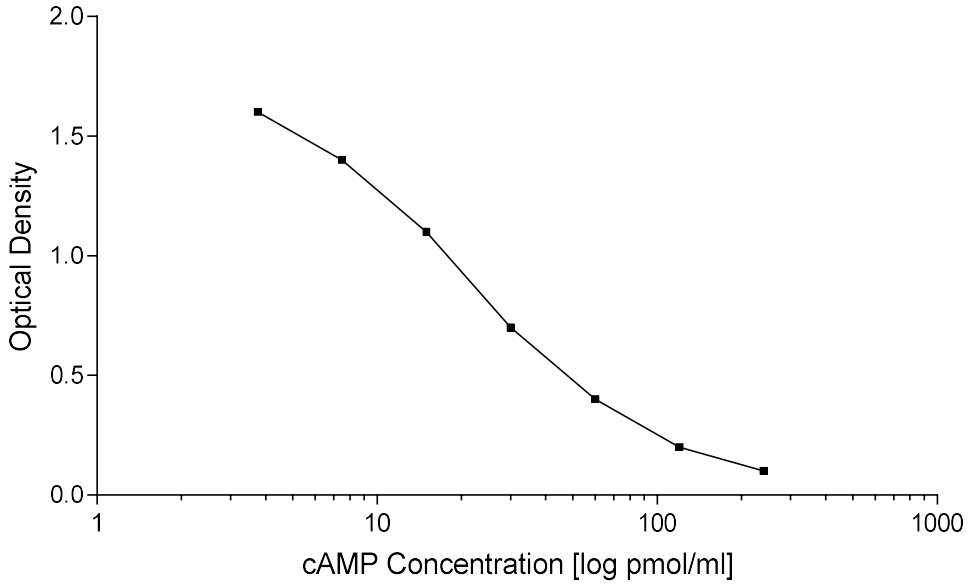

A standard curve of stock solution was prepared over a concentration range of 240-3.75 pmol/ml. The wavelength was corrected by subtracting 540 nm reading from the readings measured at 450 nm.

Figure 1.3 Graph of typical nitrophenol standard curve

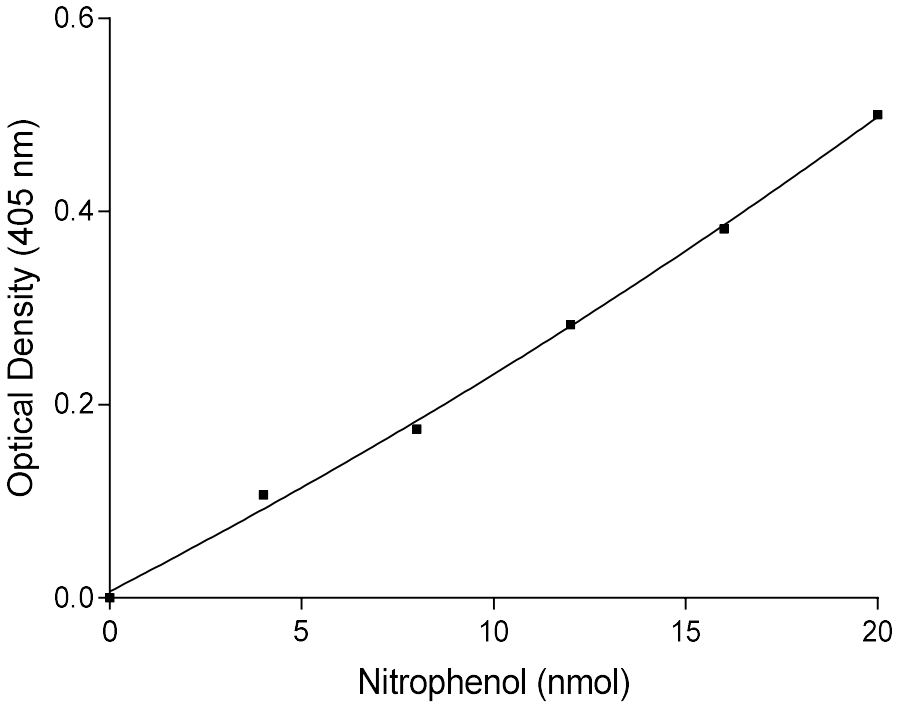

A standard curve of stock solution (2mM Nitrophenol) was prepared over a concentration range of 20-4 nmol/ml. Absorbance was measured immediately at OD=405 nm in a kinetic mode.

Figure 1.4 Graph of typical plasma ALT activity standard curve

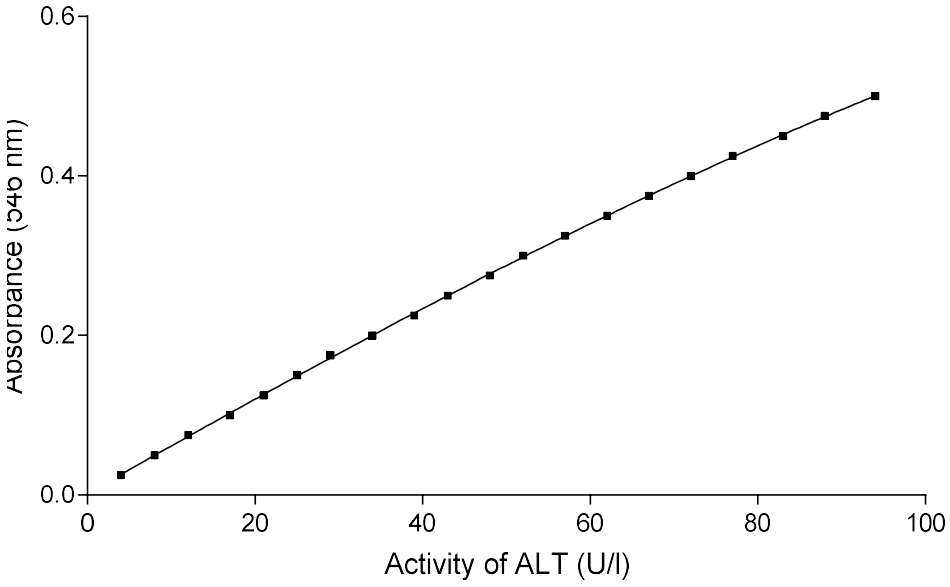

The concentration of the standards corresponded to various transaminase activities from 9 U/l to 87 U/l depending on the dilution. The standard curve was obtained by plotting the measured absorbance at 546 nm against the transaminase activities in U/l.

Chapter 3

Assessing the acute insulinotropic *in vitro* and *in vivo* effects of native fish GLP-1 peptides

3.1 Summary

The insulinotropic and antihyperglycaemic actions of GLP-1 peptides from the phylogenetically ancient sea lamprey, dogfish, ratfish, paddlefish and bowfin are compared with those of trout GLP-1 and human GLP-1 in mammalian test systems. The peptides were susceptible to DPP-IV degradation in a similar pattern as human glucagon and incretin peptides. Fish GLP-1 peptides produced a concentration-dependent stimulation of insulin release from BRIN-BD11 rat and 1.1 B4 human clonal β-cells and isolated mouse islets. Lamprey and paddlefish GLP-1 were the most potent and effective. Incubation of BRIN-BD11 cells with the GLP-1 receptor antagonist, exendin-4(9-39) attenuated the insulin-releasing activity of all peptides whereas the glucagon receptor antagonist, [desHis1,Pro4-Glu9] glucagon amide significantly decreased the activities of lamprey and paddlefish GLP-1 only. The GIP receptor antagonist GIP (6-30) Cex-K^{40} [Pal] attenuated the activity of bowfin GLP-1. All peptides (1 μM) produced significant increases in cAMP concentration in Chinese hamster lung (CHL) cells transfected with the human GLP-1 receptor but only lamprey and paddlefish GLP-1 stimulated cAMP production in human embryonic kidney (HEK293) cells transfected with the human glucagon receptor. The insulinotropic effects of lamprey and trout GLP-1 were abolished in INS-1 GLP-1 receptor knockout cells and attenuated in INS-1 GCG receptor knockout cells. Intraperitoneal administration of GLP-1 from all species except dogfish (25nmol/kg body weight) along with 18 mmol/kg body weight in mice produced significant decreases in blood glucose and increased insulin concentrations. The fish GLP-1 peptides failed to exhibited persistent glucose homeostatic effects when administered 2 hours prior to glucose challenge. Lamprey GLP-1 was most effective in suppressing the appetite in normal mice. The study has demonstrated that lamprey and paddlefish GLP-1 display

potent insulinotropic activity *in vitro* that is mediated through the GLP-1 and glucagon receptors and glucose-lowering activity *in vivo* that is comparable to that of human GLP-1.

3.2 Introduction

Glucagon-like peptide-1 (GLP-1) was first identified from the nucleotide sequence of a cDNA encoding preproglucagon in a Brockmann body (principal islet) cDNA library from the anglerfish *Lophius americanus* (Lund et al. 1982). Shortly afterwards, cDNAs encoding preproglucagon from several mammalian species including the human (Bell et al. 1983) were characterized but the incretin activity of GLP-1 was not demonstrated until it was realized that the active forms of the peptide in mammals were GLP-1(7-37) and GLP-1(7-36)amide which resemble anglerfish GLP-1 and glucagon more closely (Mojsov et al. 1987). In humans, the effects of GLP-1 and glucagon are mediated through respective interaction with the receptors GLP1R and GCGR belonging to the class B-1 (secretin receptor-like) G protein-coupled receptors that are highly specific for their native ligands (Fredriksson et al. 2003). In teleost fish, the Gcgr also binds glucagon and not GLP-1 (Chow et al. 2004) but the GLP-1-specific receptor has been lost, being replaced by a receptor that has dual selectivity for both GLP-1 and glucagon (Oren et al. 2016). In mammals, GLP-1 is multifunctional. As well as stimulating post-prandial insulin release, the peptide inhibits glucagon secretion, decreases food intake, delays gastric emptying, protects β- cells from apoptosis and has beneficial effects on cognitive impairment and cardiac function (Drucker, 2018). In contrast, GLP-1 is not an incretin hormone in teleost fish and has a glucagon-like effect on metabolism stimulating glycogenolysis, gluconeogenesis and lipolysis (Plisetskaya and Mommsen, 1996; Mommsen, 2000).

There is a unique arrangement found in the pancreas of teleosts which is represented by a large concentration of endocrine cells adjacent to the gallbladder and surrounded by a thin oval line of exocrine forming so-called Brockmann body. This almost complete separation of endocrine from exocrine tissues could potentially represent a valuable experimental model for studies of pancreatic hormones (Plisetskaya, 1989).

GLP-1 peptides have been isolated from the Brockmann bodies of a wide range of teleost species and cDNAs/ genes encoding proglucagon-derived peptides from several teleosts have been characterized [reviewed in (Irwin, 2005; Irwin and Mojsov, 2018)]. GLP-1 peptides have also been purified from a range of phylogenetically more ancient fishes: sea lamprey *Petromyzon marinus* [Petromyzontiformes] (Conlon et al. 1993), European common dogfish *Scyliorinus canicula* [Elasmobranchii] (Conlon et al. 1994), Pacific ratfish *Hydrolagus colliei* [Holocephali] (Conlon et al.1987), paddlefish *Polyodon spathula* [Acipenseriformes] (Nguyen et al. 1994), the alligator gar *Lepisosteus spatula* [Lepisosteiformes] (Pollock et al., 1988), and the bowfin *Amia calva* [Amiiformes] (Conlon et al., 1993). Characterization of a cDNA from the intestine of *P. marinus* demonstrated that the sea lamprey proglucagon gene encodes the three glucagon-related peptides (glucagon, GLP-1 and GLP-2) analogous to those encoded by the proglucagon genes of tetrapods (Irwin et al. 1999). It has been suggested that the glucagon sequence first arose in evolution approximately 1000 million years ago (MYA) while GLP-1 and GLP-2 diverged from each other approximately 700 MYA.

In the present research study, the biological activities of GLP-1 peptides from phylogenetically ancient fishes have not been investigated in detail. Consequently, the aim of the present study was to evaluate the insulinotropic properties of synthetic replicates of GLP-1 peptides from the sea lamprey, dogfish, ratfish, paddlefish, and

bowfin *in vitro* using established rat and human insulin-producing cell lines and isolated mouse to assess their acute glucose-lowering and insulin-stimulating actions *in vivo* using NIH Swiss mice. Their activities are compared with those of human GLP-1 and GLP-1 from a teleost fish, the rainbow trout *Onchorynchus mykiss* (Irwin and Wong 1995).

3.3 Materials and Methods

3.3.1 Chemical reagents and peptides

Chemical reagents that were used in this study can be found in Section 2.1.1 and Table 2.1. Synthetic human glucagon, human GLP-1, human GIP and trout GLP-1 were obtained from Synpeptide Co. Ltd. (Shanghai, China) at >95% purity which was confirmed by reversed-phase HPLC and MALDI-TOF. Lamprey GLP-1, dogfish GLP-1, ratfish GLP-1, paddlefish GLP-1, bowfin GLP-1, and exendin-4 peptides were supplied by EZBiolab Inc. (Carmel, IN, USA) in a crude form (between 10% and 50% purity). These latter peptides were purified to > 98% homogeneity by reversed-phase HPLC on a (2.2 cm x 25 cm) Vydac 218TP1022 (C-18) column. The concentration of acetonitrile in the eluting solvent was raised from 21% to 56 % or 28% to 63% over 50 min using a linear gradient. Absorbance was measured at 214 nm, and the flow rate was 6 ml/min (Section 2.2). The molecular masses of the peptides were confirmed by matrix-assisted laser desorption ionization time-of-flight mass (MALDI-TOF) spectrometry as previously described (Section 2.2). The primary structures and molecular masses of the peptides used in this study are shown in Table 2.1 and Table 3.1.

3.3.2 Assessment of metabolic stability of fish GLP-1 peptides

Lamprey GLP-1, dogfish GLP-1, ratfish GLP-1, paddlefish GLP-1, bowfin GLP-1, trout GLP-1, human GLP-1, human glucagon and human GIP were incubated in the presence of porcine DPP-IV, and peptide stability was measured over 4 hours as described in Section 2.3.1. RP-HPLC was used to identify intact peptide and degraded products the molecular masses of which were confirmed by MALDI-TOF MS as previously described (Section 2.3). The percentage intact peptide at 4 hours incubation with DPP-IV was calculated by comparison to the peak area recorded at 0 hours.

3.3.3 *In vitro* insulin release studies using BRIN-BD11 and 1.1B4 cells

The abilities of the purified synthetic peptides (0.1 nM - 3 μM; n = 8) to stimulate the rate of release of insulin from BRIN-BD11 rat clonal β-cells (McClenaghan et al., 1996) and 1.1B4 human-derived pancreatic β-cells (McCluskey et al. 2011) was determined as previously described (Section 2.5.1 and 2.5.3). In a second series of experiments, the effects of 1 μM concentrations of the (A) GLP-1 receptor antagonist, exendin-4(9-39 (Thorens et al., 1993), (B) glucagon receptor antagonist, [desHis1,Pro4-Glu9]glucagon amide (O'Harte et al., 2013), and (C) glucose-dependent insulinotropic peptide (GIP) receptor antagonist, GIP(6-30)Cex-K^{40}[Pal] (Pathak et al., 2015) on the insulin-releasing activity of the peptides (0.1 μM) were studied by incubating BRIN-BD11 cells for 20 min at 37 ˚C in Krebs-Ringer Bicarbonate (KRB) buffer, pH 7.4 supplemented with 5.6 mM glucose as previously described (Section 2.5.2). All samples were stored at −20 °C prior to measurement of insulin release by radioimmunoassay (Flatt and Bailey, 1981) as previously described (Section 2.5.7).

3.3.4 Insulin release studies using isolated mouse islets

Freshly harvested pancreatic islets from adult, male National Institutes of Health (NIH) Swiss mice (Harlan Ltd, Bicester, UK) were cultured in RPMI medium for 48 h at 37 °C in an atmosphere of 5% CO_2 and 95% air as previously described (Section 2.5.5). The islets were incubated with peptides (10 nM and 1µM; n =4) and alanine (10 mM; n =4) for 1 h at 37˚C in KRB buffer supplemented with 16.7 mM glucose. Insulin release was measured by radioimmunoassay, and the insulin content was measured by extraction with acid-ethanol.

3.3.5 Effects of peptides on cAMP production.

Chinese hamster lung (CHL) cells transfected with the human GLP-1 receptor (GLP1R) (Thorens et al. 1993) and human embryonic kidney (HEK293) cells transfected with the human glucagon receptor (GCGR) (Ikegami et al., 2001) were cultured and seeded as previously described (Section 2.6).The cells were pre-incubated for 40 minutes with KRB buffer supplemented with 0.1% (w/v) bovine serum albumin and 1.1 mmol/l glucose. A test solution containing KRB buffer supplemented with 0.1% (w/v) bovine serum albumin, 5.6 mmol/l glucose, 200 µM 3-isobutyl-1-methylxanthine (IBMX) and peptides (10 nM and 1µM) were added to the cells. After incubating for 20 min, the medium was removed, and cells were lysed before measurement of cAMP using a Parameter cAMP assay kit (R&D Systems, Abingdon, UK) according to the manufacturer's recommended protocol.

3.3.6 Insulin release studies using CRISPR/Cas9-engineered INS-1 cells

Wild-type INS-1 832/3 rat clonal pancreatic β-cells and CRISPR/Cas9-engineered cells with knock-out of the knock-out of the GLP-1 receptor (GLP-1 KO), glucagon receptor (GCG KO) and GIP receptor (GIP KO) (Naylor et al., 2016) were cultured and incubated as described for BRIN-BD11 cells with the addition of 1 mM sodium pyruvate and 50 mM 2-mercaptoethanol to the medium (Section 2.5.4). The cells were incubated with 10 nM and 1 μM concentrations of GLP-1, glucagon, GIP, and fish peptides for 20 min 37 °C in KRB buffer supplemented with 5.6 mM glucose and insulin release was measured by radioimmunoassay (Section 2.5.7).

3.3.7 *In vivo* insulin release studies

All experiments involving animals were performed in accordance with the UK Animals (Scientific Procedures) Act 1986 and EU Directive 2010/63EU and approved by Ulster University Animal Ethics Review Committee. Acute *in vivo* studies were carried out using 8-10 week-old male National Institutes of Health (NIH) Swiss mice (n = 6) maintained in environmentally controlled rooms (12:12 light/darkness cycle, 22 ± 2 ºC) with free access to a standard rodent diet (10% fat, 30% protein, 60% carbohydrate: total energy 12.99 kJ/g; Trouw Nutrition, Northwich, UK) and water (Section 2.8.1.1). After an overnight fast, glucose (18 mmol/kg body weight), either alone or together with a peptide (25 nmol/kg body weight), was administrated intraperitoneally to the animals as previously described (Section 2.8.2.1). In a second series of experiments acute duration of action studies were performed as described in Section 2.8.2.3. Blood samples were collected from a tail vein at the time points shown in Figure 3.18 and 3.19 and glucose concentrations were measured using a Bayer Counter glucose meter. Peptide administration had no apparent adverse behavioural effects on the animals.

3.3.8 Acute food consumption studies

Normal male TO mice (8-12 week-old) were used in food consumption study as previously described (Section 2.8.2.4). Mice were administrated intraperitoneal injections of either saline solution or peptides (50 nmol/kg) prior to receiving pellets of food of known weight. Food intake was then recorded over time points of 0, 30, 60, 90, 120, 150 and 180 min. Consumption of water was not restricted in this experiment.

3.3.9 Biochemical analysis

Blood was collected from the tail vein of conscious mice and analysed immediately using the Ascenacia Counter Blood Glucose Meter (Bayer, Newbury, UK). Plasma for insulin was collected, stored and assayed as described in Section 2.8.2.5.

3.3.10 Statistical analysis

Data were compared using unpaired Student's t-test (non-parametric, with two-tailed P values and 95% confidence interval) and one-way ANOVA with Bonferroni post-hoc test using GraphPad PRISM (Version 5.0 San Diego, California). Area under the curve (AUC) analysis was performed using the trapezoidal rule with baseline correction. Data are presented as mean ± S.E.M where the comparison was considered to be significantly different if $P < 0.05$.

3.4 Results

3.4.1 Purification and confirmation of molecular masses by MALDI-TOF MS

Purification was performed using multiple RP HPLC runs for each crude peptide with the original purity between 10% and 50%. The main peaks were collected as represented in Figure 3.1. All peptides were analysed by MALDI-TOF MS which

confirmed that the molecular masses corresponded very closely with their related theoretical molecular masses (Figure 3.2 and 3.3). The summary of purification and MALDI-TOF results is shown in Table 3.1.

3.4.2 Fish GLP-1 peptides stability

Human GLP-1 (Figure 3.4), human glucagon (Figure 3.5) and human GIP (Figure 3.6) were degraded into 2 major fractions after 4 hours incubation with DPP-IV. The molecular masses of these fractions corresponded to the remaining intact peptide and its truncated product cleaved at position 2 for each of the control peptides. As expected, when fish GLP-1 peptides were incubated under identical conditions, similar cleavage pattern was determined (Figures 3.7-3.12 and Table 3.2).

3.4.3. *In vitro* insulin-release studies

In the presence of 5.6 mM glucose alone, the rate of insulin release from BRIN-BD11 rat clonal β-cells was 1.02 ± 0.02 ng/10^6cells/20 min and this rate increased to 2.4 ± 0.2 ng/10^6cells/20 min during incubation with 0.1 μM human GLP-1 and to 1.4 ± 0.2 ng/10^6cells/20min during incubation with 0.1 μM glucagon. Incubation of BRIN-BD11 cells with GLP-1 peptides from all fish species produced concentration-dependent increases in the rate of insulin release (Figure. 3.13). As shown in Table 3.3, lamprey and paddlefish GLP-1 displayed the lowest threshold concentrations (minimum concentration producing a significant increase in insulin release) and the greatest responses at 3 μM concentration. These values were not significantly different from those of human GLP-1.

In the presence of 5.6 mM glucose alone, the rate of insulin release from 1.1B4 human clonal β-cells was 0.08 ± 0.01 ng/10^6cells/20min rising significantly to 0.13 ± 0.01 ng/10^6 cells/20 min and 0.24 ± 0.02 ng/10^6cells/20min during incubations with 10 nM

and 1 μM human GLP-1 respectively (Table 3.4). As shown in Figure. 3.14, incubations with GLP-1 from all fish species produced a significant increase in insulin release at 1 μM concentration and GLP-1 peptides from lamprey, paddlefish and trout produced a significant increase at 10 nM concentration. Consistent with the data obtained with BRIN-BD11 cells, the lamprey and paddlefish peptides were the most effective with the responses produced by lamprey GLP-1 at both concentrations (0.23 ± 0.01 ng/10^6cells/20min at 10 nM and 0.31 ± 0.02 ng/10^6cells/20min at 1 μM) being significantly greater than those produced by GLP-1.

The rate of insulin release from isolated mouse islets in the presence of 16.7 mM glucose alone during a 60 min incubation was 9.7 ± 1.3 % of the total insulin content of the islets rising to 16.7 ± 1.4 % in the presence of 10 nM GLP-1 and to 20.7 ± 2.5 % in the presence of 1 μM GLP-1 (Table 3.5). As shown in Figure. 3.15, GLP-1 from all species except dogfish and ratfish produced a significant increase in insulin release at both 10 nM and 1 μM concentrations. Ratfish GLP-1 was effective at 1 μM, but dogfish GLP-1 did not produce a significant increase at either concentration.

3.4.4 Receptor antagonist studies

The insulin releasing activities of human GLP-1 and all fish GLP-1 peptides were significantly attenuated when BRIN-BD11 cells were co-incubated with the GLP-1 receptor antagonist, exendin-4(9-39) (Figure 3.16 A). The activity of human glucagon and GIP were not significantly affected. The insulin releasing activities of glucagon and lamprey GLP-1 ($P < 0.001$) and paddlefish GLP-1 ($P < 0.001$) were also significantly decreased in the presence of the glucagon receptor antagonist [desHis1.Pro4-Glu9] glucagon amide (Figure 3.16 B) whereas the actions of GLP-1, GIP, and the other fish GLP-1 peptides were unaffected. Human GIP ($P < 0.001$) and bowfin GLP-1 ($P < 0.05$) were the only peptides whose insulin-releasing effects were

significantly attenuated by co-incubation with the GIP receptor antagonist GIP (6-30) Cex-K40 [Pal] (Figure 3.15 C and Table 3.6).

3.4.5 Effect of fish GLP-1 peptides on cAMP production

In the presence of 200 μM IBMX, cAMP production in CHL cells transfected with the human GLP-1 receptor was significantly stimulated by incubation with human GLP-1 and the GLP-1 peptides from lamprey, paddlefish and trout at both 10 nM and 1 μM concentrations (Figure 3.17 A). In the case of GLP-1 from dogfish, ratfish and bowfin a significant increase in cAMP production was achieved only at 1 μM concentration. Human glucagon and GLP-1 from lamprey and paddlefish, at both 10 nM and 1 μM concentrations, were the only peptides that produced a significant increase cAMP production in HEK293 cells transfected with the human glucagon receptor (Figure 3.17 B and Table 3.7).

3.4.6 Insulin release studies using CRISPR/Cas9-engineered INS-1 cells

Incubation of all fish GLP-1 peptides, as well as human GLP-1, glucagon, and GIP, at concentrations of 10 nM and 1 μM with wild-type INS-1 cells produced a significant increase in the rate of release of insulin compared with the rate in the presence of 5.6 mM glucose only (Figure 3.18 A and Table 3.8). The increases in rate in response to GLP-1 and the GLP-1 from lamprey and trout were completely abolished in the GLP-1 KO cells, and the responses to the other fish peptides were significantly attenuated (Figure 3.18 B and Table 3.8). Moreover, the increases in rate in response to glucagon and GLP-1 from lamprey and paddlefish were significantly attenuated (Figure 3.18 C and Table 3.8). In contrast, the increases in rate in response to human ($P < 0.001$) and bowfin ($P < 0.05$) GIP were significantly reduced in the GIP KO cells, but the stimulatory responses to glucagon, GIP and the other fish GLP-1 peptides were maintained (Figure 3.18 D and Table 3.8).

3.4.7 *In vivo* insulin release studies

The acute actions of human GLP-1, human glucagon and fish GLP-1 peptides on glucose homeostasis *in vivo* are shown in Figure 3.19 and Table 3.9). Blood glucose concentrations in overnight fasted NIH Swiss mice were significantly lower after receiving intraperitoneal administration of glucose (18 mmol/ kg body weight) together with all GLP-1 peptides (25nmol/kg body weight) except dogfish GLP-1 compared with mice receiving intraperitoneal glucose only (Figure 3.19 A and C). The integrated responses showed significant differences for lamprey GLP-1 ($P < 0.001$), ratfish GLP-1 ($P < 0.05$), paddlefish GLP-1($P < 0.001$), trout GLP-1 ($P < 0.001$), and bowfin GLP-1 ($P < 0.05$ compared with the glucose control. The integrated responses to GLP-1 peptides from lamprey, paddlefish and trout were not significantly different from the response to human GLP-1 (Figure 3.19 E). The concentrations of plasma insulin were significantly greater at the 15 and 30 min time points after administration of GLP-1 from lamprey, ratfish, paddlefish and trout and after 30 min in the case of bowfin GLP-1 compared with control animals receiving glucose alone (Figure 3.19 B and D). The integrated responses to all peptides except dogfish GLP-1 were not significantly different from that of human GLP-1 (Figure 3.19 F).

3.4.8 Acute duration of action studies using normal mice

As expected, fish GLP-1 peptides similarly to human GLP-1 exhibit no glucose lowering and insulinotropic effect when administrated two hours prior to a glucose challenge (Figure 3.20 and Table 3.9). In contrast, exendin-4 significantly ($P < 0.001$) reduced individual post-injection (15, 30 and 60 min) and overall 0–60 min AUC glucose values. Moreover, exendin-4 significantly ($P < 0.001$) increased individual

post-injection and overall glucose-induced insulin concentrations when administrated two hours prior to a glucose load.

3. 4. 9 Time-dependent effects of human GLP-1, human glucagon, exendin-4 and fish GLP-1 peptides on feeding in normal mice.

At a concentration of 50 nmol/kg of body weight, exendin-4 (Figure 3.21) exhibited significant ($P < 0.01$ and $P< 0.001$) effect on food intake at individual time points (30, 60, 90, 120, 150 and 180 min). Human GLP-1 and lamprey GLP-1 (Figure 3.21 A) at a similar concentration significantly ($P < 0.05$) reduced food intake at 30 min time point when compared with saline. In comparison, paddlefish GLP-1 significant ($P < 0.05$) appetite-suppressive effect at 30, 90, 120, 150 and 180 min (Figure 3.20 D). Interestingly, no effect in food intake was observed for glucagon and the other fish peptides when compared with saline only (Figure 3.21 and Table 3.10)

3.5 Discussion

GLP-1 was discovered incidentally after the cloning and sequencing of mammalian proglucagon genes and has become one of the most characterised regulatory peptides of the glucagon superfamily in the field of metabolism (Cabou et al. 2011; D'alessio 2016). GLP-1 not only exhibits insulinotropic activity *in vitro* or in healthy humans but unlike many other gastrointestinal peptides, is also remarkably effective in patients with type 2 diabetes (D'alessio 2016). The development of antidiabetic drugs based on GLP-1 system has been one of the most important and rapidly moving areas of therapeutic targets in the recent past (D'alessio 2016). In this thesis GLP-1 peptides from phylogenetically ancient fish as well as a teleost were investigated for metabolic stability, potential insulinotropic property and receptor specificity. As expected, in the presence of DPP IV human GLP-1, glucagon and GIP were cleaved at position 2 to

produce truncated products consistently with the previous studies (Authier et al. 2003; Pospisilic et al. 2001; Green et al. 2004). This effect was also observed with fish GLP-1 peptides which were largely degraded by DPP IV after 4 hours incubation. The analysis of the molecular masses of the degraded products revealed that the cleavage site of the fish GLP-1 peptides was between residues 2 and 3 similarly to that of the human proglucagon-derived peptides (Table 3.2).

The present work has also demonstrated that GLP-1 peptides from phylogenetically ancient fish and a teleost differ appreciably in potency and effectiveness in terms of their abilities to stimulate insulin release from rodent and human cells *in vitro* and lower blood glucose concentrations in mice *in vivo*. The peptides from sea lamprey, a representative of the Agnatha, or jawless fishes whose line of evolution diverged from that leading to gnathostomes at least 550 MYA, and paddlefish, an extant representative of a group of primitive Actinopterygian (ray-finned) fish whose line of evolution diverged from the sturgeons in the Cretaceous, were the most potent and effective with activities generally comparable to human GLP-1. However, these GLP-1 peptides differ from the human peptide by functioning as dual agonists at the GLP-1 and glucagon receptors. The primary structures of the GLP-1 peptides investigated in this study are compared with those of human GLP-1, glucagon, and the potent and long-acting GLP-1 receptor agonist exendin-4 (Furman, 2012), in Figure 3.22)

Structure-activity studies of human GLP-1 involving a complete alanine scan showed that the amino acids His^{1}, Gly^{4}, Phe^{5}, Thr^{7} and Asp^{9} in the N-terminal domain play an important role in binding and activation of the rat GLP1R, and Phe^{22} and Ile^{23} in the C-terminal domain are of critical importance in maintaining the conformation of the molecule that is recognized by the receptor (Adelhorst et al. 1994; Gallwitz et al. 1994). In addition, it is known that the Ala^{18}, Ala^{19}, Lys^{20}, and Leu^{26} residues of GLP-

1 interact with the GLP-1 receptors as revealed by the crystal structure of GLP-1 bound to the large N-terminal extracellular domain of the receptor (Underwood et al. 2010). It is speculated that the higher potency and efficacy of GLP-1 from lamprey, paddlefish, and trout in the mammalian test systems compared with the peptides from the other species may be explained, at least in part, by the fact that they are the only peptides that contain the Ala^{18} and Ala^{19} residues found in human GLP-1. The lower potency peptides from dogfish and ratfish contain a basic Lys residue at position 18, and bowfin GLP-1 contains a Val residue (Figure 3.22). The metabolic effects of dogfish and ratfish GLP-1 in their species of origin have not been studied, but dogfish GLP-1 has been shown to stimulate the activity of the rectal gland of North Pacific spiny dogfish *Squalus suckleyi*, increasing chloride secretion rates above baseline by approximately 16-fold (Deck et al. 2017).

The insulinotropic activity of all fish peptides in BRIN-BD11 cells was attenuated by the GLP1R antagonist, exendin-4(9-39) and all peptides stimulated cAMP production in CHL cells transfected with GLP1R demonstrating that they are capable of activating the GLP-1 receptor in mammalian test systems. However, the insulinotropic activity of lamprey GLP-1 and paddlefish GLP-1 was significantly decreased by the GCGR antagonist, [desHis1,Pro4-Glu9] glucagon amide suggesting that these peptides may act as dual agonists activating both GLP-1 and glucagon receptors. Consistent with this observation, the activity of lamprey GLP-1 was abolished in INS-1GLP1R knockout cells in a similar manner as human GLP-1, and attenuated in INS-1 GCGR knockout cells similarly to the attenuated rates of glucagon. (Figure 18). Similar pattern was observed for paddlefish GLP-1 the activity of which was significantly attenuated in INS-1 GLP-1 receptor knock out and glucagon receptor knockout cells. A comparison of the primary structures of lamprey/paddlefish GLP-1 (Figure 22) with

glucagon does provide any obvious clues in terms of the presence or absence of particular amino acid residues as to why only these peptides and not the other fish GLP-1 peptides are glucagon receptor agonists. Rather it must be assumed that only lamprey/paddlefish GLP-1 are able to adopt a stable conformation that is recognized by the receptor. Glucagon is predominantly disordered in aqueous solution but forms a stable, extended helix when bound to its receptor (Siu et al. 2013). The conformations of the fish GLP-1 peptides have yet to be determined experimentally but application of the AGADIR program, an algorithm based on the helix/coil transition theory which predicts the helical behaviour of monomeric peptides (Muñoz and Serrano, 1994), indicates that lamprey and paddlefish GLP-1 have a strong propensity to adopt a stable α-helical conformation between residues 9-28 whereas the predicted helices adopted by the dogfish, ratfish, and bowfin peptides are much less stable and extended.

The bowfin, the sole extant representative of the Amiiformes, occupies an important position in phylogeny as the surviving representatives of a group of primitive ray-finned fishes from which present-day teleosts may have evolved (Carroll, 1988). Bowfin GLP-1 contains several amino acid substitutions compared with human GLP-1 that are not seen in the other fish peptides such as Gly^{4} → Ala, Phe^{22} → Trp, Ile^{23} → Leu, and Leu^{26} → Gly (Figure 3.22). In particular, bowfin GLP-1, in common with GIP, contains an N-terminal Tyr residue and a Thr^{7} residue that is substituted by Ile. Evidence has been obtained using a chimeric GLP-1/GIP peptides that amino acids at these sites (His/Tyr^{1} and Thr/Ile^{7}) are responsible for the selective interaction toward GLP-1 and GIP receptors (Moon et al., 2010). It has been proposed that His^{1} of GLP-1 interacts with Asn^{302} in extracellular loop 2 of GLP1R and that Thr^{7} of GLP-1 has close contact with a binding pocket formed by Ile^{196} in transmembrane helix 2

and Leu^{232}, and Met^{233} in extracellular loop 1 of GLP1R (Moon et al. 2012). Despite the low overall sequence similarity between bowfin GLP-1 and GIP (Figure 3.22), the presence of Tyr^{1} and Ile^{7} in the bowfin peptide may account for the fact that the GIP receptor antagonist, GIP(6-30) Cex-K40 [pal] produced a small but significant attenuation of the insulinotropic response to bowfin GLP-1 in BRIN-BD11 cells (Figure 3.16) and the activity of the peptide was reduced in CRISPR/Cas9-engineered INS-1 cells with knock-out of the GIP receptor compared the response with wild-type INS-1 cells. Bowfin GLP displayed relatively weak insulinotropic activity compared with human GLP-1 in the mammalian systems employed in this study. Similarly, in a piscine test system, bowfin GLP-1 stimulated glycogenolysis in isolated hepatocytes from the copper rockfish *Sebastes caurinus* (Teleostei) but was 3-fold less effective and 23-fold less potent than human GLP-1 (Conlon et al. 1993). It was speculated that selective mutations in the GLP-1 molecule may be an adaptive response to the low biological potency of bowfin insulin (Conlon et al. 1991).

This Chapter has demonstrated that in agreement with *in vitro* studies, acute administration of GLP-1 from lamprey, paddlefish and trout together with glucose resulted in significant glucose lowering and insulin release in normal mice which was comparable to the effects of human GLP-1. As expected, GLP-1 from all fish species failed to exhibited persistent glucose homeostatic effects when administered 4 hours prior to glucose challenge due to the susceptibility to enzymatic degradation similarly with human GLP-1. Moreover, paddlefish GLP-1 was effective in suppressing appetite for up to 180 minutes in normal mice compared to saline control. The effects of lamprey GLP-1 on food intake were similar to human GLP-1 which significantly suppressed the appetite for up to 30 minutes after the intraperitoneal administration to mice.

To conclude, the world is currently experiencing a global pandemic of obesity-related type 2 diabetes mellitus (T2DM) and while several therapeutic options are available for treatment of patients, none is completely satisfactory (Bailey, 2018). None of the existing treatments, alone or in combination, completely normalizes blood glucose concentrations and prevents debilitating complications. Thus, there is a definite need for new types of safe and more effective anti-diabetic agents. The present study has demonstrated that GLP-1 peptides from lamprey and paddlefish, by interacting with both the GLP-1 and glucagon receptors to stimulate insulin release and lower blood glucose concentrations, have the potential for development therapeutic agents for the treatment of patients with T2DM. Pre-clinical trials involving administration of dual GLP-1/glucagon receptor agonists have shown positive results including reduction of food intake, weight loss, inhibition of glucagon release, and β-cell proliferation as well as normalization of blood glucose concentrations [reviewed in Brandt et al. 2018]. Previous work has shown that dual agonist peptides derived from dogfish glucagon possess potent insulin releasing actions *in vitro* (O'Harte et al. 2016a) and antihyperglycaemic activity in obese mice with insulin resistance and impaired glucose tolerance (O'Harte et al. 2016b). Future studies will investigate the anti-diabetic activities of long-acting peptidase-resistant analogues of lamprey and paddlefish GLP-1.

Table 3.1. Primary structures and the observed and calculated molecular masse of peptides investigated in this study.

Peptide	**Amino acid sequence**	**Calculated molecular mass, (Da)**	**Observed molecular mass, (Da)**
Lamprey GLP-1	HADGTFTNDMTSYLDAKAARDFVSWLARSDKS	3577.9	3576.5
Dogfish GLP-1	HAEGTYTSDVDSLSDYFKAKRFVDSLKSY	3330.7	3330.1
Ratfish GLP-1	HADGIYTSDVASLTDYLKSKRFVESLSNYNRKQNDRRM	4479.9	4480.2
Paddlefish GLP-1	HADGTYTSDASSFLQEQAARDFISWLKKGQ	3358.5	3357.9
Bowfin GLP-1	YADAPYISDVYSYLQDQVAKKWLKSGQDRRE	3694.1	3695.4
Trout GLP-1	HADGTYTSDVSTYLQDQAAKDFVSWLKSGRA	3418.7	3420.8
Human GLP-1	HAEGTFTSDVSSYLEGQAAKEFIAWLVKGR-NH2	3297.7	3297.9
Human glucagon	HSQGTFTSDYSKYLDSRRAQDFVQWLMNT	3482.8	3484.4
Human GIP	YAEGTFISDYSIAMDKIHQQDFVNWLLAQKGKKNDWKHNITQ	4983.6	4984.3
Exendin-4	HGEGTFTSDLSKQMEEEAVRLFIEWLKNGGPSSGAPPPS-NH2	4186.6	4186.0

Table 3.2 Summary of DPP-IV degradation results of the GLP-1-related fish peptides used in this study.

Peptide	% Degraded at 4 hours	Number of peaks	Observed MW of degraded product after 4h, Da	Proposed cleavage site
Lamprey GLP-1	90	2	3370.1	Ala^{2}-Asp^{3}
Dogfish GLP-1	89	2	3123.4	Ala^{2}-Glu^{3}
Ratfish GLP-1	83	2	4272.3	Ala^{2}-Asp^{3}
Paddlefish GLP-1	87	2	3153.3	Ala^{2}-Asp^{3}
Bowfin GLP-1	89	2	3460.3	Ala^{2}-Asp^{3}
Trout GLP-1	79	2	3212.6	Ala^{2}-Asp^{3}
Human GLP-1	86	2	3090.4	Ala^{8}-Glu^{9}
Human glucagon	24	2	3259.5	Ser^{2}-Gln^{3}
Human GIP	90	2	4749.1	Ala^{2}-Glu^{3}

Table 3.3 Effects of fish GLP-1 peptides, human GLP-1 and glucagon on the rate of insulin release from BRIN-BD11 cells.

Peptide	Threshold concentration	The effect at 3μM ng/10^6/20min	EC 50
Basal release	-	1.0 ± 0.02	-
Lamprey GLP-1	30pM**	3.9 ± 0.11	0.7nM
Dogfish GLP-1	3nM*	1.8 ± 0.08	0.1μM
Ratfish GLP-1	1nM*	2.6 ± 0.12	1.5μM
Paddlefish GLP-1	10pM*	3.7 ± 0.20	4.0nM
Trout GLP-1	30pM**	2.4 ± 0.11	7.5 nM
Bowfin GLP-1	0.3nM***	2.3 ± 0.10	1.6nM
Human GLP-1	10pM*	3.6 ± 0.17	2.1nM
Human glucagon	10nM*	2.7 ± 0.1	1.5μM

Values are mean ± S.E.M., n = 8. *P < 0.05, **P < 0.01, ***P < 0.001 compared to 5.6 mM glucose alone.

Table 3.4 Effects of fish GLP-1 peptides at 10^{-6} M and 10^{-8} M concentration on insulin secretion from 1.1 B4 cells.

Peptide name	Insulin release at 10^{-6}M	Insulin release at 10^{-8}M
None (1.4 mM glucose)	0.05 ± 0.002 **	0.05 ± 0.002 **
None (16.7 mM glucose control)	0.08 ± 0.007	0.08 ± 0.007
Lamprey GLP-1	0.31 ± 0.020 ***	0.23 ± 0.013 ***
Dogfish GLP-1	0.11 ± 0.020 **	0.09 ± 0.010
Ratfish GLP-1	0.10 ± 0.030 *	0.08 ± 0.006
Paddlefish GLP-1	0.24 ± 0.013 ***	0.16 ± 0.004 ***
Trout GLP-1	0.17 ± 0.007 ***	0.13 ± 0.008 **
Bowfin GLP-1	0.12 ± 0.006 **	0.09 ± 0.007 *
Human GLP-1	0.24 ± 0.020 ***	0.13 ± 0.008 **
Human glucagon	0.11 ± 0.002*	0.08 ± 0.006

Values are mean ± S.E.M., $n = 8$ *P < 0.05, **P < 0.01, ***P < 0.001 compared to 16.7 mM glucose alone

Table 3.5 Effects fish GLP-1 peptides on the release of insulin from islets isolated from TO Swiss mice.

Peptide	Insulin release (% of total insulin content) at 10^{-6}M	Insulin release (% of total insulin content) at 10^{-8}M
(None) 1.4 mM glucose	3.7 ± 0.1 **	3.7 ± 0.1 **
(None) 16.7 mM glucose control	9.7 ± 1.3	9.7 ± 1.3
Lamprey GLP-1	16.6 ± 1.3 **	15.6 ± 1.4
Dogfish GLP-1	13.7 ± 1.5	12.3 ± 0.9
Ratfish GLP-1	17.2 ± 1.0 **	7.2 ± 0.3
Paddlefish GLP-1	20.7 ± 2.4 **	13.1 ± 0.6*
Bowfin GLP-1	20.2 ± 1.3 ***	16.0 ± 1.5 *
Trout GLP-1	21.8 ± 1.9 **	19.2 ± 1.2 **
Human GLP-1	20.7 ± 2.5 **	16.1 ± 1.4 *
Human glucagon	15.1 ± 1.7	11.5 ± 1.3

Values are mean ± S.E.M., $n = 8$ *P < 0.05, **P < 0.01, ***P < 0.001 compared to 16.7 mM glucose alone.

Table 3.6 Summary of effect of fish GLP-1s, human GLP-1, human glucagon and human GIP on insulin secretion from BRIN-BD11 cells in the presence antagonists

Peptide, 10^{-7}	The observed reduction of peptides-stimulated insulin secretion in the presence of antagonists:		
	Exendin-4(9-39), 10^{-6}	Peptide O, 10^{-6}	(Pro^3)GIP, 10^{-6}
Lamprey GLP-1	ΔΔΔ	ΔΔΔ	No effect
Dogfish GLP-1	ΔΔ	No effect	No effect
Ratfish GLP-1	Δ	No effect	No effect
Paddlefish GLP-1	ΔΔΔ	ΔΔΔ	No effect
Bowfin GLP-1	Δ	No effect	Δ
Trout GLP-1	ΔΔΔ	No effect	No effect
Human GLP-1	ΔΔΔ	No effect	No effect
Human glucagon	No effect	Δ	No effect
Human GIP	No effect	No effect	ΔΔΔ

Values are mean ± S.E.M., n = 8 $^{\Delta}P < 0.05$, $^{\Delta\Delta}P < 0.01$, $^{\Delta\Delta\Delta}P < 0.001$ compared with the effect in the presence of respective antagonist.

Table 3.7 Summary of effect of fish GLP-1, human GLP-1, human glucagon and human GIP peptides (10^{-8} and 10^{-6} M) on cAMP production in GLP1R-transfected CHL cells, and GCGR-transfected HEK293 cells.

Peptide name	GLP-1 receptor transfected cells		GCG receptor transfected cells	
	cAMP release at 10^{-6}	cAMP release at 10^{-8}	cAMP release at 10^{-6}	cAMP release at 10^{-8}
Basal (5.6mM glucose)	4.0 ± 0.4	4.0 ±0.4	2.8 ±0.9	2.8 ±0.9
Lamprey GLP-1	16.5 ± 0.3***	14.5 ± 0.1***	10.6 ±0.1**	9.8 ±0.3**
Dogfish GLP-1	10.2 ± 0.2***	4.3 ± 0.2	2.7 ± 0.2	2.3 ± 0.2
Ratfish GLP-1	5.1 ± 0.0*	3.7 ± 0.4	3.6 ± 0.2	2.1 ± 0.8
Paddlefish GLP-1	15.0 ± 0.6***	13.1 ± 0.3**	9.2 ±0.7**	6.7 ±0.1*
Bowfin GLP-1	14.1 ± 0.3***	4.0 ± 0.1	3.2 ± 1.1	3.3 ± 0.1
Trout GLP-1	15.4 ± 0.3***	13.7 ± 0.6***	3.3 ± 0.3	2.4 ± 0.0
Human GLP-1	17.7 ± 0.2***	17.3 ± 0.3***	7.6 ± 0.2**	4.9 ± 0.4*
Human glucagon	12.3 ± 0.8 **	5.4 ± 0.4*	10.4 ± 0.3**	9.1 ± 0.4**
Human GIP	3.9 ± 0.2	3.6 ± 0.4	2.9 ± 0.4	2.8 ± 0.3

Values are mean ± S.E.M. for n = 4. *P < 0.05, ** P< 0.01 and ***P < 0.001 compared with 5.6 glucose.

Table 3.8 Summary of effects of fish GLP-1 peptides (10^{-8} and 10^{-6} M) on the rate of insulin release from wild-type INS-1 cells, CRISPR/Cas9-engineered GLP-1R KO cells, CRISPR/Cas9-engineered GIPR KO cells and CRISPR/Cas9-engineered GIPR KO cells

Peptide		Wild-type cells, % of basal control	GLP-1R KO cells, % of basal control	GCGR KO cells, % of basal control	GIPR KO cells, % of basal control
Basal (5.6mM glucose)		100 ± 2.3			
Lamprey GLP-1	10^{-6}	217.5 ± 7.5***	109.0 ± 6.1 ΔΔΔ	199.7 ± 24.6 ***	222.2 ± 7.5 ***
	10^{-8}	203. ± 9.2***	110.8 ± 7.7 ΔΔΔ	160.3 ± 19.9 *Δ	209.9 ± 11.1 ***
Dogfish GLP-1	10^{-6}	242.9 ± 7.9***	202.5 ± 12.2 *** Δ	217.1 ± 6.8***	221.6 ± 7.6 ***
	10^{-8}	199.7± 7.1***	167.5 ± 14.5 ***Δ	172.3 ± 16.8***	187.9 ± 9.2 ***
Ratfish GLP-1	10^{-6}	194.5 ± 7.6***	167.4 ± 6.4*** Δ	170.9 ± 9.8***	182.7 ± 8.8 ***
	10^{-8}	147.3 ± 6.1***	138.4 ± 2.8***	147.7± 12.7*	164.7± 8.4***
Paddlefish GLP-1	10^{-6}	259.9 ± 5.3***	226.8 ± 10.5 *** Δ	216.9 ± 24.4***	249.3 ± 9.8 ***
	10^{-8}	231.9 ± 3.5***	214.4 ± 4.1*** Δ	153.7 ± 27.9**ΔΔ	225.9 ± 10.5 ***
Bowfin GLP-1	10^{-6}	209.5 ± 6.7***	164.8 ± 9.2 *** Δ	206.9 ± 24.6 ***	192.5 ± 9.7 ***
	10^{-8}	177.8 ± 6.6***	153.8 ± 15.8**	184.3 ± 14.5***	143.7 ± 11.9* Δ
Trout GLP-1	10^{-6}	226.1 ± 5.3***	110.7 ± 6.9 ΔΔΔ	220.0 ± 20.6***	228.7 ± 11.1 ***
	10^{-8}	197.2 ± 9.3***	106.5 ± 5.4 ΔΔΔ	173.5 ± 10.0***	217.8 ± 12.3 ***
Human GLP-1	10^{-6}	213.5 ± 14.1***	102.3 ± 1.3 ΔΔΔ	222.0 ± 11.7***	213.2 ± 12.3 ***
	10^{-8}	197.1 ± 4.5***	101.1 ± 6.9 ΔΔΔ	210 ± 25.0 ***	183.5 ± 3.5***
Human glucagon	10^{-6}	215.3 ± 3.4***	252.8 ± 0.8***	159.6 ± 8.5 *** ΔΔ	181.0± 13.3 ***
	10^{-8}	172.7 ± 7.5***	194.9 ±10.9***	134.0 ± 14.4 Δ	174.0 ± 10.6 ***
Human GIP	10^{-6}	241.2 ± 10.1***	264.9 ±10.2***	231.3 ± 17.6 ***	110.1 ± 8.5 ΔΔΔ
	10^{-8}	228.8 ± 16.3***	255.4 ± 5.3***	230.1 ± 0.9***	104.4 ± 4.2 ΔΔΔ

Values are mean ± S.E.M., $n = 8$, *P < 0.05, ** P< 0.01 and ***P < 0.001 compared with 5.6 mM glucose alone. $^{\Delta}P < 0.05$, $^{\Delta\Delta}P < 0.01$, $^{\Delta\Delta\Delta}P < 0.001$ compared with effects in wild-type INS-1 cells

Table 3.9 Summary of effects of acute administration of fish GLP-1 peptides on blood glucose and plasma insulin concentrations in normal mice, including 2-hour post injection.

Peptide name	IGTT blood glucose $AUC_{0\text{-}60min}$ (mmol/l.min)	IGTT plasma insulin $AUC_{0\text{-}60min}$ (mmol/ml/min)	2 hours post saline/peptide injection, plasma insulin $AUC_{0\text{-}60min}$ (mmol/l.min)	2 hour post saline/peptide injection, plasma insulin $AUC_{0\text{-}90min}$ (ng/ml/min)
Glucose alone	991.1 ± 49.04	134.8 ± 4.23	894.3 ± 46.17	108.1 ± 4.236
Lamprey GLP-1	471.0 ± 29.79***	238.1 ± 15.25***	809.8 ± 40.48	108.2 ± 7.889
Dogfish GLP-1	833.0 ± 59.25 ΔΔ	150.5 ± 5.691 Δ	890.2 ± 59.92	119.2 ± 10.06
Ratfish GLP-1	792.9 ± 66.18*ΔΔ	164.6 ± 9.179*	831.6 ± 49.82	126.0 ± 7.245
Paddlefish GLP-1	550.6 ± 35.61***	191.5 ± 13.20**	815.8 ± 37.32	117.2 ± 2.929
Bowfin GLP-1	838.5 ± 32.00*ΔΔ	160.3 ± 7.679*	830.9 ± 19.64	103.3 ± 4.879
Trout GLP-1	573.0 ± 28.96***	164.5 ± 6.609**	811.5 ± 42.55	100.9 ± 6.990
GLP-1	476.4 ± 41.37***	186.6 ± 12.87 **	825.4 ± 32.49	101.7 ± 16.65
Glucagon	1006 ± 140.6 ΔΔ	145.9 ± 3.218 Δ	-	-
Exendin-4	-	-	369.0 ± 38.96*** ΔΔΔ	281.0 ± 16.25 ***ΔΔΔ

The values are mean ± SEM for n=6. **P<0.01 and ***P<0.001 compared to glucose alone; $^{\Delta\Delta}$ P<0.01 and $^{\Delta\Delta\Delta}$P<0.001 compared to human GLP-1

Table 3.10 Summary effects of fish GLP-1 peptides on cumulative food intake over 3 hours trained feeding in 12 h fasting normal mice.

Peptide name	Time (min)					
	30	**60**	**90**	**120**	**150**	**180**
Saline control	1.2 ± 0.03	1.7 ± 0.06	2.1 ± 0.08	2.5 ± 0.07	2.9 ± 0.07	3.3 ± 0.06
Lamprey GLP-1	0.8 ± 0.07 *	1.6 ± 0.1	2.0 ± 0.10	2.3 ± 0.19	2.6 ± 0.12	3.0 ± 0.09
Dogfish GLP-1	1.1 ± 0.09	1.6 ± 0.1	2.1 ± 0.14	2.4 ± 0.14	3.0 ± 0.20	3.3 ± 0.19
Ratfish GLP-1	1.3 ± 0.18	2.0 ± 0.3	2.4 ± 0.27	2.8 ± 0.22	3.0 ± 0.25	3.4 ± 0.17
Paddlefish GLP-1	0.7 ± 0.15 *	1.3 ± 0.2	1.5 ± 0.15 *	1.9 ± 0.23 *	2.5 ± 0.18 *	2.7 ± 0.17 *
Bowfin GLP-1	1.3 ± 0.11	1.6 ± 0.2	2.1 ± 0.19	2.4 ± 0.24	2.9 ± 0.16	3.4 ± 0.18
Trout GLP-1	1.4 ± 0.11	1.8 ± 0.2	2.1 ± 0.21	2.5 ± 0.16	3.0 ± 0.19	3.4 ± 0.08
GLP-1	0.7 ± 0.13 **	1.4 ± 0.18	2.1 ± 0.20	2.4 ± 0.13	2.7 ± 0.11	3.1 ± 0.08
Glucagon	1.3 ± 0.09	1.8 ± 0.15	2.1 ± 0.16	2.4 ± 0.18	2.6 ± 0.17	2.9 ± 0.19
Exendin-4	0.7 ± 0.13 **	1.0 ± 0.08 ***	0.9 ± 0.08 ***	1.2 ± 0.16 ***	1.2 ± 0.17 ***	1.4 ± 0.17 ***

The values are mean ± SEM for n=8. *P<0.05, **P<0.01 and ***P<0.001 compared to saline control mice treated at the same time point.

Figure 3.1. Reverse-phase HPLC purification of crude lamprey GLP-1 (A), dogfish GLP-1 (B) ratfish GLP-1 (C), paddlefish GLP-1 (D), bowfin GLP-1 (E) and exendin-4 (F) peptides using a semi-preparative Vydac C18 column.

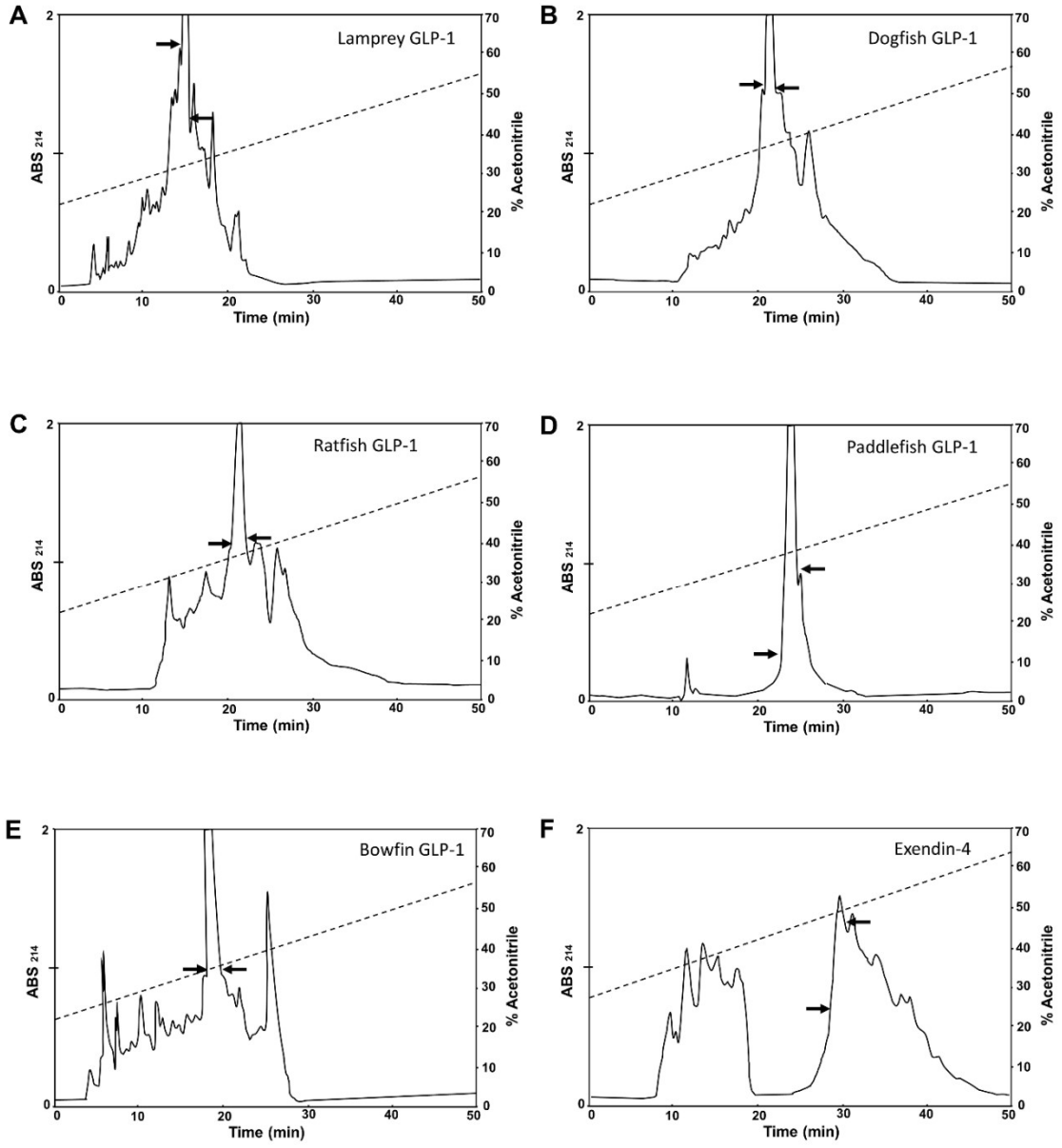

The peptides were dissolved in 15% acetonitrile (3mg/ml) and injected onto a (2.2 cm x 25 cm) Vydac 218TP1022 (C-18) column (Grace, Deerfield, IL, USA) equilibrated with 21% (or 28%) (v/v) acetonitrile and 0.1% TFA/water at a flow rate of 6.0 ml/min. The concentration of acetonitrile in the eluting solvent was raised from 21% to 56 % for the fish GLP-1 peptides and 28% to 63% for exendin-4 over 50 min using a linear gradient. Absorbance was measured at 214 nm and the black arrows show where the peak collection began and ended.

Figure 3.2 MALDI-TOF spectra of purified lamprey GLP-1 (A), dogfish GLP-1 (B) ratfish GLP-1 (C), paddlefish GLP-1 (D)

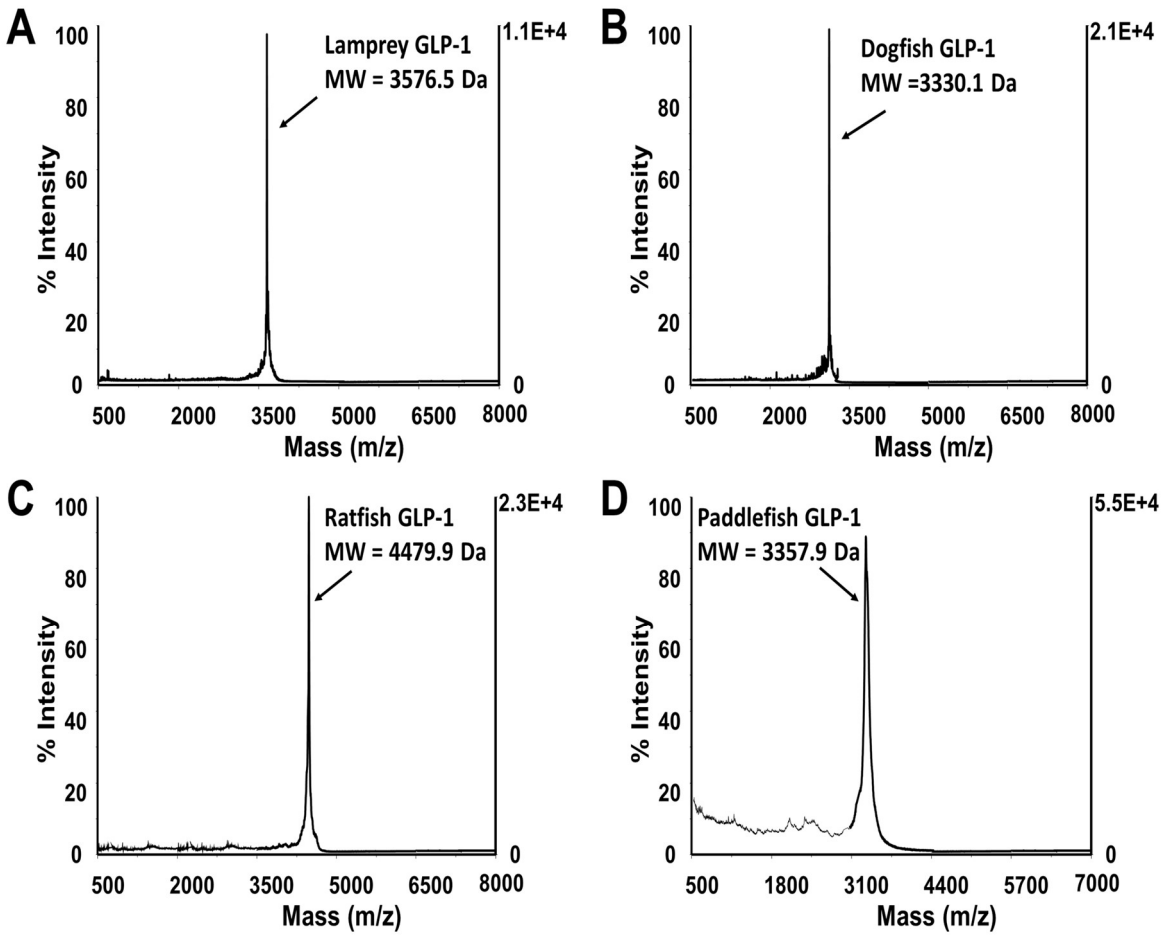

Purified peptides were mixed with α-Cyano-4-hydroxycinnamic acid on a 100 well MALDI plate before inserting into a Voyager DE Biospectrometry workstation. The mass-to-charge ratio (m/z) versus peak intensity was determined.

Figure 3.3 MALDI-TOF spectra of purified Bowfin GLP-1 (A) and trout GLP-1 (B) and Exendin-4 (C) peptides.

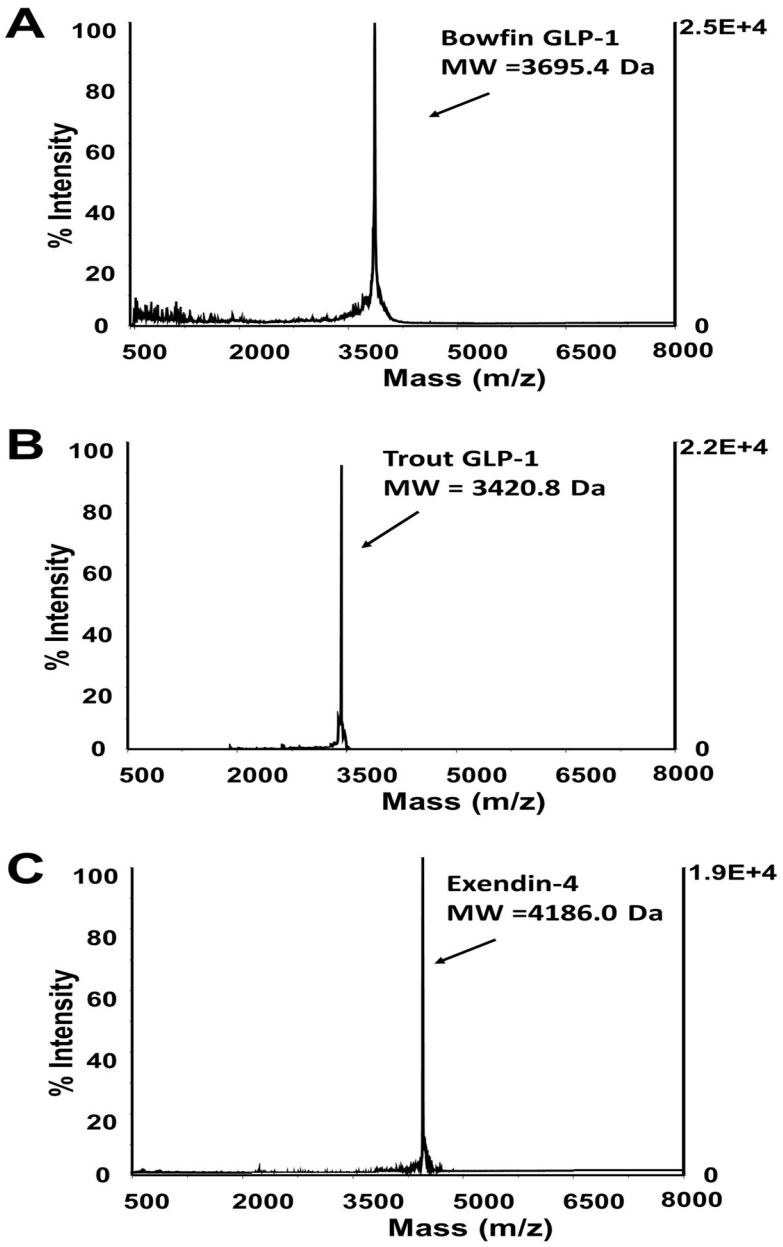

Purified peptides were mixed with α-Cyano-4-hydroxycinnamic acid on a 100 well MALDI plate before inserting into a Voyager DE Biospectrometry workstation. The mass-to-charge ratio (m/z) versus peak intensity was determined.

Figure 3.4 HPLC degradation profile of human GLP-1 following incubation with DPP-IV for 0 and 4 hours.

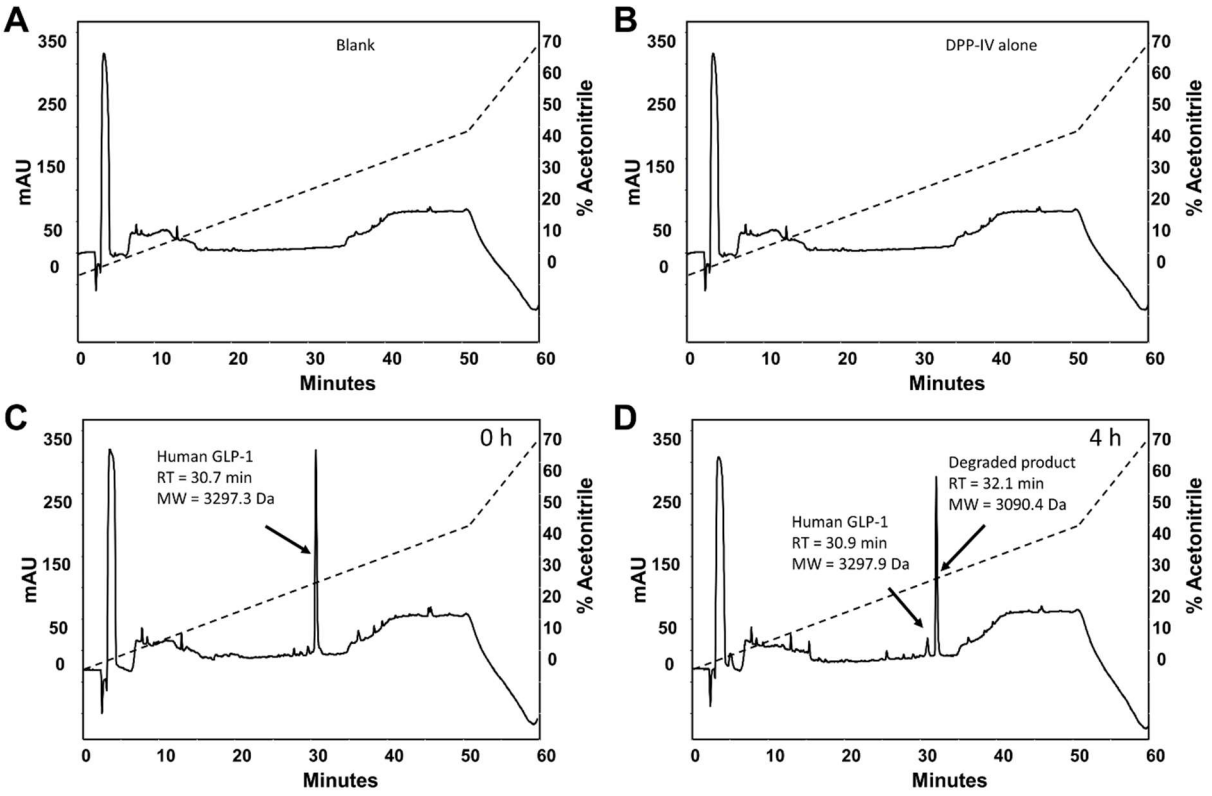

HPLC degradation study was performed with a Luna 5u C8 250x4.6mm column using gradients from 0% to 42% of acetonitrile over 50 min, and from 42% to 70% of acetonitrile over 15 min.

Figure 3.5 HPLC degradation profile of human glucagon following incubation with DPP-IV for 0 and 4 hours.

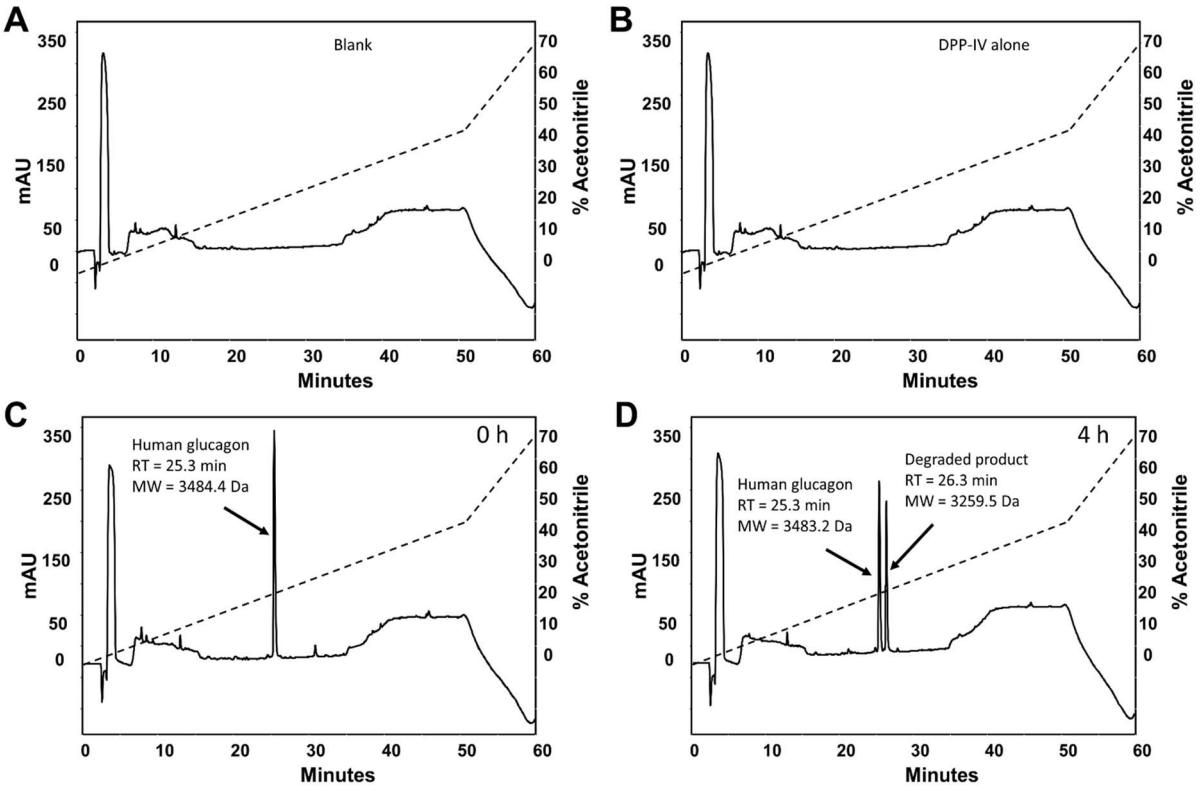

HPLC degradation study was performed with a Luna 5u C8 250x4.6mm column using gradients from 0% to 42% of acetonitrile over 50 min, and from 42% to 70% of acetonitrile over 15 min.

Figure 3.6 HPLC degradation profile of human GIP following incubation with DPP-IV for 0 and 4 hours.

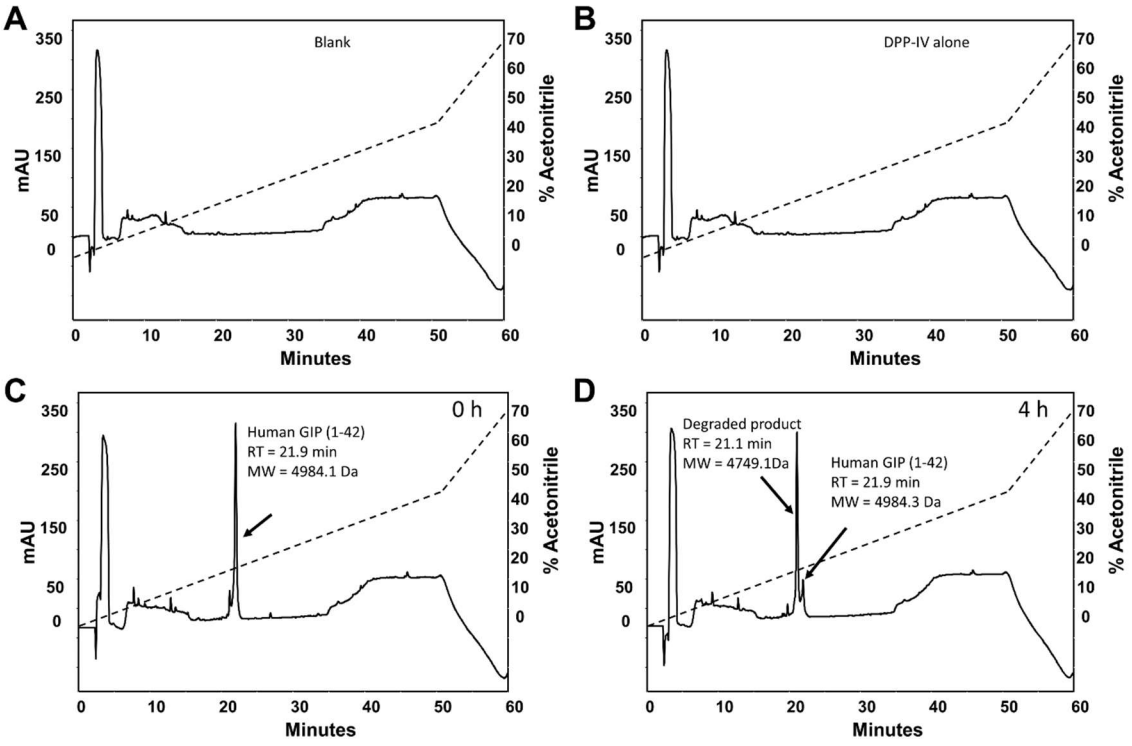

HPLC degradation study was performed with a Luna 5u C8 250x4.6mm column using gradients from 0% to 42% of acetonitrile over 50 min, and from 42% to 70% of acetonitrile over 15 min.

Figure 3.7 HPLC degradation profile of lamprey GLP-1 following incubation with DPP-IV for 0 and 4 hours.

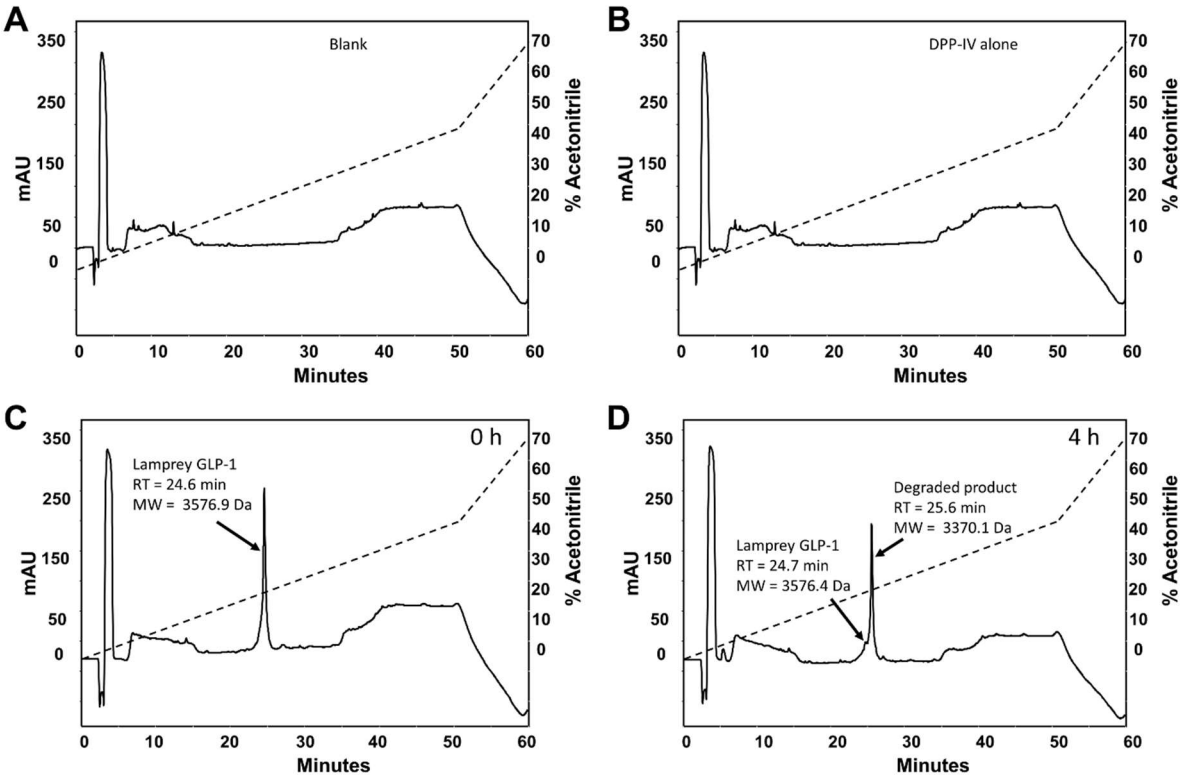

HPLC degradation study was performed with a Luna 5u C8 250x4.6mm column using gradients from 0% to 42% of acetonitrile over 50 min, and from 42% to 70% of acetonitrile over 15 min.

Figure 3.8 HPLC degradation profile of dogfish GLP-1 following incubation with DPP-IV for 0 and 4 hours.

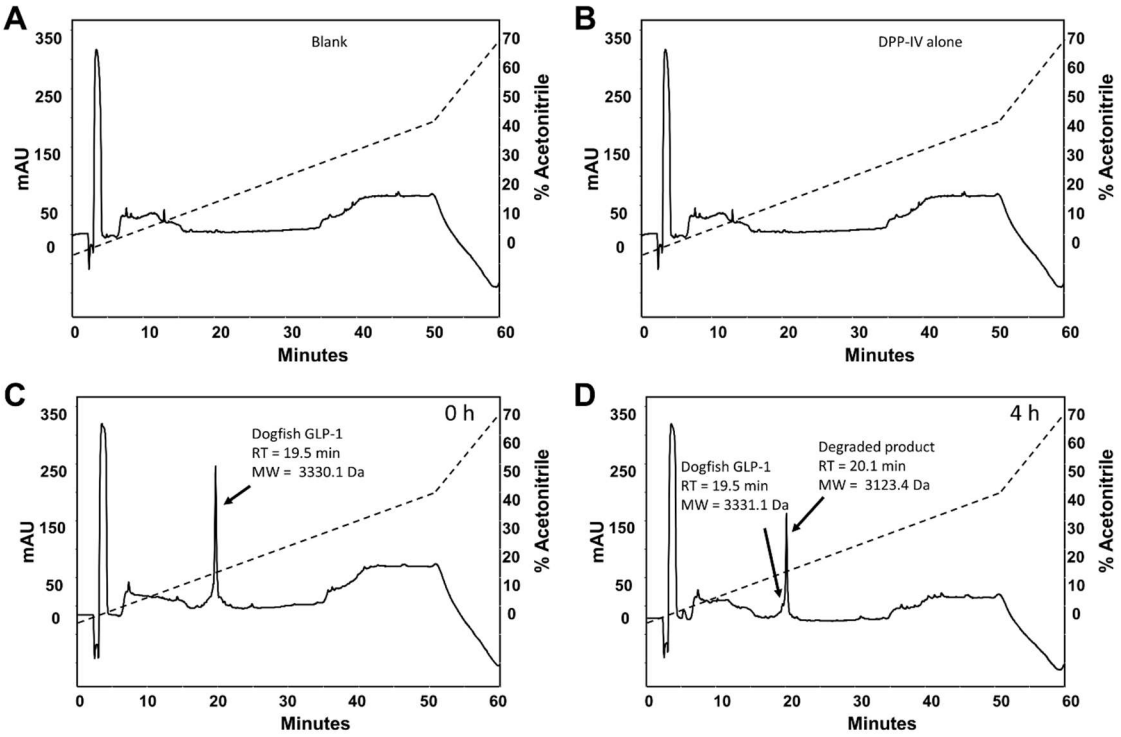

HPLC degradation study was performed with a Luna 5u C8 250x4.6mm column using gradients from 0% to 42% of acetonitrile over 50 min, and from 42% to 70% of acetonitrile over 15 min.

Figure 3.9 HPLC degradation profile of ratfish GLP-1 following incubation with DPP-IV for 0 and 4 hours.

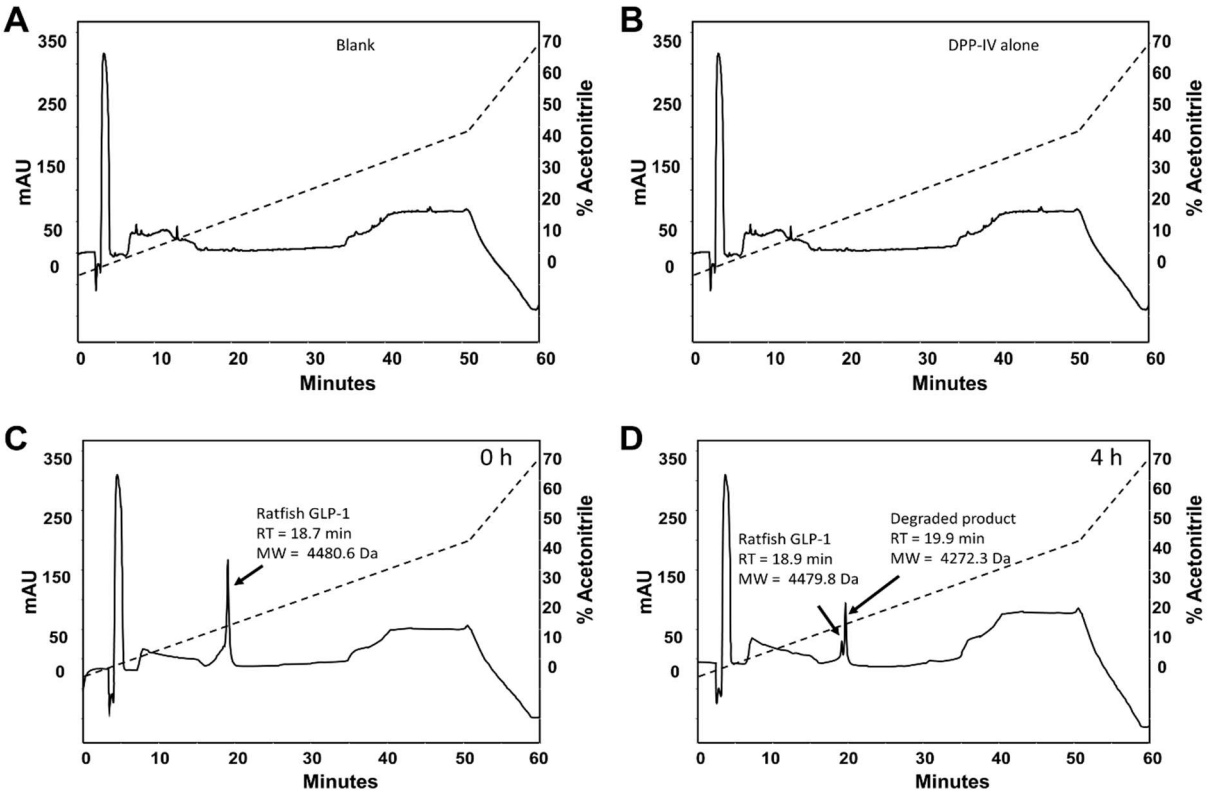

HPLC degradation study was performed with a Luna 5u C8 250x4.6mm column using gradients from 0% to 42% of acetonitrile over 50 min, and from 42% to 70% of acetonitrile over 15 min.

Figure 3.10 HPLC degradation profile of paddlefish GLP-1 following incubation with DPP-IV for 0 and 4 hours.

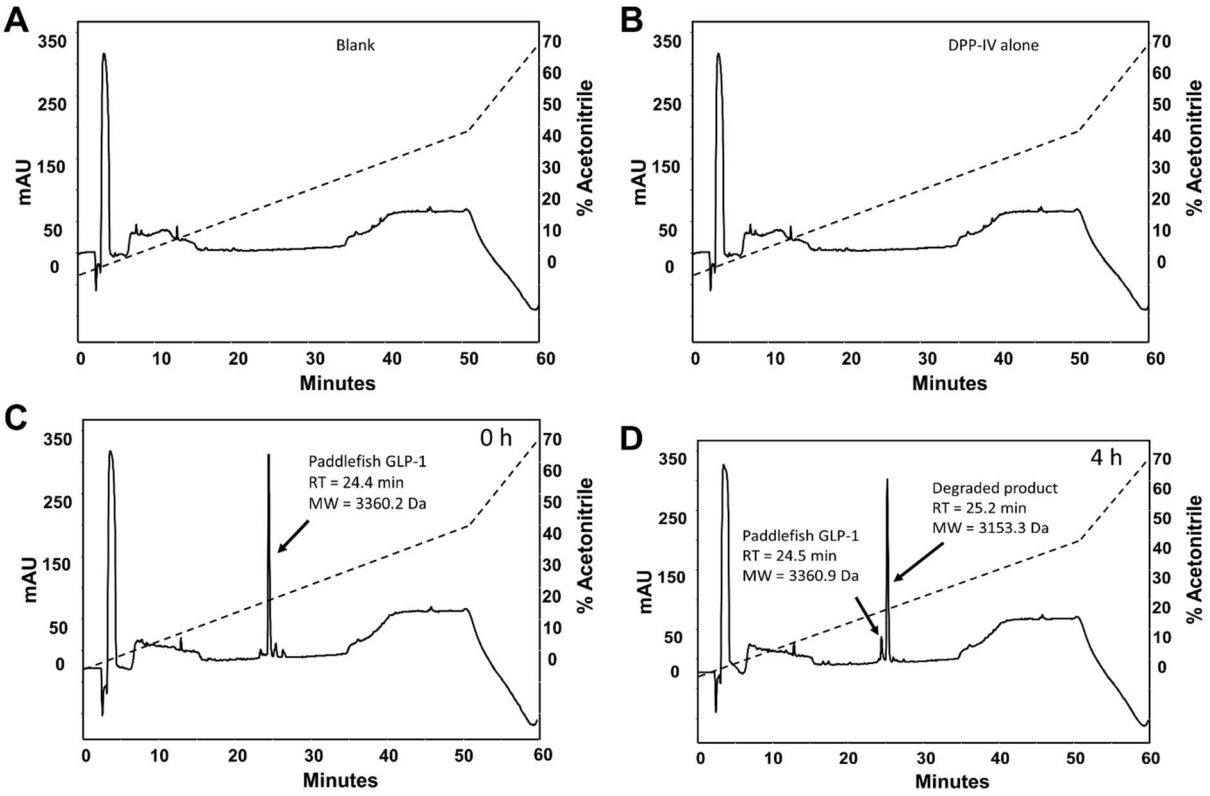

HPLC degradation study was performed with a Luna 5u C8 250x4.6mm column using gradients from 0% to 42% of acetonitrile over 50 min, and from 42% to 70% of acetonitrile over 15 min.

Figure 3.11 HPLC degradation profile of GLP-1 following incubation with DPP-IV for 0 and 4 hours.

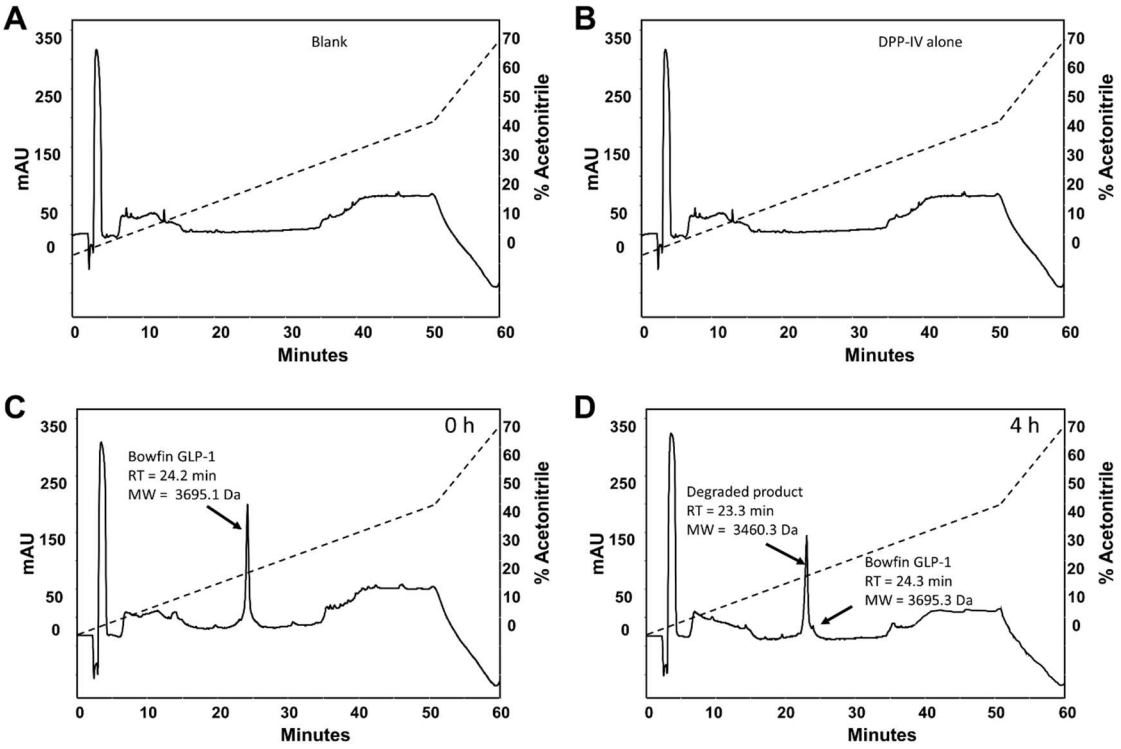

HPLC degradation study was performed with a Luna 5u C8 250x4.6mm column using gradients from 0% to 42% of acetonitrile over 50 min, and from 42% to 70% of acetonitrile over 15 min.

Figure 3.12 HPLC degradation profile of trout GLP-1 following incubation with DPP-IV for 0 and 4 hours.

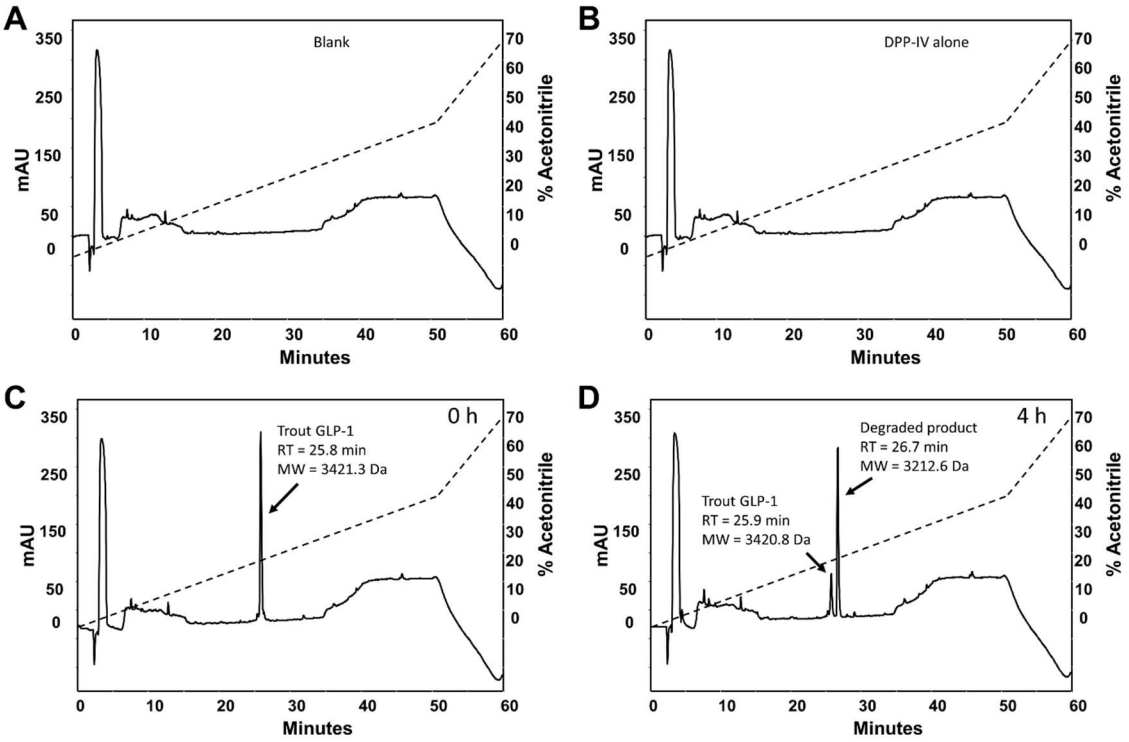

HPLC degradation study was performed with a Luna 5u C8 250x4.6mm column using gradients from 0% to 42% of acetonitrile over 50 min, and from 42% to 70% of acetonitrile over 15 min.

Figure 3.13 Effects of increasing concentrations of (A) lamprey GLP-1, (B) dogfish GLP-1, (C) ratfish GLP-1, (D) paddlefish GLP-1, (E) trout GLP-1, (F) bowfin GLP-1, (G) human GLP-1, and (H) human glucagon on insulin release from BRIN-BD11 rat clonal β-cells.

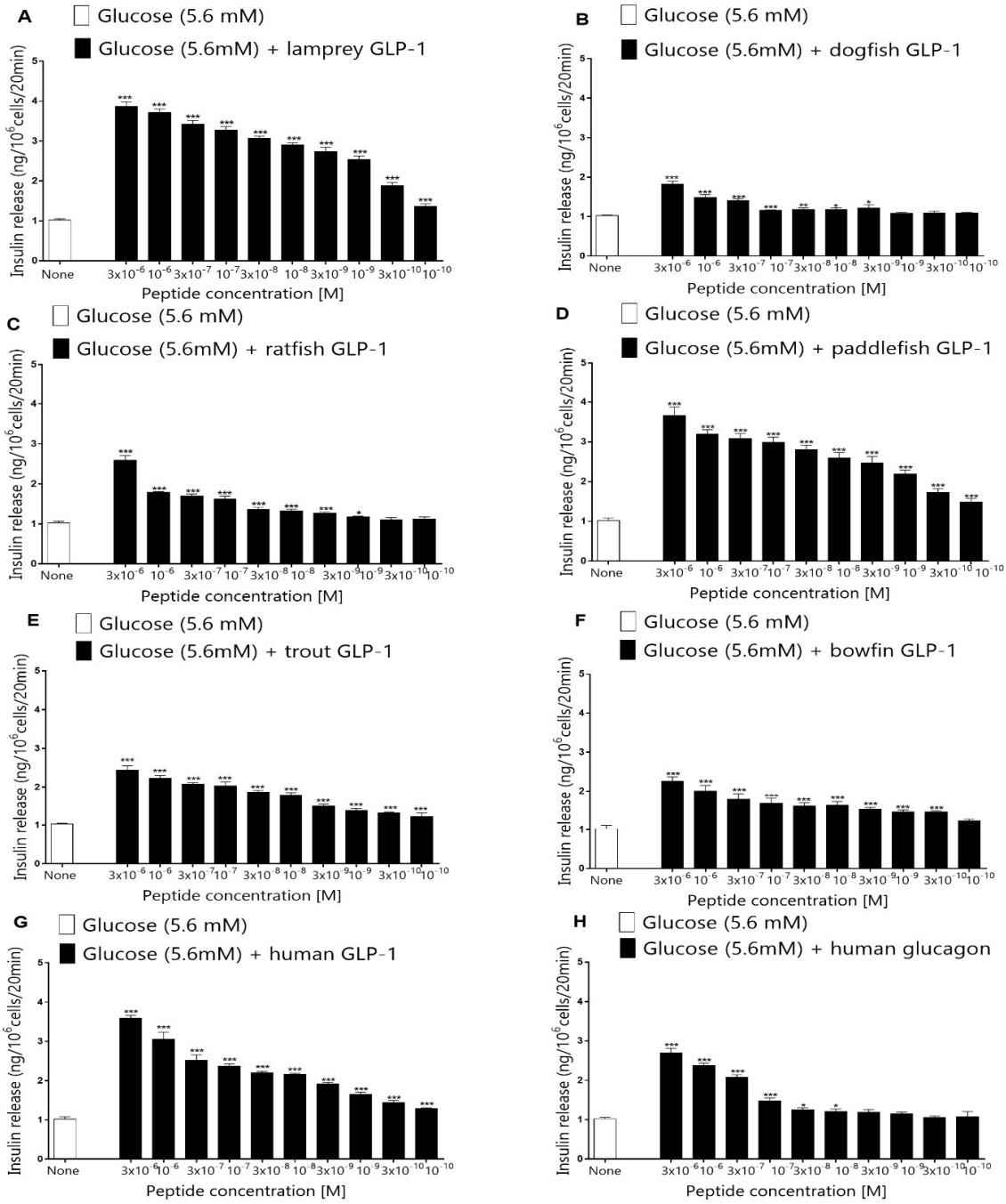

Values are mean ± S.E.M., n = 8. *P < 0.05, **P < 0.01, ***P < 0.001 compared to 5.6 mM glucose alone.

Figure 3.14 Effects of fish GLP-1 peptides at 10 nM and 1 µM concentrations on insulin release from 1.1 B4 human clonal β-cells.

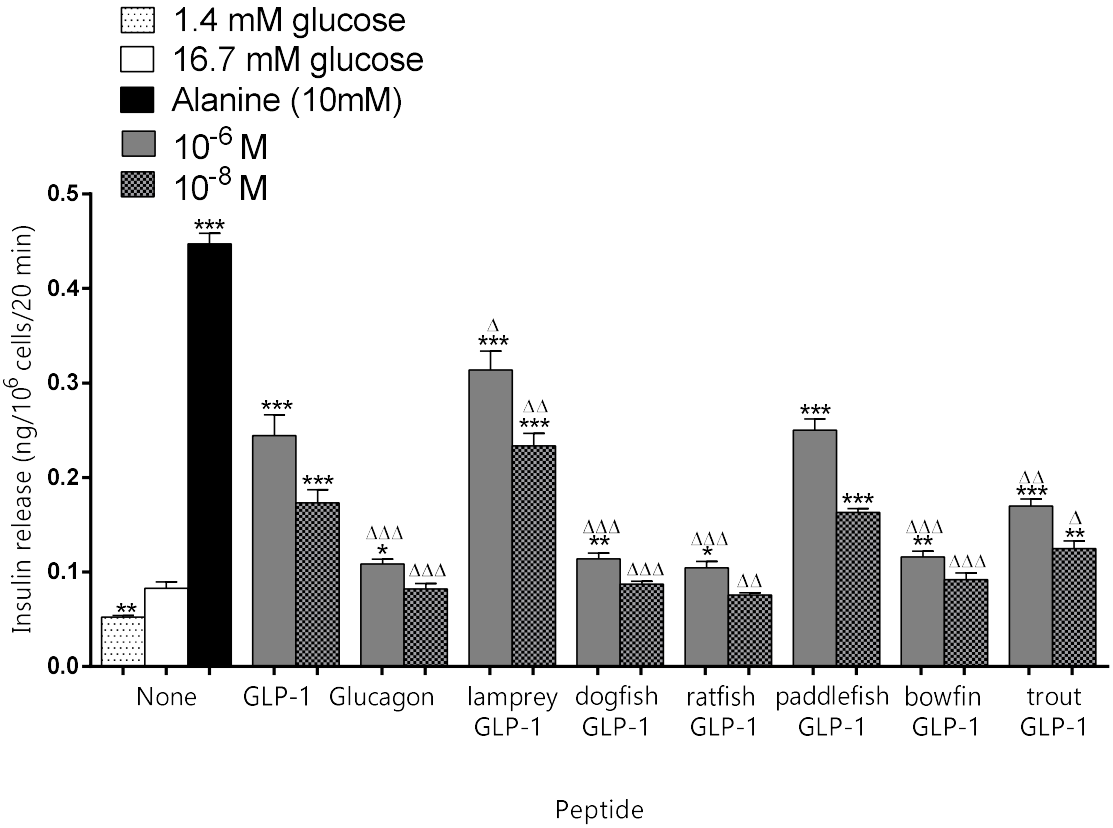

Values are mean ± S.E.M., $n = 8$ *P < 0.05, **P < 0.01, ***P < 0.001 compared to 16.7 mM glucose alone. $^{\Delta}$P < 0.05, $^{\Delta\Delta}$ P< 0.01, $^{\Delta\Delta\Delta}$ P< 0.001 compared with the response to human GLP-1.

Figure 3.15 Effects of fish GLP-1 peptides at 10 nM and 1 µM concentrations on insulin release from pancreatic islets isolated from NIH Swiss mice.

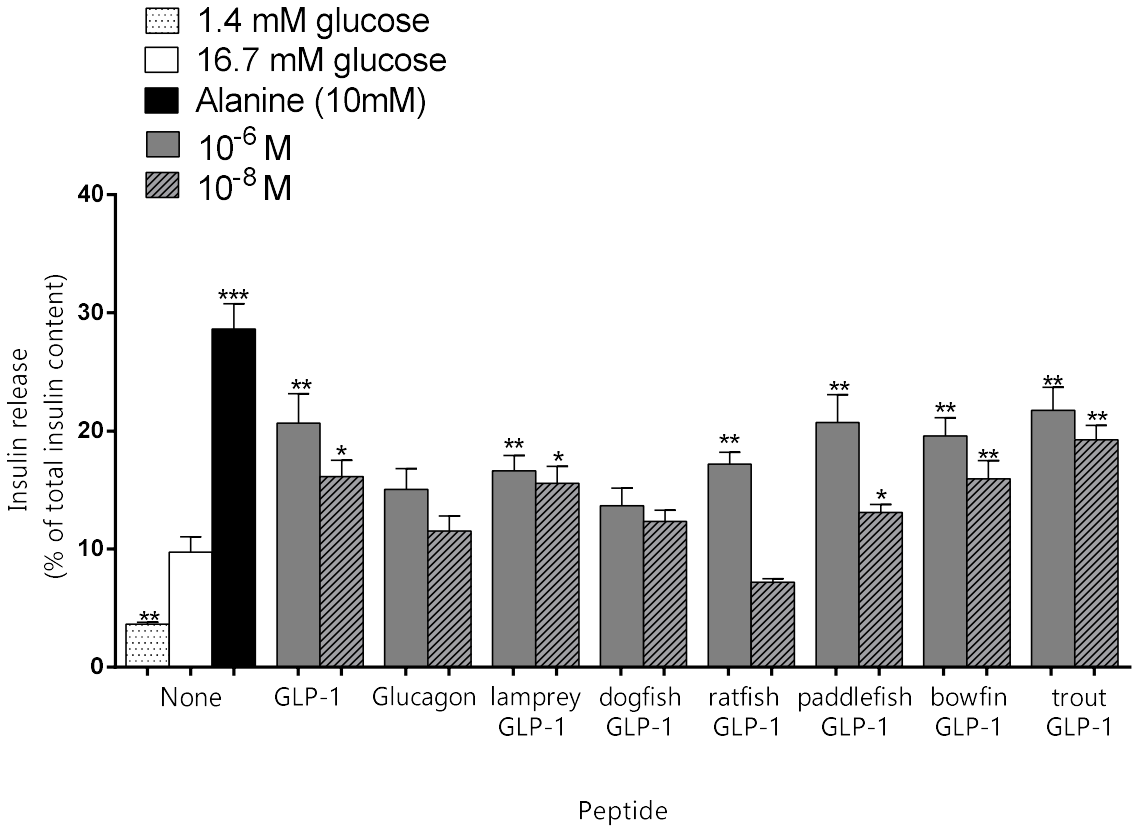

The values are mean ± SEM for n=4; *P < 0.05, **P < 0.01, ***P < 0.001 compared to 16.7mM glucose alone.

Figure 3.16 Effects of (A) the GLP-1 receptor antagonist, exendin-4(9-39), (B) the glucagon receptor antagonist [desHis1,Pro4,Glu9]glucagon amide and (C) the GIP receptor antagonist GIP(6-30)Cex-K40[Pal], on the ability of fish GLP-1 peptides (10^{-7} M) to stimulate insulin release from BRIN-BD11 cells.

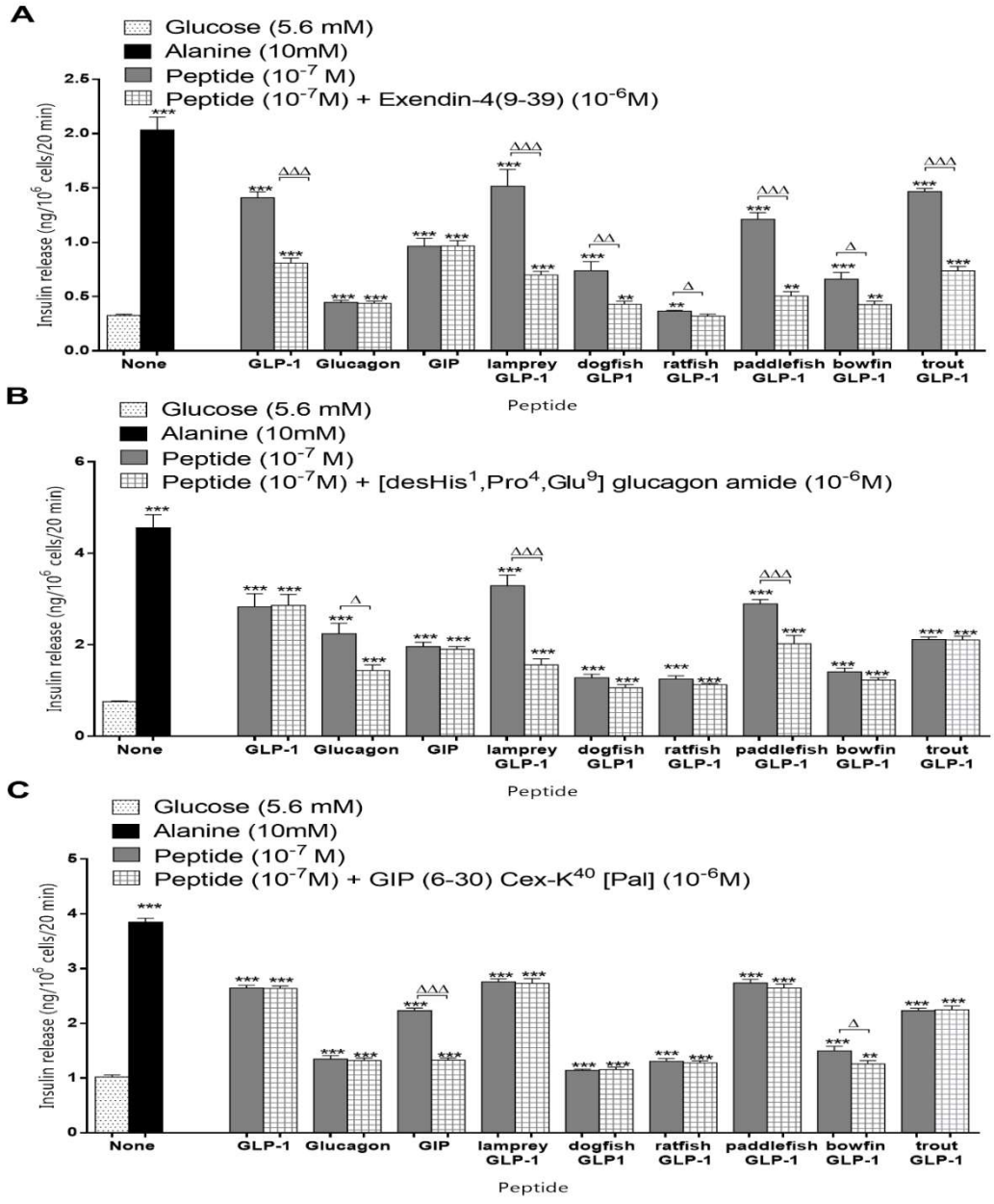

Values are mean ± S.E.M., n = 8 **P < 0.01, ***P < 0.001 compared with 5.6 mM glucose alone. $^{\Delta}$P < 0.05, $^{\Delta\Delta}$P < 0.01, $^{\Delta\Delta\Delta}$P < 0.001 compared with the effect in the presence of antagonist.

Figure 3.17 Effects of fish GLP-1 peptides (10^{-8} and 10^{-6} M) on cAMP production in (A) GLP1R-transfected CHL cells, and (B) GCGR-transfected HEK293 cells.

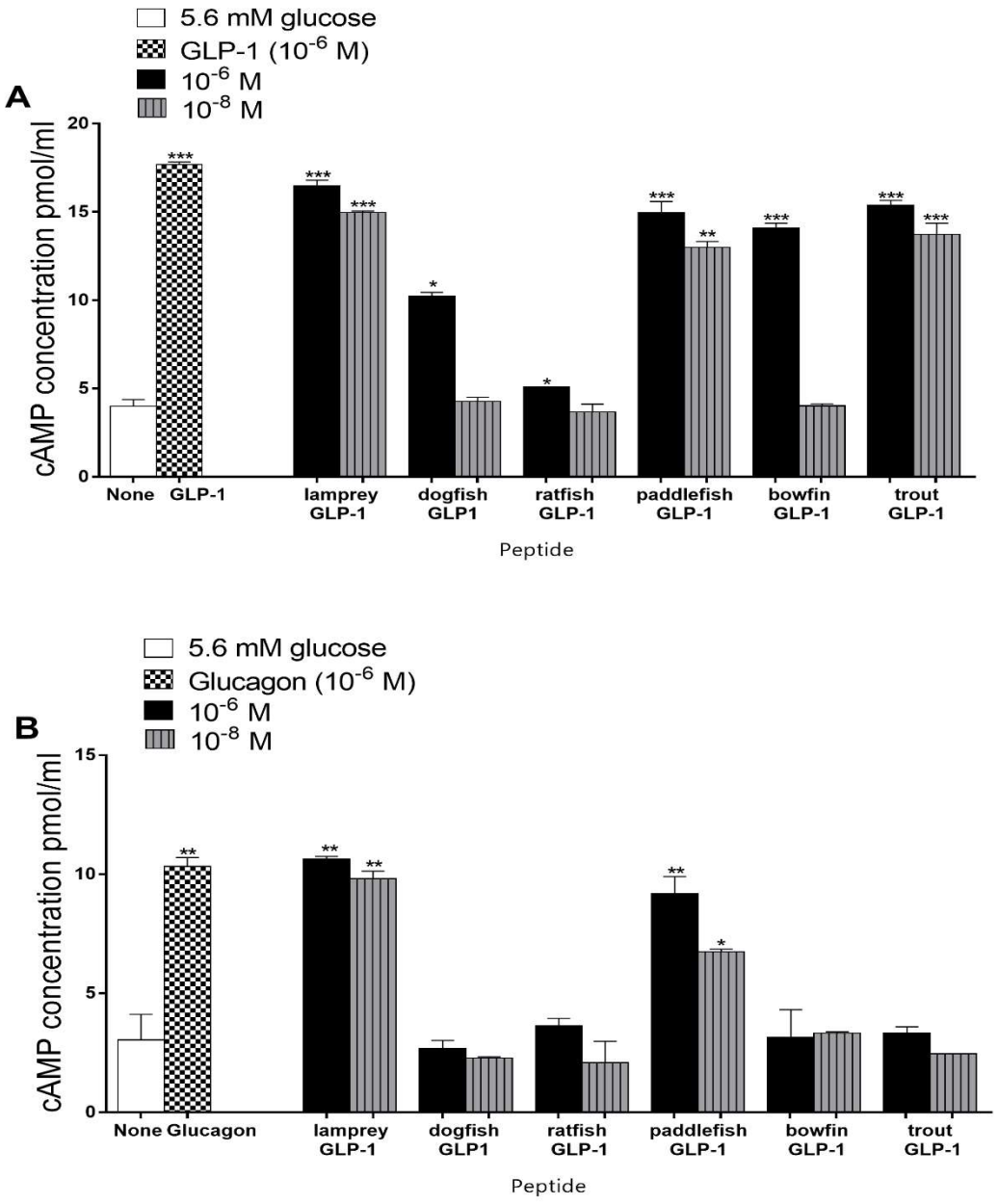

Values are mean ± S.E.M. for n = 4. *P < 0.05, ** P< 0.01 and ***P < 0.001 compared with 5.6 glucose.

Figure 3.18 Effects of fish GLP-1 peptides (10^{-8} and 10^{-6} M) on the rate of insulin release from (A) wild-type INS-1 cells, (B) CRISPR/Cas9-engineered GLP-1R knock-out cells, (C) CRISPR/Cas9-engineered GCGR knock-out cells and (D) CRISPR/Cas9-engineered GIPR knock-out cells.

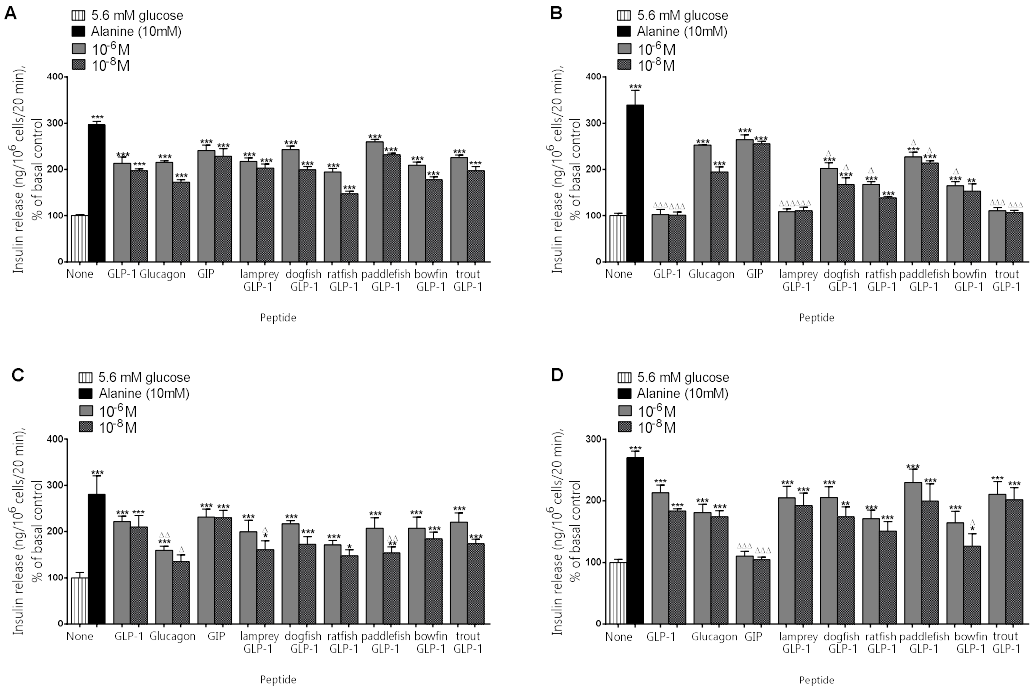

Values are mean ± S.E.M., $n = 8$, *P < 0.05, **P < 0.01 and ***P < 0.001 compared with 5.6 mM glucose alone. $^{\Delta}P < 0.05$, $^{\Delta\Delta}P < 0.01$, $^{\Delta\Delta\Delta}P < 0.001$ compared with effects in wild-type INS-1 cells.

Figure 3.19 Effects of acute administration of glucagon-related peptides (25 nmol/kg body weight) on blood glucose (panels A and C) and plasma insulin (panels B and D) concentrations in normal mice.

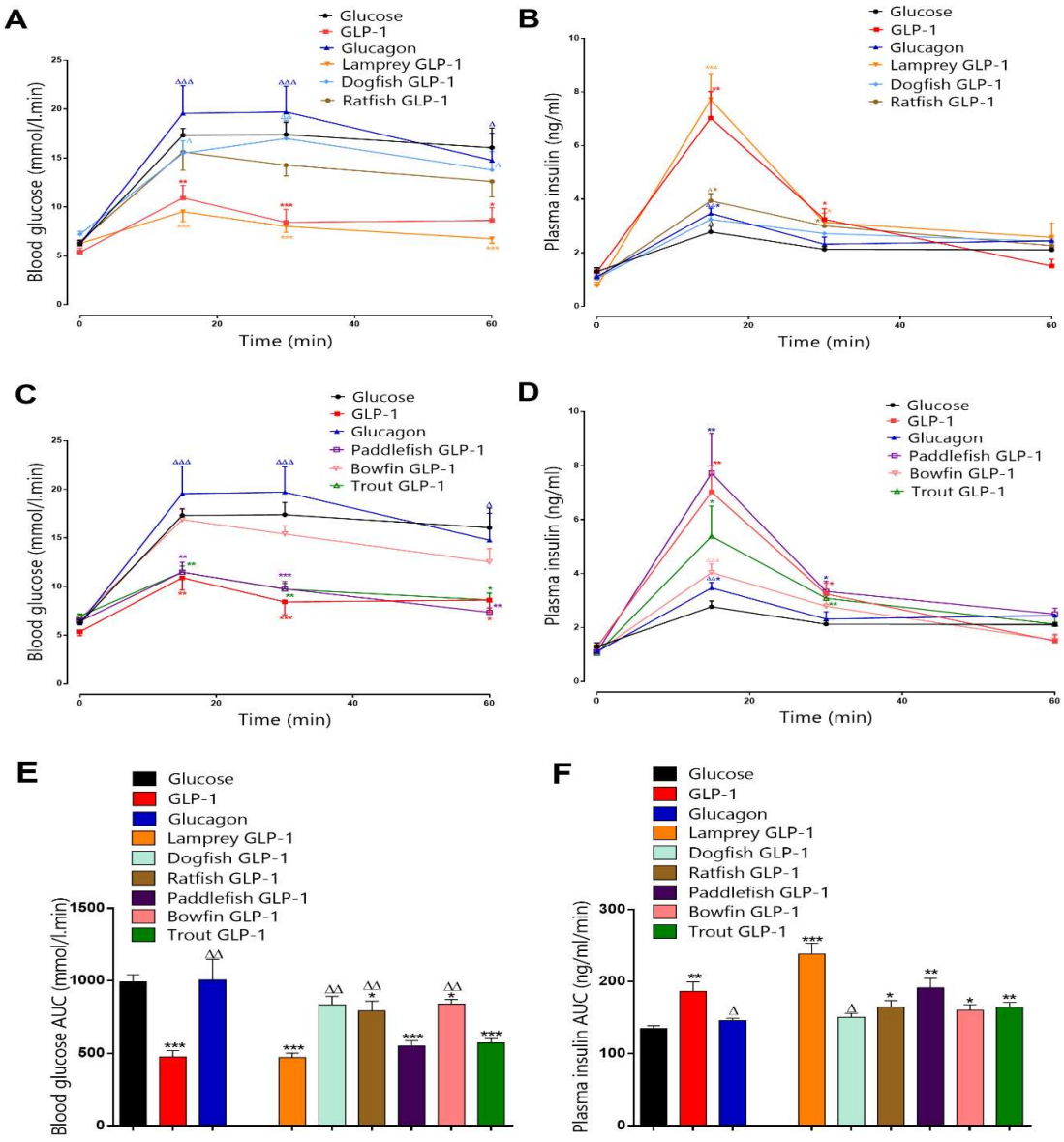

The integrated responses are shown in panels E and F. The values are mean ± S.E.M., n = 6. *P < 0.05, **P < 0.01 and ***P < 0.001 compared with glucose alone (18 mmol/kg body weight) and $^{\Delta}$ P < 0.05, and $^{\Delta\Delta}$P < 0.01 compared with the effect of GLP-1.

Figure 3.20 Effects of acute administration of fish GLP-1 peptides on blood glucose and plasma insulin concentrations in normal mice, 2 h post injection.

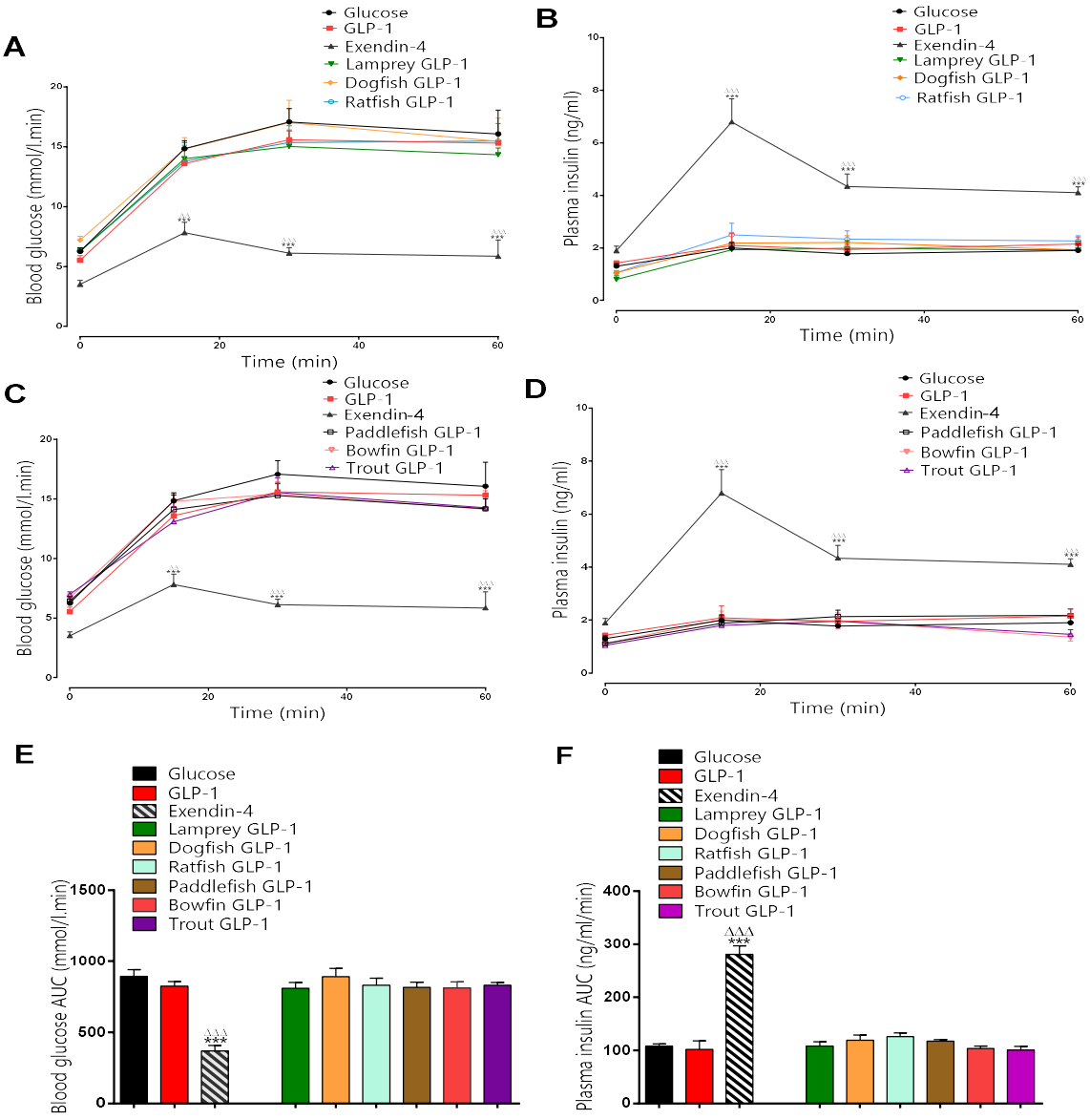

Blood glucose and plasma insulin were measured after intraperitoneal injection of glucose (18 mmol/kg body weight) 2 hours after intraperitoneal administration of 0.9% saline, exendin-4 and fish GLP-1 peptides (25 nmol/kg body weight). The integrated responses (area under the curve AUC) are shown in panels E and F. The values are mean ± SEM for n=6. **P<0.01 and ***P<0.001 compared to glucose alone; $^{\Delta\Delta}$ P<0.01 and $^{\Delta\Delta\Delta}$ P<0.001 compared to human GLP-1

Figure 3.21 Effects of fish GLP-1 peptides on cumulative food intake over 3 hours trained feeding in 12 h fasting normal mice.

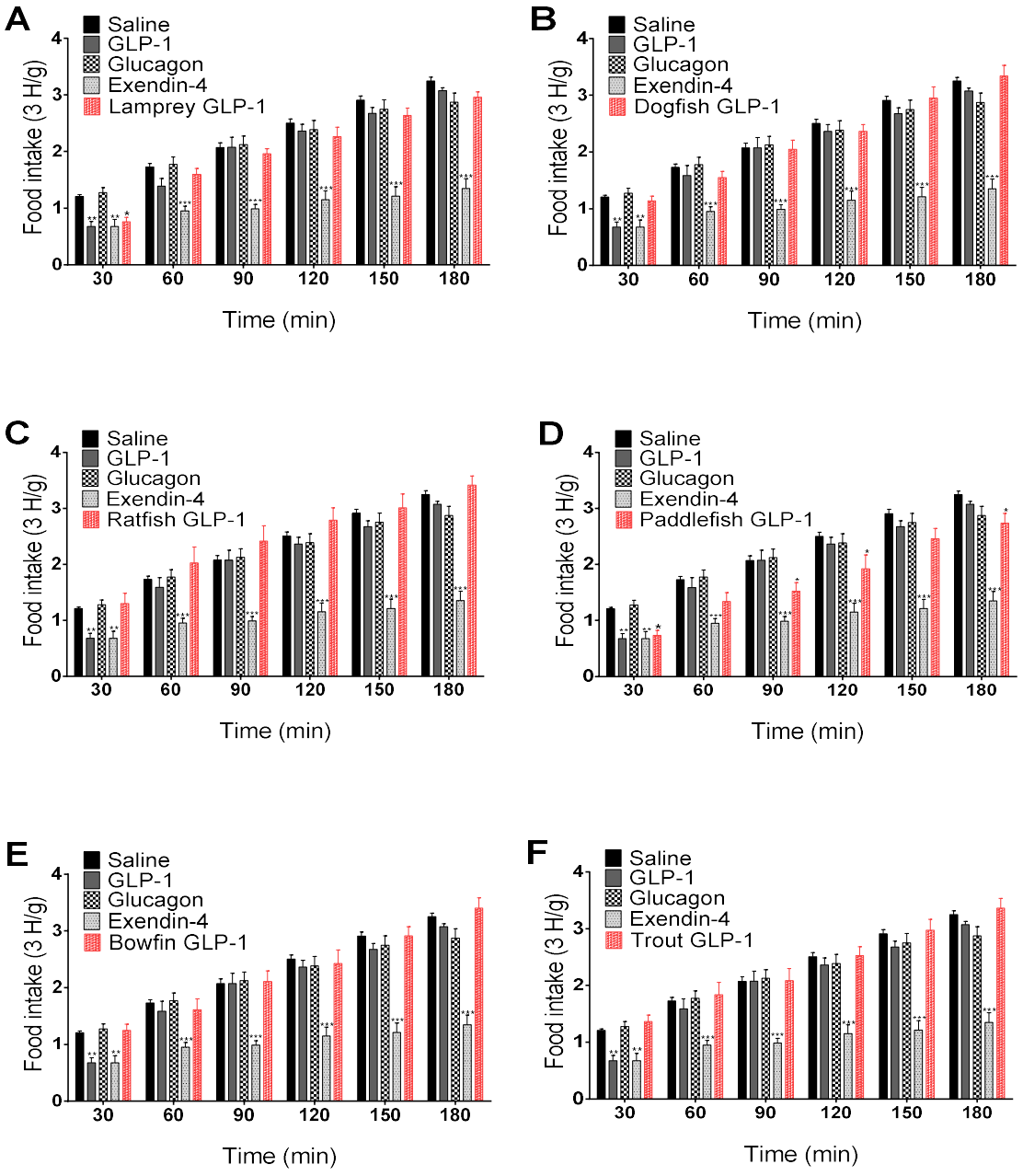

Cumulative food intake was measured after intraperitoneal administration of 50 nmol/kg peptides alongside 0.9% saline control. The values are mean ± SEM for n=8. *P<0.05, **P<0.01 and ***P<0.001 compared to saline control mice treated at the same time point.

Figure 3.22. A comparison of the primary structures of human GLP-1, glucagon, and GIP with the corresponding primary structures of exendin-4 and the fish GLP-1 peptides.

```
GLP-1             HAEGTFTSDVSSYLEGQAAKEFIAWLVKGR[a]
Exendin-4         HGEGTFTSDLSKQMEEEAVRLFIEWLKNGGPSSGAPPPS[a]
Glucagon          HSQGTFTSDYSKYLDSRRAQDFVQWLMNT
GIP               YAEGTFISDYSIAMDKIHQQDFVNWLLAQKGKKNDWKHNITQ
Lamprey GLP-1     HADGTFTNDMTSYLDAKAARDFVSWLARSDKS
Dogfish GLP-1     HAEGTYTSDVDSLSDYFKAKRFVDSLKSY
Ratfish GLP-1     HADGIYTSDVASLTDYLKSKRFVESLSNYNRKQNDRRM
Paddlefish GLP-1  HADGTYTSDASSFLQEQAARDFISWLKKGQ
Bowfin GLP-1      YADAPYISDVYSYLQDQVAKKWLKSGQDRRE
Trout GLP-1       HADGTYTSDVSTYLQDQAAKDFVSWLKSGRA

Glucagon          HSQGTFTSDYSKYLDSRRAQDFVQWLMNT
GLP-1             HAEGTFTSDVSSYLEGQAAKEFIAWLVKGR[a]
Exendin-4         HGEGTFTSDLSKQMEEEAVRLFIEWLKNGGPSSGAPPPS[a]
GIP               YAEGTFISDYSIAMDKIHQQDFVNWLLAQKGKKNDWKHNITQ
Lamprey GLP-1     HADGTFTNDMTSYLDAKAARDFVSWLARSDKS
Dogfish GLP-1     HAEGTYTSDVDSLSDYFKAKRFVDSLKSY
Ratfish GLP-1     HADGIYTSDVASLTDYLKSKRFVESLSNYNRKQNDRRM
Paddlefish GLP-1  HADGTYTSDASSFLQEQAARDFISWLKKGQ
Bowfin GLP-1      YADAPYISDVYSYLQDQVAKKWLKSGQDRRE
Trout GLP-1       HADGTYTSDVSTYLQDQAAKDFVSWLKSGRA

GIP               YAEGTFISDYSIAMDKIHQQDFVNWLLAQKGKKNDWKHNITQ
GLP-1             HAEGTFTSDVSSYLEGQAAKEFIAWLVKGR[a]
Exendin-4         HGEGTFTSDLSKQMEEEAVRLFIEWLKNGGPSSGAPPPS[a]
Glucagon          HSQGTFTSDYSKYLDSRRAQDFVQWLMNT
Lamprey GLP-1     HADGTFTNDMTSYLDAKAARDFVSWLARSDKS
Dogfish GLP-1     HAEGTYTSDVDSLSDYFKAKRFVDSLKSY
Ratfish GLP-1     HADGIYTSDVASLTDYLKSKRFVESLSNYNRKQNDRRM
Paddlefish GLP-1  HADGTYTSDASSFLQEQAARDFISWLKKGQ
Bowfin GLP-1      YADAPYISDVYSYLQDQVAKKWLKSGQDRRE
Trout GLP-1       HADGTYTSDVSTYLQDQAAKDFVSWLKSGRA
```

Sequence similarities to the human peptides are highlighted in grey. [a] denotes C-terminal α-amidation.

Chapter 4

Acute *in vitro* and *in vivo* activity studies of glucagon from phylogenetically ancient fish and a teleost with dual receptor agonistic properties

4.1 Summary

The insulinotropic and antihyperglycaemic actions of glucagon from the sea lamprey (Petromyzontiformes), paddlefish (Acipenseriformes) and trout (Teleostei) and oxyntomodulin from dogfish (Elasmobranchii) and ratfish (Holocephali) are compared with those of human glucagon and GLP-1 in mammalian test systems**.** The peptides were degraded by DPP-IV enzyme after 4 hours of incubation with the similar cleavage site to that of human glucagon. All fish peptides produced concentration-dependent stimulation of insulin release from BRIN-BD11 rat and 1.1 B4 human clonal β-cells and isolated mouse islets. Paddlefish glucagon was the most potent and effective peptide. The insulinotropic activity of paddlefish glucagon was significantly decreased after incubating BRIN-BD11 cells with the GLP1R antagonist, exendin-4(9-39) and the GCGR antagonist [desHis1,Pro4-Glu9] glucagon amide but GIPR antagonist, GIP(6-30)Cex-K^{40}[Pal] was without effect. Paddlefish glucagon (10 nM and 1 μM) produced significant increases in cAMP concentration in Chinese hamster lung (CHL) cells transfected with GLP1R and human embryonic kidney (HEK293) cells transfected with GCGR. The insulinotropic activity of the peptide was attenuated in CRISPR/Cas9-engineered GLP1R_knock-out INS-1 cells and attenuated in INS-1 GCG receptor knock-out cells but not in GIPR knock-out cells. Intraperitoneal administration of all fish peptides, except ratfish oxyntomodulin, to mice together with a glucose load produced significant decreases in plasma glucose concentrations and paddlefish glucagon produced a greater release of insulin compared with GLP-1. Paddlefish glucagon exhibited glucose lowering activity when administered 2 hours prior to a glucose load and was effecting in suppressing appetite in normal mice.

Paddlefish glucagon shares the sequences Glu^{15}-Glu^{16} and Glu^{24}-Trp^{25}-Leu^{26}-Lys^{27}-Asn^{28}-Gly^{29} with the potent GLP1R agonist, exendin-4 so may be regarded as a naturally occurring, dual-agonist hybrid peptide that may serve as a template design of new drugs for type 2 diabetes therapy.

4.2 Introduction

Patients with obesity-related diseases such as Type 2 diabetes mellitus (T2DM) often cannot be treated effectively with a single pharmaceutical agent (Bailey et al. 2018). The therapeutic potential of unimolecular dual- and triple-agonist peptides based upon the primary structures of the incretin hormones glucagon-like peptide-1 (GLP-1) and glucose-dependent insulinotropic peptide (GIP) together with glucagon is becoming increasingly apparent. Dual agonist peptides that target (A) the GLP-1 receptor (GLP1R) and the glucagon receptor (GCRG), (B) the GLP1R and the GIP receptor (GIPR), and (C) the GLP1R, GCGR, and GIPR are currently in development (reviewed in Brandt et al. 2018 and Irwin et al. 2015). Similarly, an enzymatically stable GIP/xenin hybrid peptide has been shown to enhance β-cell function and improves glucose homeostasis in mice that have been rendered insulin resistant and glucose intolerant by being fed a high fat diet (Hasib et al. 2018). A major advantage of administration of these multi-agonist peptides over their constituent monotherapies is their improved actions on blood glucose control, appetite, suppression, weight loss and hyperlipidemia/ hypercholestrolemia (Brandt et al. 2018 and Sánchez-Garrido et al. 2017).

An alternative strategy to the use of synthetic hybrid peptides is to exploit the potential of naturally occurring dual agonist peptides. Oxyntomodulin is a C-terminally extended form of glucagon that was first identified as an impurity in a commercially

available preparation of bovine/porcine glucagon (Tager et al. 1973) and is released from L-cells in the intestine in response to nutrients (Blache et al. 1988). A specific receptor for oxyntomodulin has not been identified but the peptide will activate both the GCGR and the GLP1R, although with an affinity that is appreciably less than glucagon and GLP-1 respectively, so that the peptide will stimulate insulin release and improve glucose tolerance when administered to mice (reviewed in Pocai et al. 2012 and Holst et al. 2018). Oxyntomodulin has received particular attention because of its ability at pharmacological doses to inhibit appetite and food intake (Cohen et al 2003). A GIP-oxyntomodulin hybrid peptide acting through GIP, glucagon and GLP-1 receptors exhibits promising weight reducing and anti-diabetic properties during long-term administration to high fat fed mice (Bhat et al. 2013). Recently it has been shown that glucagon from the European common dogfish dogfish *Scyliorhinus canicula* (Elasmobranchii) (Conlon et at. 1994) acts as a dual agonist at the glucagon and GLP-1 receptors and peptidase-resistant analogues showed potent insulin-releasing activity *in vitro* (O'Harte et al. 2016) and antihyperglycaemic activity in mice (O'Harte et al. 2016a). Similarly, the insulinotropic and glucose-lowering actions of zebrafish GIP in mice involve interaction with both the GLP-1 and GIP receptors (Graham et al. 2018). Glucagon has been isolated from the principal islets (Brockmann bodies) of a wide range of teleost species and the genes encoding proglucagon from several teleosts have been characterized (reviewed in Irwin et al. 2018). The peptide has also been purified from several phylogenetically more ancient fishes. Glucagon has been isolated from the islet organ of the lampreys *Petromyzon marinus*, *Lampetra fluviatilis,* and *Geotria australis* (Petromyzontiformes) [reviewed in Wang et al. 1999)] and from the pancreas of the ray *Torpedo marmorata* (Elasmobranchii), and the primitive Actinopterygian (ray-finned) fish: the N. American paddlefish *Polyodon spathula* (Polyodontidae) and

the sturgeons *Huso dauricus* and *Scaphirhynchus albus* (Acipenseriformes), the bichir *Polypterus senegalis* (Polypteriformes), the alligator gar *Lepisosteus spatula* (Lepisosteiformes), and the bowfin *Amia calva* (Amiiformes) (reviewed in Conlon et al. 1993). Components comprising glucagon extended from its COOH-terminal region by additional amino acid residues that may represent orthologs of mammalian oxyntomodulin have been purified from the pancreata of *S. canicula* (Conlon et al. 1994) and the Pacific ratfish *Hydrolagus colliei* (Holocephali) (Conlon et al. 1989). It is estimated that the Petromyzontiformes diverged from the line of evolution leading to mammals between 500 and 550 million years ago (MYA) and the Elasmobranchii diverged around 420 MYA. The divergence of the Holocephali and the Elasmobranchii is ancient (410 MYA), and the Polyodontidae are believed to have diverged from the Acipenseriformes approximately 180 MYA (Craw et al. 2012).

The biological activities and physiological roles of the proglucagon-derived peptides in the ancient fishes have not been investigated but, in teleosts, the responsiveness of hepatocytes to glucagon is limited to high concentrations while physiological concentrations of GLP-1 effectively regulate hepatic metabolism by stimulating gluconeogenesis and glycogenolysis. In contrast to mammals, GLP-1 shows very weak insulinotropic activity in teleosts (Plisetskaya et al. 1996). In the light of the promising anti-diabetic effects of dogfish glucagon (O'Harte et al, 2016 and O'Harte et al, 2016a), the aim of the present study is to compare the insulinotropic and antihyperglycemic properties of synthetic replicates of glucagons from the sea lamprey *Petromyzon marinus* (Conlon et al, 1993), paddlefish *Polyodon spathula* (Conlon et al, 1994), and rainbow trout *Onchorynchus mykiss* (Irwin et al. 1995) and oxyntomodulins from dogfish *S. canicula* (Conlon et al, 1994) and ratfish *Hydrolagus colliei* (Conlon et al. 1989) with human glucagon and GLP-1. Effects *in vitro* were

determined using established insulin-producing cell lines and isolated mouse islets and their glucose-lowering and insulin stimulating actions *in vivo* were assessed following acute administration to NIH Swiss mice. The primary structures and molecular masses of the peptides used in this study are shown in Table 4.1).

4.3 Materials and Methods

4.3.1 Chemical Reagents and Peptides

All fish glucagon peptides were obtained from EZBiolab Inc. (Carmel, IN, USA) as previously described in Section 2.1.1). Synthetic human glucagon, human GLP-1, human GIP and exendin-4 peptides were obtained and processed as described previously (Section 2.1.1). Peptides purified and subsequently characterized using MALDI-TOF MS (Section 2.2). The primary structures and molecular masses of the peptides used in this study are shown in Table 2.2 and Table 4.1.

4.3.2 Assessment of metabolic stability of fish glucagon peptides

Effect of DPP-IV on fish glucagon peptide stability was assessed as previously described in Section 2.3.

4.3.3 *In vitro* insulin release studies using BRIN-BD11 and 1.1B4 cells

In vitro insulin secretory studies were performed using BRIN-BD11 (McClenaghan et al., 1996) and 1.1B4 cells (McCluskey et al. 2011) as previously described (, Section 2.5.1 and Section 2.5.3). In a second series of experiments, the effects of 1 μM concentrations of the (A) GLP-1 receptor antagonist, exendin-4(9-39 (Thorens et al. 1993), (B) glucagon receptor antagonist, [desHis1,Pro4-Glu9] glucagon amide (O'Harte et al., 2013), and (C) glucose-dependent insulinotropic peptide (GIP)

receptor antagonist, GIP(6-30)Cex-K^{40}[Pal] (Pathak et al., 2015) on the insulin-releasing activity of the peptides (0.1 μM) were studied by incubating BRIN-BD11 cells and analysed by RIA cells as previously described (Section 2.5.2 and Section 2.5.7).

4.3.4 Insulin release studies using isolated mouse islets

Effect of fish glucagon peptides on *ex-vivo* insulin secretion were assessed using pancreatic islets from adult, male National Institutes of Health (NIH) Swiss mice (Harlan Ltd, Bicester, UK) as previously described (Section 2.5.5).

4.3.5 Effects on cAMP production.

The effect of cAMP production from Chinese hamster lung (CHL) cells transfected with the human GLP-1 receptor (GLP1R) (Thorens et al., 1993) and human embryonic kidney (HEK293) cells transfected with the human glucagon receptor (GCGR) (Ikegami et al., 2001) was assessed using a Parameter cAMP assay kit (R&D Systems, Abingdon, UK) as outlined in Section 2.6.

4.3.6 Insulin release studies using CRISPR/Cas9-engineered INS-1 cells

In vitro receptor activation studies were performed using wild-type INS-1 832/3 rat clonal pancreatic β-cells and CRISPR/Cas9-engineered cells with knock-out of the knock-out of the GLP-1 receptor (GLP-1 KO), glucagon receptor (GCG KO) and GIP receptor (GIP KO) (Naylor et al. 2016) as described in Section 2.5.4.

4.3.7 In vivo insulin release and glucose-lowering effects of peptides

Acute and persistent *in vivo* studies were carried out using male National Institutes of Health (NIH) Swiss mice as previously described (Sections 2.8.1.1, 2.8.2.1, 2.8.2.3 and 2.8.2.5). For acute IPGTT, blood glucose and plasma insulin were measured

immediately prior to (t = 0) and 15, 30 and 60 min after intraperitoneal administration of glucose alone (18 mmol/kg of body weight) or in combination with test peptides (each at 25 nmol/kg bw) in overnight fasted mice. In separate series of experiments, overnight fasted animals received either test peptides (each at 25 nmol/kg of body weight) or saline vehicle 2 hours before an intraperitoneal glucose administration (18 mmol/kg bw) and blood glucose and plasma insulin measured at 15, 30 and 60 min post glucose injection as detailed in Section 2.8.5.

4.3.8 Acute food consumption studies

Normal male TO mice were used in food consumption study as previously described (Section 2.8.2.6). Animals were administrated intraperitoneal injections of either saline solution or peptides (50 nmol/kg) prior to receiving free access to normal chow for 180 mins.

4.3.9 Biochemical analysis

Blood was collected from the tail vein of conscious mice and analysed immediately using the Ascenacia Counter Blood Glucose Meter (Bayer, Newbury, UK). Plasma for insulin was collected, stored and assayed as described in Section 2.8.2.5.

4.3.10 Statistical analysis

Data were compared using unpaired Student's t-test (non-parametric, with two-tailed P values and 95% confidence interval) and one-way ANOVA with Bonferroni post-hoc test using GraphPad PRISM (Version 5.0 San Diego, California). Area under the curve (AUC) analysis was performed using the trapezoidal rule with baseline correction. Data are presented as mean ± S.E.M where the comparison was considered to be significantly different if $P < 0.05$.

4.4 Results

4.4.1 Purification and confirmation of molecular masses by MALDI-TOF MS

Following RP-HPLC on a C-8 semi-preparative column the main peaks of peptides were collected as represented in Figure 4.1. Experimental masses detected for each peptide by MALDI-TOF MS (Figure 4.2) corresponded very closely to their theoretical masses as shown in Table 4.1.

4.4.2 Fish glucagon peptides stability

All peptides were degraded rapidly into 2 major fractions after 4 hours incubation with DPP-IV (Figures 4.3-4.7) in a similar pattern with human glucagon molecule (Figure 3.5). Interestingly, paddlefish glucagon was more stable compared to the other glucagon-related peptides investigated in this study and was degraded only by 14% (Table 4.2). The molecular masses of the fractions corresponded to the remaining intact peptide and its truncated product cleaved at position 2. The calculated percentage of degradation of each peptide is shown in Table 4.2.

4.4.3. *In vitro* insulin release studies

As illustrated in Table 4.3, the rate of insulin release from BRIN-BD11 rat clonal β-cells in the presence of 5.6 mM glucose alone was 1.02 ± 0.02 ng/10^6cells/20 min which increased to 2.4 ± 0.2 ng/10^6cells/20 min during incubation with GLP-1 (0.1 μM; $P < 0.001$). The effects of incubation with increasing concentrations of the fish glucagon-related peptides and human glucagon on insulin release are shown in Figure 4.8. All peptides produced significant and concentration-dependent increases the rate of insulin release compared with the rate in the presence of 5.6 mM glucose alone. As shown in Table 4.3, the most potent peptide was paddlefish glucagon produced a significant stimulation of insulin release ($P < 0.05$) from BRIN-BD11 cells at a

threshold concentration of 30 pM compared with 10 pM for human GLP-1 and 10 nM for human glucagon. Paddlefish glucagon was the most effective peptide producing a response at 3 μM concentrations that was not significantly different from that of GLP-1.

The rate of insulin release from 1.1B4 human clonal β-cells in the presence of 16.7 mM glucose alone was 0.08 ± 0.01 ng/10^6cells/20min. Incubation with all fish peptides significantly ($P < 0.001$) stimulated insulin release at concentrations of 1 μM compared with the rate in the presence of 16.7 mM glucose alone (Figure 4.9 and Table 4.4). Only paddlefish glucagon ($P < 0.001$) and dogfish oxyntomodulin ($P < 0.05$) produced a significant increase at 10 nM concentration. The rates of insulin release elicited by 1 μM concentrations of glucagons from lamprey and paddlefish and by dogfish oxyntomodulin were not significantly different to that produced by human GLP-1.

The rate of insulin release from mouse islets incubated for 60 min with 16.7 mM glucose was 9.7 ± 1.3 % of the total insulin content. Incubation with all peptides, except human and trout glucagon, at 1μM concentrations significantly increased the rate of insulin release compared with the rate with 16.7 mM glucose alone (Figure 4.10). Lamprey glucagon and dogfish oxyntomodulin were also effective at 10 nM concentration. The stimulatory effects of 1 μM concentrations of glucagon from lamprey and paddlefish and dogfish oxyntomodulin on insulin release were not significantly different from the effect produced by 1 μM GLP-1 (Figure 4.10 and Table 4.5).

4.4.4 Receptor antagonist studies

The *in vitro* insulinotropic activities of all peptides, except trout and human glucagon and GIP, were significantly decreased when BRIN-BD11 cells were co-incubated with

the GLP-1 receptor antagonist, exendin-4(9-39) (Figure 4.11 A). Co-incubation with the glucagon receptor antagonist [desHis1,Pro4-Glu] -glucagon amide significantly attenuated the action of all peptides except ratfish glucagon, GLP-1 and GIP (Figure 4.11 B). Human GIP was the only peptide whose stimulatory effect on insulin release was attenuated by the GIP receptor antagonist, GIP(6-30)Cex-K^{40}[Pal] (Figure 4.11 C and Table 4.6).

4.4.5 Effect of fish glucagon-related peptides on cAMP production

All peptides, except trout glucagon, at a concentration of 1 μM significantly stimulated cAMP production in CHL cells transfected with the human GLP-1 receptor (GLP1R) (Figure 4.12 A). Significant stimulation of cAMP production in HEK293 cells transfected with the human glucagon receptor (CGCR) was observed after incubating the cells with all peptides at 1 μM concentration except ratfish oxyntomodulin (Figure 4.12 B and Table 4.7).

4.4.6 Insulin release studies using CRISPR/Cas9-engineered INS-1 cells

Incubation of wild-type INS-1 cells with glucagon, GLP-1, GIP, and all fish peptides (10 nM and 1 μM) significantly increased the rate of insulin release compared with the rate in the presence of 5.6 mM glucose alone (Figure 4.13 A). The stimulatory effect on insulin release in response to incubations with lamprey glucagon, dogfish oxyntomodulin, and GLP-1 (10 nM and 1 μM) was abolished in the GLP-1 KO cells and the responses to paddlefish glucagon and ratfish oxyntomodulin were significantly attenuated compared with the effects in wild-type INS-1 cells (Figure 4.13 B and Table 4.8). Moreover, the rates of insulin release in response to human glucagon and glucagon-related fish peptides except ratfish oxyntomodulin were significantly attenuated (Figure 4.13 C and Table 4.8). In contrast, the insulin release from GIP KO

cells was significantly less that from the wild-type INS-1 cells only in the case of incubations with 10 nM and 1 μM GIP (Figure 4.13 C and Table 3.8).

4.4.7 *In vivo* insulin release studies

Acute and persistent *in vivo* effects of peptides are presented in Figure 4.14-4.15 and Table 4.9). Blood glucose concentrations of overnight fasted NIH Swiss mice were significantly lowered at time points 15, 30 and 60 min after receiving intraperitoneal administration of glucose (18 mmol/ kg body weight) along with 25 nmol/kg body weight of lamprey glucagon, dogfish oxyntomodulin, and paddlefish glucagon (Figure 4.14 A) and trout glucagon (Figure 4.14 C) compared with animals receiving glucose only. The integrated responses to the lamprey, dogfish, and paddlefish peptides were not significantly different from the response to GLP-1 (Figure 4.14 E). Concomitant with the lower blood glucose levels, the concentrations of plasma insulin were significantly greater 15 and 30 min after administration of lamprey glucagon, dogfish oxyntomodulin, and paddlefish glucagon (Figure 4.14 B), and trout glucagon (Figure 4.15 D) compared with animals receiving glucose only. The integrated insulin response to paddlefish glucagon was significantly greater than the response to human GLP-1 (Figure 4.14 F).

Interestingly, paddlefish glucagon exhibited glucose-lowering activity when administrated 2 hours prior to a glucose load. However, no insulinotropic effect was observed for paddlefish glucagon. As expected, the other fish glucagon-related were susceptible to degradation by plasma enzymes, thus exhibited no effect when administrated two hours prior to a glucose load (Figure 4.15 and Table 4.9).

4. 4. 8 Time-dependent effects of human GLP-1, human glucagon, exendin-4 and fish GLP-1 peptides on feeding in normal mice.

At a concentration of 50 nmol/kg of body weight, paddlefish glucagon significantly ($P < 0.01$ and $P < 0.001$) suppressed appetite at individual time points (30, 60, 90, 120, 150 and 180 min) in a similar pattern with exendin-4 when compared with saline only. On the other hand, human glucagon, lamprey glucagon, dogfish oxyntomodulin, ratfish oxyntomodulin and trout glucagon peptides failed to promote any significant reduction of appetite. (Figure 4.16 and Table 4.10). Human GLP-1 was effective up to 30 min post administration which could be due to its short half-life in plasma.

4.5 Discussion

In this Chapter, glucagon-related peptides from phylogenetically ancient fish as well as a teleost were investigated for metabolic stability, potential insulinotropic property and receptor specificity to extended earlier work with dogfish glucagon (O'Harte et al. 2016a and 2016b). For the stability study, DPP-IV was used to predict the cleavage site of the peptides which occurred to be between residues 2 and 3 similarly to human glucagon. (Authier et al. 2003; Pospisilic et al. 2001). Interestedly, while most of the fish peptides were degraded by 33%-47%, only paddlefish glucagon exhibited greater stability with degradation of only 14%. The receptor activation studies show that in mammalian test systems the insulinotropic actions of glucagons from the sea lamprey and paddlefish and oxyntomodulin from the dogfish are mediated through activation of both the glucagon and the GLP-1 receptors. In contrast, the effect of ratfish oxyntomodulin is mediated predominantly, if not exclusively, through interaction with the GLP-1 receptor and the effect of trout glucagon through interaction with the

glucagon receptor. No activation of the GIPR receptor by any fish peptide studied was indicated.

These conclusions are supported by consistent data involving the use of specific receptor antagonists (Figure 4.12 and Table 4.6), cells transfected with GLP1R and GCGR (Figure 4.11 and Table 4.7), and CRISPR/Cas9-engineered GLP1R knock-out and GIPR knock-out cells (Figure 4.13 and Table 4.8). Paddlefish glucagon was the most effective peptide producing a near-maximal increase in the rate of release of insulin from BRIN-BD11 rat clonal β-cells at a concentration of 3 μM that was not significantly different from that produced by human GLP-1 (Figure 4.8 D and Table 4.3). Along with dogfish oxyntomodulin, paddlefish glucagon produced the greatest responses in 1.1B4 human clonal β-cells (Figure 4.9 and Table 4.4) and, along with lamprey glucagon, in isolated mouse islets (Figure 4.10 and Table 4.5). When administered intraperitoneally to overnight-fasted mice together with a glucose load, glucagons from lamprey and paddlefish and oxyntomodulin from dogfish were equally effective as human GLP-1 in lowering blood glucose concentrations, and paddlefish glucagon produced a significantly greater insulin response than an equivalent dose of GLP-1 (Figure 4.14 and Table 4.9).

Interestingly, unlike other fish peptides, paddlefish glucagon exhibited glucose-lowering activity when administrated 2 hours prior to a glucose load (Figure 4.15 and Table 4.9). This could be due to the higher stability of the peptide which is consistent with the DPP-IV study (Figure 4.7). The percentage of degradation for paddlefish glucagon was lower compared to the other glucagon-related peptides (Table 4.2). However, no insulinotropic effect was detected for paddlefish glucagon. Moreover, paddlefish glucagon was as effective as exendin-4 in suppressing appetite over 3 hours trained feeding in 12 hours fasting normal mice.

In an extensive series of articles from the laboratory of Merrifield, the amino acids in glucagon responsible for receptor binding and signal transduction were identified (Unson et al. 1994a; 1994b; 1998; 2002). It was established that His^{1}, Asp^{9}, Ser^{11}, and Ser^{16} are involved in receptor activation and Ser^{2}, Ser^{8} and Asp^{15} are important in receptor binding (Unson et al. 1994). In addition, it was shown that the positively charged residues Lys^{12}, Arg^{17}, and Arg^{18} are necessary to ensure high biological potency by stabilizing the ligand-receptor interaction (Unson et al. 1998). Structure-activity studies of human GLP-1 have shown that the amino acids His^{1}, Gly^{4}, Phe^{6}, Thr^{7}, and Asp^{9} in the N-terminal domain play an important role in binding and activation of the GLP-1 receptor and Phe^{22} and Ile^{23} in the C-terminal domain are of critical importance in maintaining the conformation of the molecule that is recognized by the receptor (Gallwitz et al. 1994). In addition, it is known that the Ala^{18}, Ala^{19}, Lys^{20}, and Leu^{26} residues of GLP-1 interact with N-terminal extracellular domain of the receptor, and so influence binding affinity (Underwood et al. 2010). The primary structures of the fish peptides are compared with those of glucagon, oxyntomodulin, GLP-1, and the GLP1R agonist, exendin-4 that was first isolated from the venom of a reptile, the Gila monster *Heloderma suspectum* (Eng et al. 1992), in Figure 4.17.

It is apparent that the primary structure of glucagon has been better preserved during the course of evolution than that of GLP-1. The His^{1}, Asp^{9}, Ser^{11}, and Lys^{12} residues of glucagon have been conserved in all fish peptides, and a positively charged residue (Arg or Lys) is present at position 17. Similarly, the His^{1}, Gly^{4}, Phe^{5}, Asp^{9}, Phe^{22}, and Leu^{26} residues of GLP-1 have also been conserved in all fish peptides, and all peptides contain a Val residue instead of Ile at position 23. Thus, sequence differences at these sites are not responsible for the observed differences in activity and specificity of the fish peptides. The high potency of paddlefish glucagon was unexpected in view of the

fact that it contains the substitutions Ser^{8} → Asn and Ser^{16} → Glu which would be expected to reduce the ability to bind to and activate GCGR and Ala^{18} → Arg which would be expected to reduce binding affinity to GLP1R. However, the peptide contains the segments Glu^{15}-Glu^{16} and Glu^{24}-Trp^{25}-Leu^{26}-Lys^{27}-Asn^{28}-Gly^{29} in common with GLP1R agonist, exendin-4 that are not found in the other fish peptides (Figure 4.17).

Exendin-4 is both more potent and has a longer half-life in the circulation than GLP-1 and is in use in clinical practice as exenatide (Knop et al. 2017). Thus, paddlefish glucagon may be regarded as a naturally occurring glucagon/exendin-4 hybrid peptide with dual agonist activity at the glucagon and GLP-1 receptors. A previous study has shown that twice-daily administration of the hybrid peptide [S2s]glucagon-exendin-4 (31-39) to high fat-fed mice for 28 days reduced body weight, energy intake and non-fasting glucose levels, as well as increasing insulin concentrations and improving glucose tolerance and insulin sensitivity (Lynch et al. 2014). Glucagon/exendin-4 hybrid peptides have also been designed that show agonist activity at GLP1R and antagonist activity at GCGR (Pan et al. 2006).

GLP-1 and glucagon lack defined secondary structure in aqueous solution, but in membrane-mimetic environment, adopt an α-helical structure in the midsection, with flexible N- and C-terminal regions and it has been suggested that the helical structure is required for binding to their respective receptors (Pan et al, 2006) The conformations of the fish glucagons have yet to be determined experimentally but application of the AGADIR program, an algorithm based on the helix/coil transition theory which predicts the helical behaviour of monomeric peptides (Muñoz et al. 1994), indicates that paddlefish glucagon has a very strong propensity to adopt a stable α-helical conformation between residues 8-27 whereas the predicted helices adopted

by the dogfish, ratfish, and lamprey peptides are much less stable. In addition, it is suggested that the relatively weak insulinotropic activity of trout glucagon may arise from the substitutions Asp^{15} → Leu decreasing binding affinity at GCGR and Thr^{7} → Ser and Lys^{20} → Gln decreasing affinity at GLP1R.

Structure-activity relationships of the oxyntomodulin molecule have been less well studied than those of glucagon. The insulinotropic activities and receptor selectivities of ratfish and dogfish oxyntomodulin differ appreciably and it is suggested that the substitution Ser^{2} → Thr in the ratfish peptide contributes to its inability to activate GCGR and the substitutions Thr^{7} → Ser and Ala^{19} → Thr are, at least in part, responsible for its lower potency and effectiveness in stimulating GLP1R-mediated insulin release *in vitro* and weaker glucose-lowering activity *in vivo* compared with dogfish oxyntomodulin. Replacement of residues 15-23 in oxyntomodulin (Asp-Ser-Arg-Arg-Ala-Gln-Asp-Phe-Val) by the corresponding section of exendin-4 (Glu-Glu-Glu-Ala-Val-Arg-Leu-Phe-Val) resulted in an approximately 10-fold increase in binding affinity at the rat GLP-1 receptor (Druce et al. 2009), but neither dogfish not ratfish oxyntomodulins show structural similarity with exendin-4 in this region.

In conclusion, this study has extended earlier work that identified dogfish glucagon as a peptide that interacts with both the GLP-1 and glucagon receptors to stimulate insulin release and lower blood glucose concentrations (O'Harte et al. 2016) by demonstrating that glucagon-related peptides from other phylogenetically ancient fish possess similar properties. In particular, paddlefish glucagon by incorporating structural features found in exendin-4 is more potent in stimulating insulin release from rat clonal β-cells than dogfish glucagon (threshold concentration 30 pM versus 100 pM (O'Harte et al. 2016a) and provokes a greater insulin response than human GLP-1 when administered to mice.

In the light of the global pandemic of obesity-related T2DM, there is an urgent need for new types of safe and more effective anti-diabetic agents. The structure-activity properties of fish glucagon-related peptides revealed for the first time in this study will aid in the design of new therapeutic agents. In particular, paddlefish glucagon has the potential to act as a template for the development of new long-acting, peptidase-resistant analogues for the treatment of patients with the disease that display the advantages of unimolecular dual agonist peptides (Brandt et al. 2018 and Sánchez-Garrido et al. 2017).

Table 4. 1 Primary structure and molecular masses of the glucagon-related fish peptides used in this study.

Peptide	Amino acid sequence	Calculated molecular mass, (Da)	Observed molecular mass, (Da)
Lamprey glucagon	HSEGTFTSDYSKYLENKQAKDFVRWLMNA	3466.9	3466.5
Dogfish oxyntomodulin	HSEGTFTSDYSKYMDNRRAKDFVQWLMSTKRNG	3957.4	3958.5
Ratfish oxyntomodulin	HTDGIFSSDYSKYLDNRRTKDFVQWLLSTKRNGANT	4235.6	4233.6
Paddlefish glucagon	HSQGMFTNDYSKYLEEKRAKEFVEWLKNGKS	3751.1	3750.8
Human GLP-1	HAEGTFTSDVSSYLEGQAAKEFIAWLVKGR-NH2	3297.7	3297.9
Human glucagon	HSQGTFTSDYSKYLDSRRAQDFVQWLMNT	3482.8	3484.4
Human GIP	YAEGTFISDYSIAMDKIHQQDFVNWLLAQKGKKNDWKHNITQ	4983.6	4984.3
Exendin-4	HGEGTFTSDLSKQMEEEAVRLFIEWLKNGGPSSGAPPPS-NH2	4186.6	4186.0

Table 4.2 Summary of DPP-IV degradation results of the glucagon-related fish peptides used in this study.

Peptide	% Degraded at 4 hours	Number of peaks	Observed MW of degraded product, Da	Proposed cleavage site
Lamprey glucagon	42	2	3243.1	Ser^{2}-Glu^{3}
Dogfish oxyntomodulin	47	2	3734.4	Ser^{2}-Glu^{3}
Ratfish oxyntomodulin	33	2	3998.4	Thr^{2}-Asp^{3}
Paddlefish glucagon	14	2	3529.7	Ser^{2}-Gln^{3}
Trout glucagon	42	2	3289.4	Ser^{2}-Glu^{3}
Human GLP-1	86	2	3090.4	Ala^{8}-Glu^{9}
Human glucagon	24	2	3259.5	Ser^{2}-Gln^{3}
Human GIP	90	2	4749.1	Ala^{2}-Glu^{3}

Table 4.3 Effects of glucagon-related peptides on the release of insulin from BRIN-BD11 cells.

Peptide	Threshold concentration	The rate at 3 µM ng/10^6/20min	EC 50
Control (glucose alone)	-	1.02 ± 0.02	
Lamprey glucagon	3 nM	3.3 ± 0.2***	85nM
Dogfish oxyntomodulin	1 nM	2.4 ± 0.1***	23nM
Ratfish oxyntomodulin	3 nM	2.3 ± 0.2***	7.2nM
Paddlefish glucagon	30 pM	3.6 ± 0.2***	1.7nM
Trout glucagon	30 nM	1.6 ± 0.1***	0.1µM
Human glucagon	10 nM	2.7 ± 0.1***	3µM
Human GLP-1	10 pM	3.6 ± 0.2***	2.1nM

Values are mean ± S.E.M., $n = 8$ *P < 0.05, **P < 0.01, ***P < 0.001 compared to 5.6 mM glucose alone.

Table 4.4 Effects of fish proglucagon-derived peptides at 10^{-6} M and 10^{-8} M concentration on insulin secretion from 1.1 B4 cells.

Peptide name	Insulin release at 10^{-6}M	Insulin release at 10^{-8}M
1.4 mM glucose	0.05 ± 0.002 **	0.05 ± 0.002 **
16.7 mM glucose control	0.08 ± 0.007	0.08 ± 0.007
Lamprey glucagon	0.27 ± 0.010 ***	0.04 ± 0.020 ΔΔ
Dogfish oxyntomodulin	0.25 ± 0.025 ***	0.10 ± 0.006 * ΔΔ
Ratfish oxyntomodulin	0.15 ± 0.012 *** ΔΔ	0.09 ± 0.011 ΔΔΔ
Paddlefish glucagon	0.23 ± 0.010 ***	0.14 ± 0.008 ***
Trout glucagon	0.12 ± 0.009 ** ΔΔΔ	0.08 ± 0.011 ΔΔΔ
GLP-1	0.24 ± 0.020 ***	0.13 ± 0.008 **
Glucagon	0.11 ± 0.002* ΔΔΔ	0.08 ± 0.006 ΔΔΔ

Values are mean ± S.E.M., $n = 8$ *P < 0.05, **P < 0.01, ***P < 0.001 compared to 16.7 mM glucose alone. $^{\Delta}$P < 0.05, $^{\Delta\Delta}$ P< 0.01, $^{\Delta\Delta\Delta}$ P< 0.001 compared with the response to human GLP-1.

Table 4.5 Effects fish proglucagon-derived peptides on the release of insulin from islets isolated from TO Swiss mice.

Peptide	Insulin release (% of total insulin content) at 10^{-6}M	Insulin release (% of total insulin content) at 10^{-8}M
1.4 mM glucose	3.7 ± 0.1 **	3.7 ± 0.1 **
16.7 mM glucose	9.7 ± 1.3	9.7 ± 1.3
Lamprey glucagon	23.6 ± 1.1 ***	15.9 ± 0.5 **
Dogfish oxyntomodulin	21.6 ± 2.2**	18.6 ± 0.6**
Ratfish oxyntomodulin	16.4 ± 2.0 *	11.3 ± 1.1
Paddlefish glucagon	22.7 ± 1.5 ***	9.9 ± 1.3
Trout glucagon	12.9 ± 0.2	9.7 ± 0.1
Human GLP-1	20.7 ± 2.5 **	16.1 ± 1.4 *
Human glucagon	15.1 ± 1.7	11.5 ± 1.3

Values are mean ± S.E.M., $n = 8$ *P < 0.05, **P < 0.01, ***P < 0.001 compared to 16.7 mM glucose alone.

Table 4.6 Summary of effect of fish glucagon-related, human GLP-1, human glucagon and human GIP peptides on insulin secretion from BRIN-BD11 cells in the presence antagonists.

Peptide, 10^{-7}	The observed reduction of peptides-stimulated insulin secretion in the presence of antagonists:		
	Exendin-4(9-39), 10^{-6}	Peptide O, 10^{-6}	(Pro^3)GIP, 10^{-6}
Lamprey glucagon	ΔΔΔ	ΔΔΔ	No effect
Dogfish oxyntomodulin	ΔΔΔ	ΔΔ	No effect
Ratfish oxyntomodulin	ΔΔΔ	No effect	No effect
Paddlefish glucagon	ΔΔΔ	ΔΔ	No effect
Trout glucagon	No effect	ΔΔΔ	No effect
Human GLP-1	ΔΔΔ	No effect	No effect
Human glucagon	No effect	Δ	No effect
Human GIP	No effect	No effect	ΔΔΔ

Values are mean ± S.E.M., n = 8 $^{\Delta}P < 0.05$, $^{\Delta\Delta}P < 0.01$, $^{\Delta\Delta\Delta}P < 0.001$ compared with the effect in the presence of respective antagonist.

Table 4.7 Summary of effect of fish glucagon-related peptides, human GLP-1, human glucagon and human GIP (10^{-8} and 10^{-6} M) on cAMP production in GLP1R-transfected CHL cells, and GCGR-transfected HEK293 cells.

Peptide name	GLP-1 receptor transfected cells		GCG receptor transfected cells	
	cAMP release at 10^{-6}	cAMP release at 10^{-8}	cAMP release at 10^{-6}	cAMP release at 10^{-8}
Basal (5.6mM glucose)	4.0 ± 0.4	4.0 ±0.4	2.8 ± 0.9	2.8 ± 0.9
Lamprey glucagon	16.3 ± 0.5***$^{\Delta}$	14.5 ± 0.8***$^{\Delta}$	10.3 ± 0.3**	4.6 ± 0.9*$^{\Delta\Delta}$
Dogfish oxyntomodulin	14.7 ± 0.2***$^{\Delta\Delta\Delta}$	13.5 ± 0.2***$^{\Delta\Delta}$	10.9 ± 0.4**	4.1 ± 0.4*$^{\Delta\Delta\Delta}$
Ratfish oxyntomodulin	11.8 ± 0.6***$^{\Delta\Delta\Delta}$	4.5 ± 0.4 $^{\Delta\Delta\Delta}$	1.5 ± 0.1$^{\Delta\Delta\Delta}$	1.4 ± 0.6 $^{\Delta\Delta\Delta}$
Paddlefish glucagon	15.1 ± 0.1*** $^{\Delta\Delta\Delta}$	14.8 ± 0.1***$^{\Delta\Delta}$	8.2 ± 0.9**	5.4 ± 0.3*$^{\Delta\Delta\Delta}$
Trout glucagon	6.8 ± 1.4 $^{\Delta\Delta\Delta}$	5.7 ± 0.9 $^{\Delta\Delta\Delta}$	5.6 ± 0.1* $^{\Delta\Delta\Delta}$	3.2 ± 0.8 $^{\Delta\Delta\Delta}$
Human GLP-1	17.7 ± 0.2***	17.3 ± 0.3***	7.6 ± 0.2**$^{\Delta\Delta\Delta}$	4.9 ± 0.4*$^{\Delta\Delta\Delta}$
Human glucagon	12.3 ± 0.8**$^{\Delta\Delta\Delta}$	5.4 ± 0.4*$^{\Delta\Delta\Delta}$	10.4 ± 0.3**	9.1 ± 0.4**
Human GIP	3.9 ± 0.2$^{\Delta\Delta\Delta}$	3.6 ± 0.4$^{\Delta\Delta\Delta}$	2.9 ± 0.4$^{\Delta\Delta\Delta}$	2.8 ± 0.3$^{\Delta\Delta\Delta}$

Values are mean ± S.E.M. for n = 4. *P < 0.05, ** P< 0.01 and ***P < 0.001 compared with 5.6 glucose. $^{\Delta}$P < 0.05, $^{\Delta\Delta}$P < 0.01, $^{\Delta\Delta\Delta}$P < 0.001 compared with the effect of glucagon/GLP-1

Table 4.8 Summary of effects of fish GLP-1 peptides (10^{-8} and 10^{-6} M) on the rate of insulin release from wild-type INS-1 cells, CRISPR/Cas9-engineered GLP-1R KO cells, CRISPR/Cas9-engineered GIPR KO cells and CRISPR/Cas9-engineered GIPR KO cells

Peptide		Wild-type cells, % of basal control	GLP-1R KO cells, % of basal control	GCGR KO cells, % of basal control	GIPR KO cells, % of basal control
Basal (5.6mM glucose)		100 ± 2.3			
Lamprey glucagon	10^{-6}	221.7 ± 9.5***	120.7 ± 8.2 ΔΔΔ	189.3 ± 11.2 ***	188.5 ± 4.7***
	10^{-8}	202.4 ± 7.6***	103.6 ± 7.2 ΔΔΔ	134.1 ± 7.8*ΔΔ	183.2 ± 15.9***
Dogfish oxyntomodulin	10^{-6}	220.7 ± 13.1***	118.2 ± 7.6 ΔΔΔ	170.3 ± 13.5**Δ	210.0 ± 5.7***
	10^{-8}	213.2 ± 16.7***	118.9 ± 6.6 ΔΔΔ	157.0 ± 19.9*Δ	210.3 ± 10.6***
Ratfish oxyntomodulin	10^{-6}	232.1 ± 5.5***	183.7 ± 9.5 ***ΔΔ	207.6 ± 20.6***	212.0 ± 10.5***
	10^{-8}	211.4 ± 1.8***	146.8 ± 2.5 *** ΔΔΔ	197.4 ± 36.1*	195.3 ± 8.0***
Paddlefish glucagon	10^{-6}	223.2 ± 6.9***	194.3 ± 11.3 ***Δ	207.9 ± 26.6 **	210.7 ± 11.2***
	10^{-8}	184.0 ± 10.3***	161.3 ± 13.6 ***	149.1 ± 8.0** Δ	203.5 ± 13.3***
Trout glucagon	10^{-6}	238.1 ± 10.1***	236.9 ± 7.2 ***	147.4 ± 15.9*ΔΔΔ	222.1 ± 13.7 ***
	10^{-8}	240.1 ± 7.0***	192.2 ± 7.5 ***	117.8 ± 12.8 ΔΔΔ	198.3 ± 8.8 ***
Human GLP-1	10^{-6}	213.5 ± 14.1***	102.3 ± 1.3 ΔΔΔ	222.0 ± 11.7***	213.2 ± 12.3***
	10^{-8}	197.1 ± 4.5***	101.1 ± 6.9 ΔΔΔ	210 ± 25.0 ***	183.5 ± 3.5***
Human glucagon	10^{-6}	215.3 ± 3.4***	252.8 ± 0.8***	159.6 ± 8.5 *** ΔΔ	181.0± 13.3 ***
	10^{-8}	172.7 ± 7.5***	194.9 ±10.9***	134.0 ± 14.4 Δ	174.0 ± 10.6***
Human GIP	10^{-6}	241.2 ± 10.1***	264.9 ±10.2***	231.3 ± 17.6 ***	110.1 ± 8.5 ΔΔΔ
	10^{-8}	228.8 ± 16.3***	255.4 ± 5.3***	230.1 ± 0.9***	104.4 ± 4.2 ΔΔΔ

Values are mean ± S.E.M., $n = 8$, *P < 0.05, ** P< 0.01 and ***P < 0.001 compared with 5.6 mM glucose alone. $^{\Delta}P < 0.05$, $^{\Delta\Delta}P < 0.01$, $^{\Delta\Delta\Delta}P < 0.001$ compared with effects in wild-type INS-1 cells.

Table 4.9 Summary of effects of acute administration of fish glucagon-related peptides on blood glucose and plasma insulin concentrations in normal mice, including 2-hour post injection

Peptide name	IGTT blood glucose $AUC_{0\text{-}60min}$ (mmol/l.min)	IGTT plasma insulin $AUC_{0\text{-}60min}$ (mmol/ml/min)	2 hours post saline/peptide injection, plasma insulin $AUC_{0\text{-}60min}$ (mmol/l.min)	2 hour post saline/peptide injection, plasma insulin $AUC_{0\text{-}90min}$ (ng/ml/min)
Glucose alone	991.1 ± 49.0	134.8 ± 4.23	894.3 ± 46.2	108.1 ± 4.2
Lamprey glucagon	561.6 ± 62.4***	171.3 ± 6.6**	836.4 ± 34.9	95.6 ± 4.2
Dogfish oxyntomodulin	528.3± 58.3***	208.1 ± 13.5***	830.8 ± 37.4	99.9 ± 6.8
Ratfish oxyntomodulin	878.3 ± 78.1ΔΔ	151.2 ± 11.8 Δ	906.9 ± 54.1	102.7 ± 11.3
Paddlefish glucagon	466.4 ± 35.1***	239.1 ± 6.1*** Δ	720.5 ± 27.3*	119 ± 4.9
Trout glucagon	726.1 ± 34.5**ΔΔ	160.5 ± 6.5* Δ	888.6 ± 28.2	103.1± 12.2
GLP-1	476.4 ± 41.37***	186.6 ± 12.87 **	825.4 ± 32.5	101.7 ± 16.65
Glucagon	1006 ± 140.6 ΔΔ	145.9 ± 3.218 Δ	-	-
Exendin-4	-	-	369.0 ± 38.96*** ΔΔΔ	281.0 ± 16.25 ***ΔΔΔ

The values are mean ± SEM for n=6. **P<0.01 and ***P<0.001 compared to glucose alone; $^{\Delta\Delta}$ P<0.01 and $^{\Delta\Delta\Delta}$ P<0.001 compared to human.

Table 4.10 Summary effects of fish GLP-1 peptides on cumulative food intake over 3 hours trained feeding in 12 h fasting normal mice.

Peptide name	Time (min)					
	30	**60**	**90**	**120**	**150**	**180**
Saline control	1.2 ± 0.03	1.7 ± 0.06	2.1 ± 0.08	2.5 ± 0.07	2.9 ± 0.07	3.3 ± 0.06
Lamprey glucagon	1.3 ± 0.11	1.7 ± 0.2	2.1 ± 0.19	2.5 ± 0.11	2.9 ± 0.18	3.0 ± 0.11 *
Dogfish oxyntomodulin	1.3 ± 0.19	1.9 ± 0.3	2.2 ± 0.27	2.5 ± 0.22	2.7 ± 0.25	3.1 ± 0.17
Ratfish oxyntomodulin	1.3 ± 0.11	1.9 ± 0.2	2.1 ± 0.19	2.7 ± 0.11	3.1 ± 0.18	3.6 ± 0.11 *
Paddlefish glucagon	0.7 ± 0.06 **	0.8 ± 0.1***	1.2 ± 0.14 ***	1.5 ± 0.15 ***	1.8 ± 0.14 ***	2.2 ± 0.13 ***
Trout glucagon	1.4 ± 0.11	1.9 ± 0.2	2.3 ± 0.26	2.8 ± 0.26	3.1 ± 0.20	3.4 ± 0.26
GLP-1	0.7 ± 0.13 **	1.4 ± 0.18	2.1 ± 0.20	2.4 ± 0.13	2.7 ± 0.11	3.1 ± 0.08
Glucagon	1.3 ± 0.09	1.8 ± 0.15	2.1 ± 0.16	2.4 ± 0.18	2.6 ± 0.17	2.9 ± 0.19
Exendin-4	0.7 ± 0.13 **	1.0 ± 0.08 ***	0.9 ± 0.08 ***	1.2 ± 0.16 ***	1.2 ± 0.17 ***	1.4 ± 0.17 ***

The values are mean ± SEM for n=8. *P<0.05, **P<0.01 and ***P<0.001 compared to saline control mice treated at the same time point.

Figure 4.1 Reverse-phase HPLC purification of crude lamprey glucagon (A), dogfish oxyntomodulin (B) ratfish oxyntomodulin (C), paddlefish glucagon (D) and trout glucagon (E) peptides using a semi-preparative Vydac C18 column.

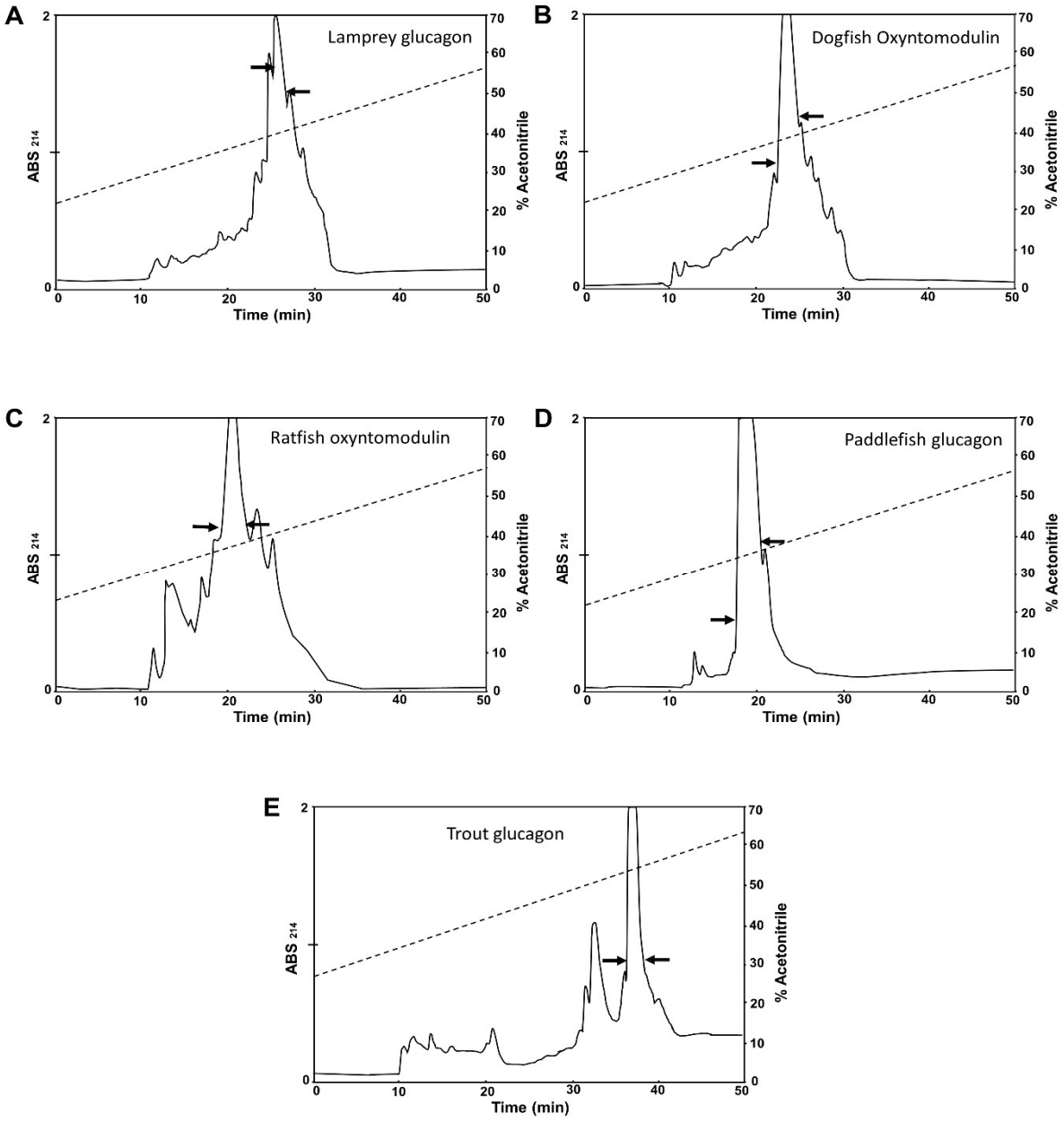

The peptides were dissolved in 15% acetonitrile (3mg/ml) and injected onto a (2.2 cm x 25 cm) Vydac 218TP1022 (C-18) column (Grace, Deerfield, IL, USA) equilibrated with 21% (or 28%) acetonitrile (v/v) and 0.1% TFA/water at a flow rate of 6.0 ml/min. The concentration of acetonitrile in the eluting solvent was raised from 21% to 56 % for the all fish glucagon peptides except trout glucagon (28% to 63%) over 50 min using a linear gradient. Absorbance was measured at 214 nm, and the black arrows show where the peak collection began and ended.

Figure 4.2 MALDI-TOF spectra of purified lamprey glucagon (A), dogfish oxyntomodulin (B) ratfish oxyntomodulin (C), paddlefish glucagon (D) and trout glucagon peptides.

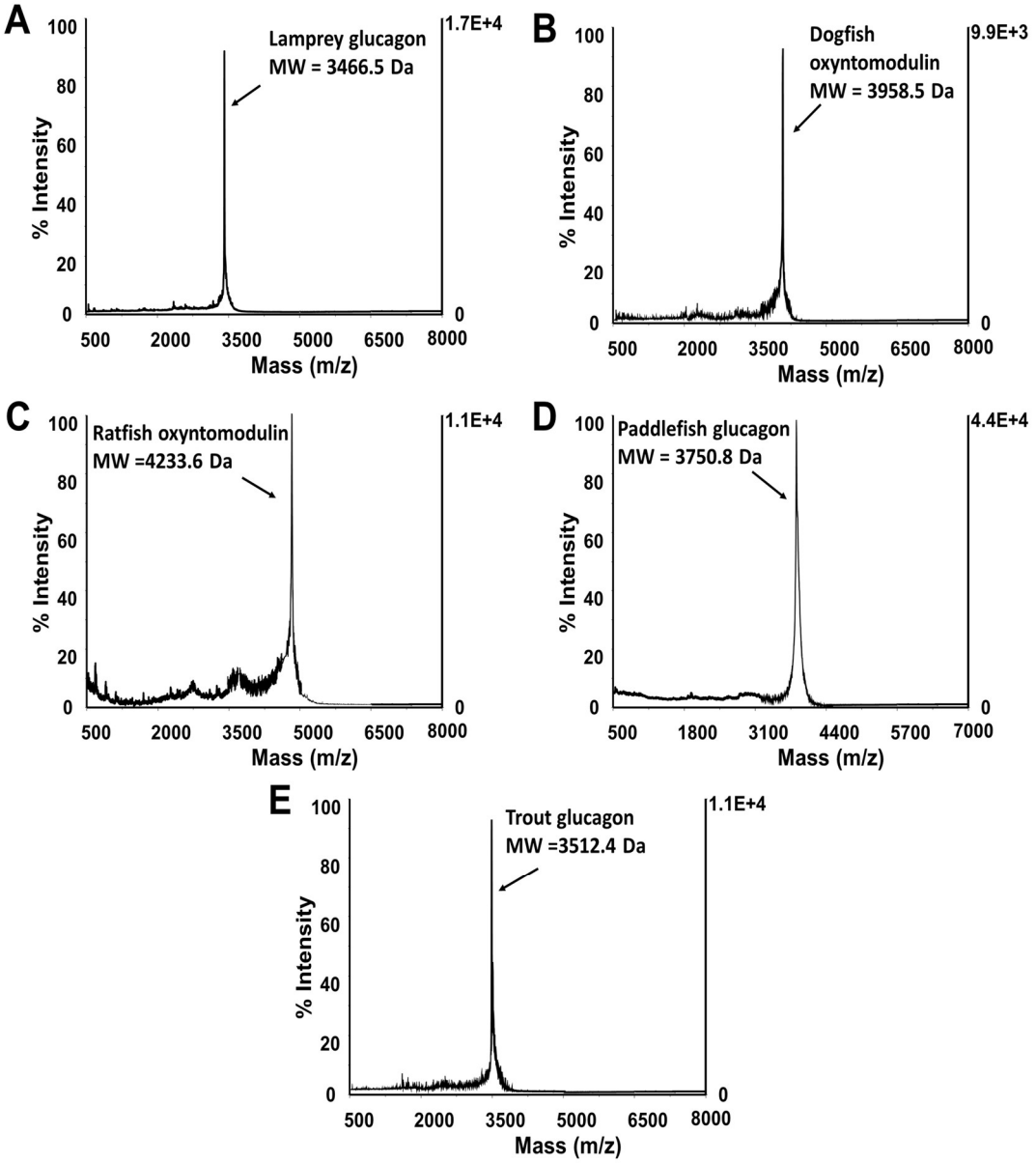

Purified peptides were mixed with α-Cyano-4-hydroxycinnamic acid on a 100 well MALDI plate before inserting into a Voyager DE Biospectrometry workstation. The mass-to-charge ratio (m/z) versus peak intensity was determined.

Figure 4.3 HPLC degradation profile of lamprey glucagon following incubation with DPP-IV for 0 and 4 hours.

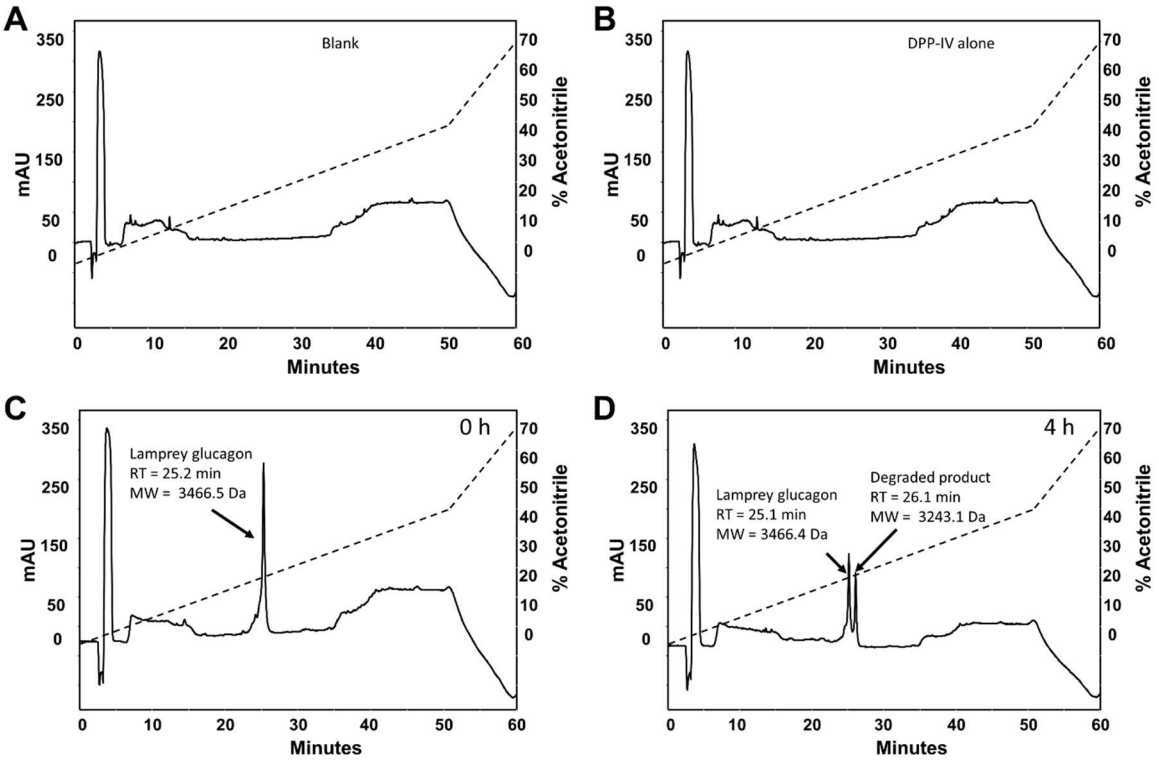

HPLC degradation study was performed with a Luna 5u C8 250x4.6mm column using gradients from 0% to 42% of acetonitrile over 50 min, and from 42% to 70% of acetonitrile over 15 min.

Figure 4.4 HPLC degradation profile of dogfish oxyntomodulin following incubation with DPP-IV for 0 and 4 hours.

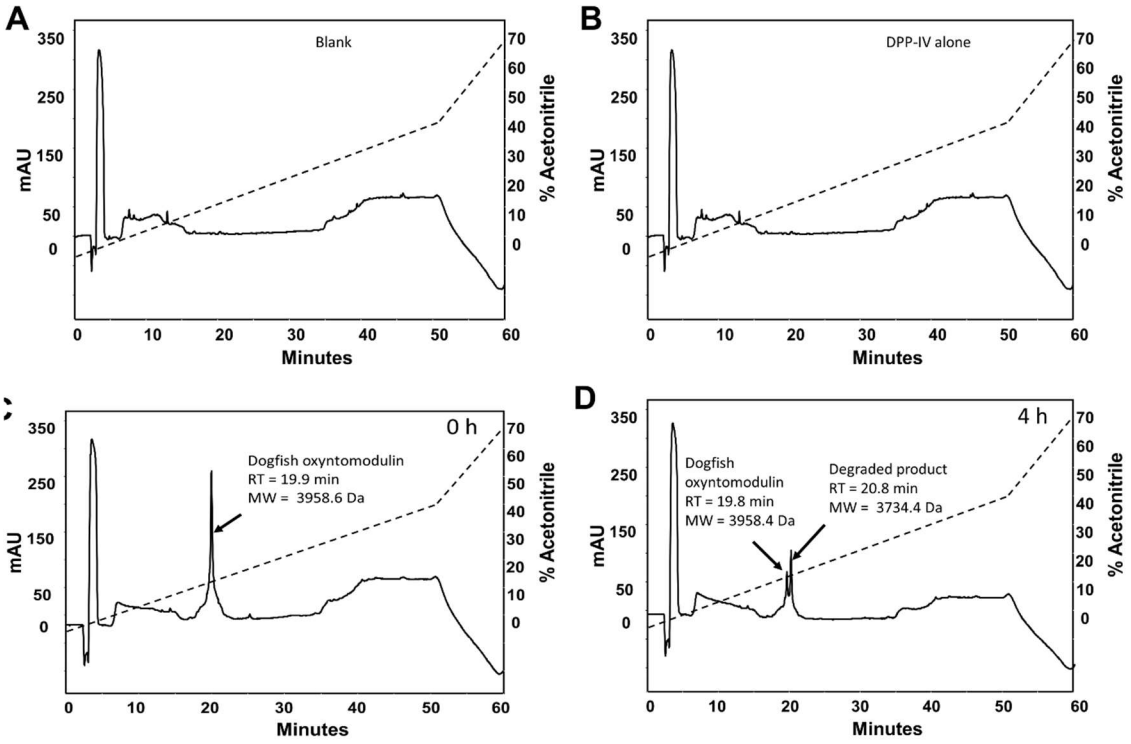

HPLC degradation study was performed with a Luna 5u C8 250x4.6mm column using gradients from 0% to 42% of acetonitrile over 50 min, and from 42% to 70% of acetonitrile over 15 min.

Figure 4.5 HPLC degradation profile of ratfish oxyntomodulin following incubation with DPP-IV for 0 and 4 hours.

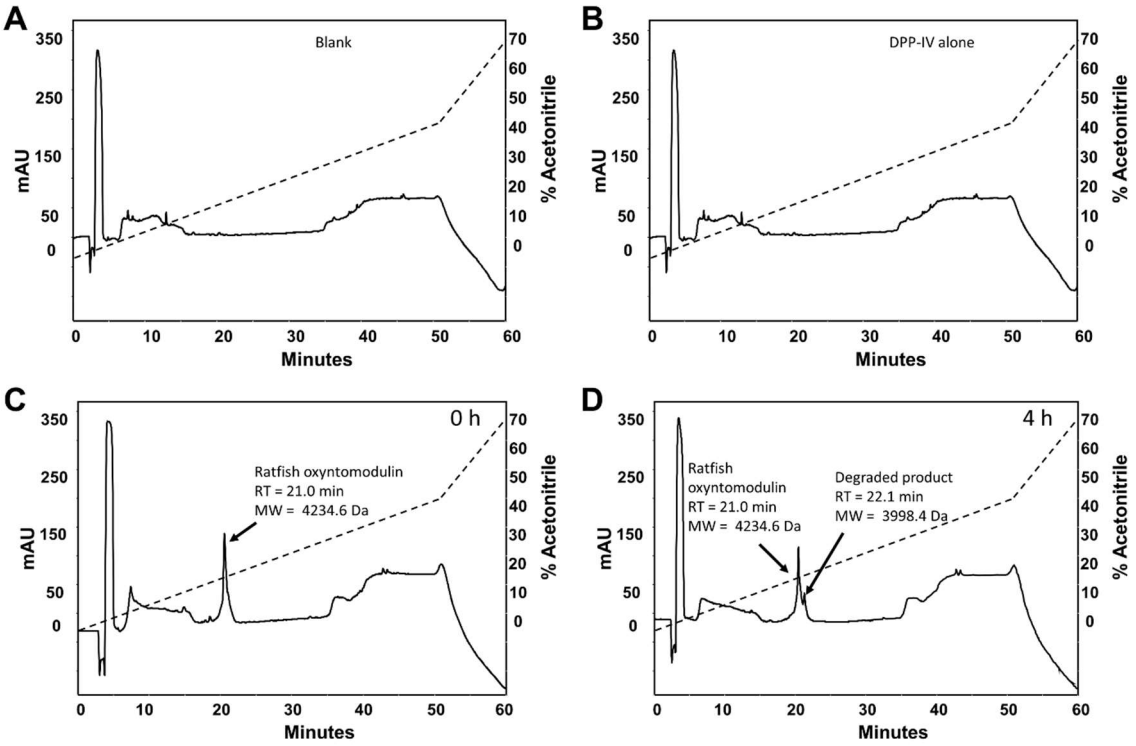

HPLC degradation study was performed with a Luna 5u C8 250x4.6mm column using gradients from 0% to 42% of acetonitrile over 50 min, and from 42% to 70% of acetonitrile over 15 min.

Figure 4.6 HPLC degradation profile of paddlefish glucagon following incubation with DPP-IV for 0 and 4 hours.

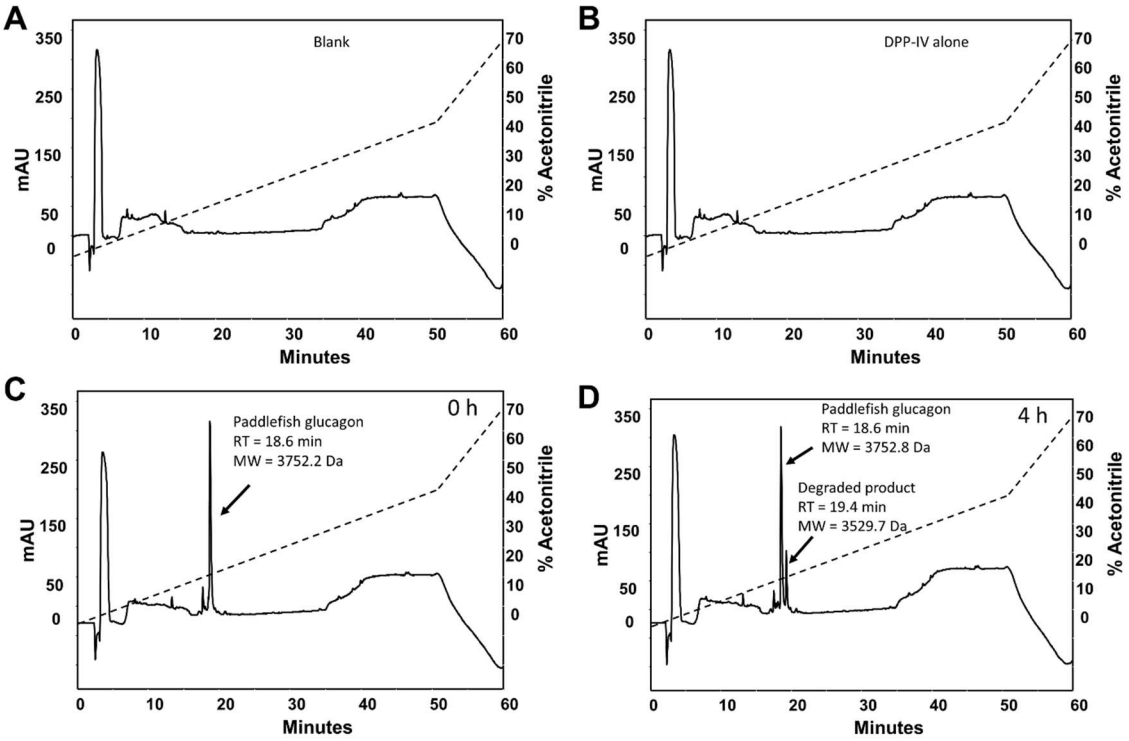

HPLC degradation study was performed with a Luna 5u C8 250x4.6mm column using gradients from 0% to 42% of acetonitrile over 50 min, and from 42% to 70% of acetonitrile over 15 min.

Figure 4.7 HPLC degradation profile of trout glucagon following incubation with DPP-IV for 0 and 4 hours.

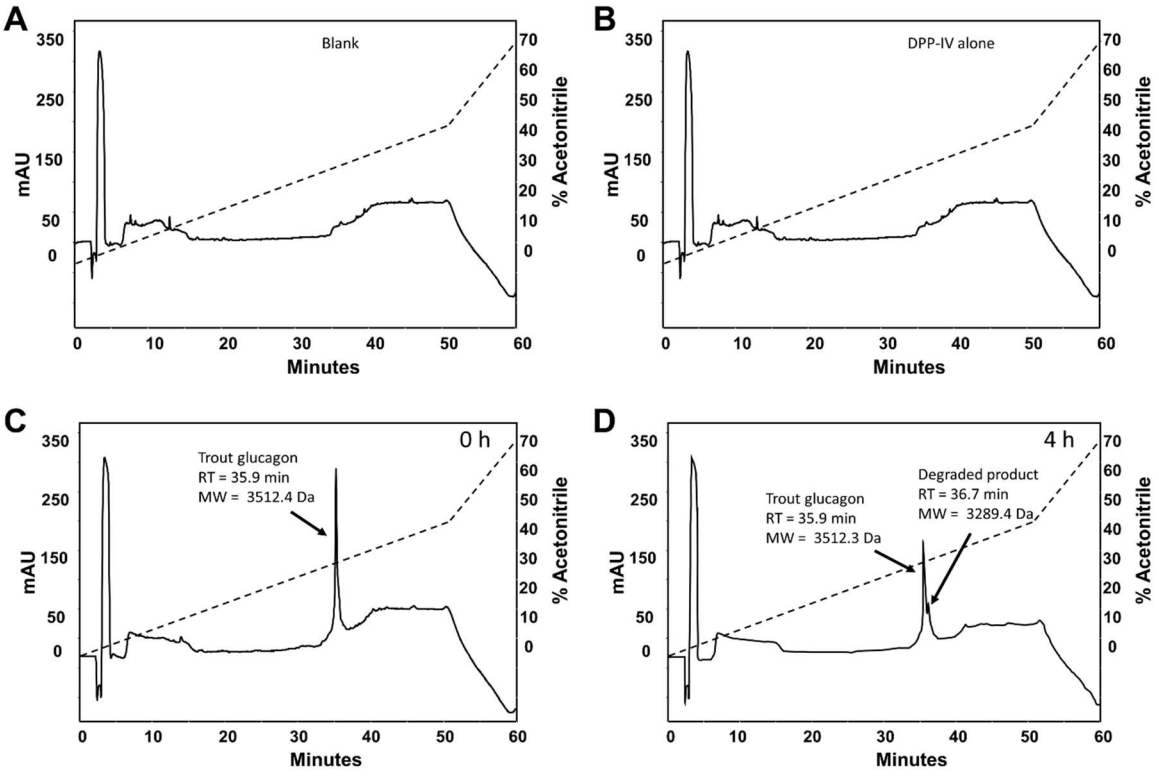

HPLC degradation study was performed with a Luna 5u C8 250x4.6mm column using gradients from 0% to 42% of acetonitrile over 50 min, and from 42% to 70% of acetonitrile over 15 min.

Figure 4.8 Effects of increasing concentrations of (A) lamprey glucagon, (B) dogfish oxyntomodulin, (C) ratfish oxyntomodulin, (D) paddlefish glucagon, (E) trout glucagon, (F) human glucagon, and (G) human GLP-1 on insulin release from BRIN-BD11 rat clonal β-cells.

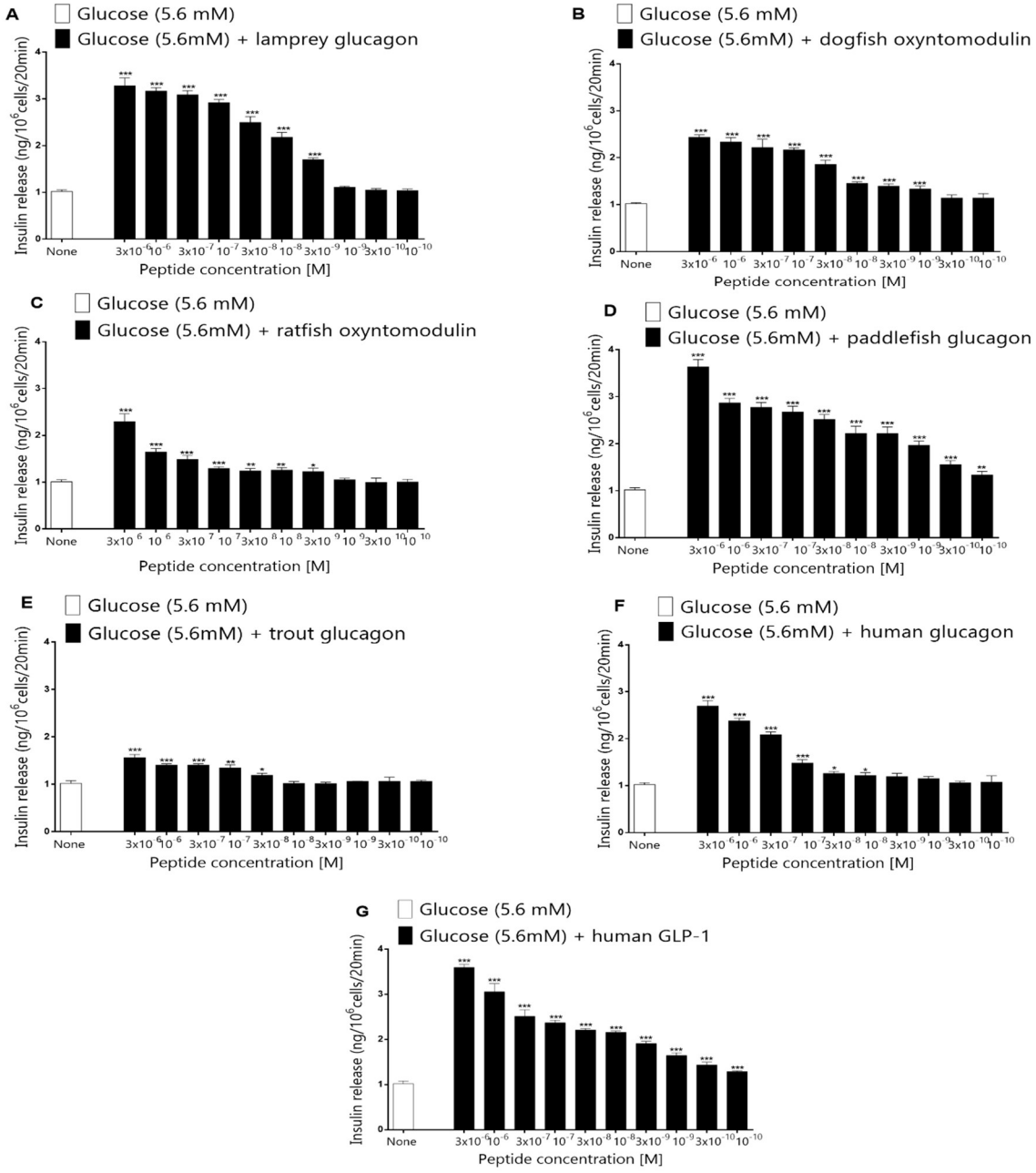

Values are mean ± S.E.M., n = 8. *P < 0.05, **P < 0.01, ***P < 0.001 compared to 5.6 mM glucose alone.

Figure 4.9 Effects of fish proglucagon-derived peptides at 10 nM and 1 μM concentrations on insulin release from 1.1 B4 human clonal β-cells.

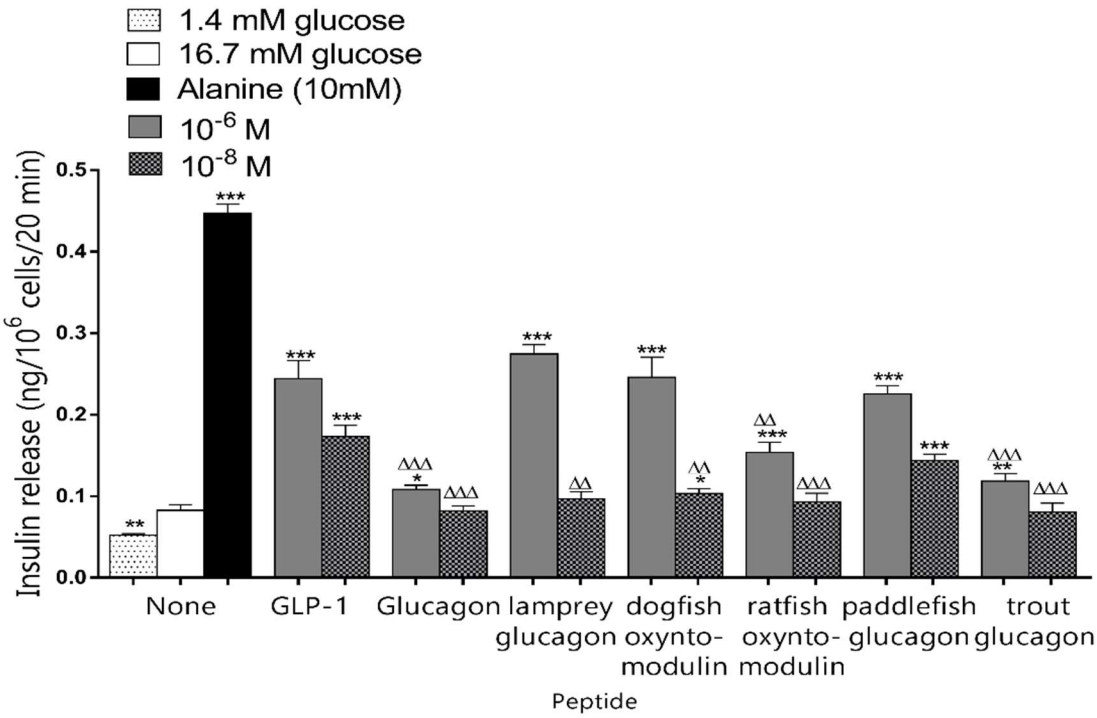

Values are mean ± S.E.M., n = 8 *P < 0.05, **P < 0.01, ***P < 0.001 compared to 16.7 mM glucose alone. $^{\Delta}$P < 0.05, $^{\Delta\Delta}$ P< 0.01, $^{\Delta\Delta\Delta}$ P< 0.001 compared with the response to human GLP-1.

Figure 4.10 Effects of fish proglucagon-derived peptides at 10 nM and 1 µM concentrations on insulin release from pancreatic islets isolated from NIH Swiss mice

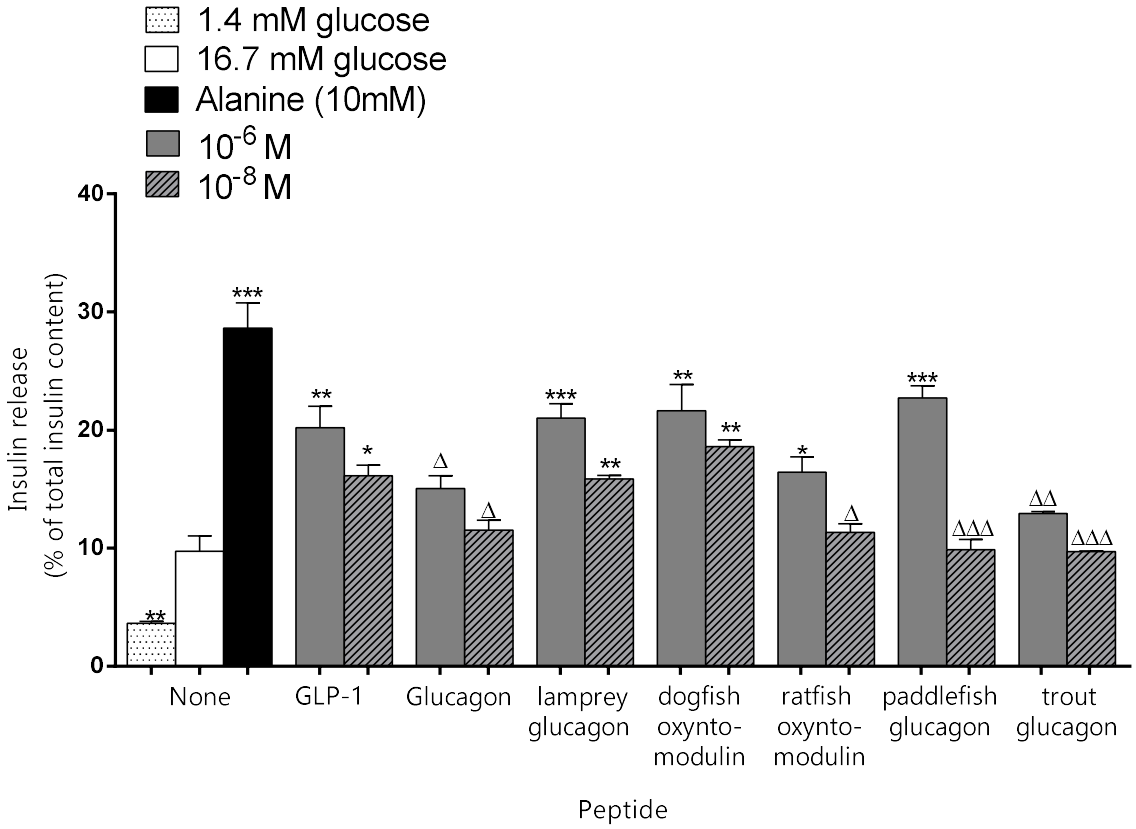

The values are mean ± SEM for n=4; *P < 0.05, **P < 0.01, ***P < 0.001 compared to 16.7mM glucose alone.

Figure 4.11 Effects of (A) the GLP-1 receptor antagonist, exendin-4(9-39), (B) the glucagon receptor antagonist [desHis1,Pro4,Glu9]glucagon amide and (C) the GIP receptor antagonist GIP(6-30)Cex-K40[Pal], on the ability of fish glucagon-related peptides (10^{-7} M) to stimulate insulin release from BRIN-BD11 cells.

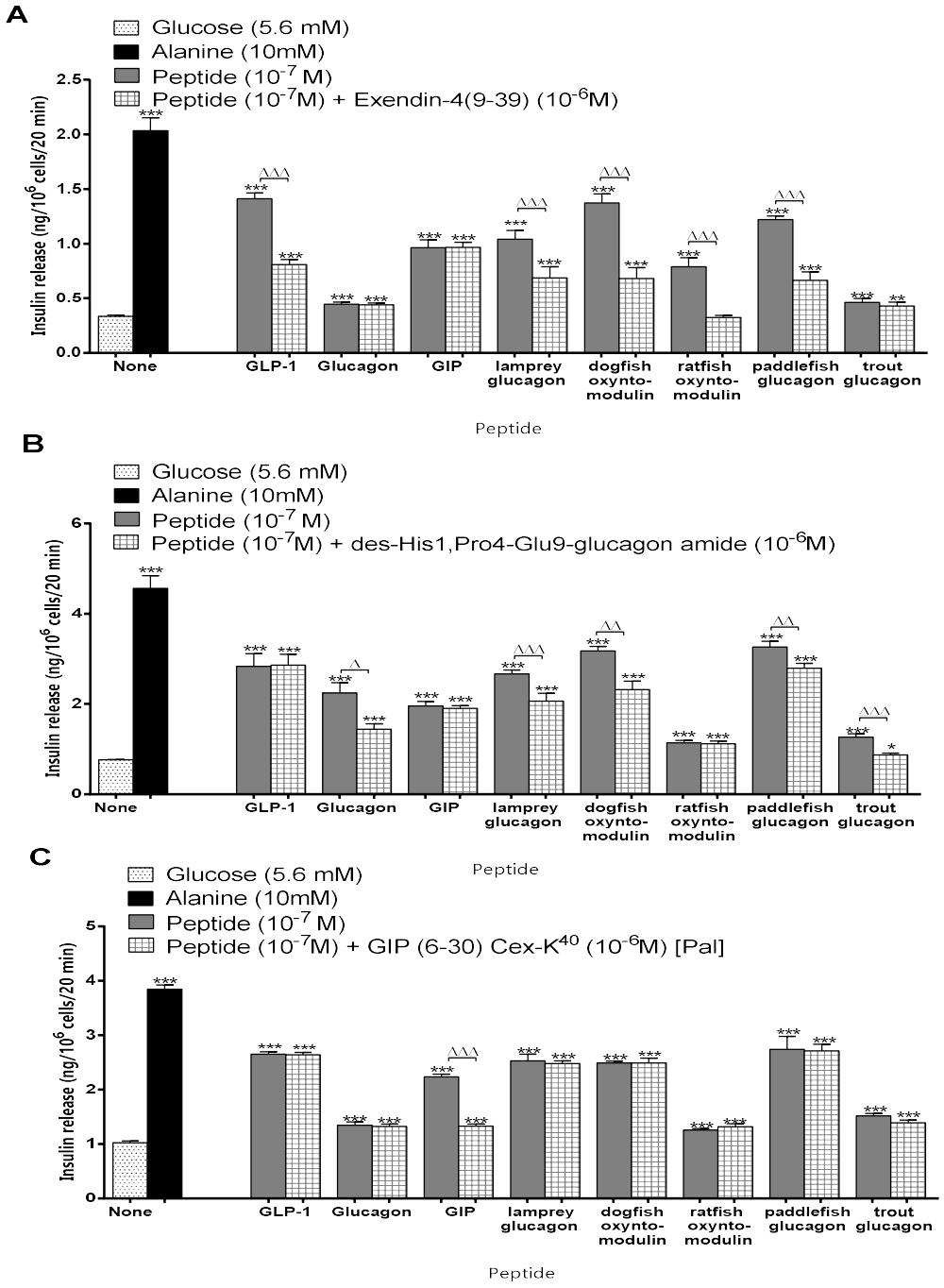

Values are mean ± S.E.M., n = 8 **P < 0.01, ***P < 0.001 compared with 5.6 mM glucose alone. $^{\Delta}$P < 0.05, $^{\Delta\Delta}$P < 0.01, $^{\Delta\Delta\Delta}$P < 0.001 compared with the effect in the presence of antagonist.

Figure 4.12 Effects of glucagon-related peptides (10^{-8} and 10^{-6} M) on cAMP production in (A) GLP1R-transfected CHL cells, and (B) GCGR-transfected HEK293 cells.

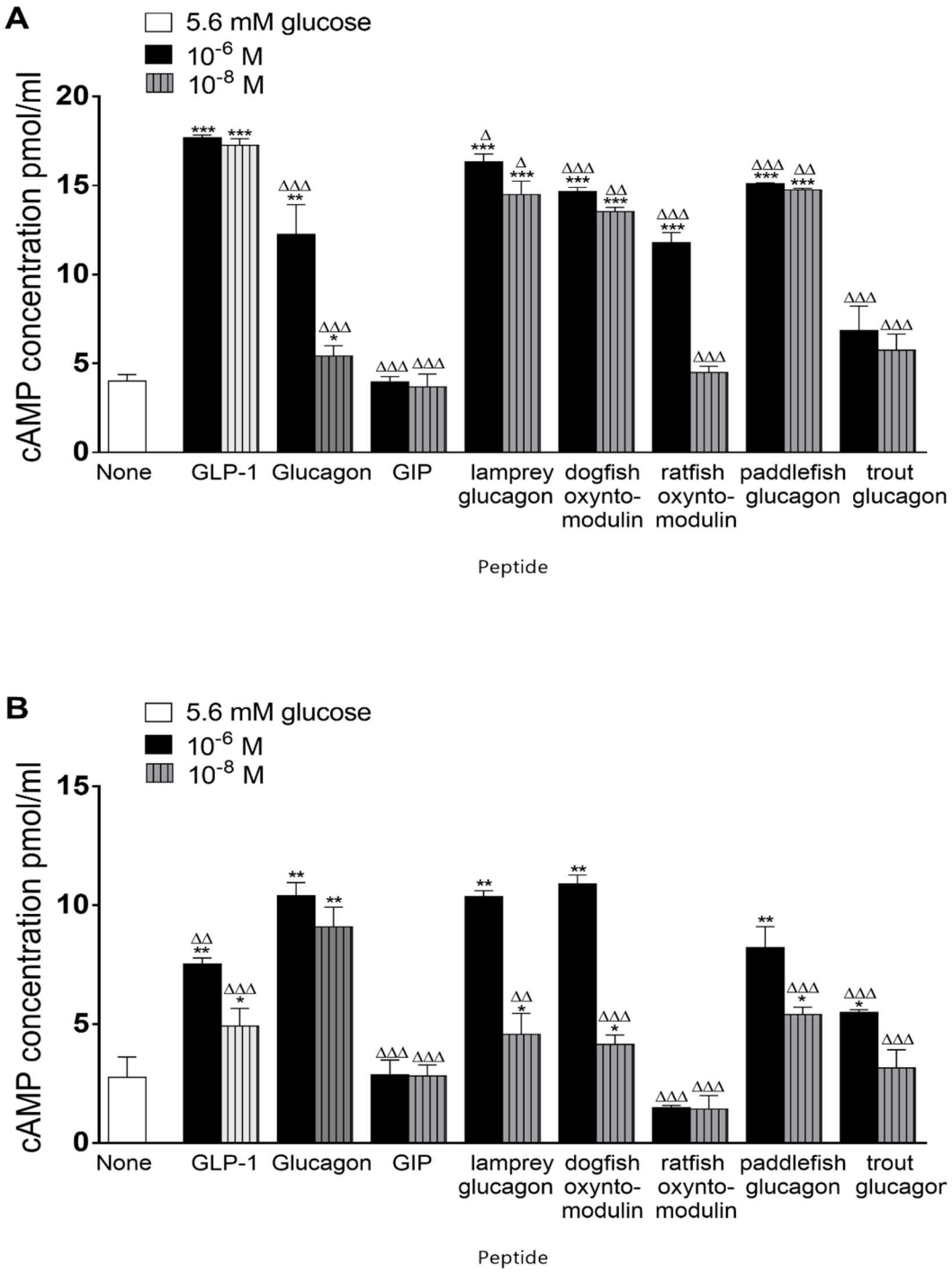

Values are mean ± S.E.M. for n = 4. *P < 0.05, ** P< 0.01 and ***P < 0.001 compared with 5.6 glucose. $^{\Delta}$P < 0.05, $^{\Delta\Delta}$P < 0.01, $^{\Delta\Delta\Delta}$P < 0.001 compared with the effect of glucagon/GLP-1

Figure 4.13 Effects of glucagon-related peptides (10^{-8} and 10^{-6} M) on the rate of insulin release from (A) wild-type INS-1 cells, (B) CRISPR/Cas9-engineered GLP-1R knock-out cells, (C) CRISPR/Cas9-engineered GCGR knock-out cells and (D) CRISPR/Cas9-engineered GIPR knock-out cells.

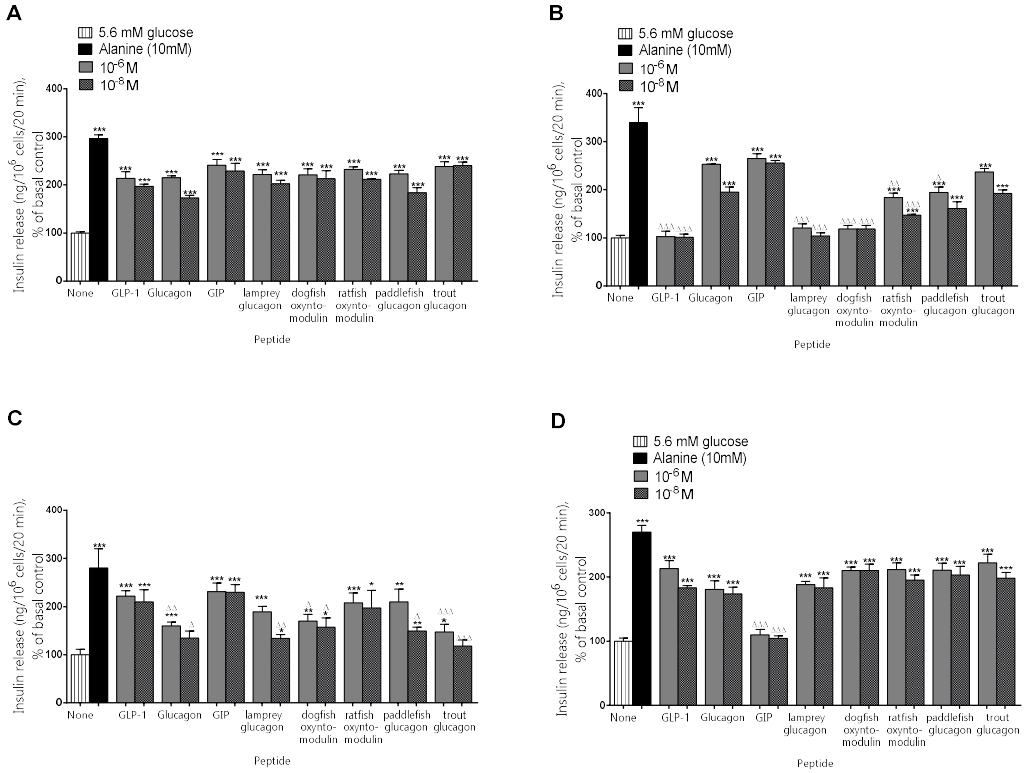

Values are mean ± S.E.M., $n = 8$, *P < 0.05, **P < 0.01 and ***P < 0.001 compared with 5.6 mM glucose alone. $^{\Delta}$P < 0.05, $^{\Delta\Delta}$P < 0.01, $^{\Delta\Delta\Delta}$P < 0.001 compared with effects in wild-type INS-1 cells.

Figure 4.14 Effects of acute administration of glucagon-related peptides (25 nmol/kg body weight) on blood glucose (panels A and C) and plasma insulin (panels B and D) concentrations in normal mice.

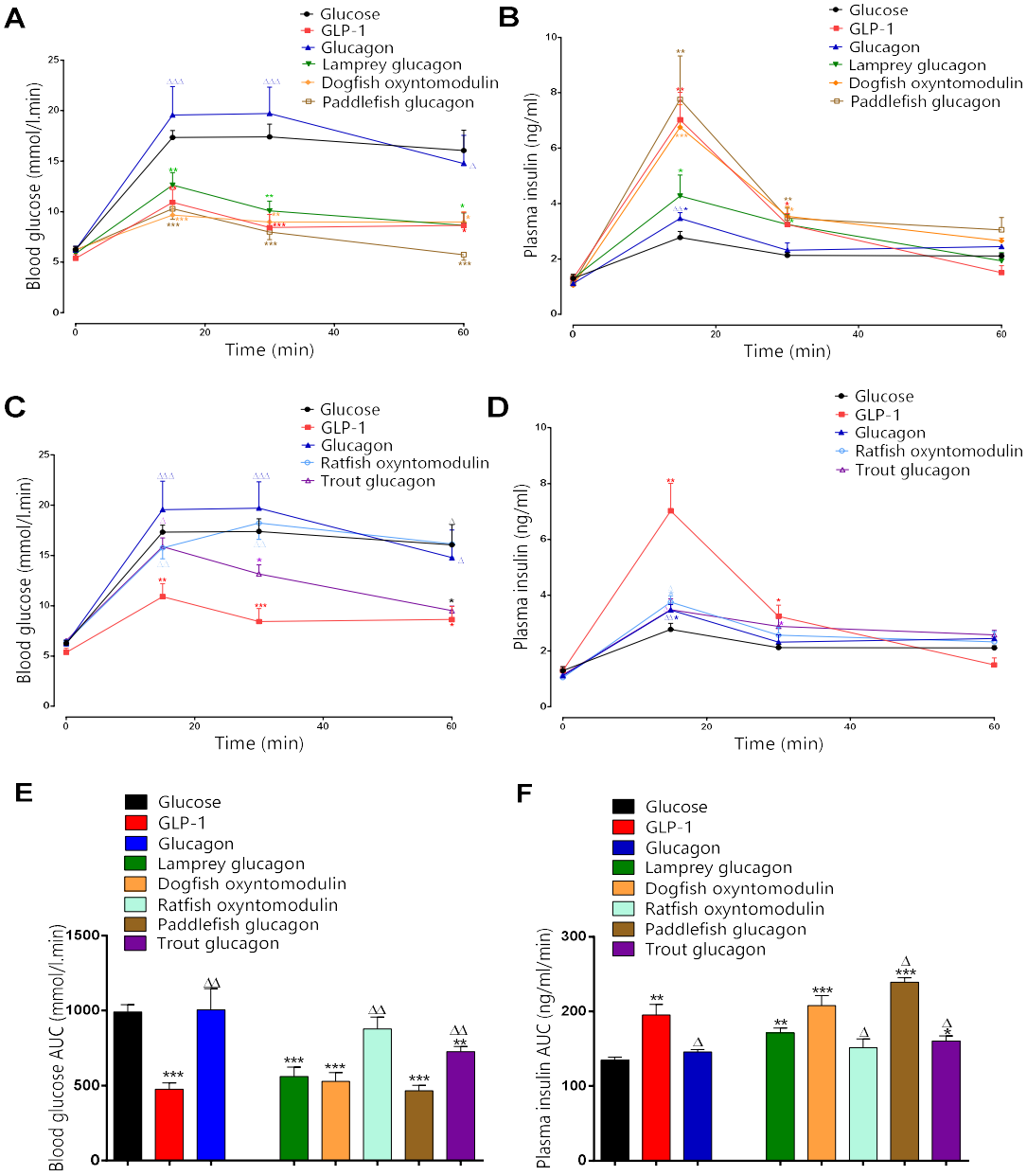

The integrated responses are shown in panels E and F. The values are mean ± S.E.M., n = 6. *P < 0.05, **P < 0.01 and ***P < 0.001 compared with glucose alone (18 mmol/kg body weight) and $^{\Delta}$P < 0.05, and $^{\Delta\Delta}$P < 0.01 compared with the effect of GLP-1.

Figure 4.15 Effects of acute administration of fish glucagon/oxyntomodulin peptides on blood glucose and plasma insulin concentrations in normal mice, 2 h post injection.

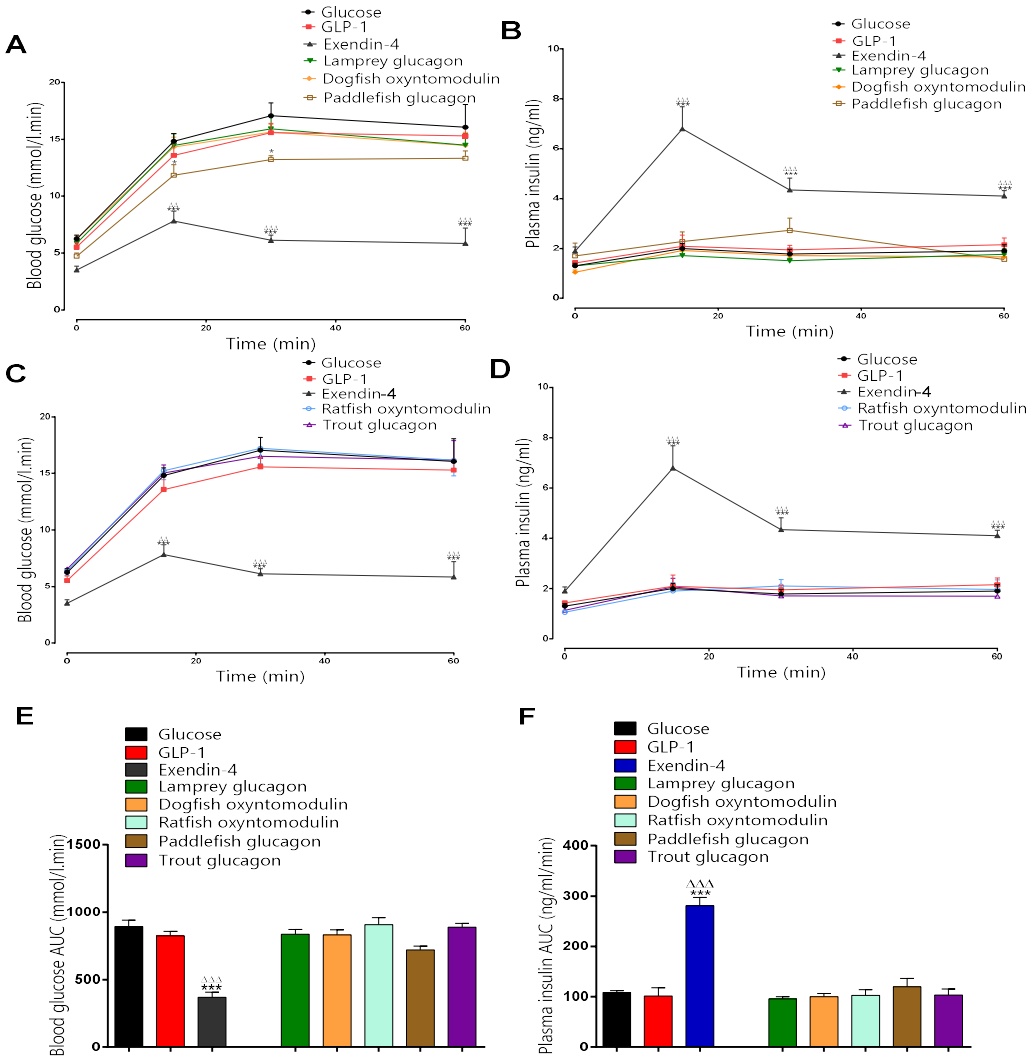

Blood glucose and plasma insulin were measured after intraperitoneal injection of glucose (18 mmol/kg body weight) 2 hours after intraperitoneal administration of 0.9% saline, exendin-4 and fish glucagon/oxyntomodulin peptides (25 nmol/kg body weight). The integrated responses (area under the curve AUC) are shown in panels E and F. The values are mean ± SEM for n=6. **P<0.01 and ***P<0.001 compared to glucose alone; $^{\Delta\Delta}$ P<0.01 and $^{\Delta\Delta\Delta}$ P<0.001 compared to human GLP-1.

Figure 4.16 Effects of fish glucagon/oxyntomodulin peptides on cumulative food intake over 3 hours trained feeding in 12 h fasting normal mice.

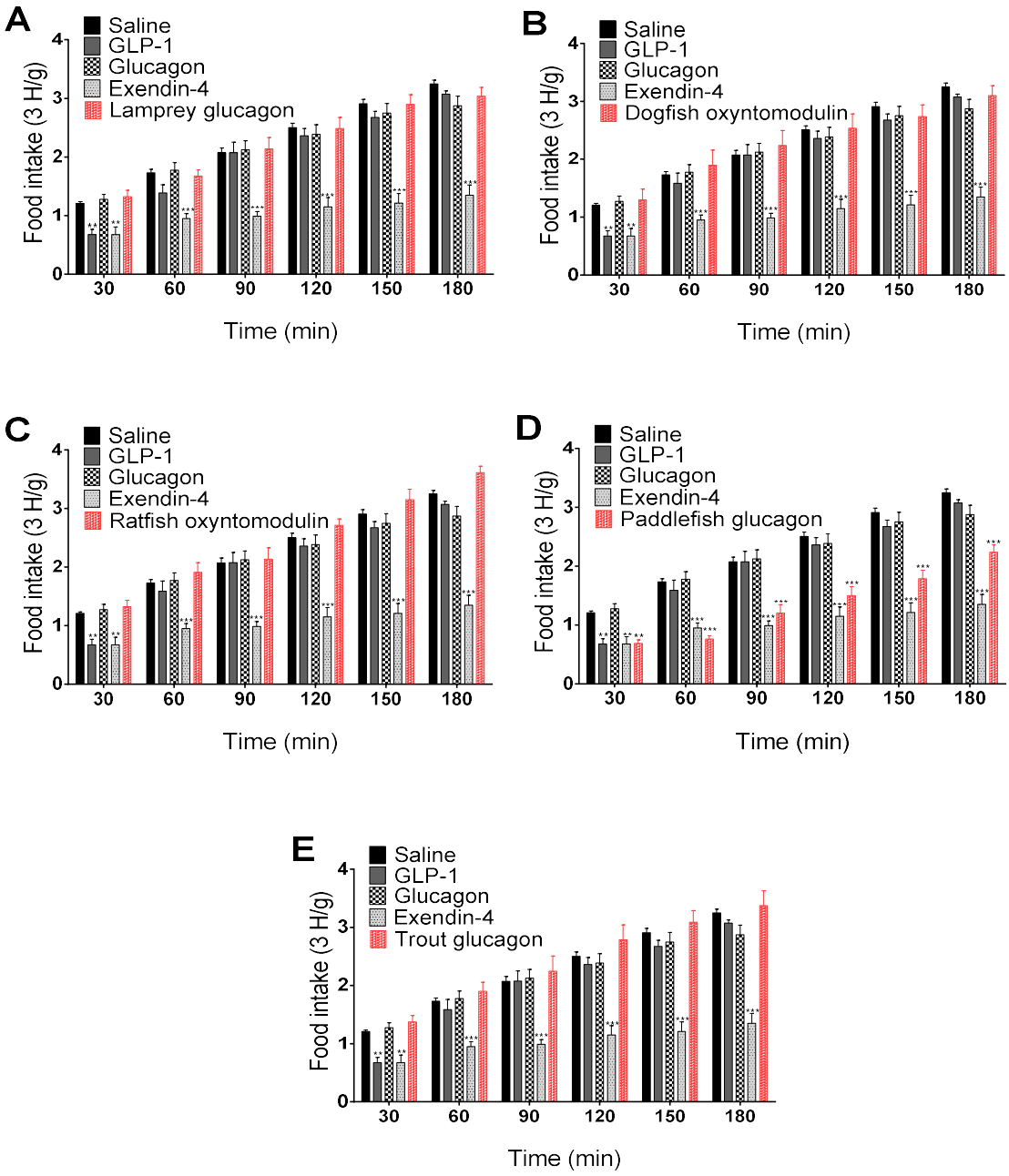

Cumulative food intake was measured after intraperitoneal administration of 50 nmol/kg peptides alongside 0.9% saline control. The values are mean ± SEM for n=8. *P<0.05, **P<0.01 and ***P<0.001 compared to saline control mice treated at the same time point.

Figure 4.17 A comparison of the primary structures of the glucagon-related fish peptides with those of human glucagon and GLP-1 and with the GLP1R agonist, exendin-4.

```
Glucagon                HSQGTFTSDY[10]SKYLDSRRAQ[20]DFVQWLMNT
Oxyntomodulin           HSQGTFTSDY SKYLDSRRAQ DFVQWLMNTKRNKNNIA
Lamprey glucagon        HSEGTFTSDY SKYLENKQAK DFVRWLMNA          (72)
Dogfish oxyntomodulin   HSEGTFTSDY SKYMDNRRAK DFVQWLMSTKRNG      (83)
Ratfish oxyntomodulin   HTDGIFSSDY SKYLDNRRTK DFVQWLLSTKRNGANT   (69)
Paddlefish glucagon     HSQGMFTNDY SKYLEEKRAK EFVEWLKNGKS        (66)
Trout glucagon          HSEGTFSNDY SKYQLERMAQ DFVQWLMNS          (72)

GLP-1                   HAEGTFTSDV[10]SSYLEGQAAK[20]EFIAWLVKGR[30]G
Exendin-4               HGEGTFTSDL SKQMEEEAVR LFIEWLKNGGPSSGAPPPS
Lamprey glucagon        HSEGTFTSDY SKYLENKQAK DFVRWLMNA          (57)
Dogfish oxyntomodulin   HSEGTFTSDY SKYMDNRRAK DFVQWLMSTKRNG      (50)
Ratfish oxyntomodulin   HTDGIFSSDY SKYLDNRRTK DFVQWLLSTKRNGANT   (40)
Paddlefish glucagon     HSQGMFTNDY SKYLEEKRAK EFVEWLKNGKS        (57)
Trout glucagon          HSEGTFSNDY SKYQLERMAQ DFVQWLMNS          (40)
```

Amino acid residues in the human peptides that have been shown to be important in receptor binding and signal transduction are shown in red. Differences in these residues are shown in green. Regions of structural similarity between paddlefish glucagon and exendin-4 are underlined. The values in parentheses show % sequence identity with the corresponding human peptides

Chapter 5

Assessing the acute and sub-chronic effects of novel enzyme resistant GLP-1 analogues derived from lamprey and paddlefish in obesity-diabetes.

5.1 Summary

Glucagon-like peptide-1 (GLP-1) molecules isolated from lamprey and paddlefish showed promising insulinotropic and glucose-lowering properties according to *in vitro* and *in vivo* studies. However, similarly to human GLP-1, these naturally occurring peptides were a subject to enzymatic degradation highlighting the need for specific modifications to prolong the half-life without affecting the biological actions. Two stable long-acting, fatty-acid linked analogues, [D-Ala^2]-lamprey GLP-1-Lys^{31}-gamma-glutamyl-pal and [D-Ala^2]-paddlefish GLP-1-Lys^{28}-gamma-glutamyl-pal, were designed and further evaluated *in vitro*, and in acute and long-term *in vivo* studies. Both stable fish GLP-1 peptide analogues significantly increased insulin secretion from BRIN-BD11 β-cells and isolated mouse islets. The peptides produced significant increases in cAMP concentration in CHL cells transfected with GLP1R and HEK293 cells transfected with GCGR. The insulinotropic effect of the fish GLP-1 analogues was decreased in CRISPR/Cas9-engineered GLP1R KO INS-1 cells and attenuated in INS-1 GCG receptor KO cells but remained unaltered in GIPR KO cells.

In vivo studies revealed that the lamprey GLP-1 analogue retained glucose-lowering and insulinotropic properties of the native peptide. In contrast, the modification of paddlefish GLP-1 resulted in the curtailment of its biological activities. Acute administration of [D-Ala^2]-lamprey GLP-1-Lys^{31}-gamma-glutamyl-pal (25 nmol/kg body weight) along with glucose (18 mmol/kg body weight) showed strong and persistent glucose lowering and insulin-releasing activities in NIH Swiss mice. Twice daily administration of [D-Ala^2]-lamprey GLP-1-Lys^{31}-gamma-glutamyl-pal to high fat-fed mice for 21 days decreased body weight, non-fasting plasma glucose and circulating insulin concentrations. Moreover, the stable analogue significantly improved glucose tolerance and insulin sensitivity with beneficial effects on islet beta-

cell area and insulin secretory responsiveness. Islet gene expression of insulin, GLUT2, Glp-1r and Gipr were also improved. Using streptozotocin-treated GluCreRosa26-YFP mice [D-Ala^{2}]-lamprey GLP-1-Lys^{31}-gamma-glutamyl-pal induced noticeable improvement in beta-cell mass including favourable effects on transdifferentiation of insulin-producing cells like liraglutide. These data highlight the potential of novel fish GLP-1 peptide analogue as therapeutic options for obesity and diabetes.

5.2 Introduction

The prevalence of type 2 diabetes (T2D) is increasing worldwide, and there is an urgent need for new cost-effective therapies that improve associated complications for the longer term (Gomez-Peralta et al. 2014; Skow et al. 2016).

The potent stimulatory effects of the intestinally derived hormone, GLP-1, on dynamics of insulin secretion was first revealed using the isolated perfused rat pancreas (Thorens et al. 1993). This insulinotropic action of GLP-1 is complemented with other unique antidiabetic functions, such as the ability to block secretion of glucagon, suppress appetite, as well as promote ß-cell proliferation and survival, thereby making it an attractive candidate for the treatment of type 2 diabetes (Furman 2009). However, native GLP-1 has a short plasma half-life (approximately two minutes) due to rapid degradation by proteases like DPP-IV and neural endopeptidase, which brings limitations to its beneficial effects (Manandhar et al. 2014). The discovery of the DPP-4 resistant exendin-4 from the venom of lizard *Heloderma suspectum* (Gila monster) and its further approval in 2005 led to the successful use and development of GLP-1 analogues exhibiting powerful antidiabetic properties which form the basis of a new therapeutically important class of drug (Tsend-Ayush

et al. 2016; Lau et al. 2018; O'Harte et al. 2016). Injectable agents, based upon the structure of human GLP-1, target gastrointestinal peptide receptors associated with appetite, insulin secretion, and energy balance. There are currently six GLP-1 receptor agonists approved for the treatment of T2D available in the market and used in combination therapies. However, dulaglutide is also licenced as monotherapy (Chaplin et al. 2016; Aroda 2018).

The incretin hormone GLP-1 is co-encoded with glucagon in the proglucagon gene which is expressed in a tissue-specific manner (Ng et al. 2010). Despite having a high degree of amino acid sequence similarity, these peptides act through distinct yet related class 2 G-protein coupled receptors, GLP1R and glucagon receptor (CGCR) respectively, to elicit important effects on glucose homeostasis, insulin secretion and energy maintenance (Moon et al. 2012; Gault et al. 2013). The post-transcriptional processing of proglucagon also gives rise to a number of other enteric peptide hormones such as oxyntomodulin (Lefèbvre 2012). The description of the proglucagon-derived peptide, oxyntomodulin, as a naturally occurring dual agonist of both GLP-1 receptors and glucagon has inspired the development of hybrids composing of multiple hormone molecules synthetically integrated into a single molecule (Elvert et al. 2018; Tschop et al. 2016; Lau et al. 2018). Stable oxyntomodulin-based peptides with specific N-terminal position 2 modifications have been recently reported to show particular promise for the treatment of diabetes (Lynch et al. 2014). Moreover, administration of triple-acting hybrid peptides with the ability to concurrently modulate GIP, GLP-1 and glucagon receptors to high fat fed mice have been shown to dramatically improve metabolic control and glycaemic status (Bhat et al. 2013a and Bhat et al. 2013b; Irwin et al. 2015).

GLP-1 and glucagon have been isolated from diverse vertebrate species from fish to mammals and are suggested to have a common evolutionary origin. Ancient fishes (lampreys and hagfishes) are the earliest known vertebrates to possess the glucagon-like sequences. Fish represent a valuable experimental model in the research of pancreatic hormones and other gastrointestinal peptides. In fish plasma, glucose levels are highly variable between species and within species, and it is suggested that glucose metabolism was adapted to long-term food deprivation conditions (Polakof et al. 2011; Cardoso et al., 2017). The extreme physiological conditions, such as extended periods of hyperglycemia or severe hypoglycemia that are considered to be pathological for mammals, hardly affect fish (Polakof et al. 2011). Interestingly, GLP-1 which is fairly conserved in vertebrates, does function as an incretin hormone in teleost fishes, acting similarly to glucagon increasing glucose levels in the blood (Mojsov 2000; Mommsen 2000; Irwin 2005). Long-acting GLP-1/glucagon receptors co-agonists derived from glucagon isolated from phylogenetically ancient fish (dogfish) have been recently reported to effectively counter hyperglycaemia and enhance both insulin secretion and action in high-fat-fed mice (O'Harte et al. 2016).

The biological activities of GLP-1 peptides from various fish species ranging from the ancient lamprey to recently evolutionary evolved rainbow trout have been investigated in Chapter 3. GLP-1 from lamprey and paddlefish were shown to act as dual agonists at the GLP-1 and glucagon receptors and were selected for further development as antidiabetic agents. Earlier results indicated that the native fish GLPs were cleaved by DPP-IV at positions 2, similarly to human GLP-1, producing smaller fragment peptides. The basic structures of the native fish peptides were thereby modified at the cleavage site by substitution of Ala at position 2 with its D-isomer to protect the molecules from DPP-IV degradation. Additionally, a gamma-glutamyl with palmitate

adjunct was added to the side-chains of the lysine residues at positions 31 for lamprey GLP-1 and at position 28 for paddlefish GLP-1 to ensure albumin binding ability and extend i*n vivo* activity. The potential beneficial metabolic effects of these two fish peptide analogues were examined in acute in vitro studies using BRIN-BD11 cells, GLP-1R-transfected CHL and glucagonR-transfected HEK293 cells and *CRISPR/Cas9*-engineered INS-1 cell lines with a specific GLP-1 or glucagon receptor KO as well as in acute and longer-term *in vivo* studies using normal and high-fat-fed mice. Further studies investigated effects of lamprey GLP-1 analogue on alpha to beta cell transdifferentiation using streptozotocin-treated GluCreRosa26-YFP mice.

5.3 Materials and Methods

5.3.1 Chemical Reagents and Peptides

Peptide analogues, [D-Ala^2]-lamprey GLP-1-Lys^{31}-gamma-glutamyl-pal and [D-Ala^2]-paddlefish GLP-1-Lys^{28}-gamma-glutamyl-pal, were obtained from Synpeptide Co. Ltd. (Shanghai, China) and purified as previously described in Section 2.1.1. Peptides analogues were subsequently characterized using MALDI-TOF MS (Section 2.2). The primary structures and molecular masses of the peptides used in this study are shown in Table 5.1. Synthetic human glucagon, human GLP-1, human GIP, oxyntomodulin, liraglutide and exendin-4 peptides were obtained and processed as described previously (Section 2.1.1).

5.3.2 Assessment of metabolic stability of fish GLP-1 analogues

Effects of DPP-IV or mouse plasma on fish GLP-1 peptide analogues stability were assessed in degradation studies as previously described in Section 2.3.

5.3.3 *In vitro* insulin release studies using BRIN-BD11 cells

In vitro insulin, secretory studies were performed using rat BRIN-BD11cell line (McClenaghan et al., 1996) as previously described (Section 2.5.1) and measured by RIA (Sections 2.5.2 and 2.5.7).

5.3.4 Insulin release studies using isolated mouse islets

Effects of [D-Ala^2]-lamprey GLP-1-Lys^{31}-gamma-glutamyl-pal and [D-Ala^2]-paddlefish GLP-1-Lys^{28}-gamma-glutamyl-pal on *ex-vivo* insulin secretion were assessed using pancreatic islets from adult, male National Institutes of Health (NIH) Swiss mice (Harlan Ltd, Bicester, UK) as previously described (Section 2.5.5).

5.3.5 Effects of peptides on cAMP production.

The effects of the fish peptide analogues on cAMP production from Chinese hamster lung (CHL) cells transfected with the human GLP-1 receptor (GLP1R) (Thorens et al., 1993) and human embryonic kidney (HEK293) cells transfected with the human glucagon receptor (GCGR) (Ikegami et al., 2001) were assessed using a Parameter cAMP assay kit (R&D Systems, Abingdon, UK) as outlined in Section 2.6.

5.3.6 Insulin release studies using CRISPR/Cas9-engineered INS-1 cells

In vitro receptor activation studies were performed using wild-type INS-1 832/3 rat clonal pancreatic β-cells and CRISPR/Cas9-engineered cells with a knock-out of either GLP-1 receptor (GLP-1 KO), glucagon receptor (GCG KO) or GIP receptor (GIP KO) (Naylor et al. 2016) as described in Section 2.5.4.

5.3.7 Effects of peptides on proliferation and apoptosis of BRIN BD11 cells

To assess the effects of the fish peptide analogues (10nM and 10μM) on beta-cell proliferation and apoptosis, BRIN-BD11 were used as previously described (Section 2.7).

5.3.8 Animals

Acute and persistent *in vivo* studies were carried out using male National Institutes of Health (NIH) Swiss mice as previously described (Sections 2.8.1.1, 2.8.2.1, 2.8.2.3 and 2.8.2.5). Normal male TO mice were used in food consumption studies as described in Section 2.8.2.6. Longer-term studies were performed using high fat fed TO mice (Section 2.8.1.2).

5.3.9 Acute *in vivo* glucose-lowering and insulinotropic effects of peptides in normal mice

For acute IPGTT studies, blood glucose and plasma insulin were measured immediately prior to (t = 0) and 15, 30 and 60 min after intraperitoneal administration of glucose alone (18 mmol/kg of body weight) or in combination with test peptides (each at 25 nmol/kg bw) in overnight fasted mice. In separate series of experiments, overnight fasted animals received either test peptides (each at 25 nmol/kg of body weight) or saline vehicle 2 or 4 hours before an intraperitoneal glucose administration (18 mmol/kg bw) and blood glucose and plasma insulin measured at 15, 30 and 60 min post glucose injection as detailed in Section 2.8.5.

5.3.10 Acute food consumption studies in normal mice

Animals were administrated intraperitoneal injections of either saline solution or peptides (75 nmol/kg) before receiving free access to normal chow for 300 mins. Food intake was measured as outlined in Section 2. 8.2.4.

5.3.11 Long-term *in vivo* studies using high-fat-fed mice

The high-fat diet was provided for 3 months before the start of the study to trigger weight gain, hyperglycaemia and insulin resistance (Section 2.8.1.2). Animals were grouped and received twice daily intraperitoneal injections saline solution for three days before administration of saline or peptides (25 nmol/kg of body weight) twice daily (09:30 and 17:00 h) over 21 days treatment period (Sections 2.8.1.2 and 2.8.3.1). The peptide treatments were commenced as follows: Group 1 (high fat control, n = 8; 0.9% NaCl, w/v; ip); Group 2 (liraglutide, n = 8; 25 nmol/kg bw; ip); Group 3 ([D-Ala^2]-lamprey GLP-1-Lys^{31}gamma-glutamyl-pal, n = 8; 25 nmol/kg bw; ip); Group 4 ([D-Ala^2]-paddlefish GLP-1-Lys^{28}-gamma-glutamyl-pal, n = 8; 25 nmol/kg bw; ip). Mice remained on a high-fat diet for the duration of the study. Non-fasting blood glucose, cumulative food intake and water intake, body weight, and insulin concentrations were monitored at 3-day intervals before daily injection of test peptides (Section 2.8.3.1). On day 21, IPGTT, OGTT (18 mmol/kg bw) and insulin sensitivity (25 U/kg bw; i.p.) tests were performed (Section 2.8.3.2 and 2.8.3.3). HOMA-β was calculated using the formula HOMA-β = 20 × fasting insulin (μIU/ml)/fasting glucose (mmol/ml) − 3.5, whereas HOMA-IR was determined using the equation HOMA-IR = fasting glucose (mmol/l) x fasting insulin (mU/l)/22.5. At the end of the experimental period, terminal non-fasted blood was collected (Section 2.8.3.5) for

measuring lipid profile (Section 2.8.3.8), plasma amylase activity (Section 2.8.3.7), ALT (Section 2.8.3.9) and glucagon levels (Section 2.8.3.11).

Bone mineral density and body tissue composition were measured using DEXA scanning (Section 2.8.3.4). The terminal analysis also included extraction of pancreatic tissue for measurement of pancreatic hormonal content (Section 2.8.3.12) and preparation of paraffin tissue blocks for immunohistochemical staining (Section 2.13.1). Islets were isolated for measurement of acute insulin secretion (Section 2.8.3.6) and determination of gene expression (Sections 2.8.3.13- 2.8.3.15).

5.3.12. Long-term in vivo studies using GluCre Rosa26-YFP mice

The animals were housed and pre-treated with streptozotocin as described in Sections 2.8.1.4, and 2.8.4 Mice (n=5) were administrated twice daily intraperitoneal injections of saline or peptides, [D-Ala^2]-lamprey GLP-1-Lys^{31}gamma-glutamyl-pal and liraglutide (25 nmol/kg of body weight) over a 10-day treatment period. Non-fasting blood glucose, food intake, water intake and body weight were monitored at 3-day intervals prior to daily injection of test peptides. Blood was collected for insulin measurements at the start and end of the experiment. The animals were sacrificed, and pancreatic tissue was removed and processed for immunohistochemistry analysis as described in Section 2.8.4.

5.3.13 Statistical analysis

Data were compared using unpaired Student's t-test (non-parametric, with two-tailed P values and 95% confidence interval) and one-way ANOVA with Bonferroni post-hoc test using GraphPad PRISM (Version 5.0 San Diego, California). Area under the curve (AUC) analysis was performed using the trapezoidal rule with baseline

correction. Data are presented as mean ± S.E.M where the comparison was considered to be significantly different if $P < 0.05$.

5.4 Results

5.4.1 Purification and confirmation of molecular masses by MALDI-TOF MS

Following RP-HPLC on a C-8 semi-preparative column the main peptide peaks of [D-Ala^2]-lamprey GLP-1-Lys^{31}gamma-glutamyl-pal and [D-Ala^2]-paddlefish GLP-1-Lys^{28}-gamma-glutamyl-pal were collected as represented in Figure 5.1. Experimental masses detected for each peptide by MALDI-TOF MS corresponded very closely with the theoretical masses as shown in Table 5.1 and Figure 5.2.

5.4.2 DPP-IV and plasma degradation studies

[D-Ala^2]-lamprey GLP-1-Lys^{31}-gamma-glutamyl-pal and [D-Ala^2]-paddlefish GLP-1-Lys^{28}-gamma-glutamyl-pal were stable to degradation after 4 h incubation with DPP-IV (Table 5.2 and Figure 5.3-5.4) whereas native fish GLP-1 peptides, as well as human GLP-1, were rapidly degraded (Chapter 3). The analogues were also resistant to degradation after 4 hours incubation with mouse plasma (Figures 5.5-5.6). Human GLP-1 was rapidly degraded (65% degradation after 4 h in plasma) (Figure 5.7 and Table 5.2).

5.4.3. *In vitro* insulin release studies

The basal rate of insulin release from BRIN-BD11 rat clonal β-cells in the presence of 5.6 mM glucose alone was 1.02 ± 0.07 ng/10^{6}cells/20 min. Incubation with human GLP-1 (0.1 μM) increased this rate to 2.4 ± 0.2 ng/10^{6}cells/20 min (Figure 5.8). In the presence of 5.6 mM glucose, [D-Ala^2]-lamprey GLP-1-Lys^{31}-gamma-glutamyl-pal and [D-Ala^2]-paddlefish GLP-1-Lys^{28}-gamma-glutamyl-pal produced a

concentration-dependent increase in the rate of insulin release from the cells (Figure 5.8). Table 5.3 compares the effects of the fish peptide analogues to their native forms and human GLP-1. The effect of [D-Ala^2]-lamprey GLP-1-Lys^{31}gamma-glutamyl-pal was similar to the native lamprey GLP-1, whereas [D-Ala^2]-paddlefish GLP-1-Lys^{28}-gamma-glutamyl-pal analogue showed inferior insulinotropic actions compared to its native form or human GLP-1.

The rate of insulin release from isolated mouse islets in the presence of 16.7 mM glucose alone during a 60 min incubation was 8.5 ± 0.5 % of the total insulin content of the islets (Table 5.4). Incubation with GLP-1 at10 nM and μM 1 raised the rate of insulin release to 14.4 ± 1.1 % and 16.4 ± 0.7 % respectively. As shown in Figure 5.9 and Table 5.4, lamprey GLP-1-derived analogue produced a significant increase in insulin release at both 10 nM and 1 μM concentrations, whereas paddlefish GLP-1-derived analogue was only effective at 1 μM.

5.4.4 Effect on fish GLP-1 analogues on cAMP production

As shown in Figure 5.10 A, [D-Ala^2]-lamprey GLP-1-Lys^{31}gamma-glutamyl-pal significantly stimulated cAMP production in CHL cells transfected with the human GLP-1 receptor in an almost identical fashion with human GLP-1 at both 10 nM and 1 μM concentrations. Similarly, [D-Ala^2]-paddlefish GLP-1-Lys^{28}-gamma-glutamyl-pal exhibited a significant effect on cAMP production at 1 μM. However the peptide had an inferior effect at 10 nM compared to human GLP-1 (Figure 5.10 B). Both of the analogues stimulated cAMP production in HEK293 cells transfected with the human glucagon receptor. However, the effect was significantly lesser than that produced by human glucagon (Figure 5.10 B and Table 5.5).

5.4.5 Insulin release studies using CRISPR/Cas9-engineered INS-1 cells

Incubation of wild-type INS-1 cells with glucagon, GLP-1, GIP and peptide analogues significantly increased the rate of insulin release at both, 10 nM and 1 μM concentrations, compared with the basal control (Figure 5.11 A and Table 5.6). The insulinotropic effects of the analogues were significantly attenuated in the GLP-1 KO and glucagon KO cells compared with their effects in wild-type INS-1 cells (Figure 5.11 B and C). In contrast, no significant alteration was observed in GIP KO apart from the abolished stimulatory effect of control human GIP at both concentrations (Figure 5.11 D).

5.4.6 Effects of stable fish GLP-1 peptides on proliferation and apoptosis of BRIN BD11 cells

As shown in Figure 5.12 proliferation was dramatically decreased ($P<0.001$) when BRIN BD11 cells were incubated with the mixture of proinflammatory cytokines compared to control cultures. Human GLP-1 and fish GLP-1 analogues (10nM and 10μM) significantly ($P<0.001$) increased proliferation of the cells in cytokine-free solution. Moreover, all peptides had a significant ($P<0.01$ $P<0.001$) protective effect on cell proliferation in the presence of cytokines. In the second series of experiments, exposure of BRIN-BD11 cells to 10nM and 10μM human GLP-1 and [D-Ala^2]-lamprey GLP-1-Lys^{31}gamma-glutamyl-pal (at 10μM) significantly ($P<0.001$- $P<0.01$) protected against cytokine-induced apoptosis (Figure 5.12).

5.4.7 *In vivo* acute insulin release and food intake studies

Blood glucose concentrations in overnight fasted NIH Swiss mice receiving intraperitoneal administration of glucose (18 mmol/ kg body weight) together with 25

nmol/kg body weight of [D-Ala^2]-lamprey GLP-1-Lys^{31}gamma-glutamyl-pal were significantly lower ($P < 0.001$) at 30 and 60 min time points compared to administration of intraperitoneal glucose alone (Figure 5.13 A and E). This peptide also potentiated ($P < 0.001$) glucose-induced insulin release compared to glucose alone (Figure 5.13 C and F) with effects greater than GLP-1 at 30 ($P < 0.05$) and 60 min ($P < 0.001$) (Figure 5.13 C).

When administered two (Figure 5.14) or four (Figure 5.15) hours prior to a glucose load [D-Ala^2]-lamprey GLP-1-Lys^{31}gamma-glutamyl-pal still significantly ($P < 0.001$) reduced individual post-injection and overall 0–60 min AUC glucose values as did exendin-4. Consistent with this insulin concentrations were persistently raised ($P < 0.01$ to $P < 0.001$) compared with glucose alone and native GLP-1 (Figure 5.14 A, C, E and F). Moreover, the effects of [D-Ala^2]-lamprey GLP-1-Lys^{31}gamma-glutamyl-pal and exendin-4 ($P < 0.05$ to $P < 0.001$) were observed in mice when administered four hours previously (Figure 5.15). In contrast, the analogue of paddlefish GLP-1, [D-Ala^2]-paddlefish GLP-1-Lys^{28}-gamma-glutamyl-pal, showed minor glucose-lowering and insulinotropic activities being less than the native fish peptide (Figure 5.13 B, D, E and F). As expected oxyntomodulin, dual glucagon/GLP-1 receptor agonist, had no glucose lowering and insulinotropic effect when administrated four hours prior to a glucose challenge (Figure 5.15 A, C, E and F).

In addition to effects on blood glucose control, [D-Ala^2]-lamprey GLP-1-Lys^{31}gamma-glutamyl-pal exhibited significant ($P < 0.01$ and $P < 0.001$) appetite suppressive actions after 150 mins of administration (Figure 5. 16). This differed considerably from the native peptide which exhibited no effect on food intake after 30 min of administration (Figure 5. 16) Moreover, [D-Ala^2]-paddlefish GLP-1-Lys^{28}-gamma-glutamyl-pal significantly ($P < 0.001$) lowered food intake after 30 mins of

administration, but was not as effective as native paddlefish GLP-1 which had a significant ($P < 0.05$ to $P < 0.001$) impact on feeding at 30 to 240 min time points (Figure 5.16).

5.4.8 Chronic effects of stable fish GLP-1 peptides on body weight, food/water intake, non-fasting plasma glucose and insulin, insulin sensitivity and insulin resistance in high-fat fed mice

[D-Ala2]-lamprey-GLP-1-Lys31gamma-glutamyl-pal, [D-Ala2]-paddlefish-GLP-1-Lys28-gamma-glutamyl-pal and liraglutide resulted in a significant change in the body weight (Figure 5.17 A and B), however only [D-Ala2]-lamprey-GLP-1-Lys31gamma-glutamyl-pal and liraglutide elicited a significant effect on accumulated food intake compared to high-fat control (Figure 5.17 C). The effect of [D-Ala2]-lamprey-GLP-1-Lys31gamma-glutamyl-pal on appetite reduction was significantly greater than liraglutide (Figure 5.17 C). No alteration was observed in water intake in any of the treated groups compared to high fat saline control (Figure 5.17 D). Chronic high fat feeding markedly increased blood glucose levels which were reduced by [D-Ala^2]-lamprey-GLP-1-Lys31gamma-glutamyl-pal (Figure 5.17 A and B). However [D-Ala^2]-paddlefish-GLP-1-Lys^{28}-gamma-glutamyl-pal and liraglutide had no noticeable effect over the 21 days (Figure 5.17 A and B). The 21-day treatment regimen with [D-Ala^2]-lamprey-GLP-1-Lys31gamma-glutamyl-pal and liraglutide significantly decreased circulating insulin compared to saline control. Exogenous insulin (day 21) induced increased glucose clearance from the circulation in [D-Ala2]-lamprey-GLP-1-Lys31gamma-glutamyl-pal-treated mice. Hence insulin sensitivity (Figure 5.18 E) and AAC (Figure 5.18 F) were significantly ($P< 0.05$) improved in this group. Moreover, HOMAR-IR values were significantly lower in animals treated with [D-Ala2]-lamprey-GLP-1-Lys31gamma-glutamyl-pal and liraglutide compared

to high-fat control (Figure 5.19 B). Beta-cell function was also improved in these groups with HOMA-β values significantly higher than control (Figure 5.19 A).

5.4.9 Chronic effects of stable fish GLP-1 peptides on glucose tolerance and pancreatic hormone content high-fat-fed mice

Following an intraperitoneal (Figure 5.20) or oral (Figure 5.18) glucose challenge on day 21, blood glucose concentrations were significant reduced ($P < 0.01$ to $P < 0.01$) at all time points in mice that were treated with [D-Ala2]-lamprey-GLP-1-Lys31gamma-glutamyl-pal compared to high fat saline control. This ultimately culminated in decreased ($P < 0.01$ to $P < 0.001$) overall 0–120 min glucose AUC values (Figure 5.20 B and Figure 5.21 B). Liraglutide treatment also reduced ($P < 0.05$) the overall glucose AUC in high fat fed mice but with slightly lesser potency than [D-Ala^2]-lamprey GLP-1-Lys^{31}-gamma-glutamyl-pal. In contrast, treatment with the second analogue, [D-Ala^2]-paddlefish GLP-1-Lys^{28}-gamma-glutamyl-pal, failed to elicit any significant effect on IPGTT and OGTT. Corresponding insulin concentrations were significantly elevated ($P < 0.05$ - $P < 0.001$) in these groups (Figure 5.20 C-D and Figure 5.21 C-D). Pancreatic insulin contents were significantly ($P < 0.05$-$P < 0.01$) reduced by all treatment regimens apart from [D-Ala^2]-paddlefish GLP-1-Lys^{28}-gamma-glutamyl-pal (Figure 5.22 B). Pancreatic glucagon was also significantly ($P < 0.05$) reduced on day 21 after the treatment with [D-Ala2]-lamprey-GLP-1-Lys31gamma-glutamyl-pal compared to high fat saline control (Figure 5.22A).

5.4.10 Chronic effects of stable fish GLP-1 peptides on blood lipid profile, amylase activity, plasma glucagon and ALT levels in high fat fed mice.

Assessment of the plasma lipid profile on day 21 showed a significant reduction ($P < 0.05$ to $P < 0.001$) in triglyceride levels and increased levels of HDL-cholesterol only in the group treated with [D-Ala^2]-lamprey GLP-1-Lys^{31}-gamma-glutamyl-pal when compared to high-fat controls (Figure 5.23 B and C). Plasma ALT was significantly ($P < 0.05$ - $P < 0.001$) decreased, whereas amylase activity was slightly but significantly ($P < 0.05$ and $P < 0.001$) elevated in all of the treatment groups compared to high-fat controls (Figure 5.24 A and B). No significant differences were noted in terms of plasma glucagon levels (Figure 5.24 C).

5.4.11 Chronic effects of stable fish GLP-1 peptides on bone density and body mass in high fat-fed mice

High-fat diet control and peptide treatment groups displayed no significant differences in bone mineral density, content and normal mass (Figure 5.25 A-D). However, a significant reduction of fat mass and body fat percentage was observed in all peptide treatment groups (Figure 5.25 D and E).

5.4.12 Chronic effects of peptide administration on ex-vivo insulin secretion from isolated mouse islets and pancreatic islet histology in high-fat-fed mice

As shown in Figure 5.26 A, islets isolated from high-fat fed and mice treated with paddlefish GLP-1 analogue exhibited a weak insulin secretory responses to stimulatory concentrations of glucose, alanine, arginine, potassium chloride, human GLP-1 and GIP. In contrast, islets isolated from animals receiving twice-daily treatment with liraglutide and lamprey GLP-1 analogue had improved insulin

secretory responses. Insulin content was less in liraglutide and lamprey GLP-1 analogues treated groups compared to controls (Figure 5.26 B).

The immunochemical staining revealed no obvious significant visual differences islet morphology between the groups treated with liraglutide and [D-Ala^2]-paddlefish GLP-1-Lys^{28}-gamma-glutamyl-pal compared to high-fat control (Figure 5.27 A-E). However, islets of the mice after a 21 day treatment with [D-Ala^2]-lamprey GLP-1-Lys^{31}-gamma-glutamyl-pal showed a significant decrease in alpha size area ($P < 0.001$) with a significant ($P < 0.5$) reduction in the larger (>25 000 μm^2) sized islets and a significant increase medium sized islets (10,000 – 25 000 μm^2) islet size compared to the control group (Figure 5.27 D and E). No significant changes in total islet area were observed in the group treated with [D-Ala2]-lamprey-GLP-1-Lys31gamma-glutamyl-pal (Figure 5.27 B). The representative images from high-fat-fed and all peptide treatment groups are represented in Figure 5.27 F-I.

5.4.13 Chronic effects of stable fish GLP-1 peptides on gene expression in high-fat-fed mice

Islet gene expression analysis revealed a significant ($P < 0.05$) decrease in expression of *Ins1* (mouse insulin 1) and a significant upregulation of *Slc2a2* (glucose transporter 2; GLUT2) as well as glucagon and GLP-1 receptor genes in animals receiving twice-daily liraglutide and lamprey GLP-1 analogue compared to high-fat control group. Furthermore, long-term administration of the lamprey GLP-1 analogue resulted in a significantly ($P < 0.05$) increased expression of *Gck* (glucokinase) and *Glp-1r* and *Gipr* receptors (Figure 5.28). Gene expression in mice after treatment with the paddlefish GLP-1 analogue was similar to high-fat control.

5.4.14 Chronic effects of [D-Ala^2]-lamprey GLP-1-Lys^{31}-gamma-glutamyl-pal on accumulative food and water intake in streptozotocin pre-treated GluCreRosa26-YFP mice

Streptozotocin treatment GluCreRosa26-YFP mice resulted in a significant ($P < 0.05$) increase in food intake on day 11 compared to untreated GluCreRosa26-YEP controls (Figure 5.29 A). No significant differences in food intake were observed in the groups treated twice daily with liraglutide or lamprey GLP-1 analogue (Figure 5.29 A). A significant ($P < 0.05$ and $P < 0.01$) increase in water intake was observed in the streptozotocin control group from day 9 (Figure 5.29 B). However, no significant differences in fluid intake were observed in mice treated with liraglutide or lamprey GLP-1 analogue (Figure 5.29 B).

5.4.15 Chronic effects of [D-Ala^2]-lamprey GLP-1-Lys^{31}-gamma-glutamyl-pal on blood glucose, body weight, plasma insulin and pancreatic hormonal content in streptozotocin pre-treated GluCreRosa26-YFP mice.

Streptozotocin significantly decreased body weight, elevated blood glucose, decreased plasma insulin, lowered pancreatic insulin and elevated pancreatic glucagon content compared to untreated control (Figure 5.30). Administration of liraglutide to streptozotocin treated GluCreRosa26-YFP mice resulted in a visible improvement but no significant change in body weight change (Figure 5.30 D). A significant decrease in body weight loss was also observed in mice treated with lamprey GLP-1. Furthermore, twice-daily administration of liraglutide or lamprey GLP-1 analogue resulted in an improved appearance but no significant decrease in blood glucose levels (Figure 5.30 A and B). Insulin levels in all groups of GluCreRosa26-YFP mice were similar before streptozotocin treatment. Liraglutide and lamprey GLP-1 analogue

increased ($P < 0.05$) plasma insulin concentrations in streptozotocin-treated mice but levels were still significantly ($P < 0.001$) lower compared to untreated control. Pancreatic insulin content was also improved by peptide treatments but remained lower than the untreated control (Figure 5.31 A). Glucagon content was significantly higher in streptozotocin groups compared with untreated controls (5.31 B).

5.4.16 Chronic effects of [D-Ala^2]-lamprey GLP-1-Lys^{31}-gamma-glutamyl-pal on islet morphology in streptozotocin pre-treated GluGre Rosa26EYFP mice

Treatment of GluCre Rosa26-YFP mice with streptozotocin resulted in a significant reduction of a number of islets, islet size and beta cell area as well as a greater percentage of smaller islets compared to untreated GluCreRosa26-YFP control mice (Figure 5.32 A, B, D and E)

Administration of liraglutide or lamprey GLP-1 analogue resulted in a significant ($P < 0.05$) improvement in the number of islets in the head and tail regions and an increase in beta cell area in the tail region and whole pancreas (Figure 5.32 A). Islet area was significantly reduced in all treatment groups compared to untreated controls (Figure 5.32 B). No significant differences were observed in alpha cell area (Figure 5.32 C). A significant decrease ($P < 0.05$ and $P < 0.01$) in the number of large and medium islets, and a significant increase ($P < 0.05$ and $P < 0.01$) in the number of small islets was observed in the treated groups.

5.4.17 Chronic effects of [D-Ala^2]-lamprey GLP-1-Lys^{31}-gamma-glutamyl-pal on islet alpha to beta cell transdifferentiation in streptozotocin-treated GluGre Rosa26-YFP mice

Administration of tamoxifen-induced the expression of the reporter protein, YFP, in alpha cells (56-73% alpha-cells expressed GFP) with the highest percentage of

expression in untreated mice (Figure 5.33 A). The number of GFP^- $glucagon^+$ alpha cells was significantly increased in peptide treatment groups (except the head region of the pancreas in mice treated with liraglutide) and STZ control compared to untreated control. (Figure 5.33 B). Moreover, GFP^+ $glucagon^-$ cells were observed in the head region of the pancreas in both peptide treatment groups (Figure 5.33 C). GFP^+ insulin+ cells were also significantly expressed in all treated groups especially in the head region of the pancreas. (Figure 5.33 D).

5.5 Discussion

Although the vertebrate incretin system is highly conserved and the proglucagon gene is expressed by all vertebrates, in fishes the function of GLP-1 as an incretin hormone is questionable. This raised the possibility that the incretin properties of GLP-1 may have evolved after the divergence of tetrapods from fish (Tsend-Ayush et al., 2016 and Mommsen, 2000). However, due to the highly conserved nature, the biologically active fish GLP-1 will bind to mammalian receptors, and mammalian hormones will act on the piscine receptors (Mommsen, 2000).

In Chapter 3 it has been demonstrated that GLP-1 peptides from phylogenetically ancient fish and a teleost appeared to exhibit a variation in the potency to stimulate insulin release from rodent and human cells *in vitro* and lower blood glucose concentrations in mice *in vivo*. GLP-1 from sea lamprey, the living fossils of ancient animals existing for over 360 million years and belonging to the superclass Cyclostomata (Xu et al. 2016), and paddlefish, a survivor of an ancient fish fauna of the Cretaceous period, over 100 MYA (Pettigrew et al. 2003) were the most potent and effective with activities generally comparable to human GLP-1. Additionally, GLP-1 from these two fish species appeared to function as dual GLP-1/glucagon receptor agonists.

In the present study, [D-Ala^2]-lamprey-GLP-1-Lys^{31}-gamma-glutamyl-pal and [D-Ala^2]-paddlefish-GLP-1-Lys^{28}-gamma-glutamyl-pal (structurally modified derivatives of lamprey and paddlefish GLP-1) have been investigated *in vitro* and *in vivo* for insulinotropic and glucose-lowering actions. These properties of analogues were compared to the effects elicited by the unmodified native fish peptides, human GLP-1, human glucagon, human GIP, human oxyntomodulin as well as long-acting antidiabetic agents such as exendin-4 (GLP-1R agonist) and liraglutide (GLP-1 analogue). Results outlined in Chapter 3, demonstrated that native lamprey and paddlefish GLP-1s were rapidly degraded in the presence of DPP-IV enzyme at position 2 (Ala^2-Asp^3), similarly to human GLP-1 molecule which is cleaved at position 2 (Ala^8-Glu^9). The stability of fish GLP-1 analogues was improved by the stereochemical configuration of an L-Ala for D-Ala at the position 2 plus the addition of acyl group. This was confirmed by HPLC results showing intact peptide peaks after 4 h incubation with DPP-IV or plasma. These observations are consistent with previous studies showing that related N-terminal modifications combat the DPP-IV cleavage and promote longer half-life of GIP, GLP-1, and glucagon (Xiao et al. 2001 and Gault et al. 2013).

Although resistant to degradation, [D-Ala^2]-paddlefish GLP-1-Lys^{28}-gamma-glutamyl-pal exhibited reduced biological activity compared to the native paddlefish GLP-1. In contrast, [D-Ala^2] lamprey-GLP-1-Lys^{31}gamma-glutamyl-pal was more potent, long-acting *in vivo* and exhibited the functional properties of the parent peptide. Previous studies investigating the stereochemical configuration of the residue susceptible the DPP-IV cleavage showed that such modification of native GLP-1 molecule appeared to have a little effect on receptor recognition and binding (Manandhar et al. 2014). Thus, the dramatic reduction in properties of paddlefish GLP-

1-derived analogue could be due to the attachment of lysine-based conjugation of a C-16 fatty acid (palmitic acid) with a glutamic acid spacer at the position 28 (Lys^{28}) which may have affected the possible active centre of the molecule. The attachment of a fatty acid chain at positions 31 (Lys^{31}) of lamprey GLP-1 appeared to be more successful in enhancing the properties of the parent molecule which was not observed in the case of the modified paddlefish GLP-1 peptide.

Acetylation is one of the commonly employed strategies to delay renal extraction of incretin analogues. Long-acting anti-hyperglycaemic agents such as liraglutide, LY315902 and naliglutide are also made by employing acetylation with the attachment of C8 and C-16 fatty acid moieties which induces plasma albumin binding (Kerr et al. 2010 and Gault et al. 2008). In the case of liraglutide, a fatty acid chain of the palmitoyl group to Lys^{26} (corresponding position 20 in fish GLP-1) through a γ-glutamyl spacer together with substitution of Lys for Arg at position 34 (corresponding position 28 in fish GLP-1).

Several other attempts of modification such as attachment of bulky metal chelators either directly to the side chain of Lys^{26} or through a linker resulted in significantly reduced binding affinity of GLP-1. A moderate loss of potency was observed after the substitution of Lys^{26} for Asn bearing *N*-acetylglucosamine (GlcNAc), *N*-acetyllactosamine (LacNAc), or α-2,6-sialyl-*N*-acetyl-lactosamine (sialyl LacNAc).

Moreover, the PEGylation of Lys^{26} with $mPEG_{2K}$ exhibited a minute effect on receptor activation (Manadhar et al. 2014). Interestingly, when lysine residue (Lys^{34}) of GLP-1 was palmitoylated with a γ-glutamyl spacer together with substitution of Lys^{26} for Arg a 2-fold decrease in potency was observed (Manadhar et al. 2014). The similar destructive effect might have occurred with paddlefish analogue due to the

fatty acids attached to lysine at position 28 (corresponding position 34 in human GLP-1) which negatively affected the biological activity of the peptide when administrated *in vivo*.

The present study demonstrates that both, lamprey and paddlefish GLP-1-derived analogues stimulated insulin secretion from clonal pancreatic BRIN-BD11 cells and isolated mouse islets, however, the effects of paddlefish GLP-1 analogue were modest in comparison to the native paddlefish GLP-1 and human GLP-1. The peptides stimulated cAMP production in the CHL cells transfected with GLP1R and the HEK293 cells transfected with glucagon receptor. In harmony with these results, the insulinotropic activities of the analogues were attenuated in the INS-1 cell lacking GLP-1 and glucagon receptors. Thus, importantly the results showed that the analogues still retained the ability to act as dual agonists for the GLP-1 and glucagon receptors similarly to the parent peptides but with lesser potency demonstrated for paddlefish GLP-1 analogue. Previous findings show that employing a secondary C-terminal fatty acid adduct to prolong biological activity of naturally occurring, oxyntomodulin, had no alteration in the ability to activate GLP-1 and glucagon receptors (Lynch et al. 2014).

The rationale as to why fish GLP-1s analogues would activate glucagon, in terms of the presence or absence of particular amino acid residues receptor, is unclear. However, their parent peptide sequences exhibited a strong propensity to adopt a stable α-helical conformation between residues 9-28 predicted by AGADIR program. The primary structures of analogues show a high degree of similarity with peptides of the same glucagon superfamily as demonstrated in Chapter 3.

Earlier in this thesis native GLP-1 from lamprey and paddlefish demonstrated insulinotropic and glucose-lowering effects. However, the peptides failed to exhibit biological actions when administrated 2 hours prior to glucose. To screen acute *in vivo* acute and long-acting properties of fish GLP-1 peptide analogues as well as positive controls, they were co-administered with glucose to normal mice. The biological *in vivo* properties of [D-Ala^2]-lamprey GLP-1-Lys^{31}gamma-glutamyl-pal appeared to be comparable with the parent peptide and human GLP-1. Notably, [D-Ala^2]-lamprey GLP-1-Lys^{31}gamma-glutamyl-pal displayed marked glucose-lowering and insulinotropic effects when administrated two and four hours prior to a glucose load, which was essentially similar to the effects of exendin-4, indicating its enhanced enzymatic stability. This suggests that the modifications did not have deleterious effects on three-dimensional peptide structure of lamprey GLP-1 analogue which retained the ability to activate G protein-coupled receptors.

In contrast, of [D-Ala^2]-paddlefish GLP-1-Lys^{28}gamma-glutamyl-pal demonstrated weaker long active potency and was not as effective. Acute intraperitoneal administration of [D-Ala^2]-lamprey GLP-1-Lys^{31}-gamma-glutamyl-pal significantly suppressed appetite in normal mice, whereas [D-Ala^2]-paddlefish GLP-1-Lys^{28}-gamma-glutamyl-pal showed less potency compared to the parent peptide. The initial results of modified lamprey GLP-1 resemble the actions of other GLP-1 related modified hormones (Flatt et al. 2009; Irwin et al. 2015) and provide a strong basis for the chronic studies using high fat-fed mice. The effectiveness of [D-Ala^2]-paddlefish-GLP-1-Lys^{28}gamma-glutamyl-pal was also examined for comparison.

In harmony with acute studies, a 21-day study treatment of high fat-fed mice with [D-Ala^2]-lamprey GLP-1-Lys^{31}-gamma-glutamyl-pal resulted in a significant

improvement of metabolic status in high-fat fed mice. This included a progressive reduction in body weight accompanied by a decrease in cumulative food intake. Although administration of liraglutide reduced in % of body weight change, it surprisingly had no apparent effect on food intake. This might reflect the ability of lamprey GLP-1 analogue to resemble the actions of glucagon which is known to have beneficial effects such as promoting lipolysis, inhibiting feeding and enhancing energy expenditure under certain conditions (O'Harte et al. 2016b). Activation of multiple biological pathways, in the case of dual-receptor agonists, offers a favourable approach for the treatment of obesity and diabetes (Sadry et al. 2013; Gault et al. 2013) Contrarily, reduction in the appetite might also be caused due to the induction of transient nausea which is one of the limitations associated with GLP-1 mimetic drugs (Lean et al. 2014). The GLP-1 analogues appeared to stimulate additional pathways involved in the activation of GLP-1 receptors in the brain mediating changes in appetite behaviour. A better understanding of these mechanisms may help in designing an effective obesity drug avoiding the side effects (Dailey et al. 2013).

Chronic administration of liraglutide and lamprey GLP-1 analogue decreased the high-fat-diet-induced insulin demand as evidenced by decreased circulating non-fasted insulin levels. Moreover, a reduction of non-fasted glucose was observed in lamprey GLP-1 treated group. Therefore, this indicates an improvement of insulin action and a reduction in overall metabolic demand leading to beta-cell rest which has been shown to dramatically improve longer-term glycaemic control (Pathak et al. 2015). Both, lamprey GLP-1 analogue and liraglutide, treatments were associated with enhanced glucose-induced insulin secretion and reduced HOMA-IR, which could be due to improved metabolic control and reversal of beta cell glucotoxicity.

DEXA scanning revealed that fat mass was significantly reduced in all treatment groups, which was not due to changes in normal mass. The levels of triglyceride, as well as LDH concentrations, were significantly improved in the group treated with lamprey GLP-1 analogue. This could be due to improved glycaemia and greater weight loss observed in this group. Consistent with the previous finding, no significant changes were observed in plasma total cholesterol after liraglutide treatment (Millar et al. 2017) or in any of the fish GLP-1 analogue treatment groups.

Levels of ALT were significantly reduced in all treatment groups showing protective effects of the peptides on diet-induced liver damage which is linked to non-alcoholic fatty liver disease (Stephenson et al. 2018)

However, all peptide treated groups exhibited slightly elevated plasma amylase activity. While it should be noted that the GLP-1 receptor agonists have been linked to the development of pancreatitis (Egan et at. 2014), this was questioned lately by LEADER randomized trial. The study reported that increased serum amylase and lipase levels were observed in the patients treated with liraglutide, but these elevations were not predictive of the development of acute pancreatitis in asymptomatic T2DM individuals (Steinberg et al. 2017).

Histological findings show a reduction in alpha cell area in the group treated with lamprey GLP-1 analogue. This appeared to be related to a lower number of larger sized and higher number of medium-sized islets, despite no alteration in the overall number of islets. In agreement with this observation, a reduction in glucagon content was observed in this group. However, no change in plasma glucagon was detected. Previous studies reported a potent glucagonostatic effect of GLP-1 on glucagon secretion in rat endocrine pancreas (Komatsu et al. 1989). Hyperglycemic clamp studies demonstrated that inhibition of glucagon secretion by GLP-1 might be

contributed to the restoration of the ability of the alpha cells to react to glucose (Vilsboll et al. 2003; Ahren et al. 1997; Hare et al. 2010) which may be seen observed in the case of lamprey GLP-1 analogue treatment.

Interestingly, none of the treatments altered beta cell area, however, a decrease of pancreatic insulin content was observed in liraglutide, and lamprey GLP-1 analogue treated group. Gene expression was also improved in the liraglutide and lamprey GLP-1 analogue treated groups, particularly the expression of insulin gene which was upregulated in the saline group due to persistently high blood glucose levels (Mosley et al. 2004). The expression of *Slc2a2* gene encoding GLU2, *Glp-1r* and *Gcgr* receptors were significantly increased in the peptide treatment groups except paddlefish GLP-1 analogue treated group which was similar to the high fat control. The overexpression of glucagon receptor may be responsible for controlling beta cell growth and differentiation (Gelling et al. 2009). Administration of lamprey GLP-1 analogue also had a positive effect on the expression of *Gipr* and glucokinase (*Gck*) genes.

Due to promising effects observed in high-fat-fed mice, lamprey GLP-1 analogue was further selected for the study using GluGre Rosa26-YFP transgenic mice bearing the transgenes Glucagon-CreER (tamoxifen-inducible tagger) and Rosa26-YFP as a reporter to label pre-existing alpha cells (Quoix et al. 2007). The animals were pre-treated with multiple doses of STZ to induce diabetes and exhibit symptoms such as reduced body weight, elevated levels of blood glucose, depletion of plasma insulin and beta cell destruction. Treatment of STZ-induced diabetic animals for ten days with liraglutide and paddlefish GLP-1 analogue resulted in improved food intake, noticeably lowered blood glucose, increased plasma insulin as well as increased beta cell area in the pancreas. Hormonal and environmental factors play an important role

in the recovery of beta-cell mass to overcome progressive beta cell loss. One of the mechanisms involves the proliferation of pre-existing beta-cells and transdifferentiation of non-beta cells to functional beta cells (Brown et al. 2015). Recent studies have highlighted the inherited beta-cell plasticity and inability to maintain a fully differentiated glucose-responsiveness and drug-responsive state (Remedi et al. 2016). Increased GLP-1 secretion exhibit a positive effect on beta cell regeneration, however, the peptide is rapidly degraded by plasma enzymes (Lee at al. 2018). Alpha cells could also be employed as a source of new beta cells to improve or reverse these processes (Thorel at al 2012). Our data show that new beta cells originated from alpha cells were significantly higher in streptozotocin-treated mice compared to normal untreated control mice. Treatment with liraglutide and lamprey GLP-1 analogue visibly improved the rate of differentiation compared to streptozotocin control favouring promotion of insulin-producing cells.

To conclude, [D-Ala^2]-lamprey-GLP-1-Lys^{31}-gamma-glutamyl-pal exhibited dual-acting effects on GLP-1 and glucagon receptors and showed potent anti-diabetic properties similar to parent peptide with prolonging plasma stability. The stable lamprey GLP-1 analogue had positive effects on body weight, insulin secretion, insulin resistance and islet morphology in high-fat-fed mice, being at least as, if not more effective than liraglutide. The study shows how modification such as acylation and the addition of gamma-glutamyl spacer may interfere with the active side of the peptide causing a reduction in biological activity as was in the case with paddlefish GLP-1 analogue. Overall, these observations provide novel and exciting findings to encourage further investigations of the lamprey GLP-1 analogue as a potential anti-diabetic agent.

Table 5.1. Primary structures and the observed and calculated molecular masse of fish GLP-1 analogue peptides investigated in this study.

Peptide	Amino acid sequence	Calculated molecular mass	Observed molecular mass
[D-Ala^{2}]-lamprey GLP-1-Lys^{31}-gamma-glutamyl-pal	HaDGTFTNDMTSYLDAKAARDFVSWL ARSD[K-gamma-glutamyl-pal]S-OH	3945.4	3947.0
[D-Ala^{2}]-paddlefish GLP-1-Lys^{28}-gamma-glutamyl-pal	HaDGTYTSDASSFLQEQAARDFISWLK[K-gamma-glutamyl-pal]GQ-OH	3726.2	3728.0
Human oxyntomodulin	HSQGTFTSDYSKYLDSRRAQDFVQWL MNTKRNKNNIA	4449.9	
Human GLP-1	HAEGTFTSDVSSYLEGQAAKEFIAWLV KGR-NH2	3297.7	3297.9
Human glucagon	HSQGTFTSDYSKYLDSRRAQDFVQWL MNT	3482.8	3484.4
Human GIP	YAEGTFISDYSIAMDKIHQQDFVNWLL AQKGKKNDWKHNITQ	4983.6	4984.3
Exendin-4	HGEGTFTSDLSKQMEEEAVRLFIEWLK NGGPSSGAPPPS-NH2	4186.6	4186.0
Liraglutide	HAEGTFTSDVSSYLEGQAAK-(γ-Glu-palmitoyl)-EFIAWLVRGRG-OH	3751.2	

Table 5. 2 Metabolic degradation studies

Peptide	% Degraded 4 h DPP-IV	% Degraded 4 h plasma	Observed MW of degraded product, Da	Proposed DPP-IV cleavage site
Lamprey GLP-1	90	-	3370.1	Ala^{2}-Asp^{3}
Paddlefish GLP-1	87	-	3153.3	Ala^{2}-Asp^{3}
[D-Ala^{2}]-lamprey GLP-1-Lys^{31}gamma-glutamyl-pal	0	0	N/A	-
[D-Ala^{2}]-paddlefish GLP-1-Lys^{28}-gamma-glutamyl-pal	0	0	N/A	-
Human GLP-1	86	65	3090.4	Ala^{8}-Glu^{9}

Table 5. 3 Effects of [D-Ala^2]-lamprey GLP-1-Lys^{31}gamma-glutamyl-pal, [D-Ala^2]-paddlefish GLP-1-Lys^{28}-gamma-glutamyl-pal, human GLP-1 and glucagon on the rate of insulin release from BRIN-BD11 cells.

Peptide	Threshold concentration	Effect at 3μM, ng/10^6/20min
Basal release	-	1.0 ± 0.02
[D-Ala2]-lamprey GLP-1-Lys31-gamma-glutamyl-pal	10pM**	3.3 ± 0.19
[D-Ala^2]-paddlefish GLP-1-Lys^{28}-gamma-glutamyl-pal	0.1nM*	2.8 ± 1.9
Human GLP-1	10pM*	3.6 ± 0.17
Human glucagon	3nM*	2.7 ± 0.10

The basal release refers to the rate of insulin release at 5.6 mM glucose alone. The threshold concentration is the minimum concentration of the peptide that produces a significant ($P < 0.05$) increase in the rate of insulin release. The values are mean ± SEM for n = 8. *P<0.5, **P<0.01, ***P<0.001 compared to 5.6 mM glucose control.

Table 5.4 Effects of [D-Ala^2]-lamprey GLP-1-Lys^{31}-gamma-glutamyl-pal and [D-Ala^2]-paddlefish GLP-1-Lys^{28}-gamma-glutamyl-pal on the release of insulin from islets isolated from Swiss mice.

Peptide	Insulin release (% of total insulin content) at 10^{-6}M	Insulin release (% of total insulin content) at 10^{-8}M
(None) 1.4 mM glucose	3.4 ± 0.4 ***	3.4 ± 0.4 ***
(None) 16.7 mM glucose control	8.5 ± 0.5	8.5 ± 0.5
[D-Ala^2]-lamprey GLP-1-Lys^{31}-gamma-glutamyl-pal	16.4 ± 0.7 ***	14.4 ± 1.1 ***
[D-Ala^2]-paddlefish GLP-1-Lys^{28}-gamma-glutamyl-pal	12.6 ± 1.8 *	8.3 ± 1.1
Human GLP-1	17.0 ± 2.1 **	14.7 ± 0.9 ***
Human glucagon	11.9 ± 1.6	8.5 ± 0.4

Values are mean ± S.E.M., n = 8 *P < 0.05, **P < 0.01, ***P < 0.001 compared to 16.7 mM glucose alone.

Table 5.5 Summary of effect of [D-Ala^2]-lamprey GLP-1-Lys^{31}gamma-glutamyl-pal, [D-Ala^2]-paddlefish GLP-1-Lys^{28}-gamma-glutamyl-pal, human GLP-1, human glucagon and human GIP peptides (10^{-8} and 10^{-6} M) on cAMP production in GLP1R-transfected CHL cells, and GCGR-transfected HEK293 cells.

Peptide name	GLP-1 receptor transfected cells		GCG receptor transfected cells	
	cAMP release at 10^{-6}	cAMP release at 10^{-8}	cAMP release at 10^{-6}	cAMP release at 10^{-8}
Basal (5.6mM glucose)	4.9 ± 0.2	4.9 ±0.2	2.5 ±0.2	2.5 ±0.2
[D-Ala^2]-lamprey GLP-1-Lys^{31}-gamma-glutamyl-pal	30.1 ± 2.0***	25.9 ± 0.8***	6.2 ±0.2***	4.7 ±0.9*
[D-Ala^2]-paddlefish GLP-1-Lys^{28}-gamma-glutamyl-pal	28.9 ± 1.4***	13.3 ± 0.9**	4.6 ± 0.8 *	4.7 ± 0.9 *
Human GLP-1	29.0 ± 0.2***	26.3 ± 1.4***	6.6 ± 0.6**	4.6 ± 0.4**
Human glucagon	17.1 ± 0.9 ***	10.7 ± 0.5***	8.9 ± 0.3**	7.5 ± 0.5**
Human GIP	5.1 ± 0.2	5.5 ± 0.6	2.8 ± 0.3	2.5 ± 0.2

Values are mean ± S.E.M. for n = 3. *P < 0.05, ** P< 0.01 and ***P < 0.001 compared with 5.6 glucose.

Table 5.6 Summary of effects of fish stable fish GLP-1 analogues (10^{-8} and 10^{-6} M) on the rate of insulin release from wild-type INS-1 cells, CRISPR/Cas9-engineered GLP-1R KO cells, CRISPR/Cas9-engineered GIPR KO cells and CRISPR/Cas9-engineered GIPR KO cells

Peptide		Wild-type cells, % of basal control	GLP-1R KO cells, % of basal control	GCGR KO cells, % of basal control	GIPR KO cells, % of basal control
Basal (5.6mM glucose)		100 ± 9.6			
[D-Ala^2]-lamprey GLP-1-Lys^{31}-gamma-glutamyl-pal	10^{-6}	215.2 ± 10.1***	147.2 ± 10.3 *** ΔΔΔ	165.1 ± 13.2** Δ	222.2 ± 7.5 ***
	10^{-8}	183.5 ± 12.4***	135.1 ± 9.7 **Δ	156.1 ± 13.7 **	209.9 ± 11.1 **
[D-Ala-^{2}] paddlefish GLP-1-Lys^{28}-gamma-glutamyl-pal	10^{-6}	162.4 ± 8.1***	128.8 ± 9.1 ** Δ	217.1 ± 6.8**	221.6 ± 7.6 ***
	10^{-8}	143.1 ± 3.3 ***	124.9 ± 4.5 **ΔΔ	172.3 ± 16.8** Δ	187.9 ± 9.2 *
Human GLP-1	10^{-6}	221.1 ± 9.8***	138.3 ± 14.5 * ΔΔΔ	222.0 ± 11.7***	231.4 ± 9.4 ***
	10^{-8}	198.9 ± 12.9 ***	114.1 ± 8.5 ΔΔΔ	210 ± 25.0 ***	187.5 ± 17.2 ***
Human glucagon	10^{-6}	225.0 ± 20.9***	211.3 ± 16.4 ***	159.6 ± 8.5 *** ΔΔ	224.0± 14.8 ***
	10^{-8}	172.2 ± 10.8***	164.2 ±16.5***	134.0 ± 14.4 Δ	175.4 ± 12.3 ***
Human GIP	10^{-6}	242.9 ± 14.2***	226.6 ±19.6***	231.3 ± 17.6 ***	125.4 ± 6.9 * ΔΔΔ
	10^{-8}	233.8 ± 18.6***	221.0 ± 29.3 ***	230.1 ± 0.9***	124.3 ± 12.6 ΔΔΔ

Values are mean ± S.E.M., $n = 8$, *P < 0.05, **P < 0.01 and ***P < 0.001 compared with 5.6 mM glucose alone. $^{\Delta}P < 0.05$, $^{\Delta\Delta}P < 0.01$, $^{\Delta\Delta\Delta}P < 0.001$ compared with effects in wild-type INS-1 cells.

Figure 5.1. Reverse-phase HPLC purification of crude [D-Ala^2]-lamprey GLP-1-Lys^{31}-gamma-glutamyl-pal (A) and [D-Ala^2]-paddlefish GLP-1-Lys^{28}-gamma-glutamyl-pal peptides using a semi-preparative Vydac C18 column.

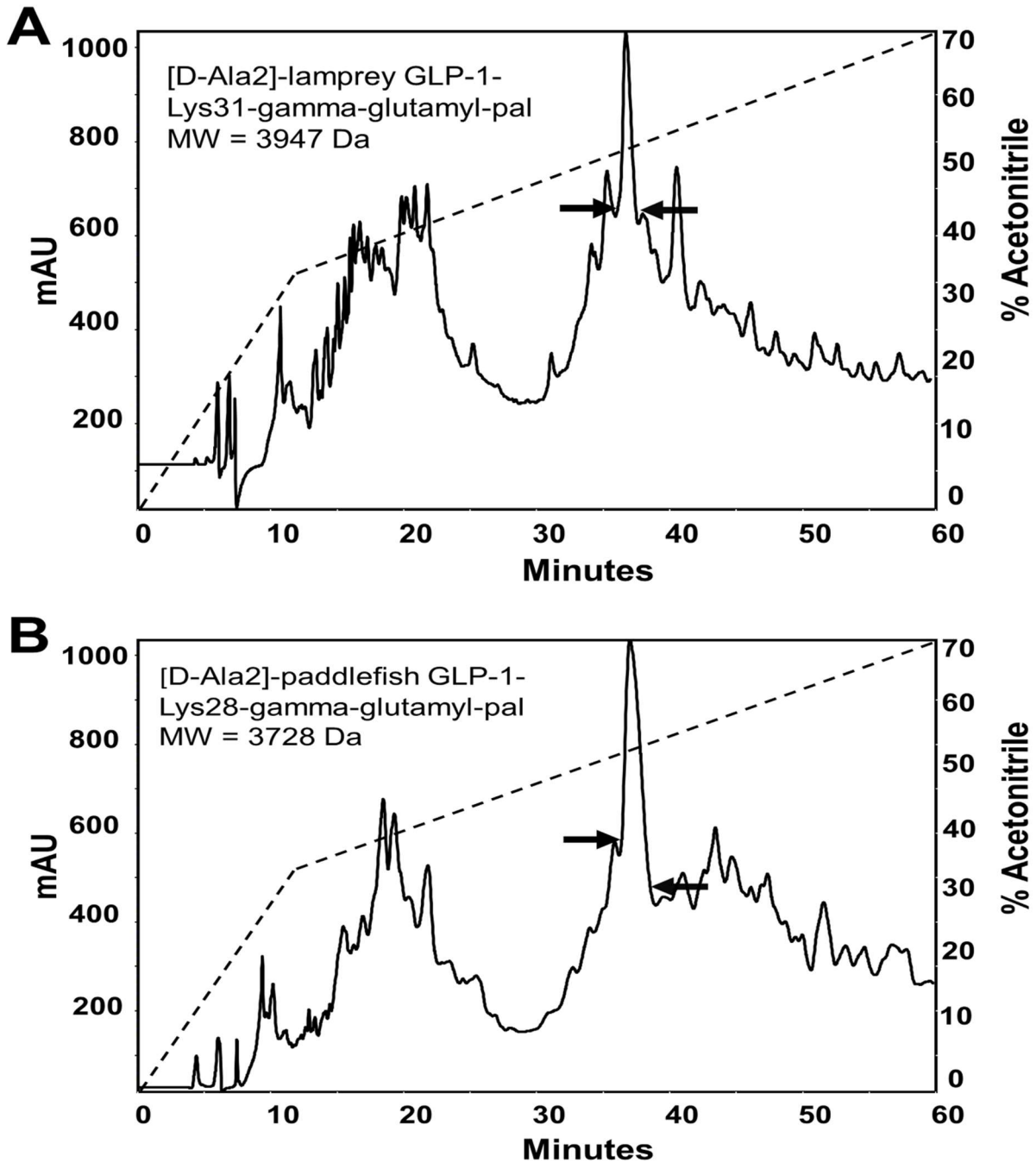

The peptides were dissolved in 15% acetonitrile (3mg/ml) and injected onto a (2.2 cm x 25 cm) Vydac 218TP1022 (C-18) column (Grace, Deerfield, IL, USA) at a flow rate of 6.0 ml/min. The concentration of acetonitrile in the eluting solvent was raised from 0% to 35 % over 10 min and from 35% to 70% over 50 min using a linear gradient. Absorbance was measured at 214 nm, and the black arrows show where the peak collection began and ended.

Figure 5.2. MALDI-TOF spectra of purified [D-Ala^2]-lamprey GLP-1-Lys^{31}-gamma-glutamyl-pal (A) and [D-Ala^2]-paddlefish GLP-1-Lys^{28}-gamma-glutamyl-pal peptides.

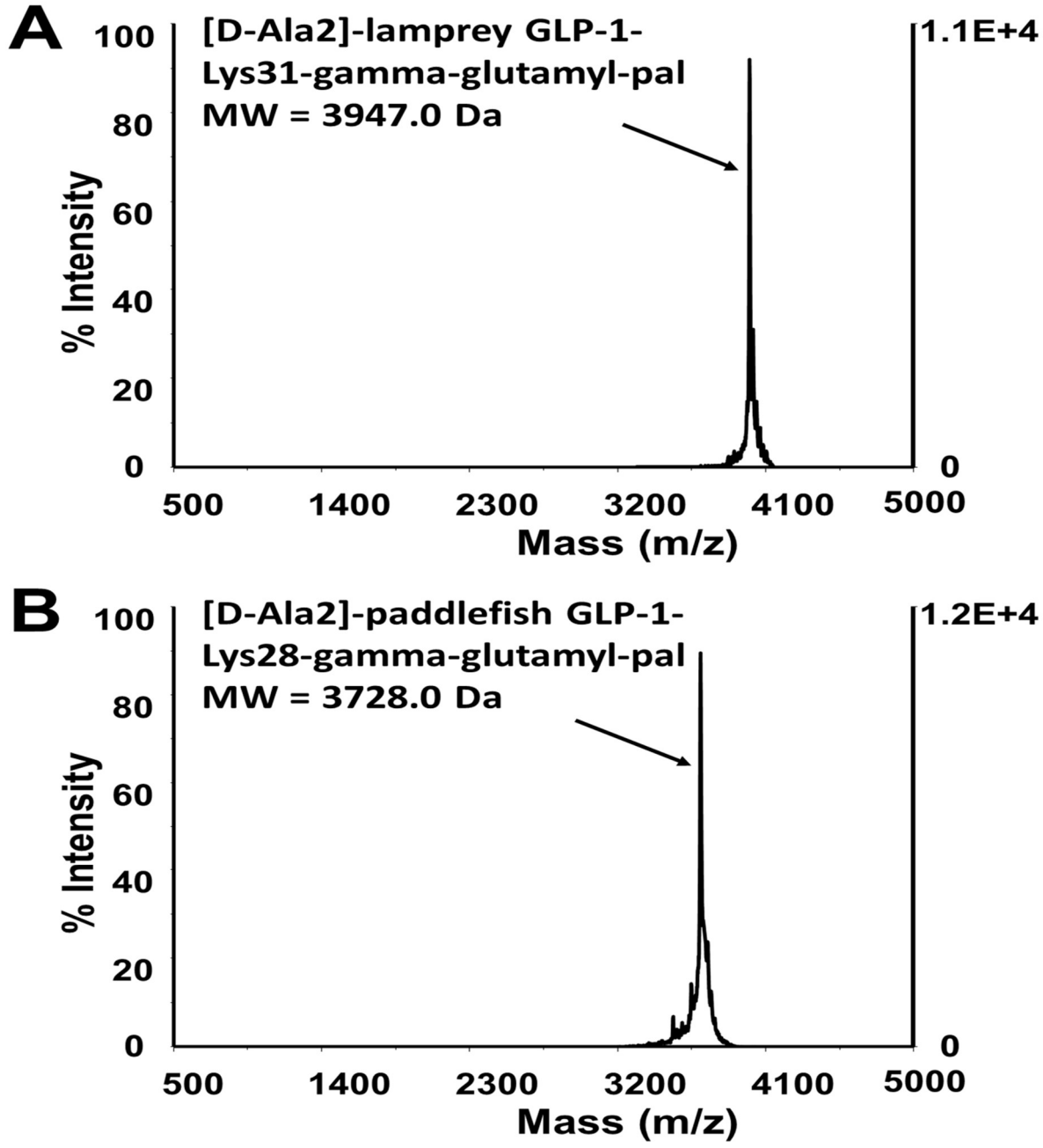

Purified peptides were mixed with α-Cyano-4-hydroxycinnamic acid on a 100 well MALDI plate before inserting into a Voyager DE Biospectrometry workstation. The mass-to-charge ratio (m/z) versus peak intensity was determined.

Figure 5.3. HPLC degradation profile of [D-Ala^2]-lamprey GLP-1-Lys^{31}-gamma-glutamyl-pal following incubation with DPP-IV for 0 and 4 hours.

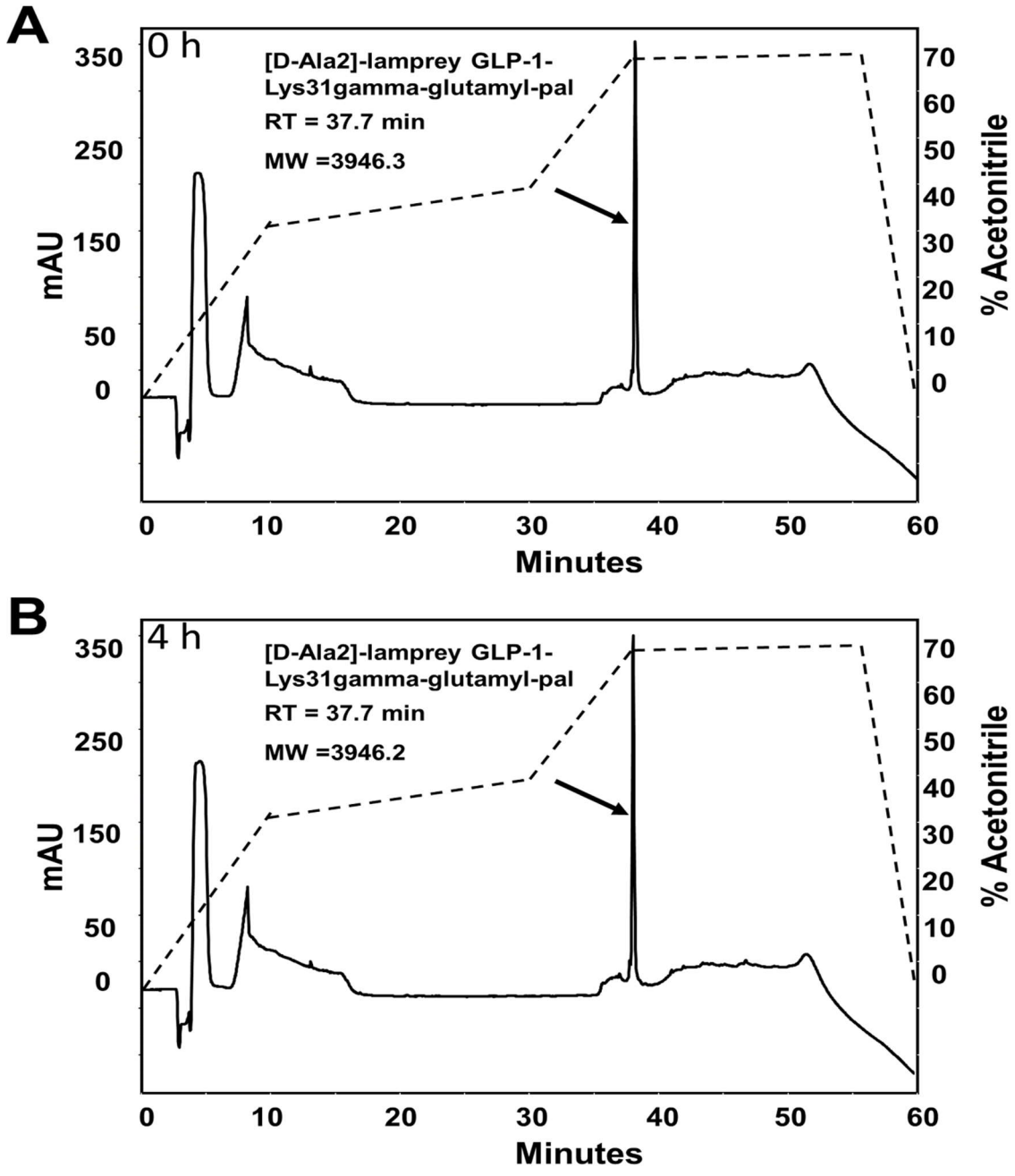

The separation was performed with a Luna 5u C8 250x4.6mm column. The dash line represents acetonitrile concentration gradient from 0% to 35% (from 0 min to 10 min), from 35% to 42% (from 10min to 30 min), from 42 to 70% (from 30 min to 35min), and 70% (from 35 min to 55 min).

Figure 5. 4 HPLC degradation profile of [D-Ala^2]-paddlefish GLP-1-Lys^{28}-gamma-glutamyl-pal following incubation with DPP-IV for 0 and 4 hours.

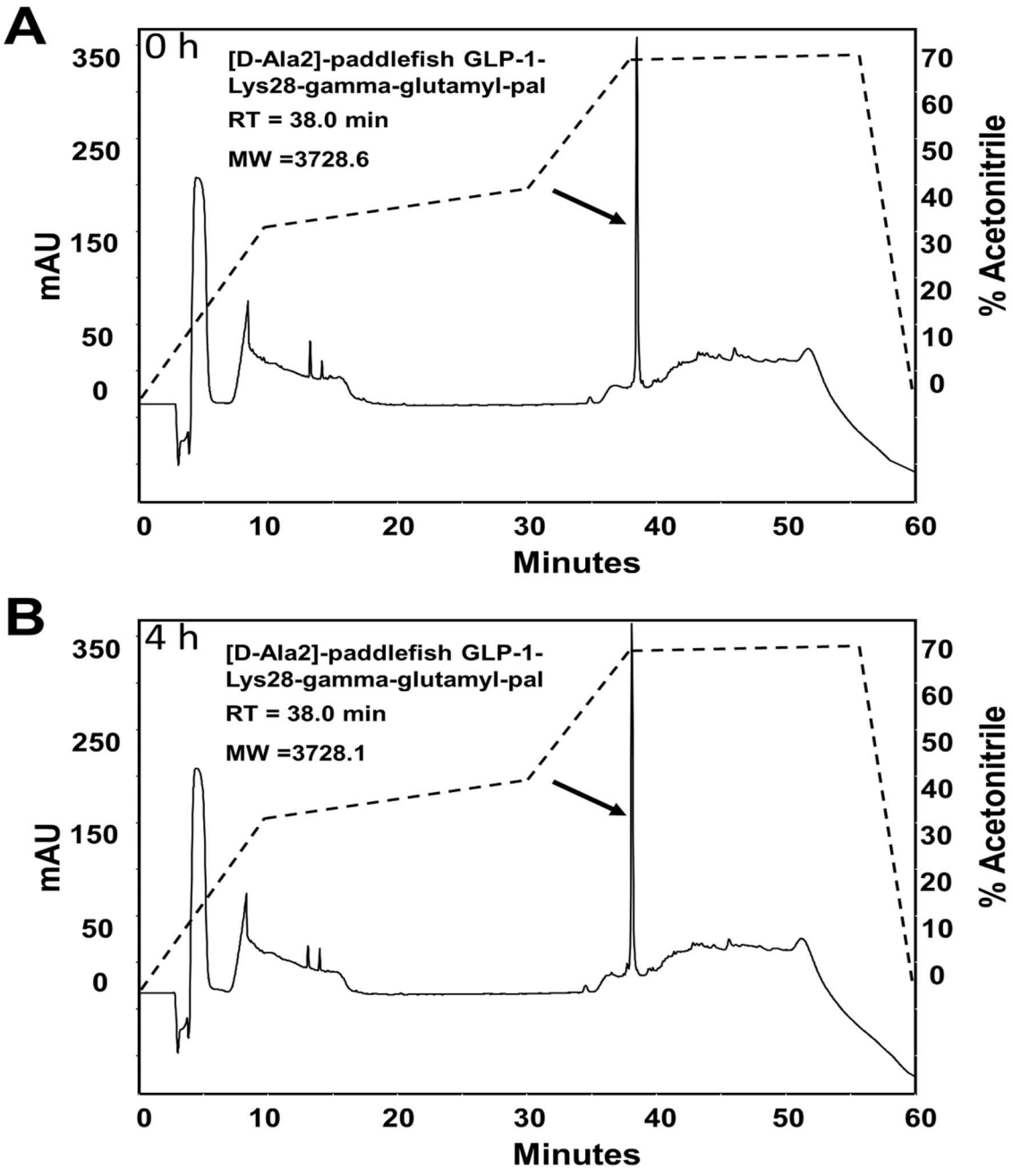

The separation was performed with a Luna 5u C8 250x4.6mm column. The dash line represents acetonitrile concentration gradient from 0% to 35% (from 0 min to 10 min), from 35% to 42% (from 10min to 30 min), from 42 to 70% (from 30 min to 35min), and 70% (from 35 min to 55 min).

Figure 5.5 HPLC result of plasma degradation of [D-Ala^2]-lamprey GLP-1-Lys^{31}-gamma-glutamyl-pal for 0 and 4 hours.

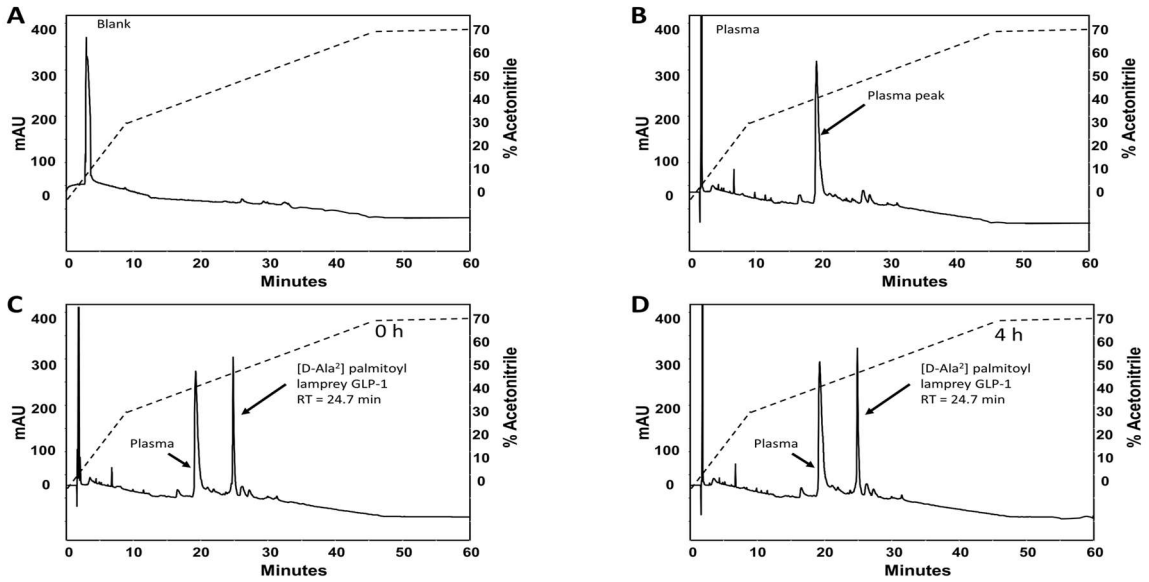

The separation was performed with a Luna 5u C8 250x4.6mm column. The dash line represents acetonitrile concentration gradient from 0% to 35% (from 0 min to 10 min), from 35% to 70% (from 10min to 45 min) and 70% (from 45 min to 60 min).

Figure 5.6 HPLC result of plasma degradation of [D-Ala^2]-lamprey GLP-1-Lys^{31}-gamma-glutamyl-pal for 0 and 4 hours

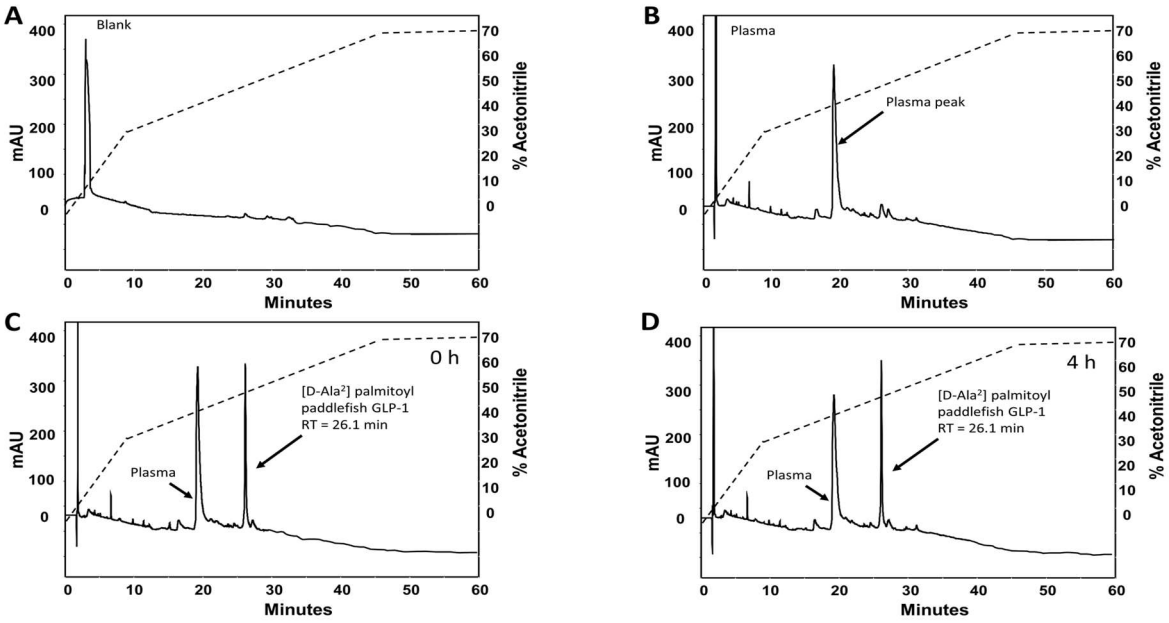

The separation was performed with a Luna 5u C8 250x4.6mm column. The dash line represents acetonitrile concentration gradient from 0% to 35% (from 0 min to 10 min), from 35% to 70% (from 10min to 45 min) and 70% (from 45 min to 60 min).

Figure 5.7 HPLC result of plasma degradation of human GLP-1 for 0 and 4 hours.

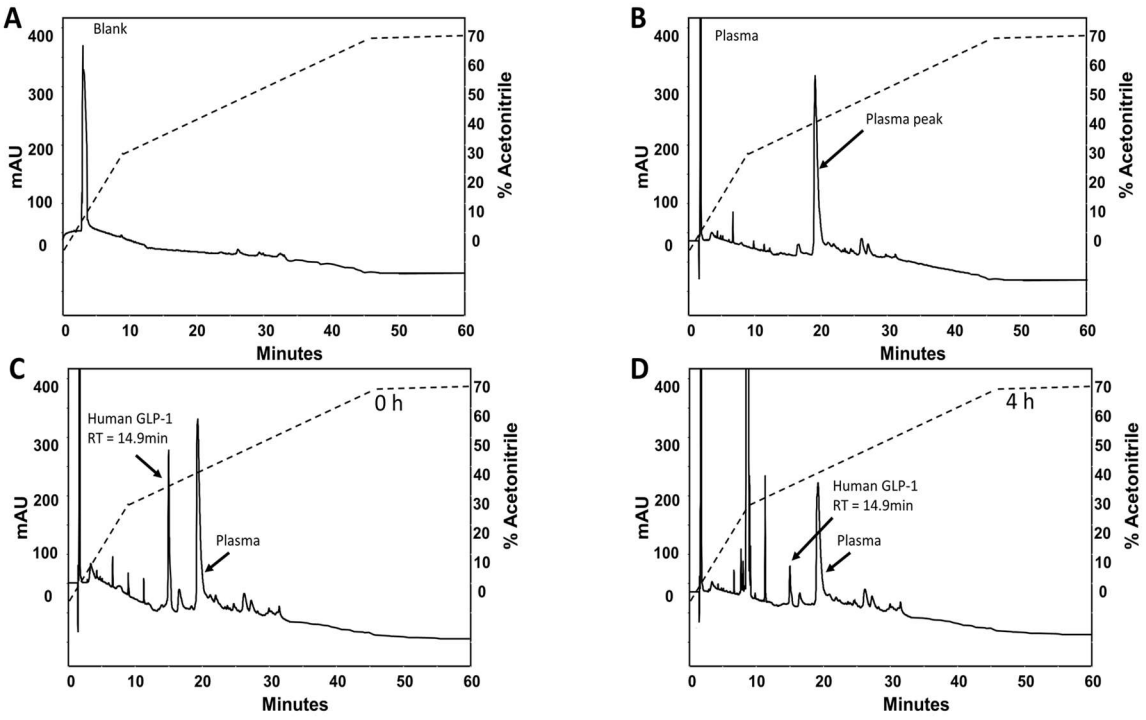

The separation was performed with a Luna 5u C8 250x4.6mm column. The dash line represents acetonitrile concentration gradient from 0% to 35% (from 0 min to 10 min), from 35% to 70% (from 10min to 45 min) and 70% (from 45 min to 60 min).

Figure 5. 8 Effects of increasing concentrations of [D-Ala^2]-lamprey GLP-1-Lys^{31}-gamma-glutamyl-pal (A) and [D-Ala^2]-paddlefish GLP-1-Lys^{28}-gamma-glutamyl-pal (B) on insulin release from BRIN-BD11 rat clonal β-cells.

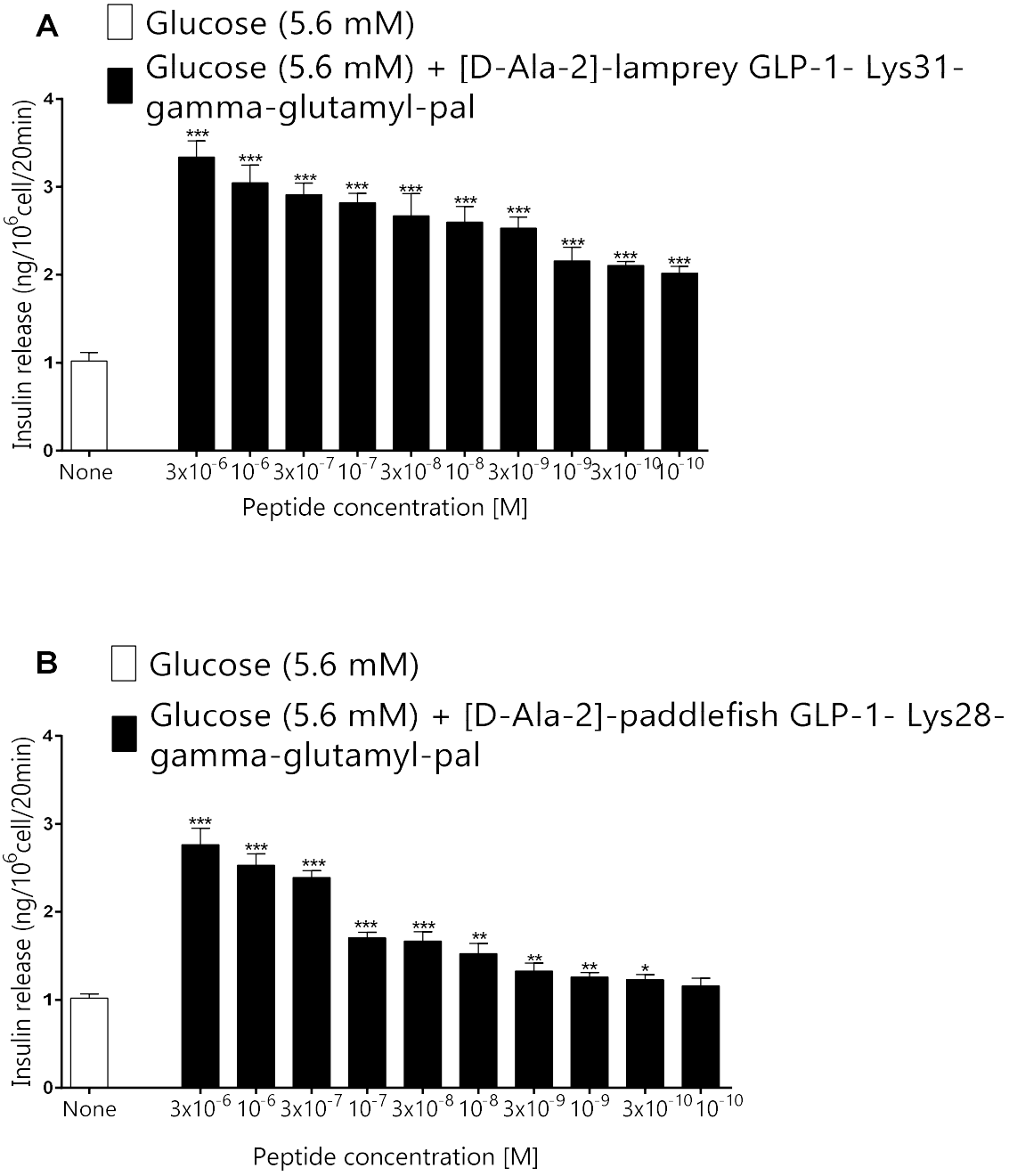

Values are mean ± S.E.M., n = 8. *P < 0.05, **P < 0.01, ***P < 0.001 compared to 5.6 mM glucose alone.

Figure 5.9 Effects of [D-Ala^2]-lamprey GLP-1-Lys^{31}gamma-glutamyl-pal and [D-Ala^2]-paddlefish GLP-1-Lys^{28}-gamma-glutamyl-pal (10^{-8} and 10^{-6} M) on insulin release from pancreatic islets isolated from NIH Swiss mice.

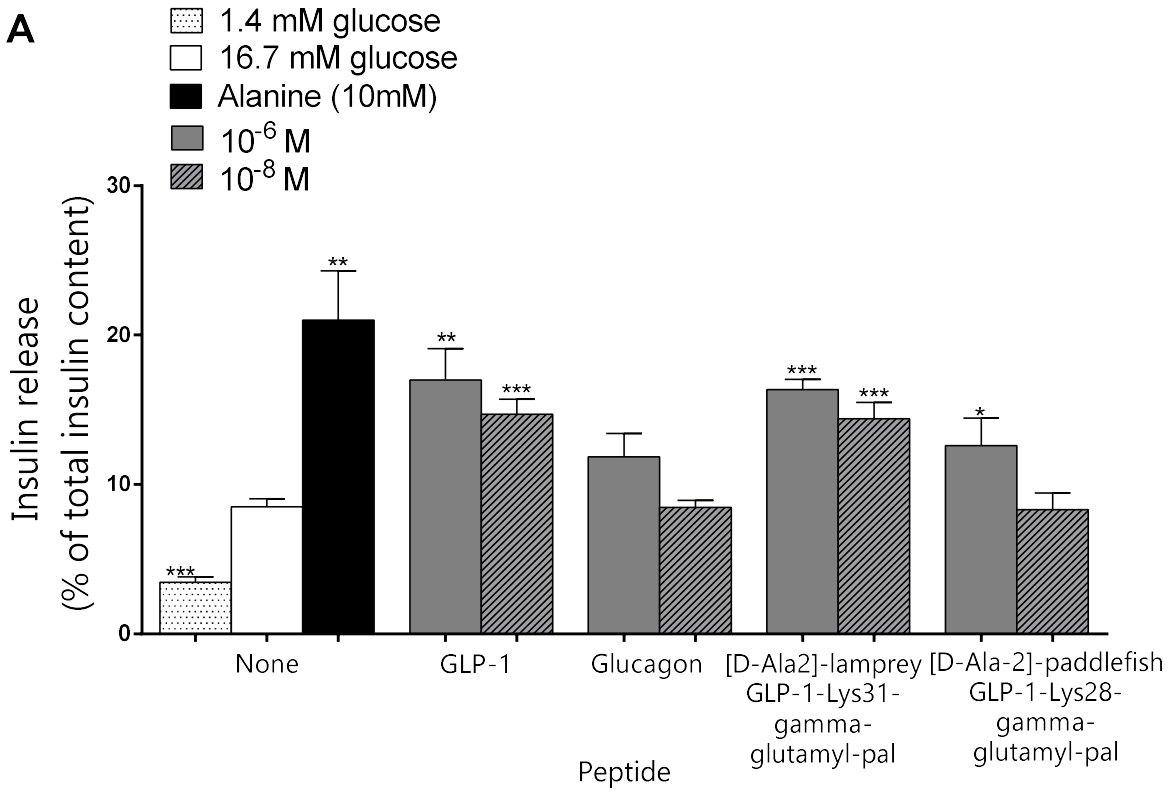

The values are mean ± SEM for n=4; *P < 0.05, **P < 0.01, ***P < 0.001 compared to 16.7mM glucose alone.

Figure 5.10 Effects of [D-Ala^2]-lamprey GLP-1-Lys^{31}gamma-glutamyl-pal and [D-Ala^2]-paddlefish GLP-1-Lys^{28}-gamma-glutamyl-pal (10^{-8} and 10^{-6} M) on cAMP production in (A) GLP1R-transfected CHL cells, and (B) GCGR-transfected HEK293 cells

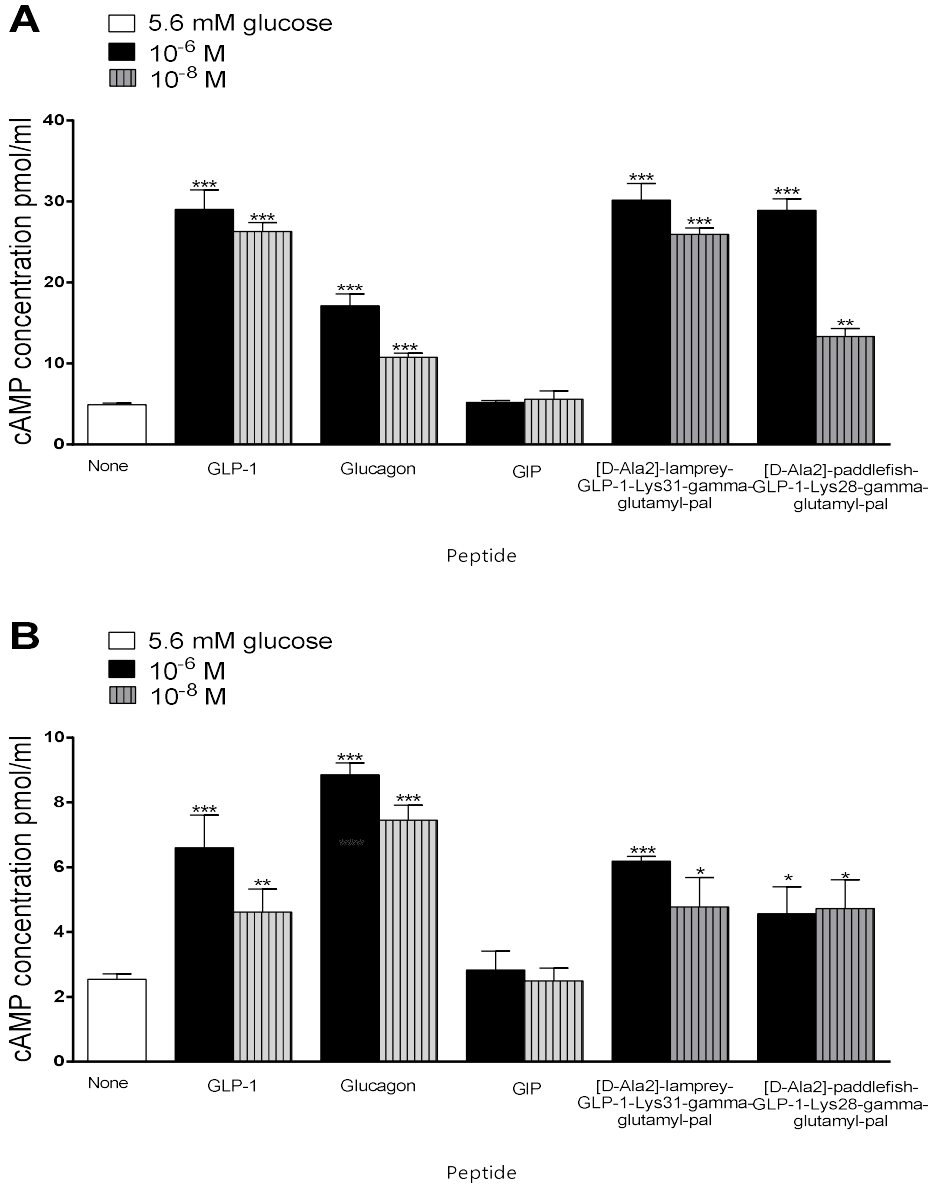

Values are mean ± S.E.M. for n = 3. *P < 0.05, ** P< 0.01 and ***P < 0.001 compared with 5.6 glucose.

Figure 5.11 Effects of [D-Ala^2]-lamprey GLP-1-Lys^{31}-gamma-glutamyl-pal peptides and [D-Ala^2]-paddlefish-GLP-1-Lys^{28}-gamma-glutamyl-pal (10^{-8} and 10^{-6} M) on the rate of insulin release from (A) wild-type INS-1 cells, (B) CRISPR/Cas9-engineered GLP-1R knock-out cells, (C) CRISPR/Cas9-engineered GCGR knock-out cells and (D) CRISPR/Cas9-engineered GIPR knock-out cells.

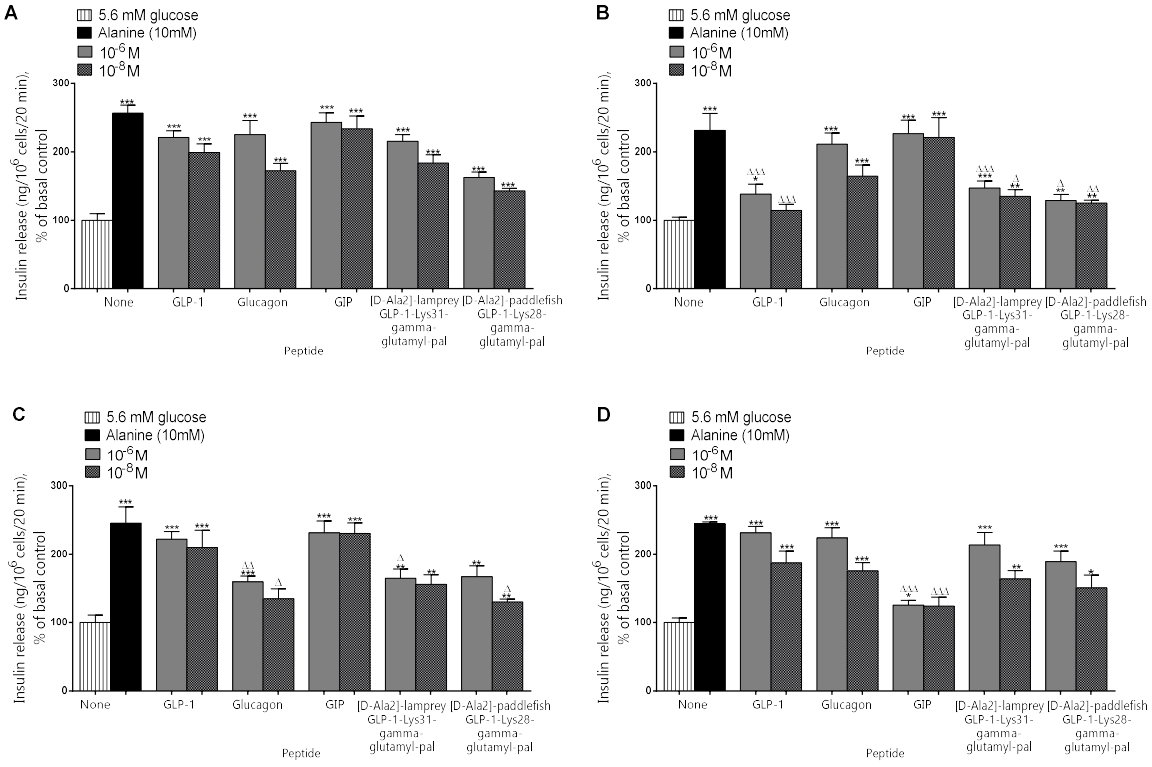

Values are mean ± S.E.M., $n = 8$, *P < 0.05, **P < 0.01 and ***P < 0.001 compared with 5.6 mM glucose alone. $^{\Delta}$P < 0.05, $^{\Delta\Delta}$P < 0.01, $^{\Delta\Delta\Delta}$P < 0.001 compared with effects in wild-type INS-1 cells.

Figure 5.12 Effects of [D-Ala^2]-lamprey GLP-1-Lys^{31}-gamma-glutamyl-pal peptides and [D-Ala^2]-paddlefish-GLP-1-Lys^{28}-gamma-glutamyl-pal (10^{-8} and 10^{-6} M) on (A) cell proliferation and (B) protection against apoptosis in rodent BRIN BD11 cells.

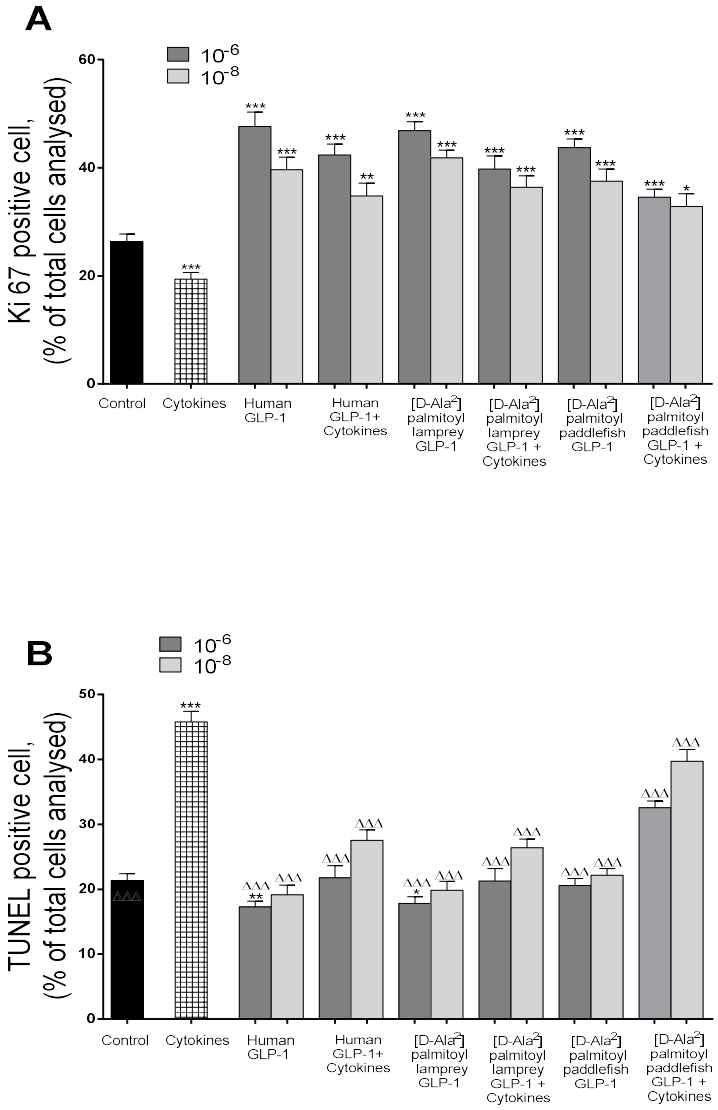

Cell were incubated (16 h) in the presence of peptides (10^{-8} and 10^{-6} M) with and without addition of cytokine cocktail. Values are mean ± S.E.M., n = 3, *P < 0.05, ** P< 0.01 and ***P < 0.001 compared with control cultures. $^{\Delta}$P < 0.05, $^{\Delta\Delta}$P < 0.01, $^{\Delta\Delta\Delta}$P < 0.001 compared with cytokine cocktail.

Figure 5.13 Effects of acute administration of lamprey GLP-1, [D-Ala^2]-lamprey GLP-1-Lys^{31}gamma-glutamyl-pal peptides (A-B), paddlefish GLP-1 and [D-Ala^2]-paddlefish GLP-1-Lys^{28}-gamma-glutamyl-pal (C-D) on blood glucose and plasma insulin in normal mice.

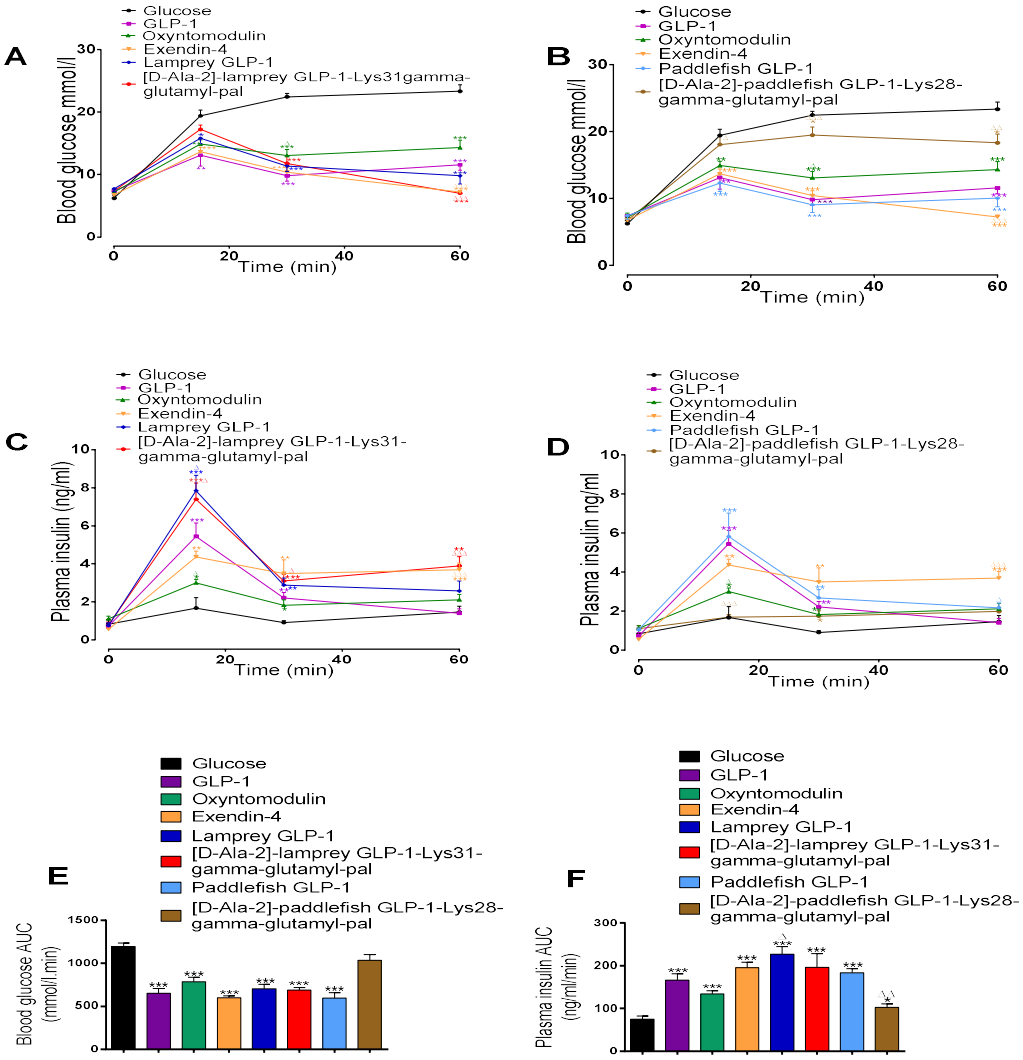

Effects of peptides (each at 25 nmol/kg body weight) on blood glucose and plasma insulin concentrations in normal mice were measured after intraperitoneal injection of glucose (18 mmol/kg body weight). The integrated responses (area under the curve AUC) are shown in panels E and F. The values are mean ± SEM for n=6. *P<0.05, **P<0.01 and ***P<0.001 compared to glucose alone; $^{\Delta}$P<0.05, $^{\Delta\Delta}$ P<0.01 and $^{\Delta\Delta\Delta}$ P<0.001 compared to human GLP-1.

Figure 5.14 Effects of acute administration of lamprey GLP-1, [D-Ala^2]-lamprey GLP-1-Lys^{31}-gamma-glutamyl-pal peptides (A-B), paddlefish GLP-1 and [D-Ala^2]-paddlefish GLP-1-Lys^{28}-gamma-glutamyl-pal (C-D) on blood glucose and plasma insulin concentrations in normal mice, 2 h post injection.

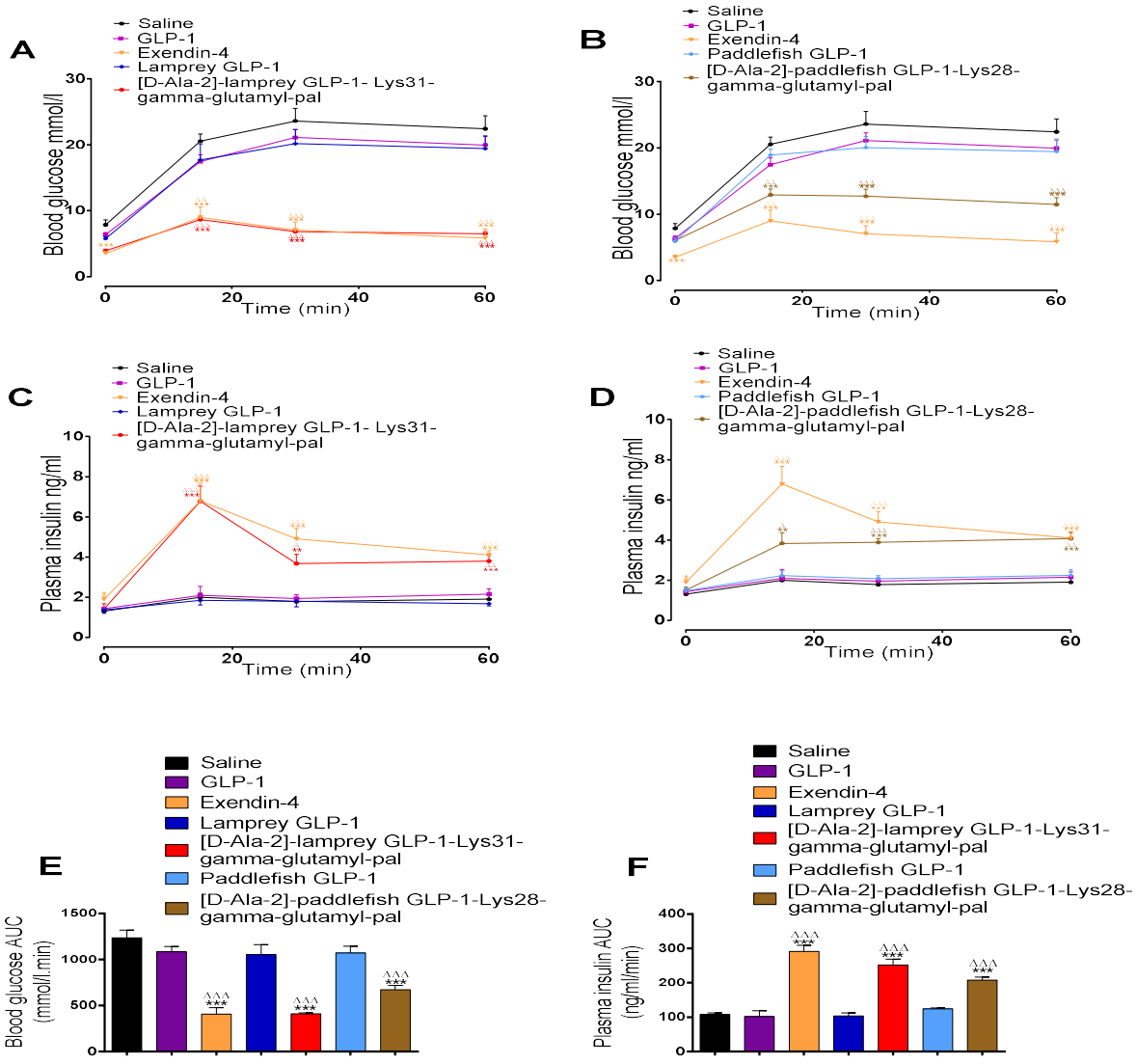

Blood glucose and plasma insulin were measured after intraperitoneal injection of glucose (18 mmol/kg body weight) 2 hours after intraperitoneal administration of 0.9% saline or peptides (25 nmol/kg body weight). The integrated responses (area under the curve AUC) are shown in panels E and F. The values are mean ± SEM for n=6. **P<0.01 and ***P<0.001 compared to glucose alone; $^{\Delta\Delta}$ P<0.01 and $^{\Delta\Delta\Delta}$ P<0.001 compared to human GLP-1.

Figure 5. 15 Effects of acute administration of lamprey GLP-1, [D-Ala^2]-lamprey GLP-1-Lys^{31}-gamma-glutamyl-pal peptides (A-B), paddlefish GLP-1 and [D-Ala^2]-paddlefish GLP-1-Lys^{28}-gamma-glutamyl-pal (C-D) on blood glucose and plasma insulin concentrations in normal mice, 4 h post injection.

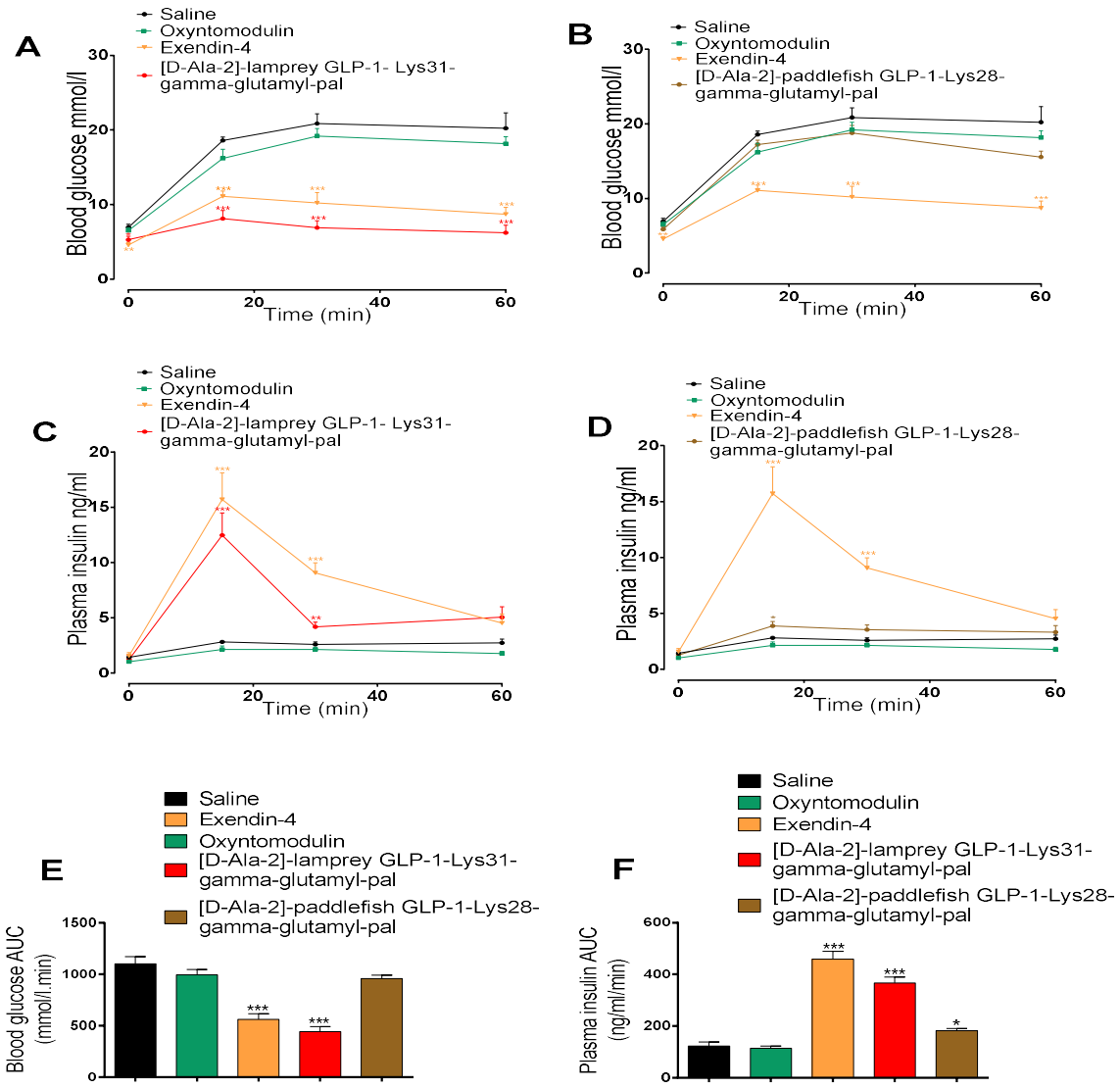

Blood glucose and plasma insulin were measured after intraperitoneal injection of glucose (18 mmol/kg body weight) 4 hours after intraperitoneal administration of 0.9% saline or peptides (25 nmol/kg body weight). The integrated responses (area under the curve AUC) are shown in panels E and F. The values are mean ± SEM for n=6. *P<0.05, **P<0.01 and ***P<0.001 compared to glucose alone; $^{\Delta\Delta}$ P<0.01 and $^{\Delta\Delta\Delta}$ P<0.001 compared to human GLP-1.

Figure 5.16 Effects of lamprey GLP-1, [D-Ala^2]-lamprey GLP-1-Lys^{31}gamma-glutamyl-pal, paddlefish GLP-1 and [D-Ala^2]-paddlefish GLP-1-Lys^{28}-gamma-glutamyl-pal on cumulative food intake over 5 hours trained feeding in 12 h fasting normal mice.

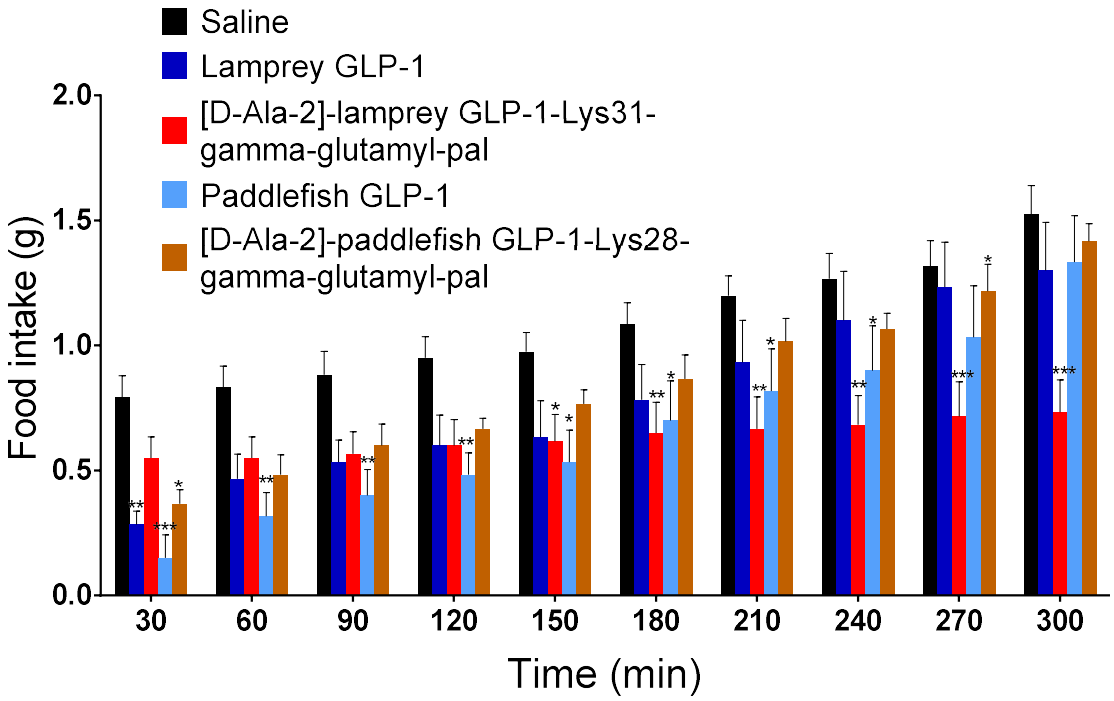

Cumulative food intake was measured after intraperitoneal administration of 75 nmol/kg peptides alongside 0.9% saline control. The values are mean ± SEM for n=8. *P<0.05, **P<0.01 and ***P<0.001 compared to saline control mice treated at the same time point.

Figure 5.17 Chronic effects of stable fish GLP-1 peptides on body weight (A), % body weight change (B), food intake (C) and water intake (D) in high fat-fed mice during 21 days study.

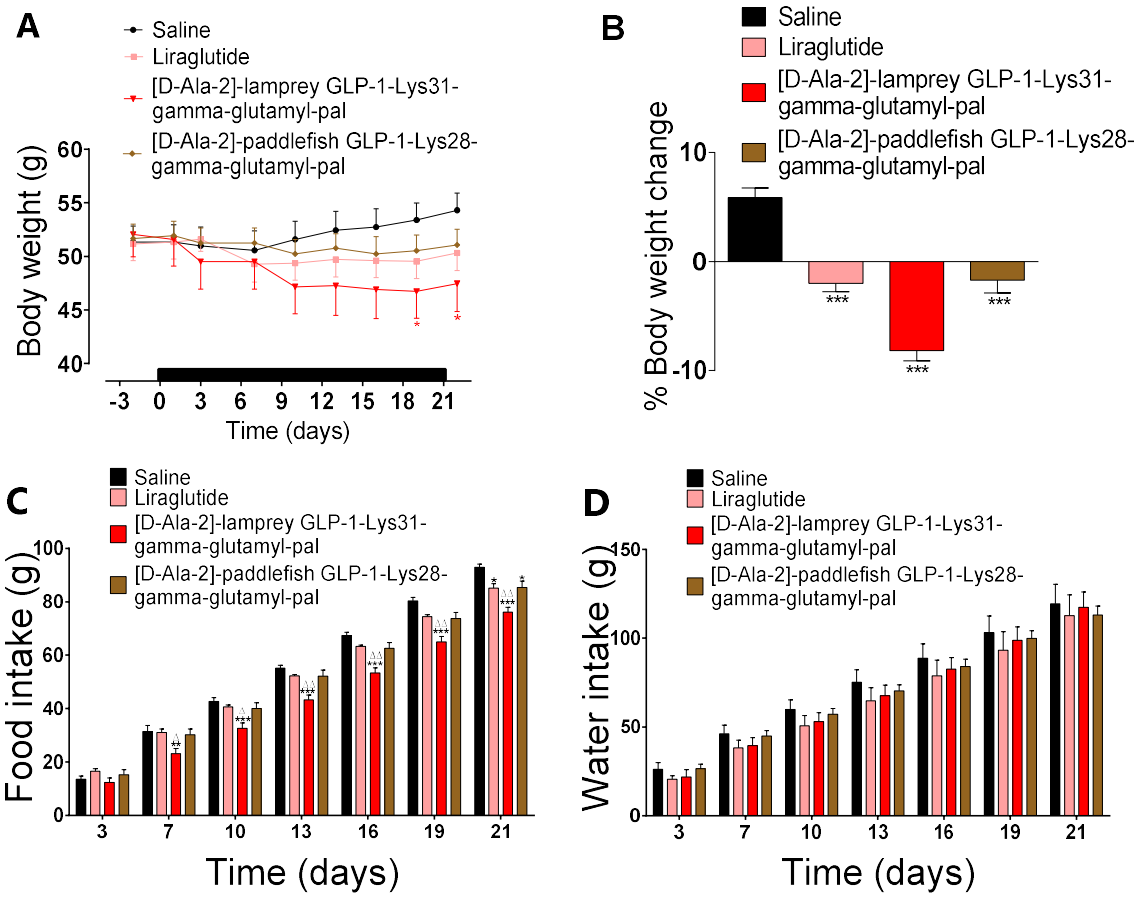

The black horizontal bar represents the treatment period. Values represent mean±SEM for 8 mice. *P<0.05, **P<0.01 and ***P<0.001 is compared with high fat treated control.

Figure 5.18 Chronic effects of stable fish GLP-1 peptides on blood glucose (A-B), plasma insulin (C-D) and insulin sensitivity during 21 days study in high fat fed mice.

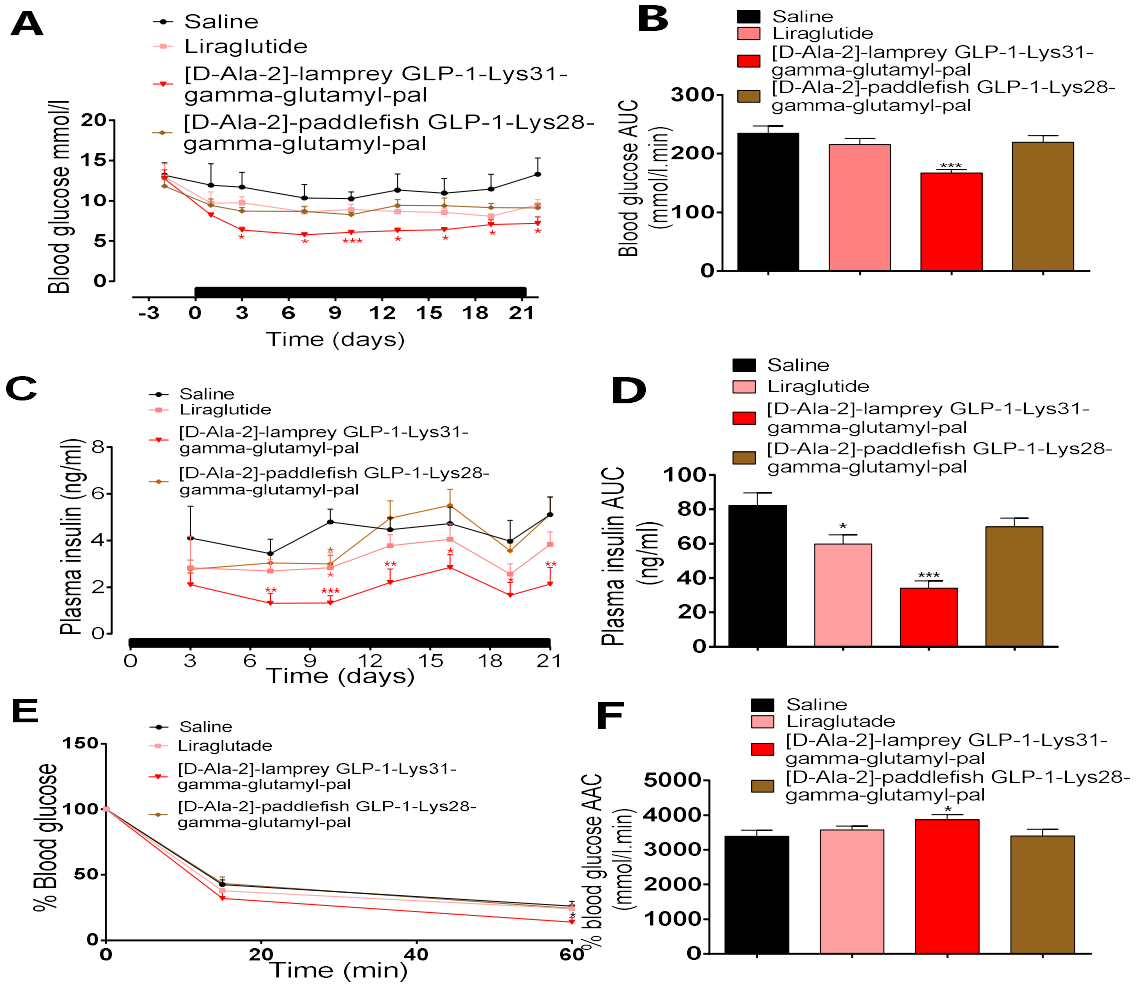

The black horizontal bar represents the treatment period. Values represent mean±SEM for 8 mice. *P<0.05, **P<0.01 and ***P<0.001 is compared with high fat treated control.

Figure 5. 19 Chronic effects of stable fish GLP-1 peptides on HOMA-β (A) and HOMA-IR (B) in high fat fed diet mice.

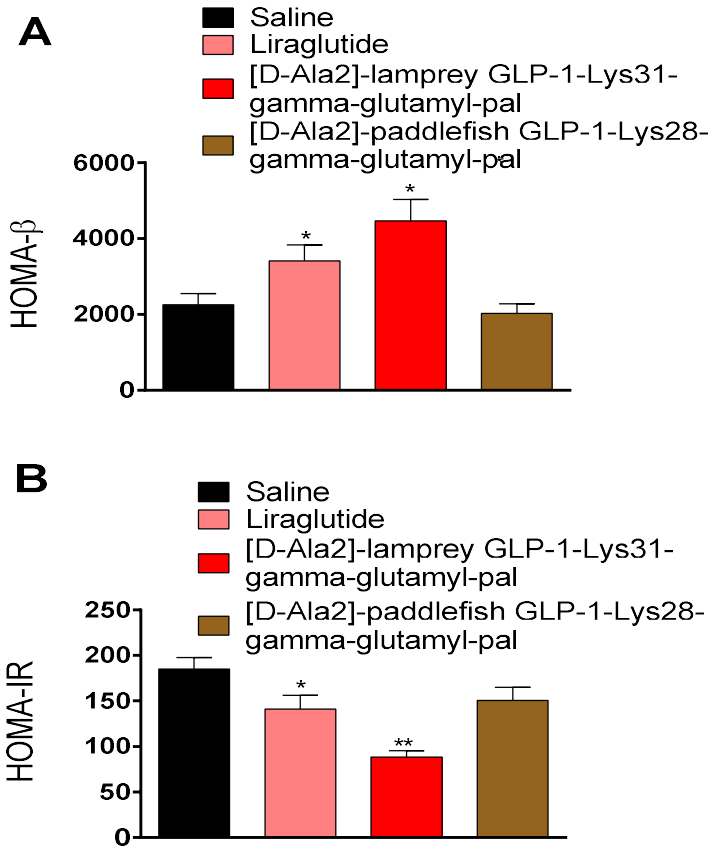

The parameters were measured on day 21 following twice-daily treatment with saline vehicle (0.9% w/v NaCl, i.p), liraglutide or fish peptide analogues (each at 25 nmol/kg of bw, i.p).

Figure 5.20 Chronic effects of stable fish GLP-1 peptides on glucose tolerance (A-B) and plasma insulin (C-D) in response to intraperitoneal administration of glucose in fasted high-fat diet fed mice.

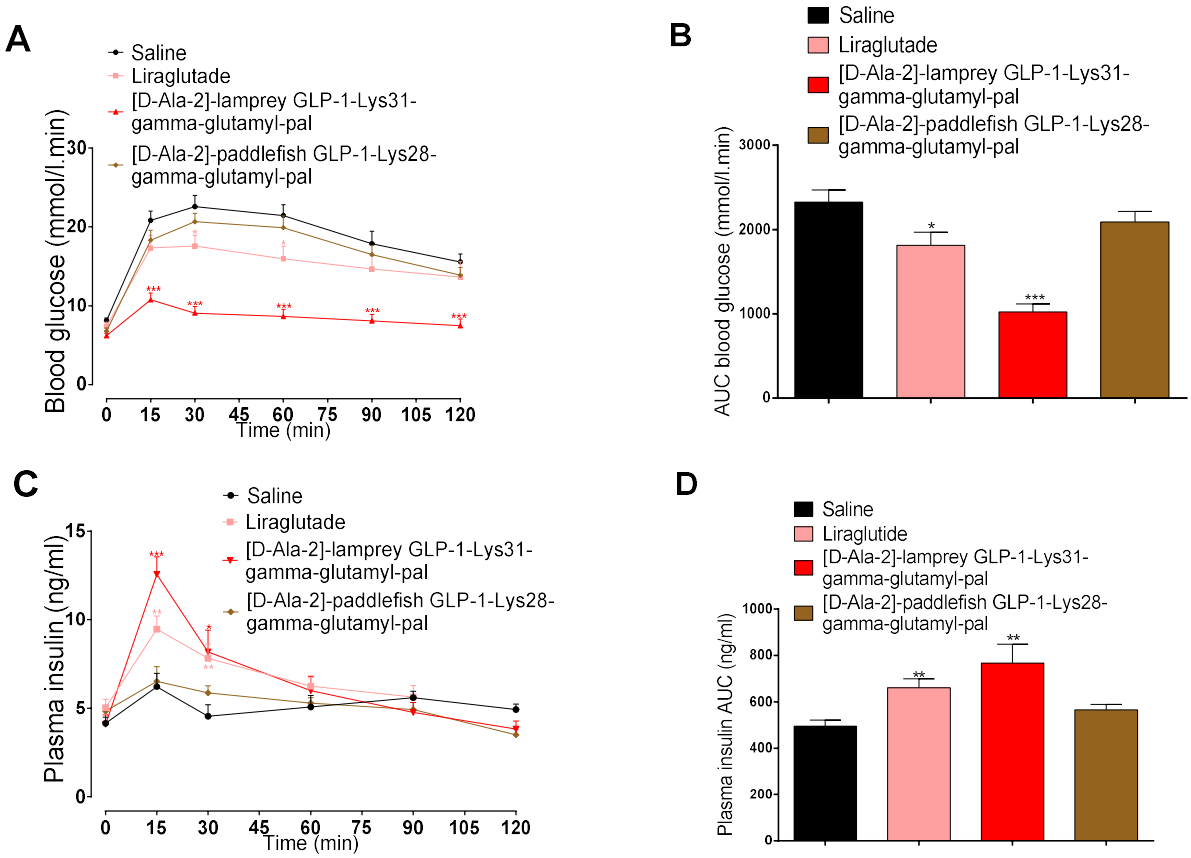

Parameters were measured prior to and after administration of glucose alone (18 mmol/kg of bw, i.p.) in animals receiving after 21 days daily treatment with saline vehicle (0.9% w/v NaCl, i.p), liraglutide or fish peptide analogues (each at 25 nmol/kg of bw, i.p.). Blood glucose and plasma insulin AUC values 0-120 min are included. The values are mean ± SEM for n=8. *P<0.05, **P<0.01 and ***P<0.001 compared to saline control.

Figure 5.21 Chronic effects of stable fish GLP-1 peptides on glucose tolerance (A-B) and plasma insulin (C-D) in response to oral administration of glucose in fasted high-fat diet fed mice.

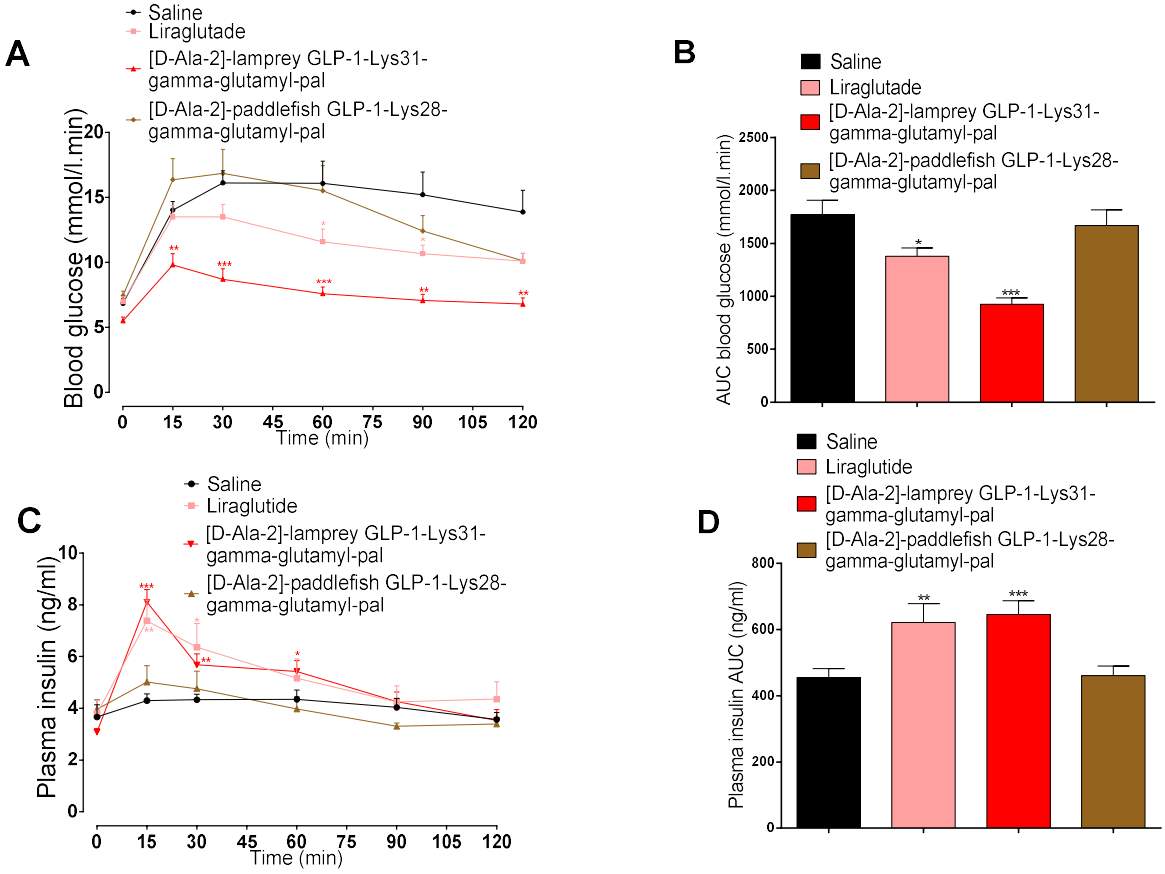

Parameters were measured prior to and after administration of glucose alone (18 mmol/kg) in animals receiving after 21 days daily treatment with saline vehicle (0.9% w/v NaCl, i.p), liraglutide or fish peptide analogues (each at 25 nmol/kg of bw, i.p.). Blood glucose and plasma insulin AUC values 0-120 min are included. The values are mean ± SEM for n=8. *P<0.05, **P<0.01 and ***P<0.001 compared to saline control.

Figure 5.22 Chronic effects of stable fish GLP-1 peptides on pancreatic glucagon (A) and pancreatic insulin (B) content in high-fat-fed diet mice.

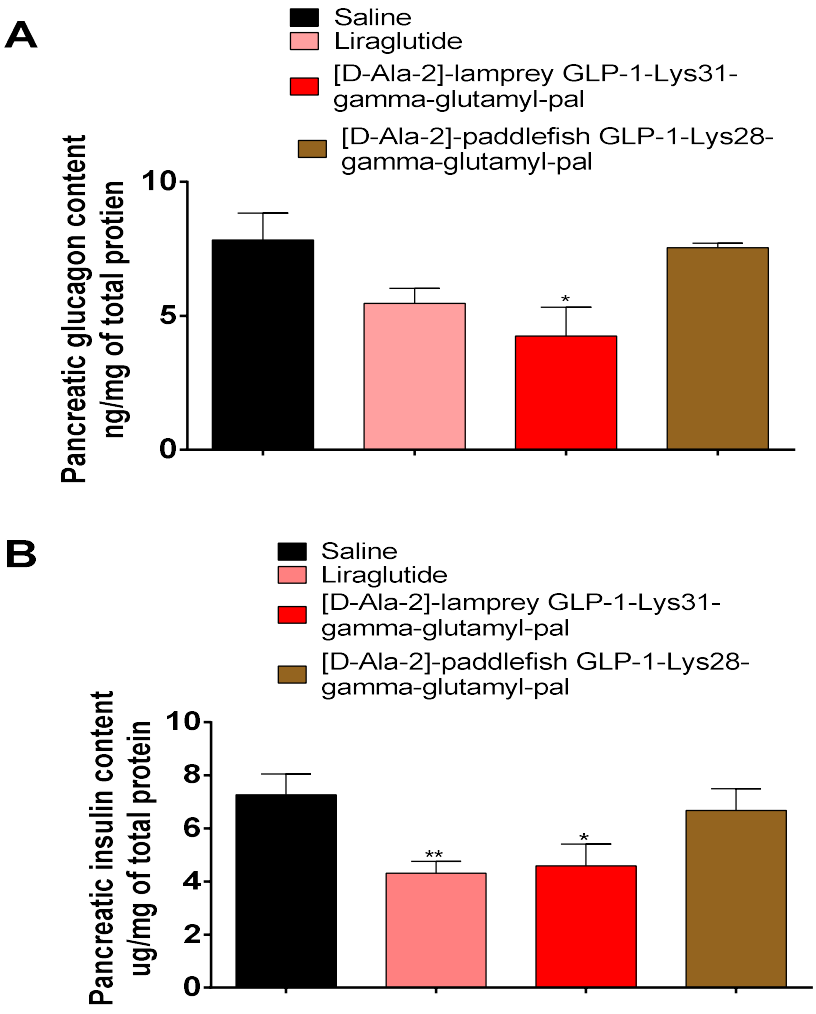

The parameters were measured on day 21 following twice-daily treatment with saline vehicle (0.9% w/v NaCl, i.p), liraglutide or fish peptide analogues (each at 25 nmol/kg of bw, i.p). Data are expressed as means ± SEMs for n=4. *P < 0.05 and ** P< 0.01 compared with high fat saline control.

Figure 5.23 Chronic effects of stable fish GLP-1 peptides on plasma total cholesterol (A), triglycerides (B), HDL-cholesterol (C), and LDL-cholesterol (D).

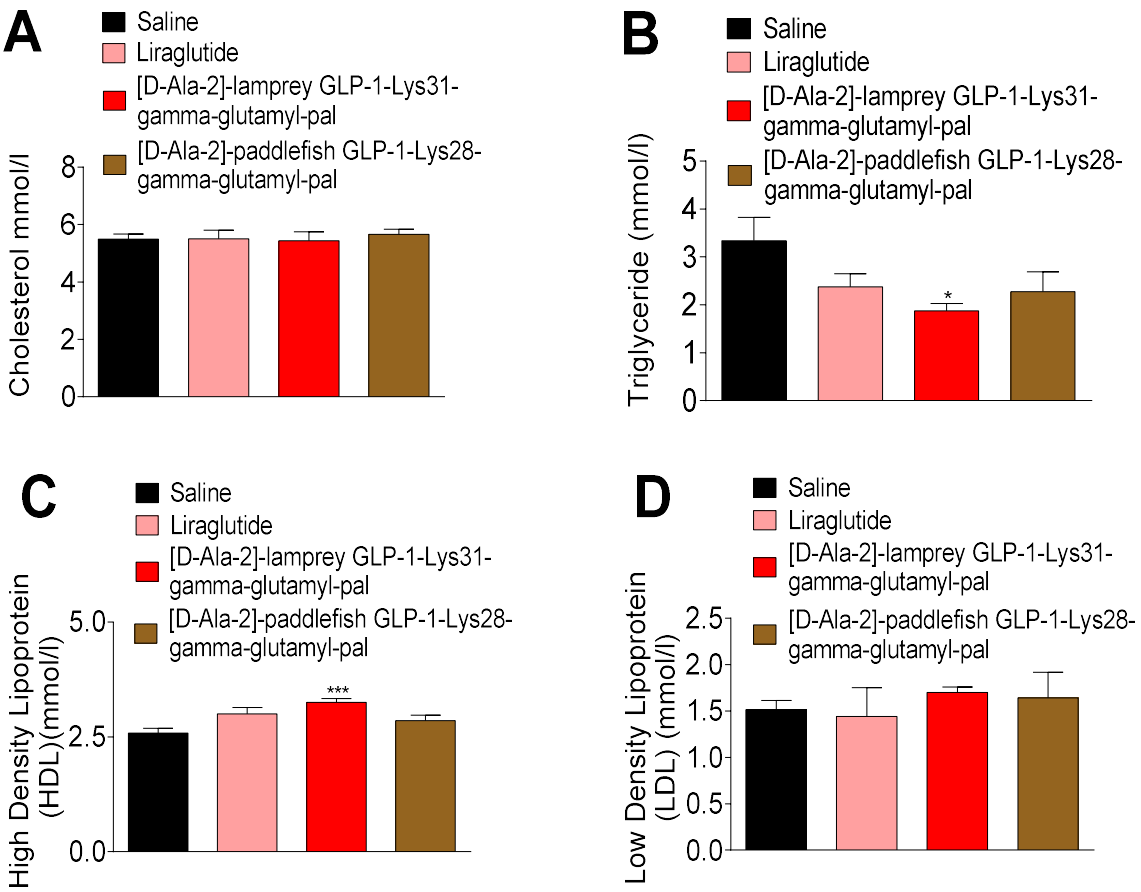

The parameters were measured on day 21 following twice-daily treatment with saline vehicle (0.9% w/v NaCl, i.p), liraglutide or fish peptide analogues (each at 25 nmol/kg of bw, i.p). Data are expressed as means ± SEMs for 8 mice. *P < 0.05 and *** P < 0.001 compared with saline control.

Figure 5.24 Chronic effects of stable fish GLP-1 peptides on (A) plasma ALT, (B) Amylase activity and (C) plasma glucagon in high-fat diet fed mice.

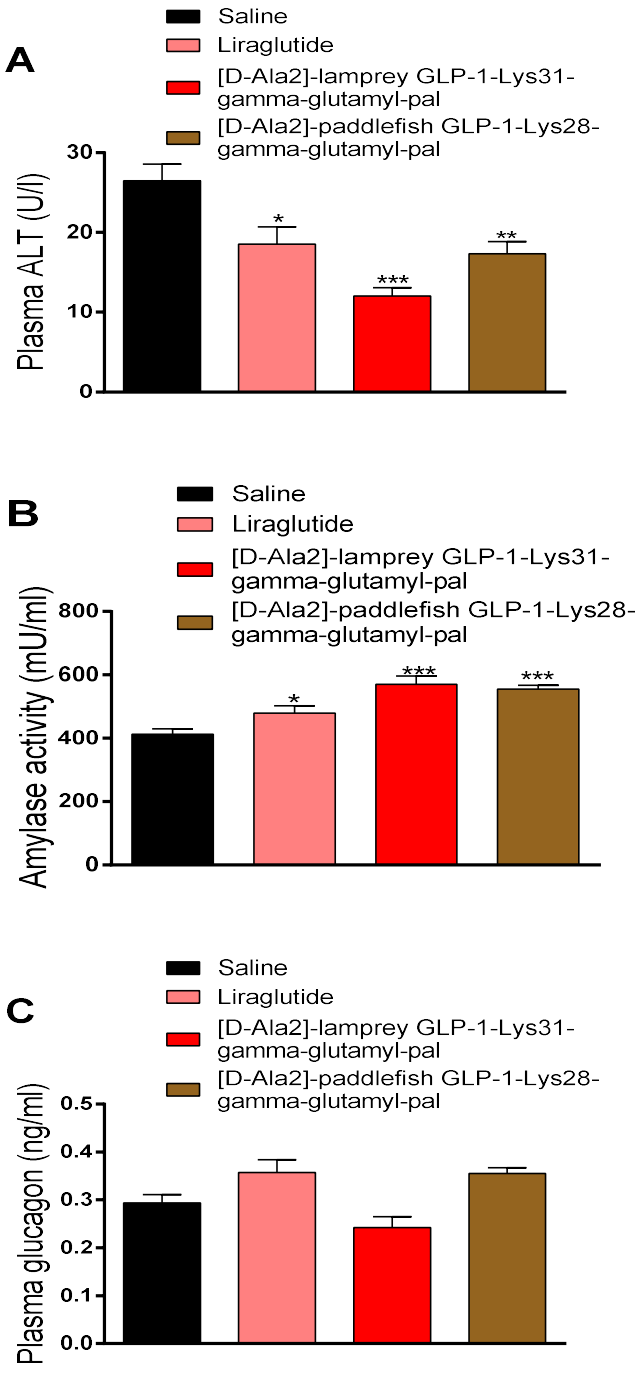

The values are mean ± SEM for n=4. *P<0.05, **P<0.01 and **P<0.01 compared to high fat control.

Figure 5.25 Chronic effects of stable fish GLP-1 peptides on (A) bone mineral density, (B) bone mineral content, (C) bone area, (D) normal body mass, (E) body fat and (F) % fat composition measured by DEXA scanning in high-fat diet fed mice.

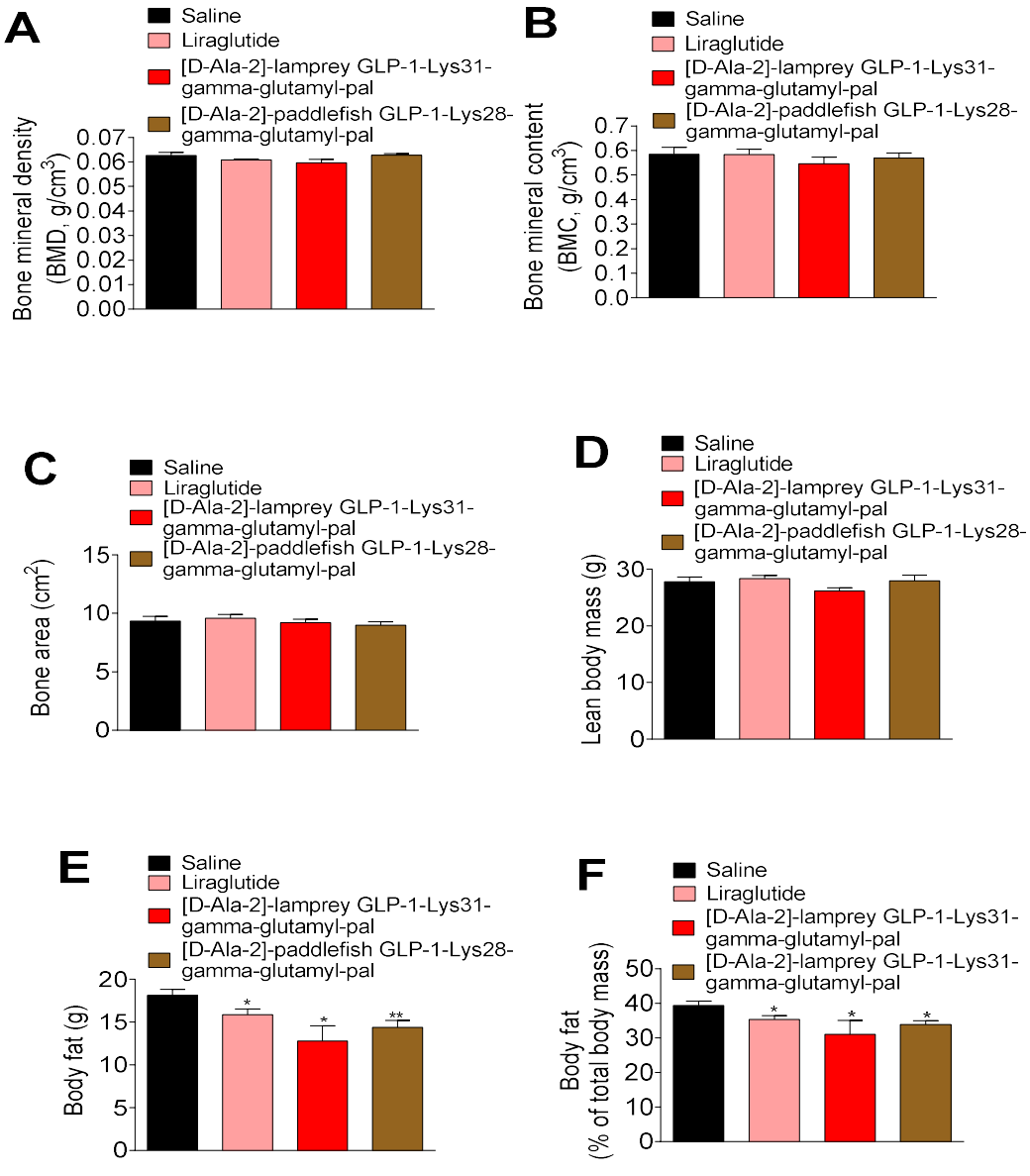

Values represent mean±SEM for 8 mice. The values are mean ± SEM for n=8. *P<0.05 and **P<0.01 compared to saline control.

Figure 5.26 Chronic effects of stable fish GLP-1 peptides on insulin secretory response from isolated islets in high-fat-fed diet mice.

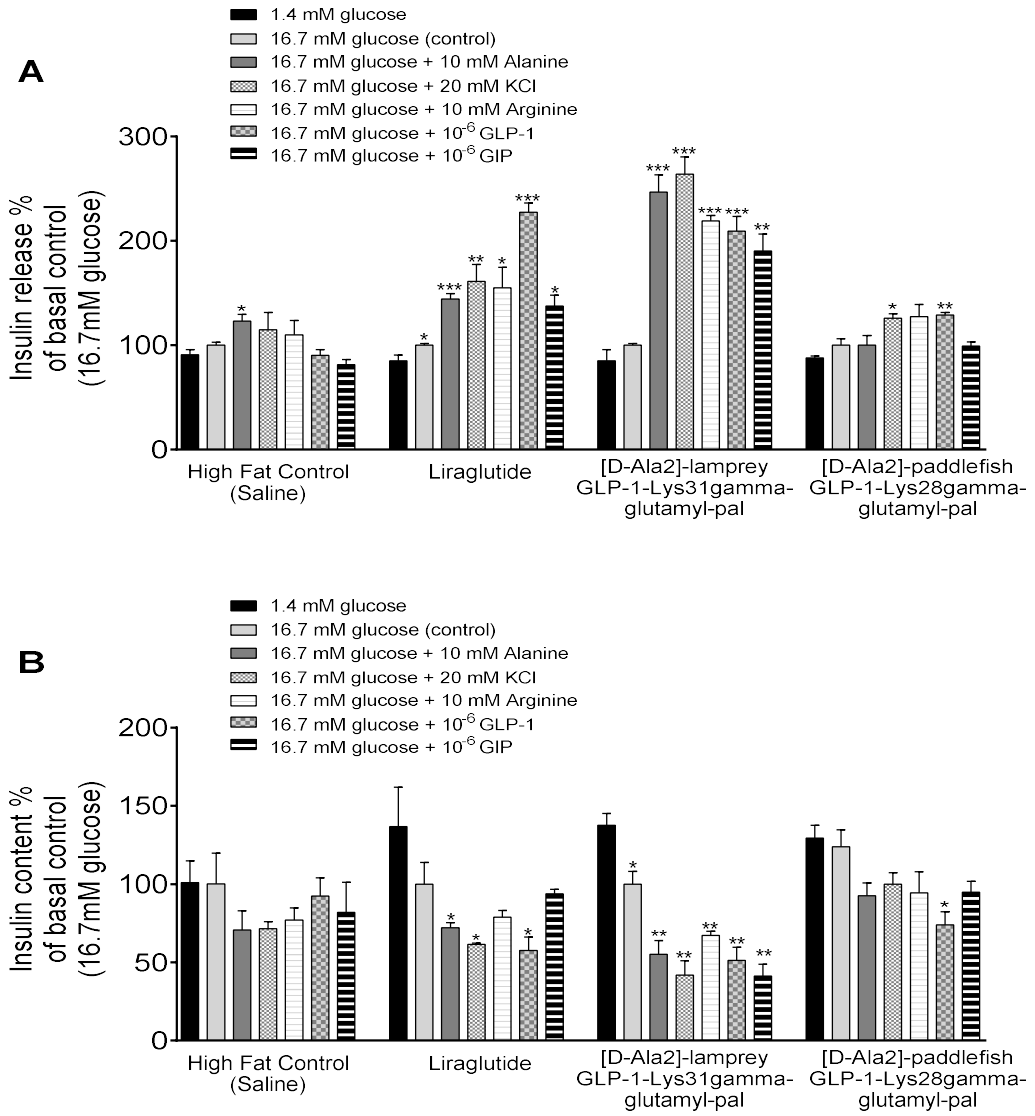

Pancreatic islets were isolated following 21 days twice-daily treatment with saline vehicle (0.9% w/v NaCl, i.p), liraglutide or fish peptide analogues (each at 25 nmol/kg of bw, i.p.). Parameters for A) insulin release and B) insulin content represent normalised values to respective control (16.7mM glucose) for each group. Values are mean±SEM for n=4. *P<0.05, **P<0.01 ***P<0.001 compared to respective 16.7mM glucose control.

Figure 5. 27 Chronic effects of stable fish GLP-1 peptides on pancreatic islet morphology in high-fat-fed mice.

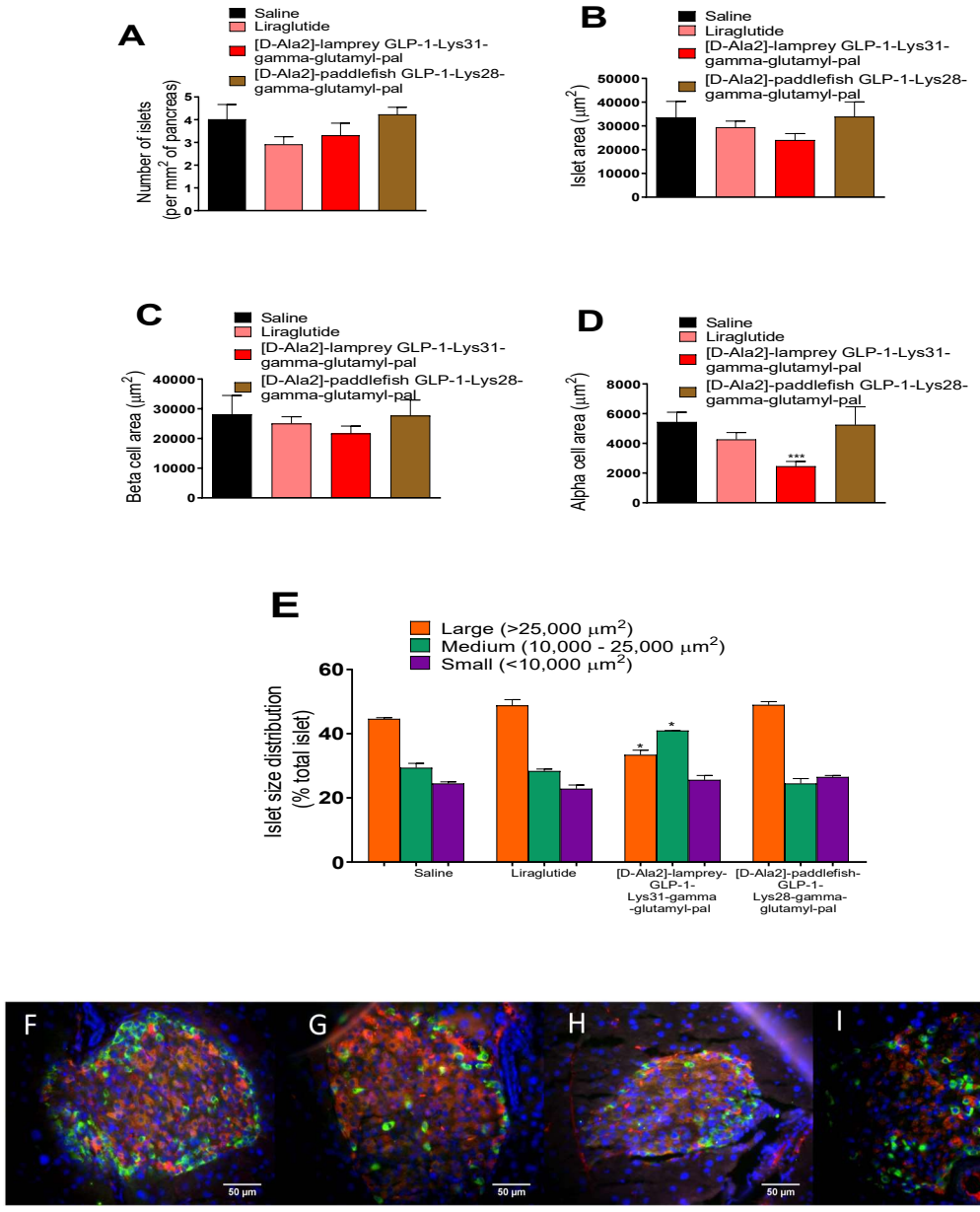

Parameters for (A) number of islets (mm), (B) islet area (μm^2), (C) beta cell area (μm^2), (D) alpha cell area (μm^2), (E) islet size distribution (% of total area) were measured on day 21 following twice-daily treatment with saline vehicle or the peptides (at 25 nmol/kg body weight. ***$P < 0.001$ compared to high-fat diet saline control. Effects of liraglutide are shown for comparison. F-I: Representative images of islets from (F) high-fat–fed mice treated with saline, (G) liraglutide, (H) [D-Ala^2]-lamprey GLP-1-Lys^{31}gamma-glutamyl-pal and (I) paddlefish GLP-1 and [D-Ala^2]-paddlefish GLP-1-Lys^{28}-gamma-glutamyl-pal hybrid. Images were analsed using Cell^F analysis software. Approximately >50 islets per mouse were analysed.

Figure 5.28 Chronic effects of stable fish GLP-1 peptides on the expression of genes involved in insulin secretion from islets in high-fat fed mice.

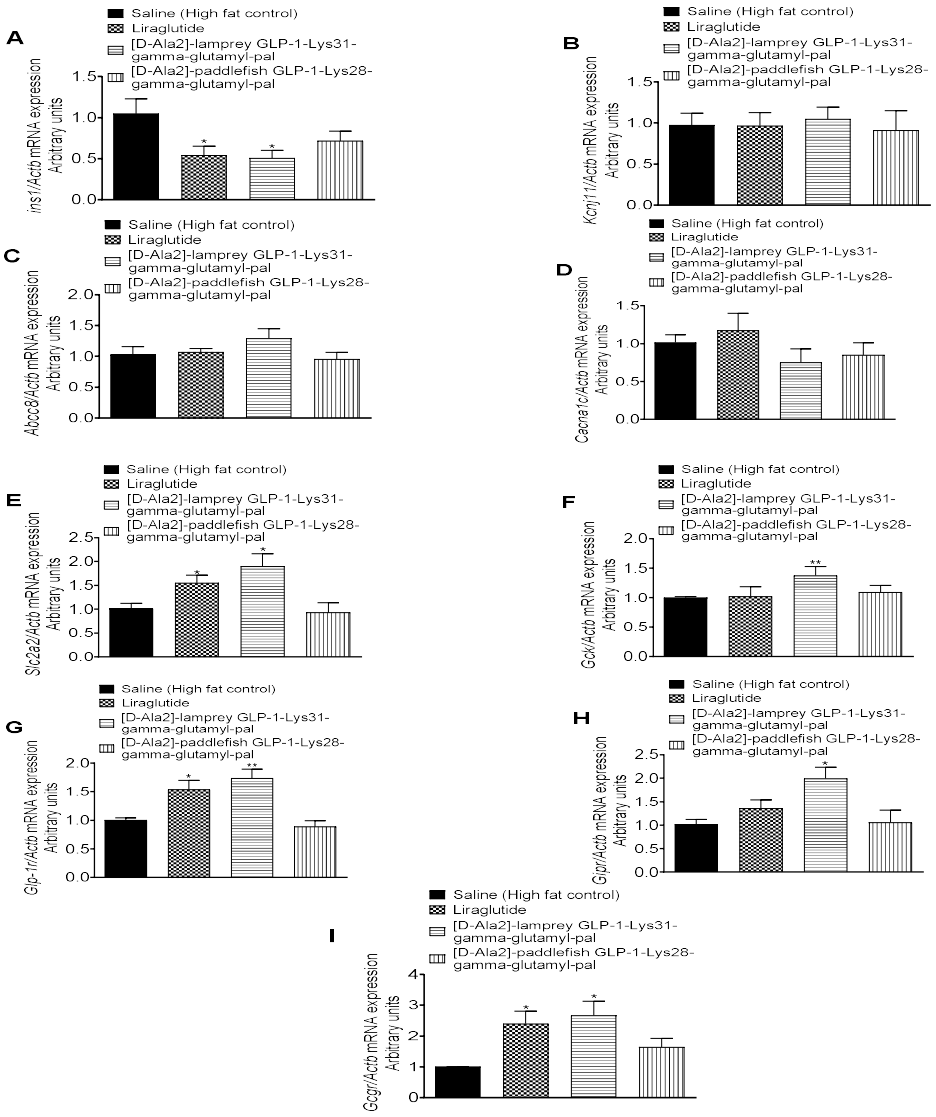

cDNA was synthesised from 1 µg of mRNA. Data were normalised to Beta-actin (Actb) gene expression used as a reference gene and analysed using the ΔΔCt method. Data are expressed as means ± SEMs for n=3. *P < 0.05, ** P< 0.01 and *** P< 0.001 compared with high fat saline control.

Figure 5.29 Chronic effects of [D-Ala^2]-lamprey GLP-1-Lys^{31}-gamma-glutamyl-pal on (A) accumulative food and (B) water intake during 11 days study in streptozotocin pre-treated GluGre Rosa26-YFP mice.

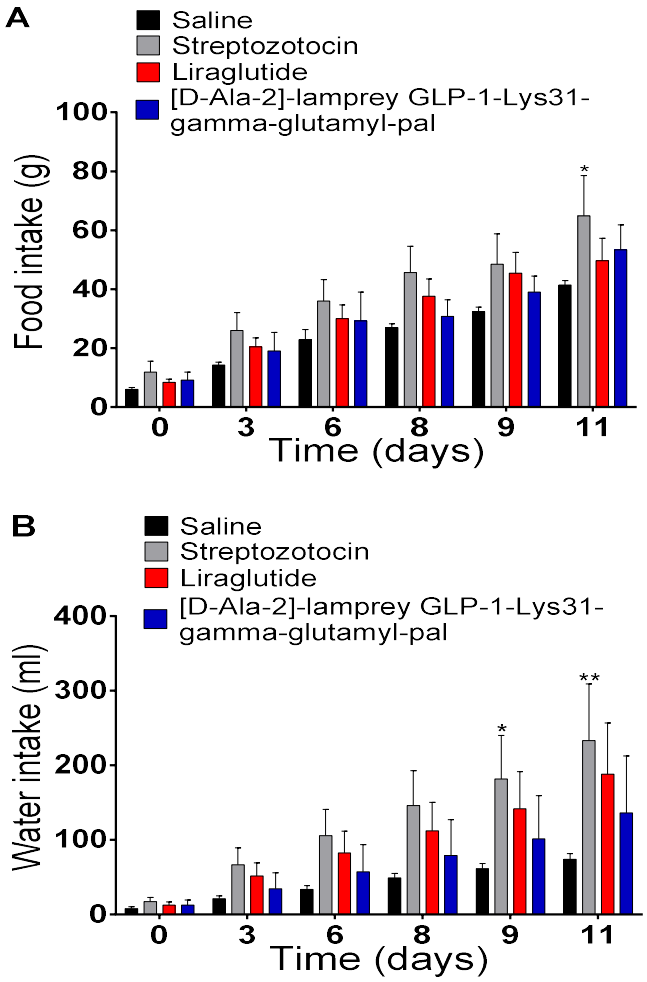

(A) Accumulative food and (B) water intake were measured during 11 days twice daily treatment with saline vehicle (0.9% (w/v) NaCl), liraglutide and [D-Ser^2]-paddlefish glucagon-Lys^{30}-gamma-glutamyl-pal (each at 25 nmol/kg bw). Values represent mean±SEM for 5 mice. *P <0.05 ** P <0.01 and ***P <0.001 is compared with normal control.

Figure 5.30 Chronic effects of [D-Ala^2]-lamprey GLP-1-Lys^{31}-gamma-glutamyl-pal on (A) blood glucose and (B) % of blood glucose change (C) body weight (D) % of body weight change and (E) plasma insulin during 11 days study in streptozotocin pre-treated GluGre Rosa26-YFP mice.

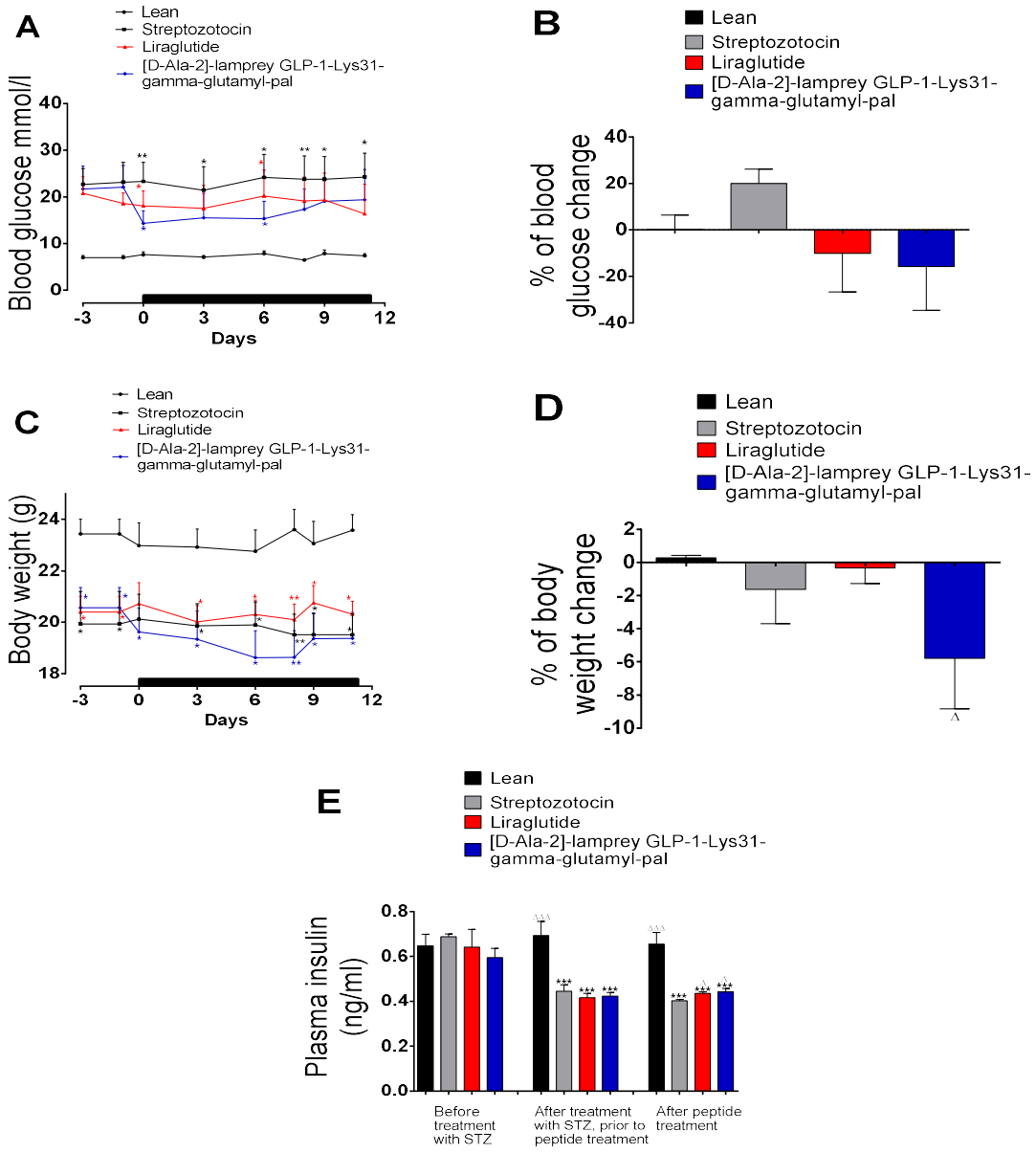

The parameters were measured during 11 days twice daily treatment with saline vehicle (0.9% (w/v) NaCl), liraglutide and [D-Ser^2]-paddlefish glucagon-Lys^{30}-gamma-glutamyl-pal (each at 25 nmol/kg bw). The black horizontal bar represents the treatment period. Values represent mean±SEM for 5 mice. *P <0.05 and ***P <0.001 is compared with normal control. $^{\Delta}$P <0.05 is compared with streptozotocin control.

Figure 5.31 Chronic effects of [D-Ala^2]-lamprey GLP-1-Lys^{31}-gamma-glutamyl-pal on pancreatic (A) insulin and (B) glucagon content during 11 days study in streptozotocin pre-treated GluGre Rosa26-EYFP mice.

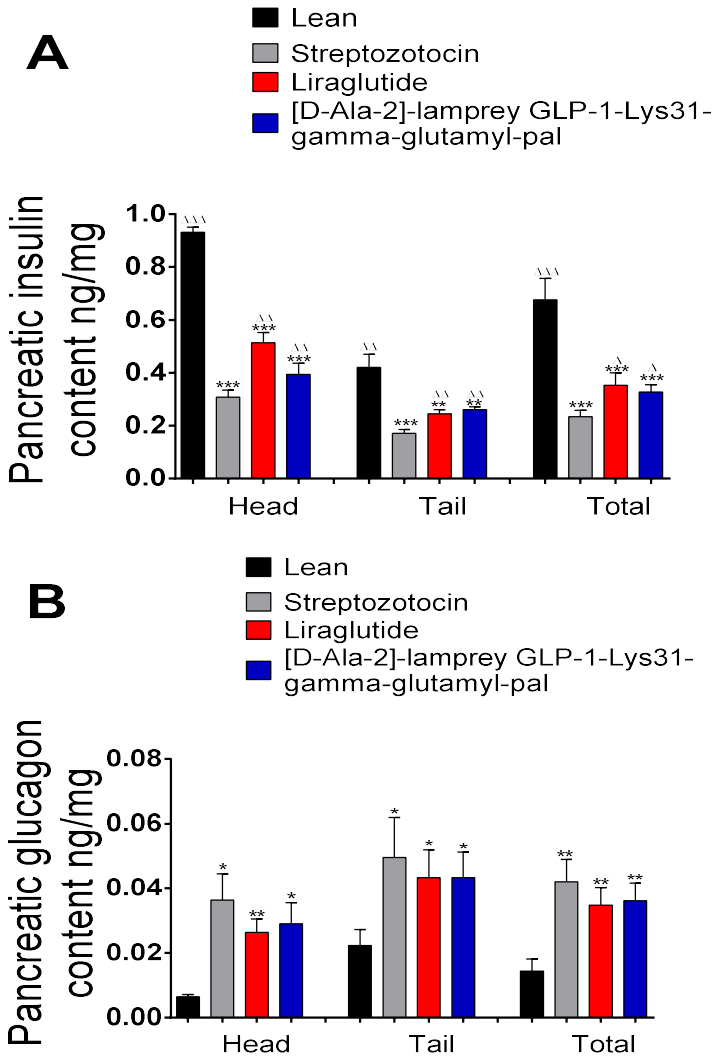

The parameters were measured during 11 days twice daily treatment with saline vehicle (0.9% (w/v) NaCl), liraglutide and [D-Ser^2]-paddlefish glucagon-Lys^{30}-gamma-glutamyl-pal (each at 25 nmol/kg bw). Values represent mean±SEM for n=3. *P<0.05 and ***P<0.001 is compared with normal control. $^{\Delta}$P<0.05, $^{\Delta\Delta}$P<0.01 and $^{\Delta\Delta\Delta}$P<0.001 is compared with streptozotocin control.

Figure 5.32 Chronic effects of [D-Ala^2]-lamprey GLP-1-Lys^{31}-gamma-glutamyl-pal on pancreatic islet morphology in GluGre Rosa26-YFP mice.

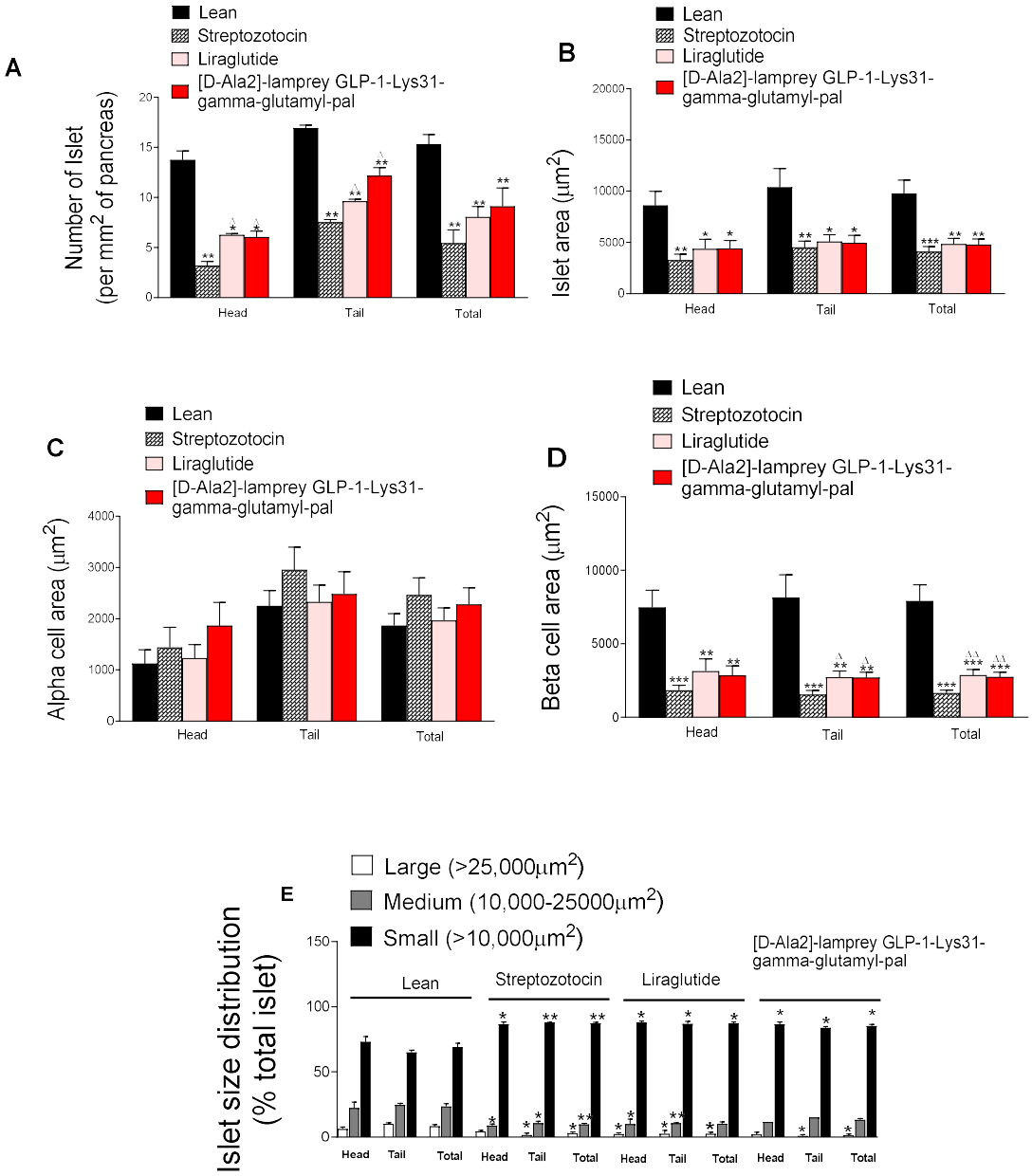

Parameters for (A) number of islets (mm), (B) islet area (µm^2), (C) beta cell area (µm^2), (D) alpha cell area (µm^2), (E) islet size distribution (% of total area) were measured on day 11 following twice-daily treatment with saline vehicle or the peptides (at 25 nmol/kg body weight. ~40-50 islets per group. The values are mean ± SEM *P<0.05, **P<0.01 and ***P<0.001 compared to untreated control; $^{\Delta}$ P<0.05 and $^{\Delta\Delta}$ P<0.05 compared to streptozotocin-treated mice.

Figure 5.33 Chronic effects of [D-Ala^2]-lamprey GLP-1-Lys^{31}-gamma-glutamyl-pal on alpha to beta cell transdifferentiation in GluGre Rosa26-YFP.

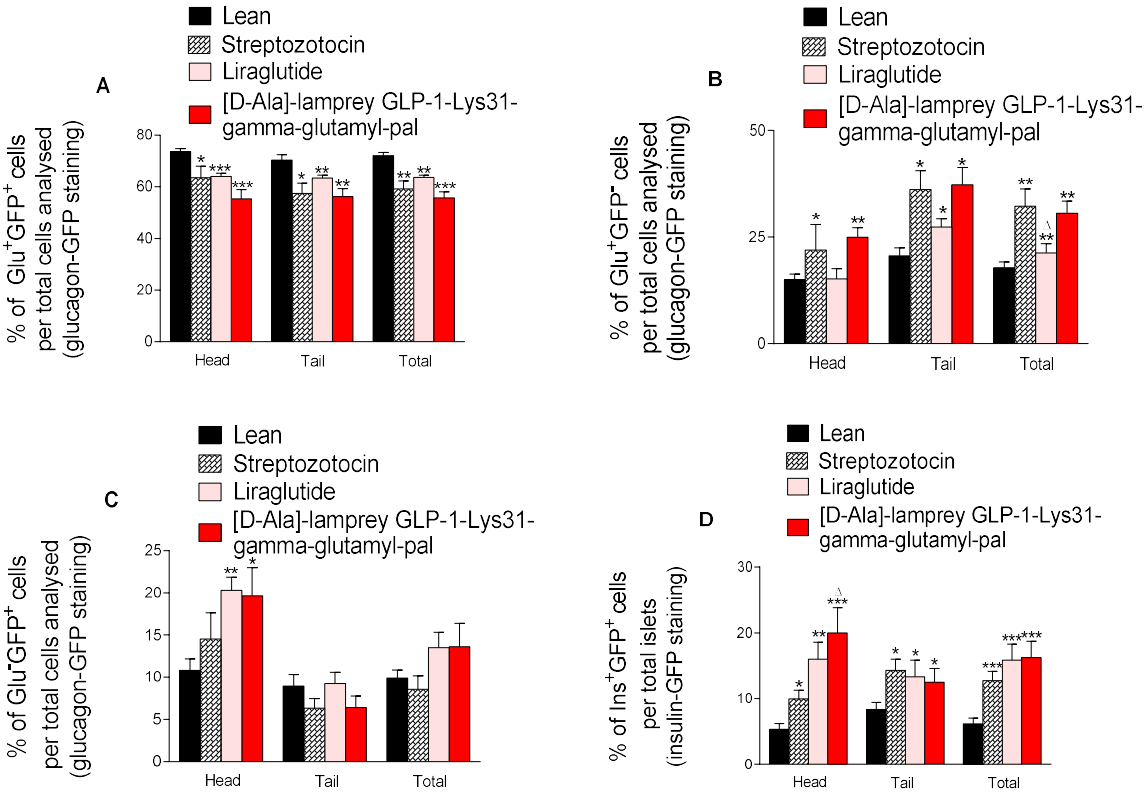

Analysis of A) Glucagon$^+$GFP$^+$ cells, B) Glu$^+$ GFP$^-$ cells, C) Glu$^-$GFP$^+$ and D) Insulin$^+$GFP$^+$ cells per total cells/islets analysed (~40-50 islets per group). The values are mean ± SEM *P<0.05, **P<0.01 and ***P<0.001 compared to untreated control; $^{\Delta}$ P<0.05 compared to streptozotocin-treated mice.

Chapter 6

Biological effects of [D-Ser^{2}]-lamprey glucagon-Lys^{30}-gamma-glutamyl-pal and [D-Ala2]-paddlefish glucagon-Lys30gamma-glutamyl-pal

6.1 Summary

This Chapter examined the insulinotropic and anti-hyperglycemic properties of novel fish analogue peptides, namely [D-Ser^2]-lamprey glucagon- Lys^{30}-gamma-glutamyl-pal and [D-Ser^2]-paddlefish glucagon-Lys^{30}-gamma-glutamyl-pal. Peptide stability was improved by several structural modifications including the stereochemical configuration of Ser at the position 2 with its D-isomer and addition of a γ-glutamyl spacer to Lys at position 30. Both analogues stimulated insulin release from BRIN-BD11 beta-cells, isolated mouse pancreatic islets and enhanced cAMP production in both, cells transfected with the human GLP-1 receptor cells transfected with the human glucagon receptor. [D-Ser^2]-paddlefish glucagon-Lys^{30}-gamma-glutamyl-pal also increased insulin release from isolated mouse islets. The insulinotropic actions of the peptides were attenuated in INS-1 cells engineered to lack GLP-1 and glucagon receptors. [D-Ser^2]-paddlefish glucagon-Lys^{30}-gamma-glutamyl-pal was found to be more effective than native peptide at acutely lowering blood glucose and elevating plasma insulin in normal mice. The peptide was selected for the 21-day study using high-fat-fed mice. Twice daily administration of [D-Ser^2]-paddlefish glucagon-Lys^{30}-gamma-glutamyl-pal reduced body weight, non-fasting plasma glucose and circulating plasma insulin, as well as significantly improving glucose tolerance and insulin resistance. [D-Ser^2]-paddlefish glucagon-Lys^{30}-gamma-glutamyl-pal significantly decreased alpha cell area and pancreatic insulin content. Molecular analysis revealed a positive long-term effect of the peptide on islet genes encoding insulin, GLUT2, and GLP-1 and GIP receptors. Studies using streptozotocin-induced diabetic GluCreRosa26-YFP mice revealed significant beta-cell transdifferentiation and regeneration. These data demonstrate that long-acting dual agonist, [D-Ser^2]-paddlefish glucagon-Lys^{30}-gamma-glutamyl-pal, exerts beneficial metabolic

properties similar to liraglutide in diabetic mice. The phylogenetically ancient fish glucagon derivative represents a novel agent with the therapeutic potential for treatment of type 2 diabetes.

6.2 Introduction

Acting as a physiological incretin hormone, glucagon-like peptide-1 (GLP-1) represents a good candidate template for the development of new drug treatments for diabetic patients (Manandhar et al. 2014). Indeed, in addition to its insulinotropic and anti-hyperglycemic benefits, GLP-1 peptide also inhibits gastric emptying, feeding and glucagon secretion via glucagon-like peptide receptor (Baggio et al. 2014).

In the last decade, a successful approach using incretin-based therapies has promoted evaluation of other glucagon-family peptides leading to the development of molecules that combine beneficial effects of core metabolic hormones into a single entity with enhanced antidiabetic properties. A large number of unimolecular co-agonists capable of activating different signalling pathways and hence minimise adverse effects due to more balanced pharmacokinetic action are in preclinical and clinical development (Brandt et al. 2017 and Pocai et al. 2009)

As such a great success was achieved in the year 2009, combining lipolytic and thermogenic properties of glucagon and insulinotropic anorectic actions of GLP-1 in a single peptide GLP-1/glucagon co-agonist with further structural modifications. The dual-acting peptide was shown to exhibit positive effects on reducing body weight, improving glucose tolerance, lipid metabolism, and liver steatosis in high-fat fed mice. Interestingly, GLP-1/glucagon co-agonist was also effective in reducing weight in GLP-1r KO mice showing the contribution of glucagon in metabolic status (Day et al. 2009 and Brandt et al. 2017).

Other studies employed naturally occurring dual-agonist oxyntomodulin sequence to design potent co-agonist peptides (Pocai et al. 2009 and Lynch et al. 2014). Furthermore, another dual GLP-1/glucagon receptor agonist, MEDI0382, was reported to have a potent *in vivo* effect on weight loss, hepatic fat content and glucose metabolism (Henderson et al. 2016).

More examples of promising *in vivo* results include a novel exendin-4 based GLP-1/glucagon co-agonist (Evers et al. 2017), as well a novel GLP-1R/GCGR dual agonist with substitution in glucagon sequence at position 22, 23 and 25 by cysteine and additional of laurate maleimide conjugation (Zhou et al. 2017). Many co-agonists currently undergo clinical trials (Brandt et al. 2017).

Amino acid sequences of the proglucagon peptide trio, glucagon and the glucagon-like peptide-1 and 2 share structural similarities which are highly maintained in the vertebrates. Studies of comparative endocrinology of secretin family of peptides, therefore, represent a novel approach for discovery and further developing novel multi-acting unimolecular peptide agonists.

Duplication of the intact gene encoding proglucagon or duplication within its gene members are extremely rare and are likely to result from the whole genome duplication. This evolutionary event began about 1 billion years ago from an ancestral glucagon exon duplication giving rise to glucagon, while GLP-1 and GLP-2 diverged from each other about 700 MYA. (Lopez et at 1984; Irwin 1999 and Irwin 2005; Ng et al. 2010). Examination of the rates of evolution for each proglucagon-derived peptide sequence uncovers an episodic nature of the evolutionary process for each hormone, leading to the sequence variation between and within vertebrate classes (Irwin 2010). Consequently, fish (Agnathans and Osteichthyes) and amphibians are

found to have multiple proglucagon sequences, either by precence of additional proglucagon genes or multiple peptide sequences within the proglucagon gene, whereas in mammals only one proglucagon-derived peptide set exists (Ng et al. 2010).

Amino acid substitutions within the sequence are fixed in the population and often reflect dramatic changes in the functions of the proglucagon-derived hormones in specific species. GLP-1 hormone is a known example of this evolutionary change showing glucagon-like functions in teleost fish but acting as incretin in mammals (Irwin 2010). Moreover, phylogenetic analysis revealed that the Class B G-protein coupled receptors (GPCRs) appeared to evolve independently before acquiring specificity for their glucagon-derived peptide ligands.

Recently it has been shown that glucagon isolated from dogfish and its derived analogues exhibited potent anti-hyperglycemic and insulinotropic effects *in vivo* as well as displayed *in vitro* and *in vivo* dual agonist activity targeting both GLP-1 and glucagon receptors (O'Harte et al. 2016). Further investigation assessing glucagon-derived peptides isolated from phylogenetically ancient and a teleost species show equally valuable data (see Chapter 4). On the basis of detailed *in vivo* and acute *in vitro* studies, Glucagon from sea lamprey and paddlefish were selected for further studies to design DPP-IV resistant synthetic analogues.

The sequences of these native fish glucagon peptides were modified by substitution of Ser at position 2 for its D-isomer and addition of a gamma-glutamyl with palmitate to the lysine residues at positions 30 for both sequences. The potential insulinotropic effects of fish peptide analogues were examined in acute *in vitro* studies using BRIN-BD11 and isolated mouse islets, cells transfected with either human GLP-1 or glucagon receptor and CRISPR/Cas9-engineered INS-1 cell line as well as in acute *in*

vivo using normal mice. The potential beneficial metabolic effects of paddlefish glucagon analogue were further examined in longer-term *in vivo* studies using high-fat-fed mice and transgenic CluCreRosa26-YFP. The activities of fish peptides analogues were compared with those of human GLP-1, GIP, glucagon, oxyntomodulin, exendin-4 and liraglutide.

6.3 Materials and Methods

6.3.1 Peptides

[D-Ser^2]-lamprey glucagon-Lys^{30}-gamma-glutamyl-pal and [D-Ser^2]-paddlefish glucagon-Lys^{30}-gamma-glutamyl-pal were obtained from Synpeptide Co. Ltd. (Shanghai, China) and purified as previously described in Section 2.1.1. Synthetic human glucagon, human GLP-1, human GIP, oxyntomodulin, liraglutide and exendin-4 peptides were obtained and purified as described previously (Section 2.1.1). Molecular masses for all peptides were subsequently confirmed using MALDI-TOF MS (Section 2.2). The structures and basic features of the peptides used in this Chapter are shown in Table 6.1.

6.3.2 Assessment of metabolic stability of fish glucagon analogues

Enzymatic effects of DPP-IV and mouse plasma on fish glucagon analogues stability were assessed in degradation studies as previously described in Section 2.3

6.3.3 *In vitro* insulin release studies using BRIN-BD11

BRIN-BD11 cells (McClenaghan et al., 1996) were used to assess in vitro insulin secretory activity of peptides as previously described (Section 2.5.1). Insulin release was measured by RIA (Section 2.5.2 and 2.5.7).

6.3.4 Insulin release studies using isolated mouse islets

Effects of fish glucagon analogues on *ex-vivo* insulin secretion were assessed using isolated pancreatic mouse islets as described in Section 2.5.5.

6.3.5 Effects of fish glucagon analogues on in vitro cAMP production.

The ability of Chinese hamster lung (CHL) cells transfected with the human GLP-1 receptor (GLP1R) (Thorens et al., 1993) and human embryonic kidney (HEK293) cells transfected with the human glucagon receptor (GCGR) (Ikegami et al., 2001) to generate cAMP production in the presence of peptides was assessed using a Parameter cAMP assay kit (R&D Systems, Abingdon, UK) as outlined in Section 2.6.

6.3.6 Insulin release studies using CRISPR/Cas9-engineered INS-1 cells

In vitro receptor activation study was performed using wild-type INS-1 832/3 rat clonal pancreatic β-cells and CRISPR/Cas9-engineered cells with the knock-out of the GLP-1 receptor (GLP-1 KO) or GIP receptor (GIP KO) (Naylor et al., 2016) or glucagon receptor (GCG KO) as described in Section 2.5.4.

6.3.7 Proliferation and apoptosis of BRIN BD11 cells

To assess the effects of peptides (10nM and 10μM) on beta-cell proliferation and apoptosis, BRIN-BD11 were used as previously described (Section 2.7).

6.3.8 Animals

Acute and persistent in vivo studies were carried out using male 8-12 week-old male National Institutes of Health (NIH) Swiss mice as outlined in Sections 2.8.1.1, 2.8.2.1, 2.8.2.3 and 2.8.2.5. Cumulative food intake was assessed as previously described

(Section 2.8.2.6). Chronic studies were evaluated using high fat fed TO mice (Section 2.8.1.2).

6.3.9 Acute in vivo studies using normal mice

For acute IPGTT studies, blood glucose and plasma insulin were measured immediately prior to (t = 0) and 15, 30 and 60 min after intraperitoneal administration of glucose alone (18 mmol/kg of body weight) or in combination with test peptides (each at 25 nmol/kg bw) in overnight fasted mice. For persistent IPGTT studies overnight fasted animals received either test peptides (each at 25 nmol/kg of body weight) or saline vehicle 2 or 4 hours before an intraperitoneal glucose administration (18 mmol/kg bw). Blood glucose and plasma insulin were subsequently measured at 15, 30 and 60 min post glucose injection as detailed in Section 2.8.5. In a separate series of experiments, cumulative food intake was assessed by administrating intraperitoneal injections to animals with either saline solution or peptides (25 nmol/kg) prior to reintroduction of normal chow for 180 mins.

6.3.10 *In vivo* long-term studies using high-fat-fed mice

Mice fed with high-fat diet for 3 months exhibited weight gain, hyperglycaemia and insulin resistance as described in Section 2.8.1.2. Animals were grouped and received twice daily intraperitoneal injections saline solution for three days prior to administration of saline or peptides (25 nmol/kg of body weight) twice daily (09:30 and 17:00 h) over 21 days (Sections 2.8.1.2 and 2.8.3.1). The peptide treatments were commenced as follows: Group 1 (high fat control, n = 8; 0.9% NaCl, w/v; ip); Group 2 (liraglutide, n = 8; 25 nmol/kg bw; ip); Group 3 ([D-Ser^{2}]-paddlefish glucagon-Lys^{30}-gamma-glutamyl-pal, n = 8; 25 nmol/kg bw; ip). Mice remained on a high-fat

diet for the duration of the study. Non-fasting blood glucose, cumulative food intake and water intake, body weight, and insulin concentrations were monitored at 3-day intervals prior to daily injection of test peptides (Section 2.8.3.1). On the final day of the study, IPGTT, OGTT (18 mmol/kg bw) and insulin sensitivity (25 U/kg bw; i.p.) tests were performed (Section 2.8.3.2 and 2.8.3.3). HOMA-β was calculated using the formula HOMA-β = 20 × fasting insulin (μIU/ml)/fasting glucose (mmol/ml) − 3.5, whereas HOMA-IR was determined using the equation HOMA-IR = fasting glucose (mmol/l) x fasting insulin (mU/l)/22.5. At the end of the experimental period, terminal non-fasted blood was collected (Section 2.8.3.5) for measuring lipid profile (Section 2.8.3.8), plasma amylase activity (Section 2.8.3.7), ALT (Section 2.8.3.9) and glucagon levels (Section 2.8.3.11).

Bone mineral density and body tissue composition of the treated animals were measures using DEXA scanning (Section 2.8.3.4). The terminal analysis also included extraction of pancreatic tissue for measurement of pancreatic hormone contents (Section 2.8.3.12) and preparation of paraffin tissue blocks for immunohistochemical staining (Section 2.13.1). Islets were also isolated for the measurement of acute insulin secretion (Section 2.8.3.6) and determination of islet gene expression (Sections 2.8.3.13- 2.8.3.15).

6.3.11. Long-term in vivo studies using GluCre Rosa26-YFP mice

Animals were housed and pre-treated with streptozotocin as described previously (Section 2.8.1.4). Mice (n=5) were administrated twice daily intraperitoneal injections of saline or peptides (25 nmol/kg of body weight) over a 10-days treatment period. Non-fasting blood glucose, food intake, water intake and body weight were monitored at 3-day intervals prior to daily injection of test peptides. Blood was collected for

insulin measurements at the start and end of the experiment. The animals were sacrificed, and pancreases were removed and stained as described previously (Section 2.8.4)

6.3.12 Statistical analysis

Data were compared using unpaired Student's t-test (non-parametric, with two-tailed P values and 95% confidence interval) and one-way ANOVA with Bonferroni post-hoc test using GraphPad PRISM (Version 5.0 San Diego, California). Area under the curve (AUC) analysis was performed using the trapezoidal rule with baseline correction. Data are presented as mean ± S.E.M where the comparison was considered to be significantly different if $P < 0.05$.

6.4 Results

6.4.1 Purification and confirmation of molecular masses by MALDI-TOF MS

Following RP-HPLC on a C-8 semi-preparative column the main peaks of peptides were collected as represented in Figure 6.1. Experimental masses detected for each peptide by MALDI-TOF MS corresponded very closely with the theoretical masses as shown in Table 6.1.

6.4.2 Assessment of metabolic stability of fish glucagon analogues

Both peptides, [D-Ser^2]-lamprey glucagon-Lys^{30}-gamma-glutamyl-pal and [D-Ser^2]-paddlefish glucagon-Lys^{30}-gamma-glutamyl-pal were stable to degradation after 4 h incubation with DPP-IV (Figures 6.3 and 6.4) and plasma (Figures 6.5 and 6.6). As expected, parent glucagon peptides and human glucagon were susceptible to rapid degradation by DPP-IV (Figures 3.5, 4.3 and 4.6). Plasma degradation of human glucagon likewise is shown in Figure 6.7 (35% degraded).

6.4.3. Acute effects of fish glucagon analogues on in vitro insulin-release

The effects of native fish glucagon peptides, human GLP-1 and human glucagon are considered in Chapter 4. Incubation with [D-Ser^2]-lamprey glucagon-Lys^{30}-gamma-glutamyl-pal and [D-Ser^2]-paddlefish glucagon-Lys^{30}-gamma-glutamyl-pal increased insulin release from the BRIN-BD11 cells in a concentration-dependent manner (Figure 6.8). A summary of the insulinotropic effects of analogues of lamprey and paddlefish glucagons together with native fish peptides and human GLP-1 is presented in Table 6.2. The rate of insulin release stimulated by [D-Ser2]-lamprey glucagon-Lys30gamma-glutamyl-pal at 3 μM was less than the parent peptide. However, the threshold concentration was superior. The effects of [D-Ser^2]-paddlefish glucagon-Lys^{30}-gamma-glutamyl-pal at 3 μM was comparable to the parent peptide and human GLP-1. However, the threshold concentration for the analogue was increased.

Surprisingly, incubation of [D-Ser^2]-lamprey glucagon-Lys^{30}-gamma-glutamyl-pal with isolated mouse islets failed to produce any significant change of insulin release. In contrast, [D-Ser^2]-paddlefish glucagon-Lys^{30}-gamma-glutamyl-pal effectively increase the rate of insulin release from the islets at 10 nM and 1 μM, which was comparable to the action of GLP-1 (Figure 6.9 and Table 6.3),

6.4.4 Effect on fish glucagon analogues on cAMP production

Incubation of CHL cells transfected with the human GLP-1 receptor with [D-Ser^2]-lamprey glucagon-Lys^{30}-gamma-glutamyl-pal resulted in significantly increased cAMP production at both 10 nM and 1 μM compared to control. However, the effect at 10nM was significantly less than human GLP-1 (Figure 6.10 A). The stimulatory effect of [D-Ser^2]-paddlefish-glucagon-Lys^{30}-gamma-glutamyl-pal was comparable to GLP-1 at both, 10 nM and 1 μM concentrations (Figure 6.10 A). Both of the analogues

stimulated cAMP production in HEK293 cells transfected with the human glucagon receptor. (Figure 6.10 B and Table 6.4).

6.4.5 Insulin release studies using CRISPR/Cas9-engineered INS-1 cells

Both analogues significantly increased the rate of insulin release in wild-type INS-1 cells at both, 10 nM and 1 μM concentrations (Figure 6.11 A and Table 6.5). Incubation of analogues with GLP-1 KO and glucagon KO cells attenuated stimulatory effects on insulin secretion compared to wild-type INS-1 cells (Figure 6.11 B and C). Incubation of fish peptide analogues with GIP KO cells showed a similar rate of insulin release compared to wild-type cells (Figure 6.11 D).

6.4.6 Effects of the peptides on proliferation and apoptosis of BRIN BD11 cells

Incubation of BRIN BD11 cells with a mixture of proinflammatory cytokines significantly ($P<0.001$) decreased proliferation when compared to control cultures. Human GLP-1 (10nM and 10μM) significantly ($P<0.001$) enhanced cell proliferation in cytokine-free solution and reversed ($P<0.01$ $P<0.001$) the negative effect of cytokines. Likewise, [D-Ser^2]-paddlefish glucagon-Lys^{30}-gamma-glutamyl-pal and [D-Ser^2]-lamprey glucagon-Lys^{30}-gamma-glutamyl-pal increased proliferation in a cytokine-fee media. In the presence of cytokines [D-Ser2]-lamprey-glucagon-Lys30-gamma-glutamyl-pal did not affect cell proliferation at 10 nM, whereas [D-Ser^2]-paddlefish glucagon-Lys^{30}-gamma-glutamyl-pal was effective at both 10nM and 10μM concentrations (Figure 6.12 A). In the second series of experiments incubation of BRIN-BD11 cells with glucagon-derived analogues and human GLP-1 (both at 10μM) resulted in a significant ($P<0.001$) protective effect against apoptosis (Figure 6.12 B).

6.4.7 Acute in vivo studies using normal mice

Acute glucose-lowering and insulinotropic effects of [D-Ser^2]-lamprey glucagon-Lys^{30}-gamma-glutamyl-pal (Figures 6.13) and [D-Ser^2]-paddlefish glucagon-Lys^{30}-gamma-glutamyl-pal (Figures 6.14) together with parent and control peptides were assessed in overnight fasted mice. Surprisingly, [D-Ser^2]-lamprey glucagon-Lys^{30}-gamma-glutamyl-pal (25 nmol/kg body weight) appeared to lose the beneficial properties of the parent peptide. Hence it failed to elicit any effects that were comparable with the positive control peptides (Figure 6.13). In contrast, [D-Ser^2]-paddlefish glucagon-Lys^{30}-gamma-glutamyl-pal significantly reduced ($P<0.05$-$P<0.001$) individual blood glucose concentrations at 15, 30 and 60 min time points and overall glucose 0-60 min compared to the admiration of 18 mmol/kg glucose alone. The effect of paddlefish glucagon analogue was not significantly different from human GLP-1 and was similar to exendin-4 and oxyntomodulin. However, native paddlefish glucagon appeared to exhibit greater glucose-lowering potential compared to human GLP-1 according to overall glucose 0-60 min integrated response to (Figure 6.14 B). These effects were associated with increased ($P<0.01$ and $P<0.001$) insulin secretory responses to human GLP-1, oxyntomodulin, exendin-4, native paddlefish glucagon and paddlefish glucagon analogue at 15 and 30 min post injection. Additionally, paddlefish glucagon analogue and exendin-4 showed improved insulin release at 60 min (Figure 6.14 C). Consistent with these results, overall 0-60 min plasma insulin AUC values were improved after the peptide treatment when compared to glucose alone controls (Figure 6.14 D).

6.4.8 Persistent effects of peptides after 2 and 4 hours on plasma glucose and insulin release in normal mice

As expected, due to rapid enzymatic degradation in plasma, native lamprey glucagon and human GLP-1 were ineffective when administrated 2 h prior a glucose load. Lamprey glucagon analogue showed a weak glucose-lowering response with a significant reduction ($P<0.05$) of blood glucose only at 60 min, which was less than potent actions of exendin-4 (Figure 6.14 A). Although the overall 0-60 min blood glucose was significantly ($P<0.05$) improved for [D-Ser2]-lamprey glucagon-Lys30gamma-glutamyl-administrated 2 h previously (Figure 6.15 B), the analogue failed to show any insulinotropic effects (Figure 6.15 C and D). In contrast, administration of [D-Ser^{2}]-paddlefish glucagon-Lys^{30}-gamma-glutamyl-pal and exendin-4 2 h prior to a glucose load (Figure 6.14) resulted in a significantly ($P<0.001$) lowered glucose concentrations at 15, 30 and 60 min time points post glucose injection (Figure 6.16 A). Interestingly, administration native paddlefish glucagon also significantly ($P<0.05$-$P<0.01$) reduced blood glucose at 15 and 30 min time point. The overall 0-60 min blood glucose AUC showed that native paddlefish glucagon was still effective when administrated 2 h prior to a glucose challenge. However, the result was less impressive than the substantial glucose-lowering actions of exendin-4 and paddlefish glucagon analogue. Corresponding glucose-induced plasma insulin responses were only significantly improved by exendin-4 and paddlefish glucagon analogue in terms of individual values at 15, 30 and 60 min post-injection as well as overall insulin 0-60 AUC values compared to saline control and human GLP-1 (Figure 6.16 C and D).

When administrated 4 h prior to a glucose load, [D-Ser^{2}]-lamprey glucagon-Lys^{30}gamma-glutamyl-pal did not show any improvement in blood glucose levels similarly to the effects of oxyntomodulin (Figure 6.17 A and B). However, the analogue slightly improved insulin secretion at 30 min and the overall 0-60 min plasma insulin response (Figure 6.17 C and D). On the other hand, exendin-4 and [D-Ser^{2}]-paddlefish glucagon-Lys^{30}-gamma-glutamyl-pal elicited a protracted glucose-lowering and insulinotropic activity when administrated 4 h prior to administration of glucose (Figure 6.18).

6.4.9 Acute in vivo food intake studies

Acute intraperitoneal administration of native lamprey glucagon at a dose of 25 nmol/kg of body weight to overnight fasted animals, did not result in a reduction of food intake over 180 min. In comparison, [D-Ser^{2}]-lamprey glucagon-Lys^{30}-gamma-glutamyl-pal significantly ($P < 0.05$) suppressed feeding at 180 min (Figure 6.18 A). Notably, the appetite suppressive effects of paddlefish glucagon and its analogue were comparable to the effects of exendin-4 which markedly ($P < 0.001$) reduced cumulative feeding rate over 180 minutes (Figure 6.19 B).

6.4.10 Chronic effects of [D-Ser^{2}]-paddlefish glucagon-Lys^{30}-gamma-glutamyl-pal on body weight, food/water intake, non-fasting plasma glucose and insulin in high fat fed mice

Twice daily administration of [D-Ser^{2}]-paddlefish glucagon-Lys^{30}-gamma-glutamyl-pal to high fat fed mice resulted in a significant ($P < 0.05$-$P < 0.001$) reduction of food intake starting from day 13 onwards when compared to high-fat control (Figure 6.20 A). However, no alteration in fluid intake was observed for any of the treatment groups (Figure 6.20 B). Chronic administration of [D-Ser^{2}]-paddlefish glucagon-Lys^{30}-

gamma-glutamyl-pal significantly lead to a reduction in body weight from day 18 onwards when compared to high-fat control (Figure 5.18 A). Indeed, both liraglutide and [D-Ser^2]-paddlefish glucagon-Lys^{30}-gamma-glutamyl-pal administration resulted in a significant ($P < 0.001$) decrease of body weight (Figure 6.21 B) compared to high-fat control. Only [D-Ser^2]-paddlefish glucagon-Lys^{30}-gamma-glutamyl-pal treatment significantly ($P < 0.001$) reduced the overall AUC glucose concentration (Figure 6.22). However, there was a notable reduction ($P < 0.05$ and $P < 0.001$) in overall plasma insulin AUC for all treatment groups as well as a reduction ($P < 0.05$) at individual time points on day 10 and day 16 for liraglutide and [D-Ser^2]-paddlefish glucagon-Lys^{30}-gamma-glutamyl-pal respectably (Figure 6.23).

6.4.11 Chronic effects of [D-Ser^2]-paddlefish glucagon-Lys^{30}-gamma-glutamyl-pal on glucose tolerance in high-fat-fed mice

Following 21 days twice daily treatment with liraglutide and [D-Ser^2]-paddlefish glucagon-Lys^{30}-gamma-glutamyl-pal a significant reduction ($P < 0.05$-$P < 0.001$) in glucose concentration was observed at individual time points, following intraperitoneal injection of glucose: 30 min for liraglutide and 15-120 min for paddlefish glucagon analogue (Figure 6.24 A). This translated to a significant reduction ($P < 0.05$-$P < 0.001$) of overall blood glucose 0-120 AUC values in these two groups (Figure 6.24 B). Glucose-stimulated insulin concentrations were also significantly increased at 15 and 30 min individual for liraglutide and at 15-60 min for [D-Ser^2]-paddlefish glucagon-Lys^{30}-gamma-glutamyl-pal treatment groups. The integrated responses of insulin release during 0-120 min showed a significant ($P < 0.01$ - $P < 0.001$) increase in all treatment groups, however [D-Ser^2]-paddlefish glucagon-Lys^{30}-gamma-glutamyl-pal treatment resulted in significantly ($P < 0.05$)

greater stimulation of insulin compared to liraglutide (Figure 6.24 C and D). In the second series of experiments, OGTT was performed. In the groups receiving twice-daily injections of liraglutide and [D-Ser^{2}]-paddlefish glucagon-Lys^{30}-gamma-glutamyl-pal there was a significant ($P < 0.05$) reduction is observed at 60, 90 and 120 min together with significantly ($P < 0.05$) lowered integrated response compared to control (Figure 6.25 A and B). Concomitant with the lower blood glucose levels, the concentrations of plasma insulin were significantly ($P < 0.05$-$P < 0.01$) greater at 15 and 30 min in liraglutide and 15 min in [D-Ser^{2}]-paddlefish glucagon-Lys^{30}-gamma-glutamyl-pal treated mice (Figure 6.25 C). The integrated insulin responses were significantly ($P < 0.05$-$P < 0.01$) greater in these treatment groups compared to high-fat mice (Figure 6.25 D).

6.4.12 Chronic effects of [D-Ser^{2}]-paddlefish glucagon-Lys^{30}-gamma-glutamyl-pal and liraglutide on insulin sensitivity, insulin resistance and pancreatic hormonal content

No significant change in blood glucose was observed in treated groups after administration of exogenous insulin (day 21) compared to high-fat control (Figure 6.26). However, HOMAR-IR values revealed improved hypoglycemic action of insulin, indicating that peptides significantly ($P< 0.05$ and $P < 0.01$) enhanced insulin sensitivity compared to high-fat control (Figure 6.27 B). Beta-cell function was also improved the peptide treated groups (Figure 27 A).

Pancreatic glucagon content of liraglutide and [D-Ser^{2}]-paddlefish glucagon-Lys^{30}-gamma-glutamyl-pal treated mice treated was not significantly different compared to high-fat control (Figure 6.28 A). In contrast, pancreatic insulin content was significantly reduced in all treated groups compared to control (Figure 6.28 B).

6.4.13 Chronic effects of [D-Ser^2]-paddlefish glucagon-Lys^{30}-gamma-glutamyl-pal and liraglutide on plasma amylase activity, plasma glucagon, ALT levels and lipid profile in high-fat-fed mice

Terminal plasma analysis showed that amylase activity was significantly ($P < 0.05$) elevated (Figure 6.29), and plasma ALT was significantly ($P < 0.05$ and $P < 0.001$) reduced (Figure 6.30) in the peptide-treated groups compared to high-fat control. Moreover, plasma glucagon concentration was not significantly different between groups (Figure 6.31).

Assessment of the terminal plasma lipid profile revealed significant ($P < 0.05$) reduction in total cholesterol and triglyceride levels the group treated with [D-Ser^2]-paddlefish glucagon-Lys^{30}-gamma-glutamyl-pal when compared to high-fat controls (Figure 6.31 A and B). Finally, LDL-cholesterol and HDL-cholesterol were not significantly different between the groups (Figure 6.32 C and D).

6.4.14 Chronic effects of [D-Ser^2]-paddlefish glucagon-Lys^{30}-gamma-glutamyl-pal on bone density and body mass in high fat-fed mice

Assessment bone mineral density and bone mineral content revealed no significant difference between the treated groups and high-fat controls (Figure 6.33 A-D). However, a significant ($P < 0.05$- $P < 0.01$) reduction of fat mass and body fat percentage was observed in the peptide treatment groups (Figure 6.33 D and E).

6.4.15 Chronic effects of [D-Ser^2]-paddlefish glucagon-Lys^{30}-gamma-glutamyl-pal and liraglutide on *ex-vivo* insulin secretion and pancreatic islet morphology in high-fat-fed mice

Islets isolated from high-fat-fed mice showed a weak insulin secretory responses to stimulatory concentrations of glucose, alanine, arginine, potassium chloride, human GLP-1 and GIP which were improved by liraglutide and paddlefish glucagon analogue treatment (Figure 6.34)

No appreciable change in islet morphology was noted between liraglutide treated group and high-fat control (Figure 6.35 A-E). In the group treated with [D-Ser^2]-paddlefish glucagon-Lys^{30}-gamma-glutamyl-pal there was a significant reduction in alpha size area ($P < 0.05$), as well as a significant increase in the amount of small (< 10,000 μm2) islets compared to controls group, was observed. However, no other alteration in the histological analysis were detected. (Figure 6.35 D and E). The representative images from high-fat–fed and all peptide treatment groups are represented in Figure 6.35 F-I.

6.4.16 Chronic effects of [D-Ser^2]-paddlefish glucagon-Lys^{30}-gamma-glutamyl-pal on the administration on gene expression in high-fat-fed mice

Twice daily administration of liraglutide and paddlefish glucagon analogue significantly ($P < 0.05$) reduced the islet expression of *Ins1* (mouse insulin 1) whereas the expression of *Slc2a2* (glucose transporter 2; GLUT2) was significantly ($P < 0.05$) upregulated compared to in high-fat control. Furthermore, liraglutide and paddlefish glucagon analogue treatment resulted in significantly ($P < 0.05$) increased the expression of GLP-1 and glucagon receptors. The fish peptide analogue also

upregulated the expression of GIP receptors, the expression of which was less in high-fat controls. (Figure 6.36).

6.4.17 Chronic effects of [D-Ser^2]-paddlefish glucagon-Lys^{30}-gamma-glutamyl-pal and liraglutide on accumulative food and water intake in streptozotocin pre-treated GluCreRosa26-YEP mice

Pre-treatment of GluCreRosa26-YFP mice with streptozotocin resulted in a significant ($P < 0.05$) increase in food intake on day 11 compared to untreated controls (Figure 6.37 A). No alterations of food intake were observed in the groups treated twice daily with liraglutide or [D-Ser^2]-paddlefish glucagon-Lys^{30}-gamma-glutamyl-pal (Figure 6.37 A). A significant ($P < 0.05$ and $P < 0.01$) increase in water intake was observed in the streptozotocin group from day 9 onwards when compared to untreated controls (Figure 6.36 B). No alterations in water intake were observed in liraglutide and [D-Ser^2]-paddlefish glucagon-Lys^{30}-gamma-glutamyl-pal treated mice (Figure 6.37 B).

6.4.18 Chronic effects of [D-Ser^2]-paddlefish glucagon-Lys^{30}-gamma-glutamyl-pal and liraglutide on blood glucose, body weight, plasma insulin and pancreatic hormonal content in streptozotocin treated GluCreRosa26-YEP mice

Streptozotocin significantly decreased body weight compared to untreated controls (Figure 6.38 A). Liraglutide induced visible however not significant improvement in body weight compared to streptozotocin controls (Figure 6.38 B). Moreover, streptozotocin significantly ($P < 0.05$) increased blood glucose at all individual time points. Administration of peptides resulted in a visible improvement but blood glucose levels were not significantly changed (Figure 6.38 C and D). Insulin levels in all groups of mice were similar before streptozotocin treatment. As expected, post streptozotocin administration significantly decreased insulin levels. Administration of

peptides significantly improved (P< 0.05) insulin status but levels were still significantly (P< 0.001) than untreated controls. Streptozoticin administration significantly reduced pancreatic insulin content which was improved by peptide treatment. However, levels achieved were still significantly lower than untreated controls (Figure 6.39 A). Glucagon contents were significantly greater than untreated mice (Figure 6.39 B).

6.4.19 Chronic effects of [D-Ser^{2}]-paddlefish glucagon-Lys^{30}-gamma-glutamyl-pal and liraglutide on islet morphology in streptozotocin treated GluGre Rosa26-YFP mice.

Treatment of GluGre Rosa26-YFP mice with streptozotocin resulted in a significant reduction of islets in head, tail and overall pancreas regions compared to untreated controls. Liraglutide treatment resulted in a significant ($P < 0.05$) improvement of the number of islets in the head and tail regions. A significant increase was also observed in the head region of the pancreas in the paddlefish glucagon analogue treatment group. The overall number of islets in the whole pancreas was significantly ($P < 0.05$ and $P < 0.01$) lower in streptozotocin and peptide treatment groups compared to untreated controls (Figure 6.40 A). Islet area was significantly reduced in all treatment groups (Figure 6.40 B). However, no significant differences were observed in the alpha cell area between all the groups including untreated controls (Figure 6.40 C). Interestingly, alpha cell area in the tail region and whole pancreas in streptozotocin controls was visibly greater than untreated mice. In the peptide treated groups, alpha cell area was similar to the untreated control (Figure 6.40 C). In contrast, beta cell area was significantly reduced in streptozotocin controls, and peptide treated groups compared to untreated mice. However, a significant improvement in beta cell area in

the tail region and total pancreas was observed in the groups treated with peptides compared to streptozotocin control (Figure 6.40 D).

Islet size distribution analysis shown a significant decrease ($P < 0.05$ and $P < 0.01$) in the number of large and medium islets, and a significant increase ($P < 0.05$ and $P < 0.01$) in the number of small islets across streptozotocin control and peptide treated groups compared to untreated controls.

6.4.20 Chronic effects of [D-Ser^{2}]-paddlefish glucagon-Lys^{30}-gamma-glutamyl-pal and liraglutide on islet alpha to beta cell transdifferentiation in streptozotocin pre-treated GluGre Rosa26-YFP mice.

The population of alpha cells that were YFP^{+} glucagon^{+} (which may also include alpha cells generated from pre-existing alpha cells) were significantly ($P < 0.05$ and $P < 0.001$) increased in untreated mice compared to the STZ-induced controls and the peptide treatment groups (Figure 6.41 A). The population of alpha cells that were YFP^{-} glucagon^{+} (new alpha cells derived from no-alpha cells) were significantly increased mostly in the tail region of the pancreas in peptide treatment groups and STZ controls compared to untreated controls. The expression of YFP^{-} glucagon^{+} cells was visibly greater in the head and tail regions together with the whole pancreas compared to liraglutide (Figure 6.41 B). Interestingly, YFP^{+} glucagon^{-} cells were expressed in the head region of the pancreas in the peptide treatment groups (Figure 6.41 C). New beta cells from alpha cells YFP^{+} insulin+ cells were also significantly increased in the head and overall pancreas in STZ control and peptide treatment groups. The expression of these cells was visibly greater in the peptide treatment groups compared to both untreated and STZ controls (Figure 6.41 D).

6.5 Discussion

Previous investigations outlined in Chapter 4 provided insight into glucagon and oxyntomodulin peptides isolated from anciently diverging lineages such as an ancient jawless fish (sea lamprey), two cartilaginous fishes (dogfish and ratfish), an early diverging ray-finned bony fish (paddlefish) and a teleost (trout). The sequences of fish glucagons and oxyntomodulins exhibit structural divergence in comparison to the sequence of mammalian glucagon. The most interesting and exciting molecule assessed in the study was paddlefish glucagon which exhibits structural similarities with the sequence of GLP-1 receptor agonist, exendin-4. Due to a unique structure and functional properties, paddlefish glucagon is suggested to be a naturally occurring hybrid glucagon/exendin-4 molecule (Graham et al. 2018).

Glucagons from lamprey and paddlefish were selected, due to their promising in vitro and in vivo insulinotropic and glucose-lowering effects, for further structural modification to design analogues with long-acting potential. In this Chapter, the properties of these two fish glucagon analogues were explored *in vitro* and acutely *in vivo* in comparison to human GLP-1, human glucagon, oxyntomodulin and exendin-4. Additionally, paddlefish glucagon was subjected to a further longer-term in *vivo study* in high-fat fed mice, and its efficacy was compared to the effects of liraglutide.

Human GLP-1 and human glucagon were promptly subjected to DPP-IV degradation at position 2 which resulted in two N-terminally truncated peptides (Chapter 3) (Mentlein et al. 1993; Authier et al. 2003; Pospisilic et al. 2001). Native lamprey and paddlefish glucagon peptides were also cleaved to metabolites, the molecular weight of which suggested the cleavage pattern at position 2. Substitution of L-Ser^2 for D-Ser^2 resulted in stable analogues which was confirmed by DPP-IV and plasma

degradation. This is consistent with previous studies employing substitution of D-isomer amino acid to confer enzyme stability and prolong plasma half-life (Lynch et al. 2014; Gault et al. 2013). An additional modification included the attachment of a gamma linker to the lysine residue at position 30 for both peptides to promote albumin binding and delay rapid renal clearance (Son et al. 2009 and Kerr et al. 2010). This modification resembles that used for the other long-acting incretin mimetics such as palmitic acid acylated GLP-1, liraglutide which have a half-life of 11-15 hours (Wajcberg et al. 2010). Based on the data retrieved from in vitro studies both fish glucagon analogues stimulated dose-dependent insulin release from BRIN-BD11 cells, however, lamprey glucagon exhibited a lower potency compared to its parent peptide.

Interestingly, only paddlefish glucagon analogue effectively induced the rate of insulin release from isolated mouse islets at the concentrations employed. Both analogues stimulated cAMP production in the CHL cells transfected with GLP1R as well as in the HEK293 cells transfected with glucagon receptor. This result was consistent with previous studies using a dogfish glucagon analogue with similar structural modification which showed the ability of the peptide to act as a dual GLP-1/glucagon agonist in these cell lines (O'Harte et al. 2016a). The insulinotropic properties of lamprey and paddlefish analogues were also attenuated in the INS-1 cell lacking GLP-1 and glucagon receptors which confirms their ability to function as a dual GLP-1 and glucagon receptor agonists. In addition, both analogues exhibited positive effects on promoting beta cell growth and protecting against apoptosis in BRIN BD11 beta-cell line.

Although the addition of gamma linker resulted in DPP-IV resistant peptides, lamprey glucagon-derived analogue exhibited no effect in acute in vivo study and a weak anti-

hyperglycemic and insulinotropic effect when administrated 2 and 4 hours prior to a glucose challenge. On the other hand, the modification of paddlefish glucagon resulted in a potent analogue which not only retained the properties of the parent peptide but also exhibited long-acting effects in reducing appetite and promoting glucose homeostasis similar to exendin-4. Acylation of GLP1 with the attachment of C8 and C16 fatty acid moieties is known to be successful in creating long-acting anti-hyperglycaemic agents (Kerr et al. 2010). However, previous observations of GLP-1-derived peptides showed that in some cases, the addition of a gamma linker resulted in a 70-fold reduction in potency for the human GLP-1 receptor (Kerr et al. 2010, Madsen et al. 2007 and Knudsen et al. 2000).

Based on the acute in vitro and in vivo finding, paddlefish glucagon analogue was selected for further long-term investigations using high-fat-fed mice and GluCreRosa26-YFP mice model. The effects of paddlefish glucagon analogue were compared to the effects of a long-acting GLP-1 derivative, liraglutide. These studies showed that twice-daily administration of paddlefish analogue for 21 days was associated with a marked decrease in overall non-fasting blood glucose, plasma insulin and pancreatic insulin content. Moreover, glycemic excursions in responses to intraperitoneal or oral glucose tolerance studies were improved which correlated with improved HOMA-IR parameters. This observation may reflect an improvement in glycaemic control and insulin resistance due to the reduction in overall metabolic demand associated with beta cell rest (Pathak et al. 2015). A similar improvement in the parameters under investigation was observed in liraglutide treatment which compares to some extent with previous findings in high-fat-fed mice (Miller et al. 2017; Buganova et al. 2017; O'Harte et at. 2018).

In addition to positive effects on glucose homeostasis, the paddlefish glucagon analogue significantly suppressed food intake and body weight. These findings are in harmony with the DEXA scan results showing a reduction in adipose tissue with unaltered, normal mass which would also be expected to contribute to the improvements of insulin sensitivity and metabolic control. A high-energy diet usually deteriorates cancellous bone parameters (Tian et al. 2017 and Shapses et al. 2012). Interestingly, GLP-1, apart from its antidiabetic and other properties, has been shown to exhibit a bone anabolic activity (Jackuliak et al. 2014). However, administration of liraglutide and paddlefish glucagon analogue at the dose employed showed no significant effects on bone mineral density after 21 days.

A high-fat diet has been shown to induced dyslipidemia with increased concentrations of plasma cholesterol, low levels of HDL cholesterol and increased levels of triglycerides (Ipsen et al. 2016). Paddlefish glucagon reduced total cholesterol and had a positive effect on decreasing circulating triglycerides in high-fat fed mice. In contrast, liraglutide failed to improve the lipid profile in high-fat fed mice. These observations contrast with other findings which showed an improvement in triglyceride levels in mice treated once daily with liraglutide (Millar et al. 2017 and O'Harte 2018).

Importantly, all treatments reduced ALT concentrations, which may indicate the protective effects of liraglutide and paddlefish glucagon analogue against liver damage (Ganz et al. 2014 and Stephenson et al. 2018). Interestingly, chronic administration of liraglutide and paddlefish glucagon analogue modestly increased levels of circulating amylase which may suggest adverse reaction leading to pancreatitis (Gier et al. 2012). Currently, there is an increase in safety concern regarding adverse effects of GLP-1 receptor agonist drugs on pancreatic and thyroid tissue, since animal studies and

analyses of drug databases link these medications to pancreatitis, pancreatic cancer, and thyroid cancer (Filippatos et al. 2014). However, several meta-analyses (Li et al. 2014 and Alves et al. 2012) and LEADER randomised trial (Steinberg et al. 2017) failed to confirm that the increase of serum amylase (caused by GLP-1 mimetics) is related to these conditions (Filippatos et al. 2014).

Chronic high-fat diet leads to developing of obesity and insulin resistance (Park et al. 2001). Increased insulin resistance elevates blood glucose levels, both due to reduced insulin-mediated glucose uptake by the peripheral tissues and due to increased hepatic glucose production. In response, beta cells compensate to cope with insulin demand by secreting more insulin per beta cell and by increasing beta cell mass via proliferation (Golson et al. 2010 and reviewed by Sachdeva et al. 2009). The histological findings revealed no significant change in any parameters in liraglutide treatment groups. However, the paddlefish glucagon analogue significantly reduced alpha cell area compared to high-fat controls. Although not significant, the beta cell area was also decreased in this group which correlated with a higher number of smaller size islets. In agreement with this observation, although no change in plasma glucagon was detected, islet insulin and glucagon contents were decreased in this group. This may be due to the restoration of the ability of the alpha cells to react to glucose which resembles beneficial action of GLP-1 (Vilsboll et al. 2009; Ahren et al. 1997; Hare et al. 2010).

A major challenge in diabetes research is understanding the multiple effects of glucose on beta cells in molecular terms, revealing the sites of dysregulation in the gene expression caused by chronically elevated glucose concentration, and finding effective drugs that will reverse these molecular abnormalities (Schuit et al. 2002). Insulin gene (*Ins1*) transcription, which is up-regulated by an increase in blood glucose levels

(Mosley et al. 2004), was shown to be decreased in the liraglutide and paddlefish glucagon analogue treated mice compared to high-fat controls. This may be due to relatively decreased glucose levels observed in the treatment groups. Moreover, the expression of *Slc2a2* gene encoding GLU2 which regulates the entry of glucose into the beta cell (Laukkanen et al. 2005), was significantly higher in the treatment groups. The disappearance of GLUC2 is a hallmarked of the beta cell glucose-unresponsiveness (Thorens et al. 1994), the improved expression observed in this study may represent the enhanced insulin sensitivity which is beneficial for the preservation of insulin secretion by the pancreatic beta cells (Laukkanen et al. 2005).

Stimulation of insulin release by GLP-1 and GIP hormones has been reported to be impaired in diabetes which also correlated to the decreased GLP-1 (*Glp-1r*) and GIP (*Gipr*) receptors expression in diabetic subjects (Xu et al. 2007). Both, liraglutide and paddlefish glucagon analogue appeared to have a positive impact on the regulation of GLP-1 compared to high-fat controls. Moreover, the treatment with the paddlefish glucagon analogue also resulted in a higher expression of *Gipr*. Interestingly, a higher expression of glucagon receptor (*Gcgr*) gene was observed in both peptide treatment groups. Previous studies suggest that glucagon may play a crucial role in pancreatic beta cell growth and differentiation. $Gcgr^{-/-}$ mice were shown to have a decreased percentage of beta cells per islets compared to control animals. Less severe hyperglycaemia was also observed in RIP-Gcg mice overexpressing the glucagon receptor in the pancreas (reduced by 20% of high-fat control) (Gelling et al. 2009).

Surprisingly, treatment with [D-Ser^{2}]-paddlefish glucagon-Lys^{30}-gamma-glutamyl-pal and liraglutide appeared to have no significant effect on the expression of genes encoding the members of potassium channel gene family (*Abcc8* and *Kcnj11*), calcium channel (*Cacna1c*) and glucokinase (*Gck*) genes.

An additional study was performed to investigate the effects of the paddlefish glucagon analogue on alpha to beta cell transdifferentiation using glucagon-CreER and Rosa26-YFP mice expressing the yellow fluorescent protein (YFP) in alpha cells (Quoix et al. 2007). These transgenic mice provide a tamoxifen-dependent Cre/loxP system due to bearing the transgenes including glucagon-CreER (a tamoxifen-inducible Cre recombinase fused to a modified form of ligand binding domain of human oestrogen receptor inserted into exon 2 of the glucagon gene) and Rosa26-YFP (a sequence loxP-STOP-loxP in the locus ROSA 26) in the genome. Administration of multiple low doses of streptozotocin resulted in the beta cell destruction, reduction of body weight, elevation of blood glucose and depletion of plasma insulin. This mimics a delayed but progressive insulitis via an immune cell-mediated mechanism (Rossini et al. 1977 and reviewed: Kobb 1987) rather than direct destruction of the beta cell using a large single dose of STZ (review: Rerup et al. 1970). Treatment with liraglutide and paddlefish glucagon analogue resulted in improved food and water intake similar to untreated mice. Moreover, the reduction of hyperglycaemia was noticeably lowered by peptide treatments. The marked destruction of pancreatic beta cells resulted in a reduction of islet area and insulin content. Hence islets of smaller sizes appeared to be more abundant in all regions of the pancreas. Absolute or relative deficiency of functional beta cells leads to impaired control of blood glucose hence causing diabetes (Lee et al. 2018). The proliferation of pre-existing beta-cells and transdifferentiation of non-beta cells to functional beta cells are a potential important pathway to overcome beta cell loss (Brown et al. 2015). Investigations using islets from diabetic humans and mice have identified the occurrence of transdifferentiation of alpha to beta cells which were suggested to be regulated by hormonal and environmental signals during the development of diabetes (Halban et al. 2014 and

Brown et al. 2015). GLP-1 is well known to have a positive effect on beta cell regeneration and differentiation (Lee at al 2018). Glucagon producing alpha cells may become a source of new beta cells during an extreme beta cell loss (Thorel at al 2012). In the present study, the proliferation of alpha cells was observed in the streptozotocin-treated animals suggesting that these cells may serve as a precursor for the regeneration of depleted beta cells.

Interestingly, lineage tracing showed that new beta cells originated from alpha cells were significantly more abundant in streptozotocin-treated mice compared to untreated transgenic mice. Treatment with liraglutide and paddlefish glucagon analogue resulted in a noticeably higher rate of differentiation compared to streptozotocin control although the effect was not significantly different. Other cells such as PP- or σ-cells could also be involved in the mechanism of new beta-cell generation (Lee et al. 2018).

To conclude, [D-Ser^{2}]-paddlefish glucagon-Lys^{30}-gamma-glutamyl-pal is a potent dual-acting agonist that activates both, GLP-1 and glucagon receptors exhibiting anti-hyperglycaemic and insulinotropic effects as well as prolonged plasma stability. Paddlefish glucagon analogue effectively improved many parameters under investigation such as body weight, insulin secretion, insulin resistance and islet morphology and gene expression in high-fat-fed mice with effects similar or superior to those of liraglutide. The fish glucagon analogue exhibits a unique naturally occurring sequence of a hybrid glucagon/exendin-4 as well as other structural modifications which make it a potential candidate to develop into an agent for treatment of diabetes.

Table 6.1 Primary structures and the observed and calculated molecular masse of fish glucagon analogue peptides investigated in this study.

Peptide	Amino acid sequence	Calculated molecular mass	Observed molecular mass
[D-Ser2]-lamprey glucagon-Lys^{30}-gamma-glutamyl-pal	HsEGTFTSDYSKYLENKQAKDFVRWLMNA[K-gamma-glutamyl-pal]	3962.6	3964.1
[D-Ser^{2}]-paddlefish glucagon-Lys^{30}-gamma-glutamyl-pal	HsQGMFTNDYSKYLEEKRAKEFVEWLKNG[K-gamma-glutamyl-pal]S-OH	4118.7	4120.0

Table 6.2 Effects of [D-Ser2]-lamprey glucagon Lys30 gamma-glutamyl-pal, [D-Ser^2]-paddlefish glucagon-Lys^{30}-gamma-glutamyl-pal, human GLP-1 and glucagon on the rate of insulin release from BRIN-BD11 cells.

Peptide	Threshold concentration	The effect at 3µM ng/10^6/20min
Basal release	-	1.0 ± 0.1
[D-Ser^2]-lamprey glucagon Lys^{30}-gamma-glutamyl-pal	0.3nM	2.4 ± 0.1
Lamprey glucagon	3nM	3.3 ± 0.2
[D-Ser^2]-paddlefish glucagon-Lys^{30}-gamma-glutamyl-pal	10pM	3.3 ± 0.2
Paddlefish glucagon	30pM	3.6 ± 0.2
Human GLP-1	10pM	3.6 ± 0.2
Human glucagon	3nM	3.1 ± 0.20

The basal release refers to the rate of insulin release at 5.6 mM glucose alone. The threshold concentration is the minimum concentration of the peptide producing a significant ($P< 0.05$) increase in the rate of insulin release. The values are mean ± SEM for n = 8. *$P<0.5$ compared to 5.6 mM glucose control.

Table 6.3 Effects fish glucagon analogues on the release of insulin from islets isolated from TO mice.

Peptide	Insulin release (% of total insulin content) at 10^{-6}M	Insulin release (% of total insulin content) at 10^{-8}M
(None) 1.4 mM glucose	3.4 ± 0.4 ***	3.4 ± 0.4 ***
(None) 16.7 mM glucose control	8.5 ± 0.5	8.5 ± 0.5
[D-Ser^{2}]-lamprey glucagon-Lys^{30}-gamma-glutamyl-pal	11.4 ± 1.3	10.2 ± 0.7
[D-Ser^{2}]-paddlefish glucagon-Lys^{30}-gamma-glutamyl-pal	13.9 ± 1.8 **	12.1 ± 1.1 *
Human GLP-1	17.0 ± 2.1 **	14.7 ± 0.9 ***
Human glucagon	11.9 ± 1.6	8.5 ± 0.4

Values are mean ± S.E.M., n = 8 *P < 0.05, **P < 0.01, ***P < 0.001 compared to 16.7 mM glucose alone.

Table 6.4 Summary of effect of fish glucagon analogues, human GLP-1, human glucagon and human GIP peptides (10^{-8} and 10^{-6} M) on cAMP production in GLP1R-transfected CHL cells, and GCGR-transfected HEK293 cells.

Peptide name	GLP-1 receptor transfected cells		GCG receptor transfected cells	
	cAMP release at 10^{-6}	cAMP release at 10^{-8}	cAMP release at 10^{-6}	cAMP release at 10^{-8}
Basal (5.6mM glucose)	4.9 ± 0.2	4.9 ±0.2	2.5 ±0.2	2.5 ±0.2
[D-Ser^2]-lamprey glucagon-Lys^{30}-gamma-glutamyl-pal	27.7 ± 0.4***	12.3 ± 0.7 ***	4.5 ± 0.9 *	3.4 ± 0.3*
[D-Ser^2]-paddlefish glucagon-Lys^{30}-gamma-glutamyl-pal	29.2 ± 0.4***	26.4 ± 1.4 ***	7.5 ± 0.5 ***	5.5 ± 0.8 **
Human GLP-1	29.0 ± 0.2***	26.3 ± 1.4***	6.6 ± 0.6**	4.6 ± 0.4**
Human glucagon	17.1 ± 0.9 ***	10.7 ± 0.5***	8.9 ± 0.3**	7.5 ± 0.5**
Human GIP	5.1 ± 0.2	5.5 ± 0.6	2.8 ± 0.3	2.5 ± 0.2

Values are mean ± S.E.M. for n = 3. *P < 0.05, ** P< 0.01 and ***P < 0.001 compared with 5.6 glucose.

Table 6.5 Summary of effects of fish glucagon analogues (10^{-8} and 10^{-6} M) on the rate of insulin release from wild-type INS-1 cells, CRISPR/Cas9-engineered GLP-1R KO cells, CRISPR/Cas9-engineered GIPR KO cells and CRISPR/Cas9-engineered GIPR KO cells

Peptide		**Wild-type cells, % of basal control**	**GLP-1R KO cells, % of basal control**	**GCGR KO cells, % of basal control**	**GIPR KO cells, % of basal control**
Basal (5.6mM glucose)		100 ± 9.6			
[D-Ser^2]-lamprey glucagon-Lys^{30}-gamma-glutamyl-pal	10^{-6}	164.0 ± 9.0 ***	134.1 ± 11.7 * $^{\Delta}$	159.0 ± 16.8*	170.9 ± 13.4 ***
	10^{-8}	158.4 ± 11.0 **	117.3 ± 14.4 $^{\Delta}$	121.2 ± 7.7 $^{\Delta}$	152.6 ± 12.7 **
[D-Ser^2] paddlefish glucagon-Lys^{30}-gamma-glutamyl pal	10^{-6}	223.7 ± 18.3***	151.3 ± 9.1 *** $^{\Delta\Delta}$	153.4 ± 11.2 ** $^{\Delta\Delta}$	231.9 ± 16.6 ***
	10^{-8}	193.5 ± 20.3 **	144.9 ± 4.5 **$^{\Delta\Delta}$	140.7 ± 12.2 **	202.1 ± 5.0 ***
Human GLP-1	10^{-6}	221.1 ± 9.8***	138.3 ± 14.5 * $^{\Delta\Delta\Delta}$	222.0 ± 11.7 ***	231.4 ± 9.4 ***
	10^{-8}	198.9 ± 12.9 ***	114.1 ± 8.5 $^{\Delta\Delta\Delta}$	210 ± 25.0 ***	187.5 ± 17.2 ***
Human glucagon	10^{-6}	225.0 ± 20.9 ***	211.3 ± 16.4 ***	159.6 ± 8.5 *** $^{\Delta\Delta}$	224.0± 14.8 ***
	10^{-8}	172.2 ± 10.8 ***	164.2 ±16.5***	134.0 ± 14.4 $^{\Delta}$	175.4 ± 12.3 ***
Human GIP	10^{-6}	242.9 ± 14.2 ***	226.6 ±19.6***	231.3 ± 17.6 ***	125.4 ± 6.9 * $^{\Delta\Delta\Delta}$
	10^{-8}	233.8 ± 18.6 ***	221.0 ± 29.3 ***	230.1 ± 0.9***	124.3 ± 12.6 $^{\Delta\Delta\Delta}$

Values are mean ± S.E.M., n = 8, *P < 0.05, ** P< 0.01 and ***P < 0.001 compared with 5.6 mM glucose alone. $^{\Delta}$P < 0.05, $^{\Delta\Delta}$P < 0.01, $^{\Delta\Delta\Delta}$P < 0.001 compared with effects in wild-type INS-1 cells.

Figure 6.1 Reverse-phase HPLC purification of crude [D-Ser^2]-lamprey glucagon-Lys^{30}-gamma-glutamyl-pal (A) and [D-Ser^2]-paddlefish glucagon-Lys^{30}-gamma-glutamyl-pal peptides using a semi-preparative Vydac C18 column.

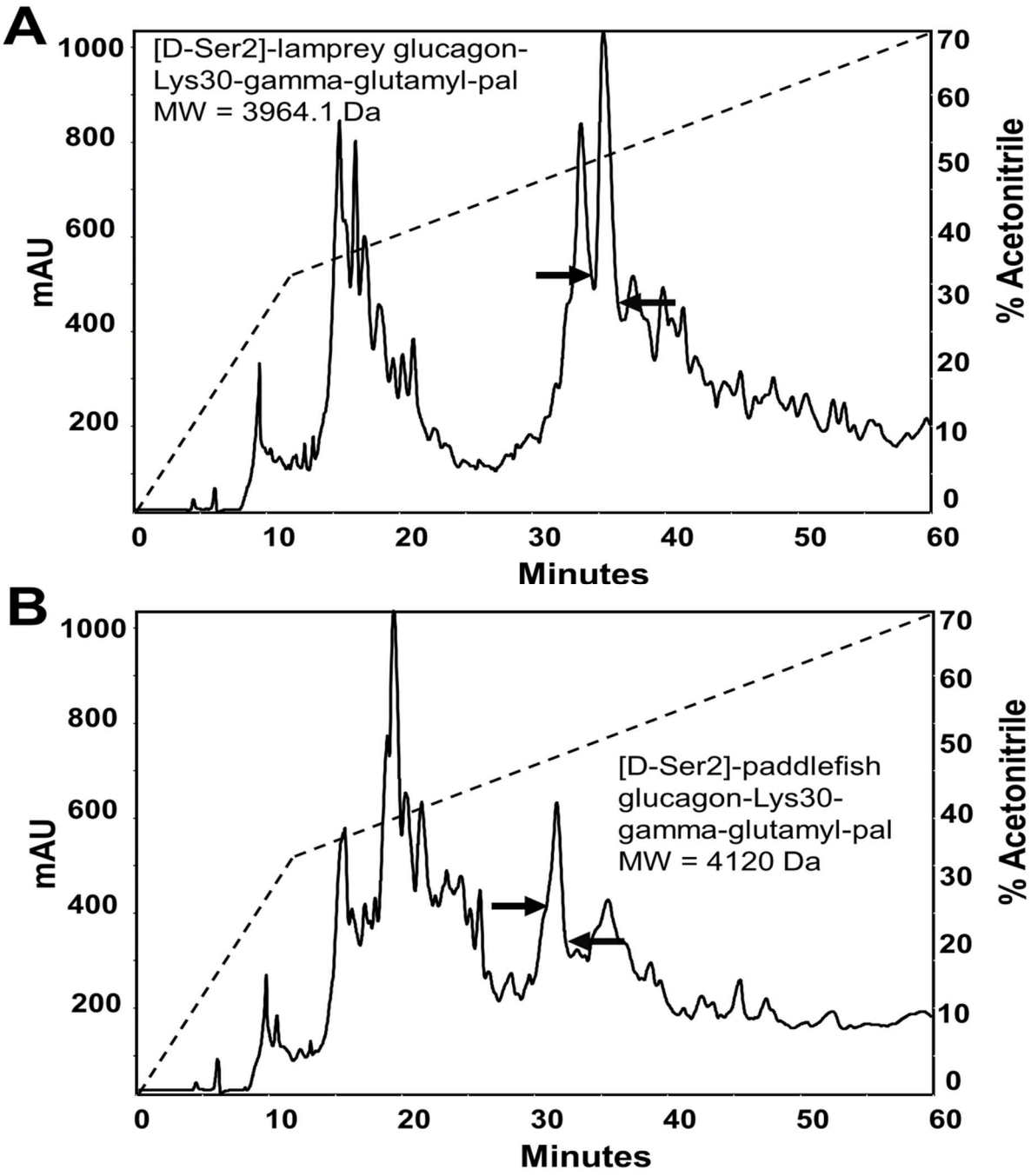

The peptides were dissolved in 15% acetonitrile (3mg/ml) and injected onto a (2.2 cm x 25 cm) Vydac 218TP1022 (C-18) column (Grace, Deerfield, IL, USA) at a flow rate of 6.0 ml/min. The concentration of acetonitrile in the eluting solvent was raised from 0% to 35 % over 10 min and from 35% to 70% over 50 min using a linear gradient. Absorbance was measured at 214 nm, and the black arrows show where the peak collection began and ended.

Figure 6.2 MALDI-TOF spectra of purified [D-Ser^{2}]-lamprey glucagon-Lys^{30}-gamma-glutamyl-pal (A) and [D-Ser^{2}]-paddlefish glucagon-Lys^{30}-gamma-glutamyl-pal peptides (B).

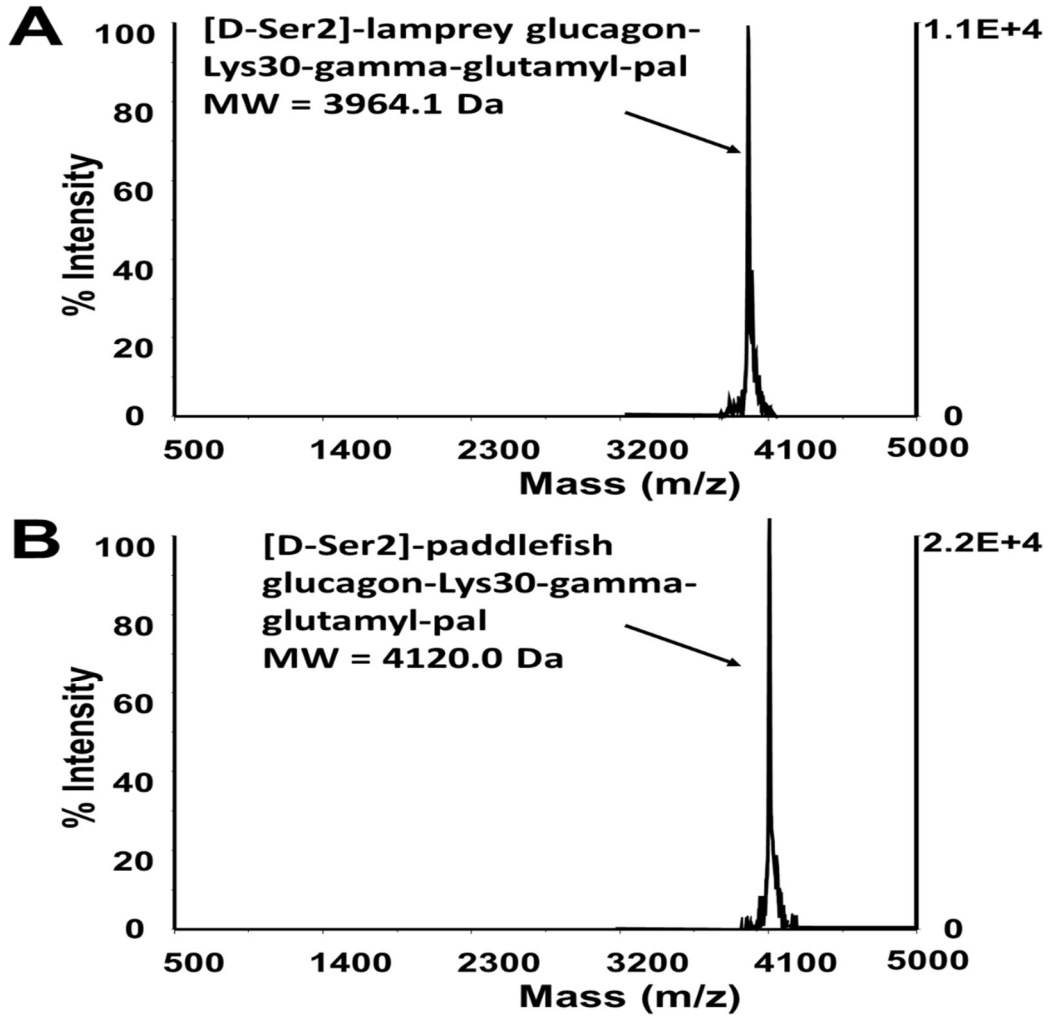

Purified peptides were mixed with α-Cyano-4-hydroxycinnamic acid on a 100 well MALDI plate before inserting into a Voyager DE Biospectrometry workstation. The mass-to-charge ratio (m/z) versus peak intensity was determined.

Figure 6. 3 HPLC degradation profile of [D-Ser^{2}]-lamprey glucagon-Lys^{30}-gamma-glutamyl-pal following incubation with DPP-IV for 0 and 4 hours.

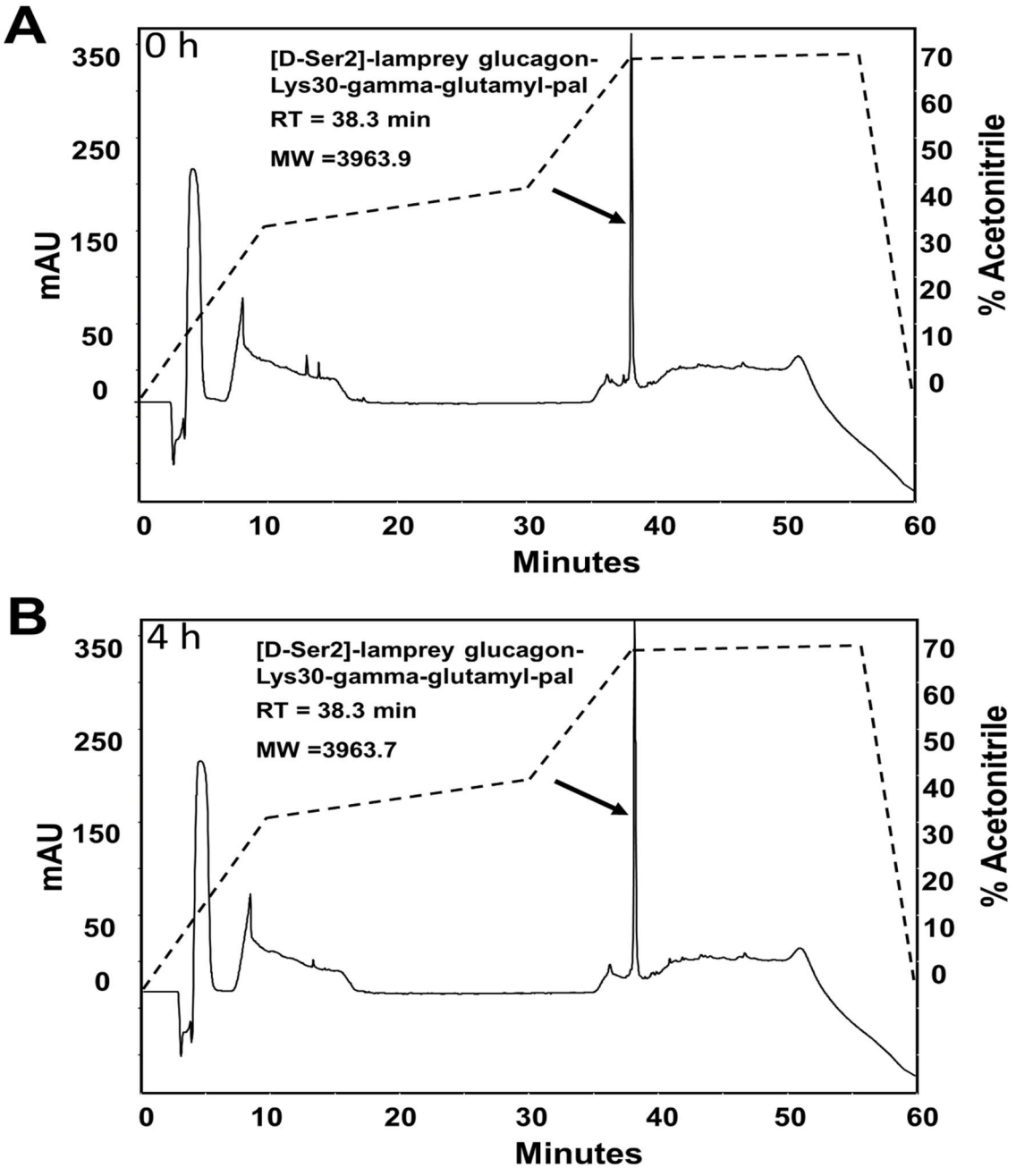

The separation was performed with a Luna 5u C8 250x4.6mm column. The dash line represents acetonitrile concentration gradient from 0% to 35% (from 0 min to 10 min), from 35% to 42% (from 10min to 30 min), from 42 to 70% (from 30 min to 35min), and 70% (from 35 min to 55 min).

Figure 6.4 HPLC degradation profile of [D-Ser^2]-paddlefish glucagon-Lys^{30}-gamma-glutamyl-pal following incubation with DPP-IV for 0 and 4 hours.

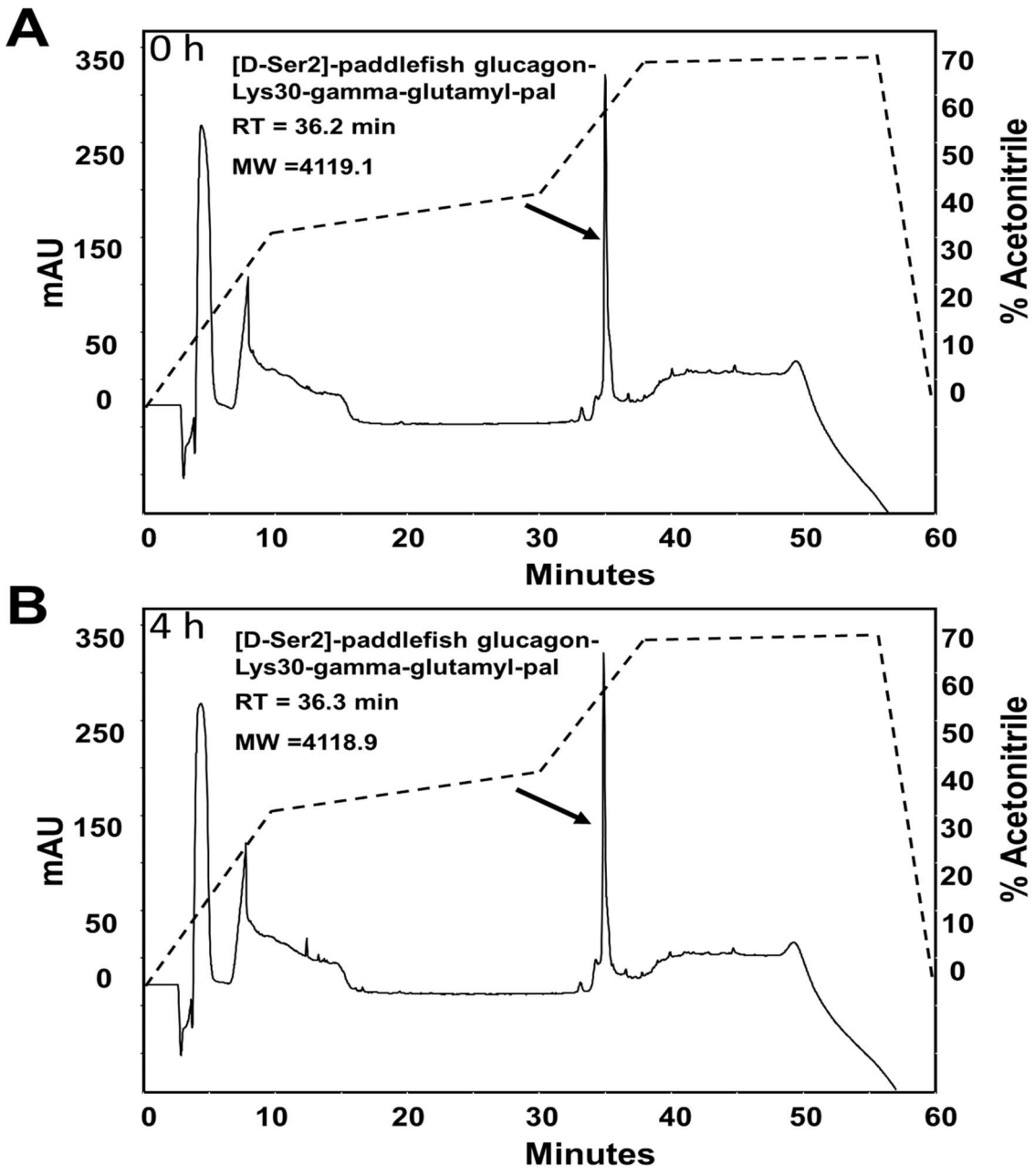

The separation was performed with a Luna 5u C8 250x4.6mm column. The dash line represents acetonitrile concentration gradient from 0% to 35% (from 0 min to 10 min), from 35% to 42% (from 10min to 30 min), from 42 to 70% (from 30 min to 35min), and 70% (from 35 min to 55 min).

Figure 6.5 HPLC result of plasma degradation of [D-Ser^{2}]-lamprey glucagon Lys^{30}-gamma-glutamyl-pal for 0 and 4 hours.

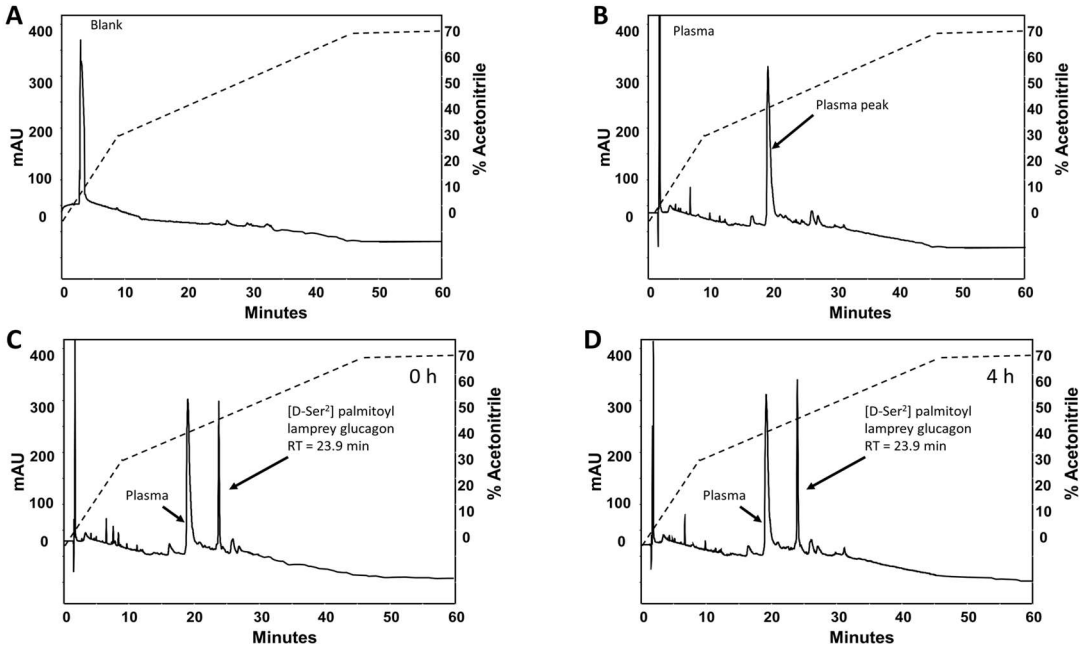

The separation was performed with a Luna 5u C8 250x4.6mm column. The dash line represents acetonitrile concentration gradient from 0% to 35% (from 0 min to 10 min), from 35% to 70% (from 10min to 45 min) and 70% (from 45 min to 60 min).

Figure 6.6 HPLC result of plasma degradation of [D-Ser^2]-paddlefish glucagon-Lys^{30}-gamma-glutamyl-pal for 0 and 4 hours.

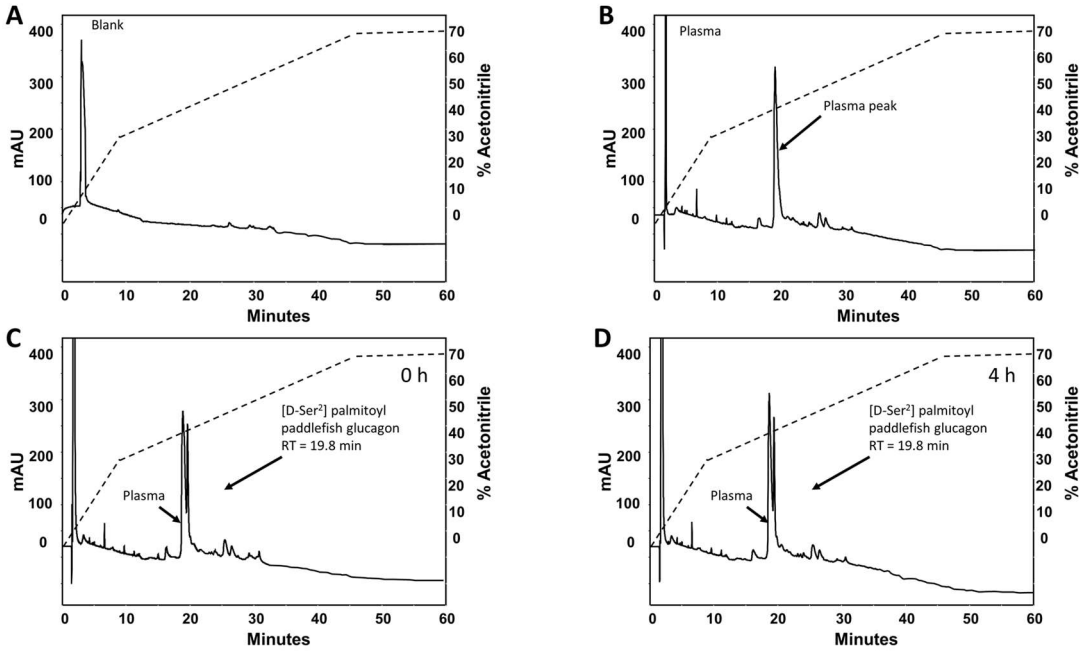

The separation was performed with a Luna 5u C8 250x4.6mm column. The dash line represents acetonitrile concentration gradient from 0% to 35% (from 0 min to 10 min), from 35% to 70% (from 10min to 45 min) and 70% (from 45 min to 60 min).

Figure 6.7 HPLC result of plasma degradation of human glucagon for 0 and 4 hours.

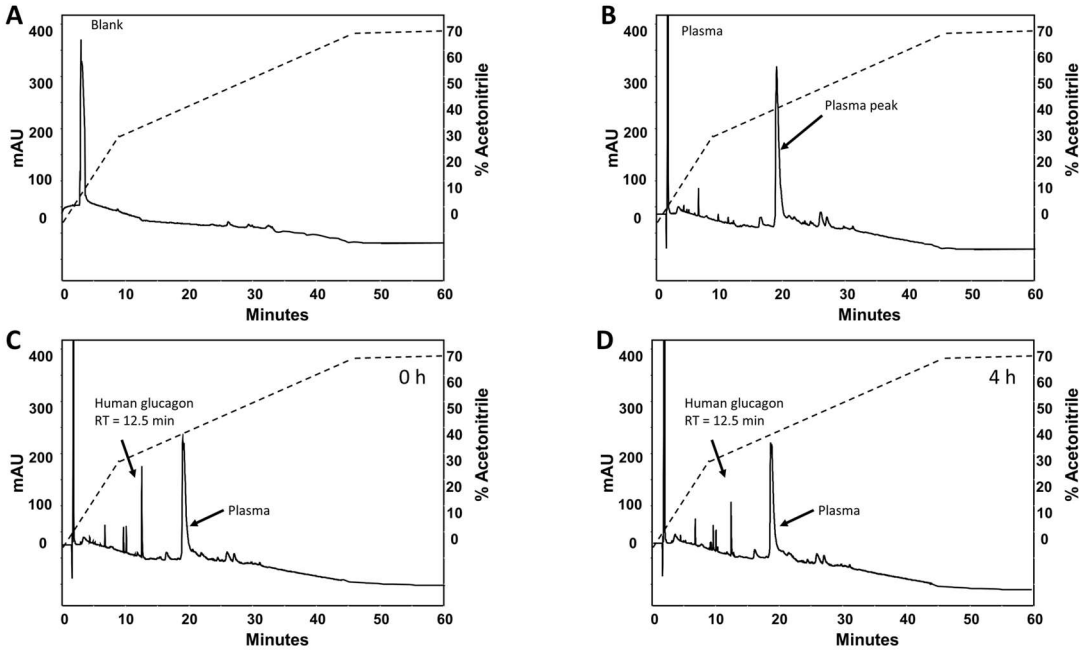

The separation was performed with a Luna 5u C8 250x4.6mm column. The dash line represents acetonitrile concentration gradient from 0% to 35% (from 0 min to 10 min), from 35% to 70% (from 10min to 45 min) and 70% (from 45 min to 60 min).

Figure 6.8 Concentration-dependent effects of (A) [D-Ser^2]-lamprey glucagon Lys^{30}-gamma-glutamyl-pal and (B) [D-Ser^2]-paddlefish glucagon-Lys^{30}-gamma-glutamyl-pal on insulin release from BRIN-BD11 rat clonal β- cells

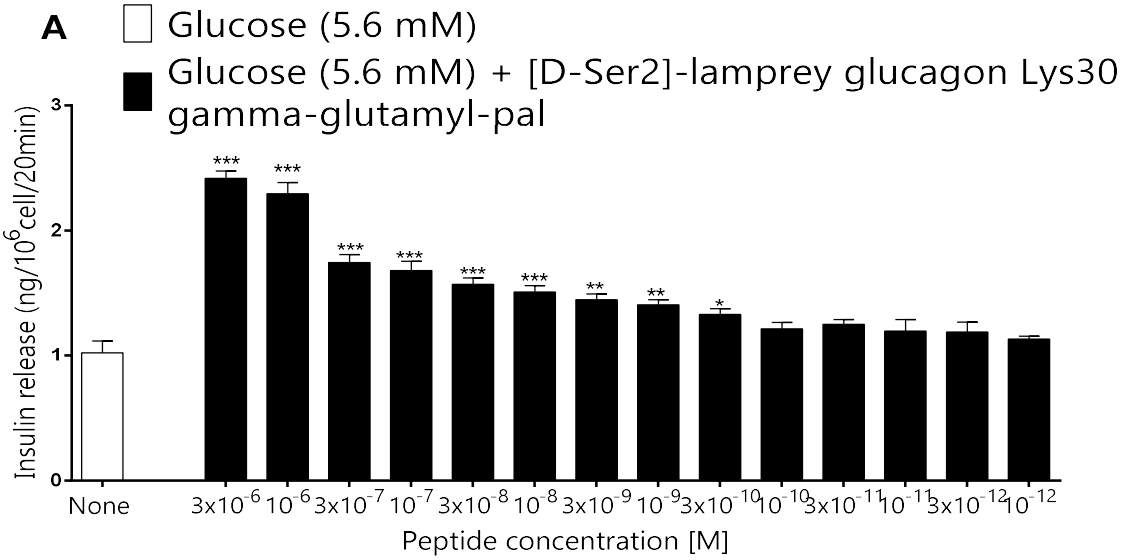

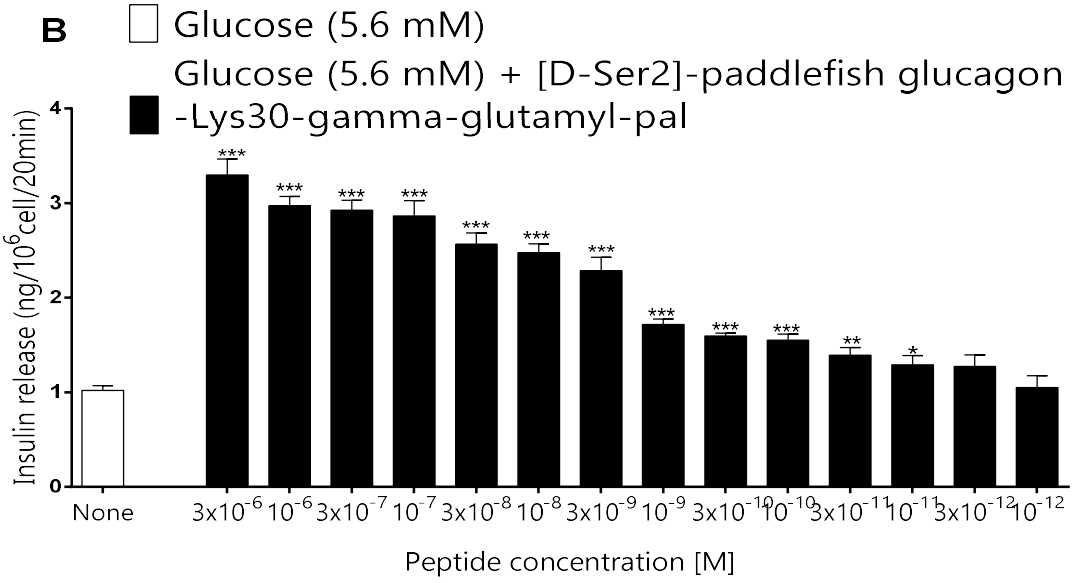

Values are mean ± S.E.M., n = 8. *P < 0.05, **P < 0.01, ***P < 0.001 compared to 5.6 mM glucose alone.

Figure 6.9 Effects of fish glucagon analogues (10^{-8} and 10^{-6} M) on insulin release from pancreatic islets isolated from NIH Swiss mice.

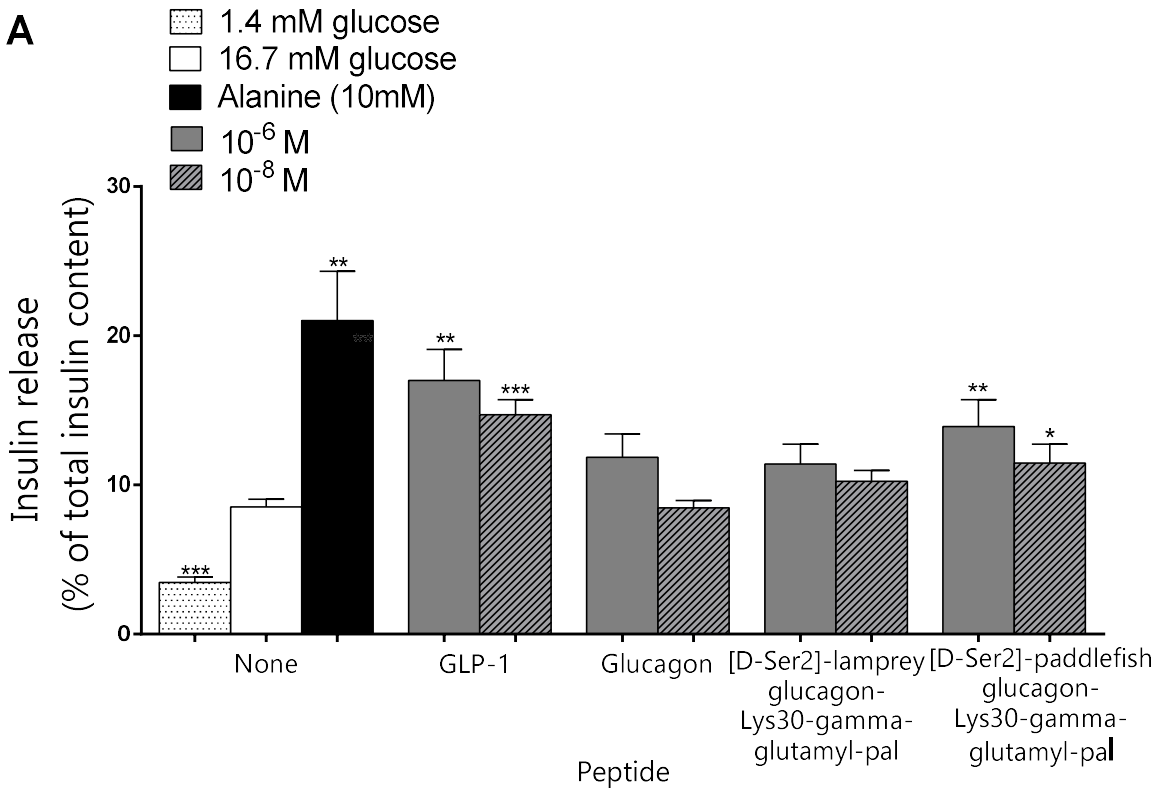

Values are mean ± S.E.M., n = 8 *P < 0.05, **P < 0.01, ***P < 0.001 compared to 16.7 mM glucose alone.

Figure 6.10 Effects of fish glucagon analogues (10^{-8} and 10^{-6} M) on cAMP production in (A) GLP1R-transfected CHL cells, and (B) GCGR-transfected HEK293 cells.

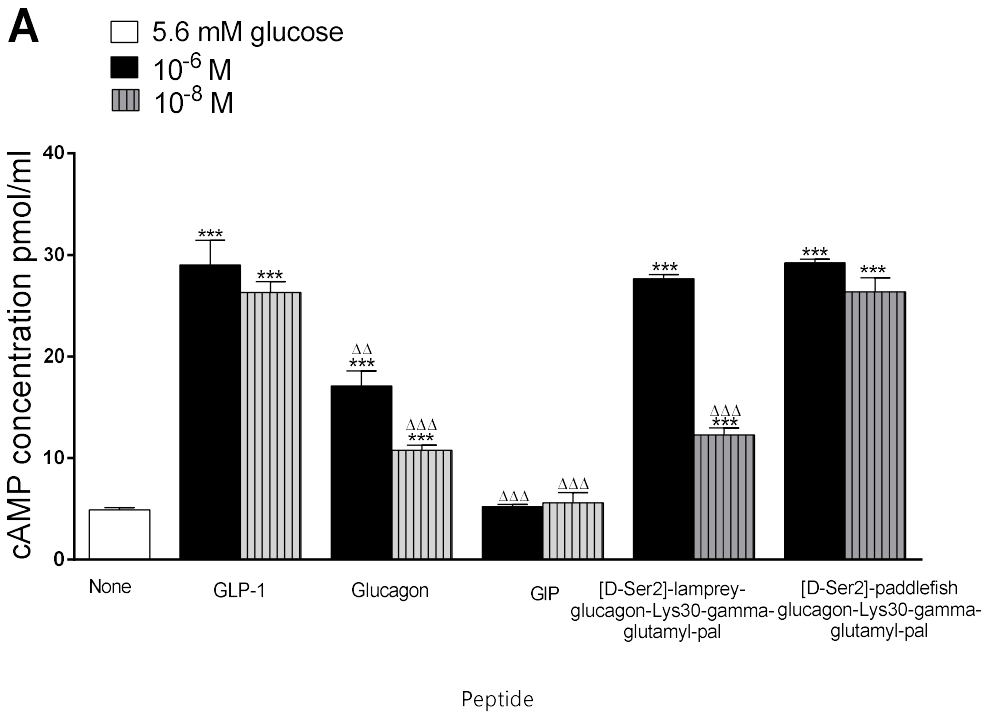

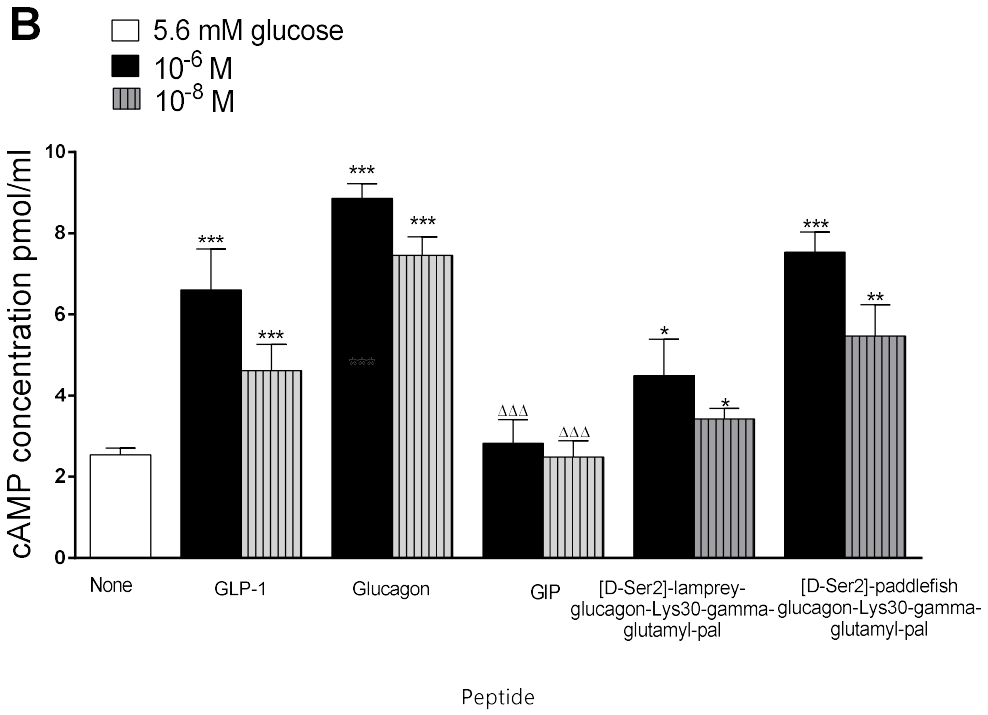

Values are mean ± S.E.M. for n = 4. *P < 0.05, ** P< 0.01 and ***P < 0.001 compared with 5.6 glucose.

Figure 6.11 Effects of fish glucagon analogues (10^{-8} and 10^{-6} M) on the rate of insulin release from (A) wild-type INS-1 cells, (B) CRISPR/Cas9-engineered GLP-1R knock-out cells, (C) CRISPR/Cas9-engineered GCGR knock-out cells and (D) CRISPR/Cas9-engineered GIPR knock-out cells.

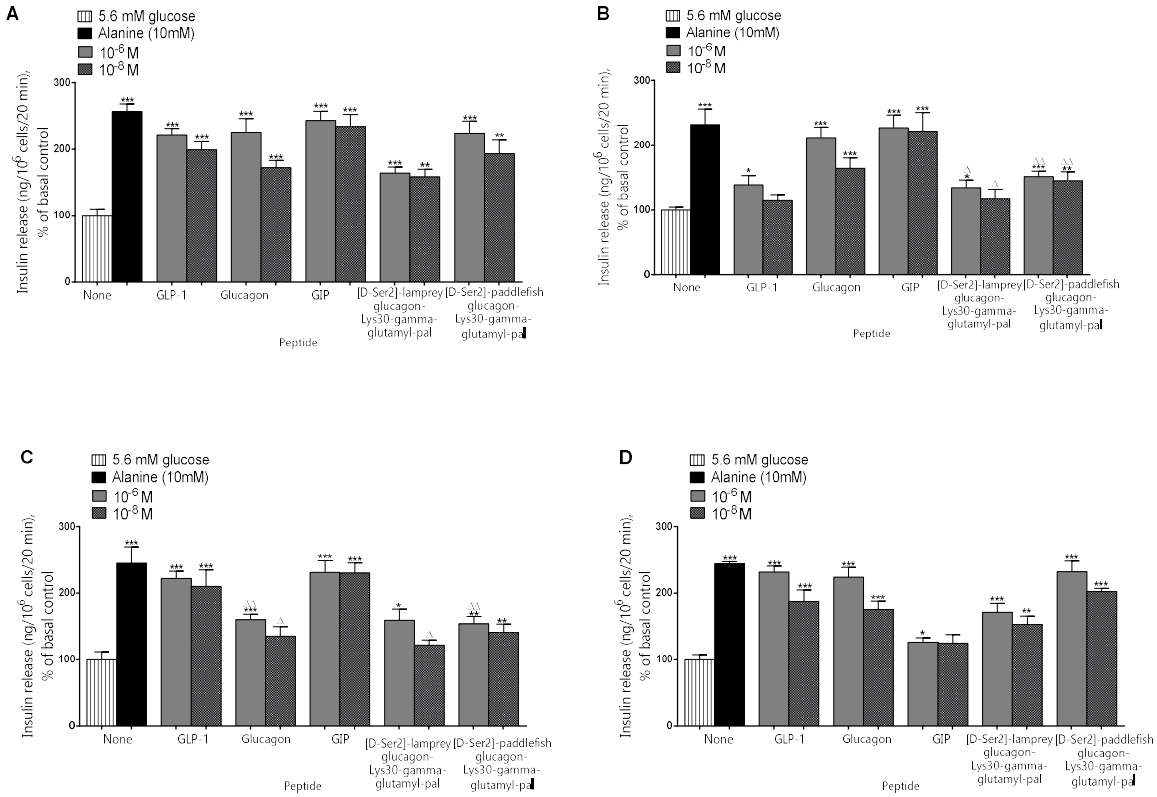

Values are mean ± S.E.M., $n = 8$, *P < 0.05, **P < 0.01 and ***P < 0.001 compared with 5.6 mM glucose alone. $^{\Delta}$P < 0.05, $^{\Delta\Delta}$P < 0.01, $^{\Delta\Delta\Delta}$P < 0.001 compared with effects in wild-type INS-1 cells.

Figure 6.12 Effects of fish glucagon analogues (10^{-8} and 10^{-6} M) on (A) cell proliferation and (B) protection against apoptosis in rodent BRIN BD11 cells.

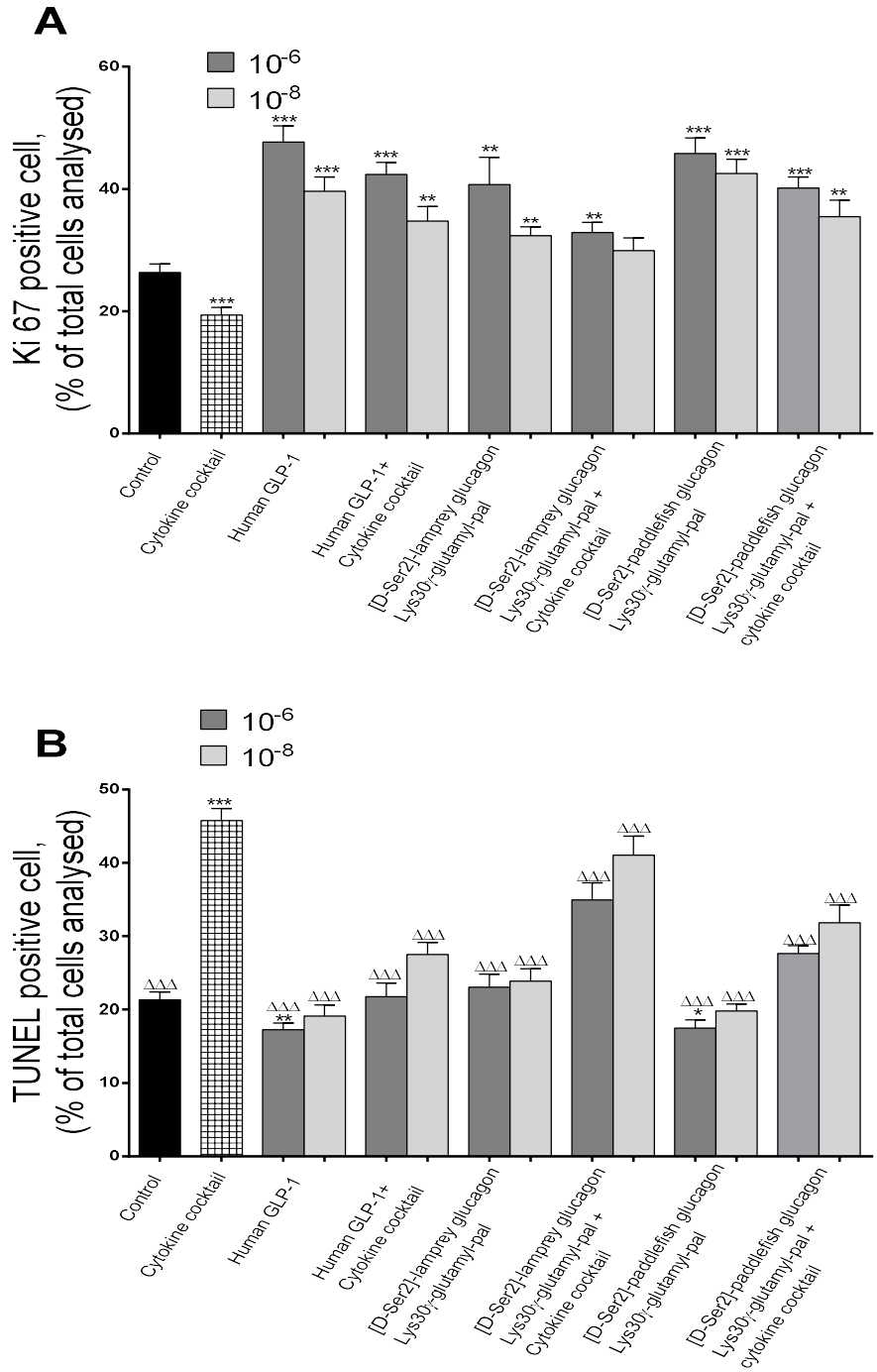

Cell were incubated (16 h) in the presence of peptides (10^{-8} and 10^{-6} M) with and without addition of cytokine cocktail. Values are mean ± S.E.M., n = 3, *P < 0.05, ** < 0.01 and ***P < 0.001 compared with control cultures. $^{\Delta}P < 0.05$, $^{\Delta\Delta}P < 0.01$, $^{\Delta\Delta\Delta}P$ < 0.001 compared with cytokine cocktail.

Figure 6.13 Effects of acute administration of lamprey glucagon and [D-Ser^2] lamprey glucagon Lys^{30}-gamma-glutamyl-pal on blood glucose (A) and plasma insulin (B) concentrations in normal mice.

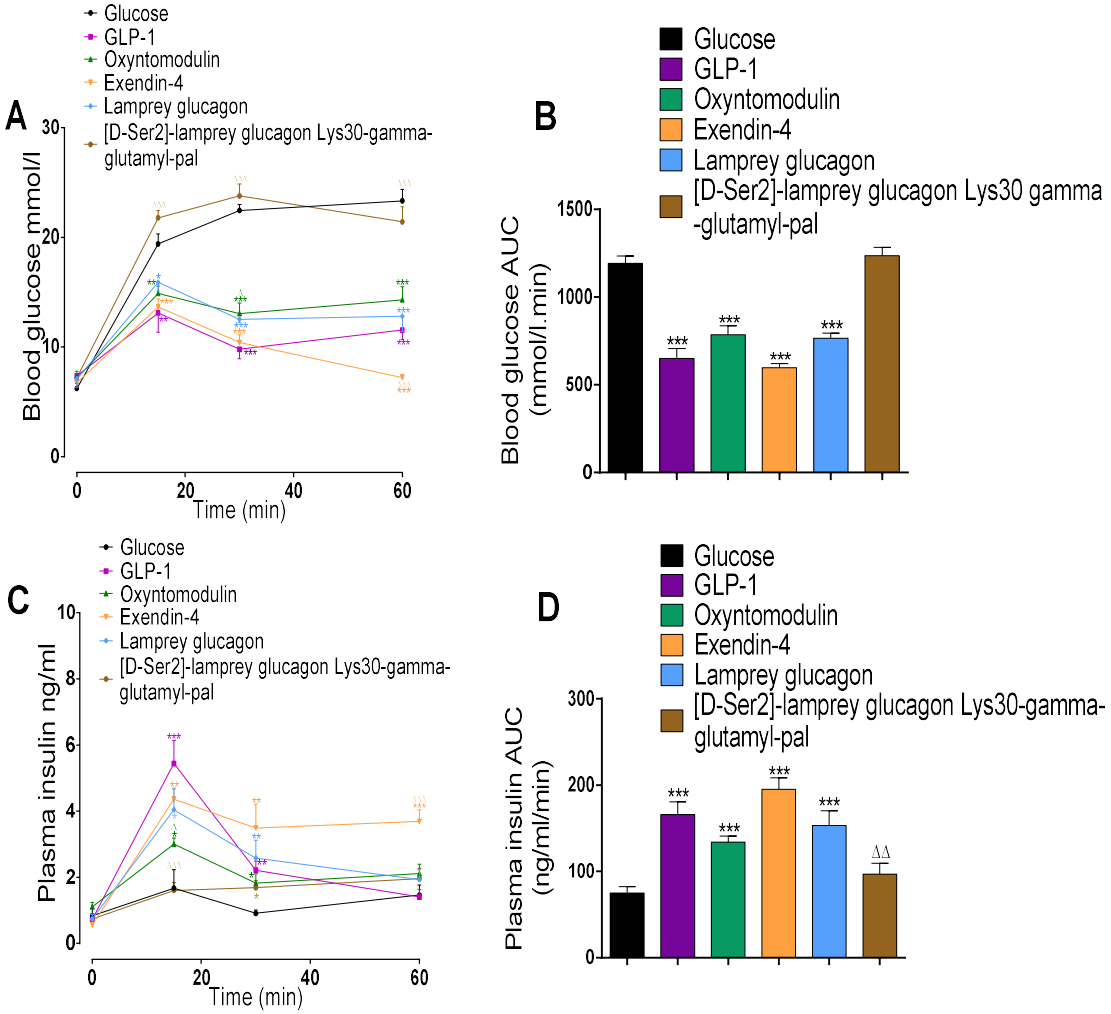

The integrated responses (area under the curve AUC) are shown in panels B and D. The values are mean ± SEM for n=6. *P<0.05, **P<0.01 and ***P<0.001 compared to glucose alone; $^{\Delta\Delta}$ P<0.01 and $^{\Delta\Delta\Delta}$ P<0.001 compared to human GLP-1.

Figure 6.14 Effects of acute administration of paddlefish glucagon and [D-Ser^2] paddlefish glucagon-Lys^{30}-gamma-glutamyl-pal on blood glucose (A) and plasma insulin (B) concentrations in normal mice.

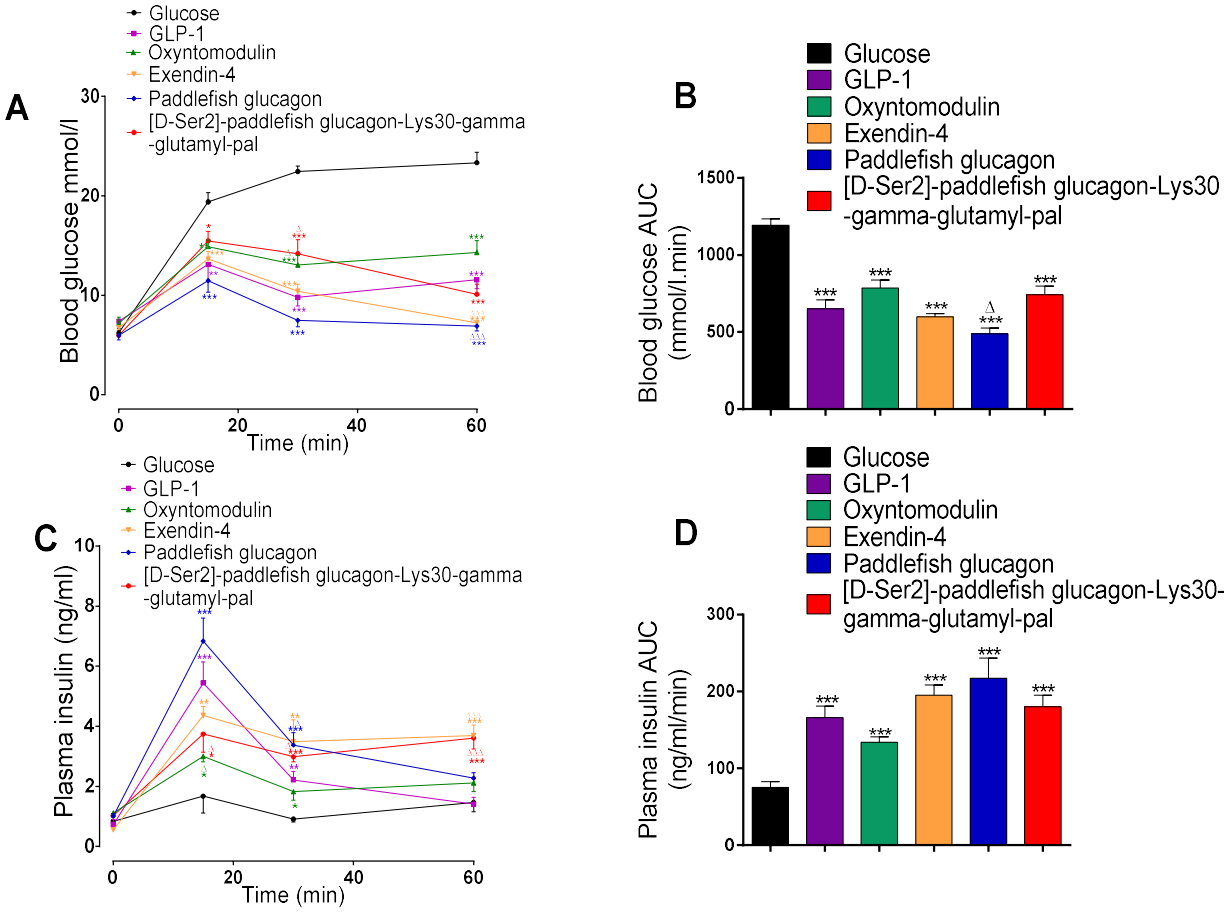

The integrated responses (area under the curve AUC) are shown in panels B and D. The values are mean ± SEM for n=6. *p<0.05, **P<0.01 and ***P<0.001 compared to glucose alone; $^{\Delta}$ P<0.05 and $^{\Delta\Delta\Delta}$P<0.001 compared to human GLP-1.

Figure 6.15 Persistent, 2 h post injection, effects of lamprey glucagon and [D-Ser^2] lamprey glucagon Lys^{30}-gamma-glutamyl-pal peptides on blood glucose (A) and plasma insulin (B) concentrations in normal mice.

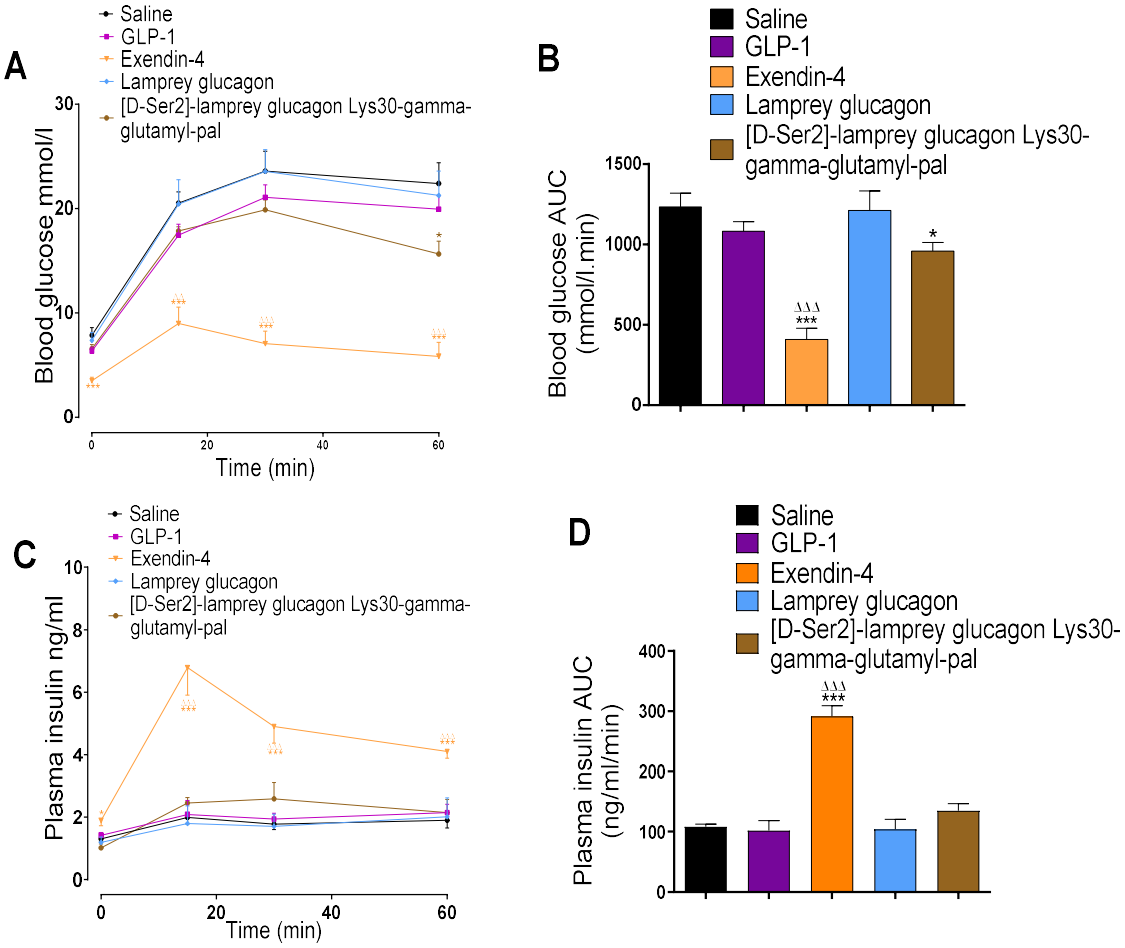

Blood glucose and plasma insulin were measured after intraperitoneal injection of glucose (18 mmol/kg body weight) 2 hours after intraperitoneal administration of 0.9% saline or peptides (25 nmol/kg body weight). The integrated responses (area under the curve AUC) are shown in panels B and D. The values are mean ± SEM for n=6. *P<0.05 and ***P<0.001 compared to glucose alone; $^{\Delta\Delta\Delta}$ P<0.001 compared to human GLP-1.

Figure 6.16 Persistent, 2 h post injection, effects of paddlefish glucagon and [D-Ser^{2}] paddlefish glucagon-Lys^{30}-gamma-glutamyl-pal peptides on blood glucose (A) and plasma insulin (B) concentrations in normal mice.

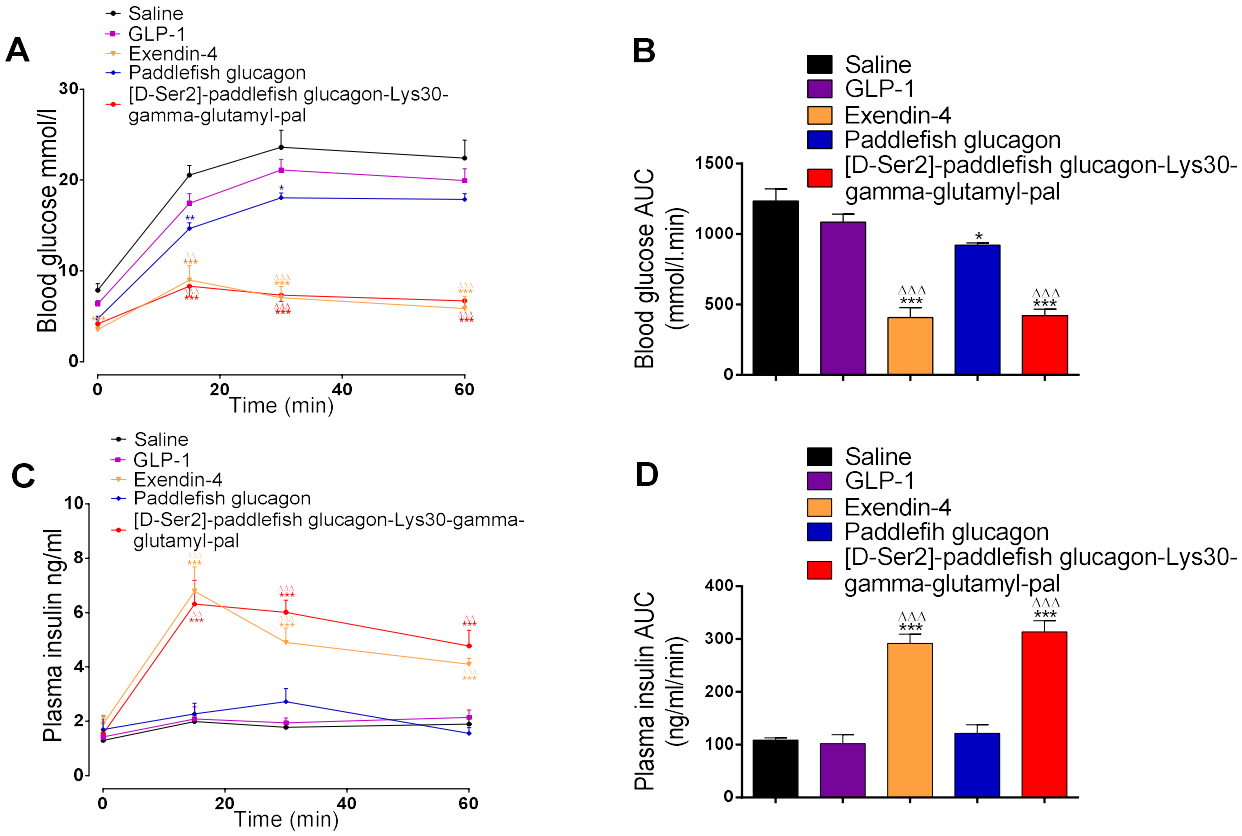

Blood glucose and plasma insulin were measured after intraperitoneal injection of glucose (18 mmol/kg body weight) 2 hours after intraperitoneal administration of 0.9% saline or peptides (25 nmol/kg body weight). The integrated responses (area under the curve AUC) are shown in panels B and D. The values are mean ± SEM for n=6. *P<0.05 **P<0.01 and ***P<0.001 compared to glucose alone; $^{\Delta\Delta\Delta}$ P<0.001 compared to human GLP-1.

Figure 6.17 Persistent, 4 h post injection, effects of [D-Ser^{2}]-lamprey glucagon Lys^{30}-gamma-glutamyl-pal on blood glucose (A) and plasma insulin (B) concentrations in normal mice.

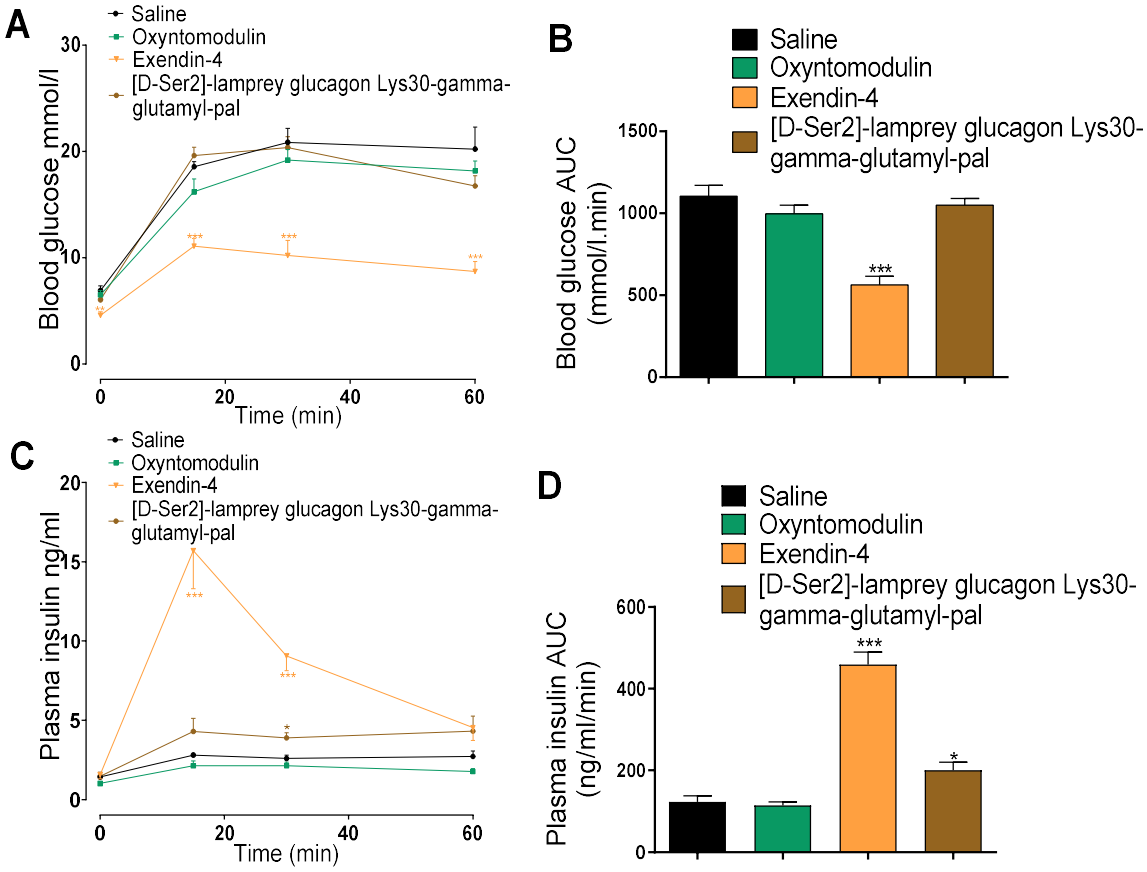

Blood glucose and plasma insulin were measured after intraperitoneal injection of glucose (18 mmol/kg body weight) 4 hours after intraperitoneal administration of 0.9% saline or peptides (25 nmol/kg body weight). The integrated responses (area under the curve AUC) are shown in panels B and D. The values are mean ± SEM for n=6. *P<0.05 and ***P<0.001 compared to glucose alone.

Figure 6.18 Persistent, 4 h post injection, effects of paddlefish glucagon and [D-Ser^2] paddlefish glucagon-Lys^{30}-gamma-glutamyl-pal peptides on blood glucose (A) and plasma insulin (B) concentrations in normal mice.

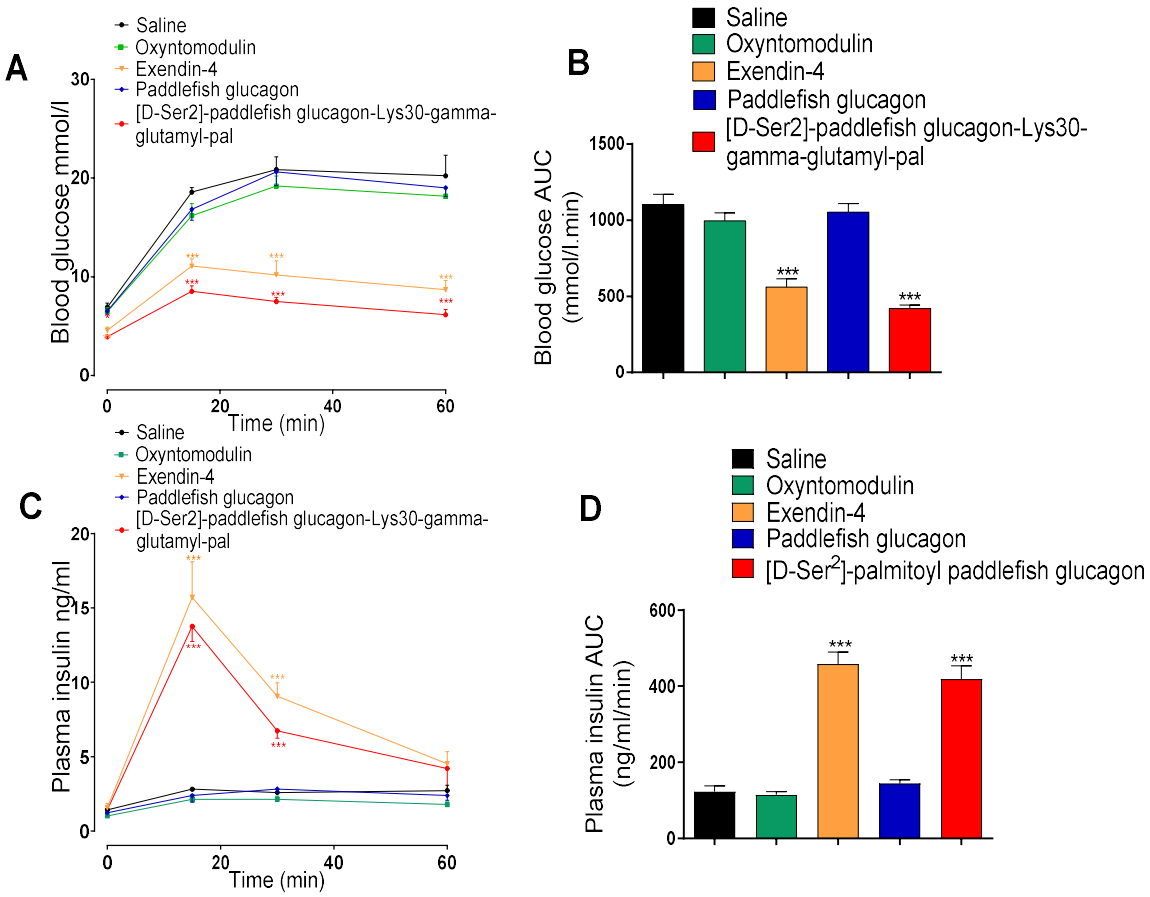

Blood glucose and plasma insulin were measured after intraperitoneal injection of glucose (18 mmol/kg body weight) 4 hours after intraperitoneal administration of 0.9% saline or peptides (25 nmol/kg body weight). The integrated responses (area under the curve AUC) are shown in panels B and D. The values are mean ± SEM for n=6. ***P<0.001 compared to glucose alone.

Figure 6.19 Effects of (A) lamprey glucagon and [D-Ser^2]-lamprey glucagon Lys^{30}-gamma-glutamyl-pal and (B) paddlefish glucagon and [D-Ser^2]-paddlefish glucagon-Lys^{30}-gamma-glutamyl-pal on cumulative food intake over 3 hours trained feeding in 12 h fasting normal mice.

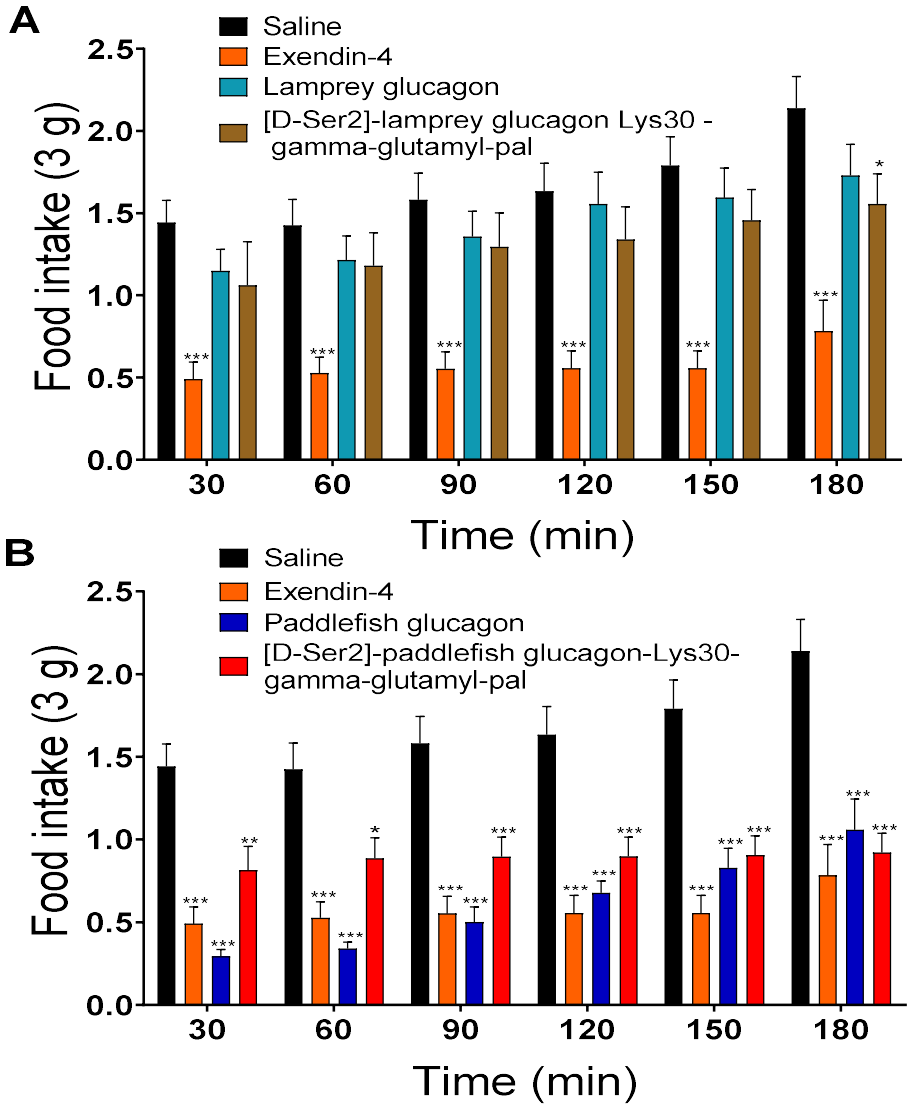

Cumulative food intake was measured after intraperitoneal administration of 25 nmol/kg peptides alongside 0.9% saline control. The values are mean ± SEM for n=8. *P<0.05, **P<0.01 and ***P<0.001 compared to saline control mice treated at the same time point.

Figure 6.20 Chronic effects of [D-Ser^2]-paddlefish glucagon-Lys^{30}-gamma-glutamyl-pal on accumulative (A) food and (B) water intake during 21 days study in high-fat-fed mice.

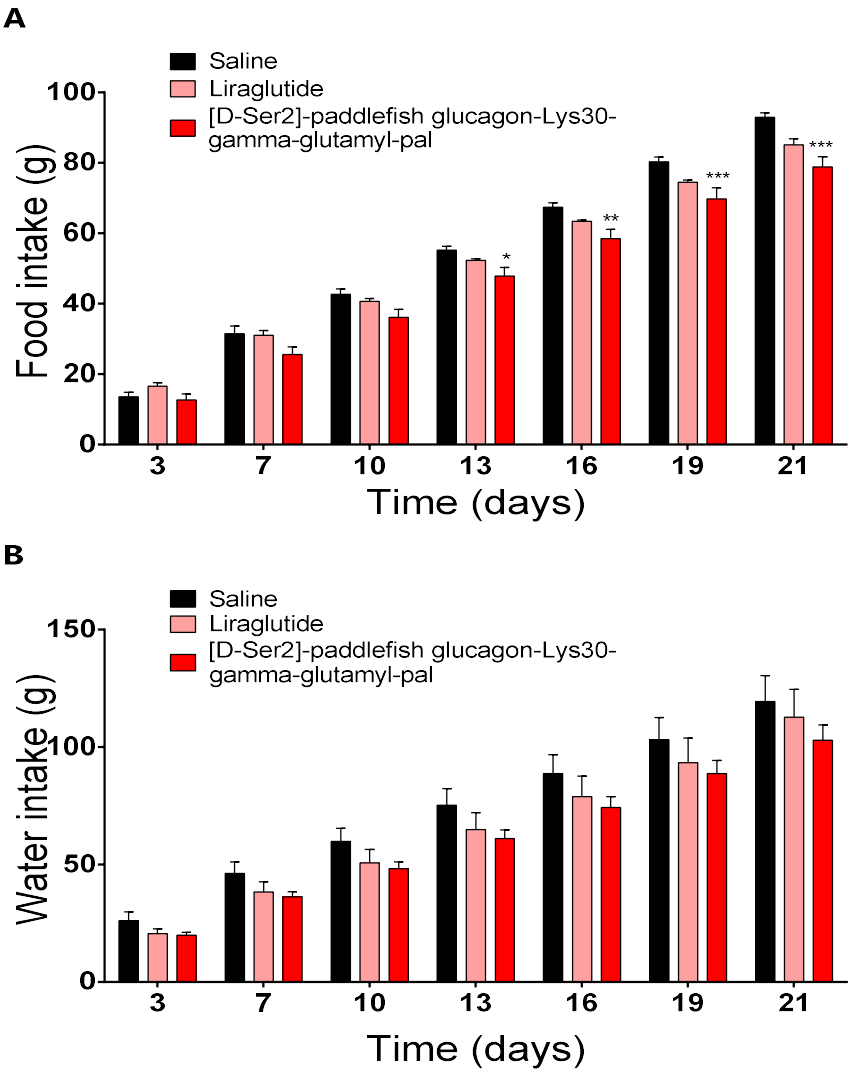

(A) Accumulative food and (B) water intake were measured during 21 days twice daily treatment with saline vehicle (0.9% (w/v) NaCl), liraglutide or [D-Ser^2]-paddlefish glucagon-Lys^{30}-gamma-glutamyl-pal (each at 25 nmol/kg bw). Values represent mean±SEM for 8 mice. *P<0.05 ** P<0.01 and ***P<0.001 is compared with high fat control.

Figure 6.21 Chronic effects of [D-Ser^{2}]-paddlefish glucagon-Lys^{30}-gamma-glutamyl-pal on body weight (A) and % body weight change (B) in high-fat-fed mice during 21 days of study.

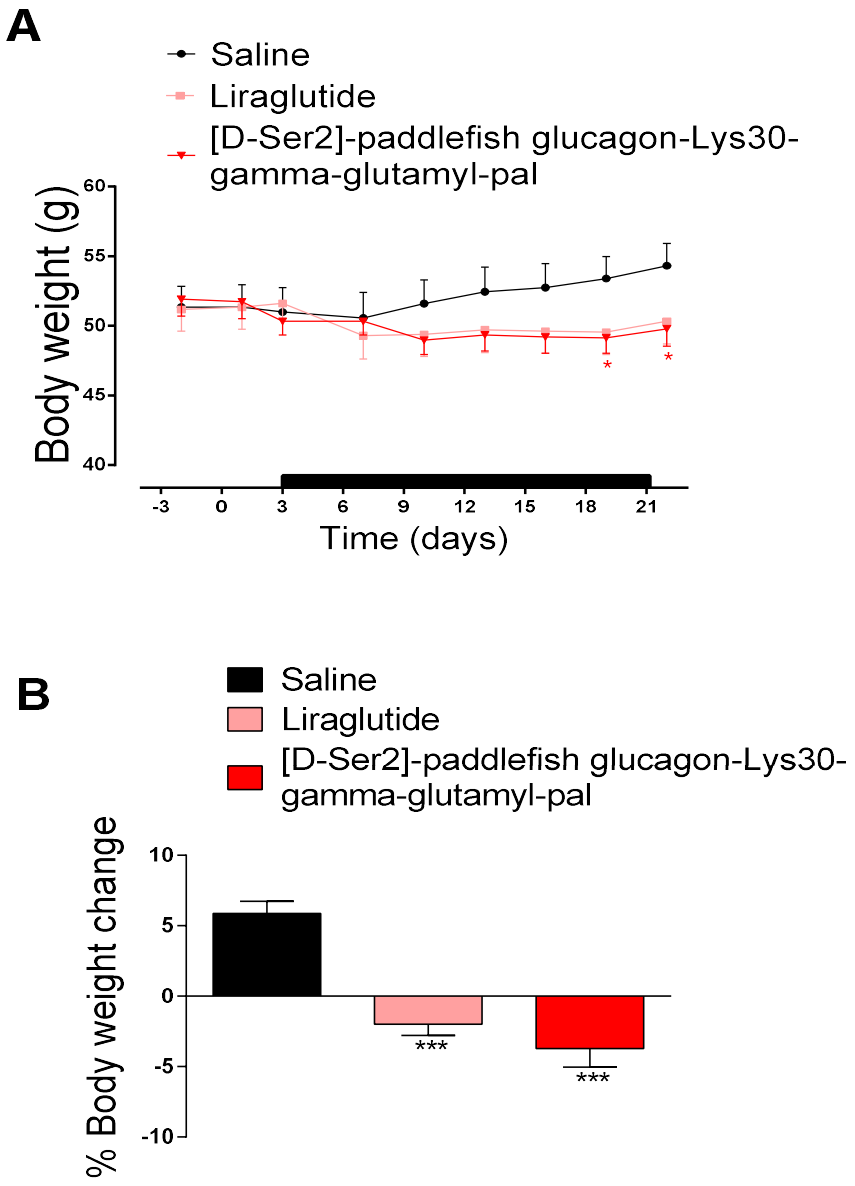

(A) Body weight and (B) % of body weight were measured during 21 days twice daily treatment with saline vehicle (0.9% (w/v) NaCl), liraglutide or [D-Ser^{2}]-paddlefish glucagon-Lys^{30}-gamma-glutamyl-pal (each at 25 nmol/kg bw). The black horizontal bar represents the treatment period. Values represent mean±SEM for 8 mice. *P<0.05, **P<0.01 and ***P<0.001 is compared with high fat control.

Figure. 6.22 Chronic effects of [D-Ser^2]-paddlefish glucagon-Lys^{30}-gamma-glutamyl-pal on non-fasting blood glucose (A) and blood glucose AUC (B) during 21 days study in high-fat-fed mice.

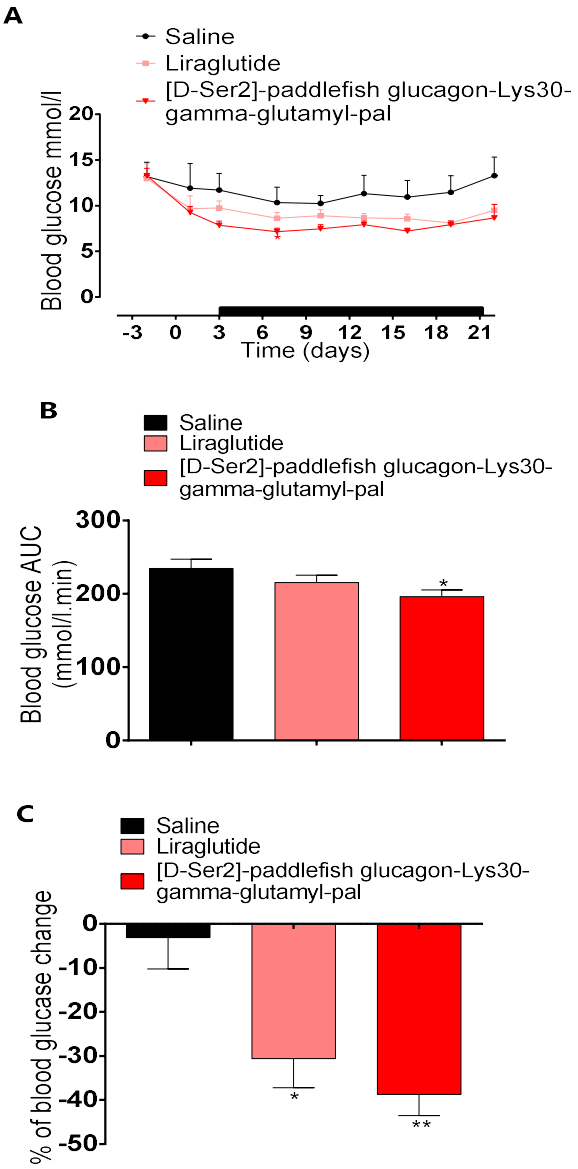

(A) Blood glucose (B) Blood glucose and AUC (C) % of blood glucose change measured during 21 days twice daily treatment with saline vehicle (0.9% (w/v) NaCl), liraglutide or [D-Ser^2]-paddlefish glucagon-Lys^{30}-gamma-glutamyl-pal (each at 25 nmol/kg bw). The black horizontal bar represents the treatment period. Values represent mean±SEM for 8 mice. *P<0.05, **P<0.01 and ***P<0.001 is compared with high fat treated control.

Figure 6.23 Chronic effects of [D-Ser^{2}]-paddlefish glucagon-Lys^{30}-gamma-glutamyl-pal on plasma insulin levels (A) and plasma insulin AUC (B) during 21 days study in high-fat-fed mice.

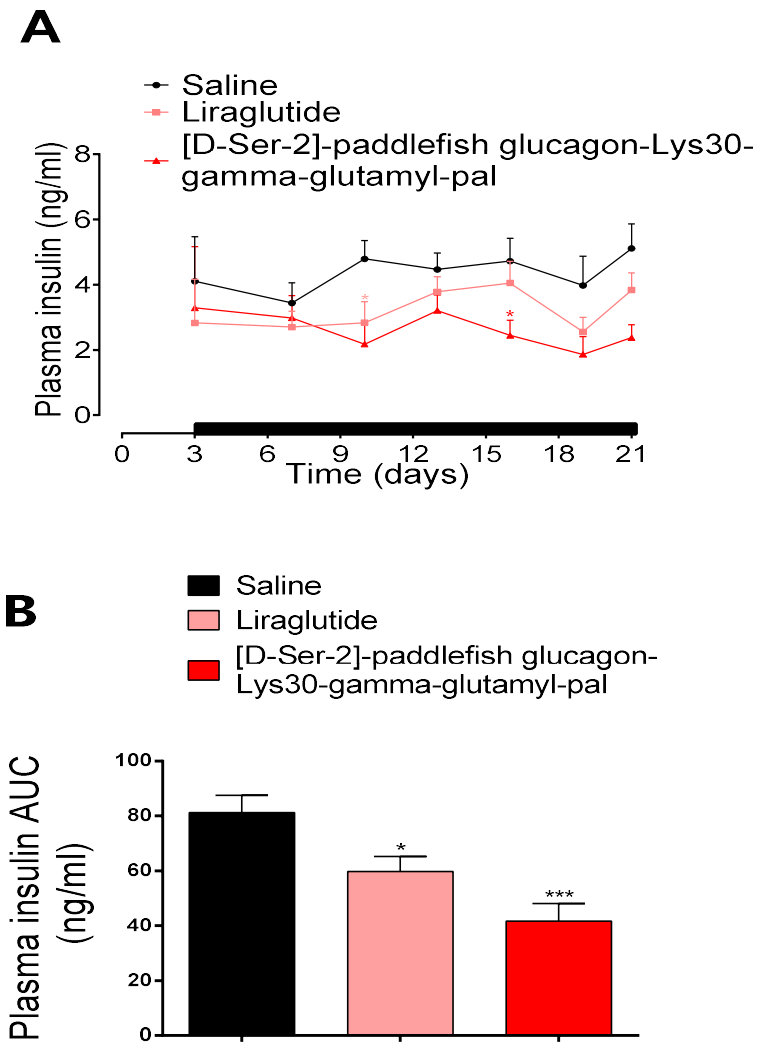

(A) Plasma insulin (B) Plasma insulin AUC measured during 21 days twice daily treatment with saline vehicle (0.9% (w/v) NaCl), liraglutide or [D-Ser^{2}]-paddlefish glucagon-Lys^{30}-gamma-glutamyl-pal (each at 25 nmol/kg bw). The black horizontal bar represents the treatment period. Values represent mean±SEM for 8 mice. *P<0.05 and ***P<0.001 is compared with high fat treated control.

Figure 6.24 Chronic effects of [D-Ser^2]-paddlefish glucagon-Lys^{30}-gamma-glutamyl-pal on glucose tolerance (A-B) and plasma insulin (C-D) in response to intraperitoneal administration of glucose in fasted high-fat diet fed mice.

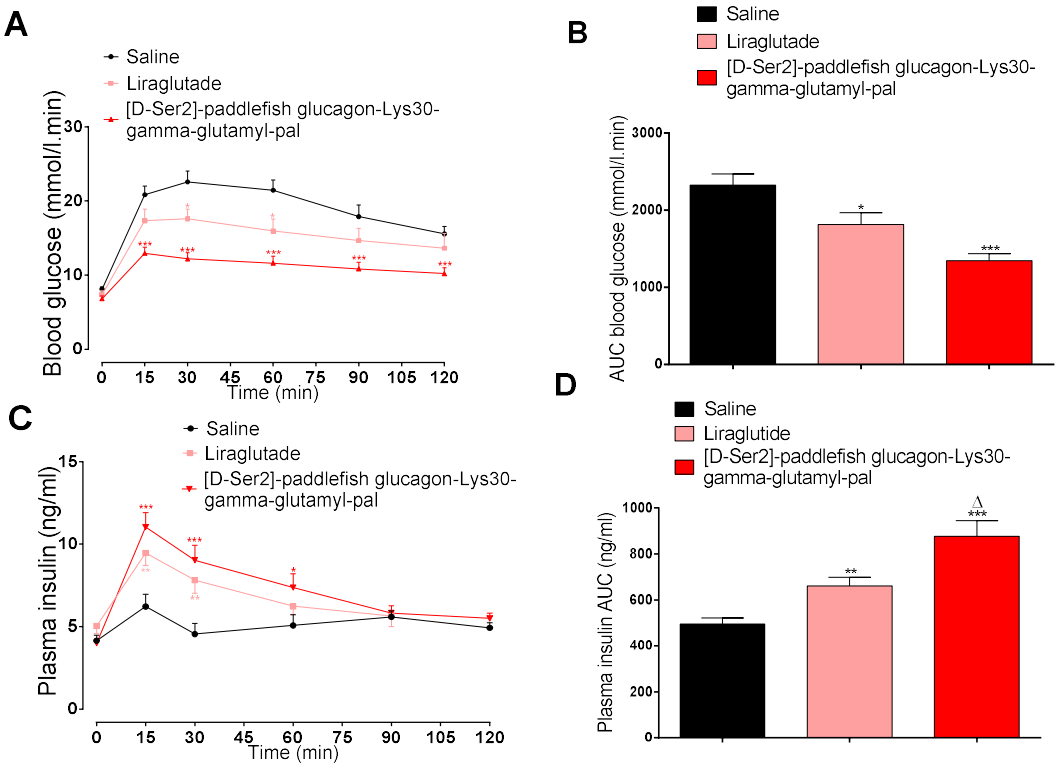

Parameters were measured prior to and after administration of glucose alone (18 mmol/kg of bw, i.p.) in animals receiving after 21 days daily treatment with saline vehicle (0.9% w/v NaCl, i.p), liraglutide or fish peptide analogue (each at 25 nmol/kg of bw, i.p.). Blood glucose and plasma insulin AUC values 0-120 min are included. The values are mean ± SEM for n=8. *P<0.05, **P<0.01 and ***P<0.001 compared to saline control. $^{\Delta}$ P<0.05 compared to liraglutide.

Figure 6.25 Chronic effects of [D-Ser^{2}]-paddlefish glucagon-Lys^{30}-gamma-glutamyl-pal on glucose tolerance (A-B) and plasma insulin (C-D) in response to oral administration of glucose in fasted high-fat diet fed mice.

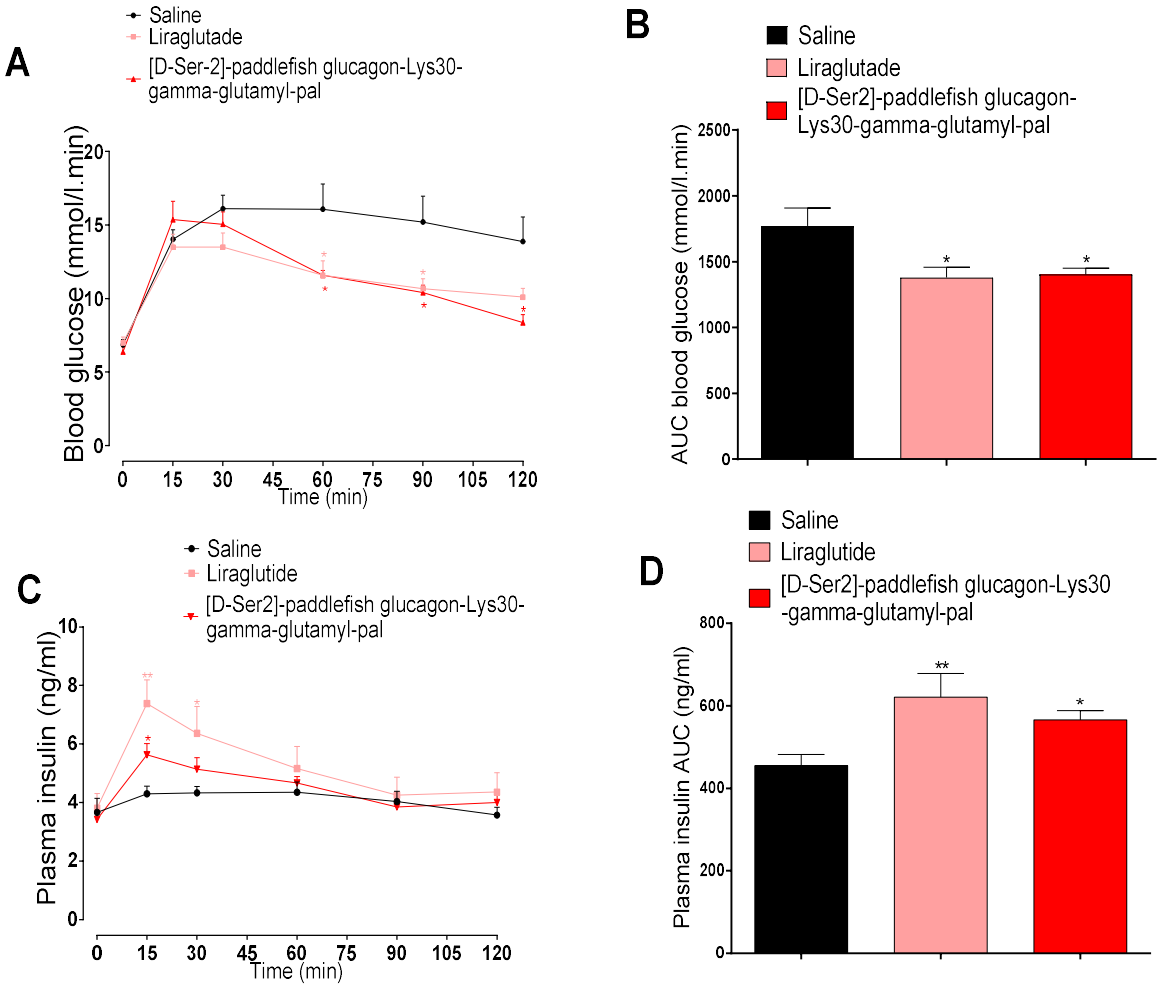

Parameters were measured prior to and after administration of glucose alone (18 mmol/kg) in animals receiving after 21 days daily treatment with saline vehicle (0.9% w/v NaCl, i.p), liraglutide or fish peptide analogues (each at 25 nmol/kg of bw, i.p.). Blood glucose and plasma insulin AUC values 0-120 min are included. The values are mean ± SEM for n=8. *P<0.05 and **P<0.01 compared to saline control.

Figure 6.26 Chronic effects of [D-Ser^{2}]-paddlefish glucagon-Lys^{30}-gamma-glutamyl-pal on insulin sensitivity in high-fat fed mice

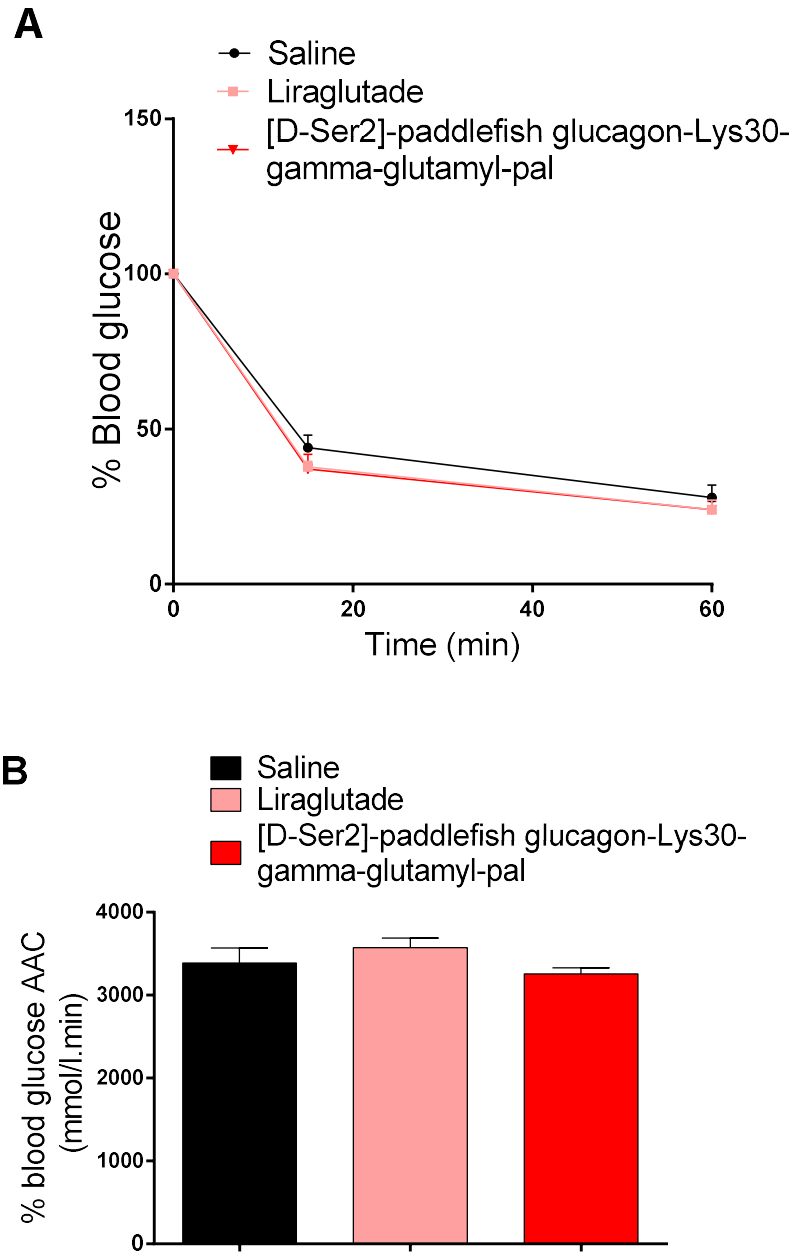

Test was performed following 21 days of twice daily intraperitoneal administration of saline vehicle (0.9% w/v NaCl, i.p), liraglutide or fish peptide analogue (each at 25 nmol/kg of bw, i.p.). Insulin (25 U/kg bw) was administrated by i.p. injection at t=0 min. % blood glucose AAC values for 0-60min are also included. Values represent mean ± SEM for 8 mice.

Figure 6.27 Chronic effects of [D-Ser^{2}]-paddlefish glucagon-Lys^{30}-gamma-glutamyl-pal on HOMA-β and HOMA-IR in high-fat–fed mice

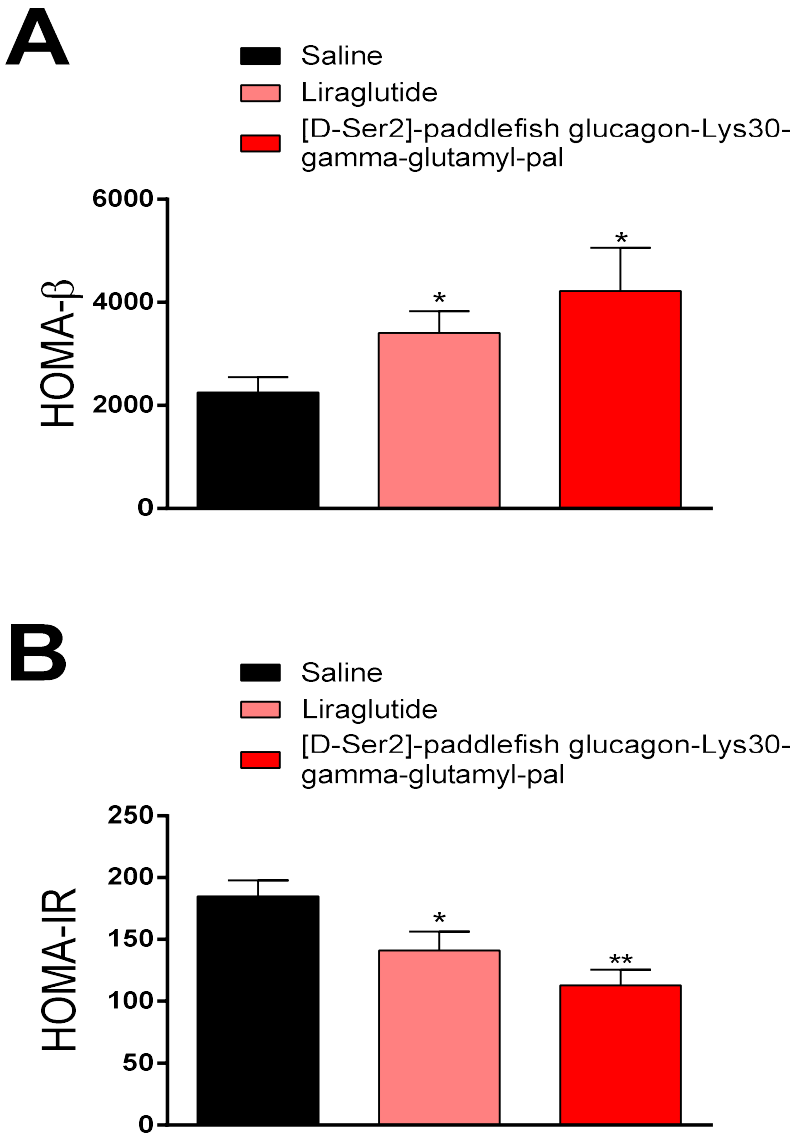

HOMA-β (A) and HOMA-IR (B) were calculated from fasting glucose and insulin concentrations. The parameters were measured on day 21 following twice-daily treatment with saline vehicle (0.9% w/v NaCl, i.p), liraglutide or fish peptide analogues (each at 25 nmol/kg of bw, i.p). Values represent mean ± SEM for 8 mice. *P<0.05 and **P<0.01 compared with high fat control group.

Figure 6.28 Chronic effects of [D-Ser2]-paddlefish glucagon-Lys30gamma-glutamyl-pal on pancreatic glucagon (A) and pancreatic insulin (B) content in high-fat-fed diet mice.

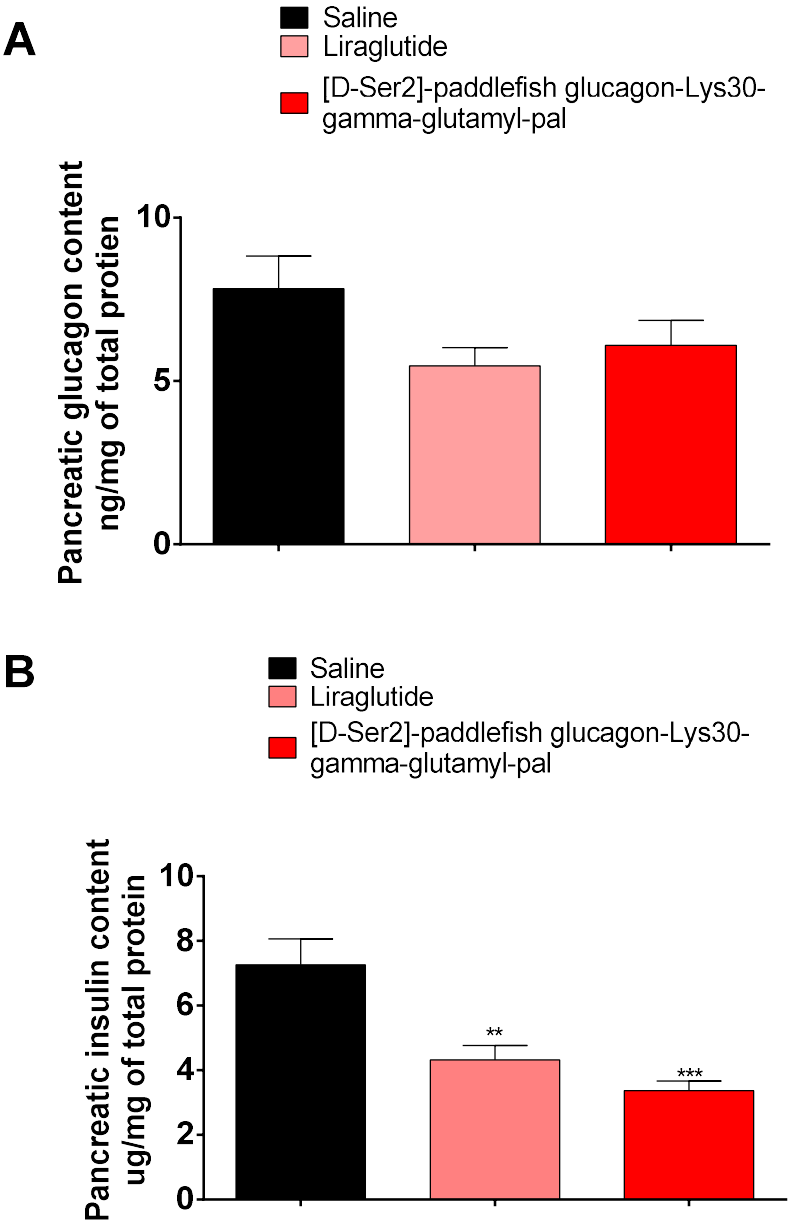

The parameters were measured on day 21 following twice-daily treatment with saline vehicle (0.9% w/v NaCl, i.p), liraglutide or fish peptide analogue (each at 25 nmol/kg of bw, i.p). Data are expressed as means ± SEMs for n=4. **P < 0.01 and *** P< 0.001 compared with saline control.

Figure 6.29 Chronic effects of [D-Ser^{2}]-paddlefish glucagon-Lys^{30}-gamma-glutamyl-pal on amylase activity in high-fat-fed diet mice

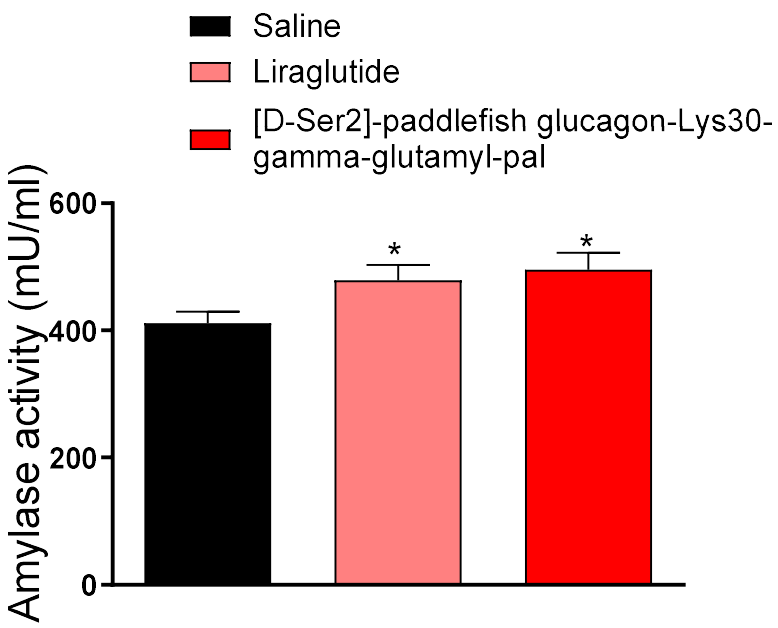

The parameters were measured on day 21 following twice-daily treatment with saline vehicle (0.9% w/v NaCl, i.p), liraglutide or fish peptide analogues (each at 25 nmol/kg of bw, i.p). Data are expressed as means ± SEMs for 8 mice.

Figure 6.30 Chronic effects of [D-Ser^{2}]-paddlefish glucagon-Lys^{30}-gamma-glutamyl-pal on plasma ALT in high-fat-fed diet mice

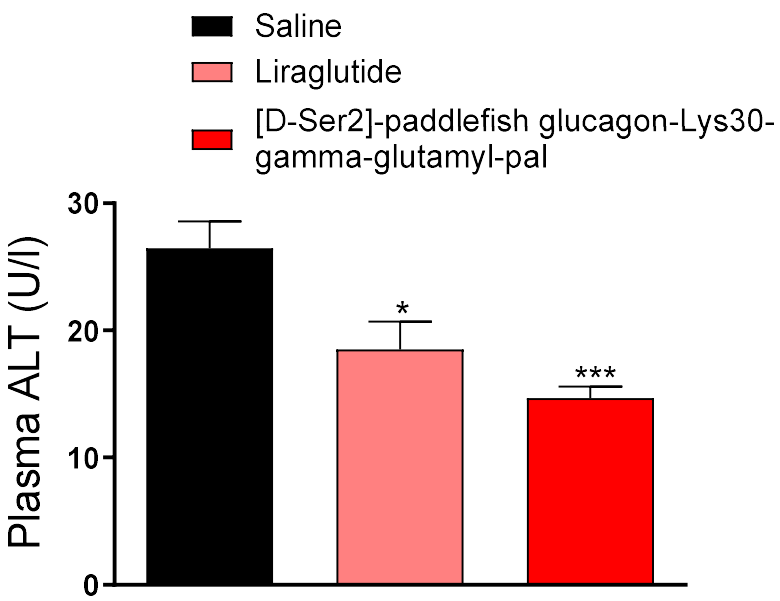

The parameters were measured on day 21 following twice-daily treatment with saline vehicle (0.9% w/v NaCl, i.p), liraglutide or fish peptide analogues (each at 25 nmol/kg of bw, i.p). Data are expressed as means ± SEMs for n=4. **P < 0.01 and *** P< 0.001 compared with saline control.

Figure 6.31 Chronic effects of [D-Ser^{2}]-paddlefish glucagon-Lys^{30}-gamma-glutamyl-pal on plasma glucagon in high-fat-fed diet mice

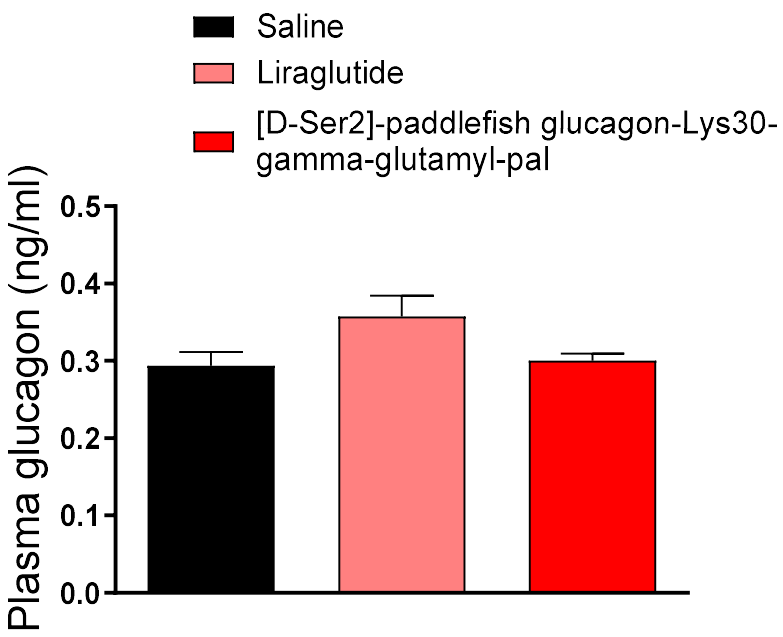

The parameters were measured on day 21 following twice-daily treatment with saline vehicle (0.9% w/v NaCl, i.p), liraglutide or fish peptide analogues (each at 25 nmol/kg of bw, i.p). Data are expressed as means ± SEMs for n=4

Figure 6.32 Chronic effects of [D-Ser^2]-paddlefish glucagon-Lys^{30}-gamma-glutamyl-pal on plasma total cholesterol (A), triglycerides (B), HDL-cholesterol (C), and LDL-cholesterol (D) in high-fat fed mice.

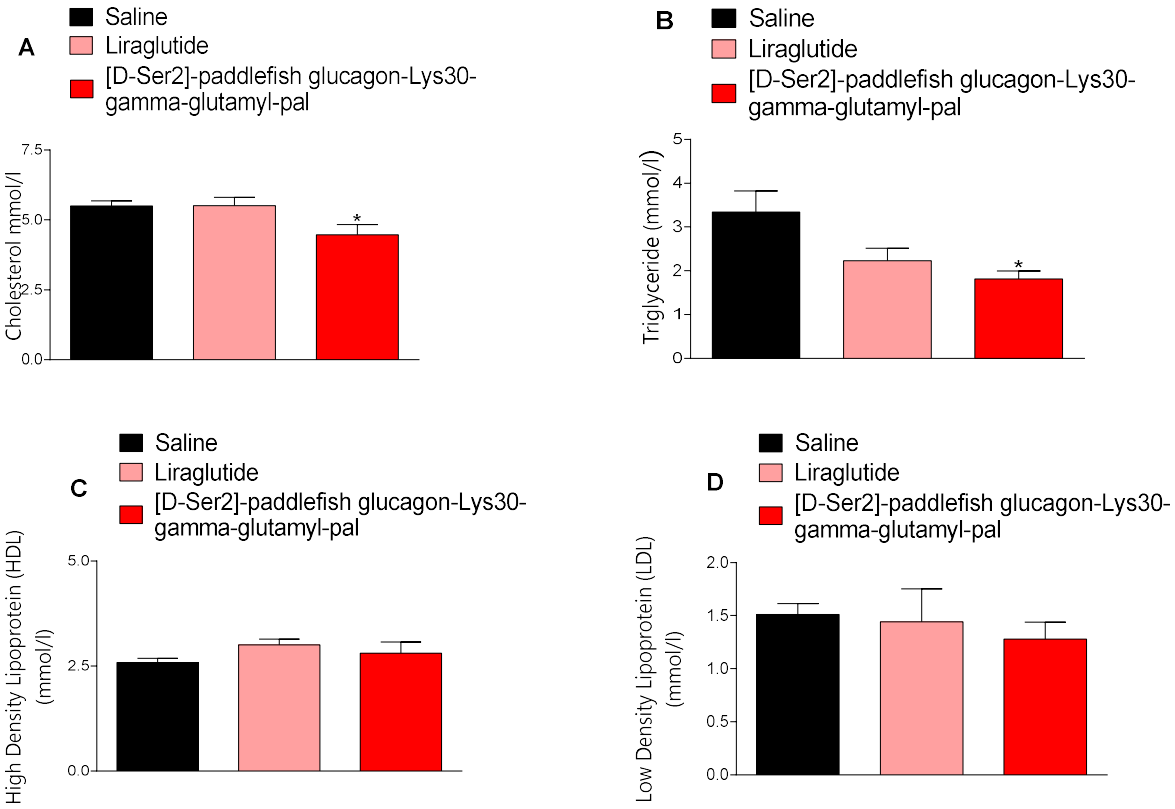

Plasma total cholesterol (A), triglycerides (B), HDL-cholesterol (C), and LDL-cholesterol (D) were measured on day 21 following twice-daily treatment with saline vehicle (0.9% w/v NaCl, i.p), liraglutide or fish peptide analogues (each at 25 nmol/kg of bw, i.p). Data are expressed as means ± SEMs for 8 mice. *P < 0.05 and *** P< 0.001 compared with saline control.

Figure 6.33 Chronic effects of [D-Ser^2]-paddlefish glucagon-Lys^{30}-gamma-glutamyl-pal on (A) bone mineral density, (B) bone mineral content, (C) bone area, (D) lean body mass, (E) body fat and (F) % fat composition measured by DEXA scanning in high-fat diet fed mice.

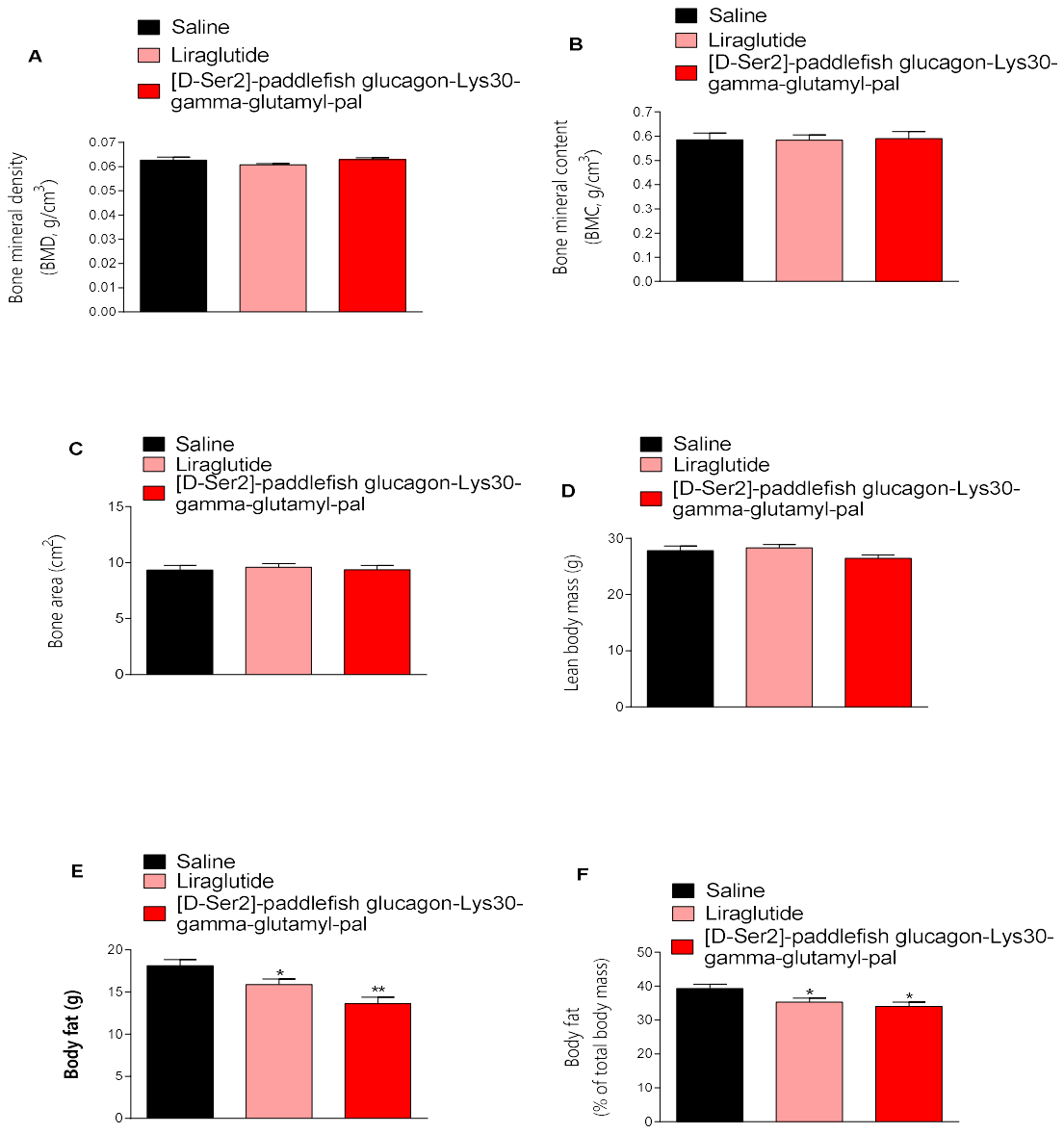

Parameters were measured by DEXA scanning after 21-days twice daily treatment with saline vehicle (0.9% (w/v) NaCl), liraglutide or [D-Ser^2]-paddlefish glucagon-Lys^{30}-gamma-glutamyl-pal (each at 25 nmol/kg bw). Values represent mean±SEM for 6-8 mice. *P<0.05 and **P<0.01 compared to high-fat control.

Figure 6.34 Chronic effects of [D-Ser^{2}]-paddlefish glucagon-Lys^{30}-gamma-glutamyl-pal on insulin secretory response from isolated islets in high-fat-fed diet mice.

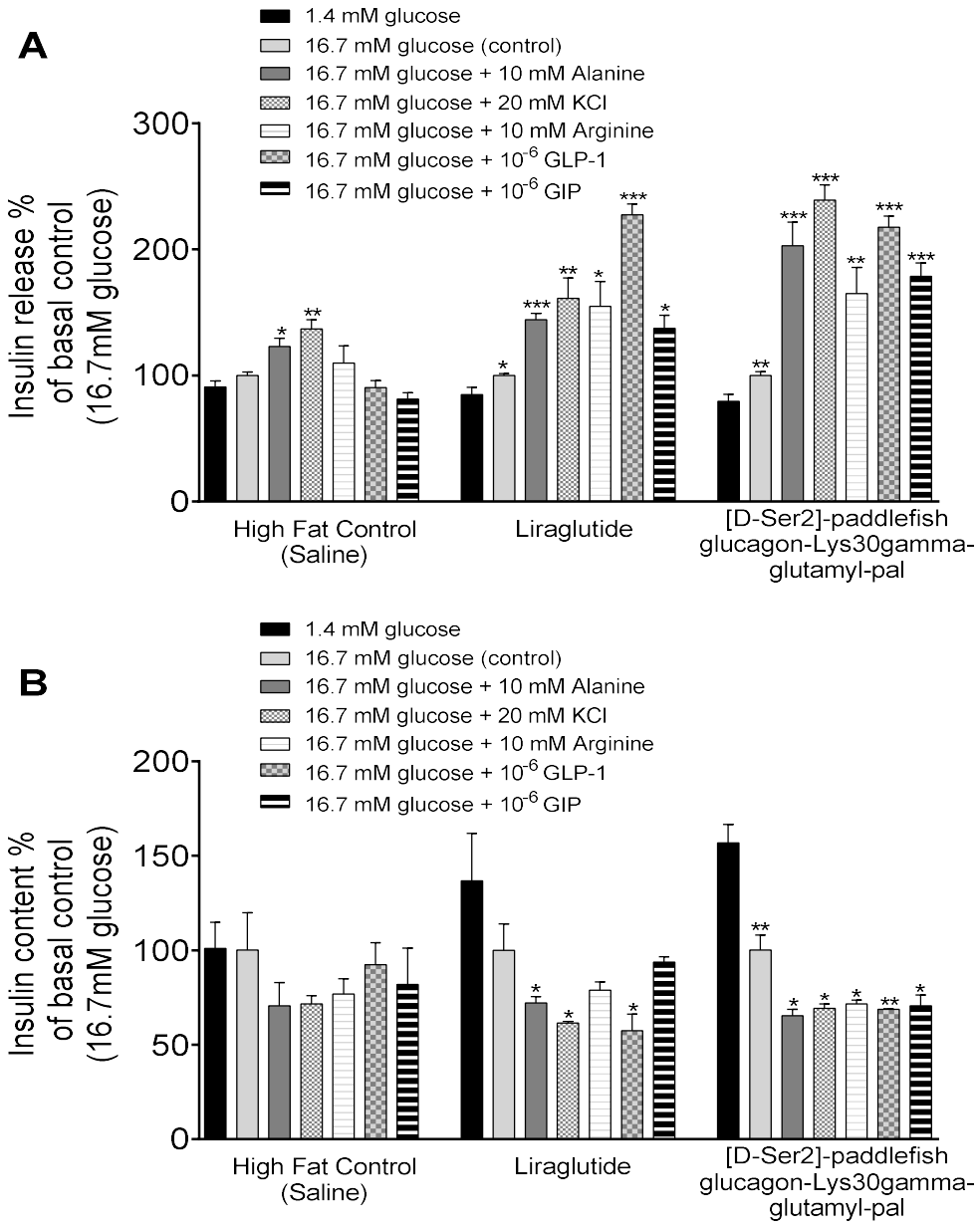

Pancreatic islets were isolated following 21 days twice-daily treatment with saline vehicle (0.9% w/v NaCl, i.p), liraglutide or fish peptide analogues (each at 25 nmol/kg of bw, i.p.). Parameters for A) insulin release and B) insulin content represent normalised values to respective control (16.7mM glucose) for each group. Values are mean±SEM for n=4. *P<0.05, **P<0.01 ***P<0.001 compared to respective 16.7mM glucose control.

Figure 6.35 Chronic effects of [D-Ser^2]-paddlefish glucagon-Lys^{30}-gamma-glutamyl-pal on pancreatic islet morphology in high-fat-fed mice.

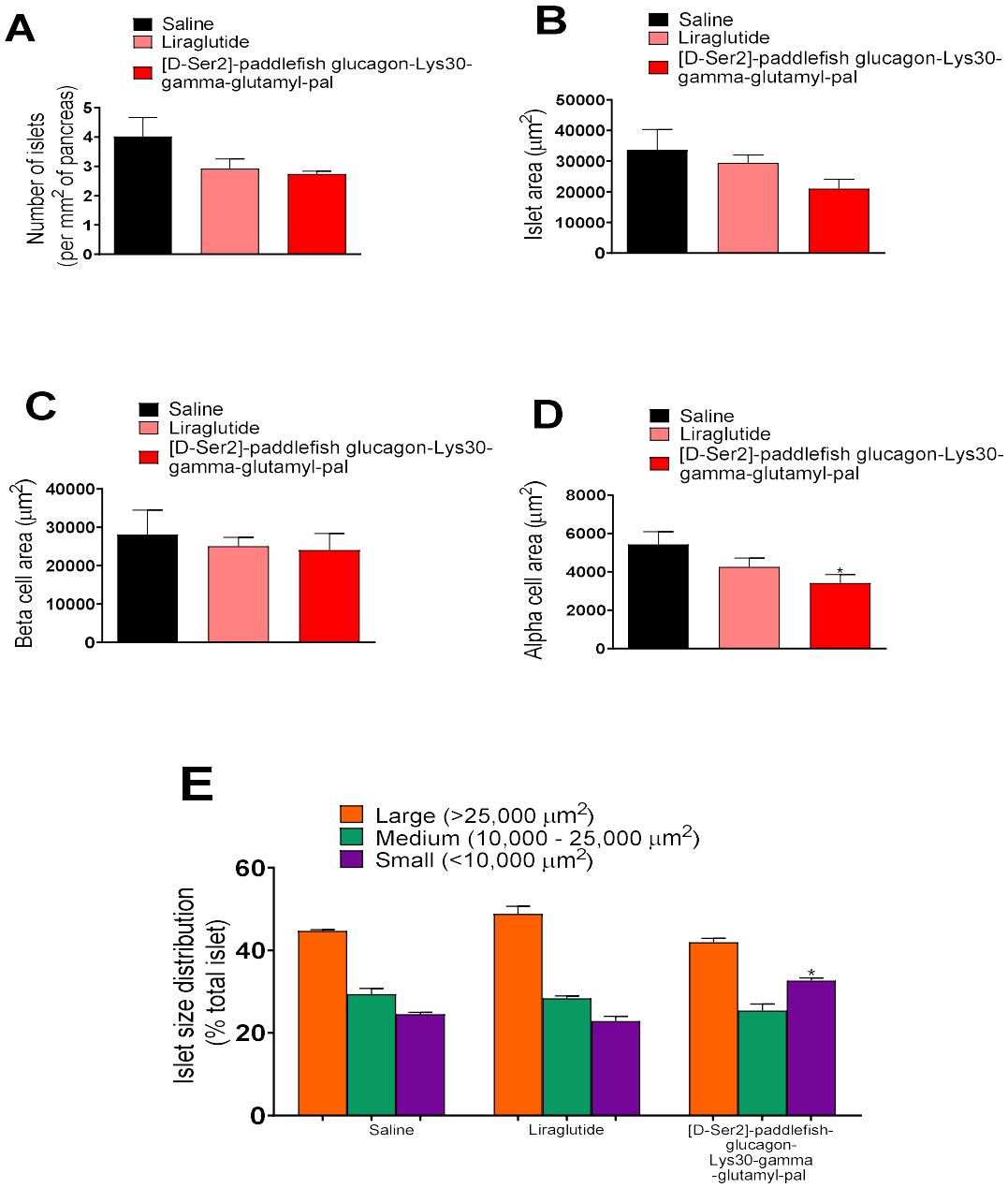

Parameters for (A) number of islets (mm), (B) islet area (µm^2), (C) beta cell area (µm^2), (D) alpha cell area (µm^2), (E) islet size distribution (% of total area) were measured on day 21 following twice-daily treatment with saline vehicle or the peptides (at 25 nmol/kg body weight. ***P < 0.001 compared to high-fat diet saline control. Effects of liraglutide are shown for comparison.

Figure 6.36 Chronic effects of [D-Ser^2]-paddlefish glucagon-Lys^{30}-gamma-glutamyl-pal on the expression of genes involved in insulin secretion from islets in high fat fed mice.

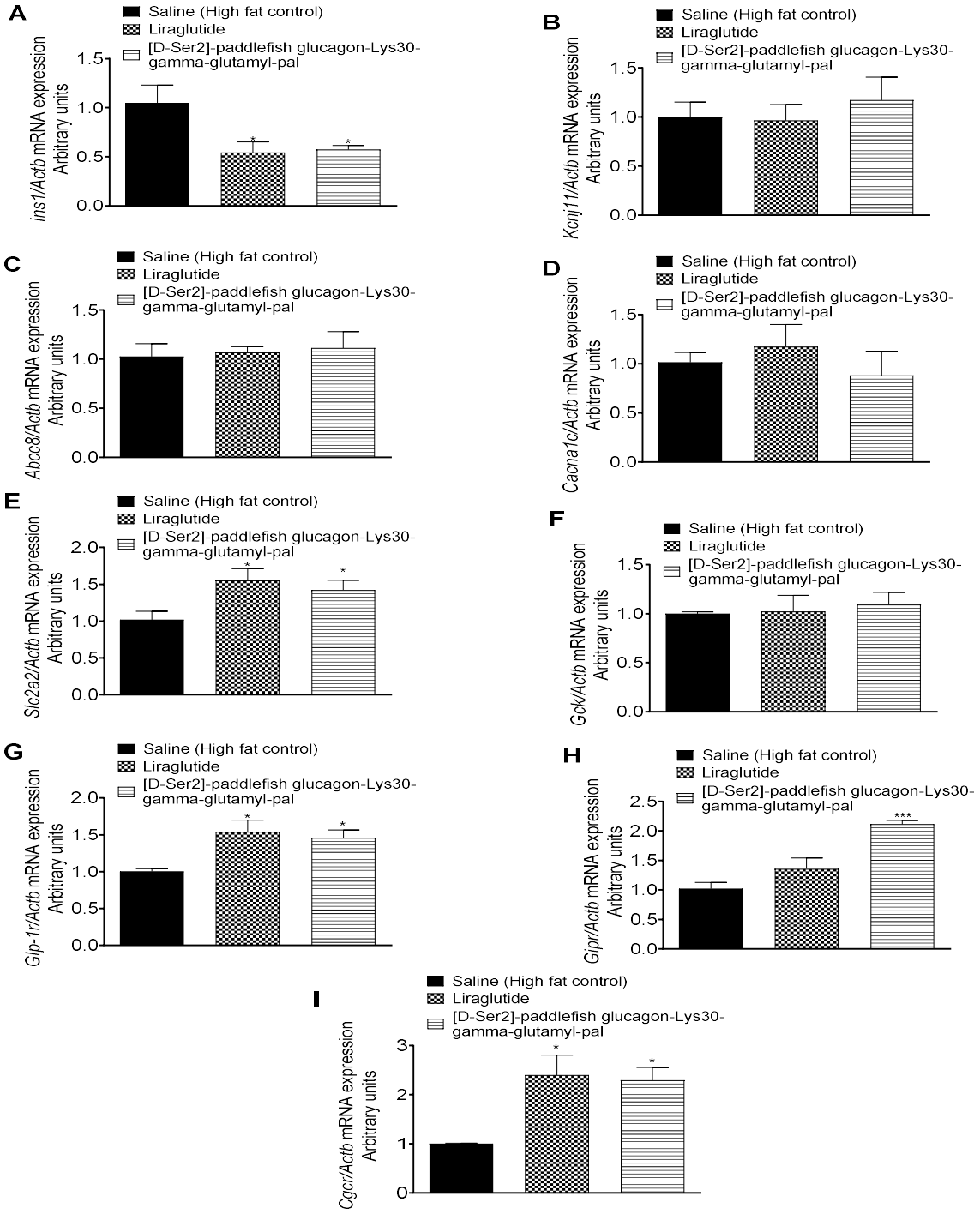

cDNA was synthesised from 1 µg of mRNA. Data were normalised to Beta-actin (Actb) gene expression used as a reference gene and analysed using the ΔΔCt method. Data are expressed as means ± SEMs for n=3. *P < 0.05, ** P< 0.01 and *** P< 0.001 compared with high fat saline control

Figure 6.37 Chronic effects of [D-Ser^{2}]-paddlefish glucagon-Lys^{30}-gamma-glutamyl-pal on (A) accumulative food and (B) water intake during 11 days study in streptozotocin treated GluGreRosa26-YFP mice.

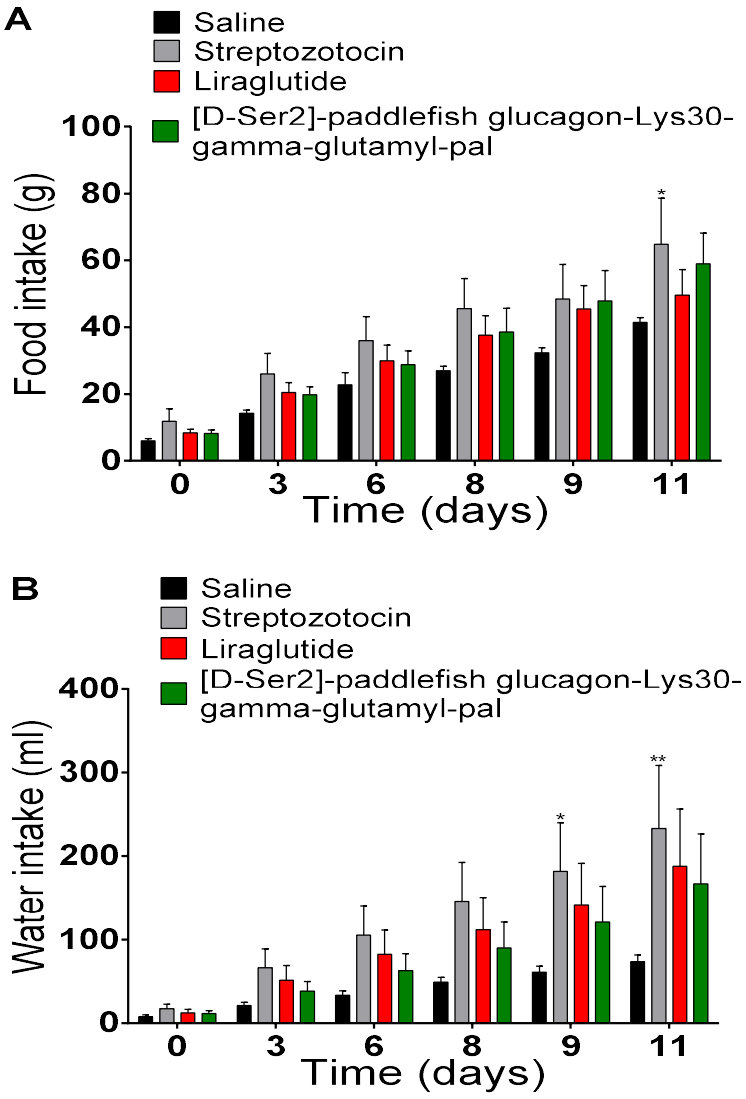

(A) Accumulative food and (B) water intake were measured during 11 days twice daily treatment with saline vehicle (0.9% (w/v) NaCl), liraglutide or [D-Ser^{2}]-paddlefish glucagon-Lys^{30}-gamma-glutamyl-pal (each at 25 nmol/kg bw). Values represent mean±SEM for 5 mice. *P<0.05 ** P<0.01 and ***P<0.001 is compared with untreated control.

Figure 6.38 Chronic effects of [D-Ser^2]-paddlefish glucagon-Lys^{30}-gamma-glutamyl-pal on (A) blood glucose and (B) % of blood glucose change (C) body weight (D) % of body weight change and (E) plasma insulin during 11 days study in streptozotocin treated GluGreRosa26-YFP mice.

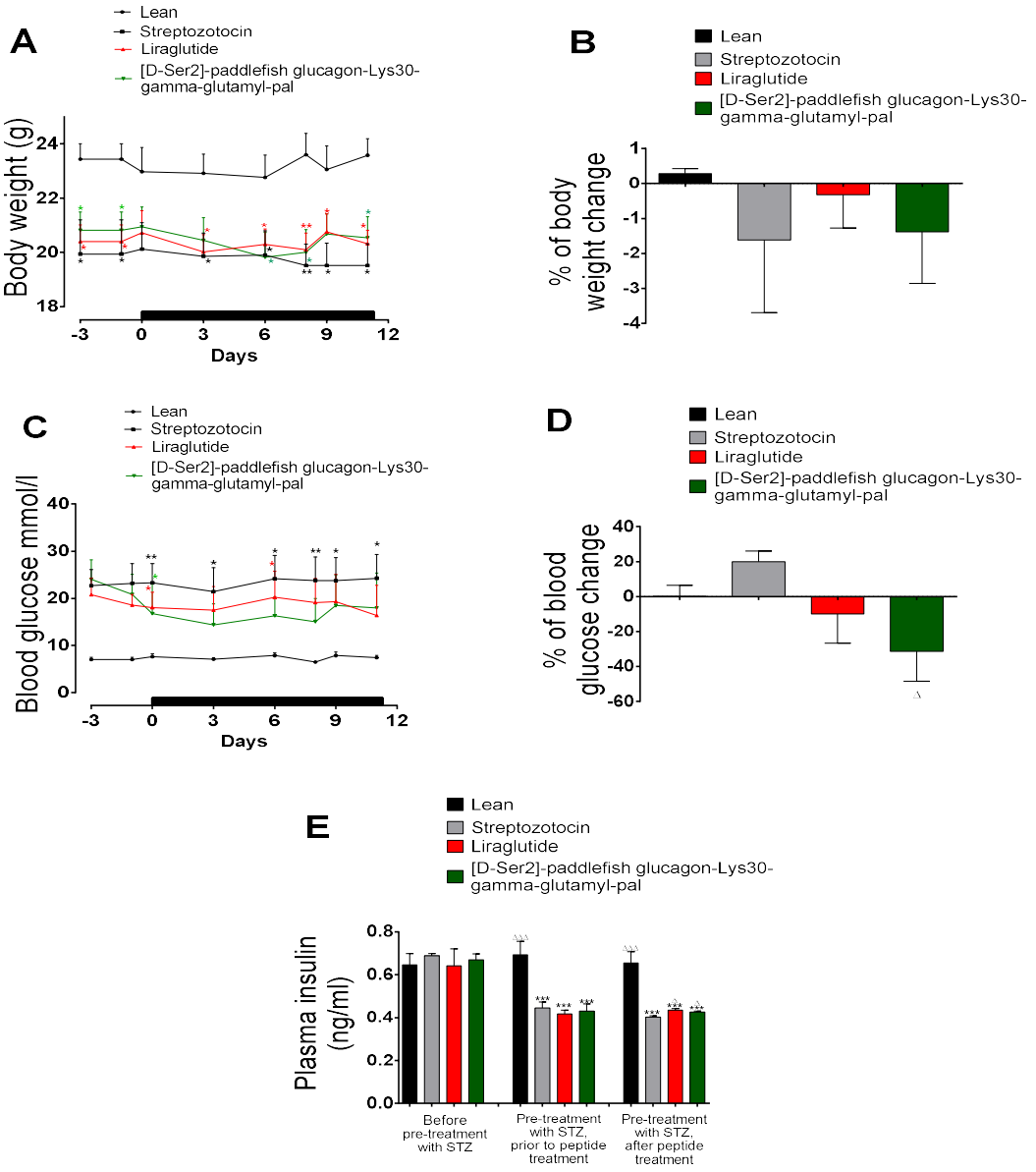

The parameters were measured during 11 days twice daily treatment with saline vehicle (0.9% (w/v) NaCl), liraglutide or [D-Ser^2]-paddlefish glucagon-Lys^{30}-gamma-glutamyl-pal (each at 25 nmol/kg bw). The black horizontal bar represents the treatment period. Values represent mean±SEM for 5 mice. *P < 0.05 and ***P <0 .001 is compared with untreated control. $^{\Delta}$P < 0.05 is compared with streptozotocin control.

Figure 6.39 Chronic effects of [D-Ser^{2}]-paddlefish glucagon-Lys^{30}-gamma-glutamyl-pal on pancreatic (A) insulin and (B) glucagon content during 11 days study in streptozotocin pre-treated GluGreRose26-YFP mice.

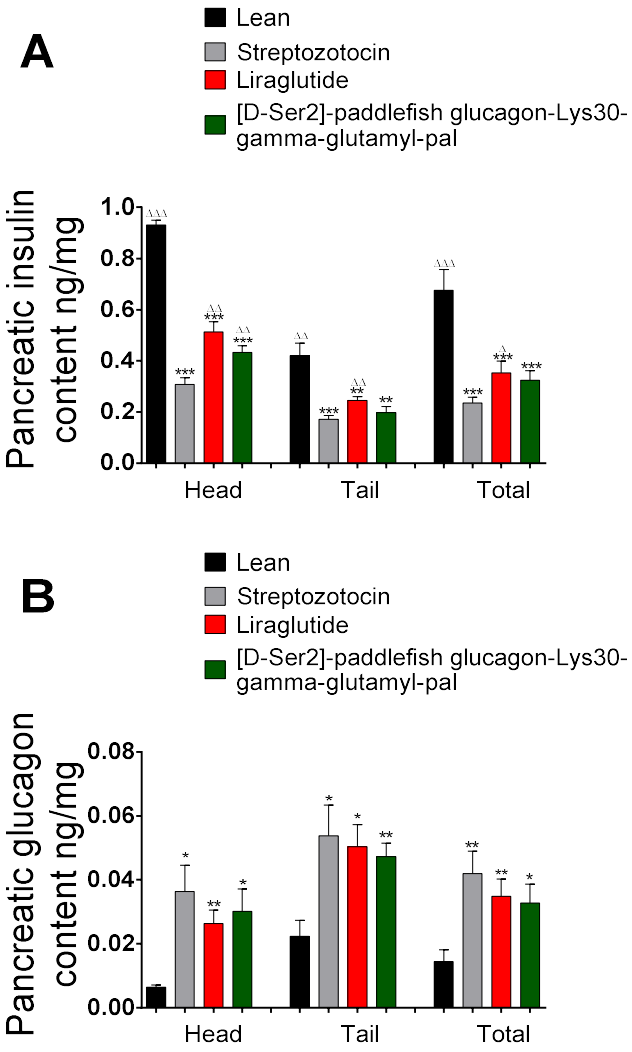

The parameters were measured during 11 days twice daily treatment with saline vehicle (0.9% (w/v) NaCl), liraglutide or [D-Ser^{2}]-paddlefish glucagon-Lys^{30}-gamma-glutamyl-pal (each at 25 nmol/kg bw). Values represent mean±SEM for n=3. *P<0.05 and ***P<0.001 is compared with untreated control. $^{\Delta}$P<0.05, $^{\Delta\Delta}$P<0.01 and $^{\Delta\Delta\Delta}$P<0.001 is compared with streptozotocin control.

Figure 6.40 Chronic effects of [D-Ser^2]-paddlefish glucagon-Lys^{30}-gamma-glutamyl-pal on pancreatic islet morphology in GluGreRosa26-YFP mice

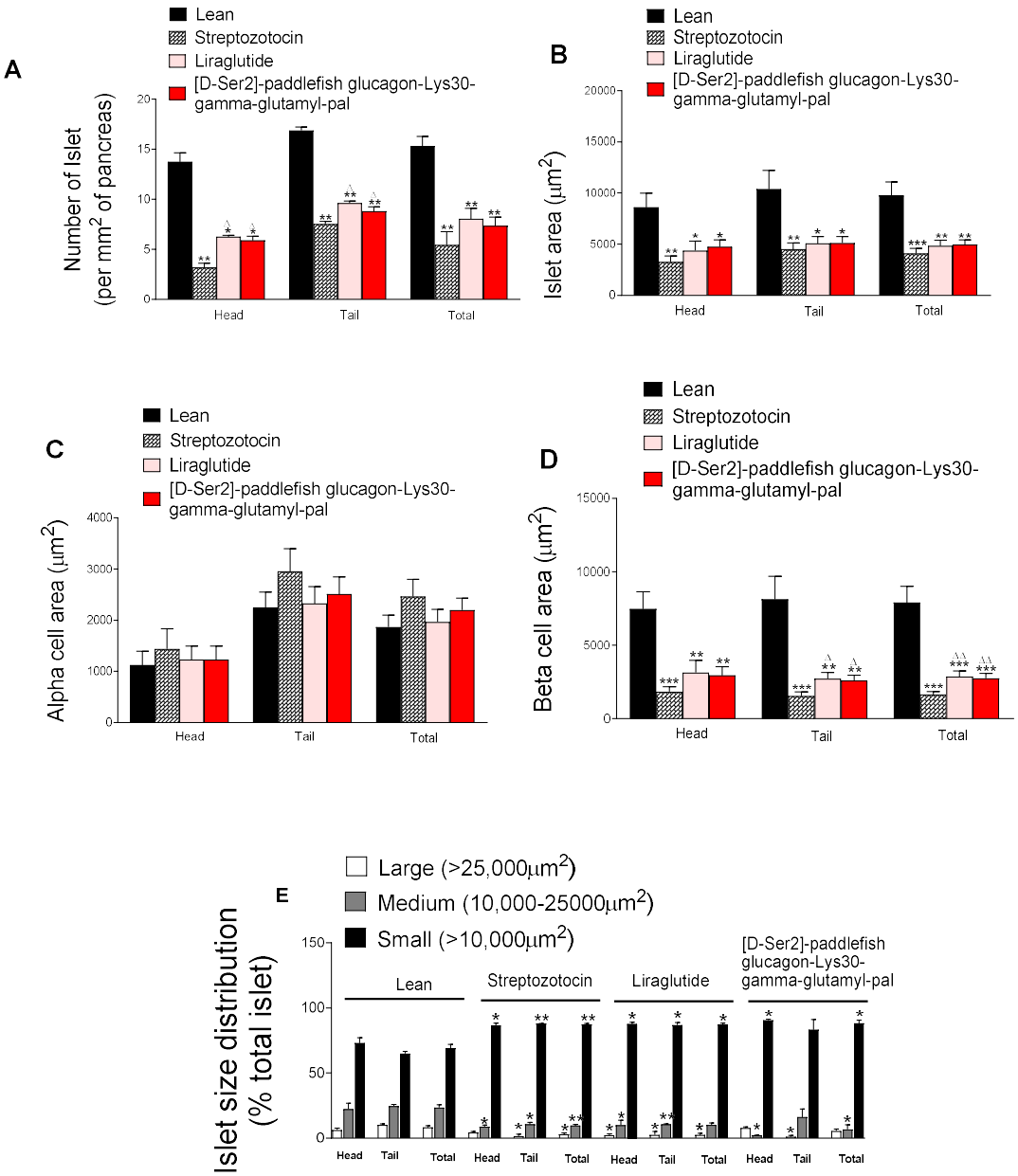

Parameters for (A) number of islets (mm), (B) islet area (μm^2), (C) beta cell area (μm^2), (D) alpha cell area (μm^2), (E) islet size distribution (% of total area) were measured on day 11 following twice-daily treatment with saline vehicle or the peptides (at 25 nmol/kg body weight. ~40-50 islets per group. The values are mean ± SEM *P<0.05, **P<0.01 and ***P<0.001 compared to untreated control; $^{\Delta}$ p<0.05 and $^{\Delta\Delta}$ P<0.05 compared to streptozotocin-treated mice.

Figure 6.41 Chronic effects of [D-Ser^2]-paddlefish glucagon-Lys^{30}-gamma-glutamyl-pal on alpha to beta cell transdifferentiation in GluGreRosa26-YFP

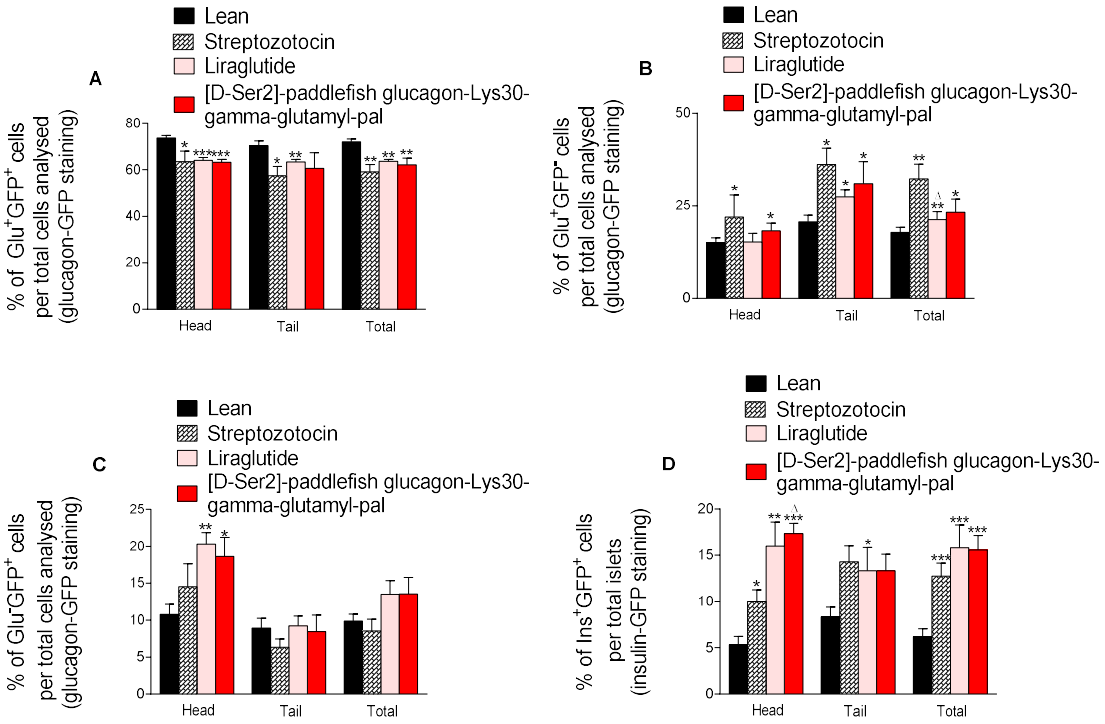

Analysis of A) Glucagon$^+$GFP$^+$ cells, B) Glu$^+$ GFP$^-$ cells, C) Glu$^-$GFP$^+$ and D) Insulin$^+$GFP$^+$ cells per total cells/islets analysed (~40-50 islets per group). The values are mean ± SEM *P < 0.05, **P < 0.01 and ***P < 0.001 compared to untreated control; $^{\Delta}$ P<0.05 compared to streptozotocin treated mice.

Chapter 7

Assessing the acute insulinotropic *in vitro* and *in vivo* effects of zebrafish GIP

7.1 Summary

Zebrafish, *Danio rerio*, (Actinopterygii, Cyprinidae) is a well-studied vertebrate genetic and developmental model system (Broughton et al. 2001). The insulinotropic properties of zebrafish GIP (zfGIP) were assessed *in vitro* using clonal pancreatic β-cell lines, and isolated mouse islets and acute effects on glucose tolerance and insulin release in vivo were evaluated in mice. The peptide produced a dose-dependent increase in the rate of insulin release from BRIN-BD11 rat clonal β-cells at concentrations ≥ 30 nM. Insulin release from 1.1 B4 human clonal β-cells and mouse islets was significantly increased by zfGIP (10 nM and 1μM). The *in vitro* insulinotropic activity of zfGIP was decreased after incubating BRIN-BD11 cells with the GLP-1 receptor antagonist, exendin-4(9-39) ($P < 0.001$) and the GIP receptor antagonist, GIP (6-30) Cex-K40 [Pal] ($P < 0.05$) but the glucagon receptor antagonist [desHis1-Pro4-Glu9]glucagon amide was without effect. zfGIP (10 nM and 1μM) produced significant increases in cAMP concentration in CHL cells transfected with the human GLP-1 receptor but was without effect on HEK293 cells transfected with the human glucagon receptor. Conversely, zfGIP, but not human GIP, significantly stimulated insulin release from CRISPR/Cas9-engineered INS-1 clonal β-cells from which the GIP receptor had been deleted. Intraperitoneal administration of zfGIP (25 and 75 nmol/kg body weight) to mice together with an intraperitoneal glucose load (18 mmol/kg body weight) produced a significant decrease in plasma glucose concentrations concomitant with an increase in insulin concentrations. The study provides evidence that the insulinotropic action of zfGIP in mammalian systems involves activation of both the GLP-1 and the GIP receptors but not the glucagon receptor.

7.2 Introduction

Glucose-dependent insulinotropic polypeptide (GIP) is a member of an extended family of structurally related regulatory peptides that includes glucagon, glucagon-like peptide-1(GLP-1), glucagon-like peptide-2, secretin, VIP, PHM, PACAP, and GHRH (McIntosh et al. 2009). In addition, a gene encoding glucagon-related peptide with structural similarity to the Gila monster venom peptides, exendin-3 and -4 is present in the genomes of a range of tetrapod taxa but is absent from zebrafish and mammals (Irwin 2012; Park et al. 2013). The peptides are related evolutionarily having arisen from an ancestral gene either by tandem duplications or as a result of ancient whole genome duplications (2R hypothesis) (Cardoso et al 2010 and Irwin et al 2011). The physiological effects of these peptides are mediated largely by interaction with a family of structurally and evolutionarily related class B (secretin–like) G-protein coupled receptors (Irwin 2014).

GIP was first isolated from a porcine intestinal extract as a 42-amino-acid peptide on the basis of its ability to inhibit gastric acid production at supraphysiological concentrations (Brown et al. 1971). Subsequently, the gene encoding the peptide has been identified in a range of mammalian species (reviewed in McIntosh et al 2009), chicken (Irwin et al 2006), the frogs *Xenopus tropicalis* and *Xenopus laevis* (Irwin et al 2006), and in a teleost, the zebrafish *Danio rerio* (Irwin et al 2006). A gene encoding a GIP-like sequence is present in the genome of the sea lamprey *Petromyzon marinus* but transcripts were not detected (Musson et al. 2011). Similarly, a GIP-like molecule has not yet been identified in an elasmobranch, but it is of interest that a mammalian GIP is a potent stimulant of cAMP production and chloride secretion in the rectal gland of the skate *Leucoraja erinacea* (Kelley et al. 2014). The predicted primary structure of zebrafish GIP (zfGIP) is only 31 amino acid residues, and it has

been speculated that the peptide is more similar to the ancestral gene product from which the glucagon family of peptides has arisen than mammalian GIP peptides (Musson et al. 2011).

GIP is described as an incretin hormone in mammals owing to its ability to promote insulin release from pancreatic β-cells at physiologically relevant concentrations. GIP is released into the circulation from intestinal enteroendocrine K- cells in response to ingestion of carbohydrates and fats and, along with GLP-1, is the major physiologic incretin in the human (Holst et al. 2016). Recent research has indicated that functionally relevant GIP is also present in the pancreatic islet cells of mice (Moffett et al. 2014).

In the zebrafish, RT-PCR and immunohistochemical studies have demonstrated that GIP expression in the intestine is restricted to cells located near the base of the vill and the peptide is located principally in endocrine cells of the pancreas (Musson et al. 2011 et al. 2009). This has led investigators to speculate that GIP may not function as an incretin in this species (Musson et al. 2011 et al. 2009). No gene that closely resembles the human GLP-1R gene has been found in the genomes of the zebrafish or other bony fish (Irwin 2014) and the fact that GLP-1 does not function as an incretin hormone in teleosts, rather as a glucagon-like stimulant of glycogenolysis and gluconeogenesis, is well established (Plisetskaya et al 1996).

The aim of the present study was to assess whether synthetic zfGIP shows potential for development into a therapeutic agent for treatment of patients with Type 2 diabetes mellitus (T2DM) by investigating its insulinotropic properties in vitro using established insulin-producing cell lines and in vivo using NIH Swiss mice. The possibility that zfGIP may function as a dual- or triple agonist in a mammalian system was investigated using selective antagonists for GIP, GLP-1, and glucagon receptors

and by using cells transfected with the human glucagon receptor (CGCR) and the GLP-1 (GLP-1R) receptor and CRISPR/Cas9-engineered INS-1 cells from which the GIPR and GLP-1R had been deleted

7.3 Materials and Methods

7.3.1 Chemical Reagents and Peptides

Chemical reagents that were used in this study can be found in Section 2.1.1 and Table 2.1. Synthetic human glucagon, human GLP-1, human GIP and trout GLP-1 were obtained from Synpeptide Co. Ltd. (Shanghai, China) at >95% purity which was confirmed by reversed-phase HPLC and MALDI-TOF.

zfGIP (YAESTIASDISKIVDSMVQKNFVNFLLNQRE)was supplied in crude form by EZBiolab Inc. (Carmel, IN, USA) and was purified to > 95% homogeneity by reversed-phase HPLC on a (2.2 cm x 25 cm) Vydac 218TP1022 (C-18) column. The concentration of acetonitrile in the eluting solvent was raised from 35% to 70% over 50 min using a linear gradient. Absorbance was measured at 214 nm, and the flow rate was 6 ml/min. The identity of the peptide was confirmed by MALDI-TOF mass spectrometry using a Voyager DE PRO instrument (Applied Biosystems, Foster City, USA) (observed molecular mass 3562.0, calculated molecular mass 3561.1). The primary structures and molecular masses of the peptides used in this study are shown in Table 2.1 and Table 7.1.

7.3.2 Assessment of metabolic stability of zfGIP

zfGIP and human GIP were incubated in the presence of porcine DPP-IV, and peptide stability was measured over 4 hours as described in Section 2.3.1. RP-HPLC was used to identify intact peptide and degraded products the molecular masses of which were

confirmed by MALDI-TOF MS as previously described (Section 2.3). The percentage intact peptide at 4 hours incubation with DPP-IV was calculated by comparison to the peak area recorded at 0 hours.

7.3.3 *In vitro* insulin release studies using BRIN-BD11 and 1.1B4 cells

In vitro insulin secretory studies were carried out using BRIN-BD11 (McClenaghan et al., 1996) and 1.1B4 cells (McCluskey et al. 2011) as previously described (Section 2.5.1 and 2.5.3). In a separate experiment, the effects of 1 μM concentrations of the (A) GLP-1 receptor antagonist, exendin-4(9-39 (Thorens et al., 1993), (B) glucagon receptor antagonist, [desHis1,Pro4-Glu9] glucagon amide (O'Harte et al., 2013), and (C) glucose-dependent insulinotropic peptide (GIP) receptor antagonist, GIP(6-30)Cex-K^{40}[Pal] (Pathak et al., 2015) on the insulin-releasing activity of the zfGIP (0.1 μM) were studied as previously described (Section 2.5.2 and 2.5.7).

7.3.4 Insulin release studies using isolated mouse islets

Effects of zfGIP on *ex-vivo* insulin secretion were assessed using pancreatic islets from adult, male National Institutes of Health (NIH) Swiss mice (Harlan Ltd, Bicester, UK) as previously described (Section 2.5.5).

7.3.5 Effects of zfGIP on cAMP production.

The effect of zfGIP on cAMP production from Chinese hamster lung (CHL) cells transfected with the human GLP-1 receptor (GLP1R) (Thorens et al., 1993) and human embryonic kidney (HEK293) cells transfected with the human glucagon receptor (GCGR) (Ikegami et al., 2001) was assessed using a Parameter cAMP assay kit (R&D Systems, Abingdon, UK) as outlined in Section 2.6.

7.3.6 Insulin release studies using CRISPR/Cas9-engineered INS-1 cells

In vitro receptor activation study was perform using wild-type INS-1 832/3 rat clonal pancreatic β-cells and CRISPR/Cas9-engineered cells with knock-out of the knock-out of the GLP-1 receptor (GLP-1 KO), glucagon receptor (GCG KO) and GIP receptor (GIP KO) (Naylor et al., 2016) as described in Section 2.5.4.

7.3.7 In vivo insulin release and glucose-lowering effects of zf GIP

Acute and persistent *in vivo* studies were carried out using male 8-12 week-old National Institutes of Health (NIH) Swiss mice as previously described (Sections 2.8.1.1, 2.8.2.1, 2.8.2.3 and 2.8.2.5). Blood glucose and plasma insulin were measured immediately prior to (t = 0), and 15, 30 and 60 min after intraperitoneal administration of glucose alone (18 mmol/kg of body weight) or in combination zfGIP (25 or 75 nmol/kg bw) in overnight fasted mice.

7.3.8 Acute food consumption studies

Normal male TO 8-12 week-old mice were used in food consumption study as previously described (Section 2.8.2.4). Animals were administrated intraperitoneal injections of either saline solution or zfGIP (50 nmol/kg) prior to receiving free access to normal chow for 180 mins.

7.3.9 Biochemical analysis

Blood was collected from the tail vein of conscious mice and analysed immediately using the Ascenacia Counter Blood Glucose Meter (Bayer, Newbury, UK). Plasma for insulin was collected, stored and assayed as described in Section 2.8.2.5.

7.3.10 Statistical analysis

Data were compared using unpaired Student's t test (non-parametric, with two-tailed P values and 95% confidence interval) and one-way ANOVA with Bonferroni post-hoc test using GraphPad PRISM (Version 5.0 San Diego, California). Area under the curve (AUC) analysis was performed using the trapezoidal rule with baseline correction. Data are presented as mean ± S.E.M where the comparison was considered to be significantly different if $P < 0.05$.

7.4 Results

7.4.1 Purification and confirmation of molecular masses by MALDI-TOF MS

Following purification, 10% and 20% of purified peptide were obtained from the original quantity of crude zfGIP. The main peaks were collected as represented in Figure 7.1 A. zfGIP was analysed by MALDI-TOF MS which confirmed the purity (Figure 7.1 B and Table 7.1).

7.4.2 zfGIP peptide stability

Human GIP (Figure 7.2 A and B) was degraded by 93% into 2 major fractions after 4 hours incubation with DPP-IV (corresponding to the cleavage at position 2). zfGIP incubated under identical conditions had a greater stability and degraded only by 35% (Figures 7.2 C and D and Table 7.2).

7.4.3. *In vitro* insulinotropic effects of zfGIP

The basal rate of insulin release from BRIN-BD11 cells in the presence of 5.6 mM glucose alone was 1.02 ± 0.02 ng/10^6cells/20 min. Incubation with GLP-1 (0.1 μM) resulted in an increase in the rate of insulin release to 2.4 ± 0.1 ng/10^6cells/20 min.

Incubation of cells with zfGIP (Figure 7.3 A) and human GIP (Figure 7.3 B) produced a concentration-dependent stimulation of insulin release. The minimum concentration showing a significant increase in the rate of insulin release compared with the basal rate) for zfGIP was 30 nM compared with a threshold concentration of 30 pM for human GIP and 10 pM for human GLP-1. The maximum rate of insulin release produced by 3 μM zfGIP was 1.7 ± 0.1 ng/10^6cells/20 min compared with a maximum rate of 3.5 ± 0.1 ng/10^6cells/20 min produced by 3 μM human GIP and 3.6 ± 0.2 ng/10^6cells/20 min produced by 3 μM human GLP-1.

The basal rate of insulin release from 1.1B4 cells in the presence of 16.7 mM glucose alone was 0.08 ± 0.01 ng/10^6cells/20min. zfGIP at concentrations of 10 nM and 1 μM significantly enhanced the rate of insulin release compared with the basal rate (Figure 7.4 A). At 1 μM concentration, the rate of release produced by zfGIP (0.14 ± 0.01 ng/10^6cells/20min) was significantly less than that produced by human GIP 0.20 ± 0.02 ng/10^6cells/20min) and GLP-1 (0.24 ± 0.02 ng/10^6cells/20min).

The basal rate of insulin release from mouse islets in the presence of 16.7 mM glucose control was 9.7 ± 1.3 % of the total insulin content of the islets released in 60 min. zfGIP at 10 nM and 1μM concentrations produced significant increases in the rate of insulin release compared with the basal control (Figure 7.4 B) The effect of 1 μM zfGIP (22.4 ± 0.8% of total insulin released in 60 min) was not significantly different from that produced by 1 μM GLP-1 (20.7 ± 2.5 % of total insulin released in 60 min).

7.4.4 Receptor antagonist studies

The *in vitro* insulinotropic activity zfGIP was significantly decreased when BRIN-BD11 cells were incubated with the peptide in the presence of the GIP receptor antagonist, GIP (6-30) Cex-K40 [Pal] ($P < 0.05$) (Figure 7.5 A) and the GLP-1 receptor antagonist, exendin-4(9-39) ($P<0.001$) (Figure 7.5 B). In contrast, the glucagon

receptor antagonist [desHis1-Pro4-Glu9] glucagon amide had no effect on the insulinotropic activity of zfGIP while significantly ($P < 0.05$) attenuating the response produced by glucagon (Figure 7.5 C).

7.4.5 Effect on zfGIP peptide on cAMP production

In the presence of 200μM IBMX, zfGIP significantly stimulated cAMP production in CHL cells transfected with the human GLP-1 receptor (GLP-1R) at a concentration of 10nM ($P<0.05$) and 1μM ($P<0.001$) (Figure 7.5 A). In marked contrast, human GIP (1 μM) was without effect on cAMP production. Glucagon produced an approximately 3-fold increase in cAMP production in HEK293 cells transfected with the human glucagon receptor (CGCR), but neither zfGIP (10 nM and 1μM) nor human GIP (1 μM) had a significant effect (Figure 7.6 B).

7.4.6 Receptor knock out studies

Wild-type INS-1 cells responded to incubation with 10 nM and 1μM concentrations of GLP-1, glucagon, GIP, and zf GIP with a significant ($P < 0.001$) increase in the rate of release of insulin compared with the rate in the presence of 5.6 mM glucose only (Figure 7.7 A). The increase in rate in response to GLP-1 was abolished in the GLP-1 KO cells, but the stimulatory responses to glucagon, GIP, and zf GIP were maintained (Figure 7.7 B). Similarly, the increase in rate in response to GIP was abolished in the GIP KO cells but not in the cells incubated with GLP-1, glucagon, and zf GIP (Figure 7.7 C).

7.4.7 *In vivo* insulin release studies

Plasma glucose concentrations in overnight fasted mice receiving glucose plus intraperitoneal administration of zfGIP (25 and 75nmol/kg body weight) were

significantly less at 15, 30 min and 60 min compared with animals receiving glucose only (Figure 7.8 A). The integrated response (area under the curve) indicated that the magnitude of the glucose-lowering effect produced by either dose of zfGIP was significantly ($P < 0.01$) less than that produced by 25 nmol/kg GLP-1 and 75nmol/kg (Figure 7.8 B). Concomitant with the lower plasma glucose levels, the concentrations of plasma insulin was significantly greater after administration of 25 nmol/kg zfGIP (30 min) and 75 nmol/kg zfGIP (15 and 30 min) compared with animals receiving glucose only (Figure 7.8 C). The integrated insulin response (Figure 7.8 D) showed that the effect of 75 nmol/kg zfGIP was comparable to that produced by 25 nmol/kg GLP-1 (7 Figure 7.8 D).

7. 4. 8 Time-dependent effects of exendin-4 and zfGIP on feeding in normal mice.

At a concentration of 50 nmol/kg of body weight, exendin-4 (Figure 7.9) exhibited significant ($P < 0.01$ and $P< 0.001$) inhibiting effect on food intake at individual time points (30, 60, 90, 120, 150 and 180 min). In contrast, zfGIP appeared to have no effect on food intake when compared with saline only (Figure 7.9).

7.5 Discussion

The global pandemic of T2DM has mandated a search for new types of therapeutic agent and several long-acting analogues of naturally occurring incretins, particularly derivatives of GLP-1, have already been adopted in clinical practice (Graaf et al. 2016). This study has provided evidence that zfGIP acts as an *in vitro* insulinotropic peptide when incubated with isolated mouse islets and with both rodent- and human-derived clonal β-cells (Figure 7.3 and 7.4). The peptide also exhibits *in vivo* glucose-lowering and insulin-releasing actions when administered to mice after a glucose load

(Figure 7.8). However, the potency and efficacy of zfGIP are appreciably less than those of human GIP and human GLP-1 so that the peptide does not show great potential for development into an agent for treatment of patients with T2DM. Treatment of high fat fed mice with a peptidase-resistant GIP-oxyntomodulin hybrid peptide was shown to lead to beneficial actions on glucose homeostasis and reduction in weight (Bhat et al. 2013). However, administration of 50 nmol/kg body weight of zfGIP to overnight fasted mice did not induce a significant change in cumulative food intake over a 3 h period (Figure 7.9) so that the peptide is unlikely to find application in promoting weight loss in obese patients with T2DM.

Synthetic dual-agonist peptides combining GLP-1 and GIP activities have been studied extensively as potential agents for T2DM therapy [Gault at al 2013 and Finan et al. 2015). The use of selective receptor antagonists has indicated that *in vitro* insulinotropic activity of zfGIP on BRIN-BD11 cells may involve activation of both the GIP and GLP-1 receptors expressed in this cell line. Insulin release elicited by the peptide was slightly but significantly decreased after incubating BRIN-BD11 cells with the GIP receptor antagonist, GIP(6-30)Cex-K40[Pal] and the GLP-1 receptor antagonist, exendin-4(9-39) suggesting that zfGIP acts as a dual agonist at both receptors. The action of the peptide was not antagonised by the glucagon receptor antagonist [desHis1-Pro4-Glu9] glucagon amide suggesting that zfGIP does not target this receptor. Consistent with this conclusion, zfGIP stimulated a significant increase in cAMP production in CHL cells transfected with the human GLP-1 receptor but not in HEK293 cells transfected with the human glucagon receptor.

CRISPR/Cas9-engineered INS-1 cells with GLP-1R and GIPR knockouts have proved to be valuable in characterizing polyagonist peptides with potential for treating patients with T2DM (Nayloe et al. 2016). Consistent with the receptor antagonist

studies, both the GLP-1R KO and the GIP KO cells responded to incubation with zfGIP with an increase in the rate of insulin release whereas the corresponding human peptides were inactive. This result shows that zfGIP is acting as a dual agonist at the GLP-1R and GIPR in INS-1 cells as well as in BRIN-BD11 cells. Our data are consistent with an earlier report by Musson and colleagues (Musson et al. 2009) that zfGIP is able to activate the rat GIP receptor but do not support their conclusion that the peptide is not able to activate the rat GLP-1 receptor. The reason for this discrepancy is difficult to determine as the origin, purity and structure of the zfGIP used in the study of Musson et al. was not reported

A comparison of the primary structure of GIP, GLP-1, and glucagon in zebrafish and human (Figure 7.10 A) demonstrates that evolutionary pressure to conserve the amino acid sequence has been appreciably less in GIP than in the other two hormones. Somewhat surprisingly in view of its proposed interaction with the human GLP-1 receptor, zfGIP shows greater structural similarity to human glucagon (11 amino acid residues) than to human GLP-1 (10 amino acid residues) (Figure 7.10 B). However, the general mechanism of activation of class B G-protein coupled receptors involves binding of the C-terminal domain of the peptide ligand to the extracellular N-terminal domain of the receptor which promotes interaction of the N-terminal region of the ligand with the juxtamembrane domain of the receptor, thereby stimulating intracellular signalling (Hoare et al. 2005 and Kirkpatrick et al. 2012). It is significant, therefore, that zfGIP shares with human/rat/mouse GLP-1 the residues Ala^{2}, Glu^{3} in the N-terminal domain and Lys^{20} and Arg^{30} in the C-terminal domain that are not found in the corresponding glucagon molecule (Figure 7.10).

The findings in this study may represent an example of a more general phenomenon that the exquisite specificity of the G protein-coupled receptors that mediate the

physiological actions of the glucagon family hormones for their ligands that is seen in mammals may have arisen relatively late in evolution. In non-tetrapod vertebrates, the receptors display a lesser degree of selectivity for the peptide, and the hormones may activate multiple receptors. While zfGIP may not activate the human glucagon receptor, it has been shown that it will activate a putative glucagon receptor from the zebrafish (Musson et al. 2013). Previous studies both *in vitro* (O'Harte et al. 2016a) and *in vivo* (O'Harte et al. 2016b) have demonstrated that glucagon from the dogfish *Scyliorhinus canicula* (Elasmobranchii) acts as a dual agonist at both the murine glucagon and GLP-1 receptors. Similarly, a receptor has been identified in the goldfish *Carassius auratus* (Teleostei) that is activated by both goldfish GLP-1 and glucagon and by human GLP-1 and glucagon (Yeung et al. 2002).

To conclude the study has investigated the properties of zfGIP in several mammalian systems in order to assess the potential value of the peptide as a template for development into an agent for the treatment of patients with T2DM. Although outside the scope of the present investigation, it is worthwhile to determine the insulin-releasing and glucose-lowering properties of zfGIP in the zebra fish to gain insight into the physiological role of GIP in teleost species.

Table 7.1 Name, amino acid sequence, acetonitrile gradient, retention time and molecular mass of zfGIP.

Name	Amino acid sequence	Gradient used, % ACN	Retention time, min	Theoretical molecular mass, Da	Observed molecular mass, Da
zfGIP	YAESTIASDISKIVDSMVQKNFVNFLLNQRE	35-70	32	3561.06	3562.00

Table 7.2 Summary of HPLC results of peptide degradation following incubation with DPP-IV.

Peptide	Theoretical Mass, Da	Number of peaks	Observed mass of peaks at 0 hr, Da	Observed mass of peaks at 4 hr, Da	% Degraded at 4 hours
Zebrafish GIP	3561.06	1	3562.00	(1) 3561.3	35
GLP-1	3297.70	2	3297.3	(1) 3297.9 (2) 3090.4	86
Glucagon	3482.80	2	3484.4	(1) 3483.2 (2) 3260.3	24
GIP (1-42)	4982.62	2	4982.2	(1) 4984.0 (2) 4749.0	93

Figure 7.1 (A) Reverse-phase HPLC purification of crude zebrafish GIP peptide using a semi-preparative Vydac C18 column and (B) MALDI-TOF spectra of purified zebrafish GIP

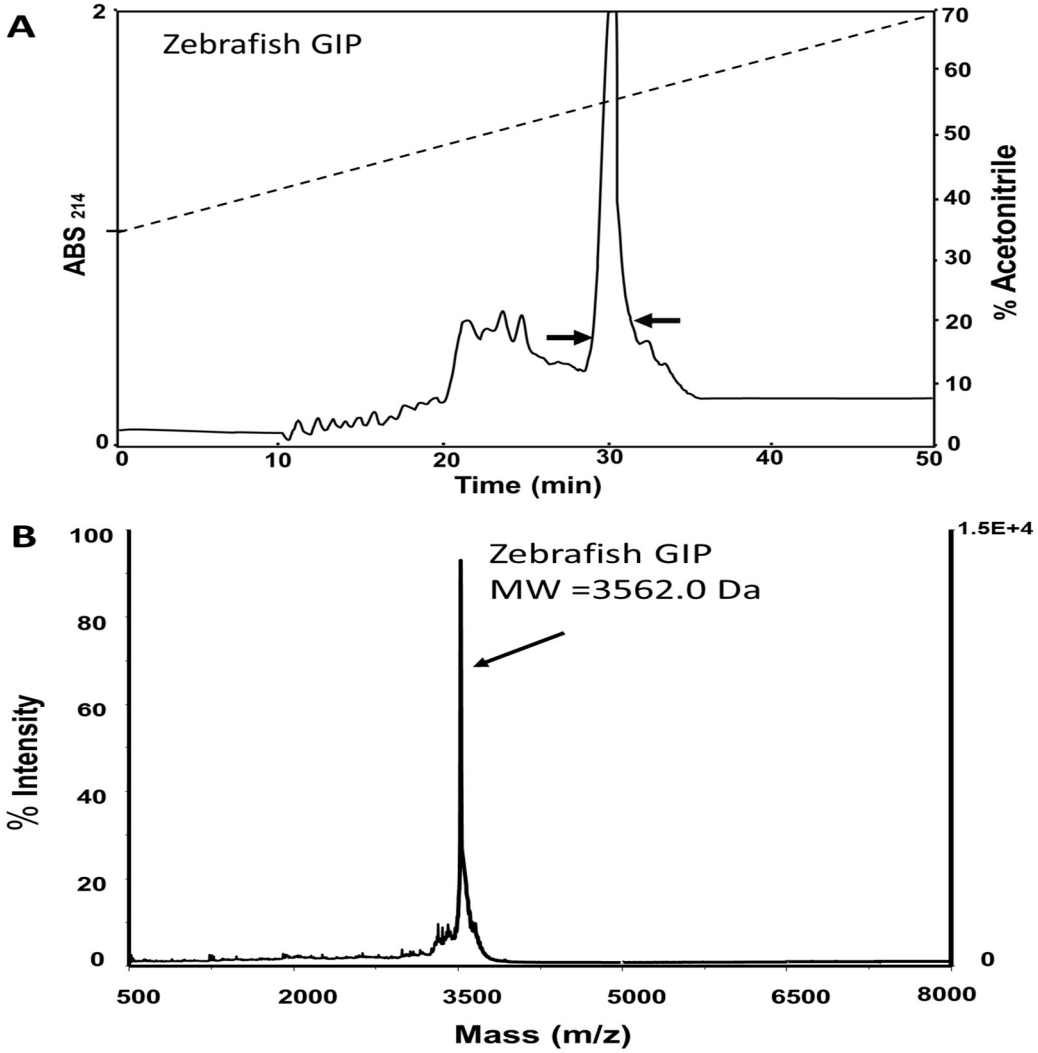

(A) The peptides were dissolved in 30% acetonitrile (3mg/ml) and injected onto a (2.2 cm x 25 cm) Vydac 218TP1022 (C-18) column (Grace, Deerfield, IL, USA) equilibrated with 35% (v/v) and 0.1% TFA/water at a flow rate of 6.0 ml/min. The concentration of acetonitrile in the eluting solvent was raised from 35% to 70 % over 50 min using a linear gradient. Absorbance was measured at 214 nm and the black arrows show where the peak collection began and ended. (B) Purified zfGIP was mixed with α-Cyano-4-hydroxycinnamic acid on a 100 well MALDI plate before inserting into a Voyager DE Biospectrometry workstation. The mass-to-charge ratio (m/z) versus peak intensity was determined.

Figure 7.2 HPLC degradation profile of (A-B) human GIP and (C-D) zf GIP following incubation with DPP-IV for 0 and 4 hour

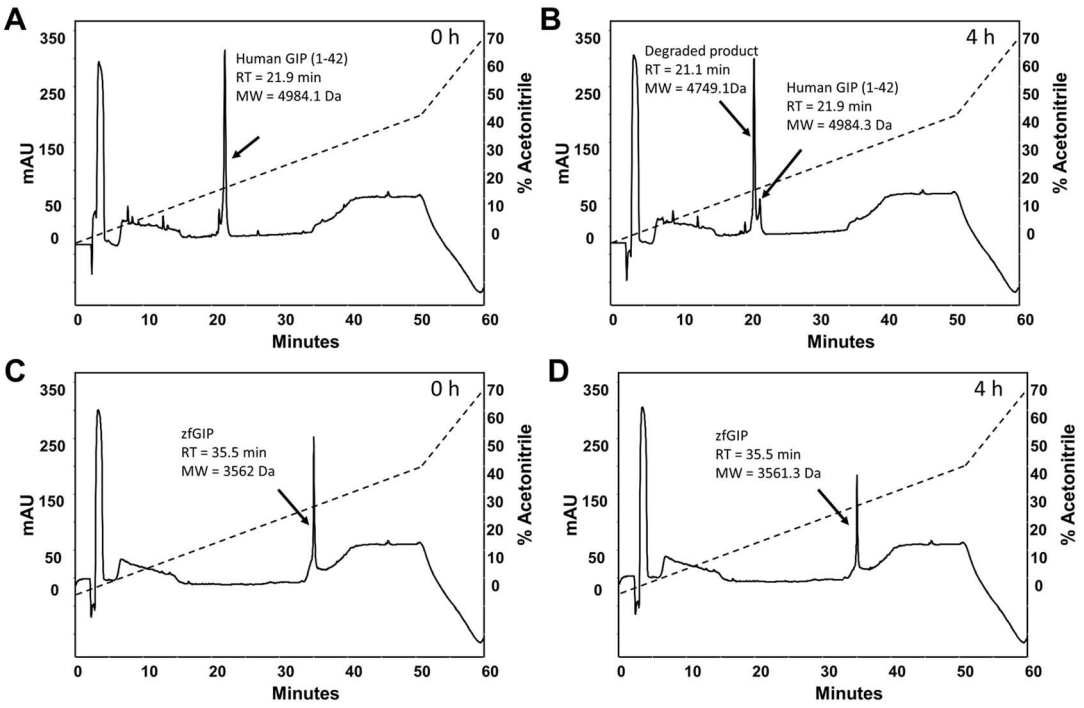

HPLC degradation study was performed with a Luna 5u C8 250x4.6mm column using gradients from 0% to 42% of acetonitrile over 50 min, and from 42% to 70% of acetonitrile over 15 min.

Figure 7.3 Concentration-dependent effects of (A) zfGIP and (B) human GIP on insulin release from BRIN-BD11 rat clonal β- cells.

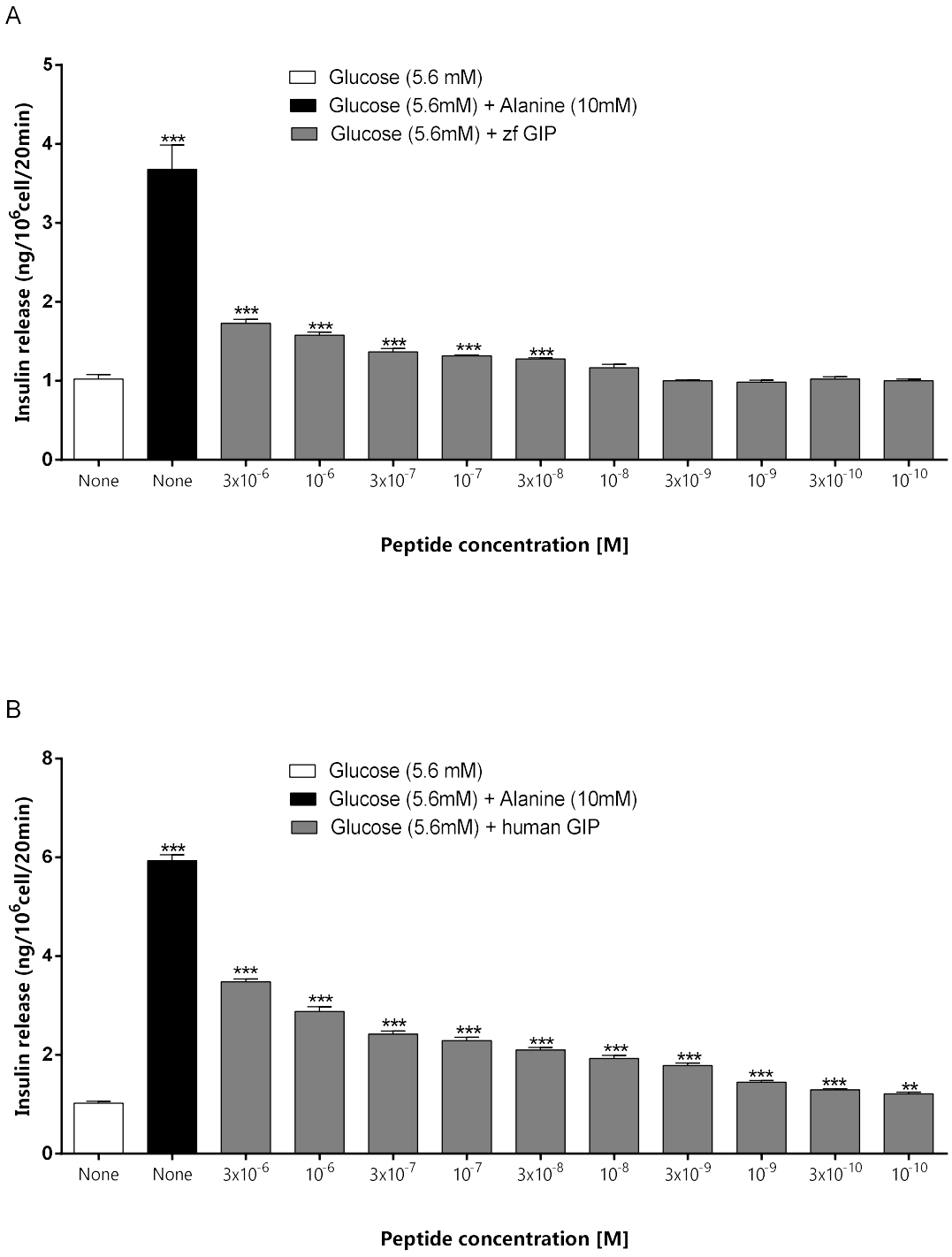

Values are mean ± S.E.M., n = 8. **P < 0.01, ***P < 0.001 compared to 5.6 mM glucose alone

Figure 7.4 Effects of zfGIP on insulin release from (A) human 1.1 B4 cells and (B) pancreatic islets isolated from NIH Swiss mice.

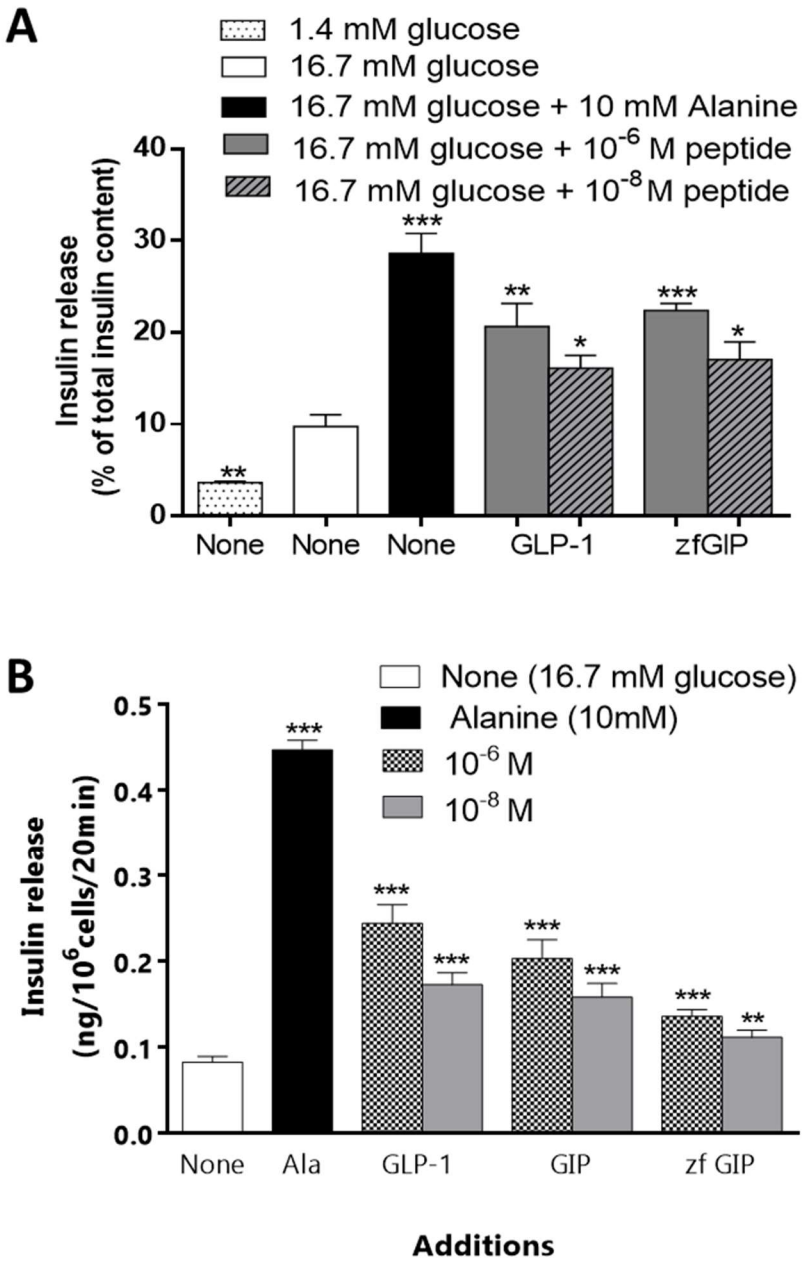

The values are mean ± SEM for n=4; *P<0.5, **P<0.01, ***P<0.001 compared to 16.7mM glucose alone.

Figure 7.5 Effects of (A) GIP receptor antagonist GIP (6-30) Cex-K40, (B) GLP-1 receptor antagonist, exendin-4 (9-39), and (C) glucagon receptor antagonist [desHis1-Pro4-Glu9] glucagon amide on the ability of zfGIP to stimulate insulin release from BRIN-BD11 cells

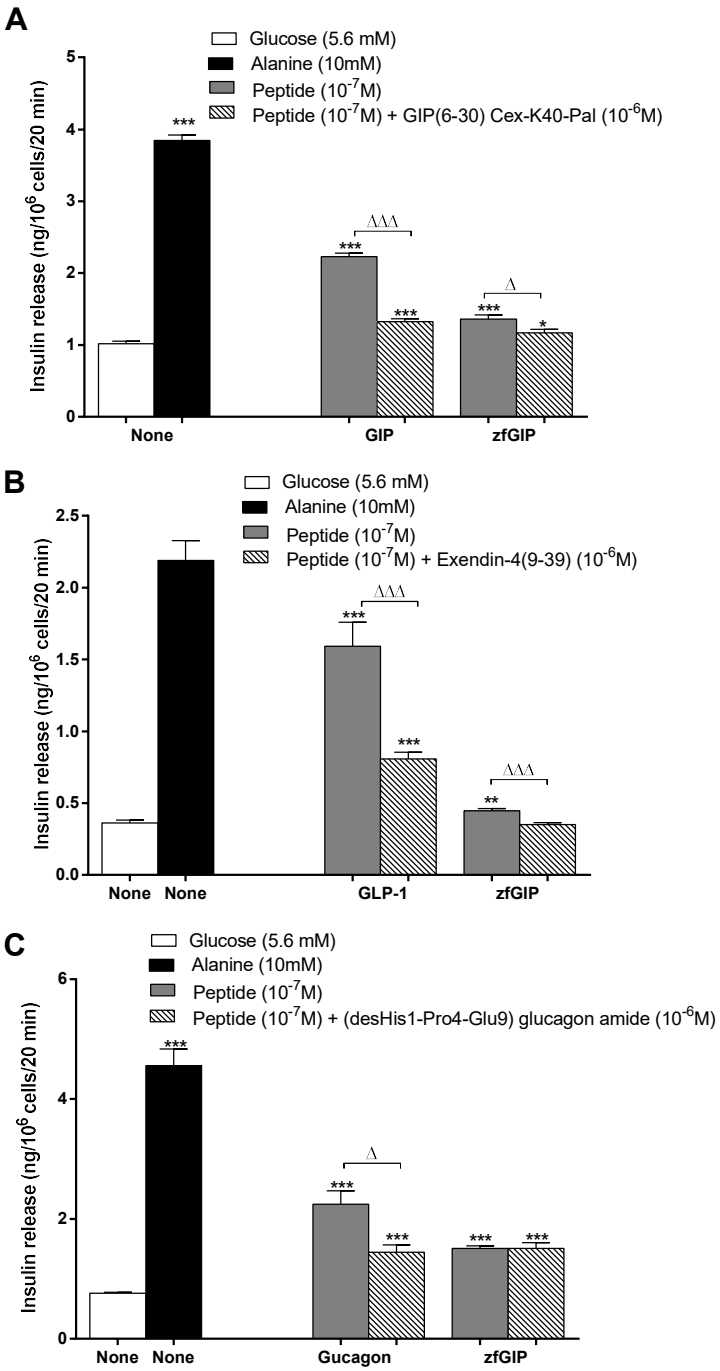

Values are mean ± S.E.M., n = 8 **P < 0.01, ***P < 0.001 compared with 16.7 mM glucose alone. Δ P ≤ 0.05, ΔΔΔp ≤ 0.001 compared with the effect in the presence of antagonist.

Figure 7.6 Effects of zfGIP on intracellular cAMP production in (A) GLP-1 receptor transfected CHL cells, and (B) glucagon receptor transfected HEK293 cells.

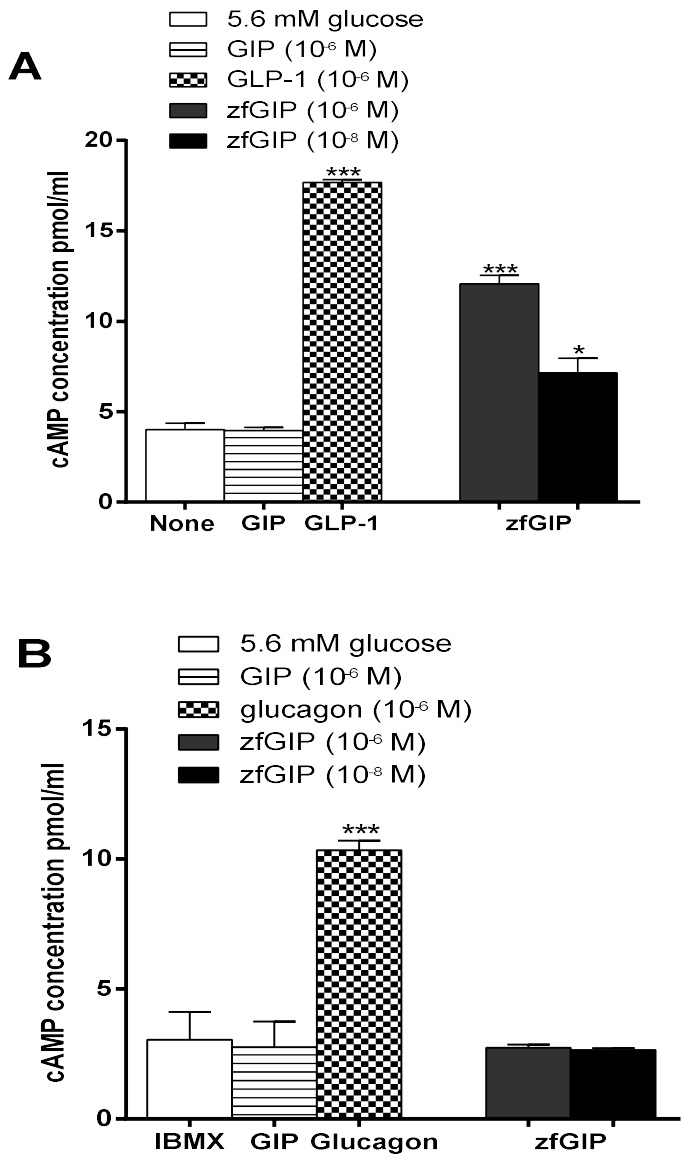

Values are mean ± SEM for N=4. *P<0.05, **P<0.01 and ***P<0.001 compared with 5.6 glucose + IBMX alone.

Figure 7.7 Effects of zfGIP on insulin release from INS-1 cells (A) native (B) GLP-1 receptor knock out (C) GIP receptor knock out cells

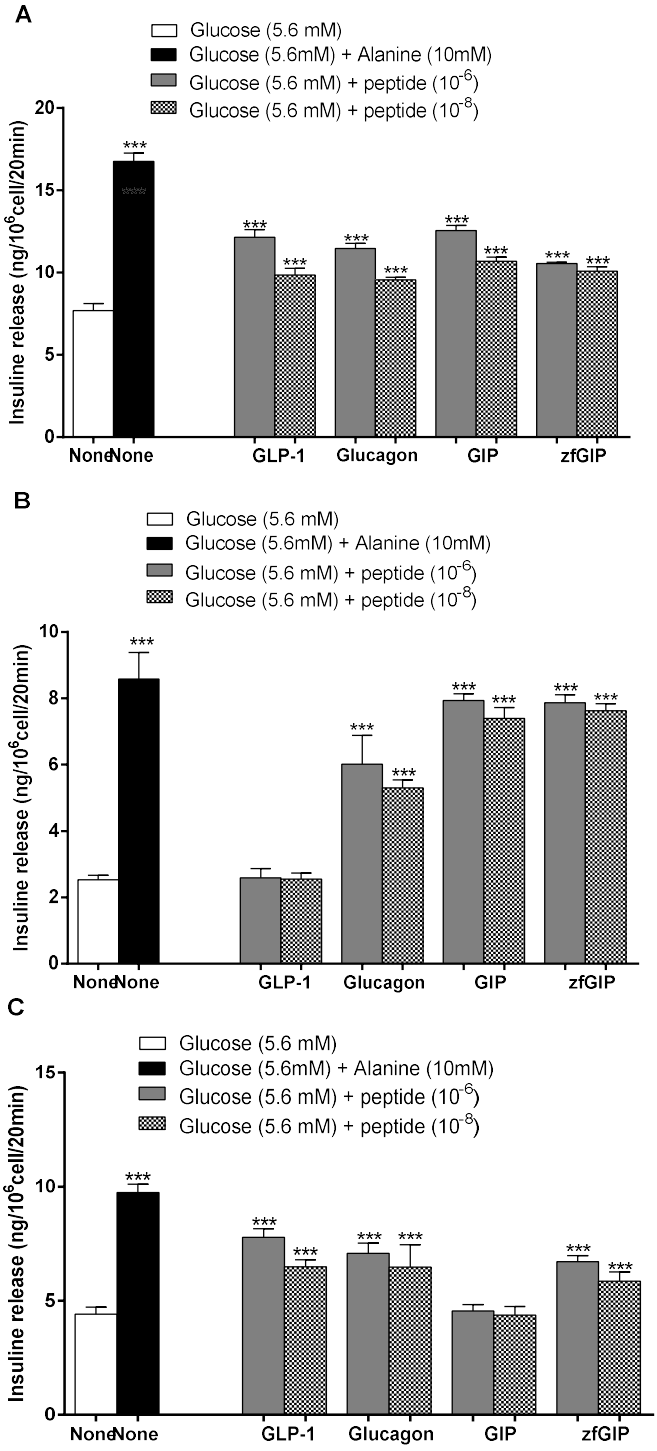

The values are mean ± SEM for n=8; ***P<0.001 compared to 5.6mM glucose alone.

Figure 7.8 Effects of acute administration of zfGIP (25 and 75 nmol/kg body weight) on plasma glucose (panel A) and plasma insulin (panel C) concentrations in mice after intraperitoneal injection of glucose (18 mmol/kg body weight).

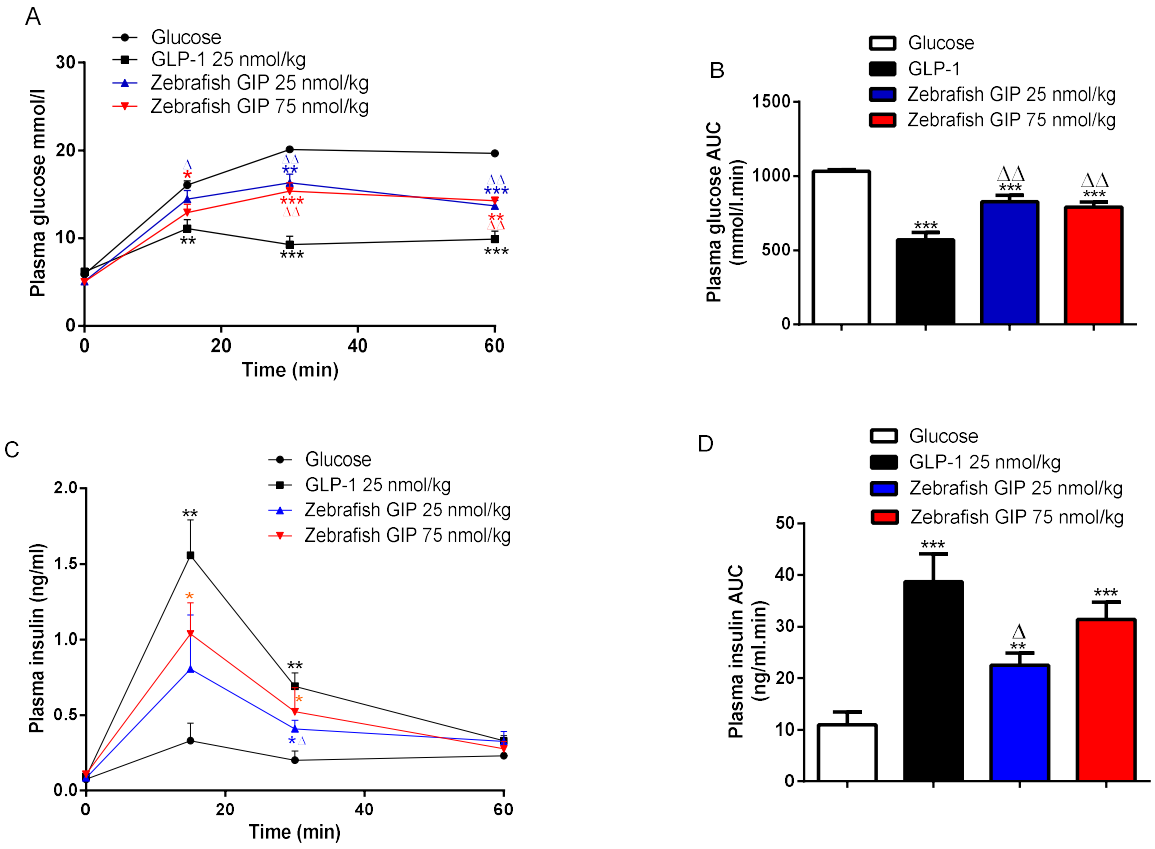

The integrated responses (area under the curve AUC) are shown in panels B and D. The values are mean ± SEM for n=6. **P<0.01 and ***P<0.001 compared to glucose alone; Δ P<0.05, ΔΔ P<0.01 and ΔΔΔ P<0.001 compared to human GLP-1.

Figure 7.9 Effects of zfGIP on cumulative food intake over 3 hours trained feeding in 12 h fasting normal mice.

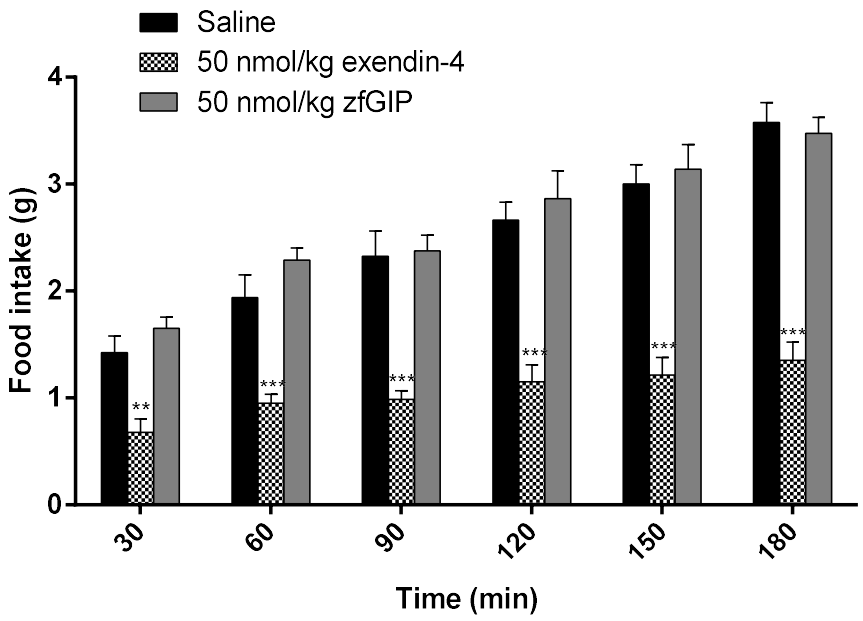

Cumulative food intake was measured after intraperitoneal administration of 50 nmol/kg zfGIP alongside 0.9% saline control. The values are mean ± SEM for n=8. **P<0.01 and ***P<0.001 compared to saline control mice treated at the same time point.

Figure 7.10 Comparison of the primary structures of zebrafish (zf) GIP, GLP-1, and glucagon with the corresponding peptides in the human, and (B) a comparison of the primary structure of zebrafish GIP with human GLP-1 and human glucagon. Sequence identity is denoted by the shading.

A

ZfGIP YAESTIASDISKIVDSMVQKNFVNFLLNQRE

Human GIP YAEGTFISDYSIAMDKIHQQDFVNWLLAQKGKKNDWKHNITQ

Zf GLP-1 HAEGTYTSDVSSYLQDQAAQRFVARLKSGQPKQE

Human GLP-1 HAEGTFTSDVSSYLEGQAAKEFIAWLVKGRG

Zf glucagon HSEGTFSNDYSKYLETRRAQDFVQWLMNA

Human glucagon HSQGTFTSDYSKYLDSRRAQDFVQWLMNT

B

ZfGIP YAESTIASDISKIVDSMVQKNFVNFLLNQRE

Human GLP-1 HAEGTFTSDVSSYLEGQAAKEFIAWLVKGRG

ZfGIP YAESTIASDISKIVDSMVQKNFVNFLLNQRE

Human glucagon HSQGTFTSDYSKYLDSRRAQDFVQWLMNT

Chapter 8

General Discussion

8.1 Diabetes Mellitus is a growing epidemic

Diabetes mellitus (DM) is one of the most common devastating metabolic diseases in nearly all countries, and its incidence continues to increase every year as a consequence of urbanization and economic growth which lead to *lifestyle* modification characterised by reduced physical activity, and high prevalence of obesity (Whiting et al. 2011). DM affects 1 in 11 adults aged 20-75 years (415 million individuals). By 2040 this number is expected to rise to 642 million (Ogurtsova et at 2017, Brandt et al. 2017 and Zheng et al. 2018). An increase in diabetes incidence and prevalence translates into a high economic impact on society affecting both the direct cost of treating the disorder including its complications and indirect costs associated the reduced productivity and the need for informal care (Jonsson et al. 1998 and Hex et al. 2012). In general, diabetic individuals have a higher risk of increased morbidity and mortality than the general population (Ogurtsova et al. 2017). According to Diabetes UK, 1 in 10 hospitalised patients have diabetes and about 15% deaths per year are linked to this condition (Hex et al. 2012). The World Health Organization (WHO) estimated that diabetes killed 1.6 million people in 2016 worldwide, up from less than 1 million in 2000, making it the 6th leading cause of global deaths (World Health Organization, 2018).

There are two main types of diabetes which are often grouped, although associated with distinct causes and costs. Type 1 diabetes (T1D) affects 10–15% of all diabetes cases and is caused by autoimmune damage of insulin-producing pancreatic β cells leading to insulin deficiency (Atkinson et al. 2012; Hex et al. 2012). Type 2 (T2D) diabetes represents 90% of all diabetic patients and is caused by insulin resistance and pancreatic β-cell dysfunction resulting in the insufficient secretion and defective insulin actions (American Diabetes Association 2009; Hex et al. 2012; Kahn et al.

2014; Zheng et al. 2018). The overall direct and indirect costs associated with this disorder were estimated at approximately £23.7bn in 2010/2011 in the UK of which 92% (£ 8.8bn direct and £13.0bn indirect) belonged to T2D.

The costs have been predicted to rise to £39.8bn by 2035/2036 which is approximately 68% greater compared to 2010/2011 and will consume 17% of all NHS budget (Kahn et al. 2014). The growth in diabetes prevalence is driven mostly by rapidly increasing cases of T2D which are closely associated with the dramatic increase in the incidence of obesity over the last three decades (Zhao et al. 2011, Gomes et al. 2013 and Kahn et al. 2014).

8.2 Justification for a new treatment

The loss of glycaemic control and progression of diabetes are believed to be linked to multiple pathophysiological and genetic factors such as impaired β-cell secretion, insulin resistance in peripheral tissues, deficiencies in the secretion of amylin and incretin hormones (particularly GLP-1) and excessive glucagon secretion as well as abnormal expression of genes that control insulin sensitivity and lipid metabolism. The chronic medical condition may also worsen due to inadequate treatment, patient noncompliance, and unhealthy lifestyle associated with obesity (Stonehouse et al. 2007).

Monotherapy with an oral medication, metformin, together with changes to lifestyle is the first line of treatment for adults with T2D and can have beneficial effects on haemoglobin HbA_{1c}, weight and cardiovascular mortality (Wise et al. 2016). However, this treatment option, as well as monotherapy with sulfonylureas, insulin or TZDs, has failed to prevent or slow the loss of β-cell function, according to the United Kingdom Prospective Diabetes Study and the ADOPT trial, and therefore become less

effective at maintaining glycaemic control over time. Therefore, many patients eventually require combined treatment to manage the condition. This, indeed, improves glycaemic control but also carries a potential risk of side effects such as weight gain associated with sulfonylurea and insulin combined therapies or gastrointestinal and oedema concerns linked to metformin and TZDs respectively (Stonehouse et al. 2007). Although newer therapeutic options, such as alpha-glucosidase inhibitors, meglitinides, amylin agonists, GLP-1 mimetics, DPP-IV inhibitors, colesevelam, bromocriptine, and most recently, SGLT2 inhibitors, are available in the market, nearly half of the population are not meeting glycaemic goal showing that the number of individuals with poor glycaemic control has not greatly decreased over the past decades (Mazzola 2012 and Cavaiola et al. 2017, Ambery et al. 2018).

None of these newer therapies exhibit similar effects as that of bariatric surgery – one of the breakthroughs in diabetes care (Laiteerapong et al. 2010 and Ambery et al. 2018). The procedure results in subsequent weight loss and normalises hyperglycaemia in >80% of patients. Moreover, it has been shown to obviate the necessity for antidiabetic drugs in up to 45% of individuals after 60 months of treatment. However, access to bariatric surgery is often limited by the health care system. As a result, more than one million individuals with morbid obesity who could potentially benefit from the procedure do not fall within the criteria (Gulliford et al. 2017). The surgery is also associated with high costs and increased risks of side effects which makes it not a viable option for most patients (Ambery et al. 2018).

Hence, new alternative research is urgently required to discover new therapeutically potent agents which could maintain glucose homeostasis, improve long-term

microvascular and neuropathic complications of diabetes, as well as have no associated side effects and be economically viable.

8.3 Unimolecular GLP-1/Glucagon Co-agonism: improvement of obesity-associated diabetes.

There has been growing evidence that sustained and moderate weight loss (>5% of initial body weight) in overweight or obese individuals with T2D results in successful outcomes of their metabolic status such as improved glycaemic control and cardiovascular risk markers (Ambery et al. 2018).

Although low carbohydrate diets in people with T2D are known to be effective for the short term improvements (Dyson 2015), the antidiabetic effects of bariatric surgery, specifically Roux-en-Y gastric bypass surgery, are not only related to the reduction of weight alone (Ambery et al. 2018). Bariatric surgery is associated with modification of secretion and action of some gut hormones and peptides (Kaska et al. 2016). This includes suppression of ghrelin, a 'hunger hormone' known to stimulate appetite and activation of incretin hormones secretion (such as GLP-1 and oxyntomodulin) resulting in the reduction of body weight. GLP-1 not only enhances glucose-induced insulin secretion from pancreatic β-cells but also slows gastric emptying, and promotes weight loss via central effects on appetite and satiety (Yamagishi et al. 2011 and Ambery et al. 2018).

Oxyntomodulin, a natural proglucagon-derived peptide that interacts with both the GLP-1 and glucagon receptors, also drives the reduction of weight similarly to GLP-1 in human and rodents but acts through an additional alternative pathway responsible for increasing energy expenditure (Li et al. 2017; Ambery et al. 2018).

Despite the known pathophysiological action of glucagon to increase hepatic glucose output in T2D, oxyntomodulin is believed to exhibit promising effects on glycaemic control and weight via the equipoise of GLP-1 and glucagon receptor agonist activity. The mechanism of action of oxyntomodulin supports the application of dual agonism in the treatment of obesity (Tillner et al. 2018). Despite many advantages as a therapeutic agent, oxyntomodulin is rapidly degraded in plasma. However, recently developed stable oxyntomodulin-based analogues with specific N-terminal position 2 modifications to protect against DPP-IV degradation, have been recently reported to show beneficial insulin secretory effects *in vitro* and improve glycaemic control, insulin secretion and appetite suppression in normal mice (Lynch et al. 2014). Moreover, long-acting analogues derived from dogfish glucagon have been recently demonstrated to act as GLP-1/glucagon receptors co-agonists with promising *in vitro* and *in vivo* results (O'Harte et al. 2016). A novel GLP-1/glucagon hybrid peptide with triple acting agonist activity at GLP-1, glucagon and GIP receptors has also been reported (Gault et al. 2013).

Clinical trials evaluating the safety, pharmacokinetics and pharmacodynamics of novel GLP-1/glucagon receptor dual agonists, highlighted the potential of these agents to reduce body weight and blood glucose in obese or overweight individuals with T2D (Ambery et al. 2018 and Tillner et al. 2018).

8.4 Exploring fish glucagon-like sequences as naturally occurring dual agonists

More than half of the 66178 species of living vertebrates are "fishes", which exhibit remarkable diversity in anatomy, morphology, physiology, behaviour trait, reproductive biology, and ecology together with their equally impressive habitat diversity (Helfman et al. 2009; Broughton et al. 2013; Ceballoset at al. 2015; Nelson

et al. 2016). Fish may be the most diverse vertebrate group, mostly to due to teleosts comprising about 96% of all extant fish species (Miya et al. 2015). Amphibians, reptiles, birds and mammals evolved after fish showing their importance in fundamental areas of vertebrate biology and evolution (Broughton et al. 2013)

Considerable differences exist between fishes and other vertebrates in proglucagon gene structure, peptide expression, peptide chemistry, and functional characteristics of the hormones produced (Plisetskaya et al. 1996).

In this thesis, insulinotropic and antihyperglycaemic properties of fish proglucagon-derived and GIP peptides were examined. Chapter 3 presents details of the structural analysis and acute *in vitro* and *in vivo* assessment of biological properties of GLP-1 peptides isolated from six different types of fish ranging from phylogenetically ancient to most recently evolved species: sea lamprey, dogfish, ratfish, paddlefish, bowfin and trout. Similar studies are shown in Chapter 4 using piscine glucagon peptides. Chapter 5 and 6 reveals long-acting proglucagon and GLP-1 analogues derived from the native lamprey and paddlefish glucagon and GLP-1 sequences. Finally, Chapter 7 presents zebrafish GIP peptide as *in vitro* dual agonist for glucagon and GLP-1 receptors.

8.4.1 Proglucagon-derived Peptides from the Agatha Superclass member (Sea Lamprey)

Lampreys, the most ancient extant vertebrates belonging to the lineage of jawless fish of the order Petromyzontiformes, express glucagon and GLP-1 only in the intestine while their endocrine pancreatic tissue appears to be devoid of glucagon-secreting α-cells (Youson et al. 1989 and Plisetskaya et al. 1996). Two proglucagon cDNAs from the intestine of the sea lamprey *Petromyzon marinus* were previously characterised

(proglucagon I and proglucagon II). Proglucagon I cDNA encodes the previously purified and characterised glucagon and GLP-1, while proglucagon II cDNA encodes a predicted GLP-2 and glucagon (Irwin et al. 1999)

Glucagon and GLP peptides, encoded by proglucagon I, were isolated and purified from sea lamprey *Petromyzon marinus* intestine in 1993 (Conlon et al. 1993). Lamprey glucagon, a 29 amino acid peptide, showed 72% and 57% sequence identity with human glucagon and GLP-1 respectively. In total 8 amino acid sequence substitutions were identified when compared lamprey with human glucagon, one of which, COOH-terminal alanine residue represents a novel structural feature that was not previously observed in the sequences of glucagon of other known species (Conlon et al. 1993). Lamprey GLP-1, a 32 amino acid peptide, appeared to be different from human GLP-1 and exhibited 16 amino acid substitutions (50 % sequence identity). The physiological roles of glucagon and GLP-1 in lampreys are poorly understood (Conlon et al. 1993). Glucose administration does not invoke insulin release in lampreys (Norris et al. 2013), and injections of mammalian glucagon had no initial effect but lowered blood glucose after 4 h post administration (Conlon et al. 1993).

In this study, the *in vitro* assessment of lamprey GLP-1 (Chapter 3) and glucagon (Chapter 4) showed that these peptides produced a significant dose-dependent stimulation of insulin-release from clonal pancreatic beta-cells, BRIN-BD11. The peptides also increased the rate of insulin release from human-derived pancreatic beta-1.1 B4 cell line and isolated mouse islets similarly to human GLP-1. The mechanism of action of the peptides was examined using potent glucagon, GLP-1 GIP antagonists, as well as various cell lines: CRISPR/Cas9-engineered glucagon-R and GLP-1R-transfected cells, and glucagon-R KO, GLP-1R KO and GIPR KO INS-1 cell lines.

The study revealed that both, glucagon-R GLP-1R were involved in the biological action of the peptides.

Acute in vivo actions of the peptides on glucose tolerance and food intake were assessed in normal mice. Intraperitoneal administration of the peptides together with glucose load showed a significant decrease in blood glucose and increased in plasma insulin levels. However, the peptides were ineffective when administrated prior a glucose load due to rapid plasma degradation which was confirmed by DPP-IV studies. No effect on food intake was observed for lamprey glucagon in normal mice. However lamprey GLP-1 suppressed the appetite at 30 min time point after peptide administration.

The potent antihyperglycaemic and insulinotropic effects of peptides, as well as their possible dual-agonist ability, distinguish them as candidates for developing into antidiabetic agents and were selected for designing long-acting analogues for further studies (Chapter 6 and 7). The amino-acid sequence substitutions that arose over 500 million years observed in the proglucagon-derived peptides have been fixed in the population giving advantages for the species and may be exportable for the therapeutic use.

8.4.2 Proglucagon-derived Peptides from Cartilaginous fishes: Dogfish and Ratfish

Only one sequence of proglucagon gene is found in Cartilaginous fishes (Ng et al. 2010). Glucagon of the primitive fishes such as representative species belonging to the Elasmobranchii subclass (i.e. dogfish) which in terms of evolution represent a

"dead-end side branch", have greater sequences similarities to human glucagon than do glucagons of teleost fishes.

Three peptides derived from the post-translational processing of proglucagon have been isolated from the pancreas of dogfish (*Scyliorhinus canicula*): glucagon (29 amino acids), GLP-1 (38 amino acids) and oxyntomodulin, originally reported as a second version of dogfish glucagon, G-33 (33 amino acids) (Conlon et al. 1993). Dogfish glucagon represents the 29 amino acid residue which was also previously isolated from the intestine (Conlon et al. 1987). The intestinally-derived version of glucagon contained one amino acid substitution at the position 28 compared to its pancreatic version, however it was later reported as an error leading to the conclusion that only one version of glucagon existed in both intestine and pancreas of dogfish (Conlon et al. 1993). The –KRNG extension in the COOH-terminal region in the dogfish oxyntomodulin is similar to the corresponding region in the 37 amino acid residue sequence of mammalian oxyntomodulin (Conlon et al. 1993). Comparison of the primary structures reveals that dogfish glucagon shares three amino acid residues (Glu^{3}, Tyr^{13}, and Lys^{20}) with human GLP-1 that are not found in human glucagon (Conlon et al. 1993 and O'Harte at al. 2016). Previous studies using dogfish glucagon and its derived analogues showed that dogfish glucagon is a potent glucagon/GLP-1 receptor co-agonist in vitro and in vivo (O'Hare at al 2016 and O'Hare at al 2016a).

The structure of dogfish GLP-1 is most similar to GLP-1 sequence from the ratfish, particularly with regard to the unusual substitutions at position 26 and 29 (Trp26 –Ser) and (Gly29–Tyr). The latter substitution is known to represent a site of proteolytic processing of proglucagon in the dogfish GLP-1 domain but not the ratfish (Conlon et al. 1993).

In ratfish, 2 forms of GLP-1 molecules exist due to the same proglucagon gene undergoes different post-transcriptional processing. This results in the generation of two structurally identical peptides one of which has an additional C-terminally extended sequence –RRM (Conlon et al. 1989). The ratfish proglucagon gene additionally encodes oxyntomodulin (originally reported as an extended version of ratfish glucagon) which shows 69% homology with human glucagon (Conlon et al. 1987). The C terminal extension sequence of ratfish oxyntomodulin has very little resemblance with the C-terminal region of mammalian intestinal oxyntomodulin (4 out of 8 matches). It is proposed that this peptide represents a major storage form of the 29-residue glucagon found in the islets (Conlon et al. 1987).

The acute the *in vitro* and *in vivo* examination of GLP-1 from dogfish and ratfish is shown in Chapter 3, whereas the results for oxyntomodulins are presented in Chapter 4. All four peptides derived from cartilaginous fishes showed dose-dependent stimulation of insulin release from BRIN-BD11. Dogfish oxyntomodulin appeared to be the most potent peptide in this peptide quartet. The promising insulinotropic activity of this peptide was also confirmed in 1.1 B4 cells and isolated mouse islets. The effects of dogfish oxyntomodulin resembled the action of human GLP-1. However, the action of dogfish oxyntomodulin was attenuated in the presence of glucagon and GLP-1 receptor antagonists ([desHis1-Pro4-Glu9]glucagon amide and exendin 9-39 respectively). Moreover, the cAMP release was observed in both glucagon and GLP-1 receptor transfected cells incubated with dogfish oxyntomodulin.

Acute in vivo studies revealed that among other proglucagon-derived peptides from cartilaginous fishes used in this study, only administration of dogfish oxyntomodulin together with a glucose load significantly decreased blood glucose and increased

plasma insulin levels in normal mice compared with the control animals which received glucose alone. All peptides ware subject of DPP-IV degradation at position 2 which corresponded to the sides of degradation of human glucagon and GLP-1 peptides.

Although divergence of elasmobranchs and holocephalans at least 300 million years ago, dogfish GLP-1 is most similar to GLP-1 from the ratfish compared to other species. This also reflected their similar less potent effects on insulin release *in vivo* and *in vitro* with no dual agonist ability detected in this study. On the other hand dogfish, oxyntomodulin was distinctively better than oxyntomodulin from ratfish which appeared to act only via GLP-1 receptor. Thus, dogfish oxyntomodulin represents an excellent dual receptor agonist candidate for further diabetes research.

8.4.3 Proglucagon-derived Peptides from Phylogenetically Ancient Actinopterygii: Paddlefish and Bowfin

The North American paddlefish, *Polyodon spathula* and the Chinese paddlefish, *Psephurus gladius* are the two living species of family Polyodontidae, the most primitive basal ray-finned fish. (Lenhardt et al. 2006). Paddlefish are closely related to the family of sturgeons (Acipenseridae). Although these two families are distinct from one another, they are frequently classified together as Chondrosteans (Nguyen et al. 1994). Paddlefish is a plankton filter-feeder and has one of the most complex digestive tube present in fishes (Weisel 1973). The pancreatic tissue of paddlefish shows the presence of some diffusion within the wall of the gut and lacks distinct segregation between pancreatic islets and the exocrine compartment. Two forms of glucagon and one molecule of GLP-1 were purified from paddlefish pancreas. Both of the paddlefish glucagon molecules contain 31 amino acid residues and show unique

structural substitutions, such as Met^{5}, Glu^{24} and Gly^{29}, not previously observed in glucagons from other species (Nguyen et al. 1994). Paddlefish glucagon also contains the segments Glu^{15}-Glu^{16} and Glu^{24}-Trp^{25}-Leu^{26}-Lys^{27}-Asn^{28}-Gly^{29} in common with GLP1R agonist, exendin-4 that are not found in the other fish peptides. Paddlefish GLP-1 appeared to be structurally similar to gar GLP-1 and shares 65% and 45% of structure similarity with human GLP-1 and glucagon respectively. In contrast, GLP-1 from bowfin, a surviving representative of a group of primitive ray-finned fishes, appeared to have an unusual structure resembling GIP due to the presence of a tyrosine residue at position 1 instead of the histidine residue that is found in all other proglucagon-derived peptides so far characterized (Conlon et al. 1993). Bowfin GLP-1 exhibited lesser glycogenolytic response than human GLP-1 (3-fold less effective) in dispersed hepatocytes from a teleost fish. It is known that the effectiveness of salmon GLP-1, in the same experiment, was similar to the effects of human GLP-1. The mechanism by which GLP-1 triggers glycogenolysis (and gluconeogenesis) in the fish liver is unknown (Conlon et al. 1993).

In terms of insulinotropic activity, paddlefish GLP-1 was more effective compared to bowfin GLP-1 ad shown in Chapter 3. Paddlefish glucagon also showed stimulation of insulin secretion from BRIN-BD11, 1.1B4 and isolated mouse islets. The secretion of insulin was suppressed to various extents after incubation of paddlefish GLP-1 and glucagon antagonists in the presence of glucagon and GLP-1 receptor antagonists ([desHis1-Pro4-Glu9] glucagon amide and exendin 9-39 respectively) but not by GIP receptor antagonist (Pro^{3}GIP). The peptides also evoked cAMP responses in glucagon and GLP-1 receptor transfected cells. The rates of insulin secretion were attenuated in glucagon and GLP-1 receptor KO cells incubated with paddlefish glucagon and GLP-

1. In contrast, the effects of bowfin GLP-1 were partially antagonised by GLP-1 and GIP receptor antagonists and significantly attenuated in GLP-1 and GIP KO cell lines.

Paddlefish GLP-1 and glucagon were equally effective in lowering blood glucose and stimulating insulin release according to acute IGTT study results. Bowfin GLP-1 exhibited weak insulinotropic and glucose-lowering *in vivo* effects. Out of all peptides, paddlefish glucagon was the most effective in suppressing appetite in normal mice the concentration of 25nmol/kg of body weight. The peptide was also less susceptible to DPP-IV degradation after 4 h incubation with the enzyme. Due to its unique structure with 15 amino acid substitutions similar to exendin-4, paddlefish may be regarded as a naturally occurring glucagon/exendin-4 hybrid peptide with dual agonist activity at the glucagon and GLP-1 receptors. A previous study reported that twice-daily administration of the hybrid peptide [S2s]glucagon-exendin-4 (31-39) resulted in a significant improvement of body weight, energy intake and non-fasting glucose parameters, accompanied by improved glucose tolerance and insulin sensitivity (Lynch et al. 2014). Naturally occurring paddlefish glucagon structure with a unique exendin-4-like substitutions could be used as a template for developing a potential therapy for type 2 diabetes. Paddlefish glucagon and GLP-1 were selected for designing novel analogues for further investigation shown in Chapter 5 and 6.

8.4.4 Trout proglucagon-derived peptides

Rainbow trout (*Oncorhynchus mykiss*) is a species of the *Salmonidae family belonging* to a basal teleost Protacanthopterygii sub-order (pikes and salmons) group that is of major ecological interest worldwide (Berthelot et al. 2014 and Wang et al. 2018). All teleosts share at least three rounds of complete or whole-genome duplication: 1R before and 2R after the divergence of lamprey from the gnathostome which is

estimated at 500–430 million years ago and a third teleost-specific (Ts3R) at the base of the teleosts ~320 million years ago (Panopoulou et al. 2005 and Berthelot et al. 2014). The whole genome duplication events are rare within animal lineages and bear evolutionary importance for the divergence of some major lineages. Only a small proportion of genes are eventually retained after this process whereas redundant copies are inactivated in a poorly understood process known as gene fractionation.

An additional and relatively recent the salmonid-specific whole genome duplication (the Ss4R autotetraploidization event) occurred 25 to 100 million years ago. Due to gene fractionation may still be ongoing in the *Salmonidae family members (Rainbow trout)*, understanding their genome structure and the factors that influence the rediploidization process are of particular interest for the research (Bobe et al. 2016).

While most teleosts have 2 proglucagon sequences (proglucagon *a* and proglucagon *b*), Salmonid fishes are known to have more than two (at least four) genes encoding proglucagon sequences as a consequence of the Ss4R (Irwin et al. 1995 and Irwin et al. 2018).

The assessment of *in vitro* insulinotropic effects of trout GLP-1 and glucagon is shown in Chapter 3 and Chapter 4 respectively. Trout GLP-1 exhibited greater insulinotropic effects in BRIN-BD11, 1.1 B4 and isolated mouse islets compared to trout glucagon. According to of the receptor studies using glucagon, GLP-1, and GIP receptor antagonists, receptor transfected cells, as well as KO cell lines, the effect of trout GLP-1 is mediated predominantly via interaction with the GLP-1 receptor and the effect of trout glucagon via activation of glucagon receptor. Although trout GLP-1 showed potent insulin-releasing activity in *vivo* and *in vitro* studies using normal mice, the

magnitudes of the maximal responses appeared to be less than those of paddlefish and lamprey GLP-1.

As a result of whole genome duplication, the trout genome contains a second proglucagon gene that encodes a GLP-1 and glucagon compared with the peptides used in this study (Irwin et al. 1995). The insulinotropic activity of these paralogues has yet to be determined.

8.4.5 Zebrafish GIP

The zf GIP gene and precursor protein appeared to be shorter compared to other vertebrate GIP genes and is missing exon 5. This results in the production of a short GIP hormone (only 31 amino acids) in zebrafish. This length is closely matching the length of proglucagon-derived hormones which may suggest that zfGIP genes (like other vertebrates) may have arisen from the ancestral gene as a result of evolutionary events, however, in tetrapods, GIP has been additionally extended (Irwin et al. 2006).

The amino acid sequence of zfGIP shares with human/rat/mouse GLP-1 the residues Ala^{2}, Glu^{3} in the N-terminal domain and Lys^{20} and Arg^{30} in the C-terminal domain which is responsible for binding of the N-terminal domain of the receptor. Chapter 7 investigates insulinotropic effects of zfGIP in a mammalian system. In vitro, zfGIP produced concentration dependent stimulation of insulin release from BRIN-BD11 cells. However, the potency and efficacy of zfGIP were noticeably less than those of human GIP and human GLP-1. The stimulatory effects of zfGIP were inhibited in the presence of GLP-1R and GIPR antagonists suggesting that the peptide acts as a dual agonist at both receptors. Further studies using receptor transfected and receptor KO cells corresponded with this result. The in vivo insulinotropic and glucose-lowering

effects of zfGIP were lesser than that of human GLP-1. The peptide was also not effective in suppressing appetite in normal mice. Thus, zfGIP peptide is unlikely to find application in promoting weight loss in obese patients with T2DM

8.4.6 Long-acting analogues derived from piscine glucagon and GLP-1 sequences

Many pathological conditions such as metabolic syndrome, obesity and diabetes cannot be sufficiently treated with a single drug strategy. The therapeutic benefits of monotherapy often coincide with an increased prevalence of unwanted adverse-effects. On the other hand, the co-administration of several independent drugs such as phentermine and topiramate to treat obesity and obesity-associated metabolic syndrome and diabetes, although showing remarkable effects on metabolism, is also not without risk. However, in the last decade, the biopharmaceutical industry has made notable progress in the development of molecules with enhanced metabolic potential whose structures represent a single entity derived from the combination of multiple key metabolic hormones. The concept of these unimolecular multiagonists is based on the ability of a single molecule simultaneously activate different signalling pathways resulting in more balanced pharmacokinetic action profile compared to loose co-administration of single hormones (Brandt et al. 2018).

Pre-clinical *in vivo* studies showed that dual glucagon/GLP-1 receptor agonists produce greater weight loss when compared to selective GLP-1R agonists such as gold standard liraglutide. The impact on body weight is due to significant suppression of appetite but may also involve increased energy expenditure. Humans studies also showed that the concomitant activation of GLP-1R protects from the potential metabolic risk and hyperglycaemic effects of GCGR activation (Elvert et al. 2018).

In this thesis, Chapter 5 and 6 present novel dual glucagon/GLP-1 receptor agonists, namely [D-Ser^2]-lamprey glucagon-Lys^{30}-gamma-glutamyl-pal, [D-Ser^2]-paddlefish glucagon-Lys^{30}-gamma-glutamyl-pal, [D-Ala2]-lamprey GLP-1-Lys^{31}gamma-glutamyl-pal and [D-Ala^2]-paddlefish GLP-1-Lys^{28}-gamma-glutamyl-pal, that were generated by using the primary structure of naturally occurring proglucagon-derived peptides from lamprey and paddlefish. All 4 analogues were resistant to metabolic degradation after 4 h incubation with mouse plasma or DPP-IV.

In vitro, insulinotropic effects of analogues assessed in this study using BRIN-BD11 cells and isolated mouse islets showed that the peptides produced a significant stimulation of insulin release. However, the effects of lamprey glucagon and paddlefish GLP-1 analogues were significantly less compared to the insulinotropic effects of native peptides. Incubation of peptides with receptor KO cells confirmed that the peptides retained the ability to activate bot glucagon and GLP-1 receptor which was also confirmed by the cAMP assay. Acute *in vivo* studies revealed that lamprey GLP-1 and paddlefish glucagon analogues were the most potent out of four peptides in glucose tolerance and food intake studies and exhibited long-acting glucose-lowering effects similar to exendin-4. Long-term benefits of analogues derived from lamprey GLP-1, paddlefish glucagon and paddlefish GLP-1 were assessed in mice with diet-induced obesity-diabetes. The results showed that a 21 days twice-daily administration of lamprey GLP-1 and paddlefish glucagon analogues significantly improved glucose tolerance and enhanced insulin sensitivity and secretion. The peptides administration also significantly reduced body weight, exhibited profound effects on biochemistry profiles and noticeably improved insulin secretory response of isolated islets from pre-treated mice and a reduced α-cell area indicating positive effects on islet function. Promising effects of the peptides on islet

transdifferentiation were also observed in GluCreRosa26-YFP mice. Thus, lamprey GLP-1 and paddlefish glucagon could be viewed as potential candidates for possible development of antidiabetic treatment.

8.5 Future studies

This thesis presented data on *in vitro* and *in vivo* insulin-releasing effects of native glucagon-related peptides from phylogenetically ancient fishes and teleosts as well as and four novel analogues derived from lamprey and paddlefish glucagon and GLP-1 which activate glucagon and GLP-1 receptors. Following future studies are essential:

1. Investigation of plasma and DPP-IV degradation of peptides for 8, 12 and 24 hours or more.
2. Dose-dependent cAMP studies.
3. Glucose uptake studies using the established pre-adipose 3T3-L1A cell line.
4. Studies of receptor specificity of peptides and their analogues using double/triple glucagon-r-KO, GLP-1r-KO and GIPr-KO mice.
5. Long-term (21, 28, 51 days) studies using *db/db* mice.
6. Receptor binding studies using RIA.
7. Designing of more structurally modified analogue based on the sequences of most promising native fish peptides.
8. Gene expression studies (intestine, adipose, liver, kidney, muscle, brain and other tissue), possibly using microarray techniques.
9. Testing of peptides and their analogues in the species of origin.
10. Western blot studies for protein expression.
11. Evaluation of toxicity, pharmacokinetics and efficacy in humans with T2D.

8.6 Concluding remarks

To summarise, this thesis demonstrated that proglucagon-derived peptides from the phylogenetically ancient fish act as dual agonists *in vitro* activating both GLP-1 and glucagon receptors. The peptides demonstrated promising insulinotropic and glucose-lowering *in vivo* activity. Based on these observations long-acting analogues were designed. Lamprey and paddlefish proglucagon-derived analogues were enzymatically resistant and exhibited positive effects on body weight, pancreatic beta cell function and insulin resistance in high fat fed mice. Positive effects on islet morphology were also observed in streptozotocin-induced model of type 1 diabetes. This research, demonstrating the concept of how naturally occurring molecules with evolutionary favourable sequence substitutions could be employed as unimolecular multi agonists for the treatment of metabolic disorders activating multiple signalling pathways. The work presented in this thesis will hopefully lead to subsequent clinical trials resulting in the generation of novel cost-effective and safe agents improving the treatment of patients with T2D.

Chapter 9

References

Abbasi, J. (2018) Oral GLP-1 analog for type 2 diabetes on the horizon. *Jama,* 320(6), 539-539.

Afroze, S., Meng, F., Jensen, K., McDaniel, K., Rahal, K., Onori, P., Gaudio, E., Alpini, G. and Glaser, S.S. (2013) The physiological roles of secretin and its receptor. *Annals of Translational Medicine,* 1(3), 29-5839.2012.12.01.

Ahlqvist, E., Storm, P., Karajamaki, A., Martinell, M., Dorkhan, M., Carlsson, A., Vikman, P., Prasad, R.B., Aly, D.M., Almgren, P., Wessman, Y., Shaat, N., Spegel, P., Mulder, H., Lindholm, E., Melander, O., Hansson, O., Malmqvist, U., Lernmark, A., Lahti, K., Forsen, T., Tuomi, T., Rosengren, A.H. and Groop, L. (2018) Novel subgroups of adult-onset diabetes and their association with outcomes: a data-driven cluster analysis of six variables. *The Lancet.Diabetes & Endocrinology,* 6(5), 361-369.

Ahmed, A.M. (2002) History of diabetes mellitus. *Saudi Medical Journal,* 23(4), 373-378.

Ahren, B., Larsson, H. and Holst, J.J. (1997) Effects of glucagon-like peptide-1 on islet function and insulin sensitivity in noninsulin-dependent diabetes mellitus. *The Journal of Clinical Endocrinology & Metabolism,* 82(2), 473-478.

Alam, S., Eqbal, K., Patel, I., Mulla, I., Ansari, S. and Ayesha, B.The history of diabetes: From olden days to discovering insulin.

Ali, O. (2013) Genetics of type 2 diabetes. *World Journal of Diabetes,* 4(4), 114-123.

Alves, C., Batel-Marques, F. and Macedo, A.F. (2012) A meta-analysis of serious adverse events reported with exenatide and liraglutide: acute pancreatitis and cancer. *Diabetes Research and Clinical Practice,* 98(2), 271-284.

Amaral, C.R., Pereira, F., Silva, D.A., Amorim, A. and de Carvalho, E.F. (2018) The mitogenomic phylogeny of the Elasmobranchii (Chondrichthyes). *Mitochondrial DNA Part A,* 29(6), 867-878.

Ambery, P., Parker, V.E., Stumvoll, M., Posch, M.G., Heise, T., Plum-Moerschel, L., Tsai, L., Robertson, D., Jain, M. and Petrone, M. (2018) MEDI0382, a GLP-1 and glucagon receptor dual agonist, in obese or overweight patients with type 2 diabetes: a randomised, controlled, double-blind, ascending dose and phase 2a study. *The Lancet,*

American Diabetes Association. (2014) Diagnosis and classification of diabetes mellitus. *Diabetes Care,* 37 Suppl 1, S81-90.

Andoh, T., Nagasawa, H. and Matsubara, T., 2000. Multiple molecular forms of glucagon and insulin in the kaluga sturgeon, Huso dauricus. *Peptides*, *21*(12), pp.1785-1792.

Andrews, P.C. and Ronner, P. (1985) Isolation and structures of glucagon and glucagon-like peptide from catfish pancreas. *The Journal of Biological Chemistry,* 260(7), 3910-3914.

Andrews, P.C., Hawke, D.H., Lee, T.D., Legesse, K., Noe, B.D. and Shively, J.E., 1986. Isolation and structure of the principal products of preproglucagon processing, including an amidated glucagon-like peptide. *Journal of Biological Chemistry*, *261*(18), pp.8128-8133.

Aroda, V.R., Rosenstock, J., Terauchi, Y., Jeppesen, O., Christiansen, E., Hertz, C.L. and Haluzik, M. (2018) *Effect and Safety of Oral Semaglutide Monotherapy in Type 2 Diabetes—PIONEER 1 Trial.*

Asmar, M., Bache, M., Knop, F.K., Madsbad, S. and Holst, J.J. (2010) Do the actions of glucagon-like peptide-1 on gastric emptying, appetite, and food intake involve release of amylin in humans? *The Journal of Clinical Endocrinology & Metabolism,* 95(5), 2367-2375.

Atkinson, M.A. (2012) The pathogenesis and natural history of type 1 diabetes. *Cold Spring Harbor Perspectives in Medicine,* 2(11), 10.1101/cshperspect.a007641.

Authier, F., Cameron, P.H., Merlen, C., Kouach, M. and Briand, G. (2003) Endosomal proteolysis of glucagon at neutral pH generates the bioactive degradation product miniglucagon-(19–29). *Endocrinology,* 144(12), 5353-5364.

Baggio, L.L. and Drucker, D.J. (2014) Glucagon-like peptide-1 receptors in the brain: controlling food intake and body weight. *The Journal of Clinical Investigation,* 124(10), 4223-4226.

Bandsma, R.H., Sokollik, C., Chami, R., Cutz, E., Brubaker, P.L., Hamilton, J.K., Perlman, K., Zlotkin, S., Sigalet, D.L., Sherman, P.M., Martin, M.G. and Avitzur, Y. (2013) From diarrhea to obesity in prohormone convertase 1/3 deficiency: age-dependent clinical, pathologic, and enteroendocrine characteristics. *Journal of Clinical Gastroenterology,* 47(10), 834-843.

Barnett, C. and Barnett, Y. (2003) Ketone Bodies.

Belfiore, A., Malaguarnera, R., Vella, V., Lawrence, M.C., Sciacca, L., Frasca, F., Morrione, A. and Vigneri, R. (2017) Insulin receptor isoforms in physiology and disease: an updated view. *Endocrine Reviews,* 38(5), 379-431.

Bell, G.I., Sanchez-Pescador, R., Laybourn, P.J. and Najarian, R.C. (1983) Exon duplication and divergence in the human preproglucagon gene. *Nature,* 304(5924), 368-371.

Bennett, W.L., Wilson, L.M., Bolen, S., Maruthur, N., Singh, S., Chatterjee, R., Marinopoulos, S.S., Puhan, M.A., Ranasinghe, P., Nicholson, W.K., Block, L., Odelola, O., Dalal, D.S., Ogbeche, G.E., Chandrasekhar, A., Hutfless, S., Bass, E.B. and Segal, J.B. (2011)

Berks, B.C., Marshall, C.J., Carne, A., Galloway, S.M. and Cutfield, J.F. (1989). Isolation and structural characterization of insulin and glucagon from the holocephalan species Callorhynchus milii (elephantfish). *Biochemical Journal*, *263*(1), pp.261-266.

Berthelot, C., Brunet, F., Chalopin, D., Juanchich, A., Bernard, M., Noël, B., Bento, P., Da Silva, C., Labadie, K. and Alberti, A. (2014) The rainbow trout genome provides novel insights into evolution after whole-genome duplication in vertebrates. *Nature Communications,* 5, 3657.

Bertin, B., Dubuquoy, L., Colombel, J. and Desreumaux, P. (2013) PPAR-gamma in ulcerative colitis: a novel target for intervention. *Current Drug Targets,* 14(12), 1501-1507.

Bhaskar, M.E., Sowmya, G., Moorthy, S., Kumar, N.S., Praveena, R. and Kumar, V. (2010) Presenting features of diabetes mellitus. *Indian Journal of Community Medicine : Official Publication of Indian Association of Preventive & Social Medicine,* 35(4), 523-525.

Bhat, V.K., Kerr, B.D., Flatt, P.R. and Gault, V.A. (2013) A novel GIP-oxyntomodulin hybrid peptide acting through GIP, glucagon and GLP-1 receptors exhibits weight reducing and anti-diabetic properties. *Biochemical Pharmacology,* 85(11), 1655-1662.

Bhat, V., Kerr, B., Vasu, S., Flatt, P. and Gault, V. (2013) A DPP-IV-resistant triple-acting agonist of GIP, GLP-1 and glucagon receptors with potent glucose-lowering and insulinotropic actions in high-fat-fed mice. *Diabetologia,* 56(6), 1417-1424.

Blind, E., Janssen, H., Dunder, K. and de Graeff, P.A. (2018) The European Medicines Agency's Approval of New Medicines for Type 2 Diabetes. *Diabetes, Obesity and Metabolism,*

Bobe, J., Marandel, L., Panserat, S., Boudinot, P., Berthelot, C., Quillet, E., Volff, J., Genêt, C., Jaillon, O. and Crollius, H.R. (2016) The rainbow trout genome, an important landmark for aquaculture and genome evolution. *In:* Anon.*Genomics in Aquaculture.* Elsevier, 21-43.

Bodnaruc, A.M., Prud'homme, D., Blanchet, R. and Giroux, I. (2016) Nutritional modulation of endogenous glucagon-like peptide-1 secretion: a review. *Nutrition & Metabolism,* 13(1), 92.

Bonnick, S.L. and Miller, P. (2013) Clinical use of bone densitometry. *In:* Anon.*Osteoporosis (Fourth Edition).* Elsevier, 1551-1571.

Boucher, J., Kleinridders, A. and Kahn, C.R. (2014) Insulin receptor signaling in normal and insulin-resistant states. *Cold Spring Harbor Perspectives in Biology,* 6(1), 10.1101/cshperspect.a009191.

Bouskila, M., Hunter, R.W., Ibrahim, A.F., Delattre, L., Peggie, M., Van Diepen, J.A., Voshol, P.J., Jensen, J. and Sakamoto, K. (2010) Allosteric regulation of

glycogen synthase controls glycogen synthesis in muscle. *Cell Metabolism,* 12(5), 456-466.

Brandt, S.J., Götz, A., Tschöp, M.H. and Müller, T.D. (2018) Gut hormone polyagonists for the treatment of type 2 diabetes. *Peptides,* 100, 190-201.

Broughton, R.E., Betancur-R, R., Li, C., Arratia, G. and Orti, G. (2013) Multi-locus phylogenetic analysis reveals the pattern and tempo of bony fish evolution. *PLoS Currents,* 5, 10.1371/currents.tol.2ca8041495ffafd0c92756e75247483e.

Broughton, R.E., Milam, J.E. and Roe, B.A. (2001) The complete sequence of the zebrafish (Danio rerio) mitochondrial genome and evolutionary patterns in vertebrate mitochondrial DNA. *Genome Research,* 11(11), 1958-1967.

Brown, M.L., Andrzejewski, D., Burnside, A. and Schneyer, A.L. (2016) Activin Enhances α-to β-Cell Transdifferentiation as a Source For β-Cells In Male FSTL3 Knockout Mice. *Endocrinology,* 157(3), 1043-1054.

Bryder, L. and Harper, C. (2013) Commentary: More than 'tentative opinions': Harry Himsworth and defining diabetes. *International Journal of Epidemiology,* 42(6), 1599-1600.

Bugáňová, M., Pelantová, H., Holubová, M., Šedivá, B., Maletínská, L., Železná, B., Kuneš, J., Kačer, P., Kuzma, M. and Haluzík, M. (2017) The effects of liraglutide in mice with diet-induced obesity studied by metabolomics. *Journal of Endocrinology,* 233(1), 93-104.

Busby, E.R. and Mommsen, T.P., 2016. Proglucagons in vertebrates: expression and processing of multiple genes in a bony fish. *Comparative Biochemistry and Physiology Part B: Biochemistry and Molecular Biology*, *199*, pp.58-66.

Byrne, C.D. (2001) Programming other hormones that affect insulin: Type 2 diabetes. *British Medical Bulletin,* 60(1), 153-171.

Cabou, C. and Burcelin, R. (2011) GLP-1, the gut-brain, and brain-periphery axes. *The Review of Diabetic Studies : RDS,* 8(3), 418-431.

Caicedo, A. (2013) Paracrine and autocrine interactions in the human islet: more than meets the eye. *In:* Paracrine and autocrine interactions in the human islet: more than meets the eye. *Seminars in cell & developmental biology.* Elsevier, 11-21.

Cardoso, J.C., Félix, R.C., Costa, C., Palma, P.F., Canário, A.V. and Power, D.M. (2018) Evolution of the glucagon-like system across fish. *General and Comparative Endocrinology,* 264, 113-130.

Cardoso, J.C., Vieira, F.A., Gomes, A.S. and Power, D.M. (2010) The serendipitous origin of chordate secretin peptide family members. *BMC Evolutionary Biology,* 10(1), 135.

Cavaiola, T.S. and Pettus, J.H. (2000) Management Of Type 2 Diabetes: Selecting Amongst Available Pharmacological Agents. *In:* De Groot, L.J., Chrousos, G., Dungan, K., Feingold, K.R., Grossman, A., Hershman, J.M., Koch, C., Korbonits, M., McLachlan, R., New, M., Purnell, J., Rebar, R., Singer, F. and Vinik, A. eds. *Endotext.* South Dartmouth (MA): MDText.com, Inc,

Cavaiola, T.S. and Pettus, J.H. (2017) Management Of Type 2 Diabetes: Selecting Amongst Available Pharmacological Agents. *In:* De Groot, L.J., Chrousos, G., Dungan, K., Feingold, K.R., Grossman, A., Hershman, J.M., Koch, C., Korbonits, M., McLachlan, R., New, M., Purnell, J., Rebar, R., Singer, F. and Vinik, A. eds. *Endotext.* South Dartmouth (MA): MDText.com, Inc,

Ceballos, G., Ehrlich, P.R., Barnosky, A.D., García, A., Pringle, R.M. and Palmer, T.M. (2015) Accelerated modern human–induced species losses: Entering the sixth mass extinction. *Science Advances,* 1(5), e1400253.

Cerf, M.E. (2013) Beta cell dysfunction and insulin resistance. *Frontiers in Endocrinology,* 4, 37.

Cernea, S. and Raz, I. (2011) Therapy in the early stage: incretins. *Diabetes Care,* 34 Suppl 2, S264-71.

Chabenne, J.R., DiMarchi, M.A., Gelfanov, V.M. and DiMarchi, R.D. (2010) *Optimization of the Native Glucagon Sequence for Medicinal Purposes,*

Cho, Y.M., Fujita, Y. and Kieffer, T.J. (2014) Glucagon-like peptide-1: glucose homeostasis and beyond. *Annual Review of Physiology,* 76, 535-559.

Chovatiya, R. and Medzhitov, R. (2014) Stress, inflammation, and defense of homeostasis. *Molecular Cell,* 54(2), 281-288.

Chow, B.K., Moon, T.W., Hoo, R.L., Yeung, C., Müller, M., Christos, P.J. and Mojsov, S. (2004) Identification and characterization of a glucagon receptor from the goldfish Carassius auratus: implications for the evolution of the ligand specificity of glucagon receptors in vertebrates. *Endocrinology,* 145(7), 3273-3288.

Conlon, J.M., Andrews, P.C., Thim, L. and Moon, T.W. (1991). The primary structure of glucagon-like peptide but not insulin has been conserved between the American eel, Anguilla rostrata and the European eel, Anguilla anguilla. *General and comparative endocrinology*, *82*(1), pp.23-32.

Conlon, J.M., Bondareva, V., Rusakov, Y., Plisetskaya, E.M., Mynarcik, D.C. and Whittaker, J. (1995) Characterization of insulin, glucagon, and somatostatin from the river lamprey, Lampetra fluviatilis. *General and Comparative Endocrinology,* 100(1), 96-105.

Conlon, J.M., Göke, R., Andrews, P. and Thim, L. (1989) Multiple molecular forms of insulin and glucagon-like peptide from the Pacific ratfish (Hydrolagus colliei). *General and Comparative Endocrinology,* 73(1), 136-146.

Conlon, J.M., Hazon, N. and Thim, L. (1994) Primary structures of peptides derived from proglucagon isolated from the pancreas of the elasmobranch fish, Scyliorhinus canicula. *Peptides,* 15(1), 163-167.

Conlon, J.M., Nielsen, P.F. and Youson, J.H. (1993a) Primary structures of glucagon and glucagon-like peptide isolated from the intestine of the parasitic phase lamprey Petromyzon marinus. *General and Comparative Endocrinology,* 91(1), 96-104.

Conlon, J.M., O'Toole, L. and Thim, L. (1987) Primary structure of glucagon from the gut of the common dogfish (Scyliorhinus canicula). *FEBS Letters,* 214(1), 50-56.

Conlon, J., Dafgård, E., Falkmer, S. and Thim, L. (1987) A glucagon-like peptide, structurally related to mammalian oxyntomodulin, from the pancreas of a holocephalan fish, Hydrolagus colliei. *Biochemical Journal,* 245(3), 851-855.

Conlon, J.M., Falkmer, S. and Thim, L., (1987). Primary structures of three fragments of proglucagon from the pancreatic islets of the daddy sculpin (Cottus scorpius). *European journal of biochemistry*, *164*(1), pp.117-122.

Conlon, J.M., Youson, J.H. and Mommsen, T.P. (1993b) Structure and biological activity of glucagon and glucagon-like peptide from a primitive bony fish, the bowfin (Amia calva). *The Biochemical Journal,* 295 (Pt 3)(Pt 3), 857-861.

Corgosinho, F.C., Dâmaso, A.R. and de Mello, M.T. (2015) Obesity, Inflammation, and Obstructive Sleep Apnea: Exercise as Therapy. *In:* Anon.*Modulation of Sleep by Obesity, Diabetes, Age, and Diet.* Elsevier, 117-126.

Creutzfeldt, W. (2005) The [pre-] history of the incretin concept. *Regulatory Peptides,* 128(2), 87-91.

Cutfield, S.M. and Cutfield, J.F., 1993. A second glucagon in the pancreatic islets of the daddy sculpin Cottus scorpius. *General and comparative endocrinology*, *91*(3), pp.281-286.

Dailey, M.J. and Moran, T.H. (2013) Glucagon-like peptide 1 and appetite. *Trends in Endocrinology & Metabolism,* 24(2), 85-91.

D'alessio, D. (2016) Is GLP-1 a hormone: Whether and When? *Journal of Diabetes Investigation,* 7, 50-55.

Das, A.K. and Shah, S. (2011) History of diabetes: from ants to analogs. *The Journal of the Association of Physicians of India,* 59 Suppl, 6-7.

Day, J.W., Ottaway, N., Patterson, J.T., Gelfanov, V., Smiley, D., Gidda, J., Findeisen, H., Bruemmer, D., Drucker, D.J. and Chaudhary, N. (2009) A new glucagon and GLP-1 co-agonist eliminates obesity in rodents. *Nature Chemical Biology,* 5(10), 749.

de Graaf, C., Song, G., Cao, C., Zhao, Q., Wang, M., Wu, B. and Stevens, R.C. (2017) Extending the structural view of class B GPCRs. *Trends in Biochemical Sciences,* 42(12), 946-960.

De Meyts, P. (2000) The Insulin Receptor and Its Signal Transduction Network. *In:* De Groot, L.J., Chrousos, G., Dungan, K., Feingold, K.R., Grossman, A., Hershman, J.M., Koch, C., Korbonits, M., McLachlan, R., New, M., Purnell, J., Rebar, R., Singer, F. and Vinik, A. eds. *Endotext.* South Dartmouth (MA): MDText.com, Inc,

Deacon, C.F. and Ahren, B. (2011) Physiology of incretins in health and disease. *The Review of Diabetic Studies : RDS,* 8(3), 293-306.

Dods, R.F. (2013) *Understanding diabetes: A biochemical perspective.* John Wiley & Sons.

Dolenšek, J., Pohorec, V., Rupnik, M.S. and Stožer, A. (2017) Pancreas Physiology. *In:* Anon.*Challenges in Pancreatic Pathology.* InTech,

Drucker, D.J. (2018) Mechanisms of action and therapeutic application of glucagon-like peptide-1. *Cell Metabolism,* 27(4), 740-756.

Drucker, D.J. and Asa, S. (1988) Glucagon gene expression in vertebrate brain. *The Journal of Biological Chemistry,* 263(27), 13475-13478.

Dupre, J. (1964) An intestinal hormone affecting glucose disposal in man. *Lancet,* 2, 672-673.

Dyson, P. (2015) Low carbohydrate diets and type 2 diabetes: what is the latest evidence? *Diabetes Therapy,* 6(4), 411-424.

Eboh, O., Osakwe, A., Otoikhian, C. and James, G. (2014) DIABETES MELLITUS A PANDEMIC SCOURGE: A REVIEW.

Echeverri, A.F. and Tobón, G.J. (2013) Autoimmune diabetes mellitus (Type 1A). *In:* Anon.*Autoimmunity: From Bench to Bedside [Internet]*. El Rosario University Press,

Egan, A.G., Blind, E., Dunder, K., De Graeff, P.A., Hummer, B.T., Bourcier, T. and Rosebraugh, C. (2014) Pancreatic safety of incretin-based drugs—FDA and EMA assessment. *New England Journal of Medicine,* 370(9), 794-797.

Eisenbarth, G.S. (2005) Type 1 diabetes mellitus. *Joslin's Diabetes Mellitus, 14th Ed.Kahn CR, Weir GC, King GL, Et Al., Eds.Lippincott Williams & Wilkins, New York,* , 399-424.

Eknoyan, G. and Nagy, J. (2005) A history of diabetes mellitus or how a disease of the kidneys evolved into a kidney disease. *Advances in Chronic Kidney Disease,* 12(2), 223-229.

El-Gohary, Y. and Gittes, G. (2018) Structure of Islets and Vascular Relationship to the Exocrine Pancreas. *Pancreapedia: The Exocrine Pancreas Knowledge Base,*

Elvert, R., Herling, A.W., Bossart, M., Weiss, T., Zhang, B., Wenski, P., Wandschneider, J., Kleutsch, S., Butty, U. and Kannt, A. (2018) Running on mixed fuel-dual agonistic approach of GLP-1 and GCG receptors leads to beneficial impact on body weight and blood glucose control: A comparative study between mice and non-human primates. *Diabetes, Obesity and Metabolism,* 20(8), 1836-1851.

Elvert, R., Herling, A.W., Bossart, M., Weiss, T., Zhang, B., Wenski, P., Wandschneider, J., Kleutsch, S., Butty, U. and Kannt, A. (2018) Running on mixed fuel-dual agonistic approach of GLP-1 and GCG receptors leads to beneficial impact on body weight and blood glucose control: A comparative study between mice and non-human primates. *Diabetes, Obesity and Metabolism,* 20(8), 1836-1851.

Erlich, H., Valdes, A.M., Noble, J., Carlson, J.A., Varney, M., Concannon, P., Mychaleckyj, J.C., Todd, J.A., Bonella, P., Fear, A.L., Lavant, E., Louey, A., Moonsamy, P. and Type 1 Diabetes Genetics Consortium. (2008) HLA DR-DQ haplotypes and genotypes and type 1 diabetes risk: analysis of the type 1 diabetes genetics consortium families. *Diabetes,* 57(4), 1084-1092.

Evers, A., Haack, T., Lorenz, M., Bossart, M., Elvert, R., Henkel, B., Stengelin, S., Kurz, M., Glien, M. and Dudda, A. (2017) Design of novel exendin-based dual glucagon-like peptide 1 (GLP-1)/glucagon receptor agonists. *Journal of Medicinal Chemistry,* 60(10), 4293-4303.

Fajans, S.S., Bell, G.I. and Polonsky, K.S. (2001) Molecular mechanisms and clinical pathophysiology of maturity-onset diabetes of the young. *New England Journal of Medicine,* 345(13), 971-980.

Fava, G. and Wu, H. (2014) Pancreatic Glucagon-Like Peptide 1: What is known. *J Diabetes Metab,* 5(397), 2.

Filippatos, T.D., Panagiotopoulou, T.V. and Elisaf, M.S. (2014) Adverse Effects of GLP-1 Receptor Agonists. *The Review of Diabetic Studies : RDS,* 11(3-4), 202-230.

Finan, B., Müller, T.D., Clemmensen, C., Perez-Tilve, D., DiMarchi, R.D. and Tschöp, M.H. (2016) Reappraisal of GIP pharmacology for metabolic diseases. *Trends in Molecular Medicine,* 22(5), 359-376.

Flatt, P., Bailey, C. and Green, B. (2009) Recent advances in antidiabetic drug therapies targeting the enteroinsular axis. *Current Drug Metabolism,* 10(2), 125-137.

Foster, D.W. and McGarry, J.D. (1982) The regulation of ketogenesis. *In:* Anon.*Metabolic Acidosis.* Pitman, London, 120-126.

Fraker, P.J. and Speck Jr, J.C. (1978) Protein and cell membrane iodinations with a sparingly soluble chloroamide, 1, 3, 4, 6-tetrachloro-3a, 6a-diphenylglycoluril. *Biochemical and Biophysical Research Communications,* 80(4), 849-857.

Frasca, F., Pandini, G., Scalia, P., Sciacca, L., Mineo, R., Costantino, A., Goldfine, I.D., Belfiore, A. and Vigneri, R. (1999) Insulin receptor isoform A, a newly recognized, high-affinity insulin-like growth factor II receptor in fetal and cancer cells. *Molecular and Cellular Biology,* 19(5), 3278-3288.

Fredriksson, R., Lagerstrom, M.C., Lundin, L.G. and Schioth, H.B. (2003) The G-protein-coupled receptors in the human genome form five main families. Phylogenetic analysis, paralogon groups, and fingerprints. *Molecular Pharmacology,* 63(6), 1256-1272.

Frias, J.P., Nauck, M.A., Van, J., Kutner, M.E., Cui, X., Benson, C., Urva, S., Gimeno, R.E., Milicevic, Z. and Robins, D. (2018) Efficacy and safety of LY3298176, a novel dual GIP and GLP-1 receptor agonist, in patients with type 2 diabetes: a randomised, placebo-controlled and active comparator-controlled phase 2 trial. *The Lancet,* 392(10160), 2180-2193.

Fu, Z., R Gilbert, E. and Liu, D. (2013) Regulation of insulin synthesis and secretion and pancreatic Beta-cell dysfunction in diabetes. *Current Diabetes Reviews,* 9(1), 25-53.

Furdell, E.L. (2008) *Fatal thirst: diabetes in Britain until insulin.* Brill.

Furman, B. (2009) Current and future incretin-based therapies for the treatment of diabetes. *Pharmaceutical Journal,* 282(7550), 521.

Gaisano, H., MacDonald, P.E. and Vranic, M. (2012) Glucagon secretion and signaling in the development of diabetes. *Frontiers in Physiology,* 3, 349.

Gannon, M., Kulkarni, R.N., Tse, H.M. and Mauvais-Jarvis, F. (2018) Sex differences underlying pancreatic islet biology and its dysfunction. *Molecular Metabolism,* 15, 82-91.

Ganz, M., Csak, T. and Szabo, G. (2014) High fat diet feeding results in gender specific steatohepatitis and inflammasome activation. *World Journal of Gastroenterology,* 20(26), 8525-8534.

Gault, V. (2018) RD Lawrence Lecture 2017 Incretins: the intelligent hormones in diabetes. *Diabetic Medicine,* 35(1), 33-40.

Gault, V.A., Irwin, N. and Flatt, P.R. (2008) GIP-based therapeutics for diabetes and obesity. *Current Chemical Biology,* 2(1), 60-67.

Gelling, R.W., Vuguin, P.M., Du, X.Q., Cui, L., Rømer, J., Pederson, R.A., Leiser, M., Sørensen, H., Holst, J.J. and Fledelius, C. (2009) Pancreatic β-cell overexpression of the glucagon receptor gene results in enhanced β-cell function and mass. *American Journal of Physiology-Endocrinology and Metabolism,* 297(3), E695-E707.

Gier, B., Matveyenko, A.V., Kirakossian, D., Dawson, D., Dry, S.M. and Butler, P.C. (2012) Chronic GLP-1 receptor activation by exendin-4 induces expansion of

pancreatic duct glands in rats and accelerates formation of dysplastic lesions and chronic pancreatitis in the Kras(G12D) mouse model. *Diabetes,* 61(5), 1250-1262.

Gillespie, K.M. (2006) Type 1 diabetes: pathogenesis and prevention. *CMAJ : Canadian Medical Association Journal = Journal De l'Association Medicale Canadienne,* 175(2), 165-170.

Giza, S., Goulas, A., Gbandi, E., Effraimidou, S., Papadopoulou-Alataki, E., Eboriadou, M. and Galli-Tsinopoulou, A. (2013) The role of PTPN22 C1858T gene polymorphism in diabetes mellitus type 1: first evaluation in Greek children and adolescents. *BioMed Research International,* 2013, 721604.

Glasauer, S.M. and Neuhauss, S.C. (2014) Whole-genome duplication in teleost fishes and its evolutionary consequences. *Molecular Genetics and Genomics,* 289(6), 1045-1060.

Golson, M.L., Misfeldt, A.A., Kopsombut, U.G., Petersen, C.P. and Gannon, M. (2010) High Fat Diet Regulation of beta-Cell Proliferation and beta-Cell Mass. *The Open Endocrinology Journal,* 4, 10.2174/1874216501004010066.

Gomes, M.d.B. (2013) Impact of diabetes on cardiovascular disease: an update. *International Journal of Hypertension,* 2013

Gosmanov, N.R., Gosmanov, A.R. and Gerich, J.E. (2000) Glucagon Physiology. *In:* De Groot, L.J., Chrousos, G., Dungan, K., Feingold, K.R., Grossman, A., Hershman, J.M., Koch, C., Korbonits, M., McLachlan, R., New, M., Purnell, J., Rebar, R., Singer, F. and Vinik, A. eds. *Endotext.* South Dartmouth (MA): MDText.com, Inc,

Graham, G.V., Conlon, J.M., Abdel-Wahab, Y.H. and Flatt, P.R. (2018a) Glucagon-like peptides-1 from phylogenetically ancient fish show potent anti-diabetic activities by acting as dual GLP1R and GCGR agonists. *Molecular and Cellular Endocrinology,*

Graham, G.V., Conlon, J.M., Abdel-Wahab, Y.H., Gault, V.A. and Flatt, P.R. (2018b) Evaluation of the insulinotropic and glucose-lowering actions of zebrafish GIP in mammalian systems: Evidence for involvement of the GLP-1 receptor. *Peptides,* 100, 182-189.

Green, B., Mooney, M., Gault, V., Irwin, N., Bailey, C., Harriott, P., Greer, B., Flatt, P. and O'Harte, F. (2004) Lys9 for Glu9 substitution in glucagon-like peptide-1 (7–36) amide confers dipeptidylpeptidase IV resistance with cellular and metabolic actions similar to those of established antagonists glucagon-like peptide-1 (9–36) amide and exendin (9–39). *Metabolism,* 53(2), 252-259.

Gulliford, M.C., Charlton, J., Prevost, T., Booth, H., Fildes, A., Ashworth, M., Littlejohns, P., Reddy, M., Khan, O. and Rudisill, C. (2017) Costs and outcomes of increasing access to bariatric surgery: cohort study and cost-effectiveness analysis using electronic health records. *Value in Health,* 20(1), 85-92.

Gupta, V. (2013) Glucagon-like peptide-1 analogues: An overview. *Indian Journal of Endocrinology and Metabolism,* 17(3), 413-421.

Gutiérrez-Rodelo, C., Roura-Guiberna, A. and Olivares-Reyes, J.A. (2017) Molecular mechanisms of insulin resistance: an update. *Gaceta Medica De Mexico,* 153(2), 214-228.

Habib, A.M., Richards, P., Cairns, L.S., Rogers, G.J., Bannon, C.A., Parker, H.E., Morley, T.C., Yeo, G.S., Reimann, F. and Gribble, F.M. (2012) Overlap of endocrine hormone expression in the mouse intestine revealed by transcriptional profiling and flow cytometry. *Endocrinology,* 153(7), 3054-3065.

Halban, P.A., Polonsky, K.S., Bowden, D.W., Hawkins, M.A., Ling, C., Mather, K.J., Powers, A.C., Rhodes, C.J., Sussel, L. and Weir, G.C. (2014) β-cell failure in type 2 diabetes: postulated mechanisms and prospects for prevention and treatment. *The Journal of Clinical Endocrinology & Metabolism,* 99(6), 1983-1992.

Hallbook, F., Lundin, L.G. and Kullander, K. (1998) Lampetra fluviatilis neurotrophin homolog, descendant of a neurotrophin ancestor, discloses the early molecular evolution of neurotrophins in the vertebrate subphylum. *The Journal of Neuroscience : The Official Journal of the Society for Neuroscience,* 18(21), 8700-8711.

Hare, K.J., Vilsboll, T., Asmar, M., Deacon, C.F., Knop, F.K. and Holst, J.J. (2010) The glucagonostatic and insulinotropic effects of glucagon-like peptide 1 contribute equally to its glucose-lowering action. *Diabetes,* 59(7), 1765-1770.

Hashimoto, H., Shintani, N., Tanida, M., Hayata, A., Hashimoto, R. and Baba, A. (2011) PACAP is implicated in the stress axes. *Current Pharmaceutical Design,* 17(10), 985-989.

Helfman, G., Collette, B.B., Facey, D.E. and Bowen, B.W. (2009) *The diversity of fishes: biology, evolution, and ecology.* John Wiley & Sons.

Henderson, S., Konkar, A., Hornigold, D., Trevaskis, J., Jackson, R., Fritsch Fredin, M., Jansson-Löfmark, R., Naylor, J., Rossi, A. and Bednarek, M. (2016) Robust anti-obesity and metabolic effects of a dual GLP-1/glucagon receptor peptide agonist in rodents and non-human primates. *Diabetes, Obesity and Metabolism,* 18(12), 1176-1190.

Henriksen, J.H. and de Muckadell, O.S. (2000) Secretin, its discovery, and the introduction of the hormone concept. *Scandinavian Journal of Clinical and Laboratory Investigation,* 60(6), 463-472.

Hex, N., Bartlett, C., Wright, D., Taylor, M. and Varley, D. (2012) Estimating the current and future costs of Type 1 and Type 2 diabetes in the UK, including direct health costs and indirect societal and productivity costs. *Diabetic Medicine,* 29(7), 855-862.

Hoist, J., Ørskov, C., Hartmann, B. and Deacon, C.F. (1997) Posttranslational processing of proglucagon and postsecretory fate of proglucagon products. *Frontiers in Diabetes,* 13, 24-48.

Holst, J.J. (2007) The physiology of glucagon-like peptide 1. *Physiological Reviews,* 87(4), 1409-1439.

Hruban, R.H., Fukushima, N. and Wilentz, R.E. (2009) Pancreas. *Modern Surgical Pathology,* 1, 867-901.

Huang, P., Altshuller, Y.M., Hou, J.C., Pessin, J.E. and Frohman, M.A. (2005) Insulin-stimulated plasma membrane fusion of Glut4 glucose transporter-containing vesicles is regulated by phospholipase D1. *Molecular Biology of the Cell,* 16(6), 2614-2623.

Hughes, L.C., Orti, G., Huang, Y., Sun, Y., Baldwin, C.C., Thompson, A.W., Arcila, D., Betancur-R, R., Li, C., Becker, L., Bellora, N., Zhao, X., Li, X., Wang, M., Fang, C., Xie, B., Zhou, Z., Huang, H., Chen, S., Venkatesh, B. and Shi, Q. (2018) Comprehensive phylogeny of ray-finned fishes (Actinopterygii) based on transcriptomic and genomic data. *Proceedings of the National Academy of Sciences of the United States of America,* 115(24), 6249-6254.

Hupfeld, C.J., Courtney, C.H. and Olefsky, J.M. (2010) Type 2 diabetes mellitus: etiology, pathogenesis, and natural history. *In:* Anon.*Endocrinology.* Elsevier/Saunders, Philadelphia, 765-787.

Inoue, J.G., Miya, M., Lam, K., Tay, B., Danks, J.A., Bell, J., Walker, T.I. and Venkatesh, B. (2010) Evolutionary origin and phylogeny of the modern holocephalans (Chondrichthyes: Chimaeriformes): a mitogenomic perspective. *Molecular Biology and Evolution,* 27(11), 2576-2586.

Ipsen, D.H., Tveden-Nyborg, P., Rolin, B., Rakipovski, G., Beck, M., Mortensen, L.W., Færk, L., Heegaard, P.M.H., Møller, P. and Lykkesfeldt, J. (2016) High-fat but not sucrose intake is essential for induction of dyslipidemia and non-alcoholic steatohepatitis in guinea pigs. *Nutrition & Metabolism,* 13(1), 51.

Irwin, D.M. (2005) Evolution of hormone function: proglucagon-derived peptides and their receptors. *AIBS Bulletin,* 55(7), 583-591.

Irwin, D.M. (2010) Evolution of genes for incretin hormones and their receptors. *In:* Anon.*Vitamins & Hormones.* Elsevier, 1-20.

Irwin, D.M. (2012) Origin and convergent evolution of exendin genes. *General and Comparative Endocrinology,* 175(1), 27-33.

Irwin, D.M., Huner, O. and Youson, J.H. (1999) Lamprey proglucagon and the origin of glucagon-like peptides. *Molecular Biology and Evolution,* 16(11), 1548-1557.

Irwin, D.M. and Wong, J. (1995) Trout and chicken proglucagon: alternative splicing generates mRNA transcripts encoding glucagon-like peptide 2. *Molecular Endocrinology,* 9(3), 267-277.

Irwin, D.M. and Zhang, T. (2006) Evolution of the vertebrate glucose-dependent insulinotropic polypeptide (GIP) gene. *Comparative Biochemistry and Physiology Part D: Genomics and Proteomics,* 1(4), 385-395.

Irwin, N. and Flatt, P.R. (2015) New perspectives on exploitation of incretin peptides for the treatment of diabetes and related disorders. *World Journal of Diabetes,* 6(15), 1285-1295.

Islam, M.S. (2002) The ryanodine receptor calcium channel of beta-cells: molecular regulation and physiological significance. *Diabetes,* 51(5), 1299-1309.

Itoh, N., Furuya, T., Ozaki, K., Ohta, M. and Kawasaki, T. (1991) The secretin precursor gene. Structure of the coding region and expression in the brain. *The Journal of Biological Chemistry,* 266(19), 12595-12598.

Jackuliak, P. and Payer, J. (2014) Osteoporosis, fractures, and diabetes. *International Journal of Endocrinology,* 2014, 820615.

Jang, H.J., Kokrashvili, Z., Theodorakis, M.J., Carlson, O.D., Kim, B.J., Zhou, J., Kim, H.H., Xu, X., Chan, S.L., Juhaszova, M., Bernier, M., Mosinger, B., Margolskee, R.F. and Egan, J.M. (2007) Gut-expressed gustducin and taste receptors regulate secretion of glucagon-like peptide-1. *Proceedings of the National Academy of Sciences of the United States of America,* 104(38), 15069-15074.

Jaskolski, M., Dauter, Z. and Wlodawer, A. (2014) A brief history of macromolecular crystallography, illustrated by a family tree and its Nobel fruits. *The FEBS Journal,* 281(18), 3985-4009.

Jo, J., Choi, M.Y. and Koh, D. (2007) Size distribution of mouse Langerhans islets. *Biophysical Journal,* 93(8), 2655-2666.

John M. Eisenberg Center for Clinical Decisions and Communications Science. (2007) Comparing Medications for Adults With Type 2 Diabetes. *In:* Anon.*Comparative Effectiveness Review Summary Guides for Clinicians.* Rockville (MD):

Jonsson, B. (1998) The economic impact of diabetes. *Diabetes Care,* 21 Suppl 3, C7-10.

Jorgens, V. and Grusser, M. (2013) Happy birthday, Claude Bernard. *Diabetes,* 62(7), 2181-2182.

Jorpes, J.E. and Mutt, V. (1973) *Secretin, cholecystokinin, pancreozymin and gastrin.* Springer.

Kacheva, S., Lenzen, S. and Gurgul-Convey, E. (2011) Differential effects of proinflammatory cytokines on cell death and ER stress in insulin-secreting INS1E cells and the involvement of nitric oxide. *Cytokine,* 55(2), 195-201.

Kahn, S.E., Cooper, M.E. and Del Prato, S. (2014) Pathophysiology and treatment of type 2 diabetes: perspectives on the past, present, and future. *The Lancet,* 383(9922), 1068-1083.

Karamanou, M., Protogerou, A., Tsoucalas, G., Androutsos, G. and Poulakou-Rebelakou, E. (2016) Milestones in the history of diabetes mellitus: The main contributors. *World Journal of Diabetes,* 7(1), 1-7.

Kaska, L., Sledzinski, T., Chomiczewska, A., Dettlaff-Pokora, A. and Swierczynski, J. (2016) Improved glucose metabolism following bariatric surgery is associated with increased circulating bile acid concentrations and remodeling of the gut microbiome. *World Journal of Gastroenterology,* 22(39), 8698-8719.

Kastin, A. (2013) *Handbook of biologically active peptides.* Academic press.

Katsarou, A., Gudbjörnsdottir, S., Rawshani, A., Dabelea, D., Bonifacio, E., Anderson, B.J., Jacobsen, L.M., Schatz, D.A. and Lernmark, Å. (2017) Type 1 diabetes mellitus. *Nature Reviews Disease Primers,* 3, 17016.

Kavvoura, F.K. and Ioannidis, J.P. (2005) CTLA-4 gene polymorphisms and susceptibility to type 1 diabetes mellitus: a HuGE Review and meta-analysis. *American Journal of Epidemiology,* 162(1), 3-16.

Kazafeos, K. (2011) Incretin effect: GLP-1, GIP, DPP4. *Diabetes Research and Clinical Practice,* 93 Suppl 1, S32-6.

Kerr, B.D., Flatt, P.R. and Gault, V.A. (2010) Effects of γ-glutamyl linker on DPP-IV resistance, duration of action and biological efficacy of acylated glucagon-like peptide-1. *Biochemical Pharmacology,* 80(3), 396-401.

Khanna, S. and Singh, T. (1971) Histology of the principal islets of a fresh water teleost, Channa punctatus (Bloch). *Cells Tissues Organs,* 78(1), 99-106.

Kilimnik, G., Zhao, B., Jo, J., Periwal, V., Witkowski, P., Misawa, R. and Hara, M. (2011) Altered islet composition and disproportionate loss of large islets in patients with type 2 diabetes. *PloS One,* 6(11), e27445.

Kim, A., Miller, K., Jo, J., Kilimnik, G., Wojcik, P. and Hara, M. (2009) Islet architecture: A comparative study. *Islets,* 1(2), 129-136.

Kim, S.H. and Park, M.J. (2017) Effects of growth hormone on glucose metabolism and insulin resistance in human. *Annals of Pediatric Endocrinology & Metabolism,* 22(3), 145-152.

Kim, W. and Egan, J.M. (2008) The role of incretins in glucose homeostasis and diabetes treatment. *Pharmacological Reviews,* 60(4), 470-512.

Knudsen, L.B., Nielsen, P.F., Huusfeldt, P.O., Johansen, N.L., Madsen, K., Pedersen, F.Z., Thøgersen, H., Wilken, M. and Agersø, H. (2000) Potent derivatives of glucagon-like peptide-1 with pharmacokinetic properties suitable for once daily administration. *Journal of Medicinal Chemistry,* 43(9), 1664-1669.

Kolb, H. (1987) Mouse models of insulin dependent diabetes: Low-dose streptozocin-induced diabetes and nonobese diabetic (NOD) mice. *Diabetes/metabolism Reviews,* 3(3), 751-778.

Komatsu, R., Matsuyama, T., Namba, M., Watanabe, N., Itoh, H., Kono, N. and Tarui, S. (1989) Glucagonostatic and insulinotropic action of glucagonlike peptide I-(7-36)-amide. *Diabetes,* 38(7), 902-905.

Kopin, A.S., Wheeler, M.B., Nishitani, J., McBride, E.W., Chang, T.M., Chey, W.Y. and Leiter, A.B. (1991) The secretin gene: evolutionary history, alternative splicing, and developmental regulation. *Proceedings of the National Academy of Sciences of the United States of America,* 88(12), 5335-5339.

Kulina, G.R. and Rayfield, E.J. (2016) The role of glucagon in the pathophysiology and management of diabetes. *Endocrine Practice,* 22(5), 612-621.

Kuraku, S. and Kuratani, S. (2006) Time scale for cyclostome evolution inferred with a phylogenetic diagnosis of hagfish and lamprey cDNA sequences. *Zoological Science,* 23(12), 1053-1064.

LaBarre, J., 1932. Sur les possibilités d'un traitement du diabète par I'incrétine. *Bull Acad R Med Belg*, *12*, pp.620-634.

Laiteerapong, N. and Huang, E.S. (2010) The public health implications of the cost-effectiveness of bariatric surgery for diabetes. *Diabetes Care,* 33(9), 2126-2128.

Lakhtakia, R. (2013) The history of diabetes mellitus. *Sultan Qaboos University Medical Journal,* 13(3), 368-370.

Laukkanen, O., Lindstrom, J., Eriksson, J., Valle, T.T., Hamalainen, H., Ilanne-Parikka, P., Keinanen-Kiukaanniemi, S., Tuomilehto, J., Uusitupa, M., Laakso, M. and Finnish Diabetes Prevention Study. (2005) Polymorphisms in the SLC2A2 (GLUT2) gene are associated with the conversion from impaired glucose tolerance to type 2 diabetes: the Finnish Diabetes Prevention Study. *Diabetes,* 54(7), 2256-2260.

Lean, M., Carraro, R., Finer, N., Hartvig, H., Lindegaard, M., Rössner, S., Van Gaal, L. and Astrup, A. (2014) Tolerability of nausea and vomiting and associations with weight loss in a randomized trial of liraglutide in obese, non-diabetic adults. *International Journal of Obesity,* 38(5), 689.

Lee, D.Y., Kim, E. and Choi, M.H. (2015) Technical and clinical aspects of cortisol as a biochemical marker of chronic stress. *BMB Reports,* 48(4), 209-216.

Lee, Y.S., Lee, C., Choung, J.S., Jung, H.S. and Jun, H.S. (2018) Glucagon-Like Peptide 1 Increases beta-Cell Regeneration by Promoting alpha- to beta-Cell Transdifferentiation. *Diabetes,* 67(12), 2601-2614.

Lefèbvre, P.J. (2012) *Glucagon III.* Springer Science & Business Media.

Lefèbvre, P. (1983) Glucagon and adipose tissue lipolysis. *In:* Anon.*Glucagon I.* Springer, 419-440.

Lenhardt, M., Hegediš, A., Mićković, B., Jeftić, V.Ž., Smederevac, M., Jarić, I., Cvijanović, G. and Gačić, Z. (2006) First record of the North American paddlefish (Polyodon spathula Walbaum, 1792) in the Serbian part of the Danube River. *Archives of Biological Sciences,* 58(3), 27-28.

Li, S., Zhao, J., Luan, J., Langenberg, C., Luben, R., Khaw, K., Wareham, N. and Loos, R. (2011) Genetic predisposition to obesity leads to increased risk of type 2 diabetes. *Diabetologia,* 54(4), 776-782.

Li, X., Zhang, Z. and Duke, J. (2014) Glucagon-like peptide 1-based therapies and risk of pancreatitis: a self-controlled case series analysis. *Pharmacoepidemiology and Drug Safety,* 23(3), 234-239.

Li, Y., Wu, K., Yu, S., Tamargo, I.A., Wang, Y. and Greig, N.H. (2017) Neurotrophic and neuroprotective effects of oxyntomodulin in neuronal cells and a rat model of stroke. *Experimental Neurology,* 288, 104-113.

Lim, G.E. and Brubaker, P.L. (2006) Glucagon-like peptide 1 secretion by the L-cell: the view from within. *Diabetes,* 55(Supplement 2), S70-S77.

Lin, F., Chen, H., Liu, J., Gao, Y., Zhang, X., Hao, J., Chen, D., Wu, H., Yuan, D., Wang, T. and Li, Z., 2015. Molecular cloning of a proglucagon in a cyprinid fish (Schizothorax prenanti): mRNA tissue distribution and quantification during periprandial changes and fasting. *Aquaculture*, *448*, pp.250-255.

Lins, P.E., Wajngot, A., Adamson, U., Vranic, M. and Efendic, S. (1983) Minimal increases in glucagon levels enhance glucose production in man with partial hypoinsulinemia. *Diabetes,* 32(7), 633-636.

Lopez, L.C., Li, W.H., Frazier, M.L., Luo, C.C. and Saunders, G.F., 1984. Evolution of glucagon genes. *Molecular biology and evolution*, *1*(4), pp.335-344.Luca, F., Perry, G. and Di Rienzo, A. (2010) Evolutionary adaptations to dietary changes. *Annual Review of Nutrition,* 30, 291-314.

Lund, P.K., Goodman, R.H., Dee, P.C. and Habener, J.F. (1982) Pancreatic preproglucagon cDNA contains two glucagon-related coding sequences arranged in tandem. *Proceedings of the National Academy of Sciences of the United States of America,* 79(2), 345-349.

Lund, P.K., Goodman, R.H., Montminy, M.R., Dee, P.C. and Habener, J.F., 1983. Anglerfish islet pre-proglucagon II: nucleotide and corresponding amino acid sequence of the cDNA. *Journal of Biological Chemistry*, *258*(5), pp.3280-3284.

Lynch, A.M., Pathak, N., Flatt, Y.E., Gault, V.A., O'Harte, F.P., Irwin, N. and Flatt, P.R. (2014) Comparison of stability, cellular, glucose-lowering and appetite supressing effects of oxyntomodulin analogues modified at the N-terminus. *European Journal of Pharmacology,* 743, 69-78.

Macfarlane, I. (2014) 1776: revolution in liverpool: Matthew Dobson discovers hyperglycaemia. *In:* 1776: revolution in liverpool: Matthew Dobson discovers hyperglycaemia. *Society for Endocrinology BES 2014.* BioScientifica

Madsen, K., Knudsen, L.B., Agersoe, H., Nielsen, P.F., Thøgersen, H., Wilken, M. and Johansen, N.L. (2007) Structure− activity and protraction relationship of long-acting glucagon-like peptide-1 derivatives: importance of fatty acid length, polarity, and bulkiness. *Journal of Medicinal Chemistry,* 50(24), 6126-6132.

Mahdizadeh, S., Khaleghi Ghadiri, M. and Gorji, A. (2015) Avicenna's Canon of Medicine: a review of analgesics and anti-inflammatory substances. *Avicenna Journal of Phytomedicine,* 5(3), 182-202.

Makman, M. H., and Sutherland, E. W., Jr. (1964). Use of liver adenyl cyclase for assay of glucagon in human gastro-intestinal tract and pancreas. Endocrinology, 75, 127-134.

Manandhar, B. and Ahn, J. (2014) Glucagon-like peptide-1 (GLP-1) analogs: recent advances, new possibilities, and therapeutic implications. *Journal of Medicinal Chemistry,* 58(3), 1020-1037.

Marin-Penalver, J.J., Martin-Timon, I., Sevillano-Collantes, C. and Del Canizo-Gomez, F.J. (2016) Update on the treatment of type 2 diabetes mellitus. *World Journal of Diabetes,* 7(17), 354-395.

Marks, V. (2018) Rebirth of the Incretin Concept: Its conception and early development. *Peptides,* 100, 3-8.

Marks, V. (1978) The enteroinsular axis. *Journal of Clinical Pathology.Supplement (Association of Clinical Pathologists),* 8, 38-42.

Matsuzaka, T. and Shimano, H. (2013) Insulin-dependent and-independent regulation of sterol regulatory element-binding protein-1c. *Journal of Diabetes Investigation,* 4(5), 411-412.

Mazzola, N. (2012) Review of current and emerging therapies in type 2 diabetes mellitus. *American Journal of Managed Care,* 18(1), S17.

McClenaghan, N.H., Barnett, C.R., Ah-Sing, E., Abdel-Wahab, Y.H., O'Harte, F.P., Yoon, T.W., Swanston-Flatt, S.K. and Flatt, P.R. (1996) Characterization of a novel

glucose-responsive insulin-secreting cell line, BRIN-BD11, produced by electrofusion. *Diabetes,* 45(8), 1132-1140.

McCluskey, J.T., Hamid, M., Guo-Parke, H., McClenaghan, N.H., Gomis, R. and Flatt, P.R. (2011) Development and functional characterization of insulin-releasing human pancreatic beta cell lines produced by electrofusion. *The Journal of Biological Chemistry,* 286(25), 21982-21992.

McIntyre N, Holdsworth CD, Turner DA. New interpretation of oral glucose tolerance. *The Lancet* (1964) 2:20–1

McDonald, N., Murray-Rust, J. and Blundell, T. (1995) The first structure of a receptor tyrosine kinase domain: a further step in understanding the molecular basis of insulin action. *Structure,* 3(1), 1-6.

Melmed, S. (2016) *Williams textbook of endocrinology.* Elsevier Health Sciences.

Mentlein, R., Gallwitz, B. and Schmidt, W.E. (1993) Dipeptidyl-peptidase IV hydrolyses gastric inhibitory polypeptide, glucagon-like peptide-1 (7–36) amide, peptide histidine methionine and is responsible for their degradation in human serum. *European Journal of Biochemistry,* 214(3), 829-835.

Mi, D., Fang, H., Zhao, Y. and Zhong, L. (2017) Birth weight and type 2 diabetes: A meta-analysis. *Experimental and Therapeutic Medicine,* 14(6), 5313-5320.

Mielke, J.G. and Wang, Y. (2011) Insulin, synaptic function, and opportunities for neuroprotection. *In:* Anon.*Progress in molecular biology and translational science.* Elsevier, 133-186.

Millar, P., Pathak, N., Parthsarathy, V., Bjourson, A.J., O'Kane, M., Pathak, V., Moffett, R.C., Flatt, P.R. and Gault, V.A. (2017) Metabolic and neuroprotective effects of dapagliflozin and liraglutide in diabetic mice. *Journal of Endocrinology,* 234(3), 255-267.

Mingrone, G. (2006) Dietary fatty acids and insulin secretion. *Scandinavian Journal of Food and Nutrition,* 50(sup2), 79-84.

Mitchell, N.S., Catenacci, V.A., Wyatt, H.R. and Hill, J.O. (2011) Obesity: overview of an epidemic. *The Psychiatric Clinics of North America,* 34(4), 717-732.

Miya, M. and Nishida, M. (2015) The mitogenomic contributions to molecular phylogenetics and evolution of fishes: a 15-year retrospect. *Ichthyological Research,* 62(1), 29-71.

Mkele, G. (2013) A review of metformin and its place in the diabetes guidelines. *South African Family Practice,* 55(6), 504-506.

Modlin, I.M. and Kidd, M. (2001) Ernest Starling and the discovery of secretin. *Journal of Clinical Gastroenterology,* 32(3), 187-192.

Mojsov, S., Weir, G.C. and Habener, J.F. (1987) Insulinotropin: glucagon-like peptide I (7-37) co-encoded in the glucagon gene is a potent stimulator of insulin release in the perfused rat pancreas. *The Journal of Clinical Investigation,* 79(2), 616-619.

Mommsen, T.P. (2000) Glucagon-like peptide-1 in fishes: the liver and beyond. *American Zoologist,* 40(2), 259-268.

Moody, T.W., Ito, T., Osefo, N. and Jensen, R.T. (2011) VIP and PACAP: recent insights into their functions/roles in physiology and disease from molecular and genetic studies. *Current Opinion in Endocrinology, Diabetes, and Obesity,* 18(1), 61-67.

Morgan, L.M., Morris, B.A. and Marks, V. (1978) Radioimmunoassay of gastric inhibitory polypeptide. *Annals of Clinical Biochemistry,* 15(1-6), 172-177.

Morgan, L., Hampton, S., Tredger, J., Cramb, R. and Marks, V. (1988) Modifications of gastric inhibitory polypeptide (GIP) secretion in man by a high-fat diet. *British Journal of Nutrition,* 59(3), 373-380.

Mosley, A.L., Corbett, J.A. and Özcan, S. (2004) Glucose regulation of insulin gene expression requires the recruitment of p300 by the β-cell-specific transcription factor Pdx-1. *Molecular Endocrinology,* 18(9), 2279-2290.

Müller, T., Finan, B., Clemmensen, C., DiMarchi, R. and Tschöp, M. (2017) The new biology and pharmacology of glucagon. *Physiological Reviews,* 97(2), 721-766.

Najjar, S.M. (2002) Regulation of insulin action by CEACAM1. *Trends in Endocrinology & Metabolism,* 13(6), 240-245.

Nakashima, K., Kaneto, H., Shimoda, M., Kimura, T. and Kaku, K. (2018) Pancreatic alpha cells in diabetic rats express active GLP-1 receptor: Endosomal co-localization of GLP-1/GLP-1R complex functioning through intra-islet paracrine mechanism. *Scientific Reports,* 8(1), 3725.

Nanditha, A., Ma, R.C., Ramachandran, A., Snehalatha, C., Chan, J.C., Chia, K.S., Shaw, J.E. and Zimmet, P.Z. (2016) Diabetes in Asia and the Pacific: Implications for the Global Epidemic. *Diabetes Care,* 39(3), 472-485.

Nathan, D.M. and DCCT/EDIC Research Group. (2014) The diabetes control and complications trial/epidemiology of diabetes interventions and complications study at 30 years: overview. *Diabetes Care,* 37(1), 9-16.

Navarro, I., Gutierrez, J., Caixach, J., Rivera, J. and Planas, J., 1991. Isolation and primary structure of glucagon from the endocrine pancreas of Thunnus obesus. *General and comparative endocrinology*, *83*(2), pp.227-232.

Nelson, J.S., Grande, T.C. and Wilson, M.V. (2016) *Fishes of the World.* John Wiley & Sons.

Ng, S.Y., Lee, L.T. and Chow, B.K. (2010) Insights into the evolution of proglucagon-derived peptides and receptors in fish and amphibians. *Annals of the New York Academy of Sciences,* 1200(1), 15-32.

Nichols, R., LEE, T.D. and Andrews, P.C. (1988). Pancreatic proglucagon processing: isolation and structures of glucagon and glucagon-like peptide from gene I. *Endocrinology*, *123*(6), pp.2639-2645.

Nie, Y., Nakashima, M., Brubaker, P.L., Li, Q.L., Perfetti, R., Jansen, E., Zambre, Y., Pipeleers, D. and Friedman, T.C. (2000) Regulation of pancreatic PC1 and PC2 associated with increased glucagon-like peptide 1 in diabetic rats. *The Journal of Clinical Investigation,* 105(7), 955-965.

Nishimoto, Y. and Tamori, Y. (2017) CIDE family-mediated unique lipid droplet morphology in white adipose tissue and brown adipose tissue determines the adipocyte energy metabolism. *Journal of Atherosclerosis and Thrombosis,* 24(10), 989-998.

Nolan, C.J., Madiraju, M.S., Delghingaro-Augusto, V., Peyot, M.L. and Prentki, M. (2006) Fatty acid signaling in the beta-cell and insulin secretion. *Diabetes,* 55 Suppl 2, S16-23.

Norris, D.O. and Carr, J.A. (2013) *Vertebrate endocrinology.* Academic Press.

Nwaneri, C. (2015) Diabetes mellitus: A complete ancient and modern historical perspective.

O'Harte, F.P., Parthsarathy, V., Hogg, C. and Flatt, P.R. (2018) Long-term treatment with acylated analogues of apelin-13 amide ameliorates diabetes and improves lipid profile of high-fat fed mice. *PloS One,* 13(8), e0202350.

O'Harte, F., Ng, M., Lynch, A., Conlon, J. and Flatt, P. (2016a) Dogfish glucagon analogues counter hyperglycaemia and enhance both insulin secretion and action in diet-induced obese diabetic mice. *Diabetes, Obesity and Metabolism,* 18(10), 1013-1024.

O'Harte, F., Ng, M., Lynch, A., Conlon, J. and Flatt, P. (2016b) Novel dual agonist peptide analogues derived from dogfish glucagon show promising in vitro insulin releasing actions and antihyperglycaemic activity in mice. *Molecular and Cellular Endocrinology,* 431, 133-144.

Ogurtsova, K., da Rocha Fernandes, J., Huang, Y., Linnenkamp, U., Guariguata, L., Cho, N., Cavan, D., Shaw, J. and Makaroff, L. (2017) IDF Diabetes Atlas: Global estimates for the prevalence of diabetes for 2015 and 2040. *Diabetes Research and Clinical Practice,* 128, 40-50.

Olokoba, A.B., Obateru, O.A. and Olokoba, L.B. (2012) Type 2 diabetes mellitus: a review of current trends. *Oman Medical Journal,* 27(4), 269-273.

Owolabi, B.O., Ojo, O.O., Srinivasan, D.K., Conlon, J.M., Flatt, P.R., Abdel-Wahab, Y.H., 2016. *In vitro* and *in vivo* insulinotropic properties of the multifunctional frog skin peptide hymenochirin-1B: a structure-activity study. Amino Acids 48, 535-544.

On, J.S. and Chow, B.K. (2016) Molecular Evolution of Pituitary Adenylyl Cyclase-Activating Polypeptide Subfamily and Cognate Receptor Subfamily. *In:* Anon.*Pituitary Adenylate Cyclase Activating Polypeptide—PACAP.* Springer, 3-17.

Oren, D.A., Wei, Y., Skrabanek, L., Chow, B.K., Mommsen, T. and Mojsov, S. (2016) Structural mapping and functional characterization of zebrafish class B G-protein coupled receptor (GPCR) with dual ligand selectivity towards GLP-1 and glucagon. *PloS One,* 11(12), e0167718.

Pais, R., Gribble, F.M. and Reimann, F. (2016) Stimulation of incretin secreting cells. *Therapeutic Advances in Endocrinology and Metabolism,* 7(1), 24-42.

Pan, C.Q., Buxton, J.M., Yung, S.L., Tom, I., Yang, L., Chen, H., MacDougall, M., Bell, A., Claus, T.H., Clairmont, K.B. and Whelan, J.P. (2006) Design of a long acting peptide functioning as both a glucagon-like peptide-1 receptor agonist and a glucagon receptor antagonist. *The Journal of Biological Chemistry,* 281(18), 12506-12515.

Paniccia, A. and Schulick, R.D. (2017) Pancreatic Physiology and Functional Assessment. *In:* Anon.*Blumgart's Surgery of the Liver, Biliary Tract and Pancreas, 2-Volume Set (Sixth Edition).* Elsevier, 66-76. e3.

Panopoulou, G. and Poustka, A.J. (2005) Timing and mechanism of ancient vertebrate genome duplications–the adventure of a hypothesis. *TRENDS in Genetics,* 21(10), 559-567.

Park, C.R., Moon, M.J., Park, S., Kim, D., Cho, E.B., Millar, R.P., Hwang, J. and Seong, J.Y. (2013) A novel glucagon-related peptide (GCRP) and its receptor GCRPR account for coevolution of their family members in vertebrates. *PLoS One,* 8(6), e65420.

Park, S., Kim, Y.W., Kim, J.Y., Jang, E.C., Doh, K.O. and Lee, S.K. (2001) Effect of high fat diet on insulin resistance: dietary fat versus visceral fat mass. *Journal of Korean Medical Science,* 16(4), 386-390.

Pathak, V., Vasu, S., Gault, V.A., Flatt, P.R. and Irwin, N. (2015) Sequential induction of beta cell rest and stimulation using stable GIP inhibitor and GLP-1 mimetic peptides improves metabolic control in C57BL/KsJ db/db mice. *Diabetologia,* 58(9), 2144-2153.

Patil, N.H. and Devarajan, P.V. (2014) Colloidal carriers for noninvasive delivery of insulin. *In:* Anon.*Colloid and Interface Science in Pharmaceutical Research and Development.* Elsevier, 411-442.

Pettigrew, J.D. and Wilkens, L. (2003) Paddlefish and platypus: parallel evolution of passive electroreception in a rostral bill organ. *In:* Anon.*Sensory Processing in Aquatic Environments.* Springer, 420-433.

Pihoker, C., Gilliam, L.K., Hampe, C.S. and Lernmark, A. (2005) Autoantibodies in diabetes. *Diabetes,* 54 Suppl 2, S52-61.

Pingitore, A., Ruz-Maldonado, I., Liu, B., Huang, G.C., Choudhary, P. and Persaud, S.J. (2017) Dynamic Profiling of Insulin Secretion and ATP Generation in Isolated Human and Mouse Islets Reveals Differential Glucose Sensitivity. *Cellular Physiology and Biochemistry : International Journal of Experimental Cellular Physiology, Biochemistry, and Pharmacology,* 44(4), 1352-1359.

Plisetskaya, E., Pollock, H., Rouse, J., Hamilton, J., Kimmel, J. and Gorbman, A. (1986) Isolation and structures of coho salmon (Oncorhynchus kisutch) glucagon and glucagon-like peptide. *Regulatory Peptides,* 14(1), 57-67.

Plisetskaya, E.M. (1989) Physiology of fish endocrine pancreas. *Fish Physiology and Biochemistry,* 7(1-6), 39.

Plisetskaya, E.M. and Mommsen, T.P. (1996) Glucagon and glucagon-like peptides in fishes. *In:* Anon.*International review of cytology.* Elsevier, 187-257.

Pocai, A. (2014) Action and therapeutic potential of oxyntomodulin. *Molecular Metabolism,* 3(3), 241-251.

Pocai, A., Carrington, P.E., Adams, J.R., Wright, M., Eiermann, G., Zhu, L., Du, X., Petrov, A., Lassman, M.E., Jiang, G., Liu, F., Miller, C., Tota, L.M., Zhou, G., Zhang, X., Sountis, M.M., Santoprete, A., Capito', E., Chicchi, G.G., Thornberry, N., Bianchi, E., Pessi, A., Marsh, D.J. and SinhaRoy, R. (2009) Glucagon-like peptide 1/glucagon receptor dual agonism reverses obesity in mice. *Diabetes,* 58(10), 2258-2266.

Polakof, S., Mommsen, T.P. and Soengas, J.L. (2011) Glucosensing and glucose homeostasis: from fish to mammals. *Comparative Biochemistry and Physiology Part B: Biochemistry and Molecular Biology,* 160(4), 123-149.

Pollock, H., Kimmel, J., Ebner, K., Hamilton, J., Rouse, J., Lance, V. and Rawitch, A. (1988) Isolation of alligator gar (Lepisosteus spatula) glucagon, oxyntomodulin, and glucagon-like peptide: amino acid sequences of oxyntomodulin and glucagon-like peptide. *General and Comparative Endocrinology,* 69(1), 133-140.

Poretsky, L. (2010) *Principles of diabetes mellitus.* Springer.

Pospisilik, J.A., Hinke, S.A., Pederson, R.A., Hoffmann, T., Rosche, F., Schlenzig, D., Glund, K., Heiser, U., McIntosh, C.H. and Demuth, H. (2001) Metabolism of glucagon by dipeptidyl peptidase IV (CD26). *Regulatory Peptides,* 96(3), 133-141.

Prasad, R. and Groop, L. (2015) *Genetics of Type 2 Diabetes-Pitfalls and Possibilities.Genes (Basel) 6: 87–123,*

Quianzon, C.C. and Cheikh, I.E. (2012a) History of current non-insulin medications for diabetes mellitus. *Journal of Community Hospital Internal Medicine Perspectives,* 2(3), 19081.

Quianzon, C.C. and Cheikh, I.E. (2012b) History of insulin. *Journal of Community Hospital Internal Medicine Perspectives,* 2(2), 18701.

Quoix, N., Cheng-Xue, R., Guiot, Y., Herrera, P.L., Henquin, J. and Gilon, P. (2007) The GluCre-ROSA26EYFP mouse: A new model for easy identification of living pancreatic α-cells. *FEBS Letters,* 581(22), 4235-4240.

Ragheb, R. and Medhat, A.M. (2011) Mechanisms of fatty acid-induced insulin resistance in muscle and liver. *J Diabetes Metab,* 2(127), 1-6.

Ralph H., H., Noriyoshi, F. and Robb E., W. (2009) Pancreas. *Modern Surgical Pathology,* 1, 867-901.

Ramachandran, A. and Snehalatha, C. (2009) Current scenario of diabetes in India. *Journal of Diabetes,* 1(1), 18-28.

Ramachandran, A., Snehalatha, C., Shetty, A.S. and Nanditha, A. (2012) Trends in prevalence of diabetes in Asian countries. *World Journal of Diabetes,* 3(6), 110-117.

Remedi, M.S. and Emfinger, C. (2016) Pancreatic β-cell identity in diabetes. *Diabetes, Obesity and Metabolism,* 18, 110-116.

Rerup, C.C. (1970) Drugs producing diabetes through damage of the insulin secreting cells. *Pharmacological Reviews,* 22(4), 485-518.

Reusch, C.E. and Padrutt, I. (2013) New incretin hormonal therapies in humans relevant to diabetic cats. *The Veterinary Clinics of North America.Small Animal Practice,* 43(2), 417-433.

Rich, S.S. and Concannon, P. (2015) Summary of the Type 1 Diabetes Genetics Consortium Autoantibody Workshop. *Diabetes Care,* 38 Suppl 2, S45-8.

Rorsman, P. and Braun, M. (2013) Regulation of insulin secretion in human pancreatic islets. *Annual Review of Physiology,* 75, 155-179.

Rose Gubitosi-Klug. (2016) Intensive Diabetes Treatment and Cardiovascular Outcomes in Type 1 Diabetes: The DCCT/EDIC Study 30-Year Follow-up. *Diabetes Care,* 39(5), 686-693.

Rosner, F. (2002) The life of Moses Maimonides, a prominent medieval physician. *Einstein Quart J Biol Med,* 19, 125-128.

Rossini, A.A., Like, A.A., Chick, W.L., Appel, M.C. and Cahill, G.F.,Jr. (1977) Studies of streptozotocin-induced insulitis and diabetes. *Proceedings of the National Academy of Sciences of the United States of America,* 74(6), 2485-2489.

Ryan, G.J., Jobe, L.J. and Martin, R. (2005) Pramlintide in the treatment of type 1 and type 2 diabetes mellitus. *Clinical Therapeutics,* 27(10), 1500-1512.

Sachdeva, M.M. and Stoffers, D.A. (2009) Minireview: meeting the demand for insulin: molecular mechanisms of adaptive postnatal ß-cell mass expansion. *Molecular Endocrinology,* 23(6), 747-758.

Sadry, S.A. and Drucker, D.J. (2013) Emerging combinatorial hormone therapies for the treatment of obesity and T2DM. *Nature Reviews Endocrinology,* 9(7), 425.

Samuel, V.T. and Shulman, G.I. (2012) Mechanisms for insulin resistance: common threads and missing links. *Cell,* 148(5), 852-871.

Sanders, L.J. (2002) From Thebes to Toronto and the 21st century: an incredible journey. *Diabetes Spectrum,* 15(1), 56-60.

Sandoval, D.A. and D'Alessio, D.A. (2015) Physiology of proglucagon peptides: role of glucagon and GLP-1 in health and disease. *Physiological Reviews,* 95(2), 513-548.

Scheen, A. (2004) Pathophysiology of insulin secretion. *In:* Pathophysiology of insulin secretion. *Annales D'endocrinologie.* Masson, 29-36.

Schmeltz, L. and Metzger, B. (2006) Diabetes/syndrome X. *In:* Anon.*Comprehensive Medicinal Chemistry II.* Elsevier Ltd.,

Schuit, F., Flamez, D., De Vos, A. and Pipeleers, D. (2002) Glucose-regulated gene expression maintaining the glucose-responsive state of beta-cells. *Diabetes,* 51 Suppl 3, S326-32.

Schuit, F.C., Huypens, P., Heimberg, H. and Pipeleers, D.G. (2001) Glucose sensing in pancreatic beta-cells: a model for the study of other glucose-regulated cells in gut, pancreas, and hypothalamus. *Diabetes,* 50(1), 1-11.

Scott, R., Tan, T. and Bloom, S. (2014) Can Bayliss and Starling gut hormones cure a worldwide pandemic? *The Journal of Physiology,* 592(23), 5153-5167.

Seetho, I.W. and Wilding, J.P. (2014) The clinical management of diabetes mellitus. *In:* Anon.*Clinical Biochemistry: Metabolic and Clinical Aspects (Third Edition).* Elsevier, 305-332.

Seewoodhary, J. and Bain, S.C. (2010) Incretin therapeutics in diabetes: 1902 to present. *West London Medical Journal,* 2(2), 15-24.

Seino, Y., Fukushima, M. and Yabe, D. (2010) GIP and GLP-1, the two incretin hormones: similarities and differences. *Journal of Diabetes Investigation,* 1(1-2), 8-23.

Sekar, R., Singh, K., Arokiaraj, A. and Chow, B. (2016) Pharmacological actions of glucagon-like peptide-1, gastric inhibitory polypeptide, and glucagon. *In:* Anon.*International review of cell and molecular biology.* Elsevier, 279-341.

Sekar, R., Wang, L. and Chow, B.K.C. (2017) Central control of feeding behavior by the secretin, PACAP, and glucagon family of peptides. *Frontiers in Endocrinology,* 8, 18.

Shah, P., Vella, A., Basu, A., Basu, R., Schwenk, W.F. and Rizza, R.A. (2000) Lack of suppression of glucagon contributes to postprandial hyperglycemia in subjects with type 2 diabetes mellitus. *The Journal of Clinical Endocrinology & Metabolism,* 85(11), 4053-4059.

Shapses, S.A. and Sukumar, D. (2012) Bone metabolism in obesity and weight loss. *Annual Review of Nutrition,* 32, 287-309.

Sharofova, M., Nuraliev, Y., Sukhrobov, P., Sagdieva, S. and Dushenkov, V. (2017) Can Avicenna Help Manage the Diabetes Epidemic in Central Asia?

Sherwood, N.M., Krueckl, S.L. and McRory, J.E. (2000) The origin and function of the pituitary adenylate cyclase-activating polypeptide (PACAP)/glucagon superfamily. *Endocrine Reviews,* 21(6), 619-670.

Simmons, K.M. and Michels, A.W. (2015) Type 1 diabetes: A predictable disease. *World Journal of Diabetes,* 6(3), 380-390.

Simsir, I.Y., Soyaltin, U.E. and Cetinkalp, S. (2018) Glucagon like peptide-1 (GLP-1) likes Alzheimer's disease. *Diabetes & Metabolic Syndrome: Clinical Research & Reviews,*

Smith, G.P. (2000) Pavlov and integrative physiology. *American Journal of Physiology-Regulatory, Integrative and Comparative Physiology,* 279(3), R743-R755.

Son, S., Chae, S.Y., Kim, C.W., Choi, Y.G., Jung, S.Y., Lee, S. and Lee, K.C. (2009) Preparation and structural, biochemical, and pharmaceutical characterizations of bile acid-modified long-acting exendin-4 derivatives. *Journal of Medicinal Chemistry,* 52(21), 6889-6896.

Sorimachi, H., Hata, S. and Ono, Y. (2013) Other calpains. *In:* Anon.*Handbook of Proteolytic Enzymes (Third Edition).* Elsevier, 2027-2038.

Spreckley, E. and Murphy, K.G. (2015) The L-cell in nutritional sensing and the regulation of appetite. *Frontiers in Nutrition,* 2, 23.

Steck, A.K. and Rewers, M.J. (2011) Genetics of type 1 diabetes. *Clinical Chemistry,* 57(2), 176-185.

Steinberg, W.M., Buse, J.B., Ghorbani, M.L.M., Orsted, D.D., Nauck, M.A., LEADER Steering Committee and LEADER Trial Investigators. (2017) Amylase,

Lipase, and Acute Pancreatitis in People With Type 2 Diabetes Treated With Liraglutide: Results From the LEADER Randomized Trial. *Diabetes Care,* 40(7), 966-972.

Stephenson, K., Kennedy, L., Hargrove, L., Demieville, J., Thomson, J., Alpini, G. and Francis, H. (2018) Updates on Dietary Models of Nonalcoholic Fatty Liver Disease: Current Studies and Insights. *Gene Expression,* 18(1), 5-17.

Stolarczyk, E., Le Gall, M., Even, P., Houllier, A., Serradas, P., Brot-Laroche, E. and Leturque, A. (2007) Loss of sugar detection by GLUT2 affects glucose homeostasis in mice. *PLoS One,* 2(12), e1288.

Stonehouse, A.H. and Maggs, D.G. (2007) Emerging therapies for type 2 diabetes. *Current Drug Therapy,* 2(2), 151-160.

Stylianou, C. and Kelnar, C. (2009) The introduction of successful treatment of diabetes mellitus with insulin. *Journal of the Royal Society of Medicine,* 102(7), 298-303.

Sun, Q. and Zhao, Z. (2017) Peptide Hormones as Tumor Markers in Clinical Practice. *In:* Anon.*The Enzymes.* Elsevier, 65-79.

Takei, Y. (2015) Secretin (Pituitary Adenylate Cyclase-Activating Polypeptide) Family. *In:* Anon.*Handbook of Hormones.* Elsevier, 140-e18-2.

Tam, J.K., Lee, L.T. and Chow, B.K. (2007) PACAP-related peptide (PRP)—molecular evolution and potential functions. *Peptides,* 28(9), 1920-1929.

Tam, J.K., Lee, L.T., Jin, J. and Chow, B.K. (2014) Molecular evolution of GPCRs: Secretin/secretin receptors. *Journal of Molecular Endocrinology,* 52(3), T1-14.

Tang, W., Cui, D., Jiang, L., Zhao, L., Qian, W., Long, S.A. and Xu, K. (2015) Association of common polymorphisms in the IL 2 RA gene with type 1 diabetes: evidence of 32,646 individuals from 10 independent studies. *Journal of Cellular and Molecular Medicine,* 19(10), 2481-2488.

Tattersall, R. (2009) *Diabetes: the biography.* Oxford University Press.

Tengholm, A. and Gylfe, E. (2017) cAMP signalling in insulin and glucagon secretion. *Diabetes, Obesity and Metabolism,* 19, 42-53.

Thorel, F., Népote, V., Avril, I., Kohno, K., Desgraz, R., Chera, S. and Herrera, P.L. (2012) Conversion of adult pancreatic α-cells to β-cells after extreme β-cell loss. *Nature,* 464(7292), 1149.

Thorens, B. and Roduit, R. (1994) Regulated expression of GLUT2 in diabetes studied in transplanted pancreatic beta cells. *Biochemical Society Transactions,* 22(3), 684-687.

Thorens, B. and Waeber, G. (1993) Glucagon-like peptide-I and the control of insulin secretion in the normal state and in NIDDM. *Diabetes,* 42(9), 1219-1225.

Tian, L. and Yu, X. (2017) Fat, sugar, and bone health: a complex relationship. *Nutrients,* 9(5), 506.

Tillner, J., Posch, M.G., Wagner, F., Teichert, L., Hijazi, Y., Einig, C., Keil, S., Haack, T., Wagner, M. and Bossart, M. (2018) A novel dual glucagon-like peptide and glucagon receptor agonist SAR425899: Results of randomized, placebo-controlled first-in-human and first-in-patient trials. *Diabetes, Obesity and Metabolism,* 21(1), 120-128.

Tipton, C.M. (2008) Susruta of India, an unrecognized contributor to the history of exercise physiology. *Journal of Applied Physiology,* 104(6), 1553-1556.

Track, N.S. (1980) The gastrointestinal endocrine system. *Canadian Medical Association Journal,* 122(3), 287-292.

Tsend-Ayush, E., He, C., Myers, M.A., Andrikopoulos, S., Wong, N., Sexton, P.M., Wootten, D., Forbes, B.E. and Grutzner, F. (2016) Monotreme glucagon-like peptide-1 in venom and gut: one gene–two very different functions. *Scientific Reports,* 6, 37744.

Tseng, C.C., Wolfe, M.M., (2004) Glucose-Dependent Insulinotropic Polypeptide (GIP). Encyclopedia of Gastroenterology, 237-243

Unger, R.H. and Cherrington, A.D. (2012) Glucagonocentric restructuring of diabetes: a pathophysiologic and therapeutic makeover. *The Journal of Clinical Investigation,* 122(1), 4-12.

Unger, R.H., Aguilar-Parada, E., Müller, W.A. and Eisentraut, A.M. (1970) Studies of pancreatic alpha cell function in normal and diabetic subjects. *The Journal of clinical investigation*, *49* (4), pp.837-848.

Unger, R.H. (1978) Role of glucagon in the pathogenesis of diabetes: the status of the controversy. *Metabolism*, *27*(11), pp.1691-1709.

Unger, R. and Orci, L. (1975) The essential role of glucagon in the pathogenesis of diabetes mellitus. *The Lancet*, *305*(7897), pp.14-16.

Unson, C.G., Wu, C., Jiang, Y., Yoo, B., Cheung, C., Sakmar, T.P. and Merrifield, R. (2002) Roles of specific extracellular domains of the glucagon receptor in ligand binding and signaling. *Biochemistry,* 41(39), 11795-11803.

Unson, C.G., Wu, C. and Merrifield, R. (1994) Roles of aspartic acid 15 and 21 in glucagon action: receptor anchor and surrogates for aspartic acid 9. *Biochemistry,* 33(22), 6884-6887.

Unson, C.G., Wu, C.R., Cheung, C.P. and Merrifield, R.B. (1998) Positively charged residues at positions 12, 17, and 18 of glucagon ensure maximum biological potency. *The Journal of Biological Chemistry,* 273(17), 10308-10312.

Unson, C.G., Wu, C.R., Fitzpatrick, K.J. and Merrifield, R.B. (1994) Multiple-site replacement analogs of glucagon. A molecular basis for antagonist design. *The Journal of Biological Chemistry,* 269(17), 12548-12551.

Ussher, J.R. and Drucker, D.J. (2012) Cardiovascular biology of the incretin system. *Endocrine Reviews,* 33(2), 187-215.

Vilsbøll, T., Krarup, T., Madsbad, S. and Holst, J.J. (2003) Both GLP-1 and GIP are insulinotropic at basal and postprandial glucose levels and contribute nearly equally to the incretin effect of a meal in healthy subjects. *Regulatory Peptides,* 114(2-3), 115-121.

Vilsbøll, T., 2009. The effects of glucagon-like peptide-1 on the beta cell. *Diabetes, Obesity and Metabolism*, *11*, pp.11-18.

Von Engelhardt, D. (1989) Outlines of historical development. *In:* Anon.*Diabetes Its Medical and Cultural History.* Springer, 3-12.

Wahba, I.M. and Mak, R.H. (2007) Obesity and obesity-initiated metabolic syndrome: mechanistic links to chronic kidney disease. *Clinical Journal of the American Society of Nephrology : CJASN,* 2(3), 550-562.

Wajcberg, E. and Amarah, A. (2010) Liraglutide in the management of type 2 diabetes. *Drug Design, Development and Therapy,* 4, 279-290.

Walton, K.L. (2009) Teaching the role of secretin in the regulation of gastric acid secretion using a classic paper by Johnson and Grossman. *Advances in Physiology Education,* 33(3), 165-168.

Wang, H. and Shen, Z. (2018) Sex Control in Aquaculture: Concept to Practice. *Sex Control in Aquaculture,* 1-34.

Wang, Y., He, S., Feng, X., Cheng, J., Luo, Y., Tian, L. and Huang, Q. (2017) Metformin: a review of its potential indications. *Drug Design, Development and Therapy,* 11, 2421.

Wang, Y., Nielsen, P.F., Youson, J.H., Potter, I.C. and Conlon, J.M. (1999) Multiple Forms of Glucagon and Somatostatin Isolated from the Intestine of the Southern-Hemisphere LampreyGeotria australis. *General and Comparative Endocrinology,* 113(2), 274-282.

Watkins, P.J., Amiel, S.A., Howell, S.L. and Turner, E. (2008) *Diabetes and its management.* John Wiley & Sons.

Weisel, G.F. (1973) Anatomy and histology of the digestive system of the paddlefish (Polyodon spathula). *Journal of Morphology,* 140(2), 243-255.

Weiss, R. and Lustig, R.H. (2014) Obesity, metabolic syndrome, and disorders of energy balance. *In:* Anon.*Pediatric Endocrinology (Fourth Edition).* Elsevier, 956-1014. e1.

White, J.R. (2014) A brief history of the development of diabetes medications. *Diabetes Spectrum,* 27(2), 82-86.

Whiting, D.R., Guariguata, L., Weil, C. and Shaw, J. (2011) IDF diabetes atlas: global estimates of the prevalence of diabetes for 2011 and 2030. *Diabetes Research and Clinical Practice,* 94(3), 311-321.

Whittaker, L., Hao, C., Fu, W. and Whittaker, J. (2008) High-affinity insulin binding: insulin interacts with two receptor ligand binding sites. *Biochemistry,* 47(48), 12900-12909.

Wilcox, G. (2005) Insulin and insulin resistance. *The Clinical Biochemist.Reviews,* 26(2), 19-39.

Wise, J. (2016) Metformin is backed as first line therapy for type 2 diabetes. *BMJ: British Medical Journal (Online),* 353

Woerle, H.J., Carneiro, L., Derani, A., Goke, B. and Schirra, J. (2012) The role of endogenous incretin secretion as amplifier of glucose-stimulated insulin secretion in healthy subjects and patients with type 2 diabetes. *Diabetes,* 61(9), 2349-2358.

Wood, A.W., Duan, C. and Bern, H.A. (2005) Insulin-like growth factor signaling in fish.

World Health Organisation. (2018) ***The top 10 causes of death***. Available at: http://www.who.int/en/news-room/fact-sheets/detail/the-top-10-causes-of-death

Wu, Y., Ding, Y., Tanaka, Y. and Zhang, W. (2014) Risk factors contributing to type 2 diabetes and recent advances in the treatment and prevention. *International Journal of Medical Sciences,* 11(11), 1185-1200.

Xiao, Q., Giguere, J., Parisien, M., Jeng, W., St-Pierre, S., Brubaker, P. and Wheeler, M. (2001) Biological activities of glucagon-like peptide-1 analogues in vitro and in vivo. *Biochemistry,* 40(9), 2860-2869.

Xu, G., Kaneto, H., Laybutt, D.R., Duvivier-Kali, V.F., Trivedi, N., Suzuma, K., King, G.L., Weir, G.C. and Bonner-Weir, S. (2007) Downregulation of GLP-1 and GIP receptor expression by hyperglycemia: possible contribution to impaired incretin effects in diabetes. *Diabetes,* 56(6), 1551-1558.

Xu, Y., Zhu, S.W. and Li, Q.W. (2016) Lamprey: a model for vertebrate evolutionary research. *Zoological Research,* 37(5), 263-269.

Yamagishi, S. and Matsui, T. (2011) Pleiotropic effects of glucagon-like peptide-1 (GLP-1)-based therapies on vascular complications in diabetes. *Current Pharmaceutical Design,* 17(38), 4379-4385.

Yang, H., Wang, Z., Xu, K., Gu, R., Chen, H., Yu, D., Xing, C., Liu, Y., Yu, L. and Hutton, J. (2012) IFIH1 gene polymorphisms in type 1 diabetes: genetic association analysis and genotype-phenotype correlation in Chinese Han population. *Autoimmunity,* 45(3), 226-232.

Yalow, R.S. and Berson, S.A., 1960. Immunoassay of endogenous plasma insulin in man. *The Journal of clinical investigation*, *39*(7), pp.1157-1175.

Yoon, J. and Jun, H. (2005) Autoimmune destruction of pancreatic β cells. *American Journal of Therapeutics,* 12(6), 580-591.

You, J., Wang, Z., Xu, S., Zhang, W., Fang, Q., Liu, H., Peng, L., Deng, T. and Lou, J. (2016) Advanced Glycation End Products Impair Glucose-Stimulated Insulin Secretion of a Pancreatic β-Cell Line INS-1-3 by Disturbance of Microtubule Cytoskeleton via p38/MAPK Activation. *Journal of Diabetes Research,* 2016

Youson, J.H. (2000) The agnathan enteropancreatic endocrine system: phylogenetic and ontogenetic histories, structure, and function. *American Zoologist,* 40(2), 179-199.

Youson, J.H. and Elliott, W.M. (1989) Morphogenesis and distribution of the endocrine pancreas in adult lampreys. *Fish Physiology and Biochemistry,* 7(1-6), 125-131.

Yuen, T.T.H., Mok, P.Y. and Chow, B.K.C., 1997. Molecular cloning of a cDNA encoding proglucagon from goldfish, Carassius auratus. *Fish Physiology and Biochemistry*, *17*(1-6), pp.223-230.

Zajac, J., Shrestha, A., Patel, P. and Poretsky, L. (2010) The main events in the history of diabetes mellitus. *In:* Anon.*Principles of diabetes mellitus.* Springer, 3-16.

Zheng, Y., Ley, S.H. and Hu, F.B. (2018) Global aetiology and epidemiology of type 2 diabetes mellitus and its complications. *Nature Reviews Endocrinology,* 14(2), 88.

Zhou, J., Cai, X., Huang, X., Dai, Y., Sun, L., Zhang, B., Yang, B., Lin, H., Huang, W. and Qian, H. (2017) A novel glucagon-like peptide-1/glucagon receptor dual agonist exhibits weight-lowering and diabetes-protective effects. *European Journal of Medicinal Chemistry,* 138, 1158-1169.

Zhou, Z., Reyes-Vargas, E., Escobar, H., Rudd, B., Rockwood, A.L., Delgado, J.C., He, X. and Jensen, P.E. (2016) Type 1 diabetes associated HLA-DQ2 and DQ8 molecules are relatively resistant to HLA-DM mediated release of invariant chain-derived CLIP peptides. *European Journal of Immunology,* 46(4), 834-845.

Zhu, X., Zhou, A., Dey, A., Norrbom, C., Carroll, R., Zhang, C., Laurent, V., Lindberg, I., Ugleholdt, R., Holst, J.J. and Steiner, D.F. (2002) Disruption of PC1/3 expression in mice causes dwarfism and multiple neuroendocrine peptide processing defects. *Proceedings of the National Academy of Sciences of the United States of America,* 99(16), 10293-10298.

Zufall, F. and Munger, S.D. (2016) *Chemosensory transduction: the detection of odors, tastes, and other chemostimuli.* Academic Press.